



University
of Glasgow

Martin, Craig Robert Leslie (2012) *Crystal engineering approaches to controlling the formation of molecular complexes and their polymorphs*. PhD thesis.

<http://theses.gla.ac.uk/3154/>

Copyright and moral rights for this thesis are retained by the author

A copy can be downloaded for personal non-commercial research or study, without prior permission or charge

This thesis cannot be reproduced or quoted extensively from without first obtaining permission in writing from the Author

The content must not be changed in any way or sold commercially in any format or medium without the formal permission of the Author

When referring to this work, full bibliographic details including the author, title, awarding institution and date of the thesis must be given

Crystal Engineering Approaches to Controlling the Formation of Molecular Complexes and their Polymorphs

Craig Robert Leslie Martin

Doctor of Philosophy Degree in Chemistry

School of Chemistry

University of Glasgow

September 2011

Supervisor: Prof Chick Wilson



**University
of Glasgow**

Declaration

The thesis has been written in accordance with the University regulations and all work presented is original and performed by the author unless otherwise stated and referenced in the text.

©Craig Robert Leslie Martin, August 2011

Craig Robert Leslie Martin

August 2011

Abstract

This work aimed to investigate and exploit the hydrogen bonds generated between heterocyclic aromatic compounds, namely benzimidazole and imidazole, and the carboxylic acid group. The flexible but robust hydrogen bonds generated have been used to create molecular complexes, using practical and relevant co-molecules. A systematic approach has been used in the selection of co-molecules on the basis of crystal engineering principles. A library of robust hydrogen bonds and primary structural motifs has been generated, which has been used to explain the solid-state assembly of the collection of molecular complexes produced in this work and in related published structures. The similarities in hydrogen bond strength, bonding motifs and proton transfer behaviour between very dissimilar molecular complexes have been remarkable. The opposite is also true in other examples, with very similar molecular complexes showing remarkable differences, but overall, a picture is built up of predictable use of crystal engineering principles in designing molecular complexes with anticipated structural and packing features.

The phenomenon of polymorphism, widely known but poorly understood, is essential to many industrial processes. A primary aim of this work was to promote and control the formation of molecular complex polymorphs through varying crystallisation conditions. Co-crystallisations involving benzimidazole with the whole series of halo-benzoic acid molecules were scrutinised and polymorphism found to be prominent throughout. Selective growth for individual forms has been achieved, offering the potential for polymorph selection, but not fully understood.

The behaviour of the protons was investigated in the molecular complexes generated; proton transfer was prevalent. This was achieved through three methods; firstly with the use of variable temperature X-ray and neutron diffraction experiments on the product, by altering the levels of pH during the crystallisation process and lastly by introducing competing acceptor sites through co-molecule selection.

A feasibility study into the use of the relatively new solvent-free crystallisation processes was undertaken. It was shown to be a successful technique in screening for polymorphs and molecular complexes.

Acknowledgements

I have to start by thanking the man who gave me this wonderful opportunity, without him I certainly would not be writing this acknowledgement today. Unfortunately he is no longer with us; even though our time together was short, you are sorely missed and will never be forgotten. This work is in memory of you, Dr Andy Parkin.

There are two people who have been equally instrumental in developing and shaping this work, I wish to thank them endlessly for all their help, guidance, support, kick up the backsides, tricky questions and opportunities, a special thanks to Chick and Lynne. I need to mention Chick's enormous generosity, nearly every word of this thesis was written on the lovely desk gifted to me, not to mention the rest of the stuff. If there is one piece of advice I got from Lynne that I will never forget, is that to never take her shot at ten pin bowling (there was too much practical stuff to mention).

Thanks to Craig Wales, Alan Martin and Smita Odedra, some of our joint work is in this thesis, and yes it was joint work even though the burden may not have been evenly split.

I need to thank some of the oldies of the Chicklets who helped me during the early years, namely Marc Schmidtmann – your knowledge is incredible, Gordon Cunningham – the most helpful person in the world, Martin Adam – thanks for teaching me the basics, and Stephen Cairns – what a great trip to Japan.

Thanks to the rest of the Chicklets for a very enjoyable four years, especially Bryan, there was never a shared pint but plenty of shared trips to the Common Rooms.

Finally and most importantly I need to thank, with all my heart, my family for all their support during my education, my beautiful wife Helen and Michael our baby boy who is full of surprises, even from day minus 8 weeks!

LIST OF FIGURES	10
LIST OF TABLES	29
LIST OF ABBREVIATIONS	34
1 INTRODUCTION	35
1.1.1 Molecular Complexes, Salts, Co-Crystals?.....	35
1.1.2 Co-crystallisation	36
1.2 Pharmaceutical Co-Crystals and Other Applications	36
1.3 Hydrogen Bonding and other Intermolecular Interactions	39
1.3.1 Strong Hydrogen Bonds.....	41
1.3.2 Moderate Hydrogen Bonds	42
1.3.3 Weak Hydrogen Bonds	43
1.3.4 Bifurcated Hydrogen Bonds.....	43
1.3.5 Hydrogen Bond Disorder	44
1.3.6 Proton Transfer	45
1.3.7 Halogen Bonds.....	47
1.3.8 π – Interactions.....	48
1.4 Crystal Engineering	49
1.5 Polymorphism	52
1.5.1 Controlling Polymorphism.....	52
1.5.1.1 Disappearing Polymorphs	53
1.5.2 Polymorphism in Co-Crystals.....	54
1.5.3 Isostructures	55
1.6 Solvent Free Co-Crystallisation	56
1.6.1 Co-Grinding/ Mechanical Mixing.....	57
1.6.2 Solvent-drop Grinding / Solvent Catalyst Method.....	57
1.6.3 Understanding the Mechanisms Involved	58
1.7 Benzimidazole	59
1.8 Imidazole	61
1.9 Aims and Objectives	62
1.10 References For Chapter 1	63
2 THEORY	68
2.1 Crystallography	68
2.1.1 The Crystal.....	68
2.1.2 The Lattice	68
2.1.3 The Unit Cell.....	69
2.1.4 The Seven Crystal Systems.....	69
2.1.5 The Fourteen Bravais Lattices	70
2.1.6 Space Groups	70
2.1.7 Theory of Diffraction.....	71
2.1.8 The Laue and Bragg Equations.....	72
2.1.9 Reciprocal Lattice	73
2.1.10 The Ewald Construction.....	74
2.1.11 Collecting X-ray Diffraction Data.....	74

2.2	Structure Solution	75
2.2.1	Fourier Transform.....	77
2.2.2	Phase Problem.....	77
2.2.3	Patterson Method	78
2.2.4	Direct Methods.....	78
2.2.5	Superflip.....	79
2.2.6	Fourier Refinement	80
2.2.7	Location of Hydrogen atoms.....	81
2.2.8	R-Values	81
2.3	Powder Diffraction	82
2.3.1	Powder Diffraction Experiments.....	83
2.3.2	Powder Diffractometers	83
2.3.3	Powder Pattern	84
2.3.4	Structure Solution from Powder X-ray Diffraction Data	85
2.4	DSC	87
2.4.1	DSC Experiments.....	88
2.5	References for Chapter 2	88
3	TECHNIQUES AND INSTRUMENTS	90
3.1	Single Crystal Formation	90
3.1.1	Solvent Evaporation Method	90
3.1.2	Solubility Phase Diagrams	92
3.1.3	Solvent-Free Co-crystallisation.....	93
3.2	Single Crystal Diffractometers	94
3.2.1	Nonius / Bruker Kappa CCD and Bruker APEX-II	95
3.2.2	Rigaku R-Axis RAPID.....	96
3.2.3	Data Collection and Structure Solution.....	97
3.3	Powder Diffraction	98
3.4	Differential Scanning Calorimetry (DSC)	99
3.5	References For Chapter 3	99
4	TOWARDS SELECTIVE MOLECULAR COMPLEX FORMATION: CHALLENGING CRYSTAL ENGINEERING	101
4.1	Introduction – Hydroxybenzoic Acids	102
4.1.1	2-Hydroxybenzoic Acid.....	102
4.1.2	3-Hydroxybenzoic Acid.....	103
4.1.3	4-Hydroxybenzoic Acid.....	105
4.1.4	2,4-Dihydroxybenzoic Acid.....	106
4.1.5	2,6-Dihydroxybenzoic Acid.....	107
4.1.6	3,4-Dihydroxybenzoic Acid.....	108
4.1.7	3,5-Dihydroxybenzoic Acid.....	108
4.2	Summary of Molecular Complexes Produced	109
4.2.1	Benzimidazolium – Proton Transfer	110
4.2.2	Potential Hydrogen Bonds and Supramolecular Synthons.....	111
4.3	Crystallographic Data	114
4.4	Structural Descriptions of the Molecular Complexes	117

4.4.1	Molecular Complex of Benzimidazolium and 2-Hydroxybenzoic Acid 1:1	117
4.4.2	Molecular Complex of Benzimidazole and 3-Hydroxybenzoic Acid 1:1	122
4.4.3	Molecular Complex of Benzimidazole and 4-Hydroxybenzoic Acid 2:1	126
4.4.4	Molecular complex of Benzimidazole 3-Hydroxybenzoic acid 2:1 Form II.....	132
4.4.5	Molecular Complex of Benzimidazole 3-Hydroxybenzoic Acid 2:1 Form I.....	137
4.4.6	Molecular Complex of Benzimidazole and 4-Hydroxybenzoic Acid 2:1 Hydrate	143
4.4.7	Molecular Complex of Benzimidazole 2-Hydroxybenzoate 1:2.....	149
4.4.8	Molecular Complex of Benzimidazole 3,5-Dihydroxybenzoic Acid 1:1	153
4.5	Solvent-Free Co-Crystallisations	158
4.5.1	Feasibility Study	159
4.5.2	Molecular Complex of Benzimidazole and 5-Chlorosalicylic Acid 1:1	163
4.5.3	Molecular Complex of Benzimidazole and L-Aspartic Acid 1:1	171
4.6	Conclusions	176
4.7	References for Chapter 4	180
4.8	Appendix	181
4.8.1	Appendix 4.A - DSC Thermograms of Solvent Free Co-crystallisations of BZN with Halo-BA....	181
4.8.2	Appendix 4.B - DSC Thermograms of Solvent Free Co-crystallisations of BZN with a Range of Co-molecules.....	183
5	SOLVENT MEDIATED MOLECULAR COMPLEX POLYMORPHISM AND ISOMORPHIC FORMATION	186
5.1	Introduction	186
5.1.1	2-Fluorobenzoic Acid	187
5.1.2	3-Fluorobenzoic Acid	188
5.1.3	4-Fluorobenzoic Acid	188
5.1.4	2-Chlorobenzoic Acid.....	189
5.1.5	3-Chlorobenzoic Acid.....	190
5.1.6	4-Chlorobenzoic Acid.....	191
5.1.7	2-Bromobenzoic Acid.....	192
5.1.8	3-Bromobenzoic Acid.....	193
5.1.9	4-Bromobenzoic Acid.....	193
5.1.10	2-Iodobenzoic Acid.....	193
5.1.11	3-Iodobenzoic Acid.....	194
5.1.12	4-Iodobenzoic Acid.....	194
5.2	Summary of Results	196
5.2.1	Benzimidazolium Ion.....	198
5.2.2	Primary Hydrogen Bonds.....	199
5.3	Crystallographic Data	202
5.4	Results and Discussion	204
5.4.1	Molecular Complex Polymorphism	204
5.4.1.1	Benzimidazole and 3-Chlorobenzoic Acid 1:1	204
5.4.1.1.1	Benzimidazole : 3-Chlorobenzoic Acid Molecular Complex 1:1 Form I.....	209
5.4.1.1.2	Benzimidazole : 3-Chlorobenzoic Acid Molecular Complex 1:1 Form II.....	213
5.4.1.2	Molecular Complex of Benzimidazole and 4-Chlorobenzoic Acid 1:1.....	218
5.4.1.3	Molecular Complex of Benzimidazole and 4-Bromobenzoic Acid 1:1.....	223
5.4.2	Isomorphism	226
5.4.2.1	Molecular Complex of Benzimidazole and 3-Bromobenzoic Acid 1:1.....	227
5.4.3	Benzimidazole and Fluorobenzoic Acid Structures	230
5.4.3.1	Molecular Complex of Benzimidazole and 2-Fluorobenzoic Acid 1:2	230
5.4.3.2	Benzimidazole and 3-Fluorobenzoic Acid	233
5.4.3.3	Molecular Complex of Benzimidazole and 4-Fluorobenzoic Acid 1:1	235

5.5	Conclusions	239
5.6	References for Chapter 5	240
5.7	Appendix	242
5.7.1	Appendix A – DSC Thermograms of the Co-crystallisation Experiments of BZN and 3-BrBA.....	242
6	INCREASING THE COMPETITION – THE INTRODUCTION OF COMPETING HYDROGEN BONDING SITES	243
6.1	Introduction	244
6.1.1	Picolinic Acid.....	244
6.1.2	3-Hydroxypicolinic Acid	245
6.1.3	6-Hydroxypicolinic Acid	245
6.1.4	Nicotinic Acid.....	247
6.1.5	Isonicotinic Acid.....	247
6.1.6	2-Nitrobenzoic Acid.....	248
6.1.7	3-Nitrobenzoic Acid.....	249
6.1.8	4-Nitrobenzoic Acid.....	250
6.2	Summary of Results	251
6.2.1	Benzimidazolium	252
6.2.2	Hydrogen Bonding Motifs and Supramolecular Synthons.....	253
6.3	Crystallographic Data	255
6.4	Structural Descriptions of the Molecular Complexes	257
6.4.1	Molecular Complex of Benzimidazole and Picolinic Acid.....	257
6.4.2	Molecular Complex of Benzimidazole and 3-Hydroxypicolinic Acid 1:1.....	262
6.4.3	Molecular Complex of Imidazole and 3-Hydroxypicolinic Acid 1:1.....	267
6.4.4	Molecular Complex of Benzimidazole and 6-Hydroxypicolinic Acid 1:1.....	271
6.4.5	Molecular Complex of Benzimidazole and 6-Hydroxypicolinic Acid Diacetic Acid Solvate 1:1:2	276
6.5	Systematic Structural Study of Nitrobenzoic acid : Benzimidazole / Imidazole Molecular Complexes	280
6.5.1	Proton Transfer	280
6.5.2	Normalisation of the Internal Bond Lengths and the Effect on Hydrogen Bond Length	281
6.5.3	Packing Effects	283
6.5.3.1	Benzimidazolium 3-Nitrobenzoate.....	283
6.5.3.2	Benzimidazolium 4-Nitrobenzoate.....	284
6.5.3.3	Imidazolium 3-Nitrobenzoate.....	285
6.5.3.4	Imidazolium 4-Nitrobenzoate.....	286
6.6	Conclusions	286
6.7	References for Chapter 6	288
7	A COMPARISON STUDY OF BENZIMIDAZOLE AND IMIDAZOLE CONTAINING MOLECULAR COMPLEXES WITH A RANGE OF RELATED CO-MOLECULES	290
7.1	Introduction – Co-molecules	291
7.1.1	2-/ 3-/ 4-Hydroxybenzoic Acid.....	291
7.1.2	4-Fluoro- / 4-Bromo- Benzoic Acid.....	291
7.1.3	Phthalic Acid.....	291
7.1.4	Isophthalic Acid	292
7.1.5	Terephthalic Acid.....	294
7.1.6	Fumaric acid.....	295

7.1.7	Succinic acid	296
7.1.8	Maleic acid.....	298
7.1.9	Malonic acid.....	299
7.1.10	Benzoic Acid.....	301
7.2	Summary of Results	302
7.2.1	Benzimidazolium, Imidazolium – Proton Transfer	304
7.2.2	Potential Hydrogen Patterns and Hydrogen Bond Motifs	305
7.3	Crystallographic Data	306
7.4	Imidazole with Mono Hydroxy Substituted Benzoic Acids	309
7.4.1	Molecular Complex of Imidazolium and 2-Hydroxybenzoic Acid 1:1	311
7.4.2	Molecular Complex of Imidazolium and 3-Hydroxybenzoic Acid 1:1	314
7.4.3	Molecular Complex of Imidazolium and 4-Hydroxybenzoic Acid 1:1	317
7.5	A Comparison of the Molecular Complexes of Imidazole and Benzimidazole with Halo Substituted Benzoic Acids	320
7.5.1	Molecular Complex of Imidazolium and 4-Fluorobenzoic Acid 1:1	323
7.5.2	Molecular Complex of Imidazolium and 4-Bromobenzoic Acid 1:1	326
7.5.3	Molecular Complex of Benzimidazole and Benzoic Acid 1:2	331
7.5.3.1	Imidazolium Benzoate 1:1	335
7.6	Molecular Complexes Containing Aromatic Dicarboxylic Acids and Benzimidazole	335
7.6.1	Molecular Complex of Benzimidazole and Phthalic Acid 1:1	336
7.6.2	Molecular Complex of Benzimidazole / Imidazole and Isophthalic Acid	340
7.6.3	Molecular Complex of Benzimidazole / Imidazole and Terephthalic Acid	343
7.7	Benzimidazole and Imidazole Molecular Complexes with Non-Aromatic Dicarboxylic Acids	347
7.7.1	Molecular Complexes of Benzimidazole and Imidazole with Fumaric Acid	349
7.7.2	Molecular Complexes of Benzimidazolium and Imidazolium with Succinic Acid	354
7.7.3	Molecular Complexes of Benzimidazolium and Imidazolium with Maleic Acid	358
7.7.4	Molecular Complexes of Benzimidazole and Imidazole with Malonic Acid	367
7.8	Conclusions	374
7.9	References for Chapter 7	376
8	CONCLUSIONS AND FUTURE WORK	378
8.1	Hydrogen Bond Patterns/ Motifs	378
8.2	Ladder Motif	381
8.3	Proton Transfer	383
8.4	Solvent-Free Crystallisation/Co-crystallisation	384
8.5	Solvent Mediated Molecular Complex Polymorphism Formation	384
8.6	Increasing the Competition – The Introduction of Competing Hydrogen Bonding Sites	386
8.7	A Comparison Study of Benzimidazole and Imidazole Containing Molecular Complexes with a Range of Related Co-Molecules	387
8.8	Halogen Bonding	388
8.9	Concluding Remarks	389

LIST OF FIGURES

Fig. 1.1 – LHS, a pharmaceutical co-crystal containing two APIs, piracetam and gentisic acid, RHS, the pharmaceutical co-crystals of 4,4'-bipyridine and 4,4'-dipyridylethan with fluoriprofen.

Fig. 1.2 – Crystal structure of the thiourea catalyst used in Stecker reactions.

Fig. 1.3 – LHS, the 1-ethyl-3-methylimidazolium hydrogen difluoride structure with the strong hydrogen bond between the fluoride ions, RHS the catena-(hydrogen maleate)-potassium structure with a strong intramolecular hydrogen bond.

Fig. 1.4 – LHS, an example of carboxylic acid and pyridyl containing molecules, 1,8-naphthalenedicarboxylic acid trans-1,2-bis(4-pyridyl)ethylene, RHS, an example of an amino acid containing complex; L-Leucine : D-valine.

Fig. 1.5 – LHS, example of a hydrogen bond containing two acceptors, RHS, extract from Jeffrey “An Introduction to Hydrogen Bonding”, a three-centered hydrogen bond with labeling of the scalar quantities; hydrogen - acceptor distance (R_1 and R_2), hydrogen bond angle (α_1 and α_2) and angle between the hydrogen bonds (α_3).

Fig. 1.6 – An example of conformational disorder in a hydrogen bonded system.

Fig. 1.7 – A reaction diagram showing amino - imino transformation (tautomerism).

Fig. 1.8 – Schematic of the most prevalent $\pi \cdots \pi$ stacking forms, LHS, off-centred, middle, T-shape, RHS, an example of a cation- π interaction, between benzene and sodium.

Fig. 1.9 – a, the carboxylic acid dimer, b, a pyrrole-2-carboxylate dimer, and c, a carboxylate hydrogen bonded to part of a pyridine molecule.

Fig. 1.10 – LHS, the bipyridine dihydroxybenzoic acid co-crystal is an example of a 1-D assembly, RHS, the 2-D assembly from the piperazine : carboxylic acid co-crystal.

Fig. 1.11 – The co-crystal polymorphs formed by carbamazepine and isonicotinamide⁹⁹.

Fig. 1.12 – Two co-crystals; LHS, tetrafluoro-1,4-diodobenzene : 1,4-thixane and, RHS, tetrafluoro-1,4-diodobenzene : 1,4-thiomorpholine, that are isostructural.

Fig. 1.13 – Extract from Trask *et al*¹⁰⁵ showing the two different packing arrangements for the co-crystal polymorphs of caffeine and glutaric acid.

Fig. 1.14 – Schematic of BZN and derivatives, left to right, BZN, thiabendazole and fuberidazole.

Fig. 1.15 – LHS, the alpha form of BZN, RHS, the beta form of BZN, middle top, secondary interaction of the alpha form, middle bottom, secondary interaction of the beta form.

Fig. 1.16 – The basic building blocks from the structures of, LHS, benzimidazolium 3-carboxyphenoxyacetate, RHS, benzimidazolium hydrogen phenylmalonate.

Fig. 1.17 – LHS, building block of the imidazolium structure with the carbon-nitrogen weak hydrogen bond circled in black, RHS, view along the *b*-axis of the extended structure of the imidazole crystal structure.

Fig. 1.18 – LHS, crystal structure of the dibenzo-18-crown-6-imidazolium complex, RHS, the structure of the imidazolium oxamate molecular complex.

Fig. 2.1 – 3-dimensional unit cell, defined in terms of the unit cell dimensions a , b , c , α , β , γ .

Fig. 2.2 – The Bragg construction for diffraction by a three-dimensional crystal structure.

Fig. 2.3 – The cubic crystal system with the directions $[hkl]$ defining a vector normal to the surface of a face.

Fig. 2.4 – The Ewald Construction.

Fig. 2.5 – X-ray atomic form factors of oxygen (blue), chlorine (green), Cl^- (magenta), and K^+ (red); smaller charge distributions have a wider form factor.

Fig. 2.6 – (a) Shows diffraction from a single crystal, (b) from a collection of four crystals, (c) from a polycrystalline sample. (d) is the resulting powder pattern from the polycrystalline sample.

Fig. 2.7 – Schematic of a traditional flat plate X-ray powder diffractometer.

Fig. 2.8 – The powder pattern of benzimidazole 5-chlorosalicylic acid obtained from structure solution with DASH (blue) and the experimental data (red). The purple line indicates the differences between the two sets of data; this is an indication of the good fit between the two.

Fig. 2.9 – Thermogram showing the three main types of event that be detected by DSC, glass transition, crystallisation and melting. For a multiple phase sample, each component will follow its own thermal profile.

Fig. 3.1 – From left to right, ReactArray Microvate, Asynt hotplate and H-tubes, the latter containing crystallisations of chloranilic acid and 3,5-dimethyl pyrazole at different stages.

Fig. 3.2 - The two-component phase diagram for the trans-cinnamic acid nicotinamide system^{3b}.

Fig. 3.3 – LHS, the three component phase diagram for the trans-cinnamic acid nicotinamide system in methanol at 20°C, RHS, in water at 20°C^{3b}. Regions 5 and 6 are areas of molecular complex/ starting material mixture, 1 a undersaturated solution, 2 and 4 is regions of solid starting material and 3 where the molecular complex is form. The letters indicate starting points of solubility curves.

Fig. 3.4 – Mortar and Pestle for use in the solvent free grinding experiments.

Fig. 3.5 –left to right, the Nonius / Bruker Kappa CCD, Bruker APEX-II and Rigaku R-Axis RAPID.

Fig. 3.6 – The working area of the Bruker APEX-II with labelling of the CCD detector, cryostream. X-ray direction and sample location.

Fig. 3.7 –The Rigaku R-Axis RAPID diffractometer with labelling of the image plate, cryostream. X-ray direction and sample location.

Fig. 3.8 – LHS, the Bruker D8 Advance used for powder X-ray diffraction; RHS, the Q200 DSC.

Fig. 4.1 – The main hydrogen bonds in the salicylic acid structure.

Fig. 4.2 – LHS – The main supramolecular synthons in the bis(2-hydroxybenzoic acid) 3,5-dimethyl-1H-pyrazole molecular complex, RHS, the tris(2-hydroxybenzoic acid) 9H-purin-6-amine molecular complex which contains two moderate hydrogen bonds between the co-molecules.

Fig. 4.3 – LHS - the main supramolecular synthon between salicylic acid and 2-amino-pyridine, RHS, the adeninium 2-hydroxybenzoate methanol molecular complex.

Fig. 4.4 – LHS, the monoclinic form of 3-hydroxybenzoic acid exhibiting the carboxylic acid dimer motif; RHS, the linear chains of the orthorhombic form of 3-hydroxybenzoic acid, the full compliment of protons was not published with the structure.

Fig. 4.5 – LHS, the 4-hydroxybenzoic acid nicotinamide supramolecular synthon. These hydrogen bond dimers are connected through a hydrogen bond between the hydroxyl and the heteroatom in the ring of the nicotinamide; RHS, the four molecule hydrogen bonded ring between 3-hydroxybenzoic acid and 4-aminopyridinium.

Fig. 4.6 – The carboxylic acid dimer motif and hydroxyl hydrogen bonds found in the structure of 4-hydroxybenzoic acid.

Fig. 4.7 – The ring system of the 2,4-dihydroxybenzoic acid structure.

Fig. 4.8 – The criss-cross pattern of the imidazolium 2,4-dihydroxybenzoate molecular complex.

Fig. 4.9 – LHS monoclinic form of 2,6-dihydroxybenzoic acid showing its carboxylic acid dimer motif, RHS orthorhombic forms of 2,6-dihydroxybenzoic acid showing a more linear pattern with single hydrogen bonds between molecules.

Fig. 4.10 – The structure of benzimidazole and 3,5-dihydroxybenzoic acid with its hydrogen bonded ring system.

Fig. 4.11 – LHS, a typical benzimidazolium molecule in which both nitrogens are protonated. RHS, the Fourier difference map generated where one of the H atoms located on a nitrogen atom has been omitted from the model, clearly showing that both nitrogen atoms are protonated.

Fig. 4.12 – Hydrogen bonding patterns that could lead to the formation of supramolecular synthons in the generation of crystal structures of the molecular complexes studied in this chapter. The potential homo-hydrogen bonds (A, B and C) and hetero-hydrogen bonds (D, E and F) that can be exhibited between a benzimidazole and carboxylic acid group. Hydrogen bonds G, H and I are those that could be generated between a benzimidazole and hydroxyl group.

Fig. 4.13 – The derivatives of hydrogen bond patterns E, F and G that occur when there has been proton transfer.

Fig. 4.14 – The benzimidazolium and 2-hydroxybenzoate ions which are generated in the molecular complex/salt, with atom labelling.

Fig. 4.15 – The main motif of the benzimidazolium 2-hydroxybenzoate molecular complex; a four molecule hydrogen bonded ring consisting of alternating co-molecules held together by partially charge assisted $N^{\delta+}-H\cdots O^{\delta-}$ hydrogen bonds. The inset shows the view along the *bc*-diagonal axis that highlights the geometric positions of the hydrogen bonded ring system.

Fig. 4.16 – LHS, the weak hydrogen bonds (-) that extend the hydrogen bonded rings, RHS displays how the rings arrange themselves into a stacking configuration due to the $C1-H\cdots O1^{\delta-}$ hydrogen bond.

Fig. 4.17 – The hydrogen bonded ring system; the main motif of the benzimidazolium 2-hydroxybenzoate molecular complex, is extended by weak hydrogen bonds (circled in red).

Fig. 4.18 – View highlighting the $C-H\cdots\pi$ interactions that extends the structure along the *ac*-diagonal.

Fig. 4.19 – View of the interactions that exist between the molecules in main motif.

Fig. 4.20 – The benzimidazolium and 3-hydroxybenzoate ions which are generated in the molecular complex, with atom labelling.

Fig. 4.21 – The 3-hydroxybenzoate molecules create chains with the mean planes of alternate molecules tilted at 104.4° from each other.

Fig. 4.22 – The 3-hydroxybenzoate molecules chains which are held together through a hydroxyl-carboxylate hydrogen bond are bridged together by hydrogen bonding through a benzimidazolium molecule. The inset shows the view along the *c*-axis, indicating that the benzimidazolium molecules sit on two distinct positions due to the twisting nature of the 3-hydroxybenzoate chains.

Fig. 4.23 – LHS - The alternating layers that exist on the *a*-face of the benzimidazole 3-hydroxybenzoate molecular complex are connected through a weak hydrogen bond on each alternate layer (red). RHS, the alternate layer is held together by a weak hydrogen bond (yellow circle) and C-H $\cdots\pi$ interactions (red circle).

Fig. 4.24 – LHS, view along the *c*-axis highlighting how the benzimidazolium molecules form into channels. RHS, view along the *b*-axis that shows the 3-hydroxybenzoate chains.

Fig. 4.25 – The different benzimidazolium molecules. From, left to right, molecules 1 and 2 hydrogen bond to one another over a glide plane, molecule 3 hydrogen bonds to itself through a inversion centre along the N6 \cdots N6 contact, molecule 4 also hydrogen bonds to itself due to an inversion centre along the N7 \cdots N7 contact. In every case a proton is split over two sites.

Fig. 4.26 – MCE³³ Fourier difference maps of the residual electron density. LHS, when the hydrogen split between nitrogen N2 and N3 is removed, RHS, when the hydrogen is removed from the N6 nitrogen (the same 50:50 split proton image is seen when the proton bonded to N7 is removed).

Fig. 4.27 – The two 4-hydroxybenzoate molecules found in the molecular complex, with associated atom labelling.

Fig. 4.28 – The 4-hydroxybenzoate molecules create chains with the molecules alternately sit on two positions.

Fig. 4.29 – LHS, view along the *a*-axis highlighting how each 4-HBA⁻ chain is involved in hydrogen bond in four different directions. RHS, view along the *b*-axis indicating the connections between each chain. bottom –view along the *c*-axis of the BZNH⁺ 4HBA⁻ molecular complex with the backbone of the structure, the 4HBA⁻ chains, being held together by the BZNH⁺ dimers that criss-cross between them.

Fig. 4.30 – The different benzimidazolium molecules: from, left to right, molecules 1 and 2 that hydrogen bond to one another with the relevant atoms labelled, and the 4-hydroxybenzoate molecule with associated atom labelling.

Fig. 4.31 – MCE³³ Fourier difference maps of the residual electron density when the hydrogen split over nitrogen N2 and N4 is removed.

Fig. 4.32 – The 3-hydroxybenzoate molecules create close-to-planar chains through a hydroxyl carboxylate hydrogen bond.

Fig. 4.33 – LHS, the 3-hydroxybenzoate molecules chains which are held together through a hydroxyl-carboxylate hydrogen are bridged together by hydrogen bonding through a benzimidazolium dimer. RHS, the view along the *a*-axis indicating the planar nature of the chains and highlighting the role of the BZNH⁺ dimer.

Fig. 4.34 – The 3-hydroxybenzoate molecules hydrogen bond along the *bc*-face which creates a sheet along the *a*-axis view along the *a*-axis indicating the planar nature of the chains and highlighting the role of the BZNH⁺ dimer.

Fig. 4.35 – The weak interactions that are used to extend the structure along the *c*-axis, C-H···O3 (red), C4-H··· O2^{δ-}(yellow) and C4-H··· O2^{δ-} (green).

Fig. 4.36 – LHS, the BZN and BZNH⁺ molecules form dimers, through a single hydrogen bond. There are two of these dimers in the reduced unit cell. RHS, the 3-HBA⁻ molecules also form single hydrogen bonded dimers.

Fig. 4.37 – The 3-hydroxybenzoate molecules create chains through a hydroxyl carboxylate hydrogen bond.

Fig. 4.38 – The 3-hydroxybenzoate molecules chains which are held together through a hydroxyl-carboxylate hydrogen bond are bridged together by four distinct hydrogen bonds of two types, a and b.

Fig. 4.39 – LHS, Form II, The ladder structure consists of stiles of 3-hydroxybenzoate molecules and rungs of hydrogen bonded dimers of BZNH⁺. RHS, Form I, The ladder structure consists of stiles of 3-hydroxybenzoate molecules and alternate rungs of hydrogen bonded dimers of BZNH⁺.

Fig. 4.40 – The ladder structure consists of stiles of 3-hydroxybenzoate molecules and the double rungs of hydrogen bonded dimers of BZNH⁺.

Fig. 4.41 – The 3-hydroxybenzoate molecules are involved in two ladders by hydrogen bonding in two directions adopting a Z and inverse Z shape (indicated by the red lines).

Fig. 4.42 –LHS, view along the *b*-axis highlighting the creation of sheets of 3-HBA⁻ molecules through weak C-H···O^{δ-} (red) and C-H···O (green) hydrogen bonds along the *a*-axis. The blue interactions represent the moderate hydrogen bonds that make up the chains of 3-HBA⁻ molecules. RHS, the weak hydrogen bonds in which the BZNH⁺ ions are involved – one C-H···O^{δ-} (yellow) and one C-H···O (yellow and circled).

Fig. 4.43 – view along the *a*-axis of the extended benzimidazolium 3-hydroxybenzoate 2:1 polymorph Form I molecular complex.

Fig 4.44 – Schematic diagram highlighting the possible hydrogen bonds that could be generated between the water molecule and the other starting materials and their charged species.

Fig. 4.45 – The BZNH⁺, BZN, 4-HBA⁻ and water molecule that are involved in the BZN BZNH⁺ 4-HBA⁻ hydrate, with atom labelling.

Fig. 4.46 – LHS, highlighting the hydrogen bonds in which the water molecule is involved. RHS, view along the *c*-axis highlighting the zigzag nature of the rungs (BZN BZNH⁺).

Fig. 4.47 – LHS, Fourier difference map in 2D and, RHS, Fourier difference map in 3D showing the possible elongation of the hydrogen atom involved in the hydrogen bond.

Fig. 4.48 – LHS –the staggered chains of 4-HBA⁻ that are held together by the stiles of BZN and BZNH⁺ in the 2:1 hydrate. Note that another BZN and BZNH⁺ group is present, oriented diagonally between the two that are shown. RHS, view along the *b*-axis of the BZN BZNH⁺ 4-HBA⁻ molecular complex showing the main motifs for comparison.

Fig. 4.49 – The short contacts that exist between the molecules in the BZN BZNH⁺ 4-HBA⁻ hydrate molecular complex. Highlighted are the areas that show the C-H---π interactions.

Fig. 4.50 – view along the *a*-axis of the BZN BZNH⁺ 4-HBA⁻ hydrate. The chains of 4-HBA⁻ molecules expand the structure along the *b*-axis (red line). The BZN BZNH⁺ group holds two chains together via

hydrogen bonding to a water molecule in one side and through hydrogen bond pattern F in the other direction (blue line).

Fig. 4.51 – The BZNH^+ 2-HBA⁻ and 2-HBA molecules which are generated in the molecular complex with atom labelling.

Fig. 4.52 – View along the *a*-axis of the main motif of the BZNH^+ 2-HBA⁻ and 2-HBA molecular complex; linear chains of 2-HBA⁻ 2-HBA pairs are held together by BZNH^+ molecules that run along the *b*-axis.

Fig. 4.53 – LHS, the C1-H \cdots O5^{δ-} weak hydrogen bonds (-) that stack the hydrogen bonded chains upon one another with the assist of two C-H \cdots π interactions (-)(-). RHS, view of the *a*-axis displays how the chains stack upon one another (-).

Fig. 4.54 – Two chains of the main motif are held by weak C-H \cdots O hydrogen bonds which are located inside the black box. Inset, A blow-up of the black box highlighting the weak C-H \cdots O hydrogen bonds.

Fig. 4.55 – The benzimidazolium and 3,5-dihydroxybenzoate molecules which are generated in the molecular complex with atom labelling.

Fig. 4.56 – The extended structure of the BZNH^+ 3,5-DHBA⁻ molecular complex which consist of chains of 3,5-DHBA⁻ molecules which are held together by BZNH^+ molecules.

Fig. 4.57 – The hydrogen bonded rings that are made up of four 3,5 DHBA⁻ molecules.

Fig. 4.58 – Two views of the 3,5 DHBA⁻ hydrogen bonded rings that expand along the *bc* diagonal and *c* dimensions.

Fig. 4.59 – The hydrogen bonds that the BZNH^+ molecule is involved with in the BZNH^+ 3,5-DHBA⁻ molecular complex, a is a partially charged assisted $\text{N}^{\delta+}\text{-H}\cdots\text{O}^{\delta-}$ hydrogen bond while b is a bifurcated hydrogen bond of two $\text{N}^{\delta+}\text{-H}\cdots\text{O}$ interactions.

Fig. 4.60 – View along the *c*-axis of an extended image of the BZNH^+ 3,5-DHBA⁻ molecular complex.

Fig. 4.61 – DSC thermograms from the product of the co-crystallisation of benzimidazole with 4-chlorobenzoic acid crystallised from propanol (-) acetone (-), ethanol (-), methanol (-) and by the solvent free method (-). The results indicate that the solvent free method replicates the more traditional evaporation technique.

Fig. 4.62 – DSC thermogram from the product of the solvent free co-crystallisation of benzimidazole with 3-chlorobenzoic acid with grinding times of 30 seconds (-), 2 minutes (-) and 5 minutes (-). The results indicate that the thermodynamic product is favoured with increasing grinding time.

Fig. 4.63 – DSC traces of the product of the solvent free co-crystallisation of benzimidazole with 3-chlorobenzoic acid grinding for 2 minutes and stored for no time (-), 24 hours (-) and 2 weeks (-). The results indicate that the thermodynamic product is favoured with increasing storage time.

Fig. 4.64 – DSC patterns of starting materials benzimidazole (-), 5-chlorosalicylic acid (-) and the co-crystallisation product of the two (-) formed by the solvent-free method.

Fig. 4.65 – DSC thermogram of the product from co-crystallisation of benzimidazole and 5-chlorosalicylic acid at 30°C in propanol (-), acetone (-), ethanol (-) and methanol (-). Inset, selective polymorph growth has been achieved for two of the co-crystal polymorphs by recrystallisation from methanol (-) Form I and ethanol (-) Form III.

Fig. 4.66 – above - Powder patterns of the products of crystallisation from three different environmental conditions to promote growth of single component of; form I (blue) using methanol at 10°C, form I and II mix phase (red) using ethanol at 10°C and form III (yellow) using ethanol at 30°C. Two different products can clearly be identified from these powder patterns, while form II is mixed with form I.

Fig. 4.66 – below – Powder x-ray diffraction pattern of benzimidazole and 5-chloro-2-hydroxybenzoic acid cocrystallised from methanol at 10°C (blue) overlaid with the simulated powder pattern from solved structure solution of form I.

Fig. 4.67 – The benzimidazolium and 5-chloro-2-hydroxybenzoate molecules which are generated in the molecular complex with atom labelling.

Fig. 4.68 – The main motif of the benzimidazolium 5-chloro-2-hydroxybenzoate molecular complex; a four molecule hydrogen bonded ring consisting of alternating co-molecules with partially charge assisted $N^{\delta+}-H\cdots O^{\delta-}$ hydrogen bonds.

Fig. 4.69 – The main motif of the benzimidazolium 5-chloro-2-hydroxybenzoate molecular complex; the four molecule hydrogen bonded ring consisting of alternating co-molecules, are expanding along the *b*-axis by a weak hydrogen bond and $\pi\cdots\pi$ stacking interactions. Inset black box– An expanded image of the $\pi\cdots\pi$ stacking interactions that connect the hydrogen bonded rings together. Inset red box– An expanded image of the $\pi\cdots\pi$ stacking interactions that connect the hydrogen bonded rings together.

Fig. 4.70 – The two weak hydrogen bonds, $C-H\cdots C$ and $C-H\cdots O$, which expand the structure along the *a*-axis.

Fig. 4.71 – The main motif of the benzimidazolium 5-chloro-2-hydroxybenzoate molecular complex; four molecule hydrogen bonded ring consisting of alternating co-molecules, are expanding along the *a*-axis by two weak hydrogen bonds, $C-H\cdots C$ and $C-H\cdots O$, that are circled in red.

Fig. 4.72 – Halogen bonds, $Cl\cdots H-C$, connect the main motif of the benzimidazolium 5-chloro-2-hydroxybenzoate molecular complex along the *c*-axis (green circle).

Fig. 4.73 – The benzimidazolium and aspartate molecules which are generated in the molecular complex with atom labelling.

Fig. 4.74 – The main hydrogen bonds within the $BZNH^+$ aspartate molecular complex create a linear chain of alternating co-molecules.

Fig. 4.75 – The amine group of the aspartate molecule is involved in three hydrogen bonds, $N3-H\cdots O1^{\delta-}$ (green), $N3-H\cdots O4^{\delta-}$ (red) and $N3-H\cdots O1^{\delta-}$ (blue).

Fig. 4.76 – The weak hydrogen bonds within the $BZNH^+$ aspartate molecular complex: bifurcated hydrogen bonds (a) and $C5-H\cdots O3^{\delta-}$ hydrogen bonds (b).

Fig. 4.77 – View along the *b*-axis of the expanded benzimidazolium aspartate molecular complex. The red line (-) indicates the chain of alternating co-molecule (Figure 4.74), the yellow box (-) indicates hydrogen bonds involving the amine group of the aspartate (Figure 4.75) and the black box is where the lesser interactions between the $BZNH^+$ molecules operate (Figure 4.76).

Fig. 4.78 – The $C-H\cdots\pi$ edge to face interactions between the $BZNH^+$ molecules.

Fig. 4.79 – The four unique hydrogen bonds that were the only hydrogen bonds in all the crystal structures in Chapter 4, in order of occurrence 1, $N^{\delta+}-H\cdots O^{\delta-}$, 2, $O-H\cdots O^{\delta-}$, 3, $N^{\delta+}-H\cdots N^{\delta+}$, 4, $O-H\cdots O$.

Fig. 4.80 – The motifs of the molecular complexes from Section 4.5 excluding benzimidazolium 4-hydroxybenzoate hydrate and benzimidazolium 3,5-dihydroxybenzoate. The three unique hydrogen bond motifs are shown, the hydrogen bonded rings (BENZH⁺ 2HBA⁻ 1:1), chains hydroxybenzoic acid dimers and the ladder motif.

Fig. 5.1 – 2-fluorobenzoic acid.

Fig. 5.2 – Basic building block of the 2-fluorobenzoic acid: 4-(1H-pyrazol-1-ylmethyl)benzamide molecular complex structure found in the CSD with a fluorine atom on one of the fluorobenzoic acid groups is disordered over two sites

Fig. 5.3 – LHS, 3-fluorobenzoic acid; RHS, 3-fluorobenzoic acid : 4-acetylpyridine molecular complex with the fluorine atom disordered over two positions (common with fluorine atoms) explaining the overlap of the hydrogen and fluorine atoms.

Fig. 5.4 – Basic building block of the 4-fluorobenzoic acid crystal structure, RHS, 4-fluorobenzoic acid.

Fig. 5.5 – Basic building block of the 4-fluorobenzoic acid : isonicotinamide molecular complex.

Fig. 5.6 - The carboxylic acid dimer that is the main supramolecular synthon in the 2-chlorobenzoic acid crystal structure; RHS, 2-chlorobenzoic acid.

Fig. 5.7 – The main building block of the 2-chlorobenzoic acid : 2-methylbenzoic acid molecular complex. Both independent molecules have the chloro and methyl substituents disordered over two sites of equal occupancy

Fig. 5.8 – Crystal structure of the 3-chlorobenzoic acid molecule; RHS, 3-chlorobenzoic acid.

Fig. 5.9 – Building block of the 3-chlorobenzoic acid 2-picoline N-oxide molecular complex.

Fig. 5.10 – Structure of 4-chlorobenzoic acid highlighting the carboxylic acid dimer being held together by a chlorine-chlorine halogen bond, RHS, 4-chlorobenzoic acid.

Fig. 5.11 – LHS, structure of the 4-chlorobenzoic acid : N,N-dimethylformamide molecular complex, RHS, 4-chlorobenzoic acid : sulfadimidine molecular complex.

Fig. 5.12 – 2-bromobenzoic acid molecule.

Fig. 5.13 – 3-bromobenzoic acid molecule.

Fig. 5.14 – The 4-bromobenzoic acid structure highlighting the carboxylic acid dimers being held together by weak C-H...O hydrogen bonds; RHS, 4-bromobenzoic acid.

Fig. 5.15 – Structure of 2-iodobenzoic acid (CSD reference - OIBZAC01); the carboxylic acid dimer is held together by iodine-iodine halogen bonds. RHS, 2-iodobenzoic acid.

Fig. 5.16 – LHS- 3-iodobenzoic acid; RHS, structure of 3-iodobenzoic acid and N-carboxymethyl-N,N'-dimethylpiperazine molecular complex.

Fig. 5.17 – The structure of 4-iodobenzoic acid; carboxylic acid dimers are held together by iodine iodine interactions. RHS, 4-iodobenzoic acid.

Fig. 5.18 – Top left, basic building block of the 3-(AMP-P) toluene 4-iodobenzoic acid solvate with CSD reference – COWHOM, top right, the 3-(AMP-P) 2,3,5,6-tetrafluoro 4-iodobenzoic acid molecular complex main hydrogen bond motif with CSD reference – COWHUS, bottom left, the molecular complex of 4-(AMP-P) 4-iodobenzoic acid which has CSD – reference COWJAA and lastly bottom right, 1-(AMP-P) 4-iodobenzoic acid with CSD reference – COWJOO.

Fig. 5.19 – LHS, a typical benzimidazolium molecule where both nitrogens are protonated; RHS, the Fourier difference map generated where the H atoms located on a nitrogen atom have been omitted from the model, clearly shows that both nitrogen atoms are protonated.

Fig. 5.20 – The potential homo-hydrogen bonds (A, B and C) and hetero-hydrogen bonds (D, E and F) that can be exhibited between a benzimidazole and carboxylic acid group.

Fig. 5.21 – The most prominent hydrogen bonds within the benzimidazole : halobenzoic acid molecular complexes: N-H \cdots N hydrogen bond (A), N-H \cdots O hydrogen bond (B) and O-H \cdots O hydrogen bond (C).

Fig. 5.22 – DSC data from the products of crystallisation of benzimidazole and 3-chlorobenzoic acid from four common solvents. Two different polymorphs can be clearly identified by two distinct melting points, but a third polymorph can also be identified in the samples crystallised from 1-propanol (1proh) and acetone. The shoulder on the principal peaks in these traces, representing the third polymorph, can be seen in the enlarged inset, taken from the acetone trace.

Fig. 5.23 – Powder patterns of the products of crystallisation from four common solvents propanol (-), acetone (-), methanol (-) and ethanol (-). Two different products can clearly be identified from these quick powder patterns (collected on the Rigaku R-axis/RAPID single crystal diffractometer) with crystallisation from propanol and acetone forming one product and methanol and ethanol the other.

Fig. 5.24 – Powder patterns of the products of crystallisation from three different environmental conditions to promote growth of single component of; form I (blue) using propanol at 10°C, form II (yellow) using acetone at ~2-4°C and form III (red) using acetone at 10°C. Three different products can clearly be identified from these powder patterns.

Fig. 5.25 – Powder pattern of benzimidazole and 3-chlorobenzoic acid Form III collected over a 33 hour period.

Fig. 5.26 – LHS, Fourier difference map of the residual electron density in BZN : 3-CIBA molecular complex with the proton associated with the carboxylic acid group removed, RHS, the BZN and 3-CIBA molecules involved in the molecular complex with associated atom labelling.

Fig. 5.27 – LHS, the main motif of the BZN : 3-CIBA Form I molecular complex; an equimolar hydrogen bonded ring system held together by N-H \cdots O and O-H \cdots N hydrogen bonds; RHS, view along the *b*-axis that highlights the spatial arrangement of the equimolar hydrogen bonded ring system.

Fig. 5.28 – View along the *a*-axis of the BZN : 3-CIBA Form I molecular complex highlighting how the chlorine-chlorine interaction connects the rings together (green circles).

Fig. 5.29 – LHS, view along the *b*-axis of the BZN 3-CIBA Form I molecular complex highlighting how the hydrogen bonded rings stack upon one another. RHS, the weak hydrogen bond, C1-H \cdots O2, which stacks the rings upon one another.

Fig. 5.30 – View along the *a*-axis of the BZN 3-CIBA Form I molecular complex. The hydrogen bonded rings, the main motif of the structure, are expanded along the *b*-axis by weak C-H \cdots O hydrogen bonds.

Fig. 5.31 – An extended view along the *a*-axis of the BZN 3-CIBA Form I molecular complex. The hydrogen bonded ring motif (blue circle), is expanded along the *b*-axis by weak C-H \cdots O hydrogen bonds (red circle) and the *ab*-diagonal by chlorine-chlorine interactions.

Fig. 5.32 – The co-molecules involved in the BZNH^{0.5+} : 3-CIBA^{0.5-} molecular complex (BZN : 3-CIBA Form II) with atom labelling.

Fig. 5.33 – LHS, a MCE Fourier difference map generated where the H atoms located on the N atom have been omitted from the model, clearly showing that the proton is split over two sites; RHS, a MCE Fourier difference map generated where the H atoms located on the carboxylic acid group have been omitted from the model, again clearly showing that this proton is split over two sites.

Fig. 5.34 – LHS, the supramolecular synthon of the BZN : 3-CIBA Form II molecular complex, co-molecule dimers, linked together through $N^{\delta+}-H\cdots O^{\delta-}$ hydrogen bonds, RHS, the main motif of the BZN : 3-CIBA Form I molecular complex, an equimolar hydrogen bonded ring system held together by $N-H\cdots O$ and $O-H\cdots N$ hydrogen bonds.

Fig. 5.35 – The secondary supramolecular synthon of the BZN : 3-CIBA Form II molecular complex that links the motifs together along the *a*-axis.

Fig. 5.36 – The lesser interactions *c*, halogen bond and *d*, $C-H\cdots\pi$ interaction, that expand the structure along the *c*-axis.

Fig. 5.37 – LHS, an extended view along the *a*-axis of the BZN : 3-CIBA Form II molecular complex. The motif, a chain of alternating co-molecule dimers (blue) is expanded along the *c*-axis via halogen bonds (green), RHS, an extended view along the *a*-axis of the BZN : 3-CIBA Form I molecular complex. The hydrogen bonded ring motif (red circle) is expanded along the *b*-axis by weak $C-H\cdots O$ hydrogen bonds (red box) and along the *ab*-diagonal by chlorine-chlorine interactions (green circle).

Fig. 5.38 – DSC thermogram of the products from benzimidazole and 4-chlorobenzoic acid co-crystallisations in acetone (-) ethanol (-), methanol (-) and propanol (-). It can clearly be seen that there are two distinct endothermic changes that relate to phase changes around 123°C and 132°C.

Fig. 5.39 – Powder patterns of the products of crystallisation from two different environmental conditions to promote growth of single component of Form I (blue) using ethanol at room temperature and a mixed phase of Forms I and II (red) using acetone also at room temperature.

Fig. 5.40 – The molecular ions, two of each co-molecule $BZNH^+$ and $4-CIBA^-$ that make up this molecular complex, with atom labelling. The numbers, 1 to 4, designate their molecule number.

Fig. 5.41 – The supramolecular synthon, the hydrogen bonded rings, involves one of each co-molecule.

Fig. 5.42 – The motif of the $BZNH^+$ and $4-CIBA^-$ molecular complex with molecules coloured that are symmetry related, i.e. molecule 1 yellow, molecule 2 red, molecule 3 green and molecule 4 blue. Highlighted by a red circle is the $BZNH^+$ molecules that further expand the structure.

Fig. 5.43 – The halogen bond and halogen- π interactions that exist between the two $4-CIBA^-$ molecules.

Fig. 5.44 – LHS, view along the *b*-axis of the $BZNH^+ : 4-CIBA^-$ molecular complex; RHS, view along the *c*-axis. Both images show the hydrogen bonded network that is held together by halogen interactions (green box and line).

Fig. 5.45 – DSC thermogram of the products of benzimidazole and 4-bromobenzoic acid co-crystallisations in acetone (-) and methanol (-). It can clearly be seen that there are two distinct endothermic changes that relate to phase changes around 123°C and 142°C.

Fig. 5.46 – Powder patterns of the products of crystallisation from four different environmental conditions to promote growth of single component of Form I (blue) using propanol and ethanol and Form II (red) using acetone and methanol all at room temperature.

Fig. 5.47 – LHS, View along the *b*-axis of the $\text{BZNH}^+ : 4\text{-BrBA}^-$ molecular complex; RHS, view along the *c*-axis. Both images show the hydrogen bonded network that is held together by halogen interactions (green box and line).

Fig. 5.48 – Powder patterns of the products of crystallisation from three different environmental conditions to promote the growth the benzimidazole : 3-bromobenzoic acid molecular complex using methanol at 10°C (red) ethanol at 10°C (blue) and acetone at 10°C (yellow).

Fig. 5.49 – LHS, the supramolecular synthon of the $\text{BZNH}^+ : 3\text{-BrBA}^-$ molecular complex, dimers of each co-molecule are connected through a $\text{N}^{\delta+}\text{-H}\cdots\text{O}^{\delta-}$ moderate hydrogen bond, RHS, the secondary supramolecular synthon of that links the motifs together along the *a*-axis.

Fig. 5.50 – View along the *a*-axis of the extended structure of the $\text{BZNH}^+ : 3\text{-BrBA}^-$ molecular complex, the motifs (blue box) are held together through weak halogen and $\text{C-H}\cdots\pi$ interactions (brown box).

Fig. 5.51 – The BZNH^+ , 2-FBA and 2-FBA^- molecules, from left to right, that make up the $\text{BZNH}^+ : 2\text{-FBA}^- : 2\text{-FBA}$ molecular complex, with atom labelling.

Fig. 5.52 – The primary hydrogen bonds within the $\text{BZNH}^+ : 2\text{-FBA} : 2\text{-FBA}^-$ molecular complex.

Fig. 5.53 – The motif of the $\text{BZNH}^+ : 2\text{-FBA} : 2\text{-FBA}^-$ molecular complex, zigzag chains between the BZNH^+ and 2-FBA^- co-molecules using the $\text{N-H}\cdots\text{O}$ form B hydrogen bond. LHS, view along the *a*-axis; RHS, view of the *b*-axis.

Fig. 5.54 – LHS, two motifs of the $\text{BZNH}^+ : 2\text{-FBA} : 2\text{-FBA}^-$ molecular complex held together along the *ac*-diagonal axis by halogen bonds (yellow circle); RHS, view of the halogen bonds, $\text{C-H}\cdots\text{F}$.

Fig. 5.55 – The $\text{C-H}\cdots\text{O}$ hydrogen bond that expands the structure along the *bc*-diagonal axis.

Fig 5.56 – top, X-ray powder diffraction patterns of benzimidazole : 3-fluorobenzoic acid (red), 3-fluorobenzoic acid (blue) and benzimidazole (green) clearly indicating a new product has been produced, bottom, DSC thermogram of the same materials; benzimidazole : 3-fluorobenzoic acid (purple), 3-fluorobenzoic acid (red) and benzimidazole (green) again indicating a new product is formed, insert, patterns of other co-crystallisations experiments.

Fig. 5.57 – LHS, the BZNH^+ and BZN dimers with atom labelling; RHS, the 4-FBA^- and 4-FBA dimers with associated labelling .

Fig. 5.58 – View along the *a*-axis of the $\text{BZN} : 4\text{-FBA}$ molecular complex, showing the main motif, a zigzag chain of dimers held together by $\text{N}^{\delta+}\text{-H}\cdots\text{O}^{\delta-}$ hydrogen bonds that expand the structure along the *ab*-diagonal axis.

Fig. 5.59 – The *a*-axis of the $\text{BZN} : 4\text{-FBA}$ molecular complex, showing the main motifs (blue line) held together along the *c*-axis by $\text{C-H}\cdots\text{F}$ halogen bonds (a and b).

Fig. 5.60 – The *a*-axis is expanded by two interactions; a $\text{C-H}\cdots\text{O}$ weak hydrogen bond (blue circle) and a $\text{C-H}\cdots\pi$ interaction (red circle).

Fig. 5.61 – Top, view along the *c*-axis of the $\text{BZN} : 4\text{-FBA}$ molecular complex which highlights the two types interactions that exist between the layers: a $\pi\cdots\pi$ stacking interaction between the BZN dimers (yellow circle) and the weak $\text{C-H}\cdots\text{O}$ hydrogen bonds (green circle) between the 4-FBA molecules, bottom LHS, $\pi\cdots\pi$ stacking interactions, bottom RHS, $\text{C-H}\cdots\text{O}$ weak hydrogen bonds.

Fig. 6.1 – The structure of picolinic acid showing the main hydrogen bonds between the molecules. Proton disorder can be seen between the carboxylic acid hydrogen bond and the weaker N-H...H-N hydrogen bond.

Fig. 6.2 –LHS, protonated picolinic acid : L-tartrate acid molecular complex; RHS, the molecular complex of picolinate and 2-amino-5-methylpyridinium, where the picolinic acid has been deprotonated.

Fig. 6.3 – Basic building block of the acetoguanaminium 3-hydroxypicolinate monohydrate molecular complex.

Fig. 6.4 – LHS, the structure of 6-hydroxypicolinic acid (2-oxo-1,2-dihydropyridine-6-carboxylic acid) and, RHS, a hydrate form.

Fig. 6.5 – The molecules involved in the 6-hydroxypicolinic acid 2-amino-5-chloropyridinium molecular complex.

Fig. 6.6 – The nicotinic acid supramolecular synthon showing the dominating O-H...N hydrogen bond.

Fig. 6.7 – LHS, 3-carboxypyridinium hydrogen (2R,3R)-tartrate molecular complex where the nitrogen has been protonated; RHS, the molecular complex 2-amino-5-methylpyridinium nicotinate, where the carboxylic group on the nicotinic acid has been deprotonated.

Fig. 6.8 – LHS, the O-H...N hydrogen bond in the crystal structure of isonicotinic acid; RHS, the molecular complex of isonicotinic acid protocatechuic acid monohydrate, with the zwitterionic form of isonicotinic acid.

Fig. 6.9 – LHS, the hydrogen bonded dimer of 2-nitrobenzoic acid with the two molecules related by an inversion centre in the middle of the hydrogen bonded ring and the nitro- groups twisted out of the plane; RHS, the molecular complex of benzimidazolium 2-nitrobenzoate bis(2-nitrobenzoic acid) showing some of the hydrogen bonds between the molecules.

Fig. 6.10 – The hydrogen bonded carboxylic acid dimer of benzimidazolium and 2-nitrobenzoic acid.

Fig. 6.11 – LHS, the supramolecular synthon of benzimidazolium and 3-nitrobenzoic acid; RHS, the supramolecular synthon of imidazolium and 3-nitrobenzoic acid.

Fig. 6.12 – The hydrogen bonded dimer of 4-nitrobenzoic acid.

Fig. 6.13 – LHS, benzimidazolium 4-nitrobenzoate molecular complex that contains the synthon $N^{\delta+}-H\cdots O^{\delta-}$, which forms into zig-zag chains; RHS, the imidazolium 4-nitrobenzoate molecular complex also forms $N^{\delta+}-H\cdots O^{\delta-}$ hydrogen bonds, which in this case assemble to form hydrogen bonded rings.

Fig. 6.14 – LHS, a typical benzimidazolium molecule where both nitrogens are protonated; RHS, the Fourier difference map generated where the H atoms located on a nitrogen atom have been omitted from the model, clearly showing that both nitrogen atoms are protonated.

Fig. 6.15 – A diffraction pattern frame from the single crystal X-ray diffraction experiment on a crystal of the benzimidazole : picolinic acid molecular complex showing the strong diffuse scattering.

Fig. 6.16 – LHS, the disordered model for the benzimidazolium picolinate hydrate molecular complex; RHS, the likely hydrogen bonded unit when considering the local ordering, i.e. with the disorder removed.

Fig. 6.17 – The water molecule connects the layers of alternately hydrogen bonded co-molecules together.

Fig. 6.18 – The main motif of the $\text{BZNH}^+ \text{PA}^-$ molecular complex is a flat chain of alternating hydrogen bonded co-molecules.

Fig. 6.19 – The water molecule, with two 0.5 occupied hydrogens (yellow) and one fully occupied hydrogen (white) connects the layers of alternately hydrogen bonded co-molecules

Fig. 6.20 – LHS, the hydrogen bonded ring (hydrogen bonds shown in blue) involving two water molecules and two picolinate molecules that connect two flat chains of hydrogen bonded $\text{BZNH}^+ \text{PA}^-$ molecules; RHS, view along the c -axis emphasising that the water molecule sits just out of the plane of the flat sheets of hydrogen bonded $\text{BZNH}^+ \text{PA}^-$ molecules.

Fig. 6.21 – LHS, the view along the c -axis of the $\text{BZNH}^+ \text{PA}^-$ molecular complex showing the herringbone layers connected by water molecules; RHS, the view along the b -axis of the $\text{BZNH}^+ \text{PA}^-$ molecular complex showing the channels of water.

Fig. 6.22 – LHS, weak $\text{C-H}\cdots\text{O}$ hydrogen bonds that lie along the a -axis; RHS, view showing that the BZNH^+ molecules lie directly parallel thus improving the chances of $\pi\cdots\pi$ stacking interactions.

Fig. 6.23 – The atom labelling for the molecular complex of benzimidazolium (LHS) and 3-hydroxypicolinate. (RHS).

Fig. 6.24 – LHS, the supramolecular synthon for the $\text{BZNH}^+ 3\text{-HPA}^-$ molecular complex; a hydrogen bonded ring system held together by partially charge assisted $\text{N}^{\delta+}\text{-H}\cdots\text{O}^{\delta-}$ and $\text{N}^{\delta+}\text{-H}\cdots\text{N}$ hydrogen bonds; RHS, the Fourier difference map (generated using MCE), where the hydrogen adjoining N2 has been removed from the model, showing the hydrogen atom to be clearly located on the N atom of the benzimidazolium molecule ion. The elongation of the electron density along the hydrogen bond illustrates the influence of the neighbouring oxygen molecule.

Fig. 6.25 – the stacking of the hydrogen bonded rings held together by π - π interactions.

Fig. 6.26 – The supramolecular synthons of the $\text{BZNH}^+ 3\text{-HPA}^-$ molecular complex, are connected by weak bifurcated hydrogen bonds (circled in red) along the c -axis. Inset shows the bifurcated weak hydrogen bond circled in red in the main figure.

Fig. 6.27 – LHS, view of the c -axis of the $\text{BZNH}^+ 3\text{-HPA}^-$ molecular complex, which indicates the interactions between the layers (circled in yellow); RHS an expanded view of the interactions that hold the layers together, with $\text{C-H}\cdots\pi$ interactions circled in yellow.

Fig. 6.28 – The intermolecular interactions in the $\text{BZNH}^+ 3\text{-HPA}^-$ molecular complex, with the supramolecular synthon circled in blue, the weak bifurcated hydrogen bonds in red and the $\text{C-H}\cdots\pi$ contacts in yellow. The π - π stacking goes into the plane of the page.

Fig. 6.29 – The atomic labelling for the two independent molecules of each type in the imidazolium 3-hydroxypicolinate molecular complex.

Fig. 6.30 – Top, view along the b -axis of the main motif of the $\text{IMDH}^+ 3\text{-HPA}^-$ molecular complex, a zigzag chain of alternate co-molecules held together by partially charge assisted hydrogen bonds; bottom, view along the a -axis of the main motif of the $\text{IMDH}^+ 3\text{-HPA}^-$ molecular complex.

Fig. 6.31 – LHS, the $\text{C-H}\cdots\text{O}^{\delta-}$ hydrogen bonds (-) along the ac -diagonal, RHS, view along the c -axis of the staggered face-to-face $\pi\cdots\pi$ stacking interactions that extend the structure along the b -axis.

Fig. 6.32 – View along the *b*-axis of the extended $\text{IMDH}^+ 3\text{HPA}^-$ molecular complex. The main motif, the zigzag chains of alternate hydrogen bonded co-molecules, is shown by the green line (-) and the weak hydrogen bonds are located within the transparent blue box (-). Inset shows the $\text{C-H}\cdots\pi$ interactions that extend the structure along the *b*-axis.

Fig. 6.33 – LHS, the benzimidazolium and 6-hydroxypicolinate molecule ions which are generated in the molecular complex, with atom labelling.

Fig. 6.34 – schematic diagram of the lactam - lactim tautomerism (imidic acid) that the 6-hydroxypicolinic acid molecule undergoes, forming 2-oxo-1,2-dihydropyridine-6-carboxylic acid.

Fig. 6.35 – The main motif of the $\text{BZNH}^+ 6\text{-HPA}^-$ molecular complex; a hydrogen bonded ring system held together by 6- HPA^- dimers (e) and partially charge assisted $\text{N}^{\delta+}\text{-H}\cdots\text{O}^{\delta-}$ (f) and $\text{N}^{\delta+}\text{-H}\cdots\text{O}$ (g) hydrogen bonds.

Fig. 6.36 – the chain of $\text{BZNH}^+ 6\text{-HPA}^-$ rings along the *b*-axis, viewed along *a*.

Fig. 6.37 – LHS, the weak hydrogen bonds $\text{C1-H}\cdots\text{O1}^{\delta-}$ and $\pi\cdots\pi$ interactions between two chains. These are two interactions that stack the chains along the *a*-axis. Middle, view along the *b*-axis showing the stacking of the chains. Highlighted in red are the interactions viewed in Figure 6.33, LHS. Circled in blue are those interactions from Figure 6.33, RHS. The interactions within the green circle are the moderate hydrogen bonds involved in the hydrogen bond ring motif. RHS, the $\text{C-H}\cdots\pi$ interactions are the blue dotted lines in the centre of the image.

Fig. 6.38 – The $\text{C-H}\cdots\text{O}^{\delta-}$ weak hydrogen bonds connect three different chains within the $\text{BZNH}^+ 6\text{-HPA}^-$ molecular complex.

Fig. 6.39 – The benzimidazolium, 6-hydroxypicolinate and acetic acid molecules which are generated in the molecular complex, with atom labelling.

Fig. 6.40 – The hydrogen bonded chains of the $\text{BZNH}^+ : 6\text{-HPA}^-$ acetic acid solvate molecular complex is a flat linear chain of alternating hydrogen bonded co-molecules.

Fig. 6.41 – The hydrogen bonding scheme in the $\text{BZNH}^+ 6\text{-HPA}^-$ acetic acid solvate molecular complex, highlighting the role of the acetic acid molecules in creating the linear chain.

Fig. 6.42 – Two motifs of the $\text{BZNH}^+ 6\text{-HPA}^-$ diacetic acid molecular complex showing how the two adjacent linear chains are connected along the *c*-axis through weak $\text{C-H}\cdots\text{O}$ hydrogen bonds (circled in red) between the acetic acid molecules; inset – expanded image of these hydrogen bonds.

Fig. 6.43 – LHS, view along the *c*-axis showing the layered nature with the weaker interactions along the *ab*-diagonal, weak hydrogen bonds (light blue) and $\pi\cdots\pi$ interactions (dark blue); middle, the $\pi\cdots\pi$ interaction (blue); RHS, the weak $\text{C-H}\cdots\text{O}$ hydrogen bonds between the acetic acid molecules.

Fig. 6.44 – The structure of the nitro group.

Fig. 6.45 – The structures of 1, benzimidazolium 4-nitrobenzoate 2, benzimidazolium 3-nitrobenzoate 3, imidazolium 3-nitrobenzoate 4, imidazolium 3-nitrobenzoate.

Fig. 6.46 – The benzimidazolium 3-nitrobenzoate molecular complex structure viewed along the *c*-axis. The spiral hydrogen bond motif runs along the *b*-axis with the weak $\text{C-H}\cdots\text{O}^{\delta-}$ hydrogen bonds (circled in red) connecting adjacent spirals.

Fig. 6.47 – The benzimidazolium 4-nitrobenzoate molecular complex structure viewed along the *c*-axis. The spiral hydrogen bond motif runs along the *b*-axis with the weak C–H \cdots O $^{\delta-}$ hydrogen bonds (circled in red) connecting adjacent spirals.

Fig. 6.48 – The imidazolium 3-nitrobenzoate molecular complex structure viewed along the *a*-axis. The hydrogen bonded rings (green boxes) are connected by weak carbon oxygen hydrogen bonds (circled in red) and $\pi\cdots\pi$ interactions (blue).

Fig. 6.49 – The imidazolium 3-nitrobenzoate molecular complex structure viewed along the *a*-axis. The hydrogen bonded rings (green boxes) are connected by weak carbon oxygen hydrogen bonds (circled in red).

Fig. 6.50 – The bifurcated hydrogen bond of the BZNH $^+$: 3-HPA $^-$ molecular complex, with the major component the N–H \cdots N hydrogen bond and minor component being N–H \cdots O.

Fig. 7.1 – Structure of phthalic acid, which is seen to exploit the carboxylic acid dimer motif.

Fig. 7.2 – LHS, crystal structure of the molecular complex of phthalic acid and benzene-1,2-dicarboxylic acid; RHS, the phthalate ion in the ionic complex formed with 2,6-dimethylpyridinium.

Fig. 7.3 – The crystal structure of isophthalic acid, which exhibits the common carboxylic acid dimer motif.

Fig. 7.4 – LHS, structure of the benzimidazole : isophthalic acid molecular complex; RHS, the structure of the imidazole : isophthalic acid molecular complex.

Fig. 7.5 – The carboxylic acid dimer that exists in all the terephthalic acid structures.

Fig. 7.6 – The imidazole : terephthalic acid molecular complex.

Fig. 7.7 – The carboxylic acid dimer motif adopted in the fumaric acid structure.

Fig. 7.8 – The ladder motif of the imidazolium hydrogen fumarate structure, with the uprights consisting of fumaric acid chains and the steps of imidazolium molecules.

Fig. 7.9 – top, the carboxylic acid dimer that is the main hydrogen bonding pattern for both polymorphs of succinic acid, with the packing shown below, LHS, triclinic form, RHS, monoclinic form.

Fig. 7.10 – Basic building block of the imidazolium succinate ionic molecular complex.

Fig. 7.11 – The structure of maleic acid Form I, showing the main hydrogen bonding pattern.

Fig. 7.12 – The hydrogen bonded ring motif of the imidazolium maleate molecular complex.

Fig. 7.13 – The basic dimeric hydrogen bonded building block of all the polymorphic forms of malonic acid.

Fig. 7.14 – The imidazolium malonate hydrate structure consists of chains of alternate co-molecules connected through the disordered water molecules.

Fig. 7.15 – The carboxylic acid dimer that is the building block of the benzoic acid structure.

Fig 7.16 – The linear chain of alternating hydrogen bonded co-molecules that exists in the imidazolium benzoate molecular complex.

Fig. 7.17 – LHS, the imidazolium molecule with 4-bromobenzoate, in which both nitrogens are protonated. RHS, the MCE Fourier difference map generated where the H atoms located on a nitrogen atom have been omitted from the model, clearly showing that both nitrogen atoms are protonated.

Fig. 7.18 – The library of hydrogen bond patterns that the molecular complexes are highly likely to adopt. E, F, G, H, I and J are all seen in other molecular complexes. The motifs are defined as the

general descriptor of these interactions; K is the ladder motif, L is the hydrogen bonded ring motif, M is the co-molecule dimer motif while N is an example of a linear chain of alternate co-molecules.

Fig. 7.19 – The imidazolium and 2-hydroxybenzoate ions which are generated in the molecular complex/salt, with atom labelling.

Fig. 7.20 – The two main hydrogen bonds within the molecular complex, a, N-H \cdots O forming pattern E and b, N-H \cdots O forming pattern F; RHS, the resulting arrow head chain of alternate co-molecules.

Fig. 7.21 – LHS, the weak C-H \cdots O hydrogen bond, c, involving the hydroxyl oxygen, RHS, the C-H $\cdots\pi$ interaction, d, that expands the structure along the *bc* diagonal.

Fig. 7.22 – LHS, the C-H \cdots O weak hydrogen bond, e, that connects two of the chains together, RHS, another C-H \cdots O hydrogen bond, f, this time expanding the structure along the *c*-axis.

Fig. 7.23 – An expanded image of the IMDH⁺ 2-HBA⁻ molecular complex showing the hydrogen bonded chains (blue line) being connected by two C-H \cdots O hydrogen bonds (red box).

Fig. 7.24 – The imidazolium and 3-hydroxybenzoate ions which are generated in the molecular complex/salt, with atom labelling.

Fig. 7.25 – LHS, an expanded view of the IMDH⁺ 3-HBA⁻ molecular complex along the *a*-axis, it can be seen that the structure is made up of hydrogen bonded boxes (red box) stacked upon each other, RHS, a expanded view of the yellow circle highlighting the corners of each box with the three hydrogen bonds that originate from this point.

Fig. 7.26 – LHS, bifurcated hydrogen bond and RHS, C-H \cdots O weak hydrogen bond that expands the stacks of boxes along the *b*-axis.

Fig. 7.27 – The imidazolium and 3-hydroxybenzoate ions which are generated in the molecular complex/salt, with atom labelling.

Fig. 7.28 – LHS, the view along the *c*-axis of the motif of the IMDH⁺ 4-HBA⁻ molecular complex, hydrogen bonded squares (red box) stack upon one another, RHS, extract from the yellow circle which shows the corners of the boxes with hydrogen bonds E, F and G highlighted.

Fig. 7.29 – View along the *a*-axis showing two stacks of boxes held together along the *c*-axis by C-H $\cdots\pi$ interactions (circled in red).

Fig. 7.30 – The double weak hydrogen bonds that expand the stacks of hydrogen bonded boxes along the *ac*-diagonal.

Fig. 7.31 – (top) The imidazolium and 4-fluorobenzoate ions which are generated in the molecular complex/salt, with atom labelling.

Fig. 7.31 – (bottom) LHS, the main motif of the IMDH⁺ 4-FBA⁻ molecular complex, a spiral chain of alternate co-molecules held together through N-H \cdots O hydrogen bonds, E and F, RHS, view along the *b*-axis of an extended spiral chain showing its cyclical nature.

Fig. 7.32 – LHS, the C-H \cdots O weak hydrogen bond that binds two spiral chains to one another, RHS, the effect the binding of the two spirals (red circle) has on the structure.

Fig. 7.33 – View along the *b*-axis of the extended structure of the IMDH⁺ 4-FBA⁻ molecular complex showing the spiral chains (highlighted in red) held together by weak hydrogen bonds (yellow lines) that connect the chains along the *a*- and *c*-axes.

Fig. 7.34 – The imidazolium and 3-bromobenzoate ions which are generated in the molecular complex/salt, with atom labelling.

Fig. 7.35 – The main motif of the $\text{IMDH}^+ 4\text{-BrBA}^-$ molecular complex, a zigzag chain of alternate co-molecules connected through moderate hydrogen bonds.

Fig. 7.36 – The motifs, zigzag chains of alternative co-molecules, are stacked upon one another along the c -axis held by weak $\text{C-H}\cdots\text{O}$ hydrogen bonds; RHS, the weak hydrogen bonds that exists between the layers.

Fig. 7.37 – The halogen bonds, $\text{C-H}\cdots\text{Br}$, that exist between the zigzag chains along the b -axis.

Fig. 7.38 – An extended image of the $\text{IMDH}^+ 4\text{-BrBA}^-$ molecular complex viewed along the a -axis, showing the main motif (blue line), the weaker $\text{C-H}\cdots\text{O}$ hydrogen bonds (red box) and the bromine halogen bonds (brown box).

Fig. 7.39 – The motif of the $\text{BZNH}^+ : \text{BA}^- : \text{BA}$ molecular complex, an $R_4^4(24)$ hydrogen bond ring system containing two of each molecule held together by $\text{N-H}\cdots\text{O}$ (a' , b' , c' , d' , f' and g') and $\text{O-H}\cdots\text{O}$ (e' and h') hydrogen bonds. The BA and BA^- molecules are labelled 1 to 4.

Fig. 7.40 – View along the c -axis highlighting the stacking behaviour of the motifs with the $\pi\cdots\pi$ interactions (red and blue ovals, and expanded in the blue and red boxes) that hold it them together.

Fig. 7.41 – The $\text{C-H}\cdots\text{O}$ weak hydrogen bond that expands the structure along the b -axis.

Fig. 7.42 – LHS, the blue shaded circles show where the $\text{C-H}\cdots\text{O}$ weak hydrogen bonds (Figure 7.41) hold the motifs together; RHS, view along the b -axis highlighting the zigzag pattern formed by the motifs.

Fig. 7.43 – LHS, the a -axis, RHS, the c -axis of the extended structure showing how the main motif (blue areas) is expanded by weak $\text{C-H}\cdots\text{O}$ hydrogen bonds (yellow areas).

Fig. 7.44 – LHS, the linear chain of hydrogen bonded alternating co-molecules is the main motif in the imidazolium benzoate structure³³; RHS, shows the cyclical nature of the motif.

Fig. 7.45 – The molecules involved in the benzimidazolium phthlate molecular complex, with atom labelling.

Fig. 7.46 – LHS, view of the main motif, linear chain of alternating hydrogen bonded co-molecules; RHS, view along the a -axis that highlights the spiral nature of the chain.

Fig. 7.47 – View along the a -axis of three motifs, spiral chains of alternating hydrogen bonded co-molecules, that are held together by $\text{C-H}\cdots\text{O}$ weak hydrogen bonds (blue circles).

Fig. 7.48 – The weak hydrogen bond, $\text{C-H}\cdots\text{O}$ (green line) and $\text{C-H}\cdots\pi$ interaction (purple line), that expand the structure along the c -axis.

Fig. 7.49 – The extended structure viewed along the a -axis, showing how the motif (red) is expanded along the b -axis by weak $\text{C-H}\cdots\text{O}$ hydrogen bonds (blue) and finally along the c -axis by $\text{C-H}\cdots\text{O}$ (green) and $\text{C-H}\cdots\text{C}$ hydrogen bonds (purple).

Fig. 7.50 – LHS, the molecules involved in the imidazolium isophthlate molecular complex; RHS, those involved in the benzimidazole isophthalic acid molecular complex, with the carboxylic acid protons in undetermined positions.

Fig. 7.51 – The main motif of the structure, a double linear chain of alternate co-molecules held together through $\text{N-H}\cdots\text{O}$ and $\text{O-H}\cdots\text{O}$ hydrogen bonds.

Fig. 7.52 – An extended structure showing the motifs (blue box) being expanded along the *c*-axis by carbon – carbon hydrogen bonds (yellow box).

Fig. 7.53 – top, the view along the *a*-axis of the chains of isophthalic acid hydrogen bonding to the imidazolium molecule, bottom, view of the *b*-axis highlighting how the imidazolium molecule hydrogen bonds to two different chains on different layers.

Fig. 7.54 – LHS, the benzimidazolium and terephthalate molecules involved in the molecular complex with atom labelling; RHS, the three main hydrogen bonds involved in the molecular complex, a' N-H...O, b' N-H...O and c' O-H...O.

Fig. 7.55 – The main motif of the benzimidazolium terephthalate molecular complex, a ladder with uprights of terephthalate molecules and rungs of benzimidazolium molecules.

Fig. 7.56 – The main motif, a ladder of terephthalic acid uprights and benzimidazole rungs, stack upon one another through C-H...O hydrogen bonds (red circle); insert, blown-up image of the C-H...O hydrogen bond.

Fig. 7.57 – The extended structure of the benzimidazolium terephthalate molecular complex viewed along the *c*-axis (LHS) and *a*-axis (RHS).

Fig. 7.58 – LHS, the linear chain of alternating co-molecules that is the motif of the molecular complex; RHS, view along the *b*-axis highlighting the spiral nature of the chain.

Fig. 7.59 – LHS, the motif, spiral chains (blue box), expands along the *b*-axis and *ac*-diagonal forming sheets; RHS, the C-H...O weak hydrogen bond (red box) connects these sheets together along the *a*-axis.

Fig. 7.60 – The benzimidazolium and fumarate ions (two protons are shown, but both have 0.5 occupancy levels) which are generated in the molecular complex/salt, with atom labelling

Fig. 7.61 – LHS, The carboxylic acid dimer of the fumaric acid structure; RHS, the hydrogen bond between the fumarate molecules of the benzimidazolium complex, with the shared proton split over the two sites.

Fig. 7.62 – The box comb chain of fumarate molecules held together by oxygen – oxygen hydrogen bonds, a' and b'. The hydrogens on the carboxylic acid groups have been removed.

Fig. 7.63 – The co-molecules arrange themselves into hydrogen bonded alternating co-molecules which expand along the *b*-axis.

Fig. 7.64 – LHS, the benzimidazolium molecules connect the fumarate chains along the *a*-axis, resulting in the layers of fumarate and alternating co-molecules interconnecting to form columns of layers, RHS.

Fig. 7.65 – the columns consisting of interconnected chains of fumarate molecules and alternating co-molecules are expanded along the *c*-axis by lesser interactions (yellow box), inset, expanded view of the lesser interactions.

Fig. 7.66 – The main motif of the imidazolium fumarate molecular complex, an amalgamation of the ladder and linear chain motifs.

Fig. 7.67 – The benzimidazolium and succinate ions which are generated in the molecular complex/salt, with atom labelling.

Fig. 7.68 – The main motif of the benzimidazolium succinate molecular complex, the ladder style with uprights of succinate ions and rungs of benzimidazolium ions.

Fig. 7.69 – the extended structure of benzimidazolium succinate molecular complex viewed along the *b*-axis, highlighting how the main motif (blue line) extends along the *c*-axis through C-H $\cdots\pi$ interactions (red box); inset, the C-H $\cdots\pi$ interaction.

Fig. 7.70 – the chain that is created through the N-H \cdots O hydrogen bonds between the co-molecules in the imidazolium succinate molecular complex.

Fig. 7.71 – The main motif of the imidazolium succinate structure, layers consisting of linear chains of alternating co-molecules that expand along the *ac*-diagonal (chains) and *a*-axis.

Fig. 7.72 – LHS, the benzimidazolium and maleate molecules which are generated in the molecular complex, with atom labelling. RHS, the Fourier difference map generated with the H atoms located on the N atoms omitted from the model; this clearly shows that both N atoms are protonated.

Fig. 7.73 – The maleic acid molecule (top) and the maleate ion (bottom) showing the differences in the bond characteristics.

Fig. 7.74 – LHS, 2D Fourier difference map, RHS, 3D Fourier difference map (MCE); both images show a slightly asymmetric location of the hydrogen atom in the intramolecular hydrogen bond of the maleate molecule.

Fig. 7.75 – The main motif of the benzimidazolium maleate molecular complex; a chain of alternating co-molecules held together by alternating charge assisted N δ^+ -H \cdots O δ^- hydrogen bonds

Fig. 7.76 – The zigzag chains that are the main synthon in the benzimidazolium maleate molecular complex are held together by weak hydrogen bonds connecting the maleate ions (insert).

Fig. 7.77 – View along the *b*-axis showing the main motif (-) of the benzimidazolium maleate molecular complex connected by the C-H \cdots O δ^- hydrogen bond from the benzimidazolium molecule (-) (insert) to make a two layer block.

Fig. 7.78 – The weak hydrogen bond between the maleate and benzimidazolium ions.

Fig. 7.79 – View along the *b*-axis of the expanded benzimidazolium maleate molecular complex. The blue line (-) indicates the planes of the main motif (Figure 7.75), the red line (-) indicates the weak hydrogen bond that holds the planes together in alternate layers (Figure 7.75) with the green line (-) indicating the other weak hydrogen bond (Figure 7.76).

Fig. 7.80 – View along the *c*-axis of the motif of the imidazolium maleate structure, showing the hydrogen bonded ring.

Fig 7.81 – LHS, the main motif, hydrogen bonded ring, are expanded by C-H \cdots O hydrogen bonds along the *ab*-diagonal (blue circle) and *ac*-diagonal (red circle); RHS, the view along the *a*-axis of an extended imidazolium maleate structure.

Fig. 7.82 – The malonate ion found in molecular complexes with (from left to right) benzimidazolium, imidazolium, imidazolium hydrate, and in its native form, with atom labelling.

Fig. 7.83 – The benzimidazolium and malonate molecules which are generated in the molecular complex, with atom labelling.

Fig. 7.84 – the main motif of the benzimidazolium malonate structure, linear chain of alternate hydrogen bonded co-molecules. Two of the motifs are connected together through carbon – oxygen hydrogen bonds (blue circle).

Fig 7.85 – RHS, the chains of motifs are held together along the *b*-axis by two alternating layers of interactions, a relatively stronger carbon – oxygen hydrogen bond (blue box), and a relatively weaker carbon – oxygen hydrogen bond (red circles); LHS, view of the *b*-axis with the interactions coloured in blocks to show the alternating layered nature.

Fig. 7.86 – the *a*-axis is expanded by two lesser interactions that stack the layers of motifs upon one-another. The shortest is a C-H···O hydrogen bond (yellow circle) while the other is a $\pi\cdots\pi$ stacking interaction between the benzimidazolium molecules (green circle). Insert LHS, the C-H···O hydrogen bond; insert RHS, the $\pi\cdots\pi$ stacking interactions.

Fig. 7.87 – The imidazolium and malonate ions which are generated in the molecular complex/salt, with atom labelling.

Fig. 7.88 – The main motif of the imidazolium malonate molecular complex, the ladder style with uprights of malonate ions and rungs of imidazolium, viewed along, LHS, the *c*-axis, middle, the *b*-axis, and RHS, the *a*-axis.

Fig. 7.89 – The motif of the structure (blue interactions) is expanded along the *b*-axis by C-H···O hydrogen bonds (green interaction) and an oxygen – oxygen interaction (red line).

Fig. 7.90 – LHS, view along the *c*-axis of the extended structure; RHS, view along the *b*-axis of the extended structure, with the main motif (blue shading) being expanded along the *b*-axis by carbon – oxygen weak hydrogen bonds (red shading).

Fig. 7.91 – LHS, extract from **Fig. 7.33**, view along the *b*-axis of the extended structure of imidazole 4-fluorobenzoate showing the spiral chains held together by halogen bonds (yellow lines) that connect the chains along the *a*- and *c*-axis; RHS, extract from **Fig. 7.68** – the carbon - carbon weak hydrogen bond that expands the benzimidazolium succinate structure along the *b*-axis.

Fig. 8.1 – The library of hydrogen bond patterns that the molecular complexes discussed in this work are highly likely to adopt: **E** ($\text{N}^{\delta+}-\text{H}\cdots\text{O}^{\delta-}$), **F** ($\text{O}-\text{H}\cdots\text{O}^{\delta-}$), **G** ($\text{N}^{\delta+}-\text{H}\cdots\text{N}^{\delta+}$) and **H** ($\text{O}-\text{H}\cdots\text{O}$). The recurrent motifs found are defined as the general descriptor of these interactions: **K** is the ladder motif, **L** is the hydrogen bonded ring motif, **M** is the co-molecule dimer motif, while **N** is an example of a linear chain of alternate co-molecules.

Fig. 8.2 – The molecular complexes that formed the ladder motif, with uprights of the carboxylic acid containing molecule and rungs of benzimidazole. From top to bottom, left to right, benzimidazolium : 3-hydroxybenzoate, benzimidazolium : 4-hydroxybenzoate 2:1, benzimidazolium: 3-hydroxybenzoate 2:1 Form I, benzimidazolium : 3-hydroxybenzoate 2:1 Form II, imidazolium : malonate, benzimidazole : terephthalate, benzimidazole : succinate and imidazolium : succinate.

LIST OF TABLES

Table 1.1 – Extract from Jeffrey “An Introduction to Hydrogen Bonding” Table 2.1, Properties of strong, moderate and weak hydrogen bonds. Relabeled in terms of the D–H...A nomenclature for donor-acceptor H bonds used in the present work.

Table 1.2 – pKa values of selected acids that are used during this research, with the name of the conjugate base. *Picolinic acid has two values as can take two forms, a neutral and a zwitterionic. This results in two pKa values for this molecule.

Table 2.1 – The seven crystal systems with the restrictions on unit cell parameters and corresponding Bravais lattice type, P primitive, C centred, I body centred, F face centred and R rhombohedral.

Table 2.3 – Typical variable count time scan set-up for SDPD.

Table 4.1 – Summary of the molecular complexes successfully generated (blue) between benzimidazole and mono-substituted hydroxybenzoic acids. Grey indicates where no molecular complex has been identified from single crystal X-ray diffraction.

Table 4.2 – Summary of the results from the co-crystallisation experiments between benzimidazole and a selection of dihydroxybenzoic acids. Blue indicates where a new molecular complex has been found from single crystal X-ray diffraction data, grey indicates where there has been none.

Table 4.3 – The three scalar quantities and bond angle of the hydrogen bonds of $N^{\delta+}-H\cdots O^{\delta-}$ and $O-H\cdots O^{\delta-}$ found in the molecular complexes presented in Section 4.5.

Table 4.4 – Crystallographic data for all the molecular complexes within chapter 4 excluding benzimidazolium and aspartate.

Table 4.5 – The inter- and intramolecular interactions with distances found in the $BZNH^+$ and $2-HBA^-$ molecular complex.

Table 4.6 – The inter- and intramolecular interactions with distances found in the $BZNH^+$ and $2-HBA^-$ molecular complex.

Table 4.7 – Bond length and bond angle data for the four different benzimidazolium molecules from the benzimidazolium 4-hydroxybenzoate molecular complex.

Table 4.8 – Bond lengths and degree of twisting of the carboxylate group from the plane of the phenyl ring, for the 4-hydroxybenzoate molecules in the benzimidazolium 4-hydroxy

Table 4.9 – The inter- and intramolecular interactions with distances found in the $BZNH^+$ 4- HBA^- molecular complex

Table 4.10 – Bond length and bond angle data for the two different benzimidazolium molecules from the benzimidazolium 3-hydroxybenzoate molecular complex.

Table 4.11 – The inter- and intramolecular interactions with distances found in the $BZNH^+$ 3 HBA^- 2:1 molecular complex.

Table 4.12 – Bond length and bond angle data for the $BZNH^+$ and BZN molecules involved in the BZN $BZNH^+$ 4- HBA^- hydrate molecular complex

Table 4.13 – The inter- and intramolecular interactions with distances found in the $BZNH^+$ 3 HBA^- 2:1 molecular complex.

Table 4.14 – The inter- and intramolecular interactions found within the $BZNH^+$ 2- HBA^- 2- HBA^- molecular complex

Table 4.15 – Internal hydrogen bond and C-O bond lengths for the 2- HBA^- ($BZNH^+$ 2- HBA^- and 2- HBA^- molecular complex), 2- HBA^- (native crystal structure, 2- HBA^- ($BZNH^+$ 2- HBA^- and 2- HBA^- molecular complex) and 2- HBA^- ($BZNH^+$ 2- HBA^- molecular complex).

Table 4.16 – The inter- and intramolecular interactions seen in the $BZNH^+$ (3,5-DIHB $^-$ molecular complex).

Table 4.17 – Results from solvent-free and solvent evaporation co-crystallisations involving benzimidazole with a range of co-molecules. SM represents starting materials while NP represents new product. Only co-crystallisation experiments with aspartic acid and 5-chlorosalicylic acid produced new molecular complexes.

Table. 4.18 – Visual Summary of the products obtained from varying the crystallisation conditions, Form I (blue), Form II (red), Form III (yellow)

Table 4.19 – All the interactions that are present in the $\text{BZNH}^+ 5\text{-Cl-2-HBA}^-$ molecular complex

Table. 4.20 – The interactions that are found within the benzimidazolium aspartate molecular complex

Table 4.21 – A comparison of the bond lengths found in the aspartate molecule in its molecular complex with benzimidazolium and those of the parent aspartic acid.

Table 5.1 – Summary of the successful (blue) and unsuccessful (grey) co-crystallisation experiments between benzimidazole and the various halobenzoic acids.

Table 5.2 – Summary of the systems where molecular complex polymorphism was confirmed by single crystal data (blue), polymorphism identified using powder data (green), no polymorphism occurred (yellow) and no molecular complex generated (grey).

Table 5.3 – A summary of the molecular complexes that have generated isomorphous structures (blue and yellow), with grey indicating no isomorphism.

Table 5.4 – The $\text{N}^{\delta+}\text{-C-N}^{\delta+}$ bond lengths and $\text{C-N}^{\delta+}\text{-C}$ bond angles for the molecular complexes discussed in Chapter 5. *Note that BZN 3-BrBa has, on average, partial ionic species of the co-molecules

Table. 5.5 – The hydrogen bond scalar quantities, donor – acceptor ($\text{D}\cdots\text{A}$), donor – hydrogen (D-H) and hydrogen – acceptor ($\text{H}\cdots\text{A}$) distances, and hydrogen bond angle ($\text{D-H}\cdots\text{A}$) for the molecular complexes discussed in Chapter 5. *Note that BZN 3-BrBa has, on average, partial ionic species of the co-molecules

Table. 5.6 – Crystallographic data for the molecular complexes discussed in Chapter 5. *Note that BZN 3-BrBa has, on average, partial ionic species of the co-molecules

Table 5.7 – The results of co-crystallisation experiments on the benzimidazole and 3-chlorobenzoic acid system in creating Form I (blue), Form II (yellow), Form III (red).

Table. 5.8 – The intermolecular interactions involved in the BZN : 3-CIBA Form I molecular complex

Table. 5.9 – The interactions that are present within the BZN : 3-CIBA Form I molecular complex

Table 5.10 – The results from the co-crystallisation experiments between benzimidazole and 4-chlorobenzoic acid with Form I (high temperature phase) shaded in blue and Form II (low temperature phase) shaded in red.

Table. 5.11 - The carbon – oxygen bond lengths within the two 4-CIBA^- molecules. re phase) in red.

Table. 5.12 – The inter- and intramolecular interactions found within the $\text{BZNH}^+ 4\text{-CIBA}^-$ molecular complex

Table 5.13 – The results from the co-crystallisation experiments between benzimidazole and 4-bromobenzoic acid with Form I (high temperature phase) shaded in blue and Form II (low temperature phase) in red.

Table 5.14 – LHS, The interactions that are involved in the molecular complex of BZN and 2-FBA, RHS, bond lengths and degree of twisting of the carboxylate group data for the 2-FBA and 2-FBA^- molecules.

Table 5.15 – The interactions found in the BZN and 4-FBA molecular complex.

Table 6.1 – Summary of the molecular complexes successfully generated (blue) between benzimidazole and imidazole with picolinic acid and its mono-substituted hydroxyl derivatives. A diverse range of products was generated including a hemihydrate and solvate.

Table 6.2 – Summary of the molecular complexes successfully generated (blue) between benzimidazole and picolinic, nicotinic and isonicotinic acids. Apart from the new molecular complex (benzimidazole : picolinic acid hydrate) only single crystals of a new hydrate of nicotinic acid was formed.

Table 6.3 – Summary of the molecular complexes found in the CSD. Blue shading corresponds to molecular complex found while grey represents no molecular complexes found.

Table 6.4 – The $N^{\delta+}$ -C- $N^{\delta+}$ bond lengths and C- $N^{\delta+}$ -C bond angles for the molecular complexes discussed in Section 6.5.

Table 6.5 - Crystallographic data for the molecular complexes discussed in Chapter 6.

Table 6.6 – The interactions involved in the $BZNH^+$ 3- HPA^- molecular complex with full data for the hydrogen bonds.

Table 6.7 – The three scalar quantities and bond angles of the hydrogen bonds and information of the interactions found in the $IMDH^+$ 3- HPA^- molecular complex

Table 6.8 – The three scalar quantities and bond angles of the hydrogen bonds with labels and information of the interactions found in the $BZNH^+$ 6- HPA^- molecular complex

Table 6.9 – The carbon-oxygen bond distances for six different molecular complexes. The numbering of the oxygen refers to Figure 6.31, with oxygens 2 and 3 always being on the same of the molecule.

Table 6.10 – The three scalar quantities and bond angles of the hydrogen bonds a, b, c, d and list of the interactions between the molecules in the benzimidazole and 6-hydroxypicolinic acid diacetic acid solvate.

Table 6.11 – Summary of the molecular complexes found on the CSD. Blue shading corresponds to molecular complexes being present, while grey represents no molecular complexes found.

Table 6.12. – List of molecular complexes where BZN = benzimidazole, IMD = imidazole, NBA = nitrobenzoic acid, HPA = hydroxypicolinic acid, HBA = hydroxybenzoic acid BrBA= bromobenzoic acid and ClBA = chlorobenzoic acid. The bond lengths C–O1, C–O2 represent the lengths in the carboxylate group and N1–C, N2–C the bond lengths between the nitrogen and central carbon in BZN and IMD. HB1 and HB2 represent the N–H···O hydrogen bond lengths between the nitrogens on the BZN or IMD and the carboxylate group.

Table 7.1. – Summary of the molecular complexes generated between cocrystallisation experiments between BZN and IMD and the mono-substituted benzoic acid series. In the Source column of the table, “New” represents complexes previously undiscovered until this research and “CSD” means the complex already been structurally determined and deposited in the CSD.

Table 7.2 – Summary of the molecular complexes that exist between IMD and BZN with aromatic dicarboxylic acids. In the Source column of the table, “New” represents molecular complexes generated for the first time during this research, “CSD” accounts for those that have already been solved while “RD” stands for re-determined, i.e. cases where a new X-ray diffraction experiment was attempted to get a improved data set than that available in the literature.

Table 7.3 – Summary of the successful cocrystallisations between IMD and mono-substituted halo-benzoic acid series with the corresponding BZN molecular complex.

Table 7.4 – Summary of the successful cocrystallisation experiments between IMD and BZN with dicarboxylic acids. In the Source column of the table, “New” represents molecular complexes generated for the first time during this research, “CSD” accounts for those that have already been solved. “RD” represents the

benzimidazole : malonic acid molecular complex structure which has been greatly improved in this work from that reported in the CSD.

Table 7.5 – Crystallographic data for the molecular complexes containing imidazolium.

Table 7.6 – Crystallographic data for the molecular complexes containing benzimidazolium. PHth represents phthalic acid i.e. TerePHth is terephthalic acid.

Table 7.7 – The three scalar quantities and bond angles of the hydrogen bonds of $N^{\delta+}-H\cdots O^{\delta-}$ and $O-H\cdots O^{\delta-}$ found in the molecular complexes presented in Chapter 7.

Table 7.8 – The three scalar quantities and bond angles of the hydrogen bonds and list of the interactions between the molecules in the $IMDH^+ 2-HBA^-$ molecular complex..

Table 7.9 – The three scalar quantities and bond angles of the hydrogen bonds and list of the interactions between the molecules in the $IMDH^+ 3-HBA^-$ molecular complex..

Table 7.10 – The three scalar quantities and bond angles of the hydrogen bonds and list of the interactions between the molecules in the $IMDH^+ 4-HBA^-$ molecular complex.

Table 7.11 – The three scalar quantities and bond angle of the hydrogen bonds of $N^{\delta+}-H\cdots O^{\delta-}$ found in the molecular complexes presented in section 7.5.

Table 7.12 - The three scalar quantities and bond angles of the hydrogen bonds and list of the interactions between the molecules in the $IMDH^+ 4-FBA^-$ molecular complex.

Table 7.13 - The three scalar quantities and bond angles of the hydrogen bonds and list of the interactions between the molecules in the $IMDH^+ 4-BrBA^-$ molecular complex.

Table 7.14 – The carbon –oxygen bond lengths of benzoic acid (BA)³² and the four benzoic acid molecules from the $BZNH^+ :BA^- : BA$ molecular complex.

Table 7.15 – The hydrogen bond data for all the moderate hydrogen bonds in the $BZNH^+ :BA^- : BA$ molecular complex.

Table 7.16 - The three scalar quantities and bond angles of the hydrogen bonds and list of the interactions between the molecules in the benzimidazolium phthalate molecular complex.

Table 7.17 – Basic crystal data for the benzimidazole : isophthalic acid molecular complex and the imidazolium isophthalate molecular complex.

Table 7.18 – The hydrogen bond data for the hydrogen bonds in the benzimidazolium terephthalate molecular complex.

Table 7.19 – Basic crystallographic data of the imidazolium terephthalate molecular complex.

Table 7.20 – The carbon oxygen bond lengths in the benzimidazolium fumarate and imidazolium fumarate molecular complex.

Table 7.21 – A list of the hydrogen bonds and interactions in the benzimidazolium fumarate molecular complex.

Table 7.22 – The carbon oxygen bond lengths in the benzimidazolium succinate and imidazolium succinate molecular complexes.

Table 7.23 – The hydrogen bond data for the hydrogen bonds in the benzimidazolium succinate molecular complex.

Table 7.24 – The hydrogen bond data for the hydrogen bonds in the benzimidazolium succinate molecular complex.

Table 7.25 – A comparison of the bond lengths found in the maleate ion in its molecular complex with benzimidazolium and those of the neutral maleic acid molecule.

Table 7.26 – Some basic crystal data for the benzimidazolium maleate molecular complex and the imidazolium maleate molecular complex.

Table 7.27 – A comparison of the bond lengths found in the malonate ions in their molecular complexes with benzimidazolium, imidazolium, imidazolium hydrate and in its native form.

Table 7.28 – The hydrogen bond geometry data and interaction details for the benzimidazolium malonate and imidazolium malonate molecular complexes.

LIST OF ABBREVIATIONS

BZN - Benzimidazole

BZNH⁺ - Benzimidazolium

IMD – Imidazole

IMDH⁺ - Imidazolium

BA – Benzoic acid

BA⁻ - Benzoate

1 Introduction

This work has concentrated on designing and creating new crystalline structures using crystal engineering principles. To achieve the new crystalline materials, be they in the form of molecular complexes, co-crystals, salts or solvates, required the use of co-crystallisation techniques while the realisation of the structures were achieved mainly through X-ray diffraction. This introduction shall discuss the basis of the project; examine the naming of the crystalline structures, introduce hydrogen bonding and other weaker intermolecular interactions, explain the use of crystal engineering and summarise some previous research into polymorphism.

1.1.1 Molecular Complexes, Salts, Co-Crystals?

Firstly, what is a co-crystal, how is it different from a molecular complex and where should the term co-crystal be used properly describe a material? These questions have come to light in recent years with its ever increasing use and its widening meaning. Authors Desiraju¹ and Dunitz² gave their respective opinions, Desiraju taking the view that a co-crystal must denote a crystal stuck together with another crystal. This implies that the term co-crystal should refer to some “multiple crystal” in which each component retains some of its individual crystal identity. In this view, two (or more) molecules co-crystallised together to form a new complex with completely new crystal identity should more correctly be called a molecular complex. Dunitz² on the other hand argued that the popularity of the term co-crystal has its reasons, “*as it provides an inelegant definition of what it is intended to describe, a crystal containing two or more components together*”. Therefore this definition would encompass a range of terms including molecular complexes, solvates and multi-component crystals. Dunitz ends by suggesting that is it so popular that it will be hard to displace, so the pragmatic approach is to stick with it. In spite of these differing views, the two authors agree on one thing, that there should always be a hyphen! There have been others who have included a definition explicitly when using the term co-crystal, for example Aakeroy³ in 2005 used the condition, “*made from reactants that are solids at ambient conditions*”, which was seized upon and used to define a pharmaceutical co-crystal in a review paper in 2006 by Zaworotko⁴, “*formed between a molecular or ionic API and a co-crystal former that is solid under ambient conditions*”. Later

Bond⁵ argues that the solid state condition should be dropped and that the term co-crystal should be seen as a synonym for *multi-component molecular crystal*. This would include all the materials suggested by Desiraju, Dunitz, Aakeroy and and Zaworotko; molecular complexes, solvates, clathrates, inclusion compounds and solid solutions, however still leaving one grey area – cases where there is not full understanding of the nature of the chemical bonding in the material. In this work, the term molecular complexes will be used to describe the vast majority of the new materials formed, including cases where there are charged species that would normally be termed a salt.

Co-crystallisation is the combination of two or more molecular components to form a new heteromeric crystalline structure where intermolecular forces, particularly hydrogen bonds, hold the constituents together. Achieving this goal depends on an understanding of the relationships between the structures of the materials involved. However the understanding of the relationships involved is still in its infancy, with the provocative quote from Maddox⁶ in 1988 still of some relevance today: “*One of the continuing scandals in the physical sciences is that it remains in general impossible to predict the structures of even the simplest crystalline solids from a knowledge of their chemical composition*”.

1.1.2 Co-crystallisation

Synthesis of molecular complexes using co-crystallisation experiments usually involves the evaporation of solvent from a solution containing the co-crystal components in a chosen stoichiometric ratio. However the method of synthesis can vary greatly depending on a range of factors from the physical form of the starting materials to the desired product outcome. The methods used during this work are discussed in Section 3.1.1, which concentrates on the solvent evaporation technique, however there are many different approaches including sublimation⁷, growth from the melt⁸, slurries⁹ and supercritical fluids¹⁰.

1.2 Pharmaceutical Co-Crystals and Other Applications

Co-crystals as a valuable material type have also become an area of emerging importance within the pharmaceutical sector, with a diverse and relevant research field in the formation of

co-crystals with an active pharmaceutical ingredient¹¹ (API). So-called pharmaceutical co-crystals, “*co-crystals that are formed between a molecular or ionic API and a co-crystal former that are solid under ambient conditions*”⁴, represent a subset of multiple component crystals that includes salts solvates, clathrates, inclusion crystals and hydrates. Crystalline APIs are preferred due to their relative ease of isolation, the rejection of impurities during the crystallisation process and the inherent stability of crystalline solids; however they also have poorer solubility and often form polymorphs, solvates and hydrates. It is thought that the use of co-crystallisation experiments will offer the ability to modify the chemical and physical properties of the API, such as solubility, stability, dissolution rate and bioavailability, without the need to make or break covalent bonds, which helps to retain their biological activity¹². This method has great potential due to the tendency of APIs to have external hydrogen bonding sites, at times numerous, available to form intermolecular interactions. These external hydrogen bonding sites can be exploited to produce new forms. Using crystal engineering principles, there is now the ability to rationally design and construct new structures and pharmaceutical co-crystals that have improved medicinal, chemical and physical properties¹³. For example, Tan¹⁴ successfully co-crystallised ethebamide (nonsteroidal anti-inflammatory drug) and gentisic acid (nonsteroidal anti-inflammatory and anti ageing properties) together to create pharmaceutical co-crystals containing two APIs. Zaworotko¹⁵ has also generated a pharmaceutical co-crystal containing two APIs, piracetam (nootropic drug) and gentisic acid (Figure 1.1 LHS), which are both polymorphic in their natural states but found to be non-polymorphic as a co-crystal. There have been numerous examples of co-crystallisations of single APIs with co-molecules utilising robust and predictable hydrogen bonds, for example the robust pyridine-carboxylic acid heterosynthon was exploited to generate pharmaceutical co-crystals of 4,4'-bipyridine and 4,4'-dipyridylethene with aspirin, ibuprofen and flurbiprofen¹⁶ (Figure 1.1 RHS) and isonicotinamide with nicotinamide (Vitamin B), clofibrate (antihyperlipidemic drug) and diclofenac (nonsteroidal anti-inflammatory)¹⁷.

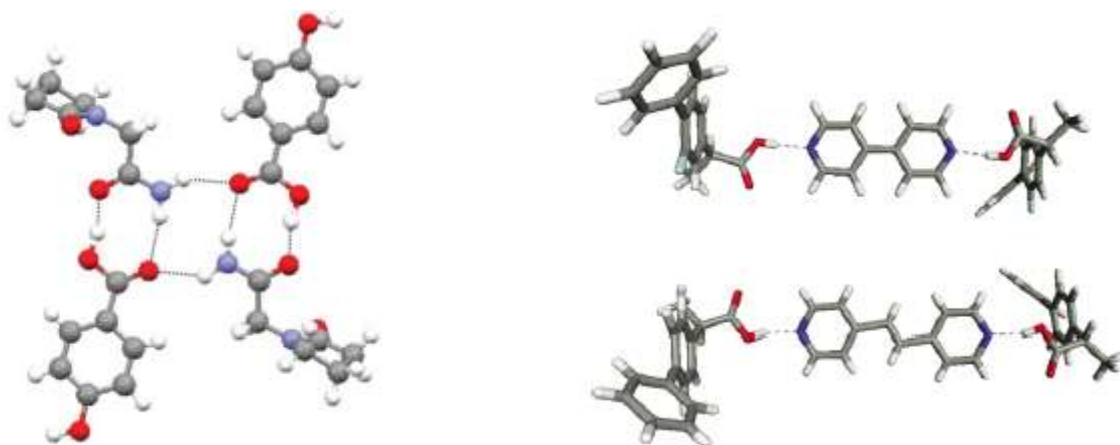


Fig. 1.1 – LHS, a pharmaceutical co-crystal containing two APIs, piracetam and gentisic acid, RHS, the pharmaceutical co-crystals of 4,4'-bipyridine and 4,4'-dipyridylethene with flurbiprofen.

Co-crystallisation also provides the opportunity to isolate or purify single component APIs during processing, with the added benefit that the co-molecule may be able to be discarded before formulation. Wales¹⁸ used multi-component crystallisation routes to form the single component of the elusive paracetamol form II, using a range of carboxylic acids and solvents. It was found to have an improved yield (100%) to those obtained with other preparation routes, with greater stability of the pure single component product.

Co-crystallisation reactions have also been used in the synthesis of organic compounds using solvent free conditions¹⁹ (see Section 1.5), which has been the subject of much recent research activity. Molecular complexes have been used in the photographic industry to create non-covalently bonded derivatives of hydroquinone which are used as the chemical that makes the latent image on the film or print visible. This method of synthesis is seen as much more environmentally friendly than traditional techniques^{20, 21}. Using organic small molecules capable of binding and activating substrates through non-covalent interactions has emerged as an important approach in organo-catalysis. This is seen as a less rigid approach than using traditional covalently bonded catalysis mechanisms and has many advantages, but also challenges²². The thiourea organo-catalyst is used to accelerate and stereochemically alter organic transformations through double hydrogen bonding interactions, for example in Stecker²³ reactions (Figure 1.2)²⁴. Co-crystals have also been used to generate compounds that have second harmonic generation properties, these non-linear optical (NLO) materials are able to combine photons effectively to generate new photons with double the energy. A number of phenol–pyridine co-crystals have been found to exhibit such properties by Byrn and co-workers²⁵.



Fig. 1.2 – Crystal structure of the thiourea catalyst used in Stecker reactions.

All the applications of co-crystallisation exploit non-covalent interactions, mainly hydrogen bonds that can form between molecules. It is this exploitation of intermolecular interactions that has been very widely researched and comes under the term crystal engineering. Even though it was first coined in 1971 by Schmidt²⁶, it was Desiraju²⁷ in 1989 that defined the term in a structural chemistry context and made popular; *“the understanding of intermolecular interactions in the context of crystal packing and the utilization of such understanding in the design of new solids with desired physical and chemical properties”*.

1.3 Hydrogen Bonding and other Intermolecular Interactions

The hydrogen bond has such a ubiquitous influence in gaseous, liquid and solid-state chemistry that its consequences were discovered well before the interaction was identified and given a name; late 19th and 20th century literature shows many references to many observations which are now known as the effects of hydrogen bonding. In 1931 Pauling wrote a general paper on the nature of the chemical bond where he discussed the $[\text{H}:\text{F}:\text{H}]^-$ ion, using the term hydrogen bond possibly for the first time. Later in 1935 he followed up these remarks with a paper on hydrogen bonds in water and ice before releasing his famous book *Nature of the Chemical Bond*²⁸ where these two statements originate; *“Under certain conditions an atom of hydrogen is attracted by rather strong forces to two atoms instead of only one, so that it may be considered to be acting as a bond between them. This is called a “hydrogen bond” ”* and *“A hydrogen atom with only one stable orbital cannot form more than one pure covalent bond and the attraction of the two atoms observed in hydrogen bond formation must be due largely to ionic forces”*.

Hydrogen bonds in the gas phase can be regarded as relatively simple interactions; however, this is not the case in the solid state. There is extensive literature, summarized by Jeffrey (1997)²⁹, using a wide range of diffraction and spectroscopic methods, indicating that the hydrogen bond in crystalline systems is a highly varied and complex interaction. It is clear that the architecture of hydrogen bonding in the solid state can be controlled by the choice of systems and substituents forming the basis, for example, of the rapidly growing field of crystal engineering and supramolecular assembly.

A hydrogen bond can be described by a donor atom, D, covalently bonded to a hydrogen atom, and an acceptor atom, A. Hydrogen bonds are formed when the electronegativity of D relative to H in a D–H covalent bond is such as to withdraw electrons and leave the proton partially unshielded. To interact with this donor D–H bond, the acceptor A must have a lone-pair or polarisable π electrons. In 2011 the IUPAC (International Union of Pure and Applied Chemistry) commissioned a task group to come up with a modern definition for the hydrogen bond. The task group was chaired by Aruan and proposed an initial recommendation for the definition of the hydrogen bond as “*The hydrogen bond is an attractive interaction between a hydrogen atom from a molecule or a molecular fragment X–H in which X is more electronegative than H, and an atom or a group of atoms in the same or a different molecule, in which there is evidence of bond formation*”³⁰. The review, seeking comments on the new definition, closed on the 31st March 2011 with the final recommendation anticipated shortly.

This simple definition does not tell the whole story, as strong hydrogen bonds are similar to covalent bonds and weak hydrogen bonds are closer to van der Waals forces in strength, with the majority of hydrogen bonds being somewhere in the middle of this range. Jeffery categorises hydrogen bonds into strong, moderate and weak in strength by use of the bond lengths, bond angles and energy associated with the hydrogen bond (Table 1.1)²⁹. These categories, are however not rigid and there may be some overlap and exceptions present.

	Strong	Moderate	Weak
D–H...A interaction	mostly covalent	mostly electrostatic	electrostatic
Bond lengths			
H...A (Å)	~1.2-1.5	~1.5-2.2	2.2-3.2
D...A (Å)	2.2-2.5	2.5-3.2	3.2-4.0
Bond angles (°)	175-180	130-180	90-150
Bond energy (kcal mol⁻¹)	14-40	4-15	<4

Table 1.1 – Extract from Jeffrey “An Introduction to Hydrogen Bonding” Table 2.1, Properties of strong, moderate and weak hydrogen bonds. Relabeled in terms of the D–H...A nomenclature for donor-acceptor H bonds used in the present work.

Even though it can be seen that hydrogen bonds are weaker than the traditional chemical bonds of metallic, ionic and covalent types, the hydrogen bond is extremely important in a wide range of materials. The presence of hydrogen bonds in materials can have a dramatic effect on their chemical and physical properties. Higher boiling and melting points in materials like water and ammonia compared to analogues such as hydrochloric acid, and the high water solubility of ammonia, are effects that are due to the hydrogen bond. Other properties affected by hydrogen bonding can be the crystal structure, viscosity, molar volume, reactivity and colour, among many others.

Hydrogen bonds play a key role in biological systems, the three-dimensional structures in proteins and nucleic acids are formed through hydrogen bonds. In these macromolecules, bonding between parts of the same macromolecule cause it to fold into a specific shape, which helps determine the molecule's physiological or biochemical role. An example is the double helical structure of DNA, which is largely held together by hydrogen bonds between base pairs that link one complementary strand to the other and enables replication.

1.3.1 Strong Hydrogen Bonds

The strong hydrogen bond can have an associated energy in excess of 40 kcal mol⁻¹ which can be of the same order as some covalent bonds and are sometimes referred to as ionic hydrogen bonds, positive- or negative-ion hydrogen bonds and low-barrier hydrogen bonds. They are formed when the proton is shared by two strong bases such as in the [F—H—F]⁻ ion (Figure 1.3)³¹ or in molecules where there is a deficiency of electron density on the donor

group or an excess of electron density on the acceptor group. This is to be expected by considering the definition, as a deficiency of electrons on the donor group will further deshield the proton, while an excess of electrons on the acceptor group increases its negative charge and thus its interaction with the proton. The proton in such strong hydrogen bonds will often sit close to the mid-point of the hydrogen bond and have a low energy barrier double well potential or a single minimum flat potential, which results in the hydrogen atom position being sensitive to external conditions such as variation of temperature and pressure or the local crystal environment³². Strong hydrogen bonds can also occur when the acceptor and donor atoms are forced by molecular configurations into much closer contact than the sum of their van der Waals radii, for example in the formation of a short intramolecular hydrogen bond in the potassium hydrogen maleate structure³³ (Figure 1.3).

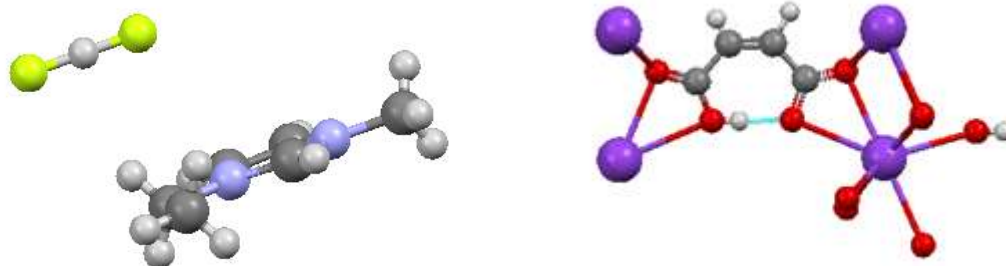


Fig. 1.3 – LHS, the 1-ethyl-3-methylimidazolium hydrogen difluoride structure with the strong hydrogen bond between the fluoride ions, RHS the *catena*-(hydrogen maleate)-potassium) structure with a strong intramolecular hydrogen bond.

1.3.2 Moderate Hydrogen Bonds

The moderate hydrogen bond, more commonly known as the normal hydrogen bond due to its extensive occurrence in nature, is formed between a neutral donor, D, and neutral atoms containing at least one lone-pair of electrons. Moderate hydrogen bonds also occur in some charged molecules. Nature extensively uses hydrogen bonds involving nitrogen and oxygen in small molecules to determine the packing and in macromolecules to influence conformation.

The hydrogen bond is very flexible and in the moderate hydrogen bond the D-H \cdots A angle can range from 130° to 180° and the D \cdots A length from 2.5Å to 3.2Å. This results in a wider variety of hydrogen bonds compared to the more rigid strong hydrogen bond, with a much wider variety of hydrogen bond donors and acceptors that can be involved. There are many

examples of intermolecular moderate hydrogen bonds between the different classes of small molecule, including carboxylic acids, amino acids, carbohydrates, purines and pyrimidines (Figure 1.4). As with strong hydrogen bonds, moderate intramolecular hydrogen bonds can also form. This was recognised by Sidgwick³⁴ (1924) as being the reason for the differences in *ortho*-, *meta*- and *para*- hydroxy and amino benzene derivatives. Moderate hydrogen bonds can also form with transition metals, these can be terminal or bridging.

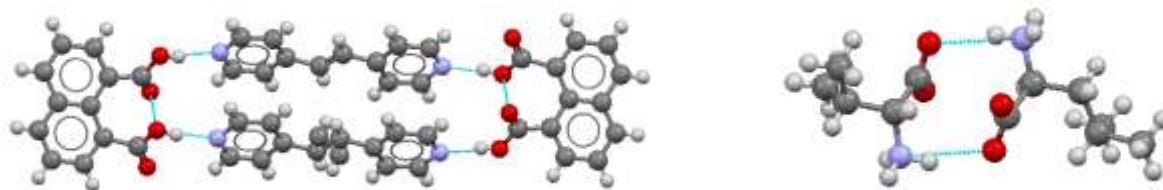


Fig. 1.4 – LHS, an example of carboxylic acid and pyridyl containing molecules, 1,8-naphthalenedicarboxylic acid trans-1,2-bis(4-pyridyl)ethylene, RHS, an example of an amino acid containing complex; L-leucine : D-valine.

1.3.3 Weak Hydrogen Bonds

There are many different varieties of interactions that come under the weak hydrogen bond classification. The most relevant to the solid state and the most controversial are hydrogen bonds involving the C–H group. These occur when the C–H group is involved in multiple bonds or attached to electron withdrawing groups. They are controversial since it is still unclear how significant they are in determining molecular configuration or packing in molecular complexes.

1.3.4 Bifurcated Hydrogen Bonds

The flexibility found in moderate and weak hydrogen bonds can support the generation of hydrogen bonds involving two acceptor sites (Figure 1.5 LHS). These are referred to as three-centred hydrogen bonds as the hydrogen is bonded to three atoms³⁵. They are more commonly known as bifurcated hydrogen bonds and are quite common with around a quarter of normal hydrogen bonds from carbohydrate and nucleic acid structures being three-centered²⁹. Bifurcated hydrogen bonds can arise when there is a proton deficiency, i.e. greater acceptor functionality than the number of hydrogen bonds available. They can range from symmetrical,

$R_1 \approx R_2$, $\alpha_1 \approx \alpha_2$ to asymmetrical, $R_1 > R_2$, $\alpha_1 > \alpha_2$ (Figure 1.5 RHS) with the latter much more common. As in single hydrogen bonds, the bifurcated hydrogen bond has geometric constraints. The three individual bonds/interactions that make up the bifurcated hydrogen bond are all attractive forces and cause the hydrogen involved to lie close to the plane made up of the donor and two acceptor atoms. An indication of this is that the closer the sum of the angles α_1 , α_2 and α_3 is to 360° , the more planar the bifurcated hydrogen bond³⁶.

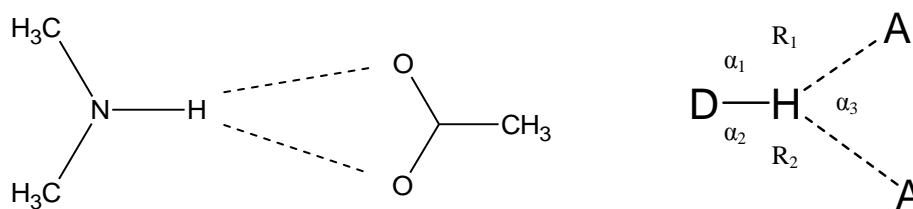


Fig. 1.5 – LHS, example of a hydrogen bond containing two acceptors, RHS, extract from Jeffrey “An Introduction to Hydrogen Bonding”, a three-centered hydrogen bond with labeling of the scalar quantities; hydrogen - acceptor distance (R_1 and R_2), hydrogen bond angle (α_1 and α_2) and angle between the hydrogen bonds (α_3).

With asymmetrical bifurcated hydrogen bonds there will be a major and minor component, with the major component being the stronger hydrogen bond. This can have properties comparable to moderate hydrogen bonds while the minor component is often more comparable to a weak hydrogen bond. In symmetrical bifurcated hydrogen bonds the two components are relatively even, with similar hydrogen bond lengths and angles. There are even examples of four-centred hydrogen bonds, with three acceptor groups, these are however extremely rare due to geometric constraints as by definition all hydrogen bonds must have a D-H \cdots A angle of greater than 90° .

1.3.5 Hydrogen Bond Disorder

Disorder in hydrogen bonds occurs when the donor and acceptor groups wholly or partially switch their functions. This can be a static effect (configurational), with split occupancy of the hydrogen atom position, or a more dynamic effect (conformational), with the proton moving position, occurring as a result of varying the temperature or pressure. Conformational disorder can occur in two situations; in strong single minimum hydrogen bonds, the hydrogen can migrate across the hydrogen bond from the donor to acceptor as the temperature is varied (e.g. in urea phosphoric acid³⁷); or when there is orientational freedom of the D-H bond and

the protons can switch bonds by means of rotation about a single covalent bond (Figure 1.6) (e.g. in cyclodextrin hydrate³⁸).

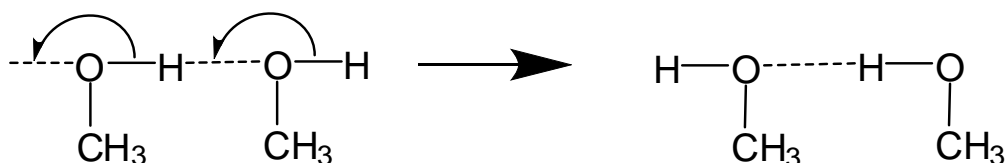


Fig. 1.6 – An example of conformational disorder in a hydrogen bonded system.

Where there are two crystallographically distinct positions in which the hydrogen can sit resulting from a double minimum potential well characteristic of moderate hydrogen bonds, and where the occupancies are not related by symmetry (e.g. 50:50 disorder across an inversion centre), the occupation of the secondary site can often be found to increase as the temperature is increased. Common examples would be enol – keto and amino – imino transformations (Figure 1.7) which do not occur in crystals but when still in solution.

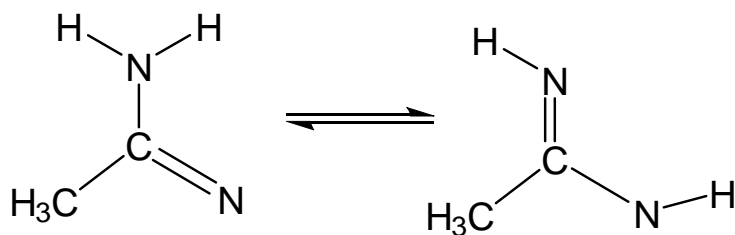


Fig. 1.7 – A reaction diagram showing amino - imino transformation (tautomerism).

1.3.6 Proton Transfer

Proton transfer is the basis of acid-base chemistry. When a hydrogen ion moves from one chemical to another, an acid-base reaction has taken place. Hydrogen bonding can promote proton transfer and in some cases restrict it; this phenomenon is considered by many as the most important property of the hydrogen bond. The ability to transmit protons and OH^- ions in water provides a catalytic mechanism for many water based reactions³⁹ and is becoming increasingly recognised as important in enzyme catalysis reactions and for transmitting ions through membranes. Proton transfer can result in hydrogen bonds between the charged species that are much stronger than the non-charged species. Charge assisted hydrogen bonds can be as much as 0.4\AA shorter than the corresponding neutral hydrogen bond and are

commonly used by crystal engineers to generate new structures of small molecules⁴⁰ and organometallics⁴¹.

When conducting co-crystallisation experiments, understanding if and when a proton will transfer is critical to understanding if a salt or co-crystal will form. It is generally accepted that a reaction of an acid with a base will be expected to form a salt if the ΔpK_a ($\Delta pK_a = pK_a(\text{base}) - pK_a(\text{acid})$) is greater than $\sim 2-3$ ⁴². A smaller ΔpK_a (less than 0) will result in co-crystal formation, therefore when the ΔpK_a is between 0 and 3 accurately predicting salt or complex formation is inconclusive and is a keen area of research⁴³. It is also not always possible to determine if a solid is a salt or co-crystal because either the proton is shared or the structure contains disordered ionized and non-ionized states. There are further limitations to the ΔpK_a rule apart from the grey area between ΔpK_a values of 0 to 3, where salt, cocrystal, shared protons or mixed ionisation states can form. The $\Delta pK_a^{50\%}$ point, where there is an equal amount of the conjugate acid to conjugate base in solution, is temperature dependent⁴⁴ which along with using non dimeric stoichiometric ratios⁴⁵ (not 1:1) has been found to produce results not in keeping with the empirical ΔpK_a rule. Table 1.2 shows the pK_a values of selected molecules that have been used during this research, values are taken from CRC handbook of Chemistry and Physics⁴⁶.

It has been found by Aakeroy⁴⁷ that proton transfer between molecules vastly decreases the probability of generating a targeted supramolecular synthon. 45% of molecular complexes generated between carboxylic acids and n-heterocycles when proton transfer has occurred resulted in unpredictable chemical or stoichiometric compositions, this drops to 5% when no proton transfer has occurred.

Acid	pKa	Conjugate Base
Benzimidazolium	5.53	Benzimidazole
Imidazolium	6.99	imidazole
Benzoic acid	4.20	benzoate
2-hydroxybenzoic acid	2.98	2-hydroxybenzoate
3-hydroxybenzoic acid	4.08	3-hydroxybenzoate
4-hydroxybenzoic acid	4.57	4-hydroxybenzoate
2-fluorobenzoic acid	3.27	2-fluorobenzoate
3-fluorobenzoic acid	3.86	3-fluorobenzoate
4-fluorobenzoic acid	4.15	4-fluorobenzoate
2-bromobenzoic acid	2.85	2-bromobenzoate
3-bromobenzoic acid	3.81	3-bromobenzoate
4-bromobenzoic acid	3.96	4-bromobenzoate
2-chlorobenzoic acid	2.90	2-chlorobenzoate
3-chlorobenzoic acid	3.84	3-chlorobenzoate
4-chlorobenzoic acid	4.00	4-chlorobenzoate
Picolinic Acid	0.99/ 5.39*	Picolinate
3-hydroxypicolinic acid	1.14	3-hydroxypicolinate

Table 1.2 – pKa values of selected acids that are used during this research, with the name of the conjugate base.

*Picolinic acid has two values as there are two parts of the molecule that can be deprotonated, the carboxylic acid and pyridine

1.3.7 Halogen Bonds

The halogen bond is an attractive interaction where the halogen atom acts as the electron density acceptor. It was introduced to name any $D \cdots X \cdots Y$ interaction in which X is the halogen (Lewis acid), D is any donor of electrons (Lewis base) and Y can be a carbon, nitrogen, halogen, etc⁴⁸. Halogen bonding is similar to hydrogen bonding in that in both types of bonding, an electron donor/electron acceptor relationship exists. The difference between the two is in what species can act as the electron donor/electron acceptor. In hydrogen bonding, a hydrogen atom acts as the electron acceptor and forms a non-covalent interaction by accepting electron density from an electron rich site (electron donor). In halogen bonding, a halogen atom is the electron acceptor. The utilisation of these bonding interactions stems from their directional preference of their positions relative to each other, of which there are two types: Type I, both $Y-X \cdots X$ angles (θ_1, θ_2) are the same and around $160 \pm 10^\circ$ or Type II, $C-X \cdots X$ angles are roughly perpendicular to each other ($\theta_1 \approx 175^\circ, \theta_2 \approx 80^\circ$).²¹ The significance of this is that the Type I arrangement lends itself to the formation crystal structures that contain inversion centres, two-fold rotation axes and mirror planes, while Type II arrangements are characteristic of two-fold screw axes or glide planes and both monoclinic and orthorhombic

space groups⁴⁹. Due to this, halogen bonding has become increasingly important in the design and engineering of molecular complexes. Nguyen⁵⁰ was the first to use the halogen bond to create targeted liquid crystals by using alkoxystilbazoles and pentafluoroiodobenzene. Meyer⁴⁸ gives a review of halogen bonds in which he describes it as a strong, specific and directional interaction and gives examples where the halogen bond prevails over other interactions including hydrogen bonding⁵¹ and $\pi\cdots\pi$ stacking⁵². Halogen bonding has also been used to separate enantiomers⁵³ and is able to bind selectively small molecules to synthetic⁵⁴ and natural receptors⁵⁵.

1.3.8 π – Interactions

There are various classifications of interactions that involve, in at least one part, the π -electrons. These all tend to be very weak interactions, however are often fundamental in the packing of the dominant structural motif in the structure. One of the common interactions is $\pi\cdots\pi$ stacking, where aromatic rings effectively stack upon one another in either a; centred, off-centred or T-shape assembly (Figure 1.8). π -stacking is instrumental within biological systems, for example in DNA π -stacking where it helps stabilise the double helix conformation and in proteins where it can help fold macromolecules⁵⁶. Cation- π interactions, also known as the Dougherty effect, is a non-covalent molecular interaction between the face of an electron-rich π system (e.g. aromatic ring) with an adjacent cation (e.g. Li^+ , Na^+) (Figure 1.8). The opposite interactions are lone pair- π interactions (also known as anion- π interactions) which involve bonding between a neutral electron-rich molecule and an electron-poor π ring. It is effectively the opposite to cation- π interactions where the charge distribution of the π system has to be reversed⁵⁷.

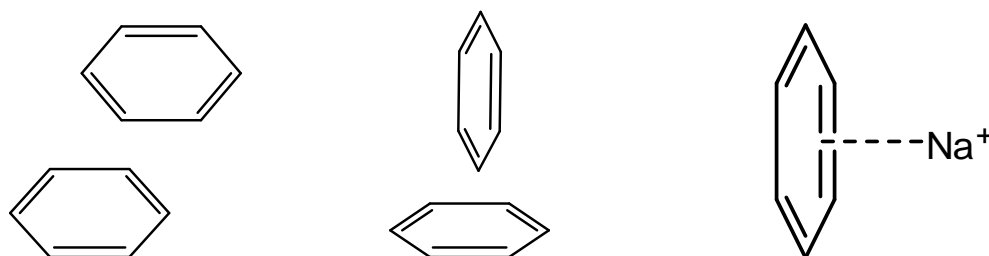


Fig. 1.8 – Schematic of the most prevalent $\pi\cdots\pi$ stacking forms, LHS, off-centred, middle, T-shape, RHS, an example of an cation- π interaction, between benzene and sodium.

1.4 Crystal Engineering

Crystal engineering is seen as the bottom-up construction of functional materials from molecular or ionic building blocks⁵⁸. These building blocks (motifs) are influenced, primarily, by relatively strong interactions which often display considerable consistency and are commonly known as supramolecular synthons. Defined as “*structural units within supermolecules which can be formed and/or assembled by known or conceivable synthetic operations involving intermolecular interactions*”⁵⁹. This area of research has accelerated in recent times after the term crystal engineering was first used by Pepinsky⁶⁰ in 1955. It is seen as a highly interdisciplinary area and attracts interest from many traditional fields including organic, inorganic, and organometallic chemistry, theoretical chemistry, crystallography and crystal growth. The area of crystal engineering is growing as it is seen as an intelligent way to: develop sophisticated devices, understand self-assembly / molecular recognition and understand the fundamental issues of nucleation and crystal growth⁶¹. Crystal engineering uses many strategies in forming supramolecular synthons; most common is using the understanding of hydrogen and coordination bonds, however more recently increasing attention has been applied to the weaker and less predictable halogen bonds⁶² and π - π interactions⁶³. These weaker and less well-defined interactions can have strong effects on the packing of the dominating structural motif, which is one area of real challenge in crystal engineering. There is a real need to improve the understanding of how the balance between the relatively strong and weak interactions influences the outcome of the crystallisation. For example, Polito⁶⁴ investigated the experimental and theoretical structures of molecules with similarly sized substituents, namely 2-methylbenzoic acid, 2-chlorobenzoic acid and a 1:1 co-crystal of these two components. All three structures contained the same primary hydrogen bond interactions creating a ribbon arrangement. However the structures were not isostructural (see Section 1.5.3) as the ribbons are arranged differently within each lattice. This simple example highlights the difficulties extrapolating from the primary hydrogen bond motif to the crystal structure. Predicting and exploiting the primary hydrogen bond, the goal of crystal engineering, was made simpler by a set of rules formalised (not exclusively devised) by Etter in 1990⁶⁵. The general rules, applying to all system, are; all good proton donors and acceptors are used in hydrogen bonding, six-membered-ring intramolecular hydrogen bonds form in preference to intermolecular hydrogen bonds and lastly the best proton donors and acceptors remaining after intramolecular hydrogen bond formation form

intermolecular hydrogen bonds to one another. There are additional rules for specific classes of functional groups. However the use of these rules explain why some of the stronger, more robust supramolecular synthons often contain the functional groups carboxylic acid⁶⁶ hydroxyl⁶⁷, amide⁶⁸ and pyridine⁶⁹ and are often found together or in mixtures creating hydrogen bond patterns that are seen in a vast array of structures. The rules also explain why a survey of the CSD revealed that hydrogen bonded molecular complexes prepared with suitable functional groups preferred to interact heteromerically rather than homomerically, i.e. best hydrogen bond donor: acceptor rule³. The common examples are N-containing heterocycle molecules with carboxylic acids, where in every case a N-H...O hydrogen bond is formed in preference to the starting materials reforming. It is possible to define the main hydrogen bond patterns in terms of 0-D, 1-D, 2-D and 3-D motifs depending on the type of intermolecular interactions that are present within and between the co-molecules. 0-D assemblies can be thought of as discrete aggregates and include: dimers, for example carboxylic acid : carboxylic acid, pyrrole-2-carboxylate : pyrrole-2-carboxylate, pyridine : carboxylic acid (Figure 1.9); trimers, for example bipyridine : carboxylic acid (1:2)⁷⁰; and tetramers, for example isonicotinamide : carboxylic acid (2:2)⁷¹.

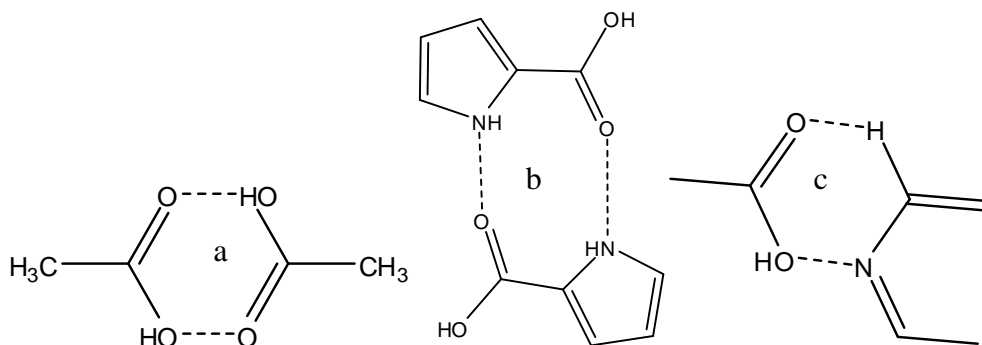


Fig. 1.9 – a, the carboxylic acid dimer, b, a pyrrole-2-carboxylate dimer, and c, a carboxylate hydrogen bonded to part of a pyridine molecule.

Co-crystals that are regarded as 1-D include those that have 1-dimensional motifs, i.e. chains and ribbons. Bipyridine : dihydroxybenzoic acid⁷² is a co-crystal with a 1-D array (Figure 1.10). 2-D assemblies are when the hydrogen bond motif is expanded in two directions, for example in the diaminotriazine : uracil⁷³ and piperazine : carboxylic acid⁷⁴ (Figure 1.10) co-crystals. Finally, the case of 3-D assemblies is when the motif expands the structure in all dimensions, examples include the iodoform : hexamethylenetetramine co-crystal⁷⁵.

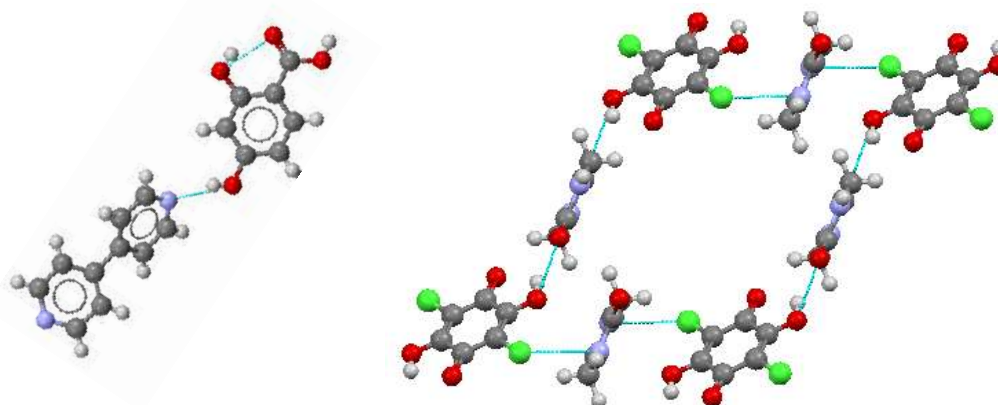


Fig. 1.10 – LHS, the bipyridine dihydroxybenzoic acid co-crystal is an example of a 1-D assembly, RHS, the 2-D assembly from the piperazine : carboxylic acid co-crystal.

Another important way to define structural motifs and patterns uses the idea that some interactions are more important than others. Etter⁷⁶ developed a system based on so-called graph-set notation that allowed structural motifs to be described in a consistent way while recognising the multiply significant interactions. The graph-set approach uses four principal motifs: chains (C), dimers (D), rings (R) and intramolecular hydrogen bonds (S) with numbers to describe: the number of atoms involved, the number of hydrogen bond donors and the number of hydrogen bond acceptors. Thus the robust carboxylic acid dimer has the graph-set notation $R_2^2(8)$, for the eight atoms that make up the ring, with two each of hydrogen bond donors and acceptors. Arguably the greatest expansion of crystal engineering has come recently in the area of metal-organic frameworks (MOF)⁷⁷. MOFs, extended metal-ligand networks with bridging organic ligands, have become an increasingly important area in chemistry with the potential to develop storage devices for hydrogen⁷⁸ and carbon dioxide storage⁷⁹, gas purification⁸⁰, gas separation⁸⁰ and catalysis⁸⁰. While it is the potential applications that drive the research in MOFs, the ability to predict or design the structures is far from fully understood⁸¹. Crystal engineering principles are being used to design MOFs synthetically, utilising not only the robust coordination interactions (metal to ligand) but also solvent selection⁸² and π -stacking interactions⁸³. Since there are many research groups from numerous specialties using crystal engineering principles to design and develop new materials, not all have been discussed here. There are however some common basic challenges that face crystal engineers, the most fundamental is the crystallisation process where there is no way of knowing if a particular recipe will form a powder, single crystal or amorphous material. There is also lack of knowledge on the role that solvent plays during the

crystallisation process, how it facilitates the nucleation process and drives the final product. The main consequence is the serendipitous nature of polymorph formation (Section 1.5) and the alternative materials obtained from the grinding technique (Section 1.6). On top of this, when crystals do form, we are unable to foretell their size, shape or space group, if they will be metastable, polymorphic or contain solvent.

1.5 Polymorphism

The area of the study of the occurrence and formation of polymorphs has been of emerging importance and debate. Polymorphism, the existence of more than one crystalline form of a compound, is an intensely studied phenomenon, yet it remains poorly understood and controlled⁸⁴. It is of critical importance to many industries, where the existence of various polymorphic forms of a material with different crystal lattices can result in different physical and chemical properties. Nowhere is this more relevant than in the pharmaceutical sector since APIs contain multiple-functional groups (therefore containing multiple sites for possible intermolecular interactions) and where polymorphism can result in changed bioactivity and bioavailability. Full characterisation of solid materials is thus critical in the determination of their ultimate use. As expected, the literature describing studies of polymorphism has grown in magnitude and detail, however, observations of polymorphism in multi-component crystals have been comparatively uncommon until recently, possibly due at least in part to the factors suggested by McCrone, that “*the number of forms known for a compound is proportional to the time and money spent in research on the compound*”⁸⁵. With the increasing time and money being spent on co-crystallisations to generate new materials, especially in the pharmaceutical sector, polymorphism has relatively recently become increasingly observed in these materials.

1.5.1 Controlling Polymorphism

There are many thousands of examples of polymorphism; with statistically 85% of all active pharmaceutical ingredients known to exhibit multiple forms⁸⁴. This has led to the development of techniques not only to screen for polymorphs but also predict if multiple forms will occur. Florence^{87, 88} has been one of the pioneers in developing an automated

parallel crystallisation approach, which can systematically set-up crystallisations using over sixty solvents, with control over solution temperature, filtration, agitation, cooling-rate and solution concentration all achievable. This technique allows for over six hundred different crystallisations to be set-up methodically. There is much emphasis on polymorph prediction as a way to reduce cost and time over the screening approach that not matter how substantial can be insufficient in exploring fully the possible crystallisation parameter space. Initial studies used a best hydrogen bond donor/acceptor approach which has now evolved into a knowledge based approach that assesses crystal stability using hydrogen bond predictions⁸⁹. The approach quantifies the likelihood of hydrogen bond formation for a specified target compound by way of probability modelling of hydrogen bonding data from known, related structures, called the logit hydrogen-bonding propensity (LHP) method. Thus, it can be used to calculate the potential for polymorphism to occur and the relative stabilities of the predicted forms. This technique has been used in biological systems, e.g. protein-ligand docking⁹⁰ and to study the Ritonavir case. In the latter “Ritonavir” story, the large scale production of an anti HIV drug, Ritonavir, was abruptly halted when new batches of the drug produced had a crystal form different to that previously observed and believed to be the most stable form – crucially more stable than the original form. This new form of the drug problematically had a decrease in solubility which entailed a loss in bioavailability. Numerous efforts were made to return to the production of the original crystal form by changing reaction conditions, removing all traces of the second form and drastically rebuilding the manufacturing facility. All this however, was to no avail. In essence, the original crystal form had “disappeared” with the new, more stable form seeding its own growth and preventing the production of the original form. The product was removed from the market and the simple tablet formulation was eventually replaced by a less convenient pre-dissolved liquid-gel capsule with a loss of over five hundred million dollars in sales and expenditure for the company⁹¹.

1.5.1.1 Disappearing Polymorphs

The Ritonavir story is not the only case of “disappearing” polymorphs. 1,2,3,5-Tetra-O-acetyl-D-ribofuranose was first prepared in Cambridge in 1946 by Howard and had a melting point of 58°C (Form A). A more rigorous study was conducted in a US laboratory by Hoepfner who found Form A and another form of higher melting point, 85°C (Form B). After

some time, Form A transformed to Form B with Form A impossible to re-produce. Crystals of Form A made in Cambridge were sent to the US, when upon opening, immediately became opaque and transformed into Form B. During this time the initial crystals of Form A in Cambridge also transformed form B. Studies in Manchester and Los Angeles by different groups went the same way, initially Form A was produced, before transforming into Form B with Form A never to be produced again. The form was deemed to be an unstable, metastable form⁹². This phenomenon of 'disappearing' polymorphs is not uncommon. For example, studies on a trimorphic dimethyl derivative, initially studied by Bürgi⁹³ reported cell constants for the compound (Form I). Bernstein re-examined the compound and after an interim of about eight months, these crystals were found no longer to diffract well. Over a three-year period, subsequent recrystallisation experiments, often preceded by a fresh synthesis of the material, resulted in the discovery of two previously unknown polymorphs, but failed to yield form I⁹⁴. After opening a new laboratory (over a kilometre away) recrystallisation using new reagents, new glassware, and a 'new' student proved successful. These examples add weight to the claims by McCrone and Woodard⁹⁵ regarding the difficulties in crystallising metastable polymorphic forms in an environment in which a more stable form has been obtained.

1.5.2 Polymorphism in Co-Crystals

The growing field of pharmaceutical co-crystals (see Section 1.1.3) (which allows the combination of an API with a co-molecule that can improve physio-chemical properties while retaining the bioactivity of the API, for example improved bioavailability⁹⁶ and shelf life⁹⁷) has inevitably led to the detection of multiple phases of these molecules. This can be seen in the increasing number of papers published in this area. Polymorphism, the existence of more than one crystalline form of multi-component crystals, has been recorded in co-crystals of 4-hydroxybenzoic acid with tetramethylpyrazine⁹⁸, chlorzoxazone with 2,4-dihydroxybenzoic acid⁹⁷ and three forms of the urea-barbituric acid co-crystal¹⁰⁰. Multiple phases have also been found in pharmaceutical co-crystals as in the case of carbamazepine (anticonvulsant and mood-stabilizing) isonicotinamide¹⁰¹ (Figure 1.11) and ethenzamide (analgesic) with 3,5-dinitrobenzoic acid¹⁰².

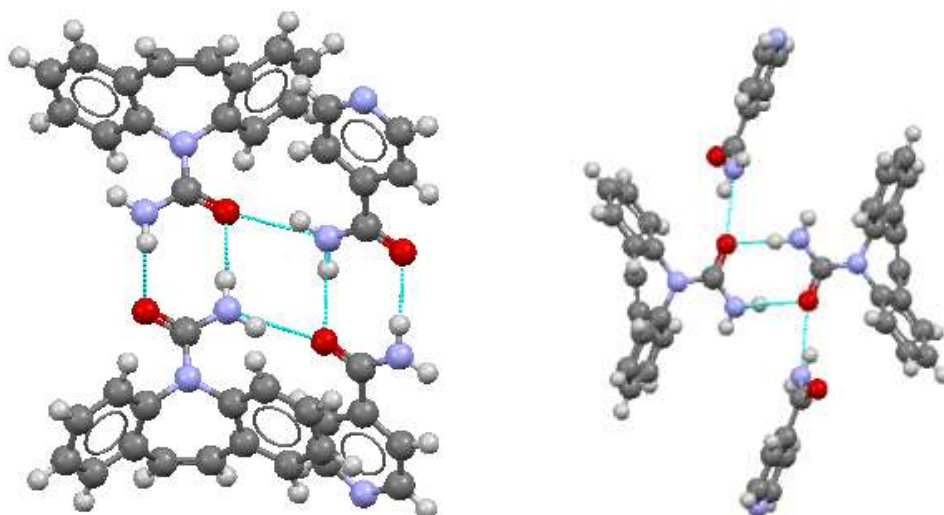


Fig. 1.11 – The co-crystal polymorphs formed by carbamazepine and isonicotinamide⁹⁹.

1.5.3 Isostructures

Two crystals are said to be *isostructural* if they have the same structure, but not necessarily the same unit cell dimensions nor the same chemical composition, and with a comparable variability in the atomic coordinates to that of the cell dimensions and chemical composition. This has been found between many structures. For example triiodoresorcinol (TIR) and triiodophloroglucinol (TIG) crystallized as orthorhombic ($P2_12_12_1$) and monoclinic ($P2_1/n$) polymorphs mediated *via* inter-halogen $I\cdots I$ interactions, where the orthorhombic and monoclinic polymorphs are isostructural¹⁰³. Recently there have even been cases of co-crystals that are isostructural; work by Jones¹⁰⁴ found this to be the case in the tetrafluoro-1,4-diodobenzene (tifb) : 1,4-thixane and tifb : 1,4-thiomorpholine co-crystals¹⁰⁴ (Figure 1.12).

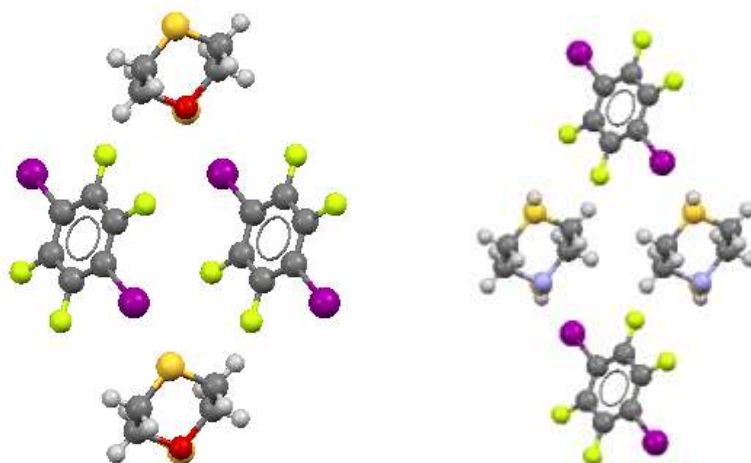


Fig. 1.12 – Two co-crystals; LHS, tetrafluoro-1,4-diiodobenzene : 1,4-thixane and, RHS, tetrafluoro-1,4-diiodobenzene: 1,4-thiomorpholine, that are isostructural.

1.6 Solvent Free Co-Crystallisation

As stated, there are various routes to generate crystalline molecular complexes, the most common being the solvent evaporation method. Over recent years, however, another area has seen an exponential increase in the interest and pace of research – the synthesis of compounds through solvent-free methods. With the emerging importance of crystal engineering in research laboratories and in industry alike, it is a natural progression in modern day science that leads us to look into greener, more environmentally-friendly ways of generating new materials. Through the green chemistry practices now being more widely adopted¹⁰⁵, crystallisation experiments can be significantly improved if the amount of waste generated and the number of auxiliary substances that are used can be reduced. This has led to developments of techniques such as solvent free co-crystallisation. Once again there are various terms used to describe the method, mostly altered based on the field the paper is directed towards. Mechanochemistry¹⁰⁶, (co-)grinding¹⁰⁷, solvent free synthesis¹⁰⁸, solid-state grinding¹⁰⁹ and solid-state synthesis¹¹⁰ are some of the terms used to describe what will be called here solvent-free co-crystallisation (see Section 3.1.2). Further to this, there are various techniques that come under the umbrella of solvent-free co-crystallisation where the method has been altered to improve or target the compounds grown, including solvent-drop grinding¹¹¹ and kneading¹¹², which uses a micro quantity of solvent; vapour digestion¹¹², wet compression¹¹² and solid-vapour reactions¹¹² where there is a mixture of the solid reactant(s) in an atmosphere of solvent(s). Solvent-free reactions can provide fast and quantitative routes to the preparation of common organic¹¹³ and inorganic compounds¹¹⁴. These methods have been predominantly used in conjunction with traditional methods to show the viability and the success of the processes with known molecules¹¹², however more importantly, these processes have been shown to be able to prepare new molecular complexes¹¹⁵ and polymorphs¹¹⁶ unobtainable from traditional methods. Solvent-free co-crystallisations have also been exploited to generate co-crystals that have subsequently undergone reactions also in the solid-state, for example concomitant [2+2] cycloaddition reactions from hydrogen bonded co-crystals of trans-1,2-bis(2-pyridyl)ethylene (2,2'-bpe) : fumaric acid and (2,2'-bpe) : mesaconic acid were reported in 2009¹¹⁷.

1.6.1 Co-Grinding/ Mechanical Mixing

The simplest techniques that come under the solvent-free umbrella are co-grinding and mechanical mixing, where the co-molecules are ground together in a pestle and mortar or a ball mill. These techniques were the focus of a review in 2007¹¹⁸ by Braga that highlighted several successful experiments. One particular example is between dicarboxylic acids of variable chain lengths with a solid base, 1,4-diazabicyclooctane. Polymorphic crystalline forms of the salt are obtained depending on preparation technique, with Form I from grinding and Form II from traditional solvent evaporation methods. James in 2006¹¹⁹ described the first solvent-free synthesis of a microporous metal-organic framework, of copper and isonicotinic acid. Previously structures of discrete coordination polymers¹²⁰ and 1-dimensional polymers¹²¹ had been formed using this technique, but this was the first example of a microporous structure. In spite of this grinding (co-grinding) and ball milling (mechanical mixing) reactions are not popular in academic laboratories (mainly due to the lack of understanding of the mechanisms and non-controllable parameters) but are widely used in industry.

1.6.2 Solvent-drop Grinding / Solvent Catalyst Method

Solvent-drop grinding is the use of a small amount of solvent to speed up solid-state reactions and to provide a lubricant for molecular diffusion, it has been described as solvent catalysis and is commonly used at industrial level. This method is generally more popular than just grinding, as the kinetics of the co-crystallisation are increased¹²² and control over the product is much more achievable, offering a wider range of applications. For example, Trask¹²³ showed how use of small amounts of an appropriate solvent can achieve control of the polymorph outcome in single component crystallisations involving anthranilic acid and succinic acid. This can also be achieved in multi-component systems, for example co-crystals of benzoic acid with diazabicyclo[2.2.2]octane and benzoic acid with 2-aminopyrimidine form different polymorphs using the solvent-drop grinding and solution based techniques, with the product of the grinding having a higher crystal density and packing coefficient¹²⁴. Pharmaceutical co-crystals have also been generated using the solvent-drop grinding method,

with polymorphic forms of the co-crystal caffeine : glutaric acid being achieved; using micro amounts of n-hexane produces Form a, while chloroform produces Form b¹⁰⁷ (Figure 1.13).

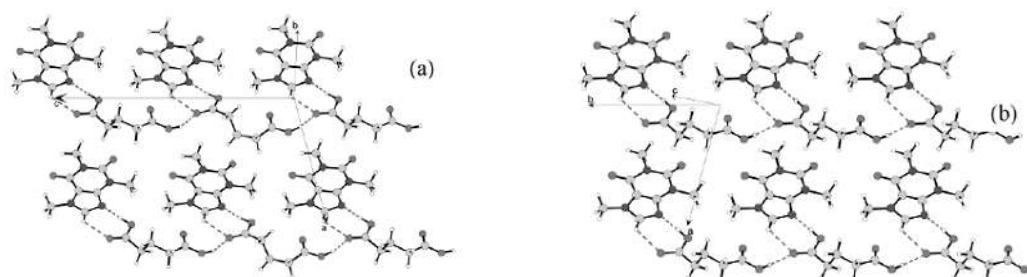


Fig. 1.13 – Extract from Trask *et al*¹⁰⁷ showing the two different packing arrangements for the co-crystal polymorphs of caffeine and glutaric acid.

1.6.3 Understanding the Mechanisms Involved

There is a lack of clear understanding on the mechanism of the grinding process, an issue that is limiting its commercial use. This can be seen from the many different postulates there have been used to explain the outcomes: for example, Kuroda¹²⁵ produced co-crystals of racemic-bis-b-naphthol : benzoquinone by solid state grinding and postulated that the shearing and molecular diffusion processes occurring during grinding generated a different adduct structure to that recovered from solution. In the work of Rastogi¹²⁶ with picric acid complexes, on the other hand, vapor diffusion was suggested as a mass transfer mechanism during solid state grinding. Shan¹²² explained solvent-drop grinding on the basis of additional degrees of freedom, enhancement of molecular collisions and formation of tiny co-crystal seeds. Rothenberg¹²⁷ has presented evidence suggesting the formation of a liquid phase in the binary phase diagram as essential to facilitate intermolecular contacts, mass transfer and chemical reaction for solid-state reactions. Recently Kaupp¹²⁸ proposed a three step solid-state mechanism, derived from atomic force microscopy studies, which involves long-range anisotropic molecular migration. Another postulate comes from Chadwick & Davey¹²⁹ in work on benzophenone and diphenylamine that was formed from co-grinding with a mortar and pestle at ambient temperature. They suggest that a melt is formed between the solid phases with “*The shear induced by the grinding and the contact between the liquid and the residual solid surfaces then induces the nucleation and growth of the co-crystal from the liquid phase, much in the same way as a synthetic chemist might scratch the wall of a reaction vessel to induce crystallization of a reaction product.*” They also go on to suggest that “*The*

closer the eutectic temperature and co-crystal melting point are, the slower will be the production rate of co-crystal and for those systems in which this temperature is above room temperature co-crystallisation will possibly require the addition of small amounts of solvent”.

1.7 Benzimidazole

Benzimidazole (BZN) is a heterocyclic aromatic organic compound made up of a fused benzene ring and imidazole molecule (Figure 1.14 LHS). BZN derivatives have been used as low use-rate, broad-spectrum fungicides that have been used commercially for the control of plant diseases since the late 1960's¹³⁰. At the time of their introduction, they represented a ground-breaking class of fungicides with unique properties including systemic and curative activity that allowed extended spray intervals¹³⁰. World-wide, BZN fungicides are registered in many countries for use on more than 70 crops including cereals, grapes, fruits and vegetables. Thiabendazole (TBZ) was the first BZN to be marketed (Figure 1.13 middle), while BZN derivatives currently commercially available include the following active ingredients: benomyl, carbendazim (MBC), thiabendazole, thiophanate, thiophanate-methyl and fuberidazole (Figure 1.14 RHS).

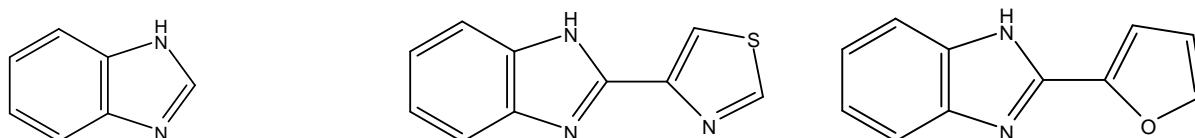


Fig. 1.14 – Schematic of BZN and derivatives, left to right, BZN, thiabendazole and fuberidazole.

There are two structurally determined polymorphs of BZN, alpha and beta, which are both orthorhombic, found within the Cambridge structural database¹³¹ (CSD – version 5.32 update May 2011). The latest version of the alpha form, which was discovered first, was published as a private communication in 2001¹³² (Figure 1.15, LHS) while the beta form was published in 2005¹³³ (Figure 1.15, RHS). The structures are similar in that the main hydrogen bond, N-H...N, is the same and that these create chains of BZN molecules. However they differ in two critical ways, firstly the alternate BZN molecules in the alpha chain are tilted at an angle of 77.49° to one another, while in the beta form the BZN molecules are head to tail. Next, the secondary interactions differ, in the alpha form, the chains connect via C-H...π interactions

involving the carbon located between the two nitrogen atoms, while in the beta form the same carbon is involved in an interaction of 3.3Å in length with a symmetry-related copy of itself.

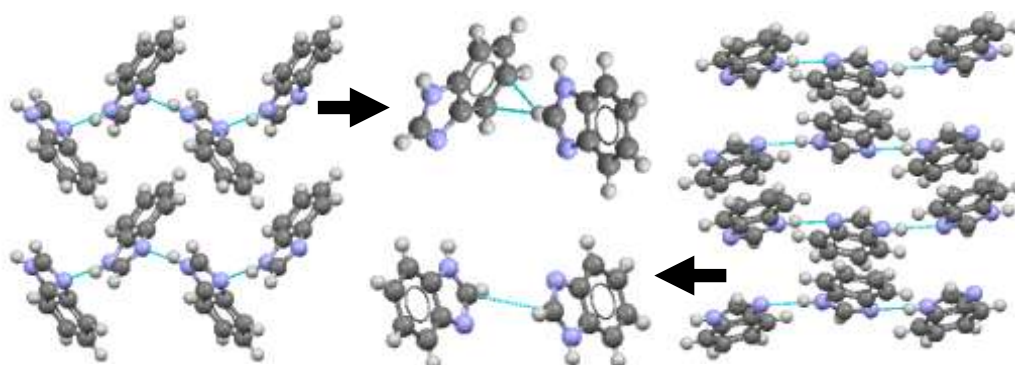


Fig. 1.15 – LHS, the alpha form of BZN, RHS, the beta form of BZN, middle top, secondary interaction of the alpha form, middle bottom, secondary interaction of the beta form.

Within the CSD, BZN is found in a wide range of organometallic complexes, for example with osmium¹³⁴, lanthanum¹³⁵ and cobalt¹³⁶ amongst many more. There are however no structures within the CSD of BZN in its native form in a complex with another small organic molecule. There may be several reasons for this. Firstly when in a basic solution with another co-molecule, BZN has a great affinity for itself, which would tend to favour its crystallising out in one of its polymorphic forms. Secondly BZN is a very good proton acceptor and in the presence of a carboxylic acid it will always deprotonate that group. The latter explains why there is a range of molecular complexes of the protonated form of BZN, benzimidazolium (BZNH⁺), for example benzimidazolium 3-carboxyphenoxyacetate¹³⁷ (Figure 1.16, LHS), benzimidazolium hydrogen phenylmalonate¹³⁸ (Figure 1.16, RHS), benzimidazolium hydrogen nitroterephthalate¹³⁸ and benzimidazolium 2-chloro-4-nitrobenzoate¹⁴⁰ among a few others. All of the structures containing BZNH⁺ contain partially charged assisted N-H...O hydrogen bonds.

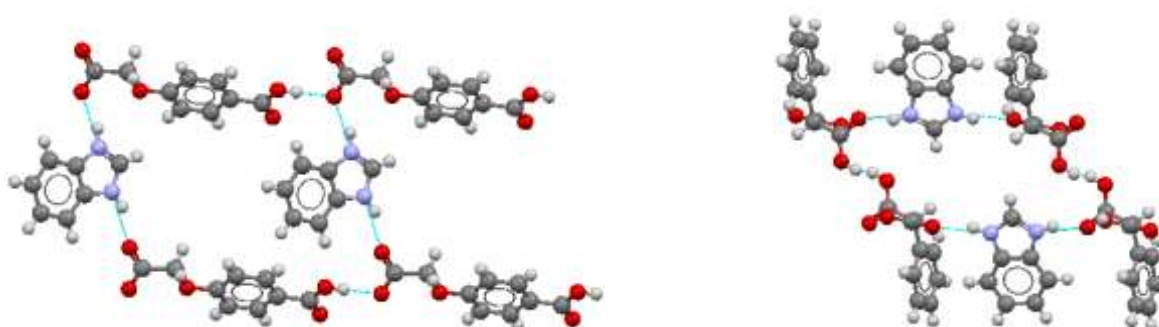


Fig. 1.16 – The basic building blocks from the structures of, LHS, benzimidazolium 3-carboxyphenoxyacetate, RHS, benzimidazolium hydrogen phenylmalonate.

1.8 Imidazole

Imidazole (IMD) is an aromatic heterocyclic and is one of the two diazoles. The term imidazole is also commonly used to refer to an IMD molecule with a substituent, which can be variable. Synthetic imidazoles are present in many fungicides and antifungal¹⁴¹, antiprotozoal, and antihypertensive medications. IMD is part of the theophylline molecule, found in tea leaves and coffee beans, which stimulates the central nervous system¹⁴². It is present in the anticancer medication mercaptopurine, which combats leukaemia by interfering with DNA activities. The crystal structure of IMD has been determined by both X-ray and neutron diffraction, the latest structure deposited within the CSD was in 2008, in a private communication¹⁴³. The structure is made up of chains of IMD molecules held together by N-H...N hydrogen bonds (Figure 1.17, LHS). These chains are then expanded by carbon – nitrogen weak hydrogen bonds utilising the carbon located between the nitrogens, and the unprotonated nitrogen (Figure 1.17 – black circle).

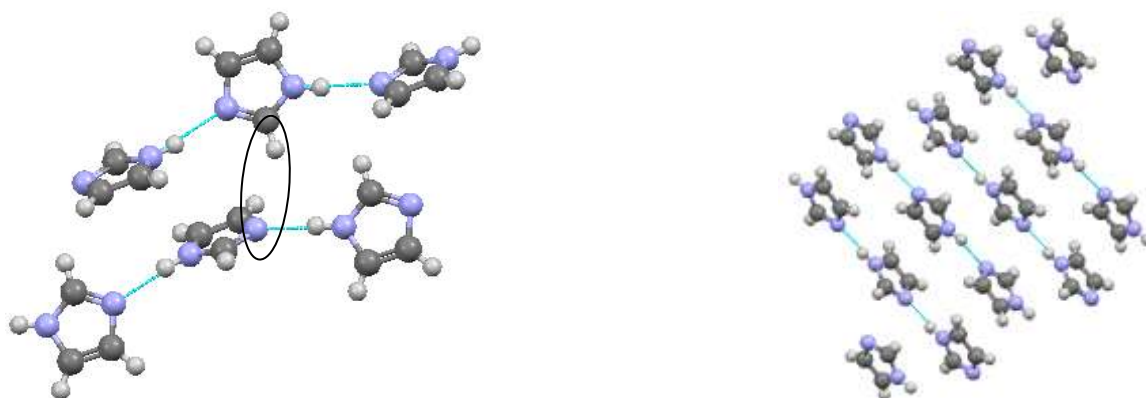


Fig. 1.17 – LHS, building block of the imidazolium structure with the carbon-nitrogen weak hydrogen bond circled in black, RHS, view along the *b*-axis of the extended structure of the imidazole crystal structure.

There are a wide range of molecular complexes and organometallic compounds containing either IMD and/or its protonated form imidazolium, IMDH^+ , deposited within the CSD. Those that are key to this research are discussed thoroughly at the appropriate stage, for example Chapter 7 discusses and compares the molecular complexes obtained from the co-crystallisation of BZN and IMD with dicarboxylic acids. As in the BZN case, there are a vast

array of organometallic complexes containing IMD, for example, with copper¹⁴⁴, nickel¹⁴⁵ and silver¹⁴⁶. There are a wide range of motivations for this research, from creating 3-dimensional supramolecular structures¹⁴⁷ to investigating its binding capabilities for use in medicines¹⁴⁸. There are currently 253 structures deposited within the CSD containing the imidazolium cation, of which 97 are defined as organic. These range from inclusion complexes with 18-crown-6¹⁴⁹ (Figure 1.18 LHS) to complexes / salts with small simple organic molecules such as oxamate¹⁵⁰ (Figure 1.18 RHS).

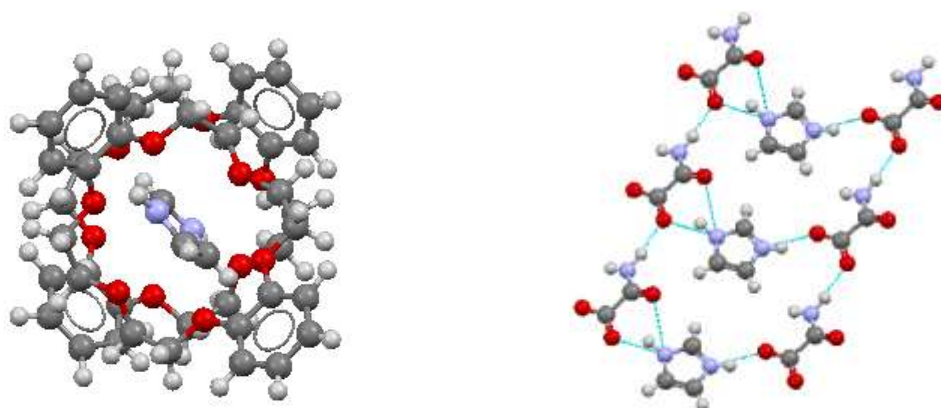


Fig. 1.18 – LHS, crystal structure of the dibenzo-18-crown-6-imidazolium complex, RHS, the structure of the imidazolium oxamate molecular complex.

1.9 Aims and Objectives

This work aimed to investigate and exploit the hydrogen bonds generated between heterocyclic aromatic compounds, namely benzimidazole and imidazole, and the carboxylic acid group. Using crystal engineering principles the projects primary objectives were to:

- generate and determine (mainly by single crystal X-ray diffraction) previously undiscovered molecular complexes
- create a library of robust hydrogen bonds to selectively generate molecular complexes
- promote and control the formation of molecular complex polymorphs through varying crystallisation conditions
- investigate unusual proton behaviour through single crystal X-ray and neutron diffraction
- explore the relatively new solvent-free crystallisation process

- use a range of analytical techniques to investigate products and reactants including X-ray powder diffraction and DSC

1.10 References For Chapter 1

- (1) G. R. Desiraju, *CrystEngComm*, 2003, **5**, 466-467.
- (2) J. D. Dunitz, *CrystEngComm*, 2003, **5**, 506-506.
- (3) C. B. Aakeroy and D. J. Salmon, *CrystEngComm*, 2005, **7**, 439-448.
- (4) P. Vishweshwar, J. A. McMahon, J. A. Bis and M. J. Zaworotko, *Journal of Pharmaceutical Sciences*, 2006, **95**, 499- 515.
- (5) A. D. Bond, *CrystEngComm*, 2007, **9**, 833-834.
- (6) J. Maddox, *Nature*, 1988, **335**, 201.
- (7) B. Sarma, S. Roy and A. Nangia, *Chemical Communications*, 2006, 4918-4920.
- (8) R. A. S. F. Chen and G. Amarasinghe, *Polymer*, 2001, **42**, 4579-4587.
- (9) V. Chégnimonhana and H. Peerhossaini, *International Journal of Refrigeration*, 2010, **33**, 1559-1568.
- (10) K. P. Johnston, S. E. Barry, N. K. Read and T. R. Holcomb, *Industrial & Engineering Chemistry Research*, 1987, **26**, 2372-2377.
- (11) S. L. Childs, *Crystal Growth & Design*, 2009, **9**, 4208-4211.
- (12) P. Vishweshwar, J. A. McMahon, J. A. Bis and M. J. Zaworotko, *Journal of Pharmaceutical Sciences*, 2006, **95**, 499- 515.
- (13) O. Almarsson and M. J. Zaworotko, *Chemical Communications*, 2004, 1889-1896.
- (14) S. u Aitipamula, P. S. Chow and R. B. H. Tan, *CrystEngComm*, 2009, **11**, 1823-1827.
- (15) P. Vishweshwar, J. A. McMahon, M. L. Peterson, M. B. Hickey, T. R. Shattock and M. J. Zaworotko, *Chemical Communications*, 2005, 4601-4603.
- (16) R. D. Bailey Walsh, M. W. Bradner, S. Fleischman, L. A. Morales, B. Moulton, N. Rodríguez-Hornedo and M. J. Zaworotko, *Chemical Communications*, 2003, 186-187.
- (17) N. B. Bathori, A. Lemmerer, G. A. Venter, S. A. Bourne and M. R. Caira, *Crystal Growth & Design*, 2011, **11**, 75-87.
- (18) L. H. Thomas, C. Wales, L. Zhao and C. C. Wilson, *Crystal Growth & Design*, 2011, **11**, 1450-1452.
- (19) M. B. J. Atkinson, S. V. S. Mariappan, D. r Bučar, J. Baltrusaitis, T. Friščić, N. G. Sinada and L. R. MacGillivray, *Proceedings of the National Academy of Science*, 2011, **1**.
- (20) A. S. Cannon, B. M. Foxman, D. J. Guarrera and J. C. Warner, *Crystal Growth & Design*, 2005, **5**, 407-411.
- (21) A. S. Cannon and J. C. Warne, *Crystal Growth & Design*, 2002, **2**, 255-257.
- (22) R. R. Knowles and E. N. Jacobsen, *Proceedings of the National Academy of Science*, 2010, **107**, 20678-60685.
- (23) A. Strecker, *European Journal of Organic Chemistry*, 2006, **75**, 27-45.
- (24) M. S. Sigman and E. N. Jacobsen, *Journal of the American Chemical Society*, 1998, **120**, 4901-4902.
- (25) K. Huang, D. Britton, M. C. Etter and S. R. Byrn, *Journal of Material Chemistry*, 1997, **7**, 713-720.
- (26) G. M. J. Schmidt, *Pure and Applied Chemistry*, 1971, **27**, 674-678.

- (27) G. R. Desiraju, *Crystal Engineering: The design of Organic Solids*, 1989.
- (28) L. Pauline, *The Nature of the Chemical Bond*, Cornwell University Press, 1993.
- (29) G. A. Jeffrey, *An Introduction to Hydrogen Bonding*, Oxford University Press, 1997.
- (30) E. Arunan, G. R. Desiraju, R. A. Klein, J. Sadlej, S. Scheiner, I. Alkorta, D. C. Clary, R. H. Crabtree, J. J. Dannenberg, P. Hobza, H. G. Kjaergaard, A. C. Legon, B. Mennucci and D. J. Nesbitt, *Pure and Applied Chemistry*, 2010.
- (31) K. Matsumoto, T. Tsudaa, R. Hagiwara, Y. Ito and O. Tamada, *Solid State Sciences*, 2002, **4**, 23-26.
- (32) C. C. Wilson, *Crystallography Reviews*, 2009, **3**, 3-59.
- (33) M. Fleck and L. Bohaty, *Zeitschrift fur Naturforsch B*, 2009, **64**, 517.
- (34) N. V. Sidgwick and R. K. Callow, *Journal of the Chemical Society, Transactions*, 1924, **125**, 527-538.
- (35) I. Rozas, I. Alkorta and J. Elguero, *The Journal of Physical Chemistry*, 1998, **102**, 9925-9932.
- (36) W. M. Latimer and W. H. Rodebush, *Journal of the American Chemical Society*, 1920, **42**, 1419-1433.
- (37) C. C. Wilson, *Acta Crystallographica section B*, 2001, **57**, 435-439.
- (38) J. Ding, T. Steiner, V. Zabel, B. E. Hingerty, S. A. Mason and W. Saenger, *Journal of the American Chemical Society*, 1991, **113**, 8081-8089.
- (39) D. Arias, L. Levi and L. Lubart, *Transactions of the Faraday Society.*, 1966, **66**.
- (40) M. D. Ward, *Chemical Communications*, 2005, 5838-5842.
- (41) S. U. Son, J. A. Reingold, G. B. Carpenter, P. T. Czech and D. A. Sweigart, *Organometallics*, 2006, **25**, 5276-5285.
- (42) K. Huang, D. Britton, M. C. Etter and S. R. Byrn, *Journal of Material Chemistry*, 1997, **7**, 713-720.
- (43) S. L. Childs, G. P. Stahly and A. Park, *Molecular Pharmaceutics*, 2006, **4**, 323-338.
- (44) T. Steiner, I. Majerz and C. C. Wilson, *Angewandte Chemie*, 2001, **40**, 2651-2654.
- (45) M. Schmidtman and C. C. Wilson, *CrystEngComm*, 2007, **10**, 177-183.
- (46) D. R. Lide, *CRC Handbook of Chemistry and Physics: A Ready-Reference Book of Chemical and Physical Data*, CRC Press, 2008.
- (47) C. B. Aakeröy, M. E. Fasulo and J. Desper, *Molecular Pharmaceutics*, 2007, **4**, 317-322.
- (48) P. Metrangolo, G. Resnati, T. Pilati, R. Liantonio and F. Meyer, *Journal of Polymer Science.*, 2006, **45**, 1-15.
- (49) G. R. Desiraju and R. Parthasarathy, *Journal of the American Chemical Society*, 1989, **111**, 8725-8726.
- (50) H. L. Nguyen, P. N. Horton, M. B. Hursthouse, A. C. Legon and D. W. Bruce, *Journal of the American Chemical Society*, 2004, **126**, 16-17.
- (51) G. Marras, P. Metrangolo, F. Meyer, T. Pilati, G. Resnati and A. Vij, *New Journal of Chemistry*, 2006, **30**, 1397-1402.
- (52) A. Farina, S. V. Meille, M. T. Messina, P. Metrangolo and G. Resnati, *Angewandte Chemie International Edition.*, 1999, **38**, 2433.
- (53) A. Mele, P. Metrangolo, H. Neukirch, T. Pilati and G. Resnati, *Journal of the American Chemical Society*, 2005, **127**, 14972-14973.
- (54) Auffinger P., Hays F.A., W. E. and H. P.S, *Proceedings of the National Academy of Science*, 2004, **101**, 16789-16794.
- (55) C. A. Hunter and J. K. M. Sanders, *Journal of the American Chemical Society*, 1990, **112**, 5525-5534.

- (56) S. Mecozzi, A. P. W. Jr and D. A. Dougherty, *Journal of the American Chemical Society*, 1996, **118**, 2307-2308.
- (57) T. J. Mooibroek, P. Gamez and J. Reedijk, *CrystEngComm*, 2008, **10**, 1501-1515.
- (58) D. Braga, *Chemical Communications*, 2003, 2751-2754.
- (59) G. R. Desiraju, *Angewandte Chemie International Edition*, 1995, **107**, 2541-2557.
- (60) R. Pepinsky, *Physical Review*, 1955, **100**, 971.
- (61) D. Braga, G. R. Desiraju, J. S. Miller, A. G. Orpen and S. L. Price, *CrystEngComm*, 2002, **4**, 500-509.
- (62) L. Brammer, G. Mi'nguez Espallargas and S. Libri, *CrystEngComm*, 2008, **10**, 1712.
- (63) M. Nishio, *CrystEngComm*, 2004, **6**, 130-158.
- (64) M. Polito, E. D'Oria, L. Maini, P. G. Karamertzanis, F. Grepioni, D. Braga and S. L. Price, *CrystEngComm*, 2008, **10**, 1848-1854.
- (65) M. Etter, *Journal of the American Chemical Society*, 1990, **23**, 120-126
- (66) Z. Yina and Z. Li, *Tetrahedron Letters*, 2006, **47**, 7875-7879.
- (67) J. A. Bis, P. Vishweshwar, D. Weyna and M. J. Zaworotko, *Molecular Pharmaceutics*, 2007, **4**, 401-416.
- (68) N.J. Babu, L.S. Reddy and A. Nangia, *Molecular Pharmaceutics*, 2007, **4**, 417-437.
- (69) P. Vishweshwar, A. Nangia and V. M. Lynch, *Journal of Organic Chemistry*, 2002, **67**, 556-565.
- (70) R. D. Walsh, M. W. Bradner, S. Fleischman, L. A. Morales, B. Moulton, N. Rodríguez-Hornedo and M. J. Zaworotko, *Chemical Communications*, 2003, 186-187.
- (71) C. Aakeröy, N. Schultheiss and J. Desper, *CrystEngComm*, 2007, **9**, 211-214.
- (72) C. Glidewell, G. Ferguson, R. M. Gregson and A. J. Lough, *Acta Crystallographica section C*, 1999, **55**, 2133.
- (73) F. H. Beijer, R. P. Sijbesma, J. A. J. M. Vekemans, E. W. Meijer, H. Kooijman and A. L. Spek, *The Journal of Organic Chemistry*, 1996, **61**, 6371-6380.
- (74) T.-J. M. Luo and G. T. R. Palmore, *Crystal Growth & Design*, 2002, **2**, 337-350.
- (75) A. Samo and M. Samo, *Chemical Physics Letters*, 1985, **114**, 423-425.
- (76) M. C. Etter, *Accounts of Chemical Research*, 1990, **23**, 120-126.
- (77) W. Yang, X. Lin, J. Jia, A. J. Blake, C. Wilson, P. Hubberstey, N. R. Champness and M. Schröder, *Chemical Communications*, 2008, 359-361.
- (78) Y. Yan, X. Lin, S. Yang, A. J. Blake, A. Dailly, N. R. Champness, P. Hubberstey and M. Schröder, *Chemical Communications*, 2009, **9**, 1025-1027.
- (79) A. R. Millward and O. M. Yaghi, *Journal of the American Chemical Society*, 2005, **127**, 17998-17999.
- (80) Czaja AU, Trukhan N and M. U., *Chemical Society Reviews*, 2009, **38**, 1284-1893.
- (81) S. L. James, *Chemical Society Reviews*, 2003, **32**, 276-288.
- (82) S. K. Ghosh and S. Kitagawa, *CrystEngComm*, 2008, **10**, 1739-1742.
- (83) C. Janiak, *Dalton Transactions*, 2000, 3885-3896.
- (84) H. G. Brittain, *Journal of Pharmaceutical Sciences*, 2007, **96**, 705-728
- (85) W. C. McCrone, *Wiley Interscience, New York*, 1965, 725-726.
- (86) P. H. Karpinski, *Chemical Engineering Technology*, 2006, **29**, 233-237.
- (87) A. J. Florence, A. Johnston, S. L. Price, H. Nowell, A. R. Kennedy and N. Shankland, *Journal of Pharmaceutical Sciences*, 2006, **95**, 1919-1930.

- (88) A. J. Florence, in *Pharmaceutical Solids*, ed. H. G. Brittain, Informa Healthcare, 2009.
- (89) P. T. A. Galek, F. H. Allen, L. Fabian and N. Feeder, *CrystEngComm*, 2009, **11**, 2634-2639.
- (90) O. Korb and P. A. Wood, *Chemical Communications*, 2010, **46**, 3318-3320.
- (91) Bauer J, Spanton S, Henry R, Quick J, Dziki W, Porter W and M. J., *Pharmaceutical Research*, 2001, **18**, 859-866.
- (92) J. D. Dunitz and J. Bernstein, *Accounts of Chemical Research*, 1995, **28**, 193-200.
- (93) H. B. Bürgi, J. D. Dunitz and C. Züst, *Acta Crystallographica section B*, 1968, **24**, 463-464.
- (94) J. Bernstein, I. Bar and A. Christensen, *Acta Crystallographica section B*, 1976, **32**.
- (95) G. D. Woodard and W. C. McCrone, *Journal of Applied Crystallography*, 1975, **8**, 342.
- (96) D. P. McNamara, S. L. Childs, J. Giordano, A. Iarriccio, J. Cassidy, M. S. Shet, R. Mannion, E. O'Donnell and A. Park, *Pharmaceutical Research*, 2006, **23**, 1888-1897.
- (97) A. V. Trask, W. D. Samuel Motherwell and W. Jones, *Crystal Growth & Design*, 2005, **5**, 1013-1021.
- (98) B. R. Sreekanth, P. Vishweshwar and K. Vyas, *Chemical Communications*, 2007, 2375-2377.
- (99) S. L. Childs and K. I. Hardcastle, *CrystEngComm*, 2007, **9**, 364-367.
- (100) M. Gryl, A. Krawczuk and K. Stadnicka, *Acta Crystallographica section B*, 2008, **64**, 623-632.
- (101) S. Aitipamula, P. S. Chow and R. B. H. Tan, *Crystal Growth & Design*, 2010, **10**, 2229-2238.
- (102) J. H. ter Horst and P. Cains, *Crystal Growth & Design*, 2008, **8**, 2537-2542.
- (103) N. K. Nath, B. K. Saha and A. Nangia, *New Journal of Chemistry*, 2008, **32**, 1693-1701.
- (104) Cincić D, Friscić T and J. W., *Chemistry - A European Journal*, 2008, **14**, 747-753.
- (105) P. T. Anastas and J. C. Warner, *Oxford University Press* 1998.
- (106) G. Kaupp, *CrystEngComm*, 2009, **11**, 388.
- (107) A. V. Trask, W. D. S. Motherwell and W. Jones, *Chemical Communications*, 2004, 890-891.
- (108) A. L. Garay, A. Pichon and S. L. James, *CrystEngComm*, 2006, **8**, 211-214.
- (109) A. V. Trask, W. D. S. Motherwell and W. Jones, *Crystal Growth & Design*, 2005, **5**, 1013-1021.
- (110) M. Nagarathinam and J. J. Vittal, *Australian Journal of Chemistry*, 2009, **63**, 589-595.
- (111) A. V. Trask, W. D. Samuel Motherwell, W. Jones, N. Shan, S. Feng, R. B. H. Tan and K. Carpenter, *Chemical Communications*, 2005, 880-882.
- (112) D. Braga and F. Grepioni, *Chemical Communications*, 2005, 3635-3645.
- (113) M. L. Cheny, G. J. McManus, J. A. Perman, Z. Wang and M. J. Zaworotko, *Crystal Growth & Design*, 2007, **7**, 616-617.
- (114) A. V. Trask, D. A. Haynes, W. D. S. Motherwell and W. Jones, *Chemical Communications*, 2006, 51-53.
- (115) R. Kuroda, Y. Imai and N. Tajima, *Chemical Communications*, 2002, 2848-2849.
- (116) S. Aitipamula, P. S. Chow and R. B. H. Tan, *CrystEngComm*, 2009, **11**, 889-895.
- (117) C. Avendano and A. Briceno, *CrystEngComm*, 2009, **11**, 408-411.
- (118) D. Braga, S. L. Giaffreda, K. a Rubini, F. Grepioni, M Curzi, L. Maini and M. Polito, *Journal of Thermal Analysis and Calorimetry*, 2007, **90**, 115-123.
- (119) L. Garay, A. Pichon and S. L. James, *Chemical Society Reviews*, 2007, **36**, 846-855.
- (120) P. J. Nichols, C. L. Raston and J. W. Steed, *Chemical Communications*, 2001, 1062-1063.
- (121) W. J. Belcher, C. A. Longstaff, M. R. Neckenig and J. W. Steed, *Chemical Communications*, 2002, 1602-1603.

- (122) N. Shan, F. Toda and W. Jones, *Chemical Communications*, 2002, 2372-2373.
- (123) A. V. Trask, W. D. Samuel Motherwell, W. Jones, N. Shan, S. Feng, R. B. H. Tan and K. Carpenter, *Chemical Communications*, 2005, 880-882.
- (124) S. Skovsgaard and A. D. Bond, *CrystEngComm*, 2009, **11**, 444-453.
- (125) R. Kuroda, Y. Imai and N. Tajima, *Chemical Communications*, 2002, 2848-2849.
- (126) R. P. Rastogi and N. B. Singh, *Journal of Physical Chemistry*, 1966, **70**, 3315-3324
- (127) Rothenberg G, Downie AP, Raston CL and S. JL., *Journal of the American Chemistry Society*, 2001, **123**, 8701-8708.
- (128) G. Kaupp, *CrystEngComm*, 2009, **11**, 388.
- (129) K. Chadwick, R. Davey and W. Cross, *CrystEngComm*, 2007, **9**, 732-734.
- (130) Wu Q, Li Y, Wang C, Liu Z, Zang X, Zhou X and W. Z, *Analytical Chimica Acta*, 2009, **638**, 139-145.
- (131) F. H. Allen, *Acta Crystallographica section B*, 2002, **58**, 380-388.
- (132) R.T.Stibrany, J.A.Potenza and H.J.Schugar, *Prviate Communication*, 2001.
- (133) S. Krawczyk and M. Gdaniec, *Acta Crystallographica section E*, 2005, **61**, 4116-4118.
- (134) I. N. Stepanenko, A. A. Krokhin, R. O. John, A. Roller, V. B. Arion, M. A. Jakupec and B. K. Keppler, *Inorganic Chemistry*, 2008, **47**, 7338-7347.
- (135) A. Zurawski, E. Wirnhier and K. M. Buschbaum, *European Journal of Inorganic Chemistry*, 2009, **2009**, 2482-2486.
- (136) J.-R. Su and D.-J. Xu, *Journal of Coordination Chemistry.*, 2006, **57**, 223-229.
- (137) X.-F. Zhang, S. Gao, L.-H. Huo and J.-G. Zhao, *Acta Crystallographica section E*, 2005, **61**, 3958-3960.
- (138) S. Ueda, T. Fukunaga and H. Ishida, *Acta Crystallographica section E*, 2005, **61**, 1845-1847.
- (139) T.-T. Pan, J.-G. Liu and D.-J. Xu, *Acta Crystallographica section E*, 2005, **61**, 3996-3997.
- (140) H. Ishida, T. Fukunaga and S. Kashino, *Acta Crystallographica section E*, 2002, **57**, 1085-1087.
- (141) L. Shargel , A. H. Mutnick , P. F. Souney and L. N. Swanson, *Lippincott Williams & Wilkins*, 2006.
- (142) G. A. Spiller, *Caffeine*, 1998.
- (142) J.R.Deschamps, J.M.Cook and Y. Teng, *Private Communication*, 2008.
- (144) Y.-X. Zhou, G.-X. Cheng, B.-L. Wu and H.-Y. Zhang, *Acta Crystallographica section E*, 2007, **63**, 2285-2286.
- (145) S. Chen, M. Li, Y. Xiao, Y. Yuan, L. Pan and L. Yuan, *CrystEngComm*, 2008, **10**, 1227-1236.
- (146) C. B. Acland and H. C. Freeman, *J. Chem. Soc. D*, 1971, 1016-1017.
- (144) L. P. Battaglia, A. Bonamartini Corradi, L. Antolini, G. Marcotrigiano, L. Menabue and G. C. Pellacani, *Journal of the American Chemical Society*, 1982, **104**, 2407-2411.
- (148) A. Kropidłowska, J. Chojnackia and B. Becker, *Journal of Inorganic Biochemistry*, 2006, **101**, 578-584.
- (149) S. Kiviniemi, A. Sillanpää, M. T. Lämsä, J. Pursiainen, M. Nissinen and K. Rissanen, *Chemical Communications*, 1999, **10**, 897-898.
- (150) C. B. Aakeröy, D. P. Hughes and M. Nieuwenhuyzen, *Journal of the American Chemical Society*, 1996, **118**, 10134-10140.

2 Theory

2.1 Crystallography

Crystallography^{1,2} is the analysis of crystalline solids using a beam of either electromagnetic radiation or particles to determine the structure of the material via diffraction - a form of elastic scattering. Crystallography is the only technique that allows the determination of the relative positions of atoms from the data, which is fundamentally different to other forms of spectroscopy (NMR, UV) that require the analyst to propose a structure and check if it matches the experimental data. This skill is still required in crystallography, but to a much lesser degree. The determination of the relative position of the atoms or ions in the structure leads to quantifying of the scalar quantities between atoms, (bond lengths, bond angles and torsion angles etc) and the relationships between the atoms (interaction distance and thus interaction type). The understanding of the structure, may it be previously undiscovered, or known but structurally undetermined (existence is known but structure is not), can lead to further studies that can utilise properties to manufacture superior materials.

2.1.1 The Crystal

A perfect crystalline solid material is made up of a large number of identical molecules or ions, which are arranged in a precisely regular way forming units which are repeated in all directions to give a highly ordered structure¹. It is only necessary to know the simplest repeating unit (unit cell) to be able to describe the crystal structure. This unit cell can be a single molecule or a more complicated building block.

2.1.2 The Lattice

Each unit cell can be mapped onto another by symmetry operations with the three basis vectors, a , b , c , describing the translation of the unit in space³. If each unit cell was described using a single point, by applying the symmetry operations, a regular repeating pattern in all 3

directions would be produced; this is called the lattice. The lattice is an abstract mathematical concept and the origin of the lattice can be any point in the crystal structure, for example on an atom or in space. It is the regular translational symmetry of crystalline materials that gives rise to discrete spots in an X-ray diffraction pattern.

2.1.3 The Unit Cell

As mentioned, the unit cell is the smallest repeating volume of the lattice and is described by the basis vectors a , b , c and three angles, α , β and γ , also called unit cell parameters (Figure 2.1). The three basis vectors enclose a shape called a parallelepiped. By convention the angle α is between vectors b and c , β between vectors a and c and γ between a and b , with the length of the basis vectors (unit cell dimensions) typically ranging from around 3\AA to 40\AA for small molecules.

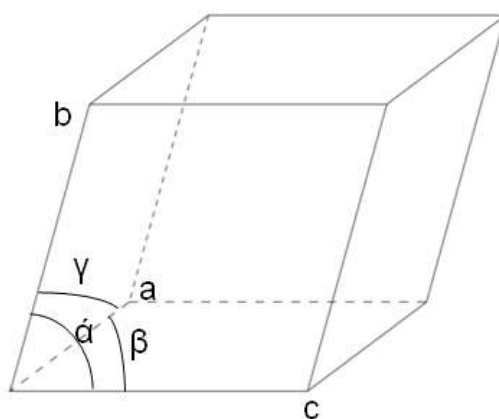


Fig. 2.1 – 3-dimensional unit cell, defined in terms of the unit cell dimensions a , b , c , α , β , γ .

2.1.4 The Seven Crystal Systems

A molecule can undergo transformations called symmetry operations, which include inversion through a point, rotation about a line, or reflection in a plane, that leave the molecule afterwards with an identical appearance⁴. Any rotation or reflection symmetry in the solid state imposes restrictions on the values of the unit cell parameters. For example, if there is a mirror plane in the crystal normal to the b -axis, the a - and c - axes must lie in this plane and hence be themselves perpendicular to the b -axis. If a 3-fold rotation axis lies parallel to the c -

axis, the angle between a and b (γ) must be 120° . Full consideration of the possible symmetry implications on the lattice results in only seven different allowed geometries, called crystal systems (Table 2.1).

Triclinic	$a \neq b \neq c$	$\alpha \neq \beta \neq \gamma \neq 90^\circ$	P
Monoclinic	$a \neq b \neq c$	$\alpha = \gamma = 90^\circ \beta \neq 90^\circ$	P + C
Orthorhombic	$a \neq b \neq c$	$\alpha = \beta = \gamma = 90^\circ$	P + C + F + I
Tetragonal	$a = b \neq c$	$\alpha = \beta = \gamma = 90^\circ$	P + I
Trigonal	$a = b \neq c$	$\alpha = \beta = 90^\circ \gamma = 120^\circ$	R
Hexagonal	$a = b \neq c$	$\alpha = \beta = 90^\circ \gamma = 120^\circ$	P
Cubic	$a = b = c$	$\alpha = \beta = \gamma = 90^\circ$	P + I + F

Table 2.1 – The seven crystal systems with the restrictions on unit cell parameters and corresponding Bravais lattice type, P primitive, C centred, I body centred, F face centred and R rhombohedral.

2.1.5 The Fourteen Bravais Lattices

A unit cell that contains one lattice point is called a primitive cell. There are times when it is beneficial to describe the unit cell with larger parameters to simplify defining the symmetry elements, in some cases 2, 3 or even 4 times the volume of the primitive cell. Such cells are called centred and contain more than one lattice point. There are eight centred lattices; **C** corresponds to a centred lattice where the second lattice point sits on either of the faces, A-face (between the b - and c - axis), B-face (between a - and c - axis) or C-face (between a - and b - axis). If the additional lattice points sit on all the faces it is labelled **F**, face centred, and has four times the volume of primitive cell, and lastly **I** represents body centred where the additional lattice point is at the centre of the cell and has double the volume of primitive³ (Table 2.1).

2.1.6 Space Groups

Within three-dimensional crystals, the presence of translation makes other kinds of symmetry possible. For example a mirror plane can be combined with a translation equal to half a cell unit repeat one of the axes instead of just a reflection; this is called a glide plane. Similarly,

combining a rotation with a translation gives a screw axis, described by the symbol 2_1 for a two fold rotation with translation half cell length. The translation is always along the axis of the rotation⁴. In a single molecule the symmetry elements pass through one point, and the combinations of symmetry elements are known as point groups. In the crystal, the symmetry elements do not necessarily pass through one point, and thus the symmetry groups are called space groups. There are exactly 230 possible arrangements of symmetry elements in the solid state and thus 230 space groups. They are all fully described in the International Tables for Crystallography Volume A⁵.

2.1.7 Theory of Diffraction

The diffraction phenomenon occurs when a wave encounters an obstacle. It is described as the apparent bending of waves around small obstacles and the spreading out of waves past small openings. The effects of diffraction of light were first observed and characterised by Francesco Maria Grimaldi⁶ in the 1600s. He coined the term diffraction, from the Latin word *diffreignere* that means “to break into pieces”.

Diffraction occurs in all waves, including water, sound, and radio and importantly here in electromagnetic waves such as X-rays. Also due to the wave-particle duality concept by which all matter exhibits both wave-like and particle-like properties, diffraction experiments can also be carried out using particles such as electrons and neutrons.

The key benefit of X-ray diffraction is that the typical wavelength of X-rays is of a similar value to the spacing between the lattices in a structure. The most widely used laboratory X-ray sources are based on molybdenum or copper targets, which yield X-rays with principal characteristic wavelengths of 0.71073\AA and 1.54184\AA respectively. Copper radiation is beneficial for a small or weakly diffracting crystals since from a typical laboratory X-ray generator, a higher flux of photons is generated in this case. It also has benefits when using crystals with larger unit cell dimensions since the longer wavelength spreads out the diffraction pattern further. However, use of a molybdenum source allows collection of data to a higher resolution and absorption effects are less serious.

2.1.8 The Laue and Bragg Equations

Every atom within a crystal structure scatters the incident X-ray beam in all directions and these scattered X-rays can undergo constructive and destructive interference. For X-rays to interfere completely constructively, the path difference must be equal to an integral number of wavelengths;

$$\text{Path difference} = a \cos \alpha - a \cos \alpha_0 = h\lambda$$

where α_0 and α are the angles of incident and diffracted beams, a is the 1-dimensional lattice spacing and h is an integer.

For a crystal, the diffracted intensity is effectively zero in all directions apart from where constructive interference has occurred. In a three dimensional array, as in crystals, there are three equations that must be met simultaneously for diffraction to occur, these are called the Laue equations;

$$a (\cos \alpha - a \cos \alpha_0) = h\lambda$$

$$b (\cos \beta - b \cos \beta_0) = k\lambda$$

$$c (\cos \gamma - c \cos \gamma_0) = l\lambda$$

Where h , k and l are integers and a , b and c are interatomic spacings. These equations provide a mathematical interpretation of diffraction geometry. However W.H. and W.L. Bragg provided a simpler, more physically meaningful interpretation, the Bragg Equation⁷;

$$n\lambda = 2 d_{hkl} \sin\theta$$

This equation showed that the crystal could be thought of as a series of parallel planes from which the incoming beam are scattered (Figure 2.2), and the Bragg equation results from the requirement for the path difference between two parallel beams to equal an integral number of wavelengths.

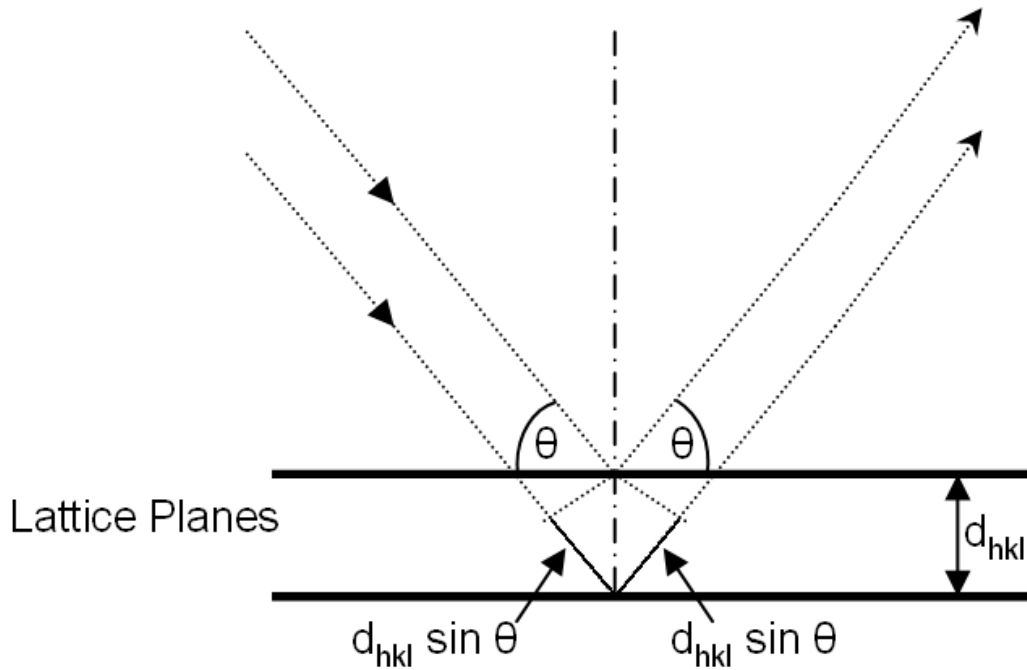


Fig. 2.2 – The Bragg construction for diffraction by a three-dimensional crystal structure.

2.1.9 Reciprocal Lattice

Each set of lattice planes is indexed using the so-called Miller indices, which define the geometry of this plane within the unit cell using three integers, h , k and l . A vector can be defined for each set of planes, with direction perpendicular to the planes, and magnitude d_{hkl} . Each Bragg reflection is thus associated with a vector, whose direction is directly linked to the unit cell. For example the (100) planes lie parallel to the bc face of the unit cell (Figure 2.3). The result is a set of vectors whose end points define a lattice with dimensions inversely related to the dimensions of the crystal lattice, the reciprocal lattice.

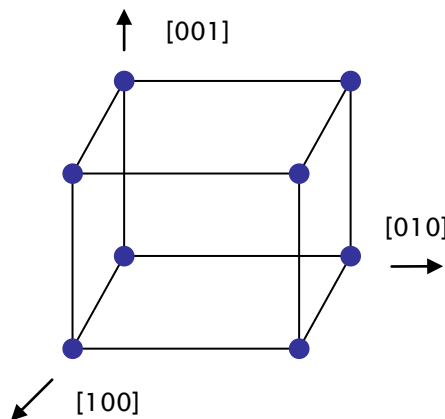


Fig. 2.3 – The cubic crystal system with the directions $[hkl]$ defining a vector normal to the surface of a face.

2.1.10 The Ewald Construction

The reciprocal lattice is very useful in describing the practical implementation of a diffraction experiment. This is seen from using the Ewald construction⁸ (Figure 2.4). Firstly consider a crystal, K , it will have a set of planes in the direct lattice shown on the LHS of the diagram. If an appropriate orientation for diffraction required by Bragg's law is achieved, d , corresponding reciprocal vectors are produced shown on the RHS of the diagram with length $1/d_{hkl}$. A circle of $1/\lambda$ is then drawn around the crystal, K , where λ is the wavelength of the radiation used (hence can be changed / tuned). Bragg's law is satisfied when the scattered vector, $d^\#$, ends on the circle; this circle is called the Ewald circle, and in 3-dimensions is called the Ewald sphere. If the scattered vector (or a reciprocal lattice point) does not lie on the sphere, Bragg's law is not satisfied and a reflection will not be observed. The orientation of the reciprocal lattice can be moved by rotating the crystal around the incident beam, or vice versa.

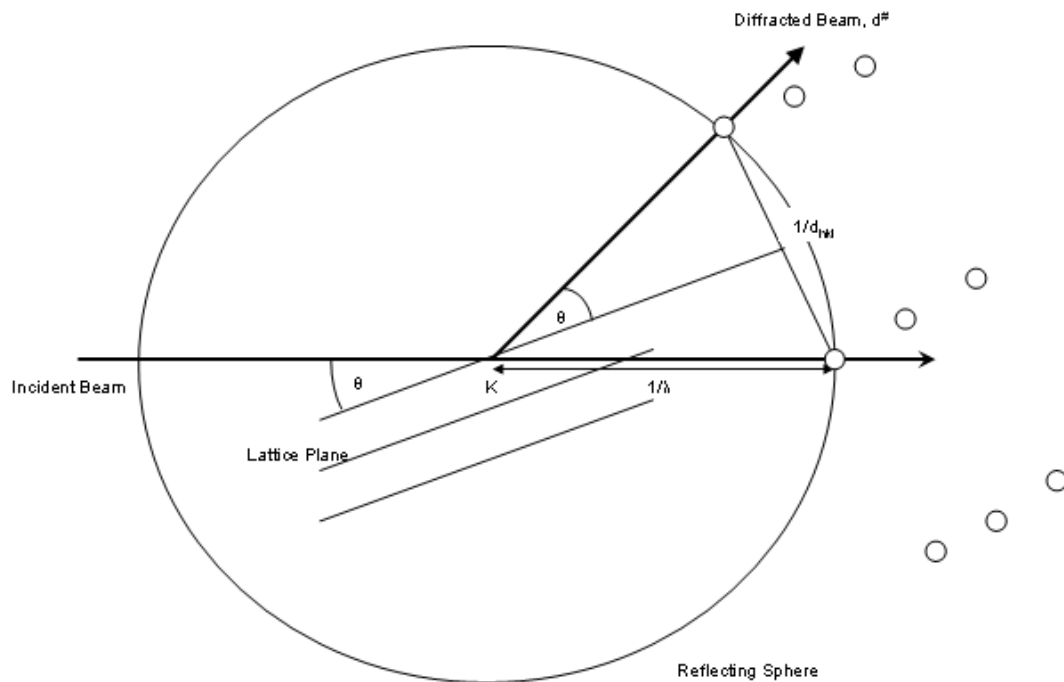


Fig. 2.4 – The Ewald Construction.

2.1.11 Collecting X-ray Diffraction Data

The first step is to determine a unit cell; this is achieved by indexing the diffraction pattern, which entails the assigning of hkl indices to each measured reflection. The space group can

then be determined by measurements of the distribution of reflection intensities, assigning a Laue group and crystal system. To narrow down the choice of possible space groups from this, systematic absences are used. Systematic absences occur in the presence of a centred lattice, glide planes or screw axes. This allows destructive interference to occur in a systematic way, therefore producing zero intensity for sets of Bragg reflections. For a centred lattice, the absences occur throughout the lattice, with a glide plane they occur in the zero layer parallel to the glide plane and for screw axis they occur on the central reciprocal lattice row parallel to the axis³. Once the unit cell and crystal system is defined, a strategy for the data collection can then be determined using the diffractometer software. The actual data collection measures anywhere between 10000 to 50000 reflections, achieved by rotating the crystal relative to the X-ray beam. A diffraction pattern always has inversion symmetry so only a hemisphere of data ever has to be measured to ensure all unique reflections are accessed. Cells with more symmetry need even less; a monoclinic cell needs less data than a triclinic one, with orthorhombic and higher symmetries requiring even less.

Over the past 40 years advancements in diffractometers have meant that a data collection can be done in a morning rather than a week, mainly down to the use of area detector systems. There are a range of these detectors; charged coupled devices (CCD), which use CCD-chips to record the X-rays as they hit the surface and image plates which undergo a reaction when struck with an X-ray that can be read by laser scanning. Both types of detectors have advantages and disadvantages. Recent advances in diffractometer technology have increasingly looked at further mechanisation of diffraction experiments, with machines that are able to take a mounted crystal from bench to structure solution.

2.2 Structure Solution

Once the reflections have been measured, the structure can be solved, i.e. the location of the atoms in the unit cell determined. Some concepts need to be accounted for before describing the method for solving the structure. Firstly, X-rays are scattered by electrons, so the electron density distribution is measured. The electrons are never stationary, with the diffraction experiments only taking a picture of the electrons at a certain time; this means the electron density is averaged out over time and over the vibrations of the atom. The structure can then be described in terms of positions and displacements of the atoms with each atom having its

own electron density distribution about its centre. Atoms are usually calculated as spherical objects, with their contributions to the X-ray scattering (atomic scattering factors) derived from quantum mechanics. Each element has a unique atomic scattering factor that decreases with increasing Bragg angle (Figure 2.5).

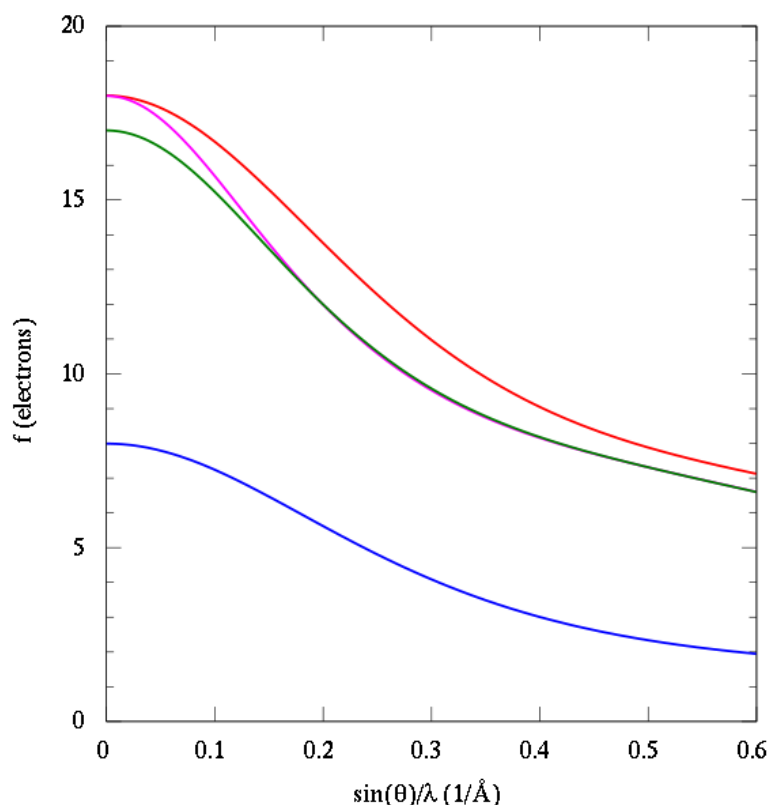


Fig. 2.5 – X-ray atomic form factors of oxygen (blue), chlorine (green), Cl⁻ (magenta), and K⁺ (red); smaller charge distributions have a wider form factor.

Since atoms are also constantly moving, known as atomic displacement, the electron density is further spread out over a larger area and usually in an unequal way (due to bonding). This effect can be described by a set of anisotropic displacement parameters, which uses six parameters and results in an ellipsoid shape for the atom. In total, the parameters that are used to describe an atom are: atomic scattering factor, x , y , z coordinates, site occupancy factors (this helps if an atom does not fully occupy a given position within the unit cell) and anisotropic displacement parameters.

The scattering amplitude, F_c , for a unit cell can be calculated from the known atomic parameters. Due to the phase shift of scattering from the different atoms in the unit cell, the scattered wave can be described by a complex quantity which is linked to the scattering

amplitudes and relative phases. All of the atoms, j , in the unit cell will have their own amplitudes and their individual phase shifts and the resultant scattered wave for the entire structure – called the structure factor – is obtained for each reflection hkl by equation 1.

$$F_{hkl}^c = \sum_j f_j [\cos 2\pi(hx_j + ky_j + lz_j) + i \sin 2\pi(hx_j + ky_j + lz_j)] \quad (1)$$

The square of the amplitude of the structure factor gives the intensity that is generated in a diffraction experiment. The phase angle can be calculated, but is not directly measurable experimentally (see 2.3.2).

2.2.1 Fourier Transform

The crystal structure that is to be determined is related to the X-ray diffraction pattern by a mathematical process called the Fourier transform, i.e. if all the individual X-ray waves are known (that is their structure factor F_o with their phases), a Fourier transform will give the electron density, therefore the structure:

$$\rho(xyz) = \frac{1}{V} \sum_{hkl} F_{hkl} \exp[-2\pi i(hx + ky + lz)] \quad (2)$$

From this the electron density, ρ , can be determined for every point x,y,z in the unit cell. V is the volume of the unit cell, F is the structure factor for the reflection with indices h, k and l . Unfortunately the experimental measurements only give the intensities of the structure factor, i.e. only the amplitudes are known and the phase information has been lost. This loss of phase information is called the phase problem.

2.2.2 Phase Problem

The phase problem arises because the diffraction experiments only collect the intensities of the reflections, with the phase information of the structure factor being lost. If the phase information can be calculated and combined with the observed structure factor values, F_o , the

resulting Fourier synthesis calculations will give the full structure (or a model which refinement methods can improve). Various methods have been devised for solving the phase problem, which for most small molecule structures is now fairly routine.

2.2.3 Patterson Method

One of the two main ways to solve the phase problem is to use the Patterson method, which basically replaces the vector from equation (2), F_{hkl} , with its square, removing the phases from the calculation (3).

$$P(uvm) = \frac{1}{V} \sum_{hkl} |F(hkl)|^2 \cos[2\pi(hu + kv + lw)] \quad (3)$$

The result is that the electron density is not calculated; the peaks on a Patterson map do not correspond to individual atoms, but to vectors between pairs of atoms. The height of Patterson peaks are related to the scattering powers of the two atoms involved in the vector, which means that this method is suited to crystals that contain heavy atoms, for example organometallics. With the heavy atoms found, approximate phases can be calculated and the remaining atoms located using difference Fourier syntheses and then refined to completion.

2.2.4 Direct Methods

Direct methods is the more common of the two techniques and makes use of the relationship between the intensities of the various reflections which lead directly to a solution of the phase problem. It is essentially a trial and error method, based on the knowledge that structure factors are linked to phases through the electron density. Characteristics of the correct electron density can be expressed as mathematical constraints on ρ (density), for example the scattering density is positive throughout and that atoms are in discrete positions. Since the ρ is linked to the structure factor by Fourier transform, constraining ρ also puts constraints on the structure factor. Since the amplitudes of the structure factor are known, the constraints are on the phases and in some cases determine the values of these directly. One of these constraints is called the triplet relationship, where when the Miller indices of three strong

reflections have well-defined relationships with one another, the values of the three phases of the reflections involved in the triplet are also related, with the probability of this relationship being proportional to the intensities of the contributing reflections. Multiple iterations of possible deduced phase sets are tried (often several hundred) and from this the best solution is picked and a density map generated. This results in a list of peaks from which fragments of the structure can often be seen, either by the user or with additional refinements by the structure solution program. There are several variables that can be changed for direct methods to improve the possibility of getting a better solution. The two main variables are the number of triplet reflections relations used or the number of variations of phase relationships attempted, both increasing the chances of finding a solution although the time required for the calculation gets progressively longer. Direct methods are very successful in solving small molecule structures and are by far the most common method used.

2.2.5 Superflip

Superflip⁸ is a relatively new method for solving the phase problem which uses the concept of charge flipping⁹, which is a mathematical algorithm that gives approximate electron densities from structure factor amplitudes. Whilst direct and Patterson methods need relatively large amounts of prior information about the material to solve the structure, charge flipping needs much less, not even chemical composition. The method uses an algorithm (4) which goes through a cycle of operations with the 0th cycle assigning random starting phases ($\varphi_{rand}(H)$) to all experimental amplitudes and making all unobserved amplitudes equal to zero.

$$F^{(0)}(H) = \{|F^{obs}(H)| \exp(i\varphi_{rand}(H)) \quad (4)$$

Where $|F^{obs}(H)|$ is the experimental structure factor. Within the algorithm all operations are performed in the whole unit cell with symmetry space group PI , therefore the origin of the structure is not fixed and the structure can emerge anywhere in the unit cell. An inverse Fourier transform is performed that calculates the electron density; from this if there is any negative electron density, the sign at this point is flipped (thus charge flipping). The next step is calculating temporary structure factors by Fourier transform and from this the calculated phases can be added to the experimental amplitudes to generate the new structure factors.

These new structure factors are then inserted in the beginning of the next cycle. The success of the operations can be monitored observing the R-value of amplitudes with respect to $|F^{obs}(H)|$. It is large in the initial cycles however once there is a sharp decrease of the R-value and this becomes steady, the process is said to have converged. The final R-values are not a measure of the quality of the structure, but merely as an indicator of convergence. Since the calculation is carried out in the *PI* space group, the actual space group still needs to be determined. This is carried out directly from the electron density after the unit cell is modelled and a list of symmetry operations that are compatible with the lattice can be drawn up and evaluated by how well they match with the electron density. From the symmetry elements that are a good match, a space group is assigned that fits best.

2.2.6 Fourier Refinement

From a partially known structure (model), a set of calculated phases can be obtained. Combining these with the observed structure factor magnitudes leads to the observed structure factors, F_o . By subtracting from each point an identical summation based on the calculated structure factor, F_c , a “difference Fourier” map can be calculated. The peaks that remain represent the missing atoms in the structure, since effectively the model calculated density has been removed from the experimental calculated electron density. With each new model, a new difference Fourier map can be calculated, this improves the phases that are used in the calculations, creating a cycle that if repeated determines the complete structure. The structure that has been achieved will describe the structure reasonably well; however there are still errors in the parameters, due to the approximations in the calculations used and in the quality of data collected; for example the experiment is not carried out at 0K so thermal parameters must be included. Therefore the calculated structure factor, F_o , does not agree with the observed values. The next step is better to match the calculated and observed structure factor values, which is done through least squares refinement. This can be used in structure refinement as the parameters are said to be over determined i.e. there are significantly more observations than parameters (for a good data set, the data/parameter ratio is typically more than 10). In addition, during the least squares refinement process, other factors affecting the agreement of model with data are optimised, including absorption corrections, which are required to account for the weakening of the X-ray beams by elastic and inelastic scattering as

they pass through the crystal; this absorption is affected by the atom types in the structure and the size and shape of the crystal,

2.2.7 Location of Hydrogen atoms

Hydrogen atoms have very little scattering power, but depending on the number of them in the structure can contribute significantly to the electron density. After the main features of the structure have been optimised by refinement, difference Fourier maps can be calculated. Using these maps it is possible to find the hydrogen atoms and to spot if an atom has been mis-assigned.

2.2.8 R-Values

In order to determine how well the model actually fits to the experimental data, residuals, normally named R-factors (5), are used. The R-factor gives the average relative deviation between the observed, F_o , and calculated, F_c , structure factors:

$$R = \frac{\sum_{hkl} |F_o| - |F_c|}{\sum_{hkl} F_o} \quad (5)$$

The higher the value of the R-factor the worse the model and data match, so the lower the better, with typical published data having R-factors around 0.02-0.07. The weighted R-factor (6) works in the same way but with weighting factors for the reflections based on the $\sigma(F^2)$ values and is directly related to the statistical quantity that is minimized in the least squares refinement. Good weighted R-factors tend to be around 0.12-0.15 (12- 15%).

$$wR_2 = \sqrt{\frac{\sum_{hkl} \omega(F_o^2 - F_c^2)^2}{\sum_{hkl} \omega(F_o^2)^2}} \quad (6)$$

A further quantity is used to measure the quality of the refinement, S (7), the goodness of fit.

$$S = \sqrt{\frac{\sum_{hkl} \omega (F_o^2 - F_c^2)^2}{m - n}} \quad (7)$$

where m is the number of reflections and n the number of parameters; the difference in these numbers gives the over determination of the structure. A good refined data set will have a S value of close to 1.

2.3 Powder Diffraction

In contrast to single crystal X-ray diffraction, powder X-ray diffraction can test the properties of a bulk sample. A powder diffraction experiment can be undertaken on a whole crystallisation experiment and be achieved to a high resolution in less than 30 minutes. Testing of bulk properties using single crystal experiments would require the diffraction of 10s of samples which would take time and may well be impossible if suitable crystals were not generated of all crystalline forms present in the sample. The benefit of analysing the bulk sample over selected single crystals is two-fold: to obtain the composition of the bulk material and to determine the degree of crystallinity of the sample. It is also possible to determine unit cell information and powder data can also sometimes lead to full structural determination. Information of the composition is vital as it can quickly find if the sample has new products, for example a molecular complex, or just starting material. Powder diffraction can also determine if the sample is pure or a mixture which is vital in identifying polymorphism in a material. The type of sample used (powders) lends a greater degree of flexibility in experimental conditions over the single crystal experiments. Using non-ambient conditions, such as high pressure, temperature or magnetic field is much easier to undertake on a powdered sample than a crystal, as single crystals are much more vulnerable to these conditions. Powder diffraction studies using non-ambient conditions can provide real time information on the kinetics of the reactions involved, phase change information and the changes of the unit cell parameters.

2.3.1 Powder Diffraction Experiments

A powder is a collection of randomly oriented crystallites; the sample is called polycrystalline. In a diffraction experiment each of these crystallites can be thought of giving rise to its own diffraction pattern, and the random orientation of the many crystallites in the experiment leads to the spots becoming spread out into rings of diffracted intensity (Figure 2.6). This generates a plot of total diffraction intensity against diffraction angle, 2θ .

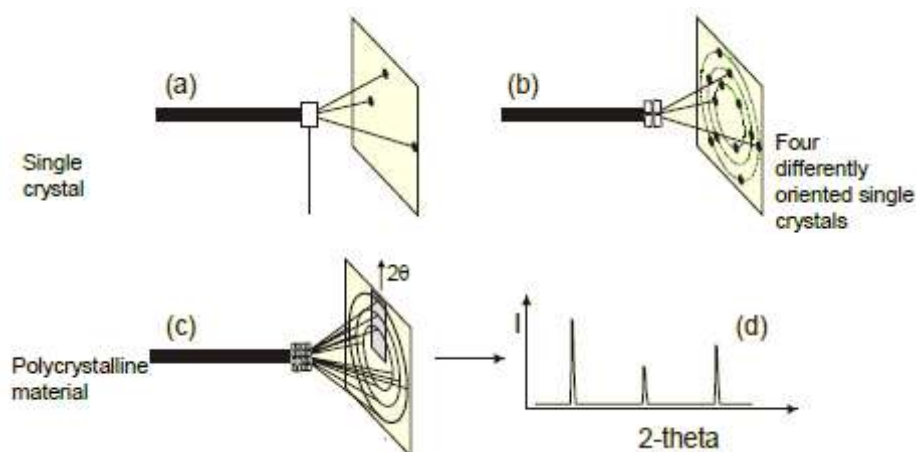


Fig. 2.6 – (a) Shows diffraction from a single crystal, (b) from a collection of four crystals, (c) from a polycrystalline sample. (d) is the resulting powder pattern from the polycrystalline sample¹⁰.

The inherent problem with powder diffraction is that the 3D intensity distribution of single crystal experiments is compressed into a 1D distribution in 2θ space. The result is a loss of information and peak overlap, with the latter being the only problem that can be resolved, to a certain extent. This peak overlap is more severe for larger and lower symmetry unit cells, and making molecular materials with chosen symmetry is still beyond crystal engineers. Therefore to reduce peak overlap, optimising experimental parameters (such as diffractometer resolution, sample quality) that will sharpen the widths of the reflections as much as possible are required.

2.3.2 Powder Diffractometers

There are a wide range of X-ray powder diffractometers available, with each instrument set-up producing advantages and disadvantages. A traditional flat plate set-up for a powder

diffractometer is shown in Figure 2.7. In this set-up the sample is scanned through an angle θ as the detector is moved through 2θ to accumulate the diffraction pattern. There are different sources and detectors with different associated properties, with the most common set-up being a sealed copper tube and a point detector with reflection geometry. As can be seen from Figure 2.7, between the source and the sample there is a divergence slit, this controls the amount of sample that is illuminated by the X-rays. It is crucial that the slit size is smaller than the sample size to ensure that diffraction intensities are useful. A similar slit is placed between the sample and the detector, the anti-scatter slit, which is used to reduce the axial divergence of the scattered X-rays. The smaller the slits, the higher the resolution, but that is at the cost of a decrease in intensity (for example, a 0.05mm detector slit will only result in $\frac{1}{4}$ of the count rate of a 0.2mm slit). The flat plate method – in which the powder sample is deposited on a flat sample holder, is prone to an effect called preferred orientation; this is when the crystallites arrange themselves into a non-random arrangement, due to their morphology. This can severely affect the diffraction intensities and skew results. The simplest way of reducing preferred orientation is to use a capillary set-up where a constantly rotating capillary tube is used to contain the sample instead of a flat plate.

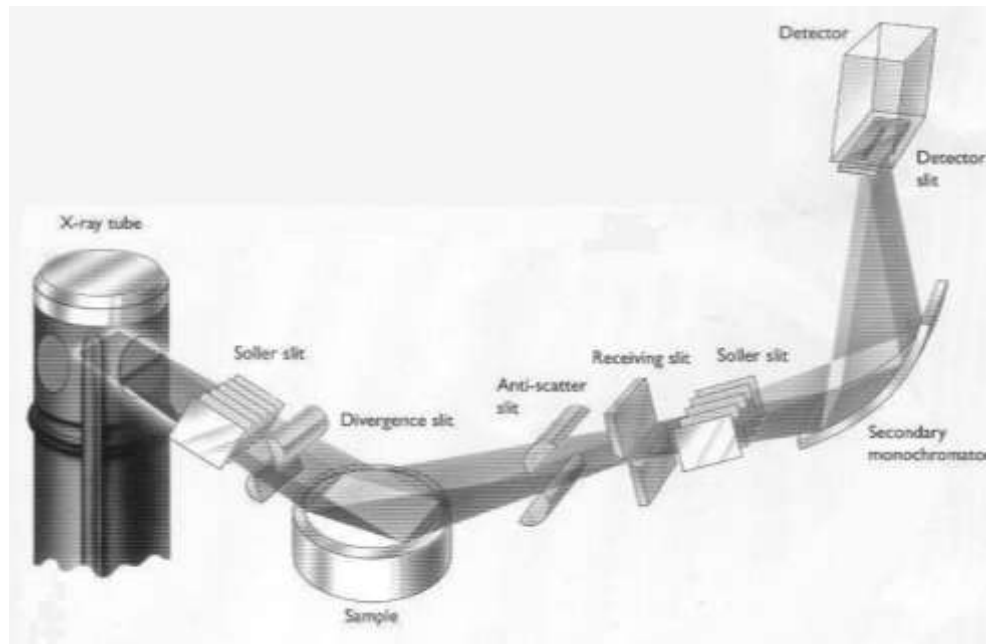


Fig. 2.7 – Schematic of a traditional flat plate X-ray powder diffractometer.

2.3.3 Powder Pattern

Information about the material is found in three distinct features of the powder pattern. The peak positions give information on the size, shape and symmetry of the unit cell. Peak intensities relate to the arrangement of scattering density within the unit cell, which relate to the unit cell contents, point group symmetry and in multi-sample experiments, the relative quantities of each phase (quantitative analysis). Lastly from the peak shape and width, information on the crystallite size and the extent of defects or strains in the sample can be determined. As discussed in Section 2.4.2, experimental factors (sources, optics, detectors) can also affect the width of the peaks.

2.3.4 Structure Solution from Powder X-ray Diffraction Data

For structure determination from powder data (SDPD), the data needs to be of the best possible quality. Recommendations to ensure this include the use of a rotating capillary set-up, small step size, varying the data collection time with angle (see Table 2.3 below for example of a variable count time strategy), and carrying out many short scans rather than one long run. Primarily the goal of these is to reduce background and at high angles of 2θ , reduce overlap of peaks and strengthen the weak signals produced.

Starting (2θ)	End(2θ)	Step size	Time (secs)
3	28	0.017	2
28	45	0.017	6
45	55	0.017	16
55	70	0.017	32

Table 2.3 – Typical variable count time scan set-up for SDPD.

There are normally several steps in the structure solution process; firstly the highest quality data possible is obtained. Unit cell parameters are then obtained from the observed peak positions. This indexing stage is performed similarly to single crystal experiments and requires careful peak fitting. The space group can be determined from systematic absences; however, where overlap between peaks at high 2θ is significant this causes difficulties with peak picking.

Next, a Pawley refinement¹¹ is performed; this method is basically a peak fitting exercise (not based upon a structural model) where only the allowed peaks that correspond to the unit cell

and the symmetry are included. If the calculated peaks are not fitting well with the observed peaks, this indicates that either the unit cell or space group is wrong or impurities are present. The Pawley refinement gives a numerical indication of the best fit that will be achieved in the Rietveld (structure) refinement stage.

There are many options for the next stage; processes similar to direct methods and Patterson synthesis can be used to solve the structure. Charge-flipping algorithms have recently been used. The SDPD method which is used in the DASH software is a direct-space structure solution method that uses information about the molecular fragments and their geometry.

The latter method works by generating a trial structure model from the molecular cell contents and compares the calculated diffraction pattern from the model to the experimental diffraction pattern. Using a simulated annealing approach, adjustments are made to the structure in a random way and for each move the agreement between the observed and calculated patterns is examined. The move is then accepted or rejected and the process is repeated until the best agreement is obtained.

Lastly, a Rietveld refinement is performed; this is a whole pattern fitting least-squares method that allows the adjustment of structural parameters such as unit cell size, fractional atomic coordinates and thermal parameters to minimise the difference between the observed (y_{obs}) and calculated (y_{calc}) patterns point by point. The quality of the model can be assessed by considering the goodness of fit (χ^2) (8) which compares the agreement factor R_{wp} against the R_{exp} which is the statistically expected value. The goodness of fit should be as close to the result of the Pawley refinement as possible.

$$\chi^2 = \frac{R_{\text{wp}}}{R_{\text{exp}}} \quad (8)$$

It is often best to use a visual inspection of the difference profile (diffraction pattern subtracted by calculated pattern) as high background can artificially lower the R_{wp} values (Figure 2.8).

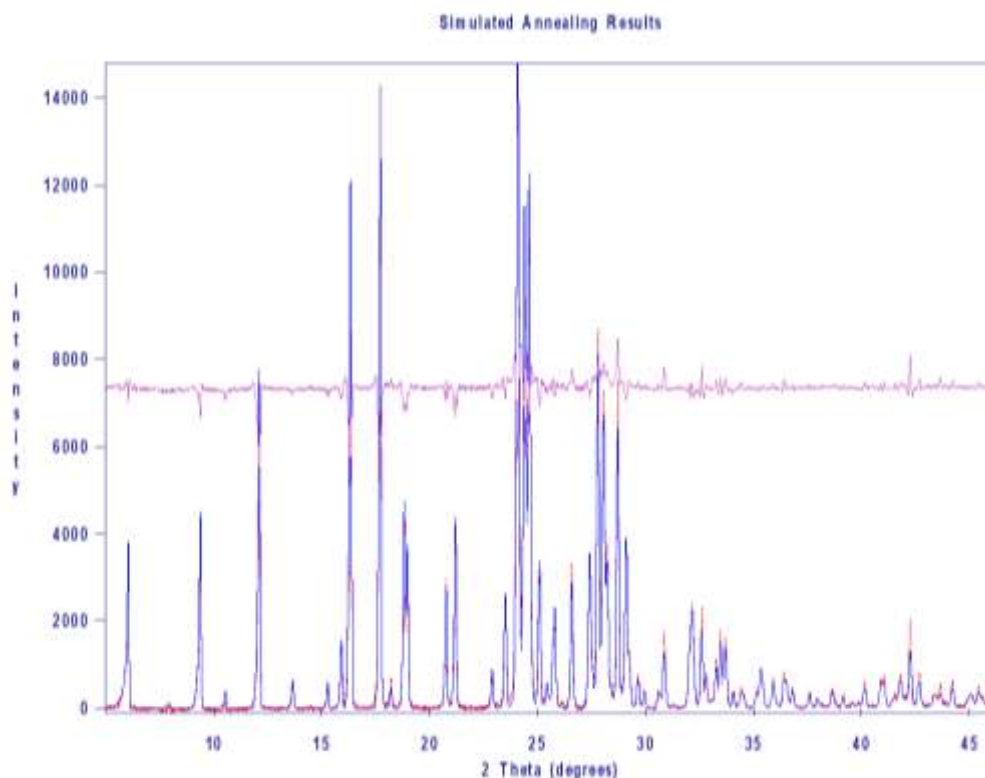


Fig. 2.8 – The powder pattern of benzimidazole 5-chlorosalicylic acid obtained from structure solution with DASH (blue) and the experimental data (red). The purple line indicates the differences between the two sets of data; this is an indication of the good fit between the two.

2.4 DSC

Differential scanning calorimetry (DSC) is a technique that investigates the thermal transitions of a material and works according to the heat flow principle. Thermal transitions are those in which there is an energy exchange with the sample environment as it is heated. This includes things like glass transitions, phase transitions, melting, and recrystallisation (Figure 2.9). DSC is a useful technique when dealing with multi-component materials as it is able to determine quickly if the sample is pure, the different phases a material adopts as a function of temperature, degree of crystallinity and, importantly, to screen for polymorphs.

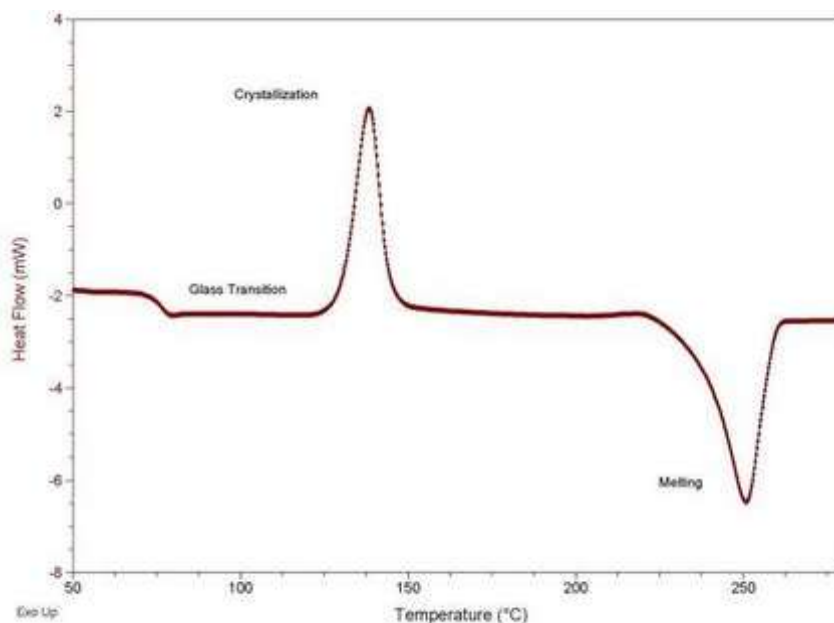


Fig. 2.9 – Thermogram showing the three main types of event that be detected by DSC, glass transition, crystallisation and melting. For a multiple phase sample, each component will follow its own thermal profile.

2.4.1 DSC Experiments

A small amount of the sample is placed in the sample pan and in parallel with an empty reference pan, they are then heated at a set rate. The difference in energy required to heat the sample pan compared to the reference pan is measured and plotted as the temperature is increased. This thermogram (normally heat flow vs. temperature) provides information on any endothermic or exothermic transitions that the sample has undergone. For example when there has been an endothermic transition (e.g. melting), the sample absorbs heat and requires an increased amount of energy to retain the same heating rate. This is represented as a negative peak in the DSC thermogram. The opposite is seen for an exothermic transition (e.g. crystallisation) where heat released by the material therefore less energy is required to keep the same heating rate so a positive peak is seen on the thermogram. The DSC scan can also be undertaken when the sample is being cooled which tends to indicate when materials recrystallise, however this is very rarely seen clearly in multi-component materials.

2.5 References for Chapter 2

- (1) W. Clegg, *Crystal Structure Determination*, Oxford Science Publications, 1998, **60**.

- (2) C. C. Wilson, *Single Crystal Neutron Diffraction From Molecular Crystals*, World Scientific, 2000.
- (3) W. Massa, *Crystal Structure Determination*, Springer, 2003.
- (4) A. J. B. William. Clegg, Jacqueline M Cole, John S O Evans, Peter Main, Simon Parsons, and David J Watkin, 2009.
- (5) T. Hahn, *International Tables for Crystallography Vol. A*, 2006.
- (6) W. L. Bragg, *Proceedings of the Cambridge Philosophical Society*, 1913, **17**, 43-57.
- (7) P. P. Ewald, *Acta Crystallographica section A*, 1969, **25**, 103-108.
- (8) L. Palatinus, G Chapuis, *Journal of Applied Crystallography*, 2007, **40**, 786-790.
- (9) G. Oszlányi and A. Süto, *Acta Crystallographica section A*, 2004, **60**, 134-141
- (10) A. J. Blake, W. Clegg and J. M. Cole, *Crystal Structure Analysis: Principles and Practice*, Oxford University Press, 2009.
- (11) G. S. Pawley, *Journal of Applied Crystallography*, 1981, **14**, 357-361.

3 Techniques and Instruments

The techniques deployed were primarily intended to prepare and characterise single crystals of previously undiscovered multi-component materials. The techniques used to grow single crystals were predominately the solvent evaporation technique with slight derivatives of this. There were a wide range of analytical techniques used to determine what materials were generated and in some cases their properties.

3.1 Single Crystal Formation

The formation of a crystal depends on the relative rates of nucleation and growth. If rate of nucleation is larger than rate of growth, the result will be generation of polycrystalline material, i.e. powder. On the other hand, if the rate of growth is too large, the crystal will undoubtedly develop defects, strains and stresses¹. Therefore the growth of the crystals is an essential stage to be optimised in sample preparation with certainly no “one size fits all” approach available. Also to be taken into consideration is the size of crystal required for the analytical technique to be used. Single crystal X-ray diffraction requires crystals of dimension typically between 0.1 – 0.4mm on a side, while neutron diffraction requires much larger crystal sizes, of volume around 1mm³.

3.1.1 Solvent Evaporation Method

The main methods for obtaining a single crystals of a material are from solution, melt or by sublimation. In this body of work, the only method used was crystallisation from solution however there are benefits to using both the melt and sublimation methods with all these methods reviewed in a paper by Hulliger². The solution method basically consisted of the dissolving of the target materials in appropriate solvent and leaving the solution to evaporate over time to produce formation of the desired materials – including the assembly of molecular complexes from multi-component solutions – and generate the required size of crystal.

Although apparently simple, there are a large variety of different variables in this method including container vessel, ratio of starting materials, selection of solvent, temperature and rate of evaporation control. There were a range of different types of glassware used including round bottom, volumetric and conical flasks, however the majority of crystallisations were conducted using a 7mm³ volume glass vial. There were also attempts made using crystallisation-specific glassware, including U- and H- tubes (Figure 3.1). There were also target materials in which different stoichiometric ratios of starting materials were required. A wide range of solvents were used to dissolve the starting materials including methanol, ethanol, propanol and acetone, with solvent selection tailored to suit the solubility of the starting materials and to try and influence the outcome of the crystallisations. Multi-component crystallisation experiments were set-up to produce complexes in which it was intended to control the proton transfer that occurs between benzimidazole and a carboxylic acid containing group, with the pH of the solvent tailored to encourage proton transfer, for example acetic acid, and to discourage transfer, for example ammonia. In some cases when starting materials dictated, a mixture of solvents was used. When trying to control the formation of polymorphs, a relatively small change in crystallisation conditions can influence the product, for example using methanol instead of ethanol, can be the difference in determining which polymorph is formed. The same can be true for temperature – there are examples in this work where a temperature difference of 10°C can be the deciding factor in selecting formation of a particular polymorph. Often the control of a constant temperature for a crystallisation, or use of a carefully controlled temperature ramp is a vital component. A wide range of temperatures were used including: 2~4°C in a cold room; 10 and 20°C using a ReactArray Microvate³ (able to programme a temperature from -30 to 160°C with ramps or constant temperature control); 30, 40 and 50°C using Asynt magnetic hotplates⁴ and the less controlled wide range of ambient temperatures achievable during the year in Glasgow (Figure 3.1).

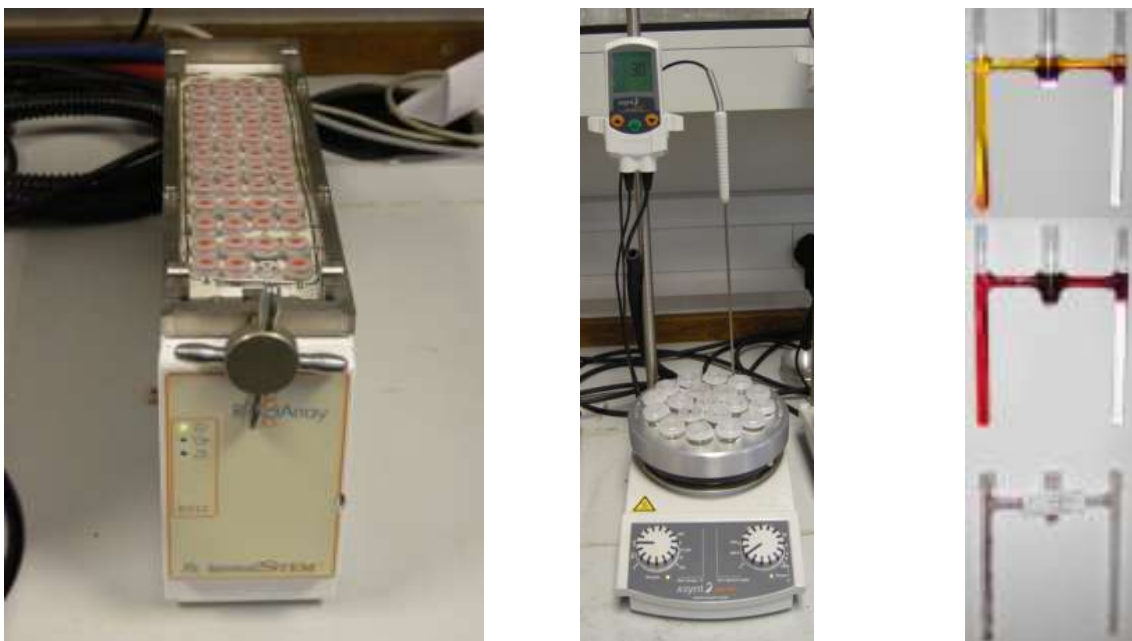


Fig. 3.1 – From left to right, ReactArray Microvate, Asynt hotplate and H-tubes, the latter containing crystallisations of chloranilic acid and 3,5-dimethyl pyrazole at different stages.

While temperature is one way to control the rate of evaporation, another is using blockers to reduce the rate of solvent loss. For the 7mm³ vials this is best achieved using the associated plastic lids, however with other glassware parafilm was used to cover. If a powdered material was the object of the crystallisation then use of a vial with no lid, with a high evaporation temperature, would produce the quickest results.

3.1.2 Solubility Phase Diagrams

It is essential that the solubilities of the starting materials are taken into account; if the solubility of the molecular complex is lower than that of the individual components, there exists a driving force for the cocrystallisation to occur⁵. Phase diagrams show when thermodynamically distinct phases occur at equilibrium with the lines indicating the conditions at which multiple phases can coexist. The phase diagram in Figure 3.2 shows that the cinnamic acid nicotinamide

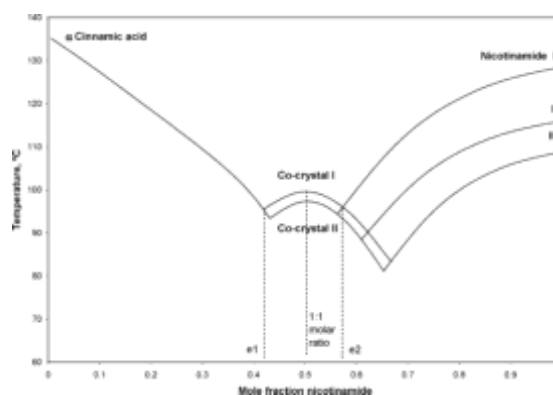


Fig. 3.2 - The two-component phase diagram for the trans-cinnamic acid nicotinamide system⁶.

co-crystal Form I will occur when there is a 1:1 molar ratio of the components. When there are a stoichiometric excess of one component (below 0.4 and above 0.7), then the starting materials are obtained. Ternary phase diagrams are required to evaluate the influence of solvents during the crystallisation and these can vary significantly on changing the solvent of crystallisation. Figure 3.3 uses the cinnamic acid nicotinamide system to highlight this; region 1 indicates an undersaturated solution, 2 is solid cinnamic acid, 4 is where solid nicotinamide is formed, 3 indicates where the molecular complex forms and 5 and 6 are mixtures of molecular complex and starting material. When both co-molecules have equal solubility in the solvent, for example in methanol for this system (Figure 3.3 LHS), the molecular complex (in a 1:1 ratio) is formed when the solubility curve of the molecular complex (b to c) crosses the molecular complex component stoichiometric line (e to f). In the case of water (Fig 3.3 RHS) where there is a wide difference in the solubilities of the two components, the region where the molecular complex is stable, is skewed giving an asymmetric phase diagram and shows that the region for co-crystal formation never crosses the 1:1 stoichiometric line (e to f) indicating that the molecular complex will not form. This indicates that a successful co-crystallisation is more likely to happen when the two components have similar solubilities⁶.

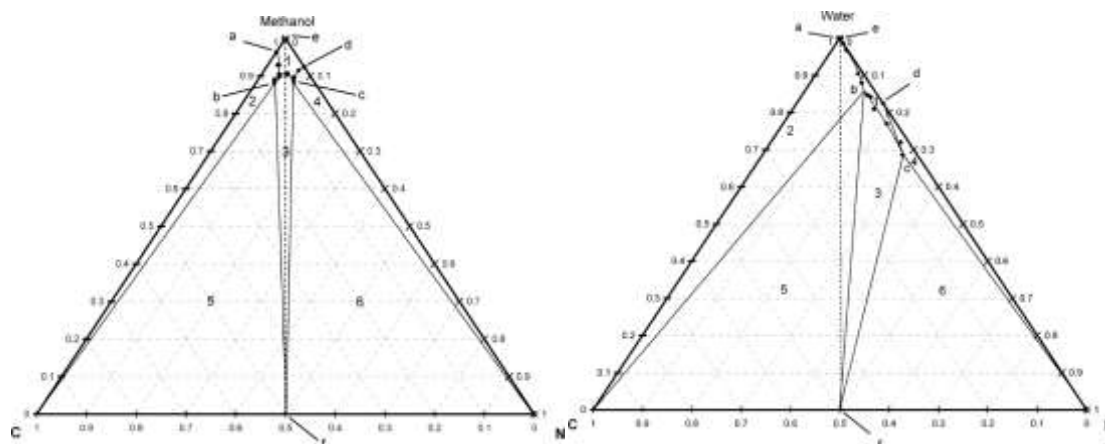


Fig. 3.3 – LHS, the three component phase diagram for the trans-cinnamic acid nicotinamide system in methanol at 20°C, RHS, in water at 20°C⁶. Regions 5 and 6 are areas of molecular complex/ starting material mixture, 1 a undersaturated solution, 2 and 4 is regions of solid starting material and 3 where the molecular complex is form. The letters indicate starting points of solubility curves.

3.1.3 Solvent-Free Co-crystallisation

Solvent-free co-crystallisation involves the grinding together of the component molecules. There are various techniques and methodologies that come under the umbrella term of solvent-free co-crystallisation (see Section 1.5), two of which were used during this research: solvent-free grinding and solvent drop grinding. Both these methods involve the grinding of the co-molecules with a mortar and pestle (Figure 3.4) for roughly three minutes, with the solvent drop grinding method including adding trace amounts of solvent. In all cases, the product was then stored at room temperature.



Fig. 3.4 – Mortar and Pestle for use in the solvent free grinding experiments.

3.2 Single Crystal Diffractometers

Once the crystals have been grown, it is necessary to determine if they are suitable for single crystal X-ray diffraction. The quickest way is to visually examine the crystals under a polarised microscope, with three aims. Firstly, to inspect the size and shape of the crystals; those that are curved, deformed, have significant secondary crystallites (small crystals attached) or have a re-entrant angle (an interior angle of a polygon that is greater than 180 degrees) should be rejected. Next, with a polarised lens in place, crystals will transmit polarised light (with exceptions including cubic crystals); those that do not can be rejected. Lastly for those crystals that do transmit polarised light, when the polariser is turned 90° the crystal will turn dark, then when turned another 90° will turn light again. This is a sign of a good quality single crystal. If during this process only half the crystal changes colour, then the crystal is likely to be twinned. When carrying out the evaluation it is essential not to damage the crystals, for example if the crystal is taken from a non-fully evaporated vial (always advised if using the solvent evaporation technique) there is a chance if solvent is within the

crystal then it may escape. If the crystal passes these tests, the next stage is to determine how it behaves on a diffractometer. Reflections need to be of strong intensity and well shaped, not split and preferably not broadened. If the diffractometer software provides a sensible unit cell which is not already published in the CSD⁷ then it is likely that an unknown structure is under investigation and a full data collection scan can be initiated.

They were three different diffractometers used in this project with two distinct types of detectors. A Nonius / Bruker Kappa with a CCD area detector⁸, a Bruker APEX-II⁹ also with a CCD area detector, and a Rigaku R-Axis RAPID¹⁰ equipped with an image plate area detector (Figure 3.5).



Fig. 3.5 –left to right, the Nonius / Bruker Kappa CCD, Bruker APEX-II and Rigaku R-Axis RAPID.

All the diffractometers used a Mo/K source with wavelength 0.71074\AA and were all capable of providing data collection temperatures down to 100K using sample cooling devices. Both the Nonius / Bruker Kappa and Rigaku R-Axis RAPID contained Oxford Cryosystems cryostream devices attached to a liquid nitrogen cylinder while the Bruker APEX-II used the Oxford Cryosystems Helix which normally operates using a gaseous nitrogen supply but can also allow access to temperatures as low as 20K using a helium source.

3.2.1 Nonius / Bruker Kappa CCD and Bruker APEX-II

There were slight differences between all the diffractometers in their set-up. The RAPID uses a 3-axis Eulerian goniometer while the Kappa and APEX II are both equipped with the kappa geometry, but the main difference is in the type of area detector used. The Charge Coupled Device (CCD) system is used in the Nonius / Bruker Kappa CCD and Bruker APEX-II (Figure 3.6) diffractometers. These use CCD-chips to record data and are based on a layer of fluorescent material, usually a gadolinium oxide sulphide which is sensitive to X-rays, with

the X-ray intensities collected very quickly. The downside to CCD detectors is that they can collect high levels of background, which can be reduced by cooling the chip to -50°C but this feature can make it unsuitable for long exposures which are needed for weakly scattering materials. These chips are large at 1024×1024 mm and have a resolution of 4096×4096 pixels. In order to collect all the reflection data the crystal must be rotated hence the detector is mounted on a 3- or 4- circle diffractometer.

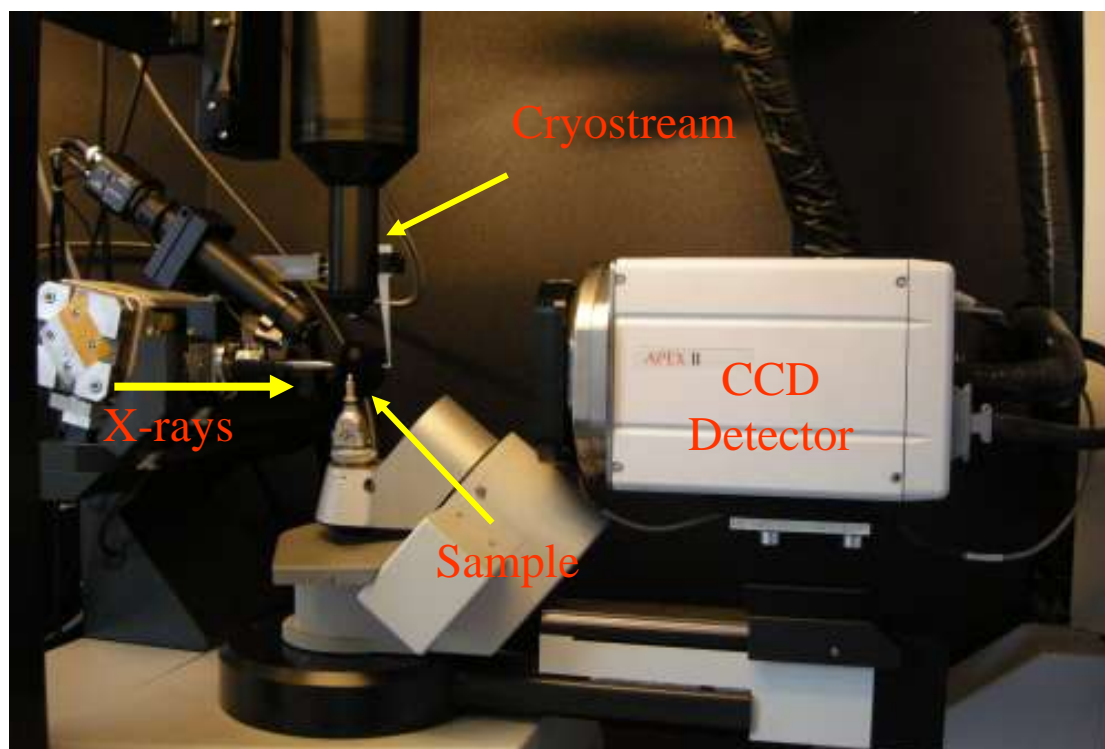


Fig. 3.6 – The working area of the Bruker APEX-II with labelling of the CCD detector, cryostream. X-ray direction and sample location.

3.2.2 Rigaku R-Axis RAPID

The Rigaku R-axis RAPID diffractometer uses a 3-axis Eulerian goniometer and has an image plate detector (Figure 3.7). The image plate has a detection size of 465mm by 258mm and works by having a layer of BaBrF doped with Eu^{2+} ; when incident X-ray quanta strike the image plate, they are converted to colour centres (free electrons in interstitial lattice sites) with the Eu^{2+} being oxidised to Eu^{3+} . The resulting image on the plate is read by a laser scanner in a similar manner to how a CD is read. The laser causes the free electrons to reduce back to Eu^{2+} , this produces an emission of photons in blue-green region of the visible spectrum, these photons can be measured using a photocell with a photomultiplier (extremely

sensitive detectors of light in the UV, Vis, near IR and electromagnetic regions which multiple the current produced by the incident light by as much as 100 million times). Once the plate has been read it is exposed to intense white light to remove any remaining colour centres and is ready for re-use. This reading process takes longer than the read-out on CCD systems, however the image plate detectors collect very low backgrounds and are almost exclusively sensitive to scattered X-ray radiation. The large detector size makes it possible to measure an entire data collection by limited rotations of the crystal, and the image plates are cheaper to manufacture than CCD systems.

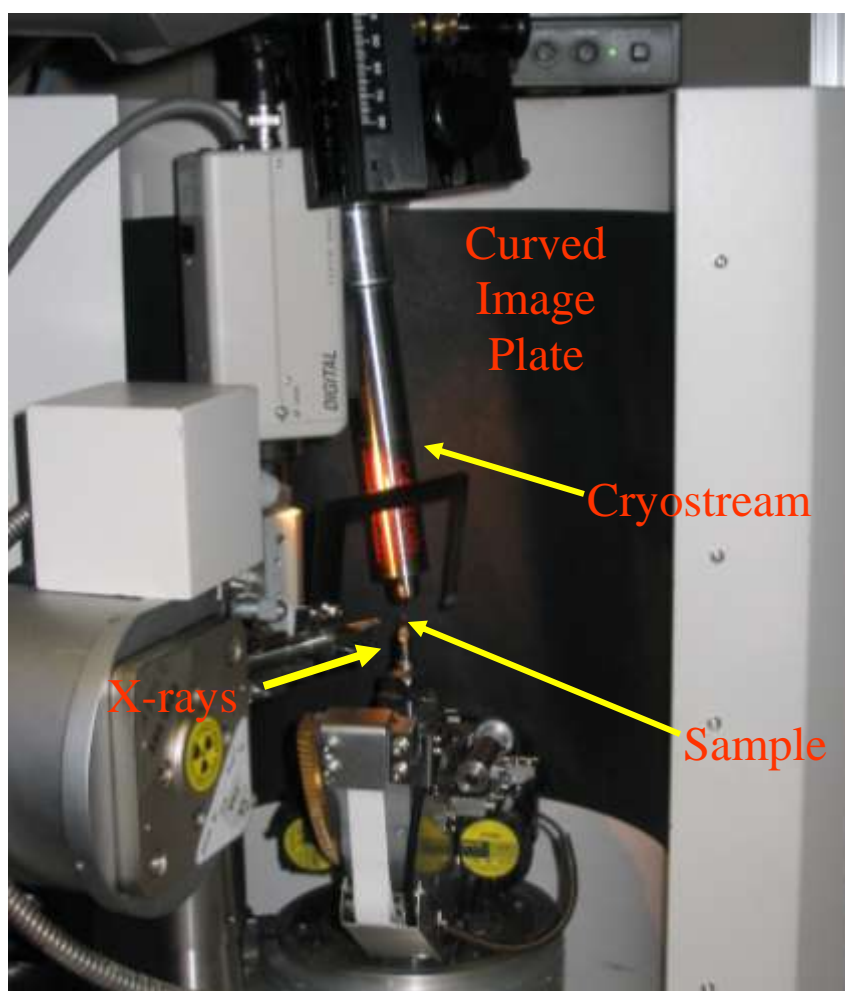


Fig. 3.7 –The Rigaku R-Axis RAPID diffractometer with labelling of the image plate, cryostream. X-ray direction and sample location.

3.2.3 Data Collection and Structure Solution

All the diffractometers have specific software that guide the user through the process of indexing to data collection, to producing the *.hkl* file that can then be used to solve the structure. In all the diffractometers the unit cell is determined by collecting a small set of frames. These frames are indexed as set out in section 2.2.4 to produce the primitive unit cell, crystal system and Bravais lattice. It is always advisable at this stage to choose the lowest possible symmetry lattice to ensure sufficient data is collected during the full data collection. A data collection strategy is then calculated, with collections typically lasting between a few hours to a day depending on the unit cell size, symmetry and atom form factors of the crystal, however in all cases a completeness level of 100% with high redundancy is always aspired to. Once the full data collection strategy has finished, the data needs to be integrated. At this stage it can be wise to re-determine the unit cell and symmetry of the crystal to ensure that weaker reflections, that may be lost in the initial quick scans, are accounted for. During the integration process the software scans a rectangular or elliptical area around the predicted position for each reflection with all the pixels summed to give the raw intensity, with the edges of the area used to estimate the background. The background is subtracted from the raw intensity to give the net reflection intensity. This net intensity is subjected to several correction methods in the data reduction program, including L_p correction, Lorentz factor, standard extinction and absorption corrections. Once these are complete a *.hkl* file is produced. The *.hkl* file is then input into a structure solution and refinement program such as CRYSTALS¹¹ or WINGX¹² to solve the structure (see section 2.3 for details of this process). Analysing the solved structure is normally achieved using a structure visualisation program such as MERCURY¹³.

3.3 Powder Diffraction

The powder diffractometer used during this research was a Bruker D8 Advance¹⁴ (Figure 3.8) equipped with a Mo/ K_α source and capillary holder. The layout is identical to that shown in Figure 3.6, using the reflection geometry but with the capillary holder instead of the flat plate. Most experiments used a capillary of diameter 0.7mm, however smaller ones were used when more accurate data was required. The typical scan range covered a 2θ range of 3 to 50° with a scan rate of roughly 1° per minute. Analysing and comparing the collected powder patterns were achieved using initially the Eva¹⁵ program supported by Bruker then latterly with

HighScore Plus¹⁶ from PANalytical. The majority of powder patterns displayed throughout the chapters are visualised from the HighScore Plus software.



Fig. 3.8 – LHS, the Bruker D8 Advance used for powder X-ray diffraction; RHS, the Q200 DSC.

3.4 Differential Scanning Calorimetry (DSC)

The DSC used was a Q200 differential scanning calorimeter from TA Instruments (Figure 3.7, right)¹⁷. Analysis of the thermograms was carried out through the Universal Analysis 2000¹⁸ software produced by TA instruments.

3.5 References For Chapter 3

- (1) W. Massa, *Crystal Structure Determination*, Springer, 2003.
- (2) J. Hulliger, *Angewandte Chemie International Edition*, 1994, **106**, 151-171.
- (3) Reactarray Microvate – <http://www.reactarray.com/>
- (4) Asynt Magnetic Hotplate Stirrer – <http://www.asynt.com/>
- (5) S. J. Nehm, B. Rodriguez-Spong, N. Rodriguez-Hornedo, *Crystal Growth and Design*, 2006, **6**, 592-600
- (6) R. A. Chiarella, R. J. Davey and M. L. Peterson, *Crystal Growth and Design*, 2006, **7**, 1223-1226
- (7) F. H. Allen, *Acta Crystallographica section B*, 2002, **58**, 380-388.
- (8) Nonius Kappa-CCD Four circle diffractometer - <http://www.nonius.nl/products/>
- (9) APEX2: Bruker AXS, 2007 - <http://www.bruker-axs.com/>
- (10) CRYSTALCLEAR: Rigaku - <http://www.rigaku.com/software/crystalclear.html>
- (11) D. J. P. Watkin, C.K., Carruthers, J.R., Betteridge, P.W., Cooper, R.I., , *Journal of Applied Crystallography*, 2003, **36**, 1487.
- (12) L. J. Farrugia, *Journal of Applied Crystallography*, 1999, **32**, 837-838.
- (13) C. F. Macrae, P. R. Edgington, P. McCabe, E. Pidcock, G. P. Shields, R. Taylor, M. Towler and J. van de Streek, *Journal of Applied Crystallography*, 2006, **39**, 453-457.

- (14) Bruker D8 Advance – http://www.bruker-axs.com/d8_advance.html
- (15) Powder Diffraction Software – <http://www.bruker-axs.com/eva.html>
- (16) Powder Diffraction Software – <http://www.panalytical.com/index.cfm?sid=212>
- (17) DSC instrument – <http://www.tainstruments.co.uk/product/>

4 Towards Selective Molecular Complex Formation: Challenging Crystal Engineering

This chapter will focus on co-crystallisation experiments with the aim of using a systematic series of related complexes to generate a library of interactions which could be used to engineer new molecular complexes.

Crystal engineering (refer to Section 1.3) is seen as the bottom-up construction of functional materials from molecular or ionic building blocks¹. These building blocks are commonly known as supramolecular synthons defined by Desiraju as “*structural units within supermolecules which can be formed and or assembled by known or conceivable synthetic operations involving intermolecular interactions*”²

Crystal engineering uses many strategies in forming supramolecular synthons; most common is using the understanding of hydrogen and coordination bonds, while more recently increasing attention has been applied to the weaker and less predictable halogen bonds³ and π - π interactions⁴.

This chapter will focus on the synthons and hydrogen bond motifs created between benzimidazole, carboxylic- and hydroxyl- functional groups. Application of a library of complexes containing identical functional groups can allow simple motifs to be engineered to form predictable structures. This chapter will also investigate the differences between the structures by studying the role of weaker interactions, the ratios of molecules in the complexes, the effects of solvates and the effects on physical properties such as densities and melting points of the complexes generated.

Lastly the chapter will investigate the use of solvent-free method of co-crystallisation. Solvent-free co-crystallisation has increasingly been of importance for crystal engineers as these processes have been found to provide a simple route to the preparation of new materials and new polymorphic and solvate forms.

4.1 Introduction – Hydroxybenzoic Acids

Hydroxybenzoic acids are very important chemicals in many areas of industry, for example, 2-hydroxybenzoic acid is the main starting material for the preparation of aspirin (2-acetoxybenzoic acid; acetylsalicylic acid). However, they are also widely used in crystal engineering studies due their ability to form predictable synthons and presence of multiple hydrogen bonding sites, reflected in the large number of hydroxybenzoic acid molecular complexes found in the CSD.

4.1.1 2-Hydroxybenzoic Acid

2-hydroxybenzoic acid, commonly known as salicylic acid, is a naturally occurring organic acid named after the Latin for willow tree, *salix*. Salicylic acid has many uses, most of which are medicinal in nature. For example it is well known for reducing aches, pains and fevers. It is also a raw material in the production of various drugs including, rubefacient (ache relief), keratolytic⁵ (treatment to remove warts) and non-steroidal anti-inflammatory drugs.

The most recent study of its structure (Figure 4.1) was carried out in 2006 by P. Munshi⁶ (CSD ref SALIAC16).

The main motif is, as might be expected, a carboxylic acid dimer reinforced by a hydroxyl – carbonyl intramolecular hydrogen bond. There are a host of molecular complexes involving salicylic acid and its de-protonated form with co-

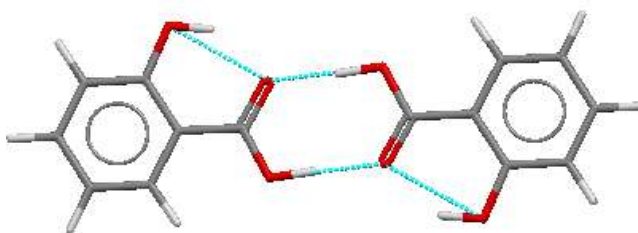


Fig. 4.1 – The main hydrogen bonds in the salicylic acid structure

molecules in the CSD, within which there is roughly a 4:3 ratio in favour of the protonated form. Salicylic acid has also been used to form coordination complexes with a range of metals, including a series of lanthanide metals, such as cerium, praseodymium, gadolinium and terbium. Of particular interest amongst the molecular complexes that are not deprotonated are those with co-molecules 3,5-dimethyl-1H-pyrazole⁷ (CSD ref^o ODOHEV) and 9H-purin-6-amine⁸ (CSD reference MUBRUD) which both contain an available basic nitrogen that might be expected to encourage de-protonation of the salicylic acid.(Figure 4.2).

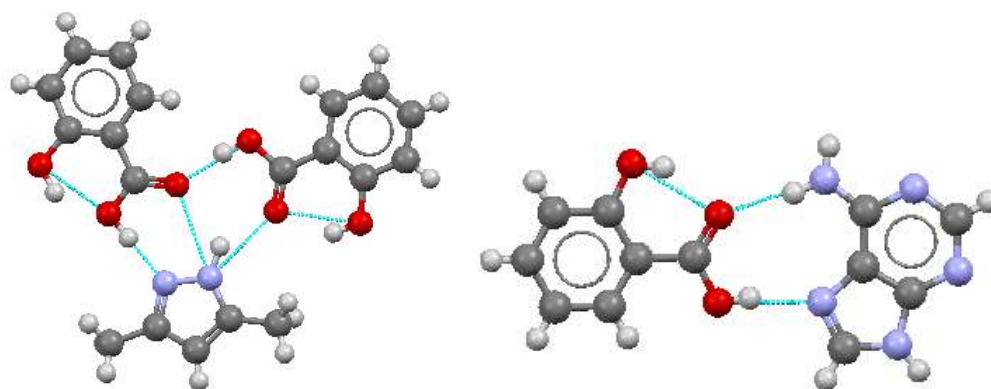


Fig. 4.2 – LHS – The main supramolecular synthons in the bis(2-hydroxybenzoic acid) 3,5-dimethyl-1H-pyrazole molecular complex, RHS, the tris(2-hydroxybenzoic acid) 9H-purin-6-amine molecular complex which contains two moderate hydrogen bonds between the co-molecules.

Of the deprotonated molecular complexes of salicylic acid (2-hydroxybenzoate) with another small organic molecule, the atom that is protonated on the second component is always a basic nitrogen. For example the 2-hydrobenzoate 2-amino-pyridine⁹ molecular complex (CSD reference SLCADB) and adeninium 2-hydroxybenzoate methanol¹⁰ (CSD reference LOLDIA) shown in Figure 4.3, both show a dimer of hydrogen bonds with proton transfer occurring.

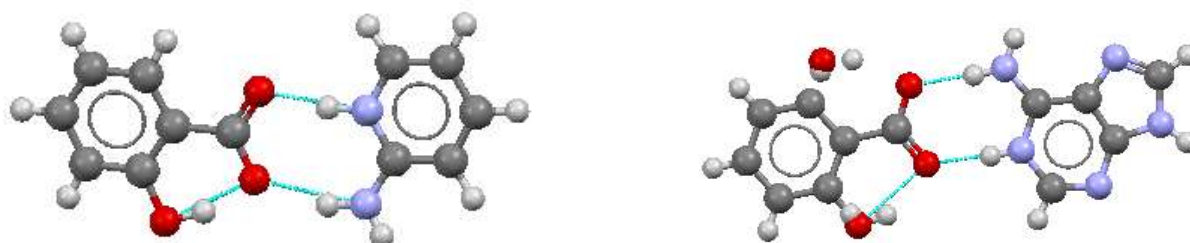


Fig. 4.3 – LHS - the main supramolecular synthon between salicylic acid and 2-amino-pyridine, RHS, the adeninium 2-hydroxybenzoate methanol molecular complex.

4.1.2 3-Hydroxybenzoic Acid

3-hydroxybenzoic is mostly used in the agrochemical sector, for example it is an ingredient in the production of the synthetic soy bean herbicide metsulfuron, broad-leaved herbicides lactofen and acifluorfen and in the creation of fungicides¹¹. It has also been used as an intermediate in the production of high-grade paints and preservatives¹².

3-hydroxybenzoic acid has two polymorphs; a monoclinic form (Figure 4.4 LHS) (CSD reference BIDLOP) and an orthorhombic form (Figure 4.4 RHS) (CSD reference BIDLOP01). These structures have two distinct hydrogen bonding motifs: the monoclinic form has the predictable carboxylic acid dimer with weaker hydrogen bonds between the hydroxyl group holding these dimers together. The orthorhombic form, on the other hand, is constructed of linear chains with the carboxylic acid groups hydrogen bonding to hydroxyl groups from two different molecules.

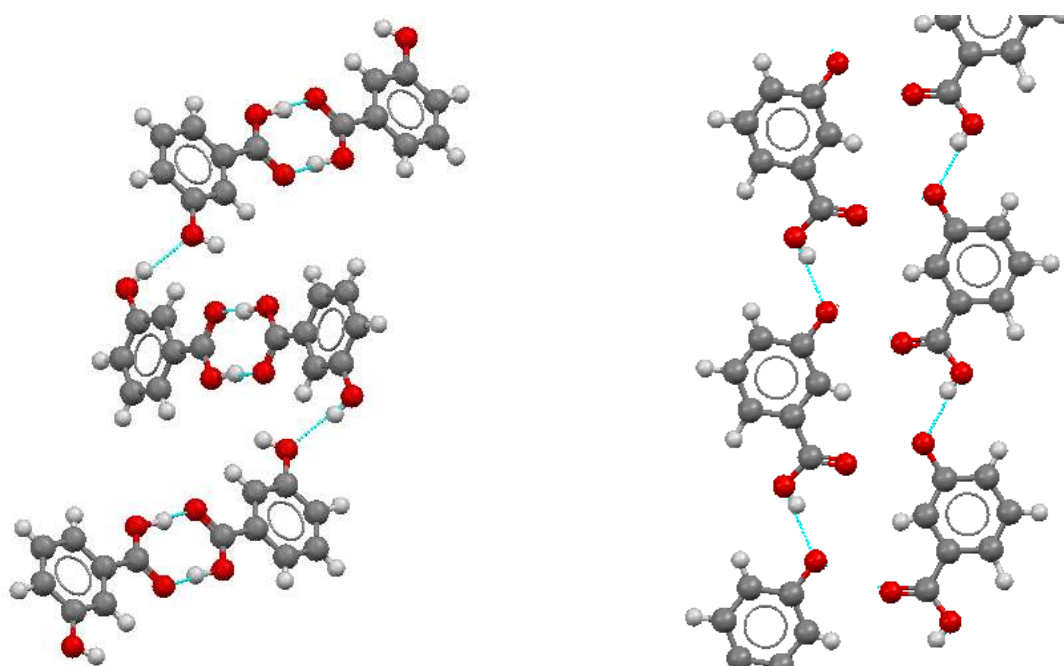


Fig. 4.4 – LHS, the monoclinic form of 3-hydroxybenzoic acid exhibiting the carboxylic acid dimer motif; RHS, the linear chains of the orthorhombic form of 3-hydroxybenzoic acid, the full compliment of protons was not published with the structure.

3-hydroxybenzoic acid has been successfully cocrystallised with a range of small organic molecules including nicotinamide (Figure 5.5) (CSD reference XAQQIQ), isonicotinamide (CSD reference LUNMEM), quinoxaline (CSD reference HONMEM), and 4,4'-bipyridine¹³ (CSD reference HONVAI). There are currently only six structures in the CSD involving the deprotonated form of 3-hydroxybenzoic acid^{14,15}. The molecular complex with 4-aminopyridinium¹⁵ (CSD reference MOYRAU) (Figure 4.5 RHS) has a hydrogen bonded ring system, R_4^4 (18), as the main motif.

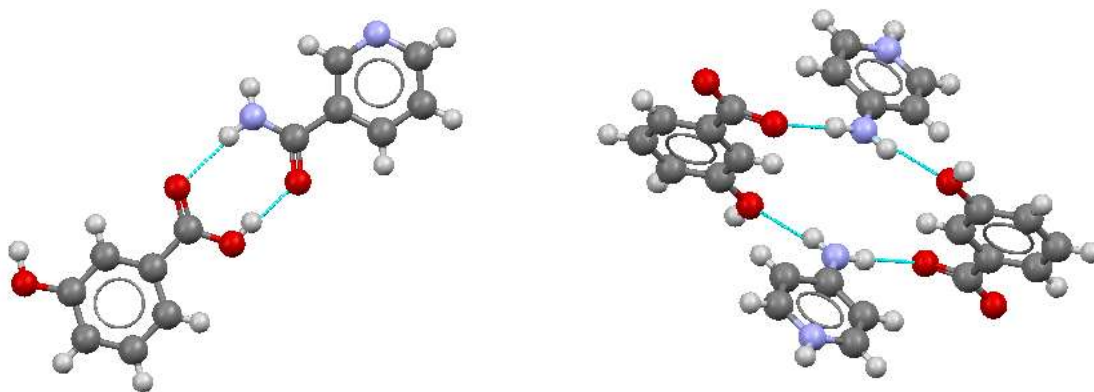


Fig. 4.5 – LHS, the 4-hydroxybenzoic acid nicotinamide supramolecular synthon. These hydrogen bond dimers are connected through a hydrogen bond between the hydroxyl and the heteroatom in the ring of the nicotinamide; RHS, the four molecule hydrogen bonded ring between 3-hydroxybenzoic acid and 4-aminopyridinium.

4.1.3 4-Hydroxybenzoic Acid

4-hydroxybenzoic acid is used in the production of parabens which are a class of chemicals that are used as preservatives in cosmetics and drugs. These compounds, and their salts, are used primarily for their bactericidal and fungicidal properties. They can be found in shampoos, commercial moisturisers, shaving gels, personal lubricants, pharmaceuticals, spray tanning solution and toothpaste.

The structure of 4-hydroxybenzoic acid was first determined in 1992 (CSD reference JOZZIH¹⁷) and has the predictable carboxylic acid dimer as the main motif with the hydroxyl groups hydrogen bonding together to generate the expanded structure (Figure 4.6).

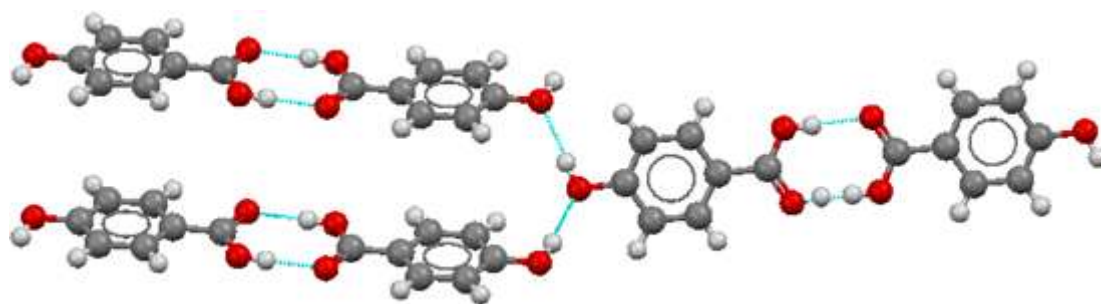


Fig. 4.6 – The carboxylic acid dimer motif and hydroxyl hydrogen bonds found in the structure of 4-hydroxybenzoic acid.

There are a host of molecular complexes where the 4-hydroxybenzoic acid exists in its natural and deprotonated form, highlighting its use in crystal engineering and MOF studies. The natural form has been cocrystallised with many other small organic molecules, namely nitrogen containing heterocyclic compounds, with the deprotonated form being found with a range of co-molecules including metals and organic molecules.

4.1.4 2,4-Dihydroxybenzoic Acid

2,4-dihydroxybenzoic acid, also known as β -resorcylic acid is a starting material for the production of dyestuffs, pharmaceuticals, reprographic chemicals, cosmetic preparations, and fine organic chemicals¹⁸. The crystal structure was intensely studied within the group in 2007¹⁹ to investigate the proton behaviour within the hydrogen bonds (CSD reference ZZZEEU01-04). The structure exhibits a 6-membered hydrogen bonded ring system, R_6^6 (36), utilising all of the potential hydrogen bonding sites (Figure 4.7).

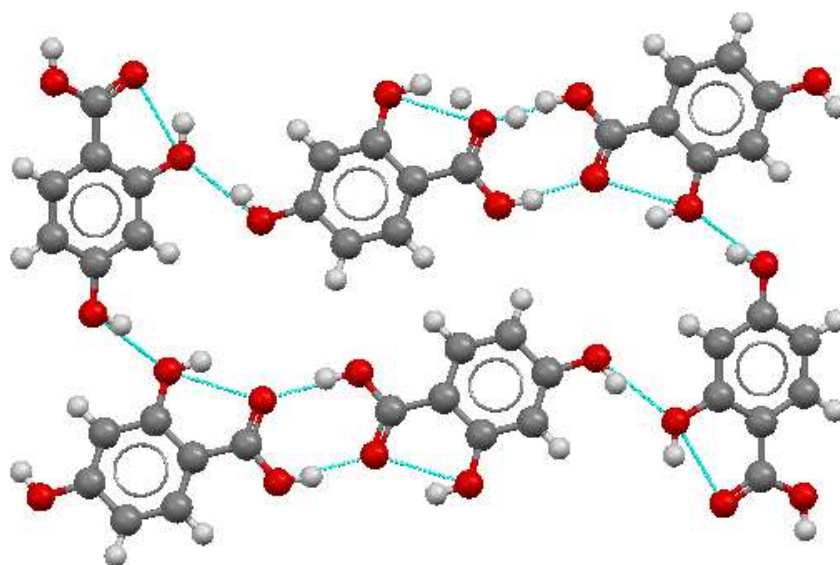


Fig. 4.7 – The ring system of the 2,4-dihydroxybenzoic acid structure.

There are a few molecular complexes with 2,4-dihydroxybenzoic acids reported; of most interest here is the protonated form with imidazole²⁰ (CSD reference HEFTUI). This complex structure basically consists of a criss-cross pattern, with each 3-dimensional box consisting of two of each of the co-molecules (Figure 4.8)

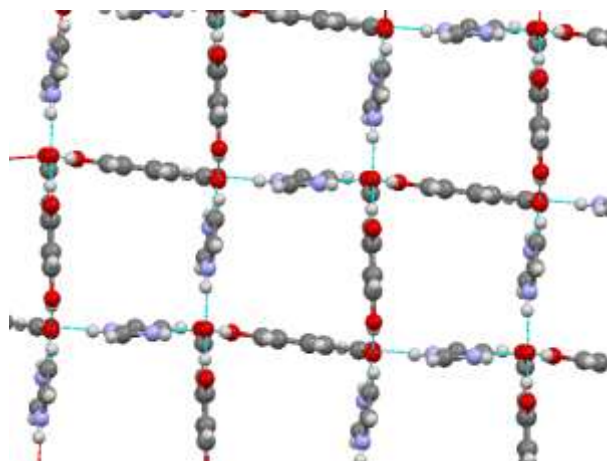


Fig. 4.8 – The criss-cross pattern of the imidazolium 2,4-dihydroxybenzoate molecular complex.

4.1.5 2,6-Dihydroxybenzoic Acid

2,6-dihydroxybenzoic acid, also known as γ -resorcylic acid, is used as an antioxidant excipient in some pharmaceutical preparations. There are two known polymorphs, a monoclinic form²¹ (Figure 4.9 LHS) (CSD reference LEZJAB01) and an orthorhombic form²² (Figure 4.9 RHS) (CSD reference LEZJAB). The monoclinic form exhibits the carboxylic acid dimer motif with the intramolecular hydrogen bonds contributing to this to the distinct dimer. In the orthorhombic form, a greater variety of hydrogen bonds is present, creating an interlinked structure. There are no molecular complexes of any form containing 2,6-dihydroxybenzoic acid in the CSD.

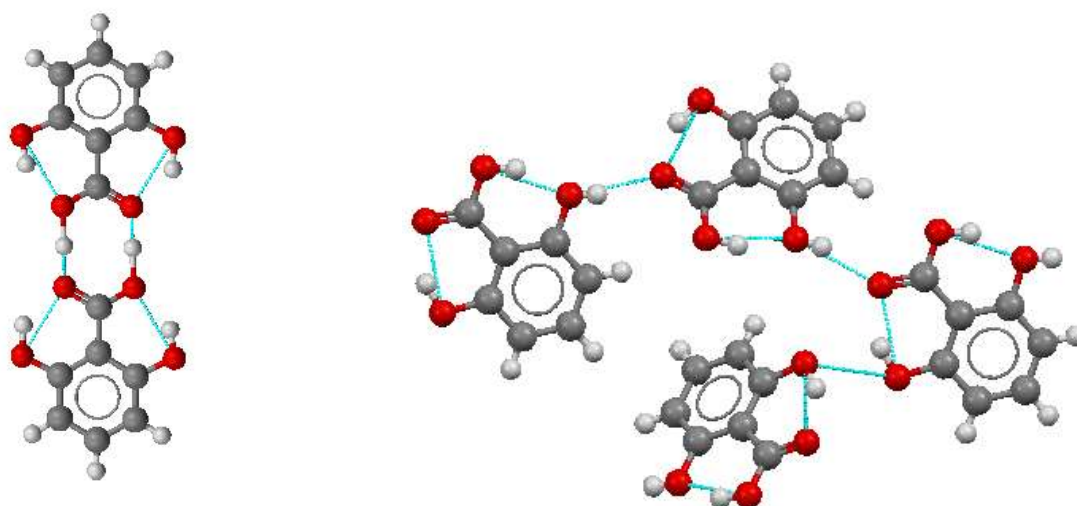


Fig. 4.9 – LHS monoclinic form of 2,6-dihydroxybenzoic acid showing its carboxylic acid dimer motif, RHS orthorhombic forms of 2,6-dihydroxybenzoic acid showing a more linear pattern with single hydrogen bonds between molecules.

4.1.6 3,4-Dihydroxybenzoic Acid

3,4-dihydroxybenzoic acid, also known as protocatechuic acid, is used as an anticancer agent. It has mixed effects on normal and cancer cells in in vitro and in vivo studies²³. 3,4-dihydroxybenzoic acid has been reported to induce apoptosis of human leukemia cells, as well as malignant HSG1 cells taken from human oral cavities, but found to have mixed effects on TPA-induced mouse skin tumours^{24,25}. Depending on the amount of 3,4-dihydroxybenzoic acid and the time before application, it can have the effect of reducing or enhancing tumour growth²⁶. Only the structure of the hydrate form is reported (CSD reference BIJDON03)²⁷ and 3,4-dihydroxybenzoic acid is also reported within a cadmium complex²⁸ (CSD reference RUMDAE).

4.1.7 3,5-Dihydroxybenzoic Acid

3,5-dihydroxybenzoic acid, also known as α -resorcylic acid, is used as an intermediate for the synthesis of many pharmaceuticals and in synthetic resins. The crystal structure of 3,5-dihydroxybenzoic acid has yet to be reported, however it is known to form molecular complexes with other small organic molecules including BZN²⁹ (CSD reference XAZMIV). This molecular complex forms in a 1:1 ratio; the reported structure determination is at room temperature. The main motif in this structure is a hydrogen bonded ring system R_4^4 (22) (Figure 4.10). Proton transfer has occurred with the carboxylic acid group losing a hydrogen to the initially non-protonated nitrogen on the benzimidazole.

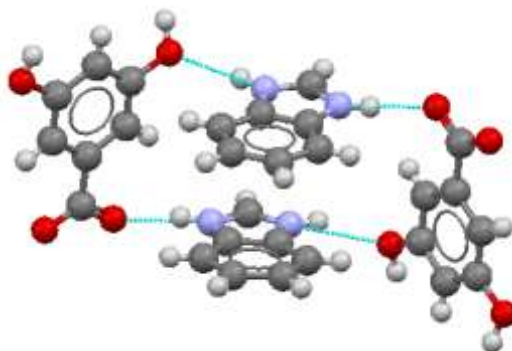


Fig. 4.10 – The structure of benzimidazole and 3,5-dihydroxybenzoic acid with its hydrogen bonded ring system.

4.2 Summary of Molecular Complexes Produced

Co-crystallisation experiments have produced an array of molecular complexes of BZN with mono-hydroxybenzoic acids, polymorphic forms of starting materials, and one di-hydroxybenzoic acid molecular complex.

The BZN and mono-substituted benzoic acids crystal structures have been analysed primarily using single crystal X-ray diffraction due to the facile precipitation of single crystals. Single crystal neutron diffraction data collected on the VIVALDI instrument at the ILL facility in Grenoble, France were also obtained for a range of these complexes. The aim of the neutron experiments was to allow accurate location of the hydrogen atoms and investigation of the extended hydrogen bonded networks and proton transfer effects present in these systems.

The hydroxybenzoic acid : benzimidazole molecular complexes exhibited an increased level of complexity, with the potential to adopt different ratios of co-molecules to BZN. The BZN molecule is an efficient hydrogen atom abstractor from carboxylic acid groups, however the presence of an additional hydrogen bond donor in the form of a hydroxyl group, introduces competition for hydrogen bonding with the carboxylate group. The complexes found are summarised in Table 4.1, illustrating the diverse range of molecular complexes obtained.

Benzimidazole	1:1 - ratio	1:2 - ratio	2:1 - ratio
2-hydroxybenzoic Acid	Blue	Blue	Grey
3-hydroxybenzoic Acid	Blue	Grey	Two Polymorphs
4-hydroxybenzoic Acid	Grey	Blue	Blue

Table 4.1 – Summary of the molecular complexes successfully generated (blue) between benzimidazole and mono-substituted hydroxybenzoic acids. Grey indicates where no molecular complex has been identified from single crystal X-ray diffraction.

The main aim of this work was to engineer molecular complexes with predictable hydrogen bonded units using knowledge of previously obtained motifs. The mono-substituted hydroxybenzoic acids co-crystallisation experiments gave a diverse library of such motifs and attempts were made to make molecular complexes with a range of di- substituted benzoic acids, in attempts to explore the robustness of the motifs found. However, in these

experiments only 3, 5-dihydroxybenzoic acid successfully generated crystals of a molecular complex (Table 4.2).

	2,4-diOH-BA	2,6-diOH-BA	3,4-diOH-BA	3,5-diOH-BA
Benzimidazole				

Table 4.2 – Summary of the results from the co-crystallisation experiments between benzimidazole and a selection of dihydroxybenzoic acids. Blue indicates where a new molecular complex has been found from single crystal X-ray diffraction data, grey indicates where there has been none.

As a further level of complexity, it is clear that even using the most apparently predictable motifs, structural diversity is frequently found; also reported here are the formation of polymorphs of the molecular complex of benzimidazole and 3-hydroxybenzoic acid, induced by solvent effects.

Experiments involving solvent free co-crystallisations were successful in verifying the ability of this relatively new technique to produce known forms, and in addition highlighted potential new molecular complexes. This method led to two new structurally determined molecular complexes: benzimidazolium 5-chloro-2-hydroxybenzoate and benzimidazolium aspartate.

4.2.1 Benzimidazolium – Proton Transfer

In cases where the crystallisation product is in a 1:1 stoichiometric ratio of benzimidazole and a carboxylic acid containing molecule, the benzimidazole is protonated through hydrogen transfer from the carboxylic acid group onto the normally unprotonated nitrogen atom in the five-membered ring, creating a benzimidazolium molecule (BZNH^+) (Figure 4.11). The result of the proton transfer on the benzimidazolium molecule is a delocalisation of the charge across the five-membered ring, reflected in the equalisation of the internal bond lengths $\text{N}^{\delta+}\text{-C}$ and bond angles $\text{C-N}^{\delta+}\text{-C}$. The delocalisation of the charge has the effect of creating a partial positive charge on both nitrogens. This effect has been reported in many structures involving BZN and IMD.

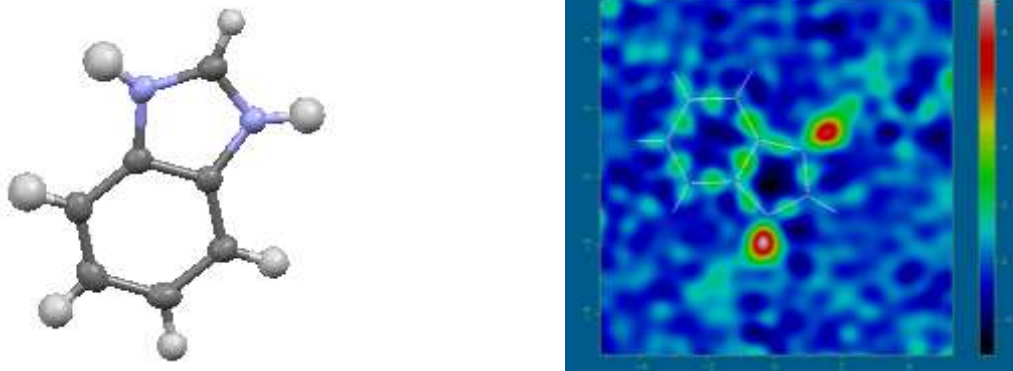


Fig. 4.11 – LHS, a typical benzimidazolium molecule in which both nitrogens are protonated. RHS, the Fourier difference map generated where both the H atoms located on a nitrogen atom has been omitted from the model, clearly showing that both nitrogen atoms are protonated.

The consequence for the co-molecule that has been deprotonated is the creation of a negative charge, which is delocalised over the carboxylic acid group resulting in equalisation of the C-O and C=O bond lengths in the carboxylate group.

4.2.2 Potential Hydrogen Bonds and Supramolecular Synthons

Consideration of the co-molecules involved in these sets of results would point to a series of possible hydrogen bond patterns and supramolecular synthons that could be generated (Figure 4.12). All of these hydrogen bond patterns have many examples in the CSD and have been of interest in their own right.

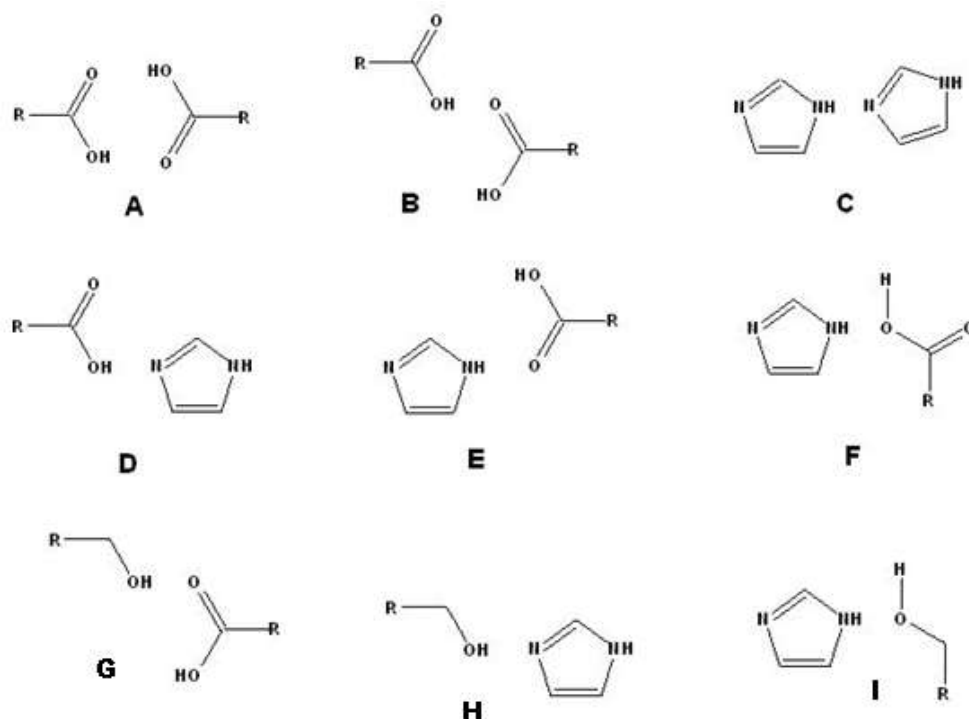


Fig. 4.12 – Hydrogen bonding patterns that could lead to the formation of supramolecular synthons in the generation of crystal structures of the molecular complexes studied in this chapter. The potential homo-hydrogen bonds (A, B and C) and hetero-hydrogen bonds (D, E and F) that can be exhibited between a benzimidazole and carboxylic acid group. Hydrogen bonds G, H and I are those that could be generated between a benzimidazole and hydroxyl group.

The formation of the molecular ion species in many of the molecular complexes reduces the potential hydrogen bonds from those depicted in Figure 4.12, for example the homo-hydrogen bonds A, B and C. Consequentially it also promotes the charged derivatives of certain hydrogen bonds, namely E, F and G (Figure 4.13). These hydrogen bond patterns utilise the charged species in the creation of the hydrogen bonds, which are inherently stronger. There are examples of hydrogen bond patterns E, F and G through-out the molecular complexes generated in this chapter and Table 4.3 bonds summarises the full hydrogen bond data.

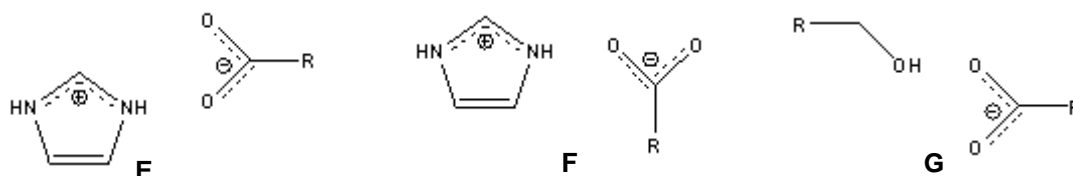


Fig. 4.13 – The derivatives of hydrogen bond patterns E, F and G that occur when there has been proton transfer.

Molecular Complexes		BZNH ⁺ 2-HBA ⁻	BZNH ⁺ 3-HBA ⁻	BZNH ⁺ 4-HBA ⁻	BZN BZNH ⁺ 3-HBA ⁻ II	BZN BZNH ⁺ 3-HBA ⁻ I	BZN BZNH ⁺ 4-HBA ⁻ hydrate	BZNH ⁺ 2- HBA ⁻ 2-HBA	BZNH ⁺ 3,5-HBA ⁻
Hydrogen Bonds									
N ^{δ+} - H...O ^{δ-} E and F	D...A(Å)	2.646(1) 2.621(1)	2.700(1) 2.697(1)	2.689(3) 2.717(2)	2.751(2) 2.748(2)	2.644(2) 2.814(2)	2.641(2)	2.709(2) 2.672(1)	2.700(1)
	D-H(Å)	0.99(2) 0.99(2)	0.88(1) 0.90(1)	0.91(3) 0.93(3)	0.84(3) 0.94(3)	0.92(2) 0.98(2)	0.96(3)	0.91(3) 0.91(2)	0.92(2)
	H...A(Å)	1.67(2) 1.64(2)	1.82(1) 1.80(1)	1.78(3) 1.79(3)	1.93(3) 1.81(3)	1.68(2) 1.89(2)	1.72(3)	1.81(3) 1.80(2)	1.79(2)
	D-H...A angle(°)	169(2) 171(2)	178(1) 173(1)	173(3) 170(3)	165(3) 177(2)	165(2) 177(2)	161(2)	173(2) 161(2)	167(2)
	D...A(Å)	-	2.654(1)	2.602(2) 2.605(2)	2.660(2)	2.540(1) 2.565(1)	2.634(2)	2.605(1)	2.625(1) 2.640(1)
	D-H(Å)	-	0.87(1)	1.02(3) 0.94(3)	0.92(3)	0.97(2) 1.02(2)	0.91(3)	0.99(2)	0.92(2) 0.95(2)
	H...A(Å)	-	1.79(1)	1.60(3) 1.69(3)	1.74(3)	1.57(2) 1.55(2)	1.72(3)	1.62(2)	1.70(2) 1.69(2)
	D-H...A angle(°)	-	172(1)	166(3) 166(3)	178(3)	173(2) 179(2)	174(3)	174(2)	177(2) 178(2)
O- H...O ^{δ-} G	D...A(Å)	-	2.654(1)	2.602(2) 2.605(2)	2.660(2)	2.540(1) 2.565(1)	2.634(2)	2.605(1)	2.625(1) 2.640(1)
	D-H(Å)	-	0.87(1)	1.02(3) 0.94(3)	0.92(3)	0.97(2) 1.02(2)	0.91(3)	0.99(2)	0.92(2) 0.95(2)
	H...A(Å)	-	1.79(1)	1.60(3) 1.69(3)	1.74(3)	1.57(2) 1.55(2)	1.72(3)	1.62(2)	1.70(2) 1.69(2)
	D-H...A angle(°)	-	172(1)	166(3) 166(3)	178(3)	173(2) 179(2)	174(3)	174(2)	177(2) 178(2)

Table. 4.3 – The three scalar quantities and bond angle of the hydrogen bonds of N^{δ+}-H...O^{δ-} and O-H...O^{δ-} found in the molecular complexes presented in Section 4.5.

4.3 Crystallographic Data

Compound	BZNH ⁺ 2-HBA ⁻	BZNH ⁺ 3-HBA ⁻	BZNH ⁺ 4-HBA ⁻
Formula	C ₇ N ₂ H ₇ , C ₇ O ₃ H ₅	C ₇ N ₂ H ₇ , C ₇ O ₃ H ₅	C ₄₂ N ₃₆ H ₈ O ₃₆
ΔpKa (1:1)	4.01	2.91	2.42
Crystallisation Conditions	Methanol, room temperature	Acetone, 40°C	Methanol, ~-2-4°C
Molecular weight / gmol ⁻¹	256.26	256.26	748.80
Temperature (K)	100	100	100
Space Group	<i>P</i> 2 ₁ / <i>c</i>	<i>P</i> <i>b</i> <i>c</i> <i>n</i>	<i>P</i> 2 ₁ / <i>c</i>
<i>a</i> (Å)	7.2866(1)	19.7452(3)	15.2728(3)
<i>b</i> (Å)	6.6937(1)	8.6372(1)	12.0727(2)
<i>c</i> (Å)	25.0118(4)	14.6758(2)	20.6951(3)
α (°)	90	90	90
β (°)	95.428(1)	90	107.3180(10)
γ (°)	90	90	90
Volume (Å ³)	1214.46(3)	2502.86(6)	3642.86(11)
<i>Z</i>	4	8	4
θ range (°)	1.636-27.740	2.063-27.496	1-27.507
Completeness (%)	98.5	99.5	99.5
Refln Collected	42532	63734	53918
Independent	2801	2852	8314
Refln (obs.I>2sigma(I))	2334	2844	6261
R _{int}	0.0624	0.0247	0.0607
Parameters	220	220	657
GooF on F ²	0.981	1.0031	1.0800
R ₁ (Observed)	0.0384	0.0329	0.0607
R ₁ (all)	0.0482	0.0358	0.0886
wR ₂ (all)	0.1015	0.0847	0.1241

Compound	BZN BZNH⁺ 3- HBA⁻ II	BZN BZNH⁺ 3- HBA⁻ I	BZN BZNH⁺ 4- HBA⁻ hydrate
Formula	C ₂₁ H ₁₈ N ₄ O ₃	C ₂₁ H ₁₈ N ₄ O ₃	C ₂₁ H ₂₀ N ₄ O ₄
ΔpKa (1:1)	2.91	2.91	2.42
Crystallisation Conditions	Methanol, 2~4°C	Ethanol, 2~4°C	Ethanol, 2~4°C
Molecular weight / gmol⁻¹	374.39	747.79	392.41
Temperature (K)	100	100	110
Space Group	<i>P 2₁/c</i>	<i>P 2₁/c</i>	<i>P 2₁</i>
<i>a</i> (Å)	8.0799(7)	13.90550(10)	5.81540(10)
<i>b</i> (Å)	17.5606(15)	18.7934(2)	15.2726(3)
<i>c</i> (Å)	13.3960(11)	15.4338(2)	11.0557(2)
<i>α</i> (°)	90	90	90
<i>β</i> (°)	103.432(4)	114.3120(6)	102.9910(10)
<i>γ</i> (°)	90	90	90
Volume (Å³)	1848.7(3)	3675.65(7)	956.79(3)
Z	4	4	2
θ range (°)	1.946-28.805	1.448-27.486	1.890-27.211
Completeness (%)	98.5	99.9	99.6
Refn Collected	53224	81887	23409
Independent	4753	8386	2304
Refln (obs.I>2σ(I))	4737	4720	2222
R_{int}	0.0607	0.089	-
Parameters	329	645	342
GooF on F²	1.1017	0.8340	1.0103
R₁ (Observed)	0.0589	0.0397	0.0259
R₁ (all)	0.0705	0.0979	0.0272
wR₂ (all)	0.1285	0.0941	0.0657

BZNH⁺ 2-HBA 2-HBA⁻	BZNH⁺ 3,5-HBA⁻	BZNH⁺ 5-CL-2-HBA⁻	benzimidazolium aspartate
C ₇ N ₂ H ₇ , C ₇ O ₃ H ₅ , C ₇ O ₃ H ₆	C ₇ N ₂ H ₇ , C ₇ O ₅ H ₇	C ₇ N ₂ H ₇ , C ₇ O ₃ Cl H ₄	C ₇ N ₂ H ₇ , C ₄ O ₄ H ₆ N ₁
2.55	1.49		3.54
Acetone, ~2-4°C	Methanol/water, room temperature	Methanol, 40°C	Methanol/water, room temperature
394.38	272.26	290.70	251.24
100	100	100	100
<i>P -1</i>	<i>P b c n</i>	<i>P 2₁/c</i>	<i>P 2₁</i>
8.1123(5)	16.2063(14)	11.1639(14)	8.871(5)
8.6367(5)	10.5665(11)	3.8182(4)	5.076(3)
14.0347(8)	14.6614(11)	29.310(3)	12.324(7)
98.618(3)	90	90	90
104.238(3)	90	97.238(4)	103.221(7)
99.515(3)	90	90	90
921.15(10)	2510.7(4)	1239.4(2)	540.2(5)
2	8	4	2
1.528- 32.381	3.050-27.479	3.152-27.483	3.206- 27.479
99.0	99.9	99.6	99.8
32185	5260	16061	7174
6529	2885	10142	1380
5984	2880	7229	1299
0.054	0.0247	0.0624	0.021
334	229	225	215
1.2168	1.0006	1.1056	1.0267
0.0573	0.0350	0.0391	0.0257
0.0641	0.0379	0.0599	0.0270
0.1718	0.0930	0.1237	0.0655

Table. 4.4 – Crystallographic data for all the molecular complexes within chapter 4 excluding benzimidazolium and aspartate.

4.4 Structural Descriptions of the Molecular Complexes

4.4.1 Molecular Complex of Benzimidazolium and 2-Hydroxybenzoic Acid 1:1

Previous results indicate that benzimidazole will abstract a proton from the carboxylic acid group of the 2-hydroxybenzoic acid. There is a potential for the proton to come from the hydroxyl group however, this would be highly unlikely due to the inability of the negative charge, which would be generated, to be delocalised over connecting atoms thus forming an unstable phenoxide anion. Therefore the formation of a benzimidazolium 2-hydroxybenzoate salt can be predicted. In terms of the predicted hydrogen bond scheme, if the molecular ratio is 1:1 then this rules out the possible hydrogen bonds of types A, B, C, D and H.

With the formation of the benzimidazolium ion, there would then be competition for the primary hydrogen bond from this molecule between hydrogen bond types E, F and I (Figure 12). There are examples of all of these in the literature, however hydrogen bond E is much more prolific. There is also likely to be competition from the homo-hydrogen bonds, mainly A and B, as the carboxylic acid dimer is a very robust and dependable motif.

With the hydroxyl group in the 2-position, it is most likely, as in its natural structure, to hydrogen bond to the double bonded oxygen on the carboxylic acid group. There will be potential for it to be involved in weak hydrogen bonds with a motif similar to that seen in hydrogen bond I.

There are many competing factors, however it would be reasonable to predict the formation of the charged species with the main hydrogen bonds being of forms E, F, G or I.

Structure Description

The molecular ions, BZNH^+ and 2-hydroxybenzoate (2-HBA^-) form a 1:1 molecular complex, or salt. The molecular complex was obtained using the solvent evaporation method, with a 1:1 stoichiometric mixture of BZN (12mg) and 2-hydroxybenzoic acid (2-HBA) (14mg) dissolved in the minimum amount of methanol followed by evaporation at room temperature.

The crystals generated were cubic shaped and colourless. Single crystal X-ray diffraction data were obtained using a Bruker-Nonius Kappa CCD diffractometer at 100K, equipped with graphite monochromated Mo K α radiation ($\lambda = 0.71073 \text{ \AA}$). The structure was solved using SIR92³⁰ within the CRYSTALS³¹ program. The crystallographic data are summarised in Table 4.4 with the interactions involved in the molecular complex outlined in Table 4.5.

In the molecular complex, the BZN molecule is protonated through hydrogen transfer from the carboxylic acid group on the 2-HBA, as described in section 4.2.1 (Figure 4.14). The result is that the internal bond lengths are now normalised, to N1 ^{δ^+} -C1 1.325(3) \AA and N2 ^{δ^+} -C1 1.326(3) \AA , and bond angles to C1-N1 ^{δ^+} -C2 108.05(19) $^\circ$ and C1-N2 ^{δ^+} -C7 108.31(18) $^\circ$.

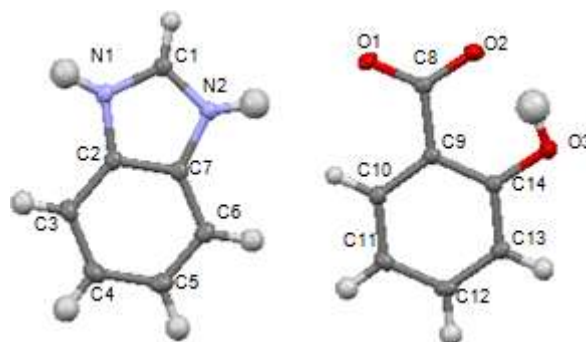


Fig. 4.14 – The BZNH⁺ and 2-HBA⁻ ions which are generated in the molecular complex/salt, with atom labelling.

Interaction	Length (\AA) (D \cdots A(\AA))	For Hydrogen Bonds		
		D-H(\AA)	H \cdots A(\AA)	D-H \cdots A angle($^\circ$)
O3 \cdots O2	2.551(3)	0.93(2)	1.69(2)	153(“)
N1 \cdots O2	2.622(1)	0.99(2)	1.64(2)	171(2)
N2 \cdots O2	2.646(1)	0.99(2)	1.67(2)	169(2)
C1 \cdots O1	3.092(1)	0.97(1)	2.15(1)	164(1)
C13 \cdots O3	3.296(1)	0.97(2)	2.62(1)	125(1)
C5 $\cdots\pi$	3.676	-	-	-

Table 4.5 – The inter- and intramolecular interactions with distances found in the BZNH⁺ and 2-HBA⁻ molecular complex

The 2-HBA molecule in its native crystal structure (Section 4.1.1) is configured such that there is an intramolecular hydrogen bond between the hydroxyl and carboxylic acid groups. Within the molecular complex with BZNH⁺ this intramolecular hydrogen bond persists despite the proton transfer of a hydrogen atom to the benzimidazole. The intramolecular hydrogen bond is shorter than found in the native crystal structure with an O \cdots O distance of 2.551(3) \AA (c.f. O \cdots O distance of 2.6191(3) \AA). This is due to the intramolecular hydrogen bond being charged assisted, a result of the deprotonation of the 2-HBA and is similar to that

found in other 2-HBA⁻ molecular complexes reported in the CSD. The negative charge is found to be delocalised over the carboxylic acid group indicated by the normalisation of the bond lengths in the carboxyl group, C8- O1^{δ-} 1.264(1)Å and C8- O2^{δ-} 1.273(1)Å.

The supramolecular synthon in the benzimidazolium 2-hydroxybenzoate molecular complex is constructed through partially charge assisted N^{δ+}-H...O^{δ-} hydrogen bonds between both the nitrogens of the BZNH⁺ and oxygens of the carboxylic acid group, a derivative of hydrogen bond motif E (Figure 12). These are of moderate strength, the distances being 2.622(1)Å (a) and 2.649(1)Å (b) (see Table 4.3 for full details), and arrange themselves into a four molecule hydrogen bonded ring consisting of alternating co-molecules that can be described by the graph set notation symbol R_4^4 (16). This hydrogen bonded ring system is the main motif of the system and contains two of each co-molecule (Figure 4.15).

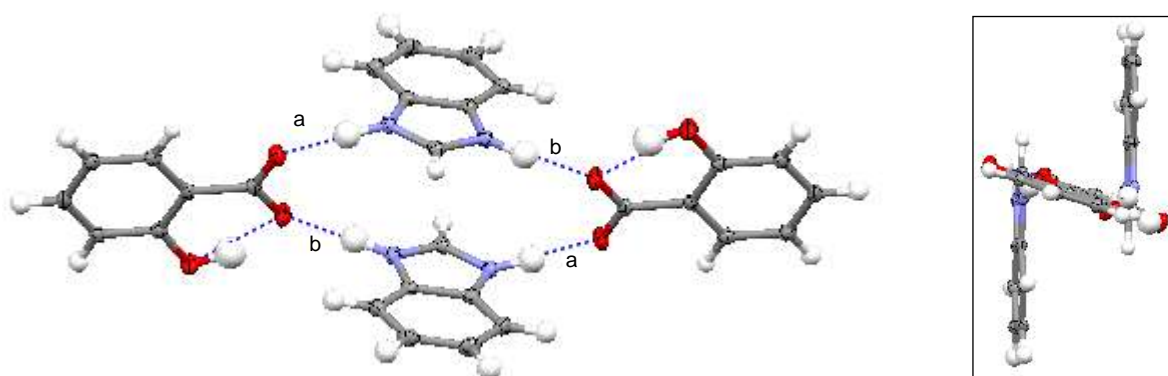


Fig. 4.15 – The main motif of the benzimidazolium 2-hydroxybenzoate molecular complex; a four molecule hydrogen bonded ring consisting of alternating co-molecules held together by partially charge assisted N^{δ+}-H...O^{δ-} hydrogen bonds. The inset shows the view along the *bc*-diagonal axis that highlights the geometric positions of the hydrogen bonded ring system.

There are three interactions that connect the hydrogen bonded rings together. The most influential is a weak hydrogen bond from a carboxylate oxygen to the carbon sandwiched between the nitrogens on the benzimidazole. The C1-H...O1^{δ-} hydrogen bond is 3.092(1)Å in length and connects the hydrogen bonded rings as seen in Figure 4.16.

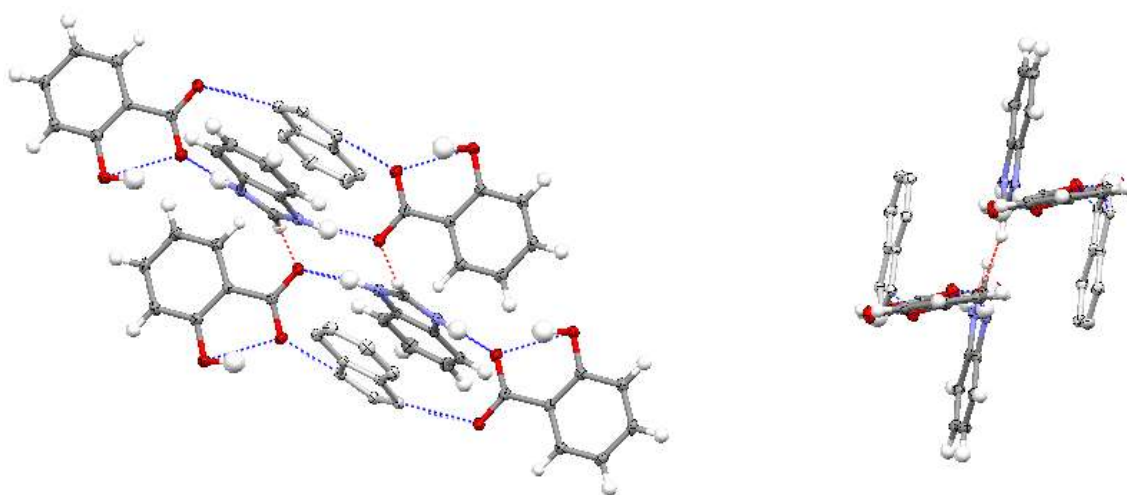


Fig. 4.16 – LHS, the weak hydrogen bonds (-) that extend the hydrogen bonded rings, RHS displays how the rings arrange themselves into a stacking configuration due to the C1-H \cdots O1 $^{\delta-}$ hydrogen bond.

The hydroxyl oxygen is only involved in one intermolecular interaction, which is with a methine group on another 2-HBA $^-$ molecule. This weak hydrogen bond of length 3.296(1)Å expands the hydrogen bonded ring along the *-ac diagonal* (Figure 4.17).

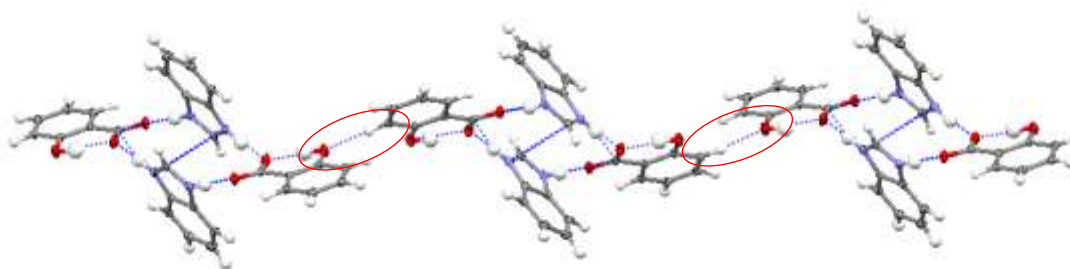


Fig. 4.17 – The hydrogen bonded ring system; the main motif of the benzimidazolium 2-hydroxybenzate molecular complex, is extended by weak hydrogen bonds (circled in red).

The last interaction that extends the hydrogen bonded ring system is a set of C-H \cdots π contacts that extends the structure along the *ac-diagonal*. These contacts have a length of 3.676 Å from C5 to a centroid between C13 and C14 (Figure 4.18).

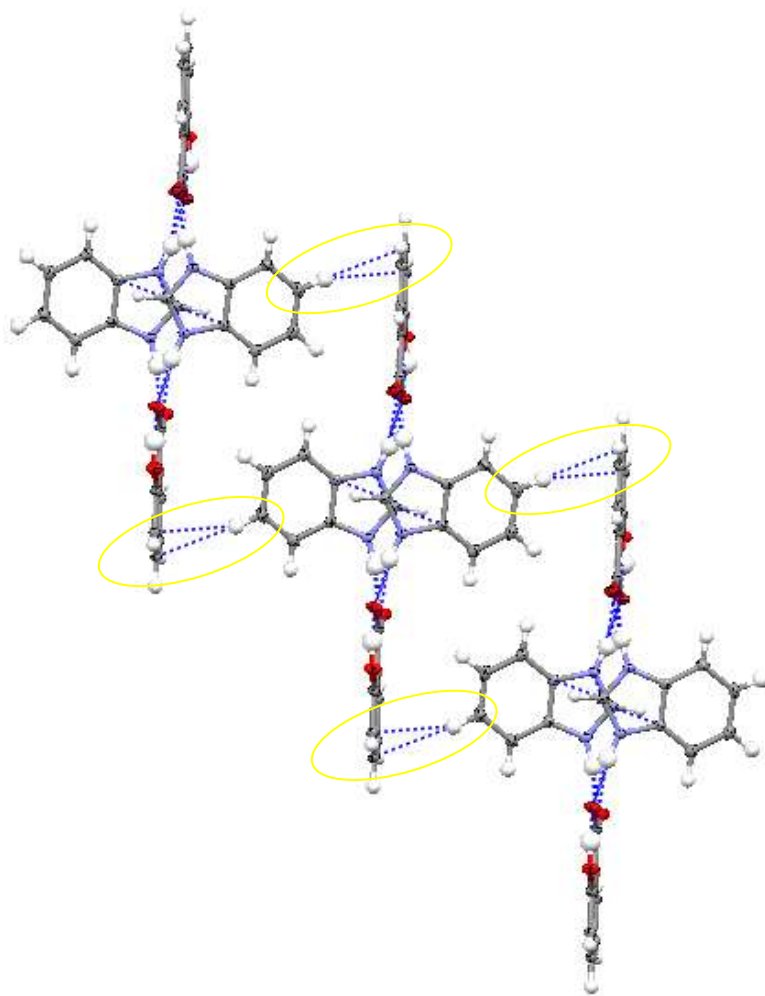


Fig. 4.18 – View highlighting the C-H $\cdots\pi$ interactions that extends the structure along the *ac*-diagonal.

These three interactions, the C1-H \cdots O1 $^{\delta-}$ and C13-H \cdots O3 hydrogen bonds and C-H $\cdots\pi$ contacts, expand the main motif of the structure, the hydrogen bonded ring R_4^4 (16), into the extended structure. There are other interactions in the molecular complex, however these complement the interactions that have already been mentioned. For example there are $\pi\cdots\pi$ stacking contacts between BZNH $^+$ molecules which are in the same hydrogen bonded ring system. These contacts have a relatively short distance for $\pi\cdots\pi$ stacking (3.179 Å) and in all probability are a consequence of the hydrogen bonded ring system (Figure 4.19).

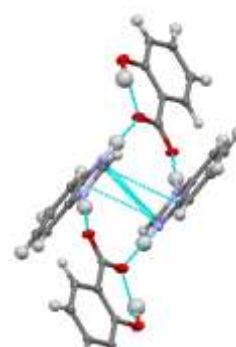
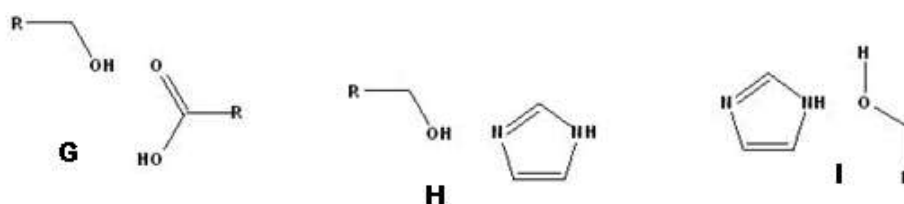


Fig. 4.19 – View of the interactions that exist between the molecules in main motif.

4.4.2 Molecular Complex of Benzimidazole and 3-Hydroxybenzoic Acid 1:1

From the benzimidazolium 2-hydroxybenzoate structure it can be seen that the hydrogen bond E is the most prominent in the molecular complex. Initial consideration of the benzimidazole and 3-hydroxybenzoic acid structure would suggest this could also be the same. Firstly it can safely be assumed there will be proton transfer creating the charge species of the co-molecules.

When the hydroxyl group is in the meta position, there is a greater potential for this group to be involved in a primary hydrogen bond that influences the structure. This increases the potential for hydrogen bond patterns G, H and I to be the more prominent in comparison to the benzimidazole and 2-hydroxybenzoic acid structure (Extract from Fig 4.11). Of these, hydrogen bond H would not be feasible due to the proton transfer and hydrogen bond G would be inherently stronger than I due to the strength of the hydrogen bond acceptor.



Extract from Fig 4.11 – Potential hydrogen bond patterns involving the hydroxyl group on the 3-hydroxybenzoic acid. G shows the potential hydrogen bond between the hydroxyl and carboxyl groups, H shows the potential hydrogen bond between the nitrogen lone pair and the hydrogen on the hydroxyl group and I shows the potential hydrogen bond between the oxygen lone pair and the hydrogen on the hydroxyl group.

For this potential molecular complex, there are two competing hydrogen bonds that may prevail. Hydrogen bond E, as seen in the BZNH^+ 2-HBA $^-$ molecular complex, could again create hydrogen bonded rings, whereas if hydrogen bond G is the primary bond, this could potentially create chains of 3-hydroxybenzoic acid molecules.

Structure Description

A 1:1 molecular complex containing the molecular ions, BZNH^+ and 3-hydroxybenzoate (3-HBA $^-$) was obtained using the solvent evaporation method, with a 1:1 stoichiometric mixture of BZN (12mg) and 3-hydroxybenzoic acid (3-HBA) (14mg) dissolved in the minimum amount of acetone followed by evaporation at 10°C using an Asynt hotplate. The crystals

generated were block shaped and colourless. Single crystal X-ray diffraction data were obtained using a Bruker-Nonius Kappa CCD diffractometer at 100K, equipped with graphite monochromated Mo K α radiation ($\lambda = 0.71073 \text{ \AA}$). The structure was solved using SIR92³⁰ within the CRYSTALS³¹ program. The crystallographic data are summarised in Table 4.4 with the interactions involved in the molecular complexed outlined in Table 4.6

As described in Section 4.2.1, the BZN molecule is protonated through hydrogen transfer from the carboxylic acid group on the 3-HBA molecule (Figure 4.20). This is reflected in the

equalisation of the internal bond lengths, N1 $^{\delta+}$ -C1 1.3298(14)(3) \AA and N2 $^{\delta+}$ -C1 1.3255(14) \AA , and bond angles, C1-N1 $^{\delta+}$ -C2 108.55(9) $^{\circ}$ and C1-N2 $^{\delta+}$ -C7 108.50(9) $^{\circ}$. The negative charge on the deprotonated 3-HBA molecule is found to be delocalised over the carboxylic acid group, indicated by the normalisation of the bond lengths in the carboxyl group, C8-O1 $^{\delta-}$ 1.2702(12) \AA and C8-O2 $^{\delta-}$ 1.2603(12) \AA .

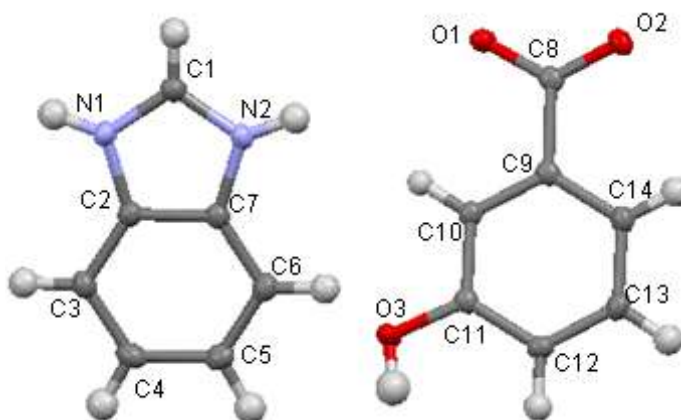


Fig. 4.20 – The benzimidazolium and 3-hydroxybenzoate ions which are generated in the molecular complex, with atom labelling.

Interaction	Length (\AA) (D \cdots A(\AA))	For Hydrogen Bonds		
		D-H(\AA)	H \cdots A(\AA)	D-H \cdots A angle($^{\circ}$)
O3 \cdots O1	2.645(1)	0.87(1)	1.79(1)	172(1)
N1 \cdots O1	2.697(1)	0.90(1)	1.80(1)	173(1)
N2 \cdots O2	2.700(1)	0.88(1)	1.82(1)	173(1)
C1 \cdots O2	3.091(1)	0.93(1)	2.21(1)	157(1)
C5 \cdots O3	3.298(1)	0.95(1)	2.60(1)	131(1)
C3 $\cdots\pi$	3.501	-	-	-

Table 4.6 – The inter- and intramolecular interactions with distances found in the BZNH $^+$ and 2-HBA $^-$ molecular complex

There are two primary hydrogen bonds in the benzimidazolium 3-hydroxybenzoate molecular complex. Both are similar in length and both play a pivotal role in the structure. They are slight modifications of hydrogen bond patterns F and G (from Figure 12) due to the introduction of the charged species. Hydrogen bond G, which corresponds to the O3-H \cdots O1 $^{\delta-}$ hydrogen bond, is 2.6544(15)Å in length (see Table 4.3 for full details) and creates long chains of 3-HBA $^-$ molecules along the *c*-axis. The mean planes of alternate 3-HBA $^-$ molecules lie at angles of 104.4° to each other and always hydrogen bond through the O1 atom of the carboxylic acid group (Figure 4.21).

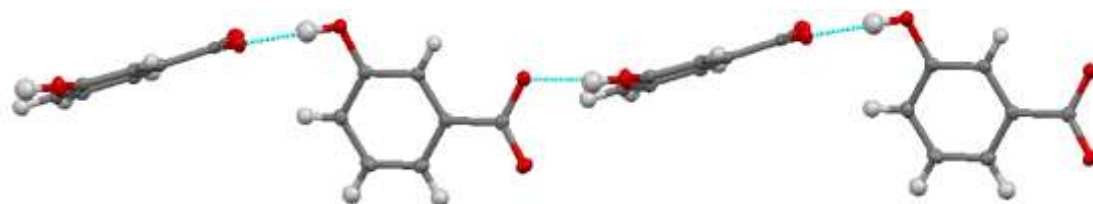


Fig. 4.21 – The 3-hydroxybenzoate molecules create chains with the mean planes of alternate molecules tilted at 104.4° from each other.

The derivative of hydrogen bond pattern F comprises two distinct N1 $^{\delta+}$ -H \cdots O1 $^{\delta-}$ and N2 $^{\delta+}$ -H \cdots O2 $^{\delta-}$ hydrogen bonds with lengths 2.6996(15)Å and 2.6972(15)Å, respectively (refer to Table 4.3 for full details). These moderate hydrogen bonds have the role of holding the chains of 3-HBA $^-$ to one another which extends the structure along the *b*-axis (Figure 4.22).

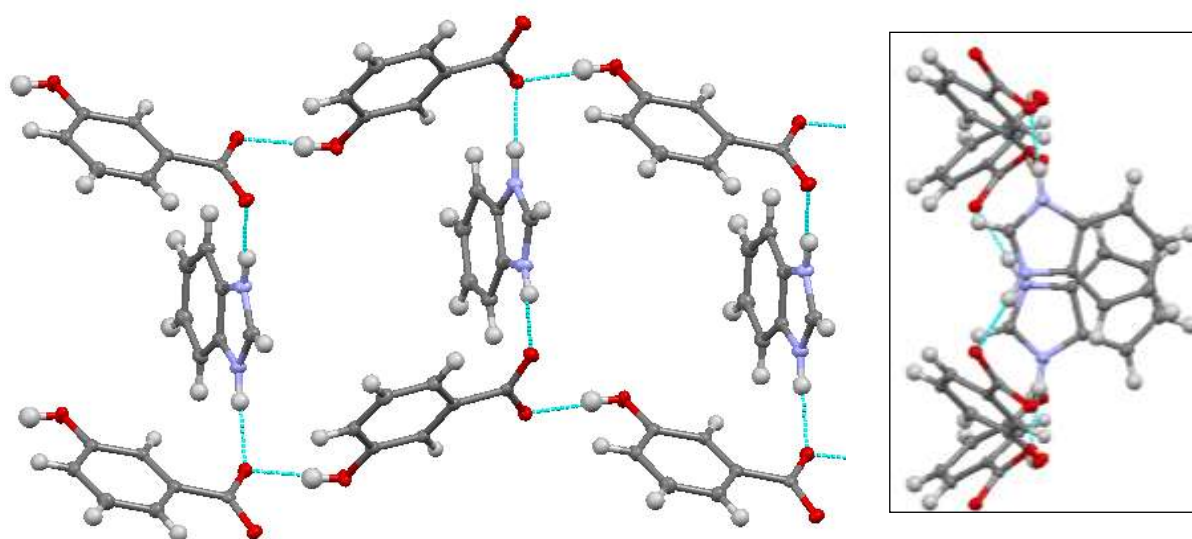


Fig. 4.22 – The 3-hydroxybenzoate molecules chains which are held together through a hydroxyl-carboxylate hydrogen bond are bridged together by hydrogen bonding through a benzimidazolium molecule. The inset

shows the view along the *c*-axis, indicating that the benzimidazolium molecules sit on two distinct positions due to the twisting nature of the 3-hydroxybenzoate chains.

While the two main hydrogen bonds, G which creates the chains of 3-HBA⁻ molecules and F which uses the BZNH⁺ as a bridge between the chains, create a sheet along the *bc* face, it is the role of weaker interactions that extend the structure along the *a*-axis. The *a*-axis is configured in a layered type network, with the weaker interactions filling the gaps in an alternating arrangement.

One of the layers uses a weak hydrogen bond that links the carbon sandwich between the two nitrogens of the BZNH⁺ and an oxygen of the carboxylate group, C1-H \cdots O2 ^{δ^-} , that is 3.0913(15)Å in length (Figure 4.23 LHS). The other layer uses a weak hydrogen bond between the hydroxyl oxygen and a carbon from BZNH⁺, C5-H \cdots O3 ^{δ^-} with length 3.2985(15)Å and a C-H \cdots π interaction of around 3.501Å (Figure 4.23 RHS).

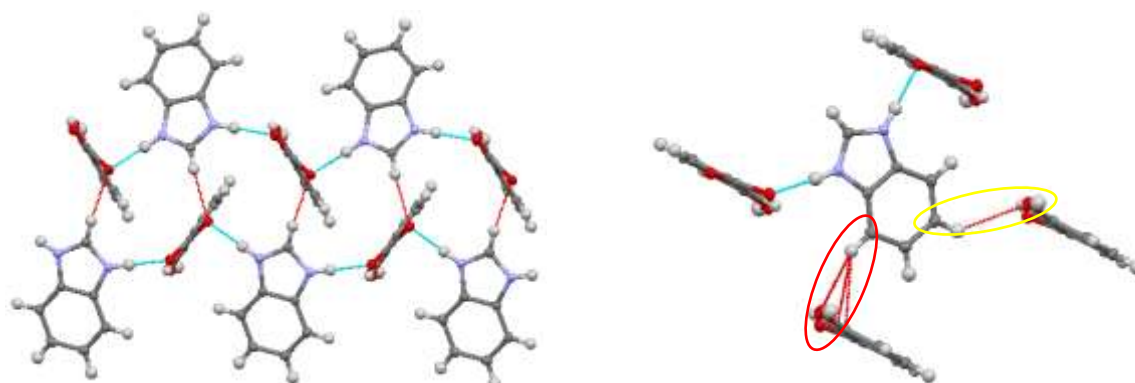


Fig. 4.23 – LHS, The alternating layers that exist on the *a*-face of the benzimidazolium 3-hydroxybenzoate molecular complex are connected through a weak hydrogen bond on each alternate layer (red). RHS, the alternate layer is held together by a weak hydrogen bond (yellow circle) and C-H \cdots π interactions (red circle).

The extended structure of the BZNH⁺ 3-HBA⁻ molecular complex can be seen in Figure 4.24. The supramolecular synthon, comprising 3-HBA⁻ chains, is easily identified in both images with the chains arranging into a zigzag formation (note there are no interactions between the chains, all interactions are through BZNH⁺ molecules). All the BZNH⁺ molecules lie in the channels of the chains like a ladder with around 3.598Å separating each molecule (seen in Figure 4.24 RHS). They sit in four different geometric positions, all “facing” outwards into a box shape, with the benzene part overlapping in the middle (seen in Figure 4.24 LHS).

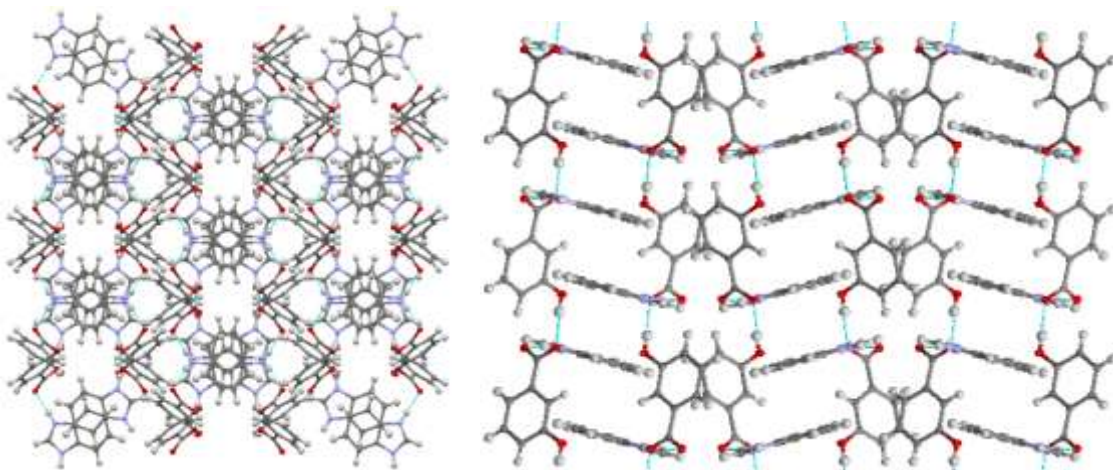


Fig. 4.24 – LHS, view along the c -axis highlighting how the benzimidazolium molecules form into channels. RHS, view along the b -axis that shows the 3-hydroxybenzoate chains.

4.4.3 Molecular Complex of Benzimidazole and 4-Hydroxybenzoic Acid 2:1

After the discovery of the BZNH^+ 3-HBA^- molecular complex, it was predicted that the co-crystallisation of BZN and 4-HBA would be as successful. As ever proton transfer would be inevitable and with the hydroxyl group moving to the 4-position, hydrogen bonding through this group would be readily available. A structure very similar to the BZNH^+ 3-HBA^- molecular complex would be predicted with an extension between the BZNH^+ molecules most likely due to the increase in distance between 4-hydroxybenzoate molecules a result of the positioning of the hydroxyl group.

Structure description

The molecular ions, BZNH^+ and 4-hydroxybenzoate (4-HBA^-) form a 2:1 molecular complex. The molecular complex was obtained using the solvent evaporation method, with a 1:1 stoichiometric mixture of BZN (6.8mg) and 4-hydroxybenzoic acid (4-HBA) (8.8mg) dissolved in the minimum amount of methanol followed by evaporation at $\sim 2\text{-}4^\circ\text{C}$ in the walk-in cold room. The crystals generated were block shaped and colourless. Single crystal X-ray diffraction data were obtained using a Rigaku R-axis/RAPID image plate diffractometer at 100K, equipped with graphite monochromated Mo $K\alpha$ radiation ($\lambda = 0.71073 \text{ \AA}$). The structure was solved using SUPERFLIP³² within the CRYSTALS³¹ program. The crystallographic data are summarised in Table 4.4.

As in Section 4.2.1, BZNH^+ molecules are generated through proton transfer from the carboxylic acid group on the 4-HBA molecule onto the normally unprotonated nitrogen atom on the BZN molecules. However the stoichiometric ratio in this case is two BZNH^+ molecules to every one 4-HBA^- , therefore it would be chemically impossible for all nitrogen atoms to be fully protonated if only the carboxylic group is de-protonated, which is the case. The result is that four of the nitrogens are bonded to partially occupied hydrogens, i.e. a proton is shared between BZN molecules (Figure 4.25). In one case the two half protons are bonded to nitrogens N6 and N7 that are hydrogen bonded to themselves ($\text{N6}\cdots\text{H}$ (50%) $\cdots\text{N6}'$; $\text{N7}\cdots\text{H}$ (50%) $\cdots\text{N7}'$) through an inversion centre, this accounts for one proton. The other proton is split in the hydrogen bond between the nitrogens N2 and N3. This proton is best resolved to a occupancy level of 0.4:0.6 in favour of nitrogen N2 (Figure 4.26). The result of the proton transfer on the BZNH^+ molecules, even though they are only partially protonated, is a delocalisation of the charge across the five-membered ring, reflected in the equalisation of the internal bond lengths and angle (Table 4.7). It was first thought that the nitrogens bonded to the partially occupied protons would be those that have been protonated, however this is unjustifiable for two reasons; firstly all the internal bond lengths and angles are normalised and secondly the partially protonated nitrogens are all hydrogen bonded to other partially protonated nitrogens therefore initially one of these nitrogens would have been unprotonated but which one cannot be identified.

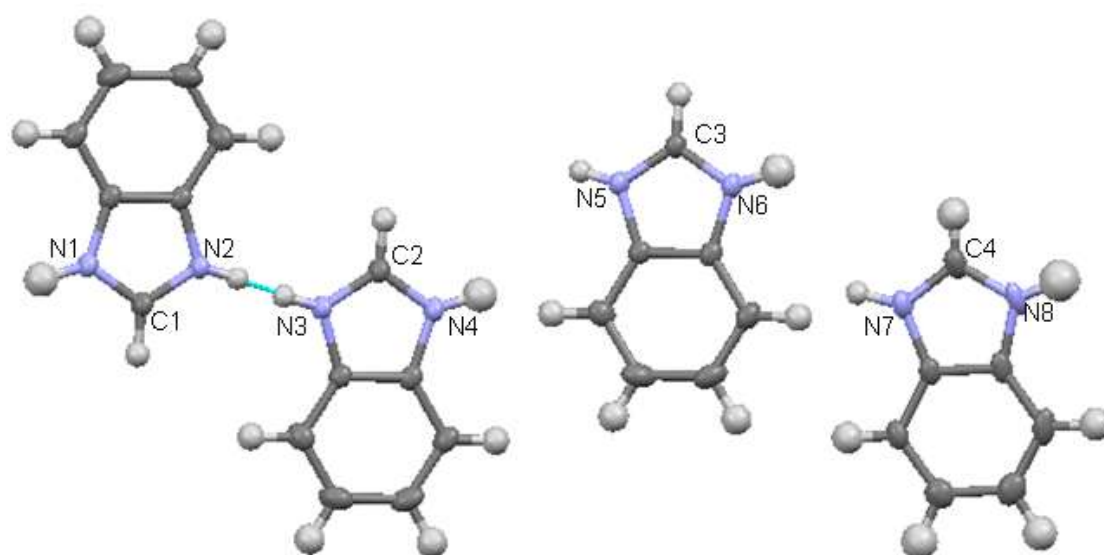


Fig. 4.25 – The different benzimidazolium molecules. From, left to right, molecules 1 and 2 hydrogen bond to one another over a glide plane, molecule 3 hydrogen bonds to itself through a inversion centre along the $\text{N6}\cdots\text{N6}$ contact, molecule 4 also hydrogen bonds to itself due to an inversion centre along the $\text{N7}\cdots\text{N7}$ contact. In every case a proton is split over two sites.

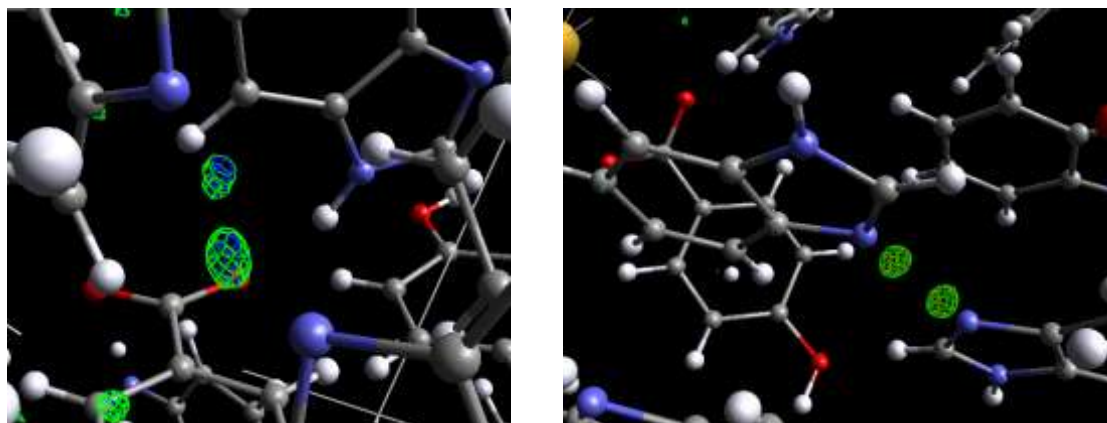


Fig. 4.26 – MCE³³ Fourier difference maps of the residual electron density. LHS, when the hydrogen split between nitrogen N2 and N3 is removed, RHS, when the hydrogen is removed from the N6 nitrogen (the same 50:50 split proton image is seen when the proton bonded to N7 is removed).

	Molecule 1	Molecule 2	Molecule 3	Molecule 4
N-C (Å)	N1-C1 1.346(3)	N3-C2 1.327(3)	N5-C3 1.339(3)	N7-C4 1.323(3)
C-N (Å)	C1-N2 1.323(3)	C2-N4 1.341(3)	C3-N6 1.322(3)	C4-N8 1.344(3)
C-N-C (°)	N1 107.17(19)	N3 106.6(2)	N5 107.23(19)	N7 106.8(2)
C-N-C (°)	N2 106.0(2)	N4 107.83(19)	N6 106.45(19)	N8 107.8(2)

Table 4.7 – Bond length and bond angle data for the four different benzimidazolium molecules from the benzimidazolium 4-hydroxybenzate molecular complex.

The 4-HBA⁻ molecules have a simpler role in this molecular complex. There are two distinct 4-HBA⁻ molecules in the structure, with the extent of the twisting of the carboxylate group their distinguishing feature. As explained the carboxylic acid group has been deprotonated which creates a negative charge that is delocalised over the carboxylate group, as seen by the normalisation of the bond lengths in the carboxyl group (Figure 4.28, Table 4.6).

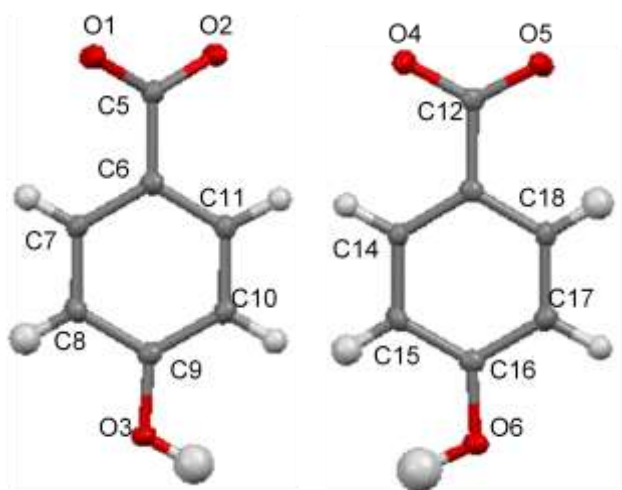


Fig. 4.27 – The two 4-hydroxybenzoate molecules found in the molecular complex, with associated atom labelling.

Molecule	1	2
C-O(Å)	C5-O1 1.253 (3)	C12-O4 1.271(3)
C-O(Å)	C5-O1 1.271(3)	C12-O5 1.258(2)
Twisting (°)	3.13	23.06

Table 4.8 – Bond lengths and degree of twisting of the carboxylate group from the plane of the phenyl ring, for the 4-hydroxybenzoate molecules in the benzimidazolium 4-hydroxybenzoate molecular complex.

Interaction	Length (Å) (D...A(Å))	For Hydrogen Bonds		
		D-H(Å)	H...A(Å)	D-H...A angle(°)
O3...O2	2.605(3)	1.02(3)	1.60(3)	166(3)
O6...O4	2.602(3)	0.94(3)	1.69(3)	166(3)
N2...N3	2.675(3)	1.01(6)	1.67(6)	173(6)
N6...N6	2.682(3)	0.82(4)	1.86(4)	178(5)
N8...O4	2.717(2)	0.93(3)	1.79(3)	170(3)
N4...O1	2.695(2)	0.95(3)	1.78(3)	163(3)
N1...O5	2.689(3)	0.91(3)	1.78(3)	173(3)

Table 4.9 – The inter- and intramolecular interactions with distances found in the BZNH⁺ and 4-HBA⁻ molecular complex

The main motif of the BZNH⁺ 4HBA⁻ molecular complex is, as expected, very similar to that in BZNH⁺ 3HBA. These are two main differences which have a profound effect on the extended structure. The primary hydrogen bond is a derivative of pattern G (Figure 4.12) which corresponds to the hydroxyl carboxylate hydrogen bond. There are two of these hydrogen bonds, the main hydrogen bonds in the molecular complex with lengths O3-H...O2^{δ-} 2.605(3)Å and O6-H...O4^{δ-} 2.602(3)Å (refer to Table 4.3 for full details).

They link to create chains of 4-HBA⁻ molecules along the *a*-axis and the mean planes of alternating molecules lie at an angle of 29.96° to one another (Figure 4.28). By comparison the chains created in the BZNH⁺ 3HBA⁻ molecular complex have longer lengths (2.6544(15)Å) and lie to a greater degree of interplanar angle to one another (104.4 °) (Figure 4.21).

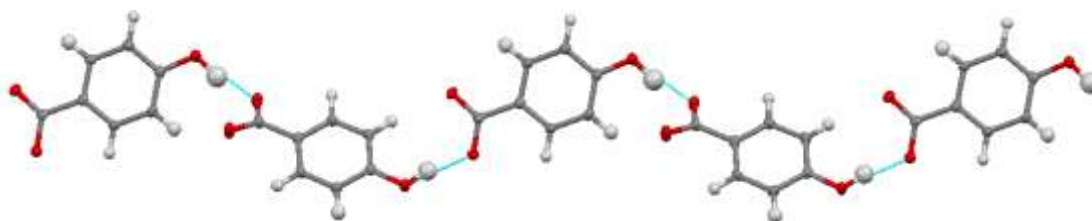


Fig. 4.28 – The 4-hydroxybenzoate molecules create chains with the molecules alternately sitting on two positions.

The derivative of pattern F, which is the N^{δ+}-H···O^{δ-} and N^{δ+}-H···O^{δ-} hydrogen bonds have lengths ranging from 2.689Å to 2.717Å (refer to Table 4.9 for details). These three moderate strength hydrogen bonds have the role of holding the chains of 4-HBA⁻ to one another, exactly the same as in the BZNH⁺ 3HBA⁻ molecular complex. However, there are two differences, of which one might be expected whereas the other adds complexities to the structure. The expected difference is in with the introduction of the extra BZNH⁺, which has led to the molecular complex adopting hydrogen bond C (Figure 4.12), N^{δ+}-H···H- N^{δ+}. These BZNH⁺ dimers have lengths of N2^{δ+}-H···H- N3^{δ+} 2.675(3) Å, N6^{δ+}-H···H- N6^{δ+} 2.682(3) Å and N7^{δ+}-H···H- N7^{δ+} 2.737(3) Å which compares favourably to the N-H···N distance of 2.884Å found in the BZN structure (CSD ref – BZDMAZ04)³⁴. Secondary, it is not simply the case that two chains of 4HBA⁻ are held together by the BZNH⁺ dimers creating sheets. Instead, in this structure each chain is connected to four other chains through the dimers (Figure 4.29 LHS). Moving through the chain, each alternate 4-HBA⁻ molecule hydrogen bonds in opposite directions thus every other 4HBA⁻ molecule is involved in one ladder structure (Figure 29 RHS). This creates a criss-cross pattern for the extended structure (Figure 29 bottom). There are a host of weaker interactions in this molecular complex, however none are thought to be significant enough to influence the structure.

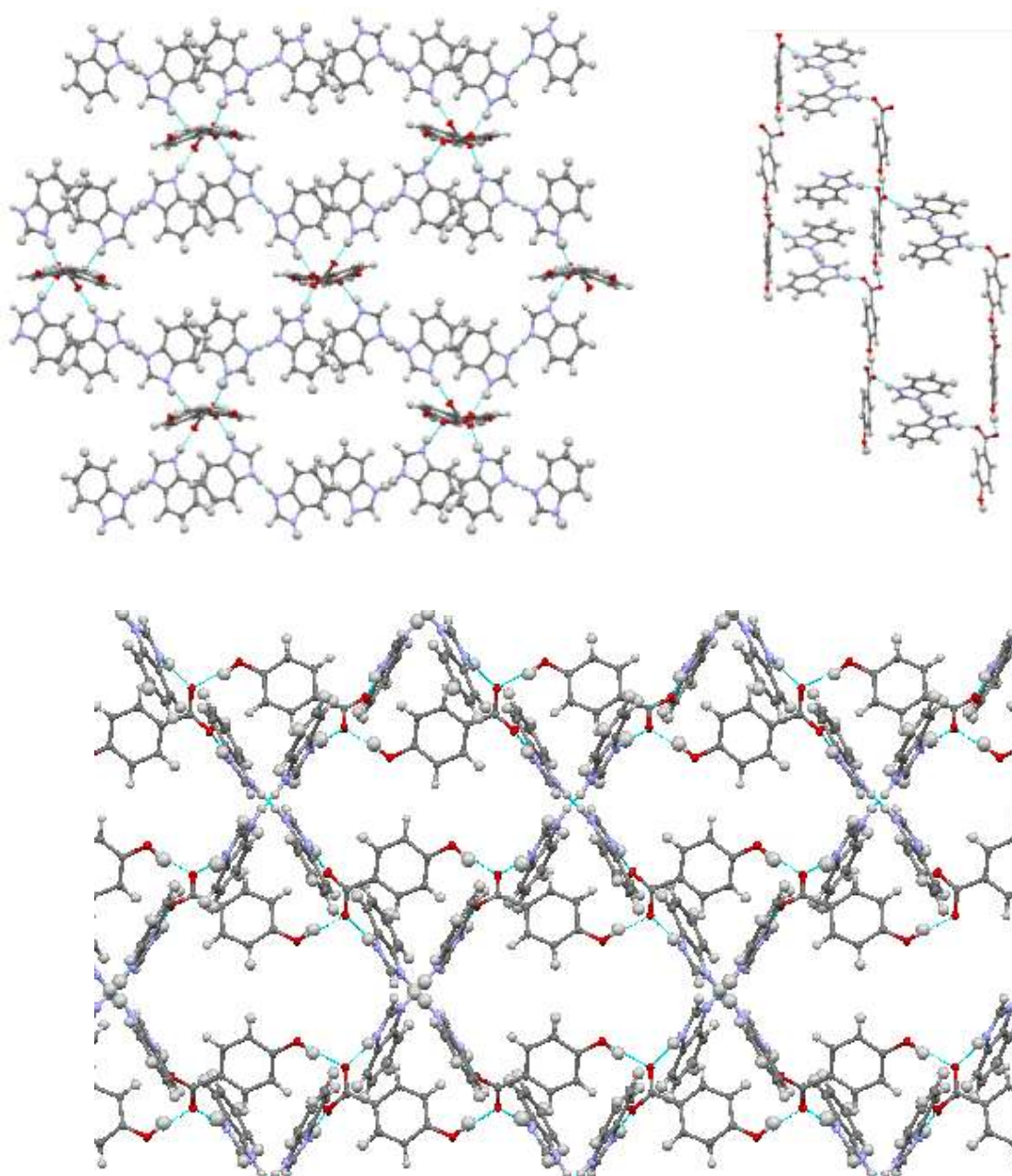


Fig. 4.29 – LHS, view along the a -axis highlighting how each 4-HBA^- chain is involved in hydrogen bond in four different directions. RHS, view along the b -axis indicating the connections between each chain. bottom – view along the c -axis of the $\text{BZNH}^+ 4\text{HBA}^-$ molecular complex with the backbone of the structure, the 4HBA^- chains, being held together by the BZNH^+ dimers that criss-cross between them.

Effect of Stoichiometric ratio

The $\text{BZNH}^+ 4\text{HBA}^-$ molecular complex always adopts a 2:1 stoichiometric ratio no matter the ratio of the initial starting materials used: 1:1, 2:1 or 1:2. The use of excess 4-hydroxybenzoic acid results in a hydrate of the 4-HBA starting material, the $\text{BZNH}^+ 4\text{HBA}^-$ 2:1 complex and

in some cases the $\text{BZNH}^+ 4\text{HBA}^-$ hydrate molecular complex being formed. Experiments using these ratios were also set-up for both 2-HBA and 3-HBA. As can be seen from Table 1.1, successful molecular complexes were generated for both 2-HBA and 3-HBA. The experiments between BZN and 3-HBA in a 2:1 ratio generated two polymorphs which differ in many aspects including the bonding motifs.

4.4.4 Molecular complex of Benzimidazole 3-Hydroxybenzoic acid 2:1 Form II

The trends in the other related structures indicates that this structure will adopt a structure similar to $\text{BZNH}^+ 4\text{HBA}^-$ molecular complex which has supramolecular synthons of chains of 4HBA^- using the hydrogen bond pattern G. These chains are connected to BZNH^+ by partially charge assisted hydrogen bonds of form F. Further, homo-hydrogen bond C might be expected to connect the two BZNH^+ molecules into dimers.

Structure Description

The molecular ions, BZNH^+ and 3-hydroxybenzoate (3-HBA^-) form a 2:1 molecular complex with one another. The molecular complex was obtained using the solvent evaporation method, with a 2:1 stoichiometric mixture of BZN (24 mg) and 3-hydroxybenzoic acid (3-HBA) (16 mg) dissolved in the minimum amount of methanol followed by evaporation at $\sim 2\text{-}4^\circ\text{C}$ using the walk in cold room. The crystals generated were block shaped and colourless. Single crystal X-ray diffraction data were obtained using a Bruker ApexII diffractometer at 100K, equipped with graphite monochromated Mo $K\alpha$ radiation ($\lambda = 0.71073 \text{ \AA}$). The structure was solved using SUPERFLIP³² within the CRYSTALS³⁰ program. The crystallographic data are summarised in Table 4.4.

In this molecular complex, the BZN molecules are protonated forming BZNH^+ molecules as described in section 4.2.1. However the stoichiometric ratio is two BZNH^+ molecules to one 3-HBA^- , the result is two of the nitrogens are bonded to partially occupied hydrogens, i.e. a proton is shared between BZN molecules (Figure 4.30). The proton is split in the hydrogen bond between the nitrogens N2 and N4 with the best model (lowest concluding R-factor) having occupancy levels of 0.55:0.45 in favour of nitrogen N2 (Figure 4.31). The result of the proton transfer on the BZNH^+ molecules, even though they are only partially protonated,

is a delocalisation of the charge across the five-membered ring, reflected in the equalisation of the internal bond lengths and angle (Table 4.10). As in the previous molecular complex it was first thought that the nitrogens bonded to the partially occupied protons would be those that have been protonated, however this is unjustifiable for two reasons; firstly all the internal bond lengths and angles are normalised and secondly the partially protonated nitrogens are all hydrogen bonded to other partially protonated nitrogens therefore initially one of these nitrogens would have been unprotonated but which one cannot be identified.

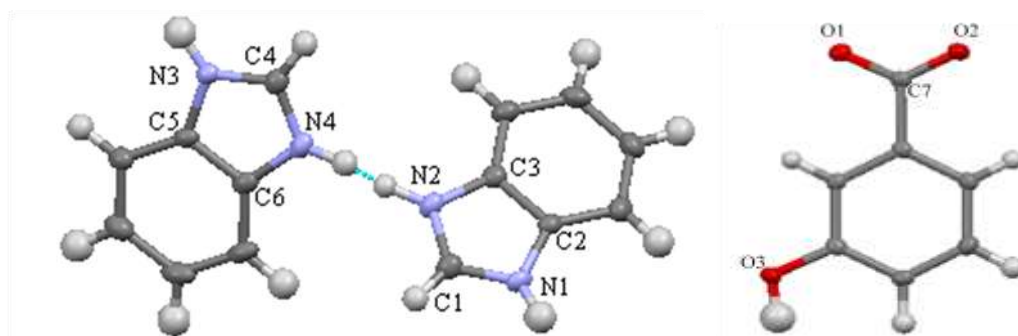


Fig. 4.30 – The different benzimidazolium molecules: from, left to right, molecules 1 and 2 that hydrogen bond to one another with the relevant atoms labelled, and the 4-hydroxybenzoate molecule with associated atom labelling.

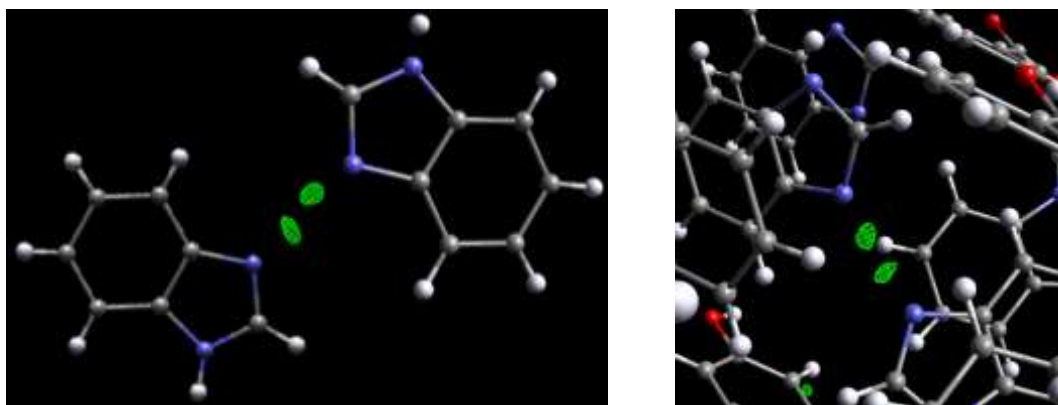


Fig. 4.31 – MCE³³ Fourier difference maps of the residual electron density when the hydrogen split over nitrogen N2 and N4 is removed.

	Molecule 1		Molecule 2	
Bond Lengths (Å)	N3-C4	1.342(2)	N2-C1	1.320(2)
	N4-C4	1.322(2)	N1-C1	1.341(3)
Bond Angle (°)	C5-N3-C4	107.63(16)	C2-N1-C1	107.55(16)
	C6-N3-C4	106.79(16)	C3-N2-C1	106.00(16)

Table 4.10 – Bond length and bond angle data for the two different benzimidazolium molecules from the benzimidazolium 3-hydroxybenzoate molecular complex.

Interaction	Length (Å) (D...A(Å))	For Hydrogen Bonds		
		D-H(Å)	H...A(Å)	D-H...A angle(°)
N2...N4	2.676(3)	0.88(5)/0.94(5)	1.75(5)/1.80(5)	175(5)/171(5)
O3...O2	2.660(3)	0.92(3)	1.74(3)	178(3)
N1...O1	2.751(3)	0.84(3)	1.93(3)	165(3)
N3...O1	2.748(3)	0.94(3)	1.81(3)	177(2)
O3...C	3.446(3)	0.95(2)	2.50(2)	174(2)
O2...C4	3.420(3)	0.97(2)	2.51(2)	156(2)
O2...C1	3.338(3)	0.95(2)	2.42(2)	161(2)

Table 4.11 – The inter- and intramolecular interactions with distances found in the BZNH⁺ 3HBA⁻ 2:1 molecular complex.

The 3HBA⁻ molecule has been deprotonated with a proton from the carboxylic acid group transferring to the BZN, leading to a negative charge that is delocalised over the carboxylate group, C7-O1 1.269(2)Å and C7-O2 1.256(2)Å.

The main motif of the BZNH⁺ 3HBA⁻ 2:1 molecular complex is, as expected, a hybrid of the BZNH⁺ 3HBA⁻ 1:1 and BZNH⁺ 4HBA⁻ 2:1 molecular complexes. It is expected because it might be predicted that the extra BZN molecule would behave as in the BZNH⁺ 4HBA⁻ 2:1 structure, forming a BZNH⁺ dimer. The supramolecular synthons will thus be identical to the BZNH⁺ 3HBA⁻ 1:1 structure and a ladder type molecular complex would be formed.

The main hydrogen bond is a derivative of synthon G (Figure 4.12) which corresponds to the hydroxyl carboxylate hydrogen bond. This hydrogen bond, O3-H...O2, is 2.660(3)Å in length and forms chains along the *c*-axis (refer to Table 4.3 for full details) as seen in Figure 4.32. The molecules all lie on the same plane with the carboxylate group slightly twisting out of the plane by ~16°. The close planarity of the molecules in the chain in this case is in contrast to the chains created in the BZNH⁺ 3HBA⁻ 1:1 molecular complex, which lie at a greater angle to one another (104.4 °) (Figure 4.21).

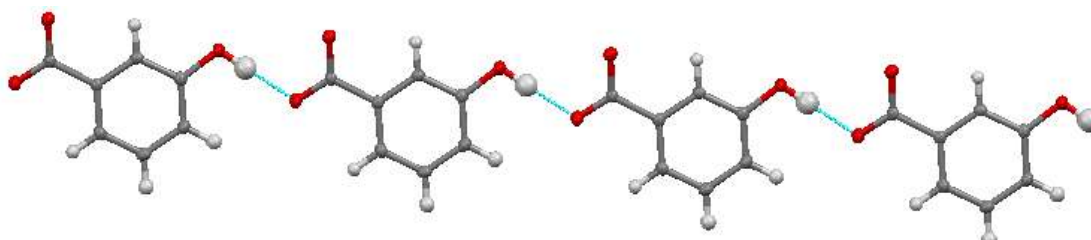


Fig. 4.32 – The 3-hydroxybenzoate molecules create close-to-planar chains through a hydroxyl carboxylate hydrogen bond.

The derivative of hydrogen bond pattern F corresponds to the hydrogen bonds $N1^{\delta+}-H\cdots O1^{\delta-}$ and $N3^{\delta+}-H\cdots O1^{\delta-}$, which have lengths $2.751(3)\text{\AA}$ and $2.748(3)\text{\AA}$ respectively (refer to Table 3.11 for all the interactions within the molecular complex). These moderate hydrogen bonds have the role of holding the chains of 3-HBA^- to one another, exactly the same as in the $\text{BZNH}^+ 3\text{HBA}^-$ 1:1 molecular complex, but are longer in length by $\sim 0.05\text{\AA}$. As expected, the introduction of the extra BZNH^+ has led to the molecular complex adopting hydrogen bond pattern C (Figure 4.12), $N^{\delta+}-H\cdots H-N^{\delta+}$. This BZNH^+ dimer has hydrogen bond length $N2^{\delta+}-H\cdots H-N4^{\delta+}$ 2.676\AA which is identical to the dimers found in the $\text{BZNH}^+ 4\text{HBA}^-$ molecular complex ($2.675(3)\text{\AA}$ and $2.682(3)\text{\AA}$) (Figure 4.33 RHS).

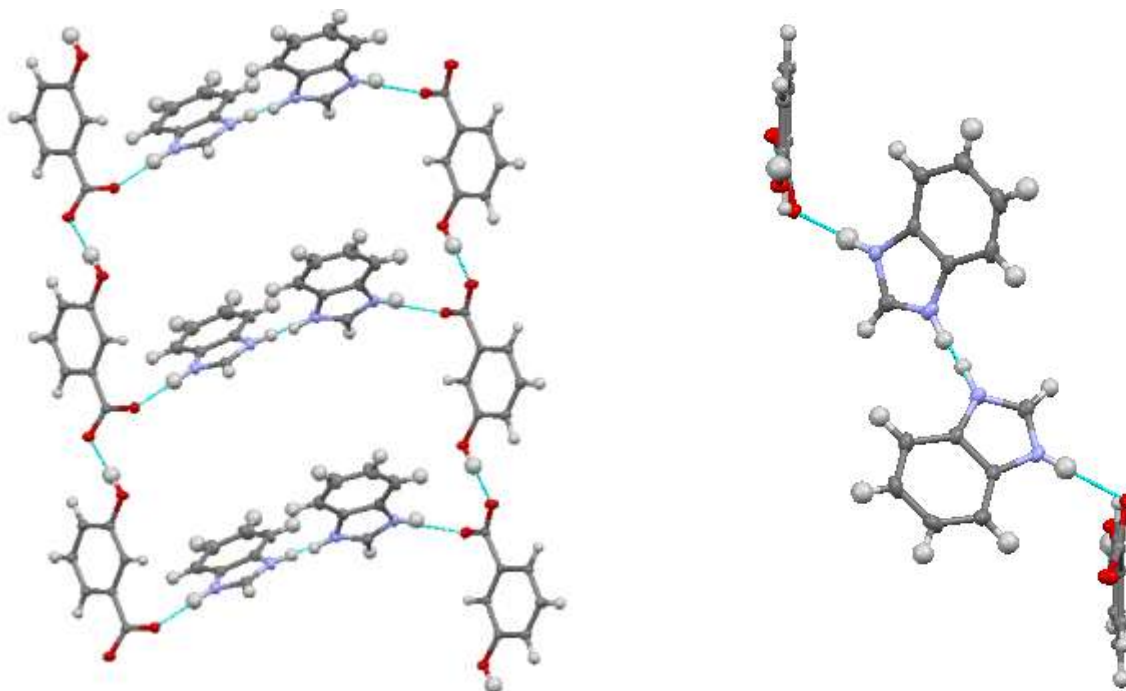


Fig. 4.33 – LHS, the 3-hydroxybenzoate molecules chains which are held together through a hydroxyl-carboxylate hydrogen are bridged together by hydrogen bonding through a benzimidazolium dimer. RHS, the view along the *a*-axis indicating the planar nature of the chains and highlighting the role of the BZNH^+ dimer.

The 3-HBA⁻ chains run along the *a*-axis, the dimers joins this motif to the next one creating ladders. These ladders are further extended along *bc*-face as every 3-HBA⁻ molecule hydrogen bonds to two different BZN⁺ dimers (Figure 4.34).

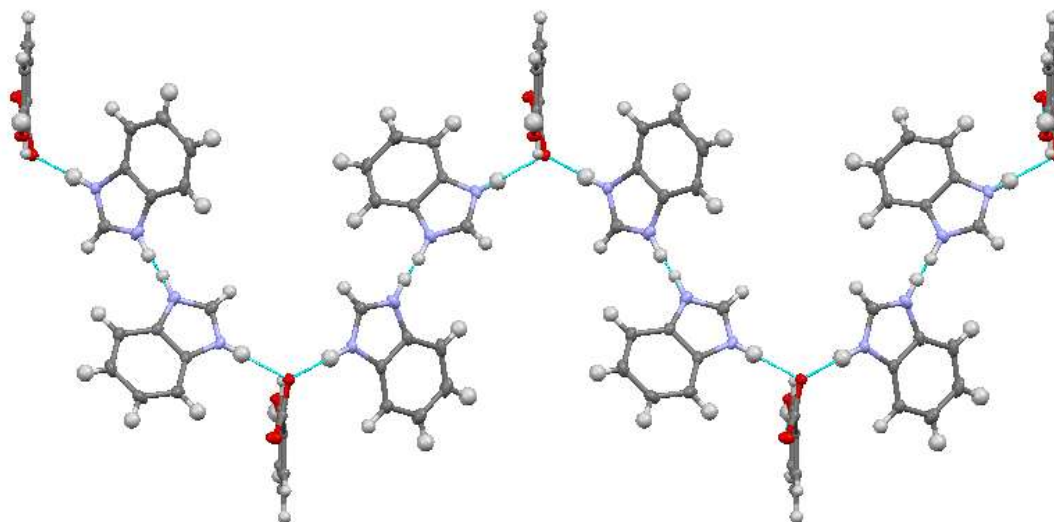


Fig. 4.34 – The 3-hydroxybenzoate molecules hydrogen bond along the *bc*-face which creates a sheet along the *a*-axis view along the *a*-axis indicating the planar nature of the chains and highlighting the role of the BZNH⁺ dimer.

This structure contains three weak hydrogen bonds that cooperate together to extend the packing along the *c*-axis (Figure 4.35). One is a hydrogen bond involving the oxygen of the hydroxyl group and a carbon from a 3HBA⁻ molecule, C-H···O3, that has length 3.446(3)Å and has been circled in red in Figure 4.35. The other two are C-H···O^{δ-} weak hydrogen bonds involving the carbons sandwiched between the nitrogens on the BZNH⁺ and the oxygen of the carboxylate that is involved in the chain motif, O2. They have lengths C4-H··· O2^{δ-} 3.420(3)Å and C1-H··· O2^{δ-} 3.338(3)Å and are circled in yellow and green.

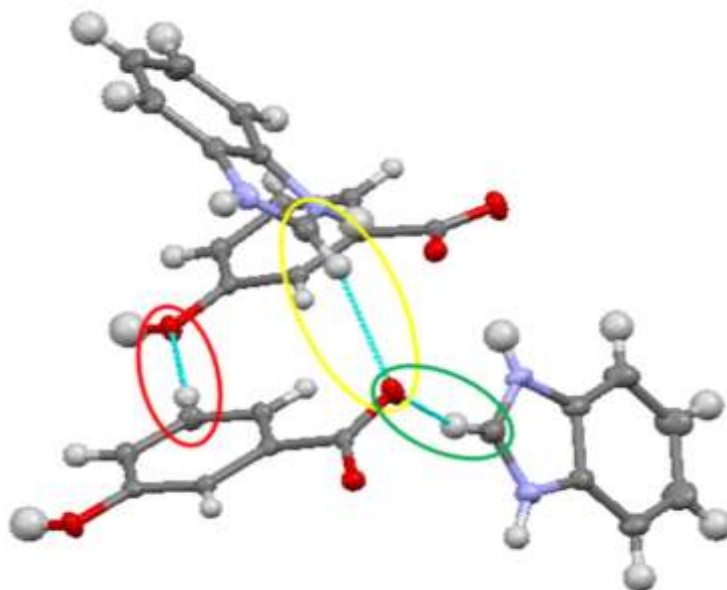


Fig. 4.35 – The weak interactions that are used to extend the structure along the *c*-axis, C-H···O3 (red), C4-H··· O2^{δ-}(yellow) and C4-H··· O2^{δ-} (green).

4.4.5 Molecular Complex of Benzimidazole 3-Hydroxybenzoic Acid 2:1 Form I

The serendipitous discovery of a polymorph of benzimidazolium 3-hydroxybenzoate was due to poor data collected from samples of the initial molecular complex. This meant that further unit cells scans were carried out, resulting in three different unit cells being discovered in crystals of benzimidazole and 3-hydroxybenzoic acid in a 2:1 mixture. However only the two discussed were reproducible as single crystals, with polymorph II forming greater quality crystals than Form I. Form II was discussed in Section 4.5.4 above, Form I is discussed here.

Structure description

The molecular ions, BZNH⁺ and 3-hydroxybenzoate (3-HBA⁻) form a 2:1 molecular complex, shown by unit cell screening to be a different polymorph from that discussed above (Form II). The molecular complex was obtained using the solvent evaporation method, with a 2:1 stoichiometric mixture of BZN (6.8mg) and 3-hydroxybenzoic acid (3-HBA) (8.8mg) dissolved in the minimum amount of ethanol followed by evaporation at ~2-4°C using a walk in cold room. The crystals generated were block shaped and colourless. Single crystal X-ray diffraction data were obtained using a Bruker ApexII diffractometer at 100K, equipped with graphite monochromated Mo K α radiation ($\lambda = 0.71073 \text{ \AA}$). The structure was solved using

SUPERFLIP³² within the CRYSTALS³¹ program. The crystallographic data are summarised in Table 4.4.

In this molecular complex, half of the BZN molecules are protonated as described in section 4.2.1, forming BZNH^+ molecules. Since there are four BZN molecules in the reduced unit cell, the result is that two of the BZNs have been protonated while two remain unprotonated. The result of the proton transfer on the BZNH^+ molecules, is a delocalisation of the charge across the five-membered ring, reflected in the equalisation of the internal bond lengths, 1.332(2)Å and 1.326(2)Å and angles 108.0(1)° and 108.0(1)° (Figure 4.36 LHS). The BZN molecules where no protonation has occurred retains distinct single and double bond characteristics with bond lengths 1.312(2)Å and 1.334(2)Å and bond angles 104.7(1)° and 106.8(1)°. The other BZN and BZNH^+ molecules in the unit cell have bond angles and lengths within the error range of the measurements given above.

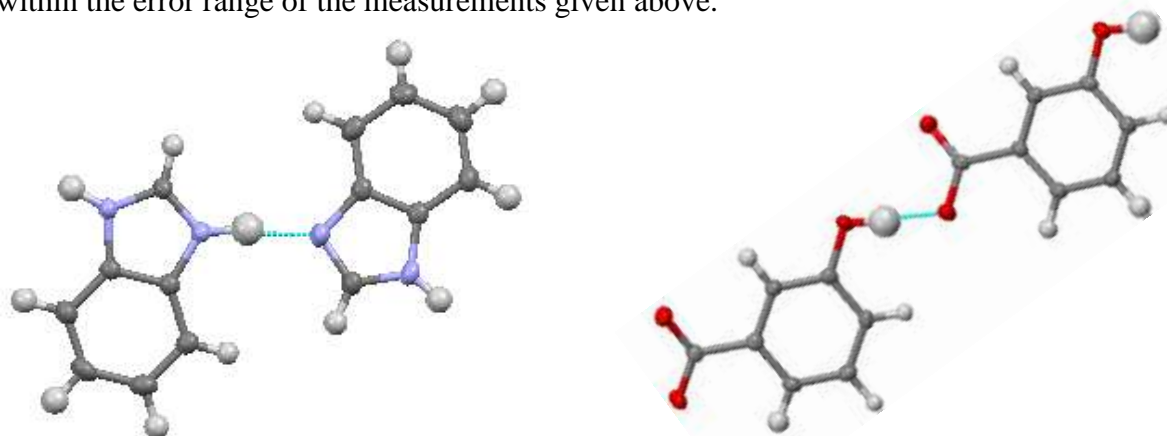


Fig. 4.36 – LHS, the BZN and BZNH^+ molecules form dimers, through a single hydrogen bond. There are two of these dimers in the reduced unit cell. RHS, the 3-HBA^- molecules also form single hydrogen bonded dimers.

The two distinct 3HBA molecules within the unit cell have both been deprotonated with a proton from each carboxylic acid group transferring to two of the BZN molecules. The consequence is the normalisation of the bond lengths in the carboxyl group, 1.265(2)Å and 1.246(2)Å (Figure 4.36 RHS). The bond lengths of the other 3-HBA^- molecules within the unit cell are within the errors of measurements and are consistent with the geometry found in the Form II polymorph.

The main motif of the $\text{BZNH}^+ 3\text{HBA}^- 2:1$ Form I molecular complex is the same as the $\text{BZNH}^+ 3\text{HBA}^- 2:1$ Form II molecular complex. The primary hydrogen bond is a derivative of synthon G (Figure 4.12) which corresponds to the hydroxyl carboxylate hydrogen bond. This

hydrogen bond, O-H \cdots O, is 2.540(1)Å in length and forms chains along the *ac*-diagonal axis (see Table 4.3 for full details). The planes of the benzene rings of the molecules in the chain tilt with respect to one another by 19.1° (Figure 4.37). However the twist of the carboxylate group plane and the benzene ring is 15.7° for both molecules in Form I. For comparison, the chains created in the BZNH⁺ 3HBA⁻ 2:1 Form II molecular complex have hydrogen bond lengths of 2.660(3)Å and lie on the same plane, with the carboxylate group slightly twisting out of the ring plane by ~15.9° (Figure 4.32).

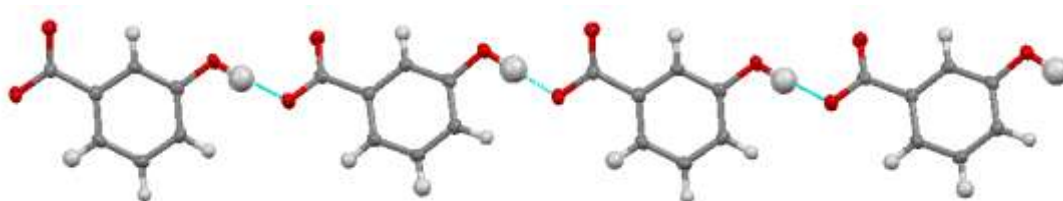


Fig. 4.37 – The 3-hydroxybenzoate molecules create chains through a hydroxyl carboxylate hydrogen bond.

These chains are then held together, as in the other polymorph, by BZN dimers using the derivative of hydrogen bond F. Contrary to the Form II polymorph however, the chains are also linked using hydrogen bond pattern I. The hydrogen bonds involved correspond to N^{δ+}-H \cdots O^{δ-}(carboxylate oxygen; a) and N^{δ+}-H \cdots O(hydroxyl oxygen; b) (Figure 4.38). These hydrogen bonds have lengths of 2.632(2)Å (a), and 2.913(2)Å (b) and can clearly distinguish the charged assisted hydrogen bonds which are shorter than those involving the hydroxyl group (refer to Table 4.3 for full details). It is also worth noting the hydrogen bond lengths of the Form II polymorph, which are two N^{δ+}-H \cdots O^{δ-}(carboxylate oxygen) hydrogen bonds of length 2.751(3)Å and 2.748(3)Å respectively, sitting close to the middle of the range of the hydrogen bonds in Form I.

The BZN - BZNH⁺ dimers adopt a derivative of hydrogen bond C (Figure 4.12), N^{δ+}-H \cdots N. These have lengths of 2.710(2)Å and 2.709(2)Å which is slightly longer than found in polymorph Form II with length 2.676(3)Å.

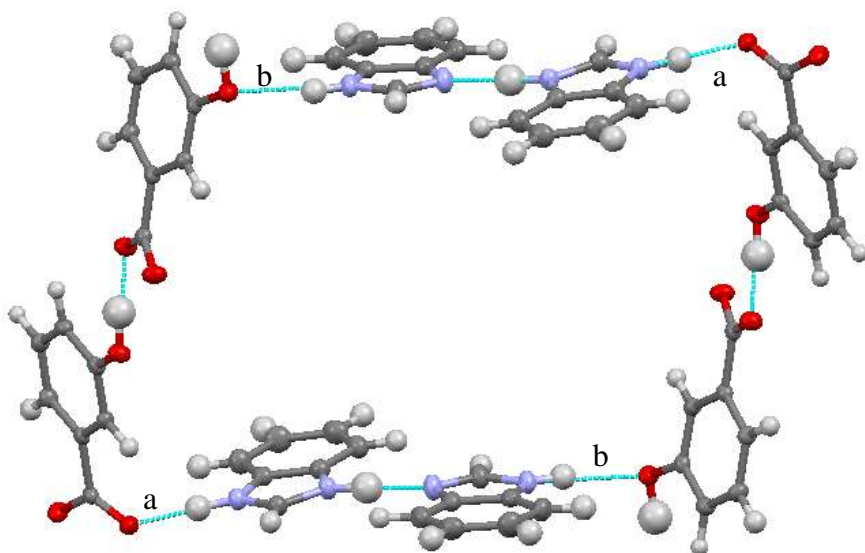


Fig. 4.38 – The 3-hydroxybenzoate molecules chains which are held together through a hydroxyl-carboxylate hydrogen bond are bridged together by four distinct hydrogen bonds of two types, a and b.

There are marked differences between the ladder motifs of Forms I & II, with Form II having stiles of 3-hydroxybenzoate molecules and consecutive rungs of hydrogen bonded dimers of BZNH^+ . While Form I, on the other hand, has alternate rungs of hydrogen bonded dimers (Figure 4.39).

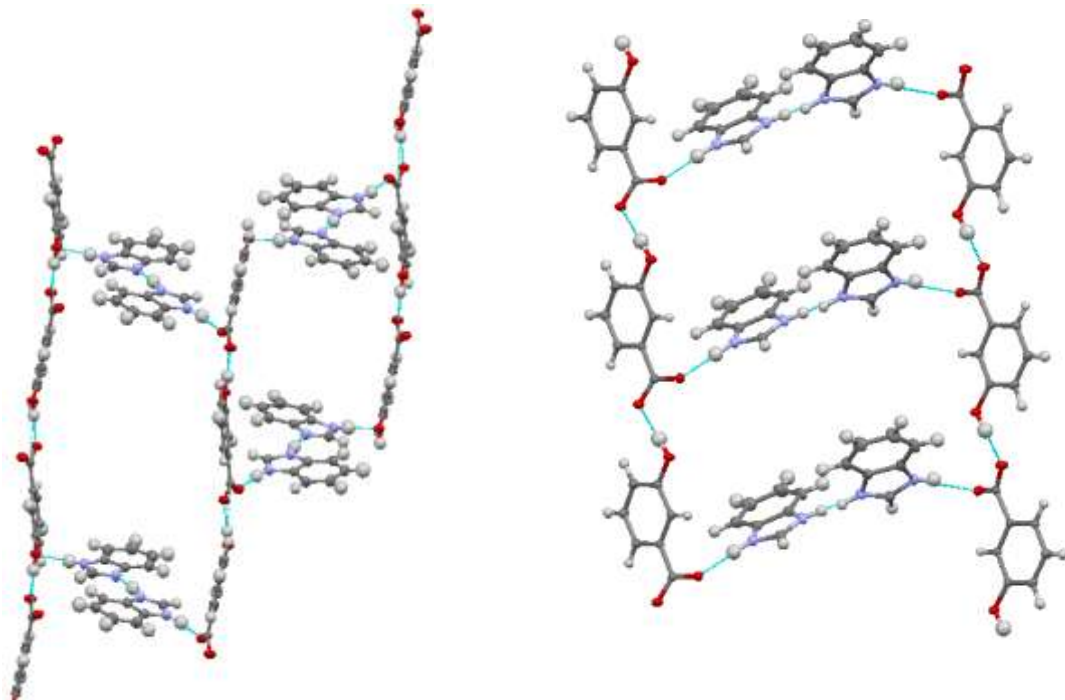


Fig. 4.39 – LHS, Form II, The ladder structure consists of stiles of 3-hydroxybenzoate molecules and rungs of hydrogen bonded dimers of BZNH^+ . RHS, Form I, The ladder structure consists of stiles of 3-hydroxybenzoate molecules and alternate rungs of hydrogen bonded dimers of BZNH^+ .

The ladder description can be extended, to reveal a “double” step, due to the hydroxyl along with the carboxylate group assisting in the hydrogen bonding (Figure 4.40). This double step occurs as one chain of 3-HBA⁻ molecules is involved in two ladders, as in the BZNH⁺ 4-HBA⁻ structure. This expands the structure indefinitely along the *ac*-diagonal. Advancing through the chains, each alternate 4-HBA⁻ has hydrogen bonding connections in the shape of a Z, while the other has the inverse shape Σ (Figure 4.41).

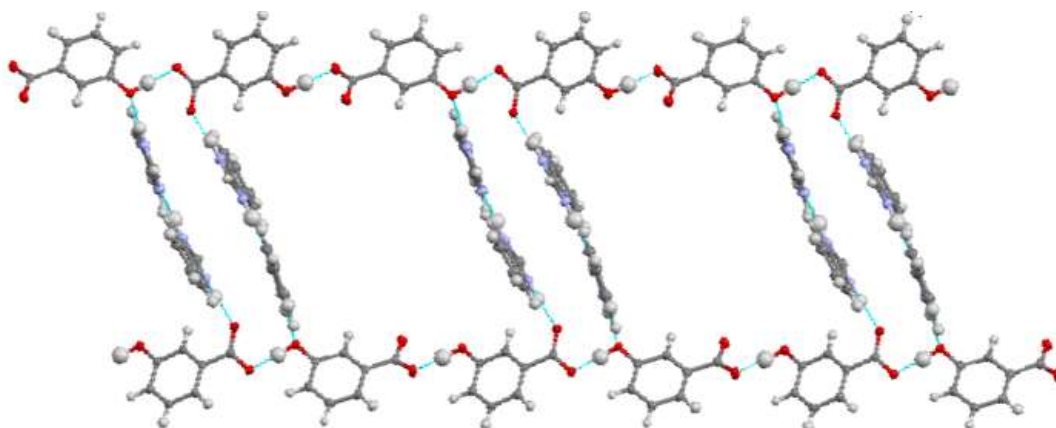


Fig. 4.40 – The ladder structure consists of uprights of 3-hydroxybenzoate molecules and the double rungs of hydrogen bonded dimers of BZNH⁺.

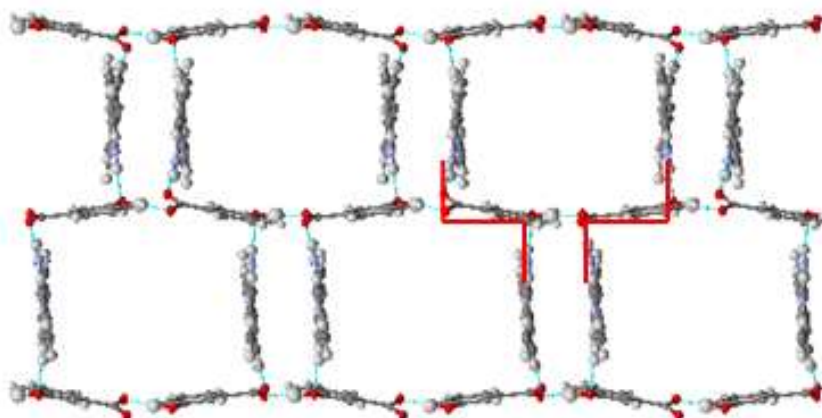


Fig. 4.41 – The 3-hydroxybenzoate molecules are involved in two ladders by hydrogen bonding in two directions adopting a Z and inverse Z shape (indicated by the red lines).

The structure also contains various weaker interactions, three of which assist in forming sheets of 3-HBA⁻ molecules along the *a*-axis. Firstly the 3-HBA⁻ molecules hydrogen bond to one another via C-H^{δ+}⋯O^{δ-} and C-H^{δ+}⋯O hydrogen bonds of lengths 3.240(2)Å and 3.433(2)Å, respectively (Figure 4.42 LHS). These are linear in geometry and arrange themselves into a hydrogen bonded ring. The BZNH⁺ (not the unprotonated form) also assist in the creation of

the sheets by bonding to two different 3-HBA⁻ molecules that are adjacent to one another (Figure 4.42 LHS). This involves hydrogen bonds to one 3-HBA⁻ through the predictable N^{δ+}-H···O^{δ-} synthon, then a further hydrogen bond to an adjacent 3-HBA⁻ molecule. These are already hydrogen bonding via the weak hydrogen bonds mentioned above, with a C-H···O^{δ-} interaction involving the carbon sandwiched between the two nitrogens and deprotonated oxygen (Figure 4.42 RHS). This weak hydrogen bond has a length of 3.186(2)Å. Another hydrogen bond, also involving the BZNH⁺, is made from a carbon to the hydroxyl oxygen on the 3-HBA⁻ (Figure 4.42 RHS). This C-H···O hydrogen bond has length 3.429(2)Å and again assists in creating the sheets of 3-HBA⁻ molecules

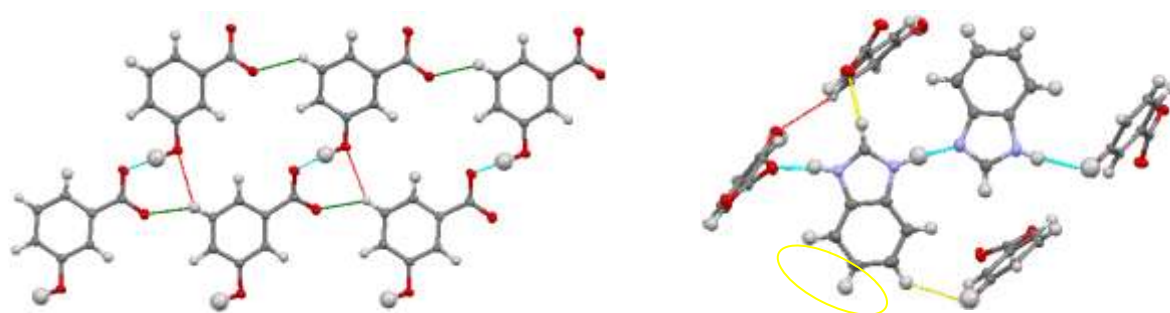


Fig. 4.42 –LHS, view along the *b*-axis highlighting the creation of sheets of 3-HBA⁻ molecules through weak C-H···O^{δ-} (red) and C-H···O (green) hydrogen bonds along the *a*-axis. The blue interactions represent the moderate hydrogen bonds that make up the chains of 3-HBA⁻ molecules. RHS, the weak hydrogen bonds in which the BZNH⁺ ions are involved – one C-H···O^{δ-} (yellow) and one C-H···O (yellow and circled).

There are other interactions in the structure of the benzimidazolium 3-hydroxybenzate 2:1 polymorph Form I, however they only assist the major interactions that have already been mentioned. The extended structure can be seen in Figure 4.43, with the 3-HBA⁻ molecules creating chains, these chains connected together along the *b*-axis via the BZN-BZNH⁺ molecules with the weaker interactions extending the structure along the *a*-axis.

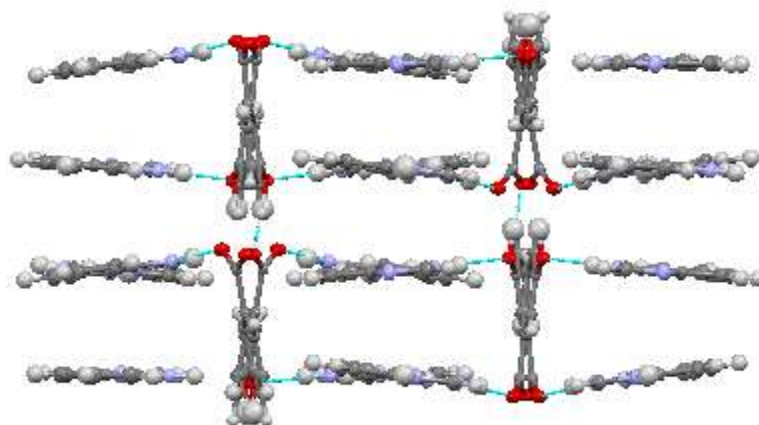


Fig. 4.43 – view along the *a*-axis of the extended benzimidazolium 3-hydroxybenzoate 2:1 polymorph Form I molecular complex.

4.4.6 Molecular Complex of Benzimidazole and 4-Hydroxybenzoic Acid 2:1 Hydrate

The crystallisation attempts on benzimidazole and 4-hydroxybenzoic acid also resulted in a hydrate of the 2:1 molecular complex being formed. The crystal was obtained from ethanol at ~2-4°C and were flat plates in shape and colourless. Single crystal X-ray diffraction data were obtained using a Bruker-Nonius Kappa CCD diffractometer at 110K, equipped with graphite monochromated Mo K α radiation ($\lambda = 0.71073 \text{ \AA}$). The structure was solved using SIR92³⁰ within the CRYSTALS³¹ program. The crystallographic data are summarised in Table 4.4.

The introduction of a water molecule brings a large number of possible supramolecular synthons which are shown in Figure 4.44. However there are only a couple of designs that would use every possible interaction site.

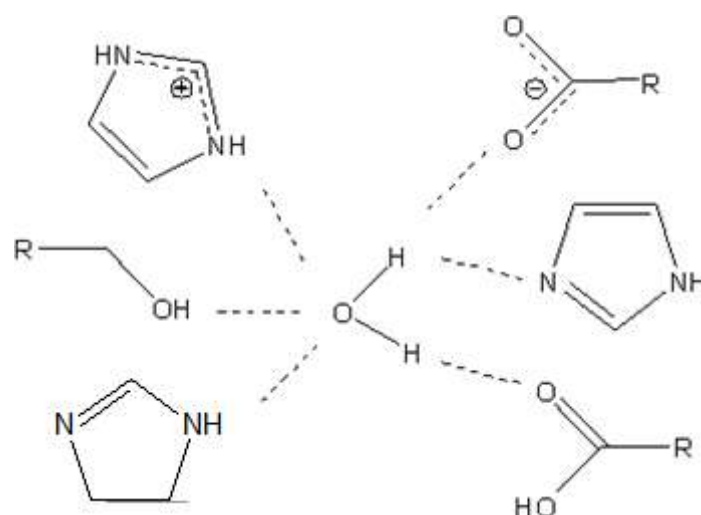


Fig. 4.44 – Schematic diagram highlighting the possible hydrogen bonds that could be generated between the water molecule and the other starting materials and their charged species.

In this molecular complex BZNH^+ molecules are formed through proton transfer from the carboxylic acid group on the 4-HBA molecule onto the normally unprotonated nitrogen atom. However with the stoichiometric ratio being two BZN molecules to every one 4-HBA, it would be chemically impossible for all nitrogen atoms to be fully protonated if only the carboxylic group is deprotonated, which is the case. Thus one BZN molecule is left unprotonated. The result of the proton transfer on the BZNH^+ molecule, is a delocalisation of the charge across the five-membered ring, reflected in the equalisation of the internal bond lengths and angles (Table 4.12). The BZN molecule where no protonation has occurred retains distinct single and double bond character (Figure 4.45). The intra- and intermolecular interactions are listed in Table 4.13.

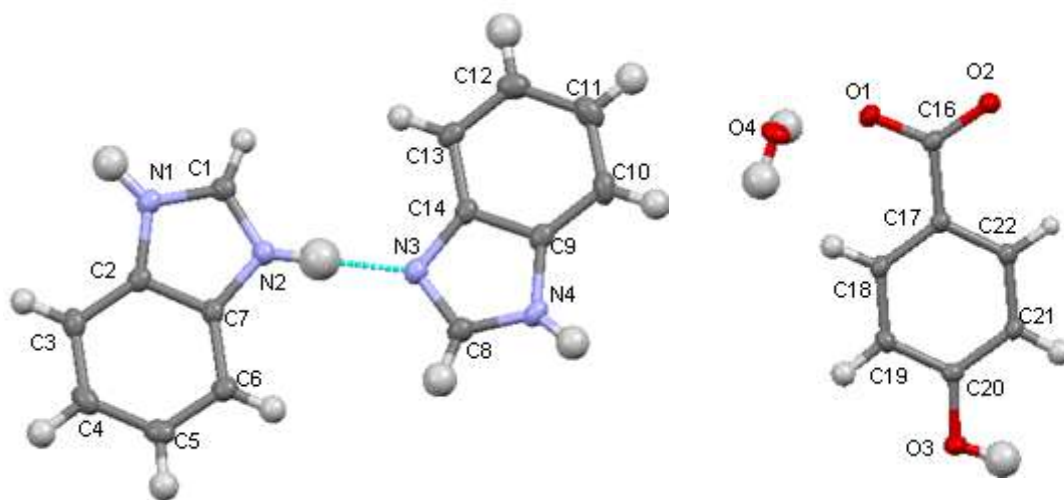


Fig. 4.45 – The BZNH^+ , BZN, 4-HBA^- and water molecule that are involved in the $\text{BZN BZNH}^+ 4\text{-HBA}^-$ hydrate, with atom labelling.

	BZNH⁺		BZN	
Bond Lengths (Å)	N1-C1	1.331(2)	N3-C8	1.321(2)
	N2-C2	1.328(2)	N4-C8	1.347(3)
Bond Angle (°)	C2-N1-C1	108.0(0)	C14-N3-C8	104.7(1)
	C7-N2-C1	106.7(1)	C9-N4-C8	107.0(2)

Table 4.12 – Bond length and bond angle data for the BZNH⁺ and BZN molecules involved in the BZN BZNH⁺ 4-HBA⁻ hydrate molecular complex.

Interaction	Length (Å) (D...A(Å))	For Hydrogen Bonds		
		D-H(Å)	H...A(Å)	D-H...A angle(°)
O4...O1	2.765(2)	0.92(3)	1.86(3)	168(3)
O4...O2	2.805(2)	0.86(2)	1.96(3)	168(3)
N4...O4	2.719(2)	0.88(3)	1.84(2)	172(2)
N1...O2	2.641(2)	0.96(3)	1.72(3)	161(2)
N2...N3	2.702(2)	0.99(3)	1.71(3)	176(3)
O3...O2	2.635(2)	0.91(3)	1.72(3)	174(3)
C1...π	3.350	-	-	-
O8...π	3.323	-	-	-

Table 4.13 – The inter- and intramolecular interactions with distances found in the BZNH⁺ 3HBA⁻ 2:1 molecular complex.

The 4HBA⁻ molecule has been deprotonated with a proton from the carboxylic acid group transferring to the BZN. This deprotonation leads to a negative charge that is delocalised over the carboxylate group, as seen by the normalisation of the bond lengths in the carboxyl group, C16-O1 1.262(2)Å and C16-O2 1.258(2)Å.

Figure 4.46 shows how the water molecule positions itself between two linear chains of 4-HBA⁻ and the BZN. It results in every possible hydrogen bond interaction site of the water molecule being utilised. All these hydrogen bonds are of moderate strength: O4-H...O1^{δ-} 2.765(2)Å, O4-H...O2^{δ-} 2.805(2)Å and N4^{δ+}-H...O4 2.719(2)Å (Figure 4.46 LHS). The water molecule does not significantly disturb the main motifs compared with those found in to

the non-hydrated form; there are still linear chains of 4-HBA⁻ held together by dimers of BZN. There is also minimal difference between the calculated densities with 1.362 g.cm⁻³ for the hydrate and 1.365 g.cm⁻³ for the non-hydrate. However the introduction of the water molecule has resulted in two key differences: one is that the rungs of the ladder now have a zig-zag formation (Figure 4.46 RHS) and it expands the structure in two directions, while the packing in the third direction is through the chains of 4-HBA⁻.

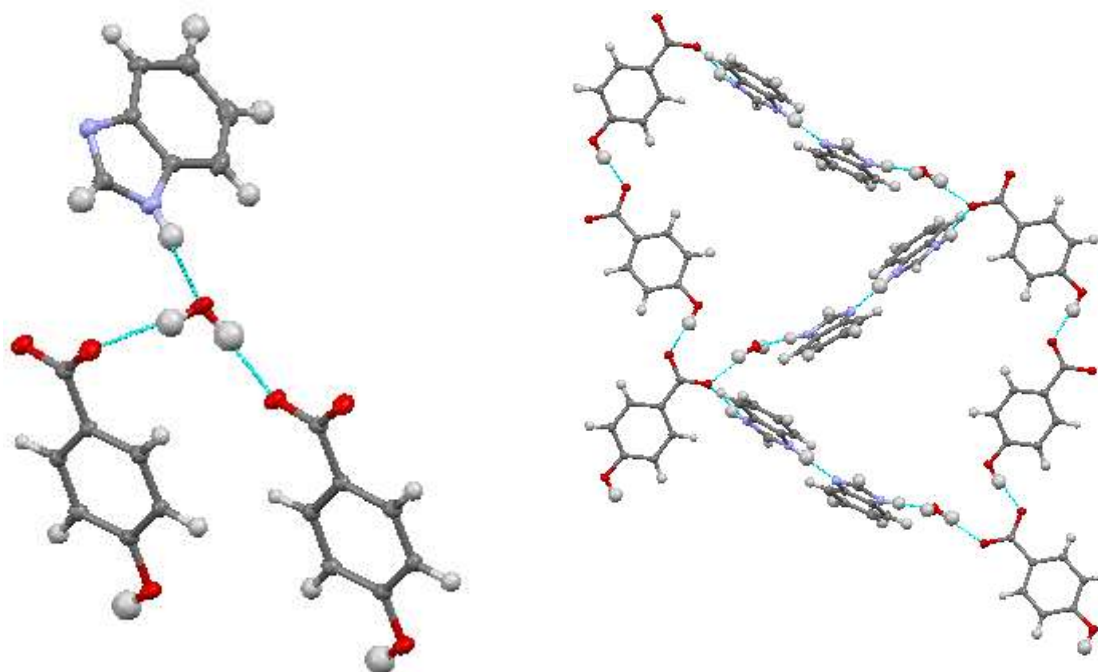


Fig. 4.46 – LHS, highlighting the hydrogen bonds in which the water molecule is involved. RHS, view along the *c*-axis highlighting the zigzag nature of the rungs (BZN BZNH⁺).

The hydrogen bond connecting the BZN and BZNH⁺ molecules has a distance of N2^{δ+}-H...N3, 2.702(2)Å which is similar to that found in the non-hydrated form. As seen in the other structures the hydrogen involved in the hydrogen bond shows signs of elongation (Figure 4.47).

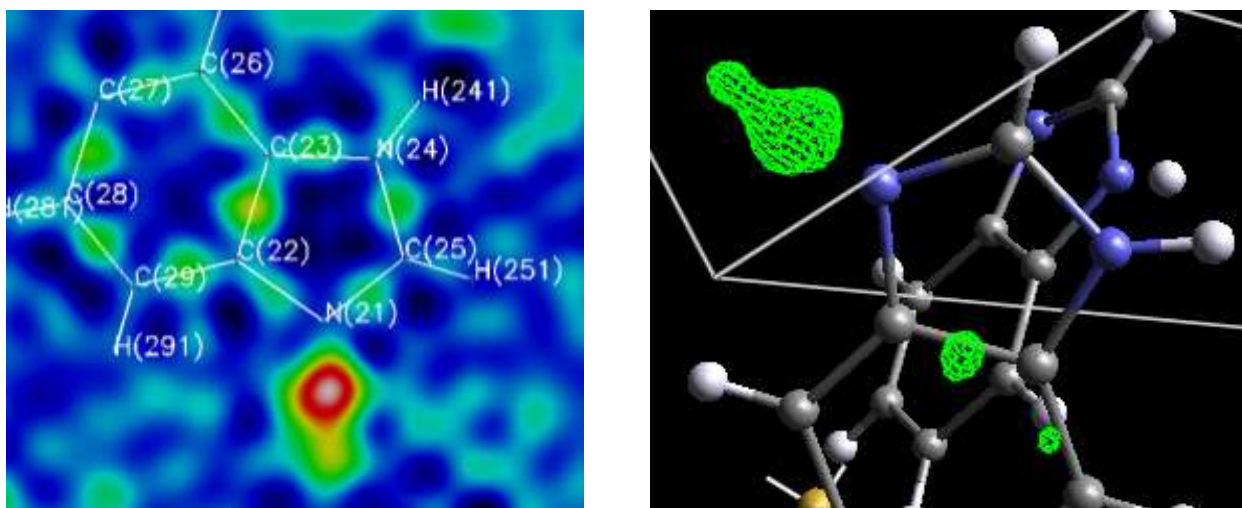


Fig. 4.47 – LHS, Fourier difference map in 2D and, RHS, Fourier difference map in 3D showing the possible elongation of the hydrogen atom involved in the hydrogen bond.

The 4-HBA⁻ chains form via hydroxyl – carboxylate O3–H⁺⋯O2^{δ-} hydrogen bonds of length 2.635(2)Å (refer to Table 4.3 for full details). They are slightly longer than the same hydrogen bond in the non-hydrated structure (2.603(3)Å) and form with a greater degree of staggered geometry (Figure 4.48).

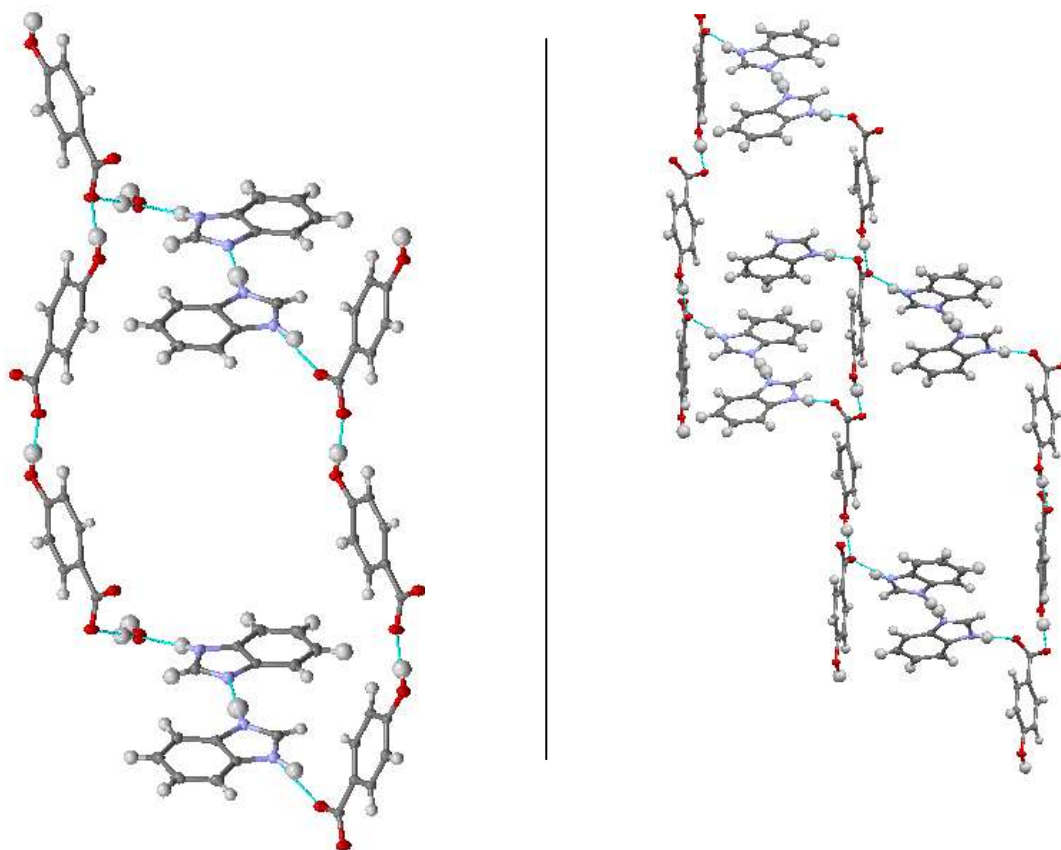


Fig. 4.48 – LHS, the staggered chains of 4-HBA⁻ that are held together by the stiles of BZN and BZNH⁺ in the 2:1 hydrate. Note that another BZN and BZNH⁺ group is present, oriented diagonally between the two that are

shown, RHS, view along the *b*-axis of the BZN BZNH⁺ 4-HBA⁻ molecular complex showing the main motifs for comparison.

This structure contains various weaker interactions however none are significant and only assist the stronger hydrogen bonds. For example there are C-H... π interactions between a carbon of the benzimidazole and the benzene ring of the benzoic acids (Figure 4.49) with distances ranging from approximately 3.323 Å (purple boxes) to 3.560Å and 3.771Å (yellow boxes). However as can be seen, these molecules are also connected through hydrogen bonds via the water molecule.

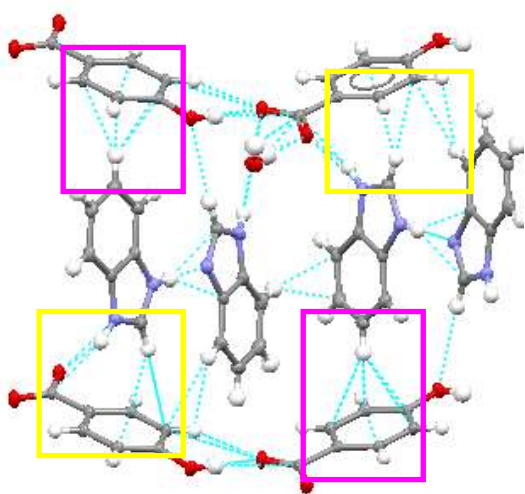


Fig. 4.49 – The short contacts that exist between the molecules in the BZN BZNH⁺ 4-HBA⁻ hydrate molecular complex. Highlighted are the areas that show the C-H... π interactions.

As expressed, the water molecule expands the structure in two directions, one with the aid of the BZN BZN⁺ group to connect two chains of 4-HBA⁻ molecules and in the other direction by hydrogen bonding to two 4-HBA⁻ molecules from two separate chains. The chains expand the structure in the third dimension. Figure 4.50 is an extended image of the structure which highlights the main interactions.

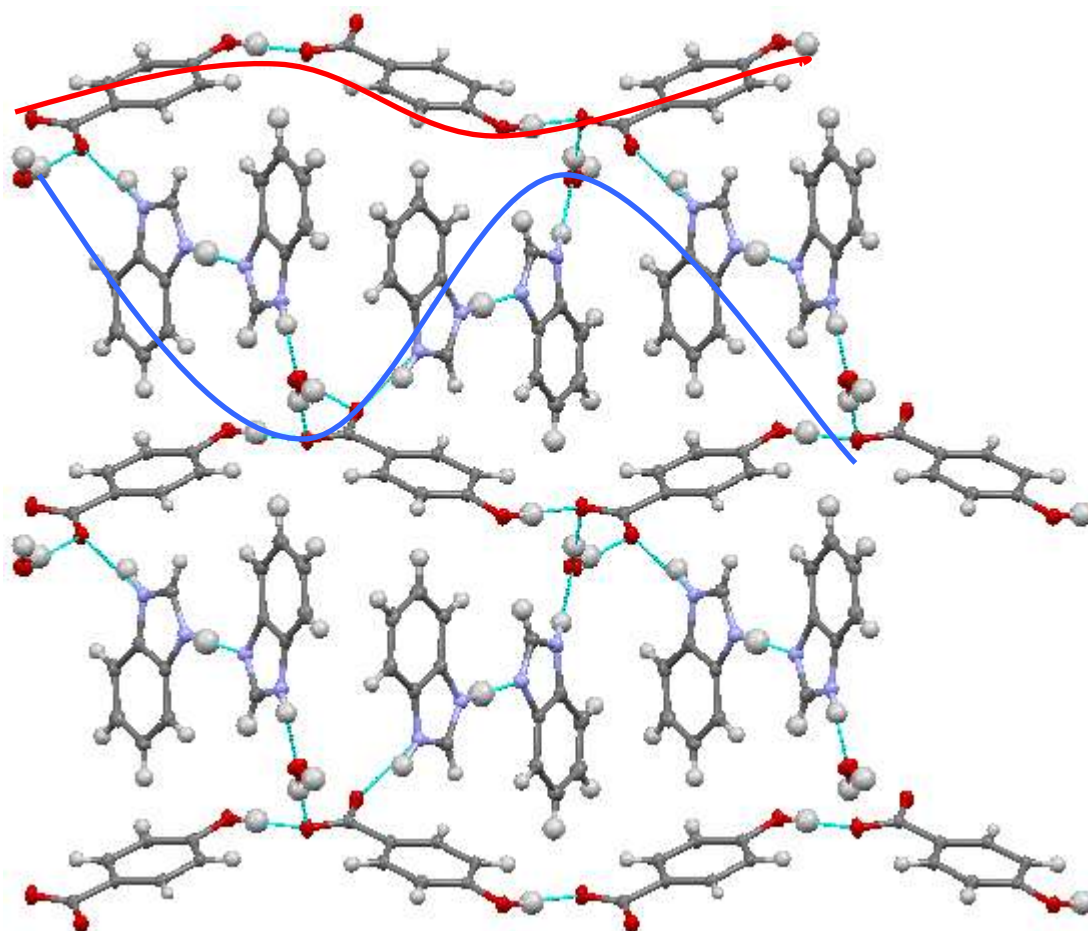


Fig. 4.50 – view along the *a*-axis of the BZN BZNH⁺ 4-HBA⁻ hydrate. The chains of 4-HBA⁻ molecules expand the structure along the *b*-axis (red line). The BZN BZNH⁺ group holds two chains together via hydrogen bonding to a water molecule in one side and through hydrogen bond pattern F in the other direction (blue line).

4.4.7 Molecular Complex of Benzimidazole 2-Hydroxybenzoate 1:2

Molecular ions, BZNH⁺ and 2-hydroxybenzoate(2-HBA⁻) and molecule 2-hydroxybenzoic acid (2-HBA) form a 1:1:1 molecular complex with one another. The molecular complex was obtained using the solvent evaporation method, with a 1:2 stoichiometric mixture of BZN (12mg) and 2-hydroxybenzoic acid (2-HBA) (28mg) dissolved in the minimum amount of acetone followed by evaporation at 2~4°C. The crystals generated were plate shaped and colourless. Single crystal X-ray diffraction data were obtained using a Bruker ApexII CCD diffractometer at 100K, equipped with graphite monochromated Mo K α radiation ($\lambda = 0.71073 \text{ \AA}$). The structure was solved using SIR92³⁰ within the CRYSTALS³¹ program. The crystallographic data are summarised in Table 4.4. A BZNH⁺ molecule is created through proton transfer as discussed in Section 4.2.1 (Figure 4.51). The charge on the BZNH⁺

molecule is delocalised across the five-membered ring, reflected in the equalisation of the internal bond lengths, N1^{δ+}-C1 1.325(2)Å and N2^{δ+}-C1 1.325(2) Å, and bond angles, C1-N1^{δ+}-C2 108.5(1)° and C1-N2^{δ+}-C7 108.2(1)°.

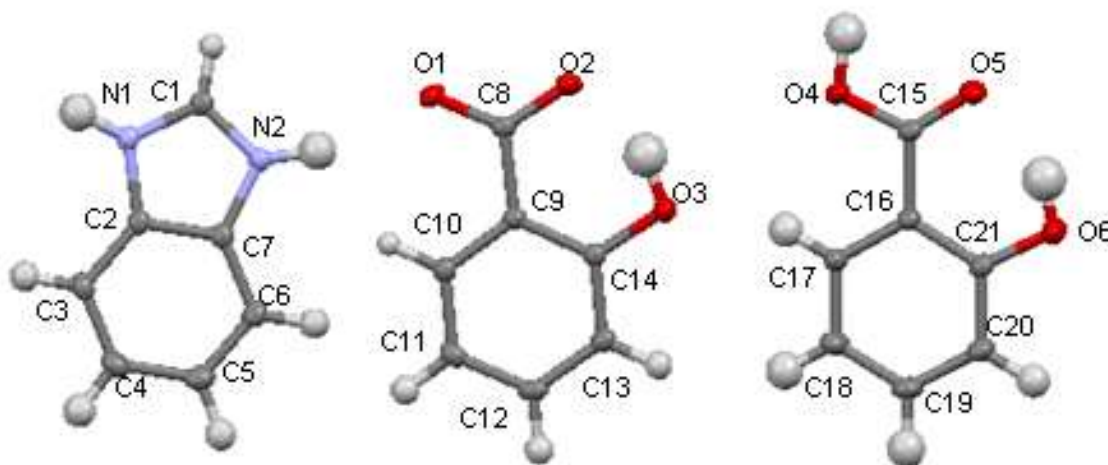


Fig. 4.51 – The BZNH⁺ 2-HBA⁻ and 2-HBA molecules which are generated in the molecular complex with atom labelling.

Interaction	Length (Å) (D...A(Å))	For Hydrogen Bonds		
		D-H(Å)	H...A(Å)	D-H...A angle(°)
O6...O5	2.624(2)	0.88(2)	1.83(3)	150(3)
O3...O2	2.555(2)	0.92(3)	1.69(3)	155(3)
O4...O1	2.605(1)	0.99(2)	1.62(2)	1.74(2)
N2...O1	2.709(2)	0.91(3)	1.81(3)	173(2)
N1...O2	2.672(1)	0.91(2)	1.80(2)	161(2)
C1...O5	3.091(1)	0.94(2)	2.21(2)	157(2)
C10...π	3.780(2)	-	-	-
C13...π	3.541(2)	-	-	-
C13...O6	3.642(2)	0.98(3)	2.66(3)	175(2)
C20...O3	3.562(2)	1.00(3)	2.57(3)	171(2)

Table. 4.14 – The inter- and intramolecular interactions found within the BZNH⁺ 2-HBA⁻ 2-HBA molecular complex

The 2-HBA molecule in its native crystal structure (refer to Section 4.1.1) is configured such that there is an intramolecular hydrogen bond between the hydroxyl and carboxylic acid groups. Within the molecular complex with BZNH⁺ this intramolecular hydrogen bond persists in both 2-HBA⁻ and 2-HBA despite the proton transfer of a hydrogen atom to the benzimidazole. The intramolecular hydrogen bond is shorter in the 2-HBA⁻ than the 2-HBA,

as would be expected due to the carboxylate group containing a negative charge creating a charged assisted hydrogen bond. Table 4.15 highlights the differences in these internal hydrogen bonds and bond lengths and compares then with the native 2-HBA molecule and that 2-HBA⁻ found in the BENZH⁺ 2-HBA⁻ 1:1 molecular complex. It can be seen that the negative charge is found to be delocalised over the carboxylate group and the resulting effect on the intramolecular hydrogen bond is profound in comparison to the protonated form.

	2-HBA	2-HBA (native)	2-HBA⁻	2-HBA⁻ (1:1)
Internal H-bond (Å)	2.624(2)	2.622Å	2.555(2)	2.551(3)
Bond Lengths (Å)	1.234(2)	1.2450(3)	1.274(2)	1.273(1)
	1.325(2)	1.3113(3)	1.262(2)	1.264(1)

Table 4.15 – Internal hydrogen bond and C-O bond lengths for the 2-HBA (BZNH⁺ 2-HBA⁻ and 2-HBA molecular complex), 2-HBA(native crystal structure, 2-HBA(BZNH⁺ 2-HBA⁻ and 2-HBA molecular complex) and 2-HBA⁻ (BZNH⁺ 2-HBA⁻ molecular complex).

The structure of the BZNH⁺ 2-HBA⁻ 2-HBA molecular complex is more similar to the structures of 3-HBA and 4-HBA than to that of the BZNH⁺ 2-HBA⁻ molecular complex. The motif is a chain that runs along the *b*-axis (Figure 4.52). This chain is made up of pairs of 2-HBA⁻ and 2-HBA using hydrogen bonds G (Figure 4.12) being held together by BZNH⁺ molecules using bonds of pattern E. For comparison the BZNH⁺ 2-HBA⁻ molecular complex motif is a four molecule hydrogen bonded ring consisting of alternating co-molecules, while the 3-HBA and 4-HBA molecular complexes have ladder style structures. The 2-HBA⁻ and 2-HBA pairs are connected through a moderate hydrogen bond between the carboxylic acid and carboxylate groups, O4-H...O1⁻ with length 2.605(1)Å. They are two distinct type E hydrogen bonds, both are N^{δ+}-H...O^{δ-} interactions however the oxygens involved differ. The N2^{δ+}-H...O1^{δ-} hydrogen bond has length 2.709(2)Å and the N1^{δ+}-H...O2^{δ-} hydrogen bond has length 2.672(1)Å (refer to Table 4.14 for full interactions list).

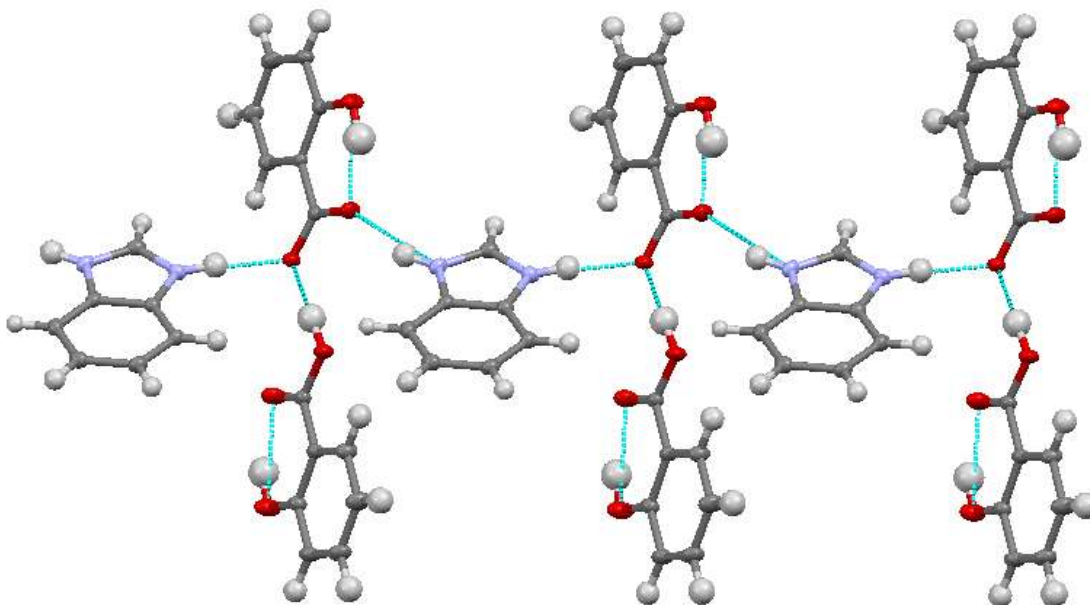


Fig. 4.52 – View along the *a*-axis of the main motif of the BZNH⁺ 2-HBA⁻ and 2-HBA molecular complex; linear chains of 2-HBA⁻ 2-HBA pairs are held together by BZNH⁺ molecules that run along the *b*-axis.

There are a few weaker interactions that connect the chains together. The most influential is a weak hydrogen bond from a carboxylic oxygen to the carbon sandwiched between the nitrogens on the benzimidazole. The C1-H \cdots O5 ^{δ^-} hydrogen bond is 3.091(1)Å in length and connects the chains as seen in Figure 4.53. Two C-H \cdots π interactions assist these weak hydrogen bonds in stacking the chains (Figure 4.53 RHS), these are of length C10-H \cdots π 3.780(2)Å and C13-H \cdots π 3.541(2)Å.

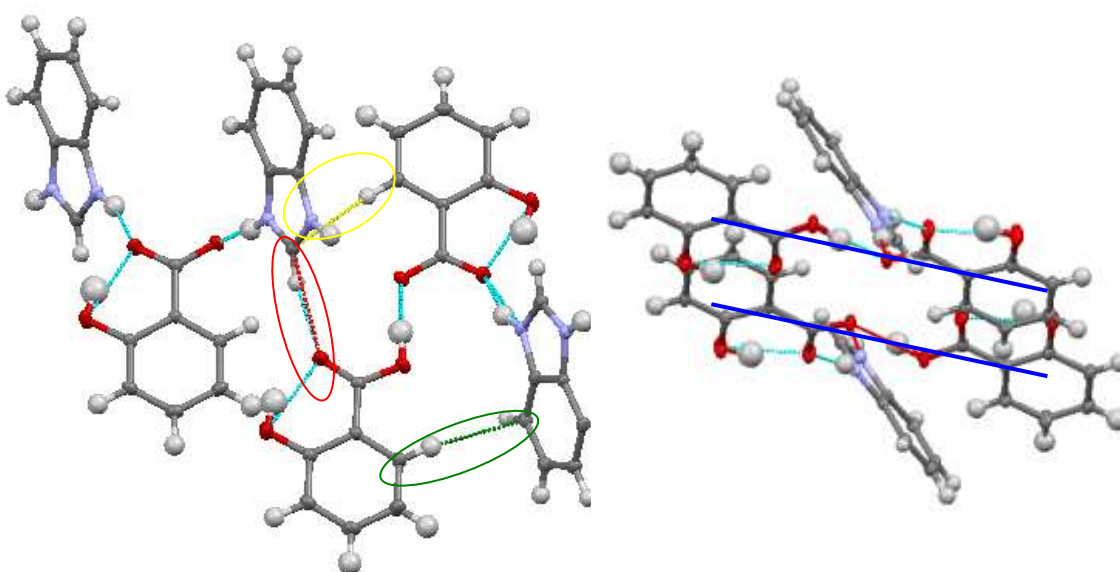


Fig. 4.53 – LHS, the C1-H \cdots O5 $^{\delta-}$ weak hydrogen bonds (-) that stack the hydrogen bonded chains upon one another with the assist of two C-H \cdots π interactions (-)(-). RHS, view of the *a*-axis displays how the chains stack upon one another (-).

Expanding the chain along the *c*-axis are C-H \cdots O hydrogen bonds involving the hydroxyl group from one of the 2-HBA 2-HBA $^-$ molecules and a C-H group of the other (Figure 4.54). These are very weak hydrogen bonds with lengths C13-H \cdots O6, 3.642(2)Å (a), C20-H \cdots O3, 3.562(2)Å (b) (Figure 4.54 inset).

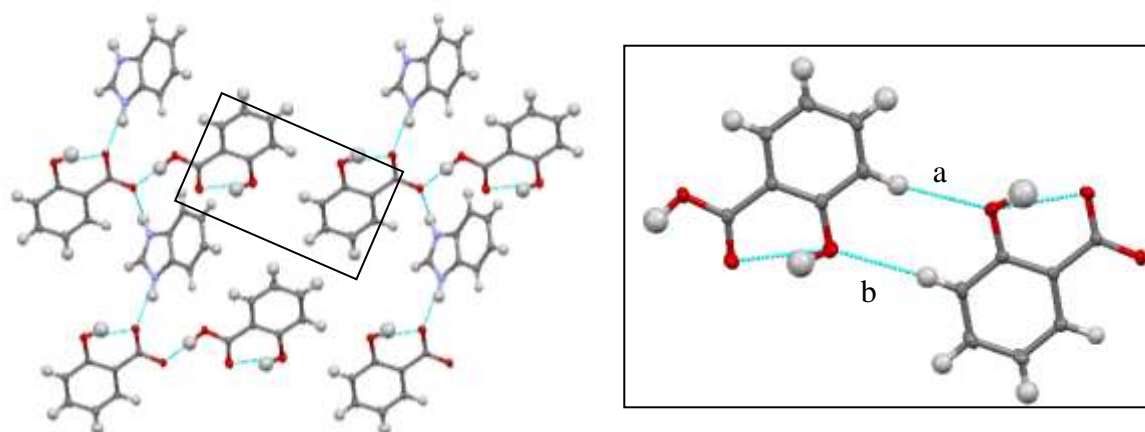


Fig. 4.54 – Two chains of the main motif are held by weak C-H \cdots O hydrogen bonds which are located inside the black box. Inset, a blow-up of the black box highlighting the weak C-H \cdots O hydrogen bonds.

4.4.8 Molecular Complex of Benzimidazole 3,5-Dihydroxybenzoic Acid 1:1

The crystal structure of the molecular complex benzimidazolium 3,5-dihydroxybenzoate has already been published in Acta Crystallographica Section E²⁹, however the experiment reported in that work was undertaken at room temperature. As mentioned previously, experiments with the other di-hydroxybenzoic acids, 2,4-, 2,6- and 3,4- did not produce single crystal molecular complexes with benzimidazole or its derivatives. The aim of using the di-hydroxybenzoic acids was to use the library of motifs and supramolecular synthons that have been created in the study of the other complexes presented, to understand the hydrogen bonding patterns that could be found when there are a greater number of potential donor and acceptor sites. Unfortunately only the structure of a single example, benzimidazolium 3,5-dihydroxybenzoate molecular complex, has been obtained. The structure is discussed here.

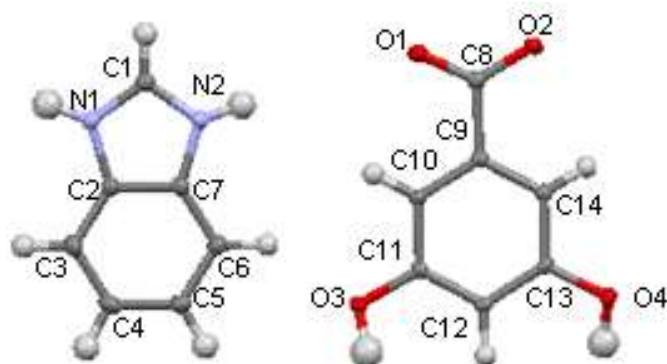


Fig. 4.55 – The benzimidazolium and 3,5-dihydroxybenzoate molecules which are generated in the molecular complex with atom labelling.

Interaction	Length (Å) (D...A(Å))	For Hydrogen Bonds		
		D-H(Å)	H...A(Å)	D-H...A angle(°)
O1...O4	2.640(1)	0.95(2)	1.69(2)	177(2)
O2...O3	2.625(1)	0.92(2)	1.70(2)	178(2)
N2...O2	2.700(1)	0.92(2)	1.79(2)	167(2)
N1...O3	2.893(1)	0.89(2)	2.31(2)	123(1)
N1...O4	2.813(1)	0.89(2)	1.99(2)	153(1)

Table 4.16 – The inter- and intramolecular interactions seen in the BZNH^+ (3,5-DIHB $^-$) molecular complex

The molecular ions, BZNH^+ and 3,5-dihydroxybenzoate(3,5-DIHB $^-$) form a 1:1 molecular complex. This was produced using the solvent evaporation method, with a 1:1 stoichiometric mixture of BZN (12mg) and 3,5-dihydroxybenzoic acid (3-HBA) (16mg) dissolved in the minimum amount of a methanol/water mixture followed by evaporation at room temperature. The crystals generated were cubic shaped and colourless. Single crystal X-ray diffraction data were obtained using a Rigaku R-axis/RAPID image plate diffractometer at 100K, equipped with graphite monochromated Mo $K\alpha$ radiation ($\lambda = 0.71073 \text{ \AA}$). The structure was solved using SIR92³⁰ within the CRYSTALS³¹ program. The crystallographic data are summarised in Table 4.4. The BZNH^+ molecule is created as discussed in Section 4.2.1 (Figure 4.55). The result of the proton transfer on the BZNH^+ molecule is a delocalisation of the charge across the five-membered ring, $\text{N1}^{\delta+}\text{-C1}$ 1.328(1) \AA and $\text{N2}^{\delta+}\text{-C1}$ 1.328(1) \AA , and bond angles, $\text{C1-N1}^{\delta+}\text{-C2}$ 108.89(9) $^\circ$ and $\text{C1-N2}^{\delta+}\text{-C7}$ 108.80(9) $^\circ$. The negative charge on the 3,5-DIHB $^-$ molecule is delocalised over the carboxylic acid group, $\text{C8-O1}^{\delta-}$ 1.250(1) \AA and $\text{C8-O2}^{\delta-}$ 1.276(1) \AA .

The increase in the amount of potential hydrogen bonding sites has led to an increase in complexity of the structure obtained. The extended structure can be described very much like the other hydrobenzoic acid molecular complexes, a ladder style structure with uprights of 3,5-DHBA⁻ and rungs of BZNH⁺ molecules (Figure 4.56).

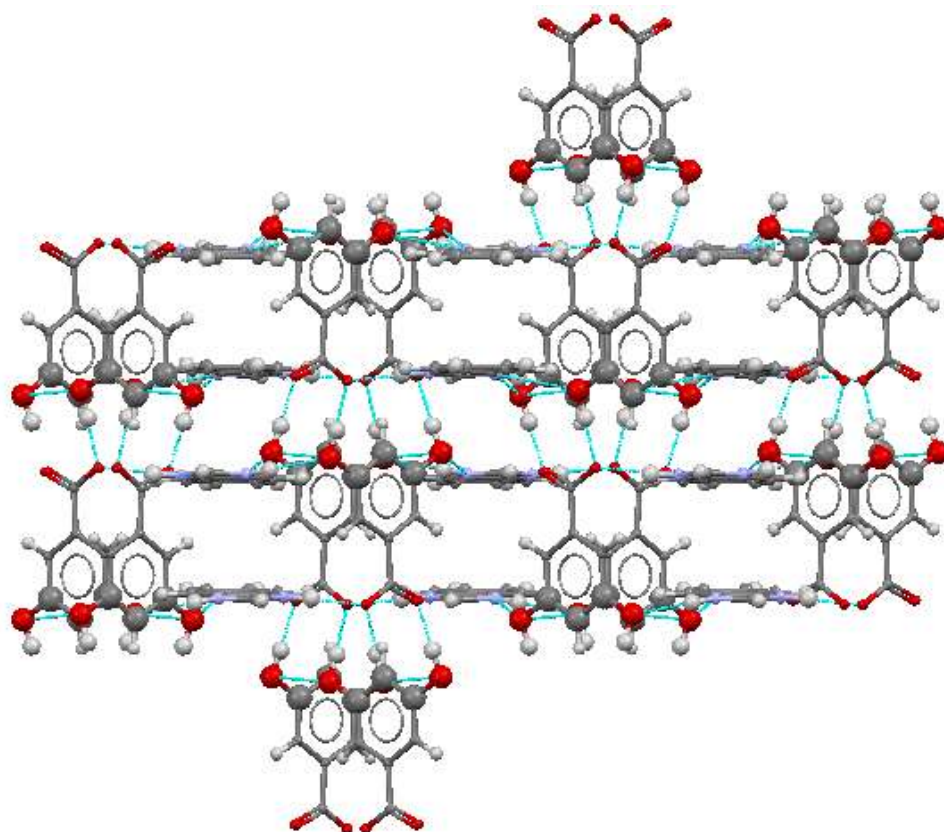


Fig. 4.56 – The extended structure of the BZNH⁺ 3,5-DHBA⁻ molecular complex which consist of chains of 3,5-DHBA⁻ molecules which are held together by BZNH⁺ molecules.

The uprights of the ladder are created by hydrogen bonded rings of 3,5-DHBA⁻ molecules, described by graph set notation as R_4^4 (24) (Figure 4.57). There are two moderate hydrogen bonds that hold the rings together, O-H \cdots O $^{\delta-}$ 2.640(1)Å (a) and O-H \cdots O $^{\delta-}$ 2.625(1)Å (b). Every 3,5-DHBA⁻ molecule is the top, bottom, left or right part of each ring (Figure 4.58) and expands the structure along the *ba* diagonal and *c* dimensions (refer to Table 4.16 for full details).

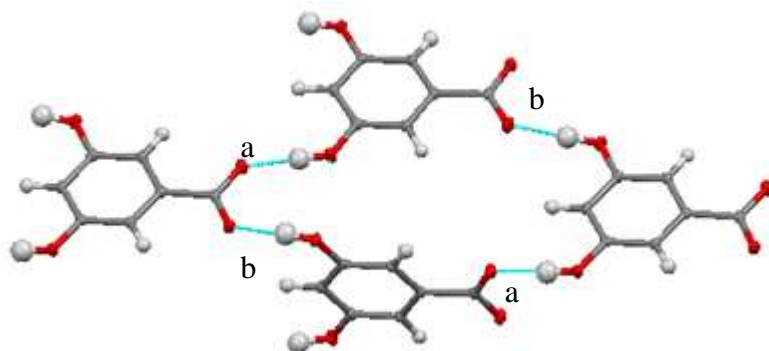


Fig. 4.57 – The hydrogen bonded rings that are made up of four 3,5 DHBA⁻ molecules.

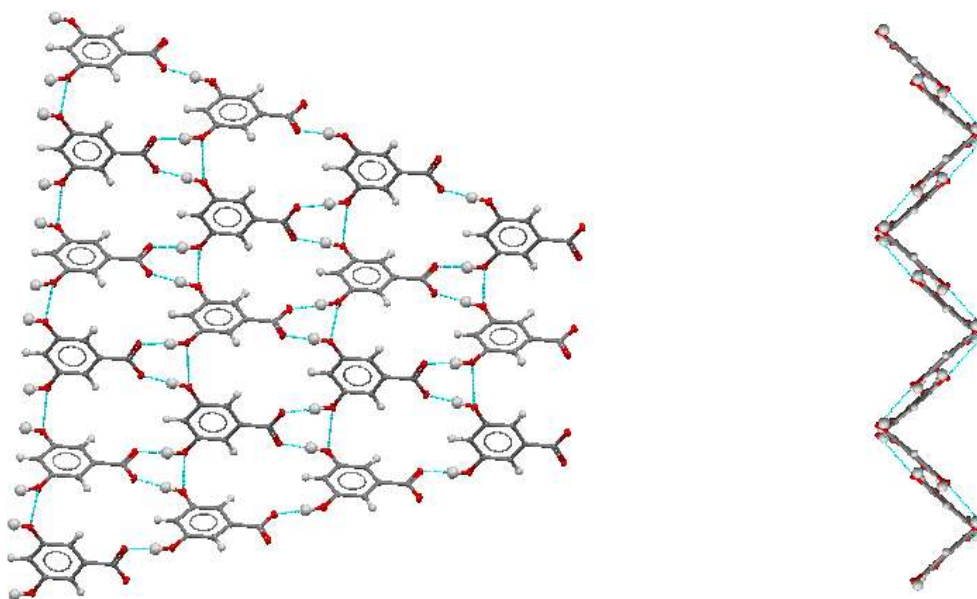


Fig. 4.58 – Two views of the 3,5 DHBA⁻ hydrogen bonded rings that expand along the *bc* diagonal and *c* dimensions.

The BZNH⁺ molecules hold the 3,5 DHBA⁻ chains together through hydrogen bonding to the carboxylate group in one direction (Figure 4.59 a) and a bifurcated hydrogen bond to two hydroxyl groups in the other direction (Figure 4.59 b). The single hydrogen bond is of moderate strength and has a greater degree of charged assistance than the bifurcated hydrogen bond, which is also of moderate strength. The single hydrogen bond is of length N2^{δ+}-H····O2^{δ-} 2.700(1)Å and the bifurcated hydrogen bonds are N1^{δ+}-H····O3 2.893(1)Å and N1^{δ+}-H····O4 2.813(1)Å. These hydrogen bonds expand the structure along the *a*-axis.

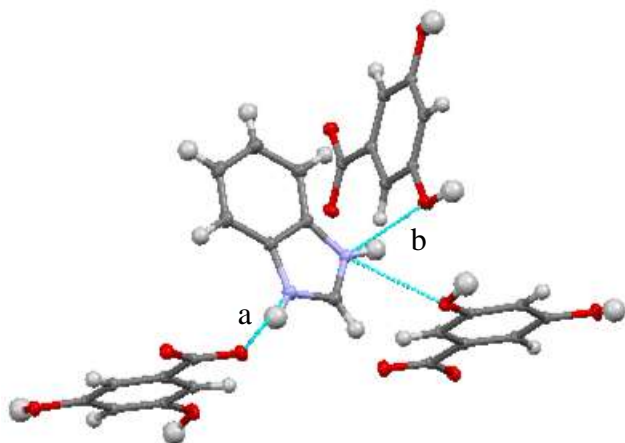


Fig. 4.59 – The hydrogen bonds that the BZNH^+ molecule is involved with in the BZNH^+ 3,5-DHBA $^-$ molecular complex, a is a partially charged assisted $\text{N}^{\delta+}\text{-H}\cdots\text{O}^{\delta-}$ hydrogen bond while b is a bifurcated hydrogen bond of two $\text{N}^{\delta+}\text{-H}\cdots\text{O}$ interactions.

None of the weaker interactions within the BZNH^+ 3,5-DHBA $^-$ molecular complex are significant in defining the packing, they all assist the hydrogen bonds that have already been mentioned. Figure 4.60 is another extended image of the structure, it clearly shows the zig zag chains of 3,5-DHBA $^-$ molecules that extend the structure along the b and c axis, while the BZNH^+ molecules hold these zigzag chains together along the a -axis.

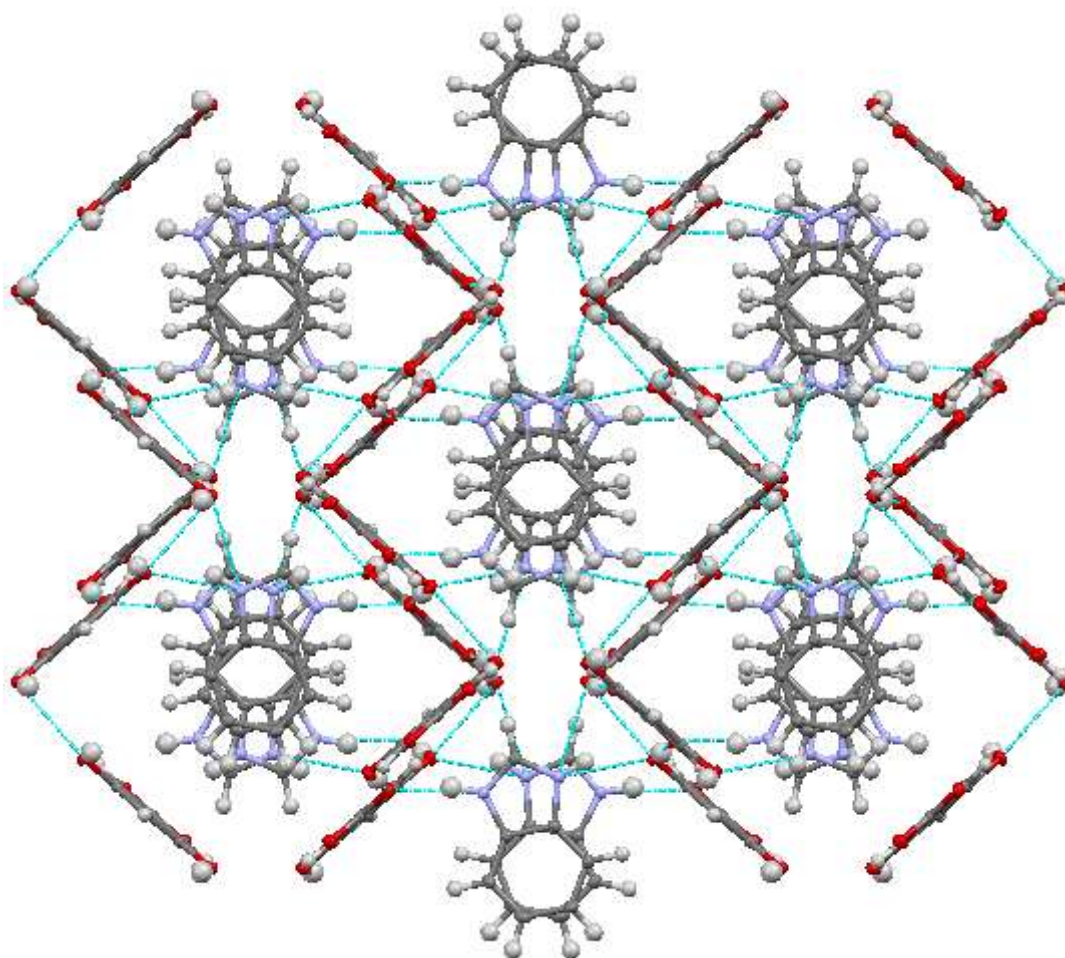


Fig. 4.60 – View along the *c*-axis of an extended image of the BZNH⁺ 3,5-DHBA⁻ molecular complex.

4.5 Solvent-Free Co-Crystallisations

As discussed in the introduction (Section 1.5) solvent-free co-crystallisation involves the mechanical grinding together of the components. There are various techniques and methodologies that come under the umbrella term of solvent free co-crystallisation, two of which were used during this research: solvent-free grinding and solvent drop grinding. Both these methods involve the grinding of the co-molecules with a mortar and pestle for roughly three minutes, with the solvent drop grinding method including adding micro-amounts of solvent. The product was then stored at room temperature.

As this technique was relatively new with only a limited number of papers published when this research was started, the initial aim was to investigate the effectiveness and limits of the technique. Initial studies concentrated on already discovered and researched molecular complexes, particularly between benzimidazole and halo-benzoic acids.

4.5.1 Feasibility Study

The initial experiments using solvent free co-crystallisations were carried out to test its feasibility. This was assessed on a range of halo-benzoic acids co-crystallised with benzimidazole. These had already been studied using the traditional evaporation crystallisation techniques (see Chapter 5) in some detail. A range of experimental conditions were studied in the solvent-free attempts, including variations in time of grinding, amount of sample used and after storage temperature.

Solvent free grinding experiments were carried out on BZN with co-molecules 3- and 4-chlorobenzoic acid, 3- and 4- bromobenzoic acid and 3- and 4- fluorobenzoic acid. Grinding was carried out for three minutes then the product stored for at least 24 hours at room temperature. The analysis of these experiments was by DSC and it was found that the solvent free experiments replicated well the solvent evaporation technique (Figure 4.61; see Appendix 4.A for more evidence).

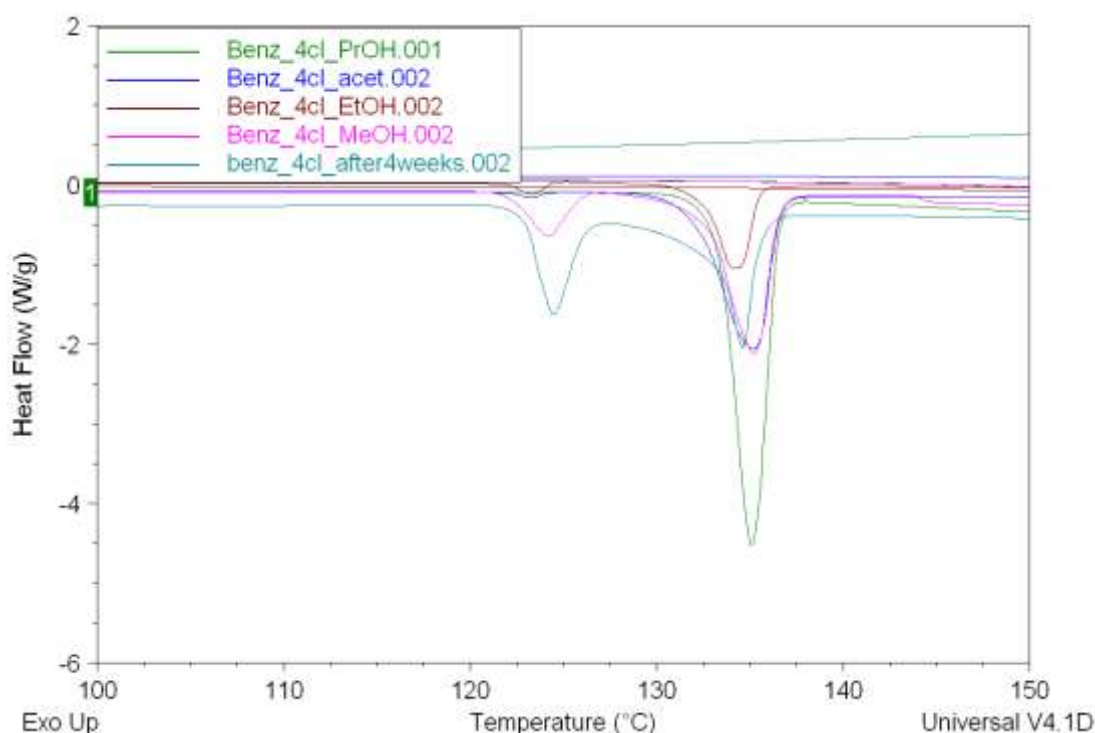


Fig. 4.61 – DSC thermograms from the product of the co-crystallisation of benzimidazole with 4-chlorobenzoic acid crystallised from propanol (-) acetone (-), ethanol (-), methanol (-) and by the solvent free method (-). The results indicate that the solvent free method replicates the more traditional evaporation technique.

Further studies to test the technique involved varying the grinding time and storage time after sample preparation. These experiments were carried out on the benzimidazole and 3-chlorobenzoic acid molecular complexes as these were found to have at least two polymorphs and a possibly third observed in powder diffraction and DSC data; a multi-phase product such as this is obviously more of a challenge and potentially of more interest. Figure 4.62 shows the full DSC trace of the products from grinding benzimidazole and 3-chlorobenzoic acid together for 30 seconds, 2 minutes and 5 minutes. It can clearly be seen that when longer grinding times are used the outcome favours the thermodynamic product (e.g the most stable polymorph) and the resulting product is more uniform. It has been found that the molecular complexes prepared using solvent free grinding tend to be less crystalline and thus show broader peaks in both DSC and X-ray powder diffraction data.

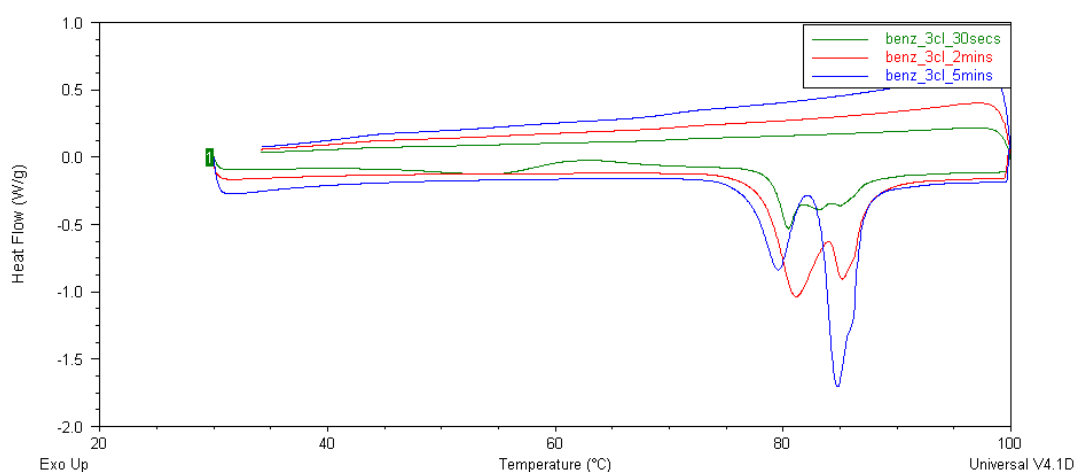


Fig. 4.62 – DSC thermogram from the product of the solvent free co-crystallisation of benzimidazole with 3-chlorobenzoic acid with grinding times of 30 seconds (-), 2 minutes (-) and 5 minutes (-). The results indicate that the thermodynamic product is favoured with increasing grinding time.

The stability of the product of solvent free crystallisations was tested by analysing the product regularly over a 6 month period. Figure 4.63 displays the DSC traces of the solvent free grinding experiments of benzimidazole and 3-chlorobenzoic acid, for a grinding time of 2 minutes. It was found that the longer the product was stored the greater chance the thermodynamic product would prevail, thus highlighting product stability issues.

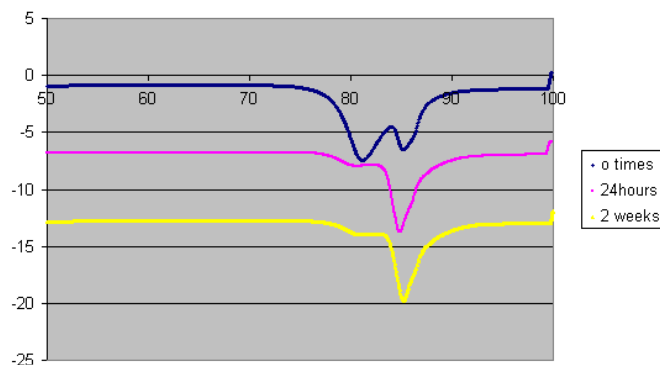


Fig. 4.63 – DSC traces of the product of the solvent free co-crystallisation of benzimidazole with 3-chlorobenzoic acid grinding for 2 minutes and stored for no time (-), 24 hours (-) and 2 weeks (-). The results indicate that the thermodynamic product is favoured with increasing storage time.

These experiments testing the solvent free co-crystallisation technique underline that this technique is capable of producing molecular complexes that the traditional solvent evaporation method can produce. It also highlights that this method has the potential to reveal rapidly the different phases / polymorphs that the system can produce.

A wider study was then undertaken on a much greater range of co-molecules (Table 4.17). From the solvent-free co-crystallisation results it can be seen that there was a potential for three new molecular complexes of benzimidazole having been produced, with aspartic acid, 5-chlorosalicylic acid and glycine. The tradition solvent evaporation method mirrored the solvent-free results, by producing two new molecular complexes, benzimidazolium aspartate and benzimidazole and 5-chlorosalicylic acid, that also produced different polymorphs (Figure 4.64). It also concurred with the solvent-free in the negative results and the unsuccessful co-crystallisations of benzimidazole and glycine produced an oil (see appendix 4.B).

Co-Molecule	Solvent Free Method	Solvent Evaporation Technique	
	DSC	DSC	Single Crystal
ascorbic acid	SM	SM	-
aspartic acid	NP	NP	NP
Cysteine	SM	SM	-
glutamic acid	SM	SM	-
Glycine	NP	Oil produced	-
Histidine	SM	SM	-
Guanosine	SM	SM	-
Thymine	SM	SM	SM
Creatine	SM	SM	SM
5-chlorosalicylic acid	NP	NP	NP
D-Valine	SM	SM	-
Isobartituric acid	SM	insoluble	-
D-alanine	SM	SM	SM
Cytidine	SM	SM	SM
Alenine	SM	SM	SM
Thymidine	SM	SM	-
Uracil	SM	SM	SM
Guanine	SM	insoluble	-
acetlysalicylic acid	SM	SM	-

Table 4.17 – Results from solvent-free and solvent evaporation co-crystallisations involving benzimidazole with a range of co-molecules. SM represents starting materials while NP represents new product. Only co-crystallisation experiments with aspartic acid and 5-chlorosalicylic acid produced new molecular complexes.

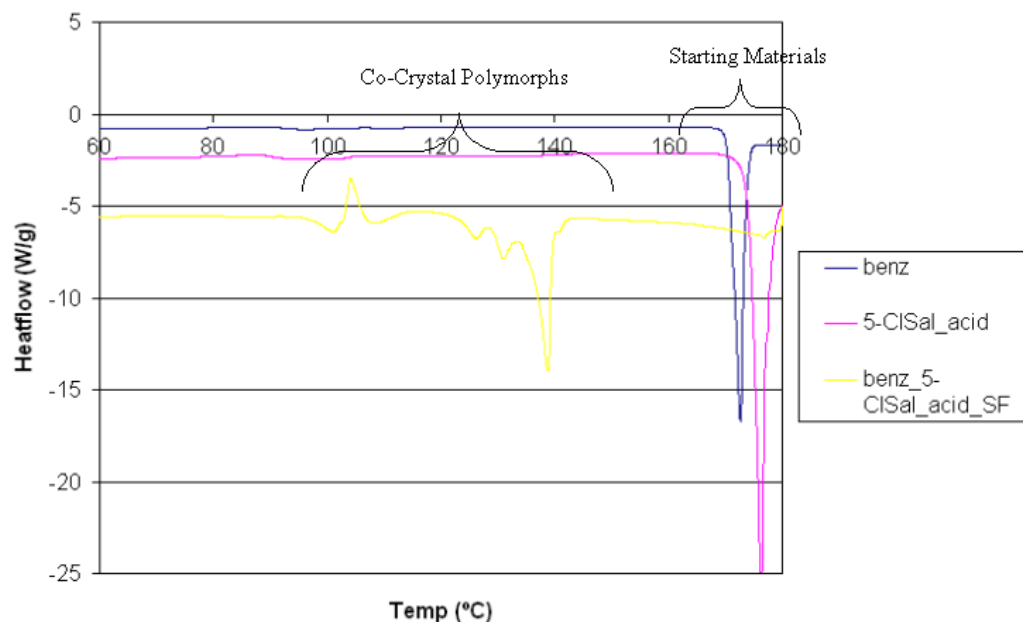


Fig. 4.64 – DSC patterns of starting materials benzimidazole (-), 5-chlorosalicylic acid (-) and the co-crystallisation product of the two (-) formed by the solvent-free method.

4.5.2 Molecular Complex of Benzimidazole and 5-Chlorosalicylic Acid 1:1

Guided by the successful solvent free experiments, solvent evaporation experiments were set-up on the target systems using four common solvents, methanol, ethanol, propanol and acetone. From these initial experiments it could be seen from the DSC thermogram of the products that there were at least three polymorphs present and that selective growth could be achieved for two of them (Figure 4.65)

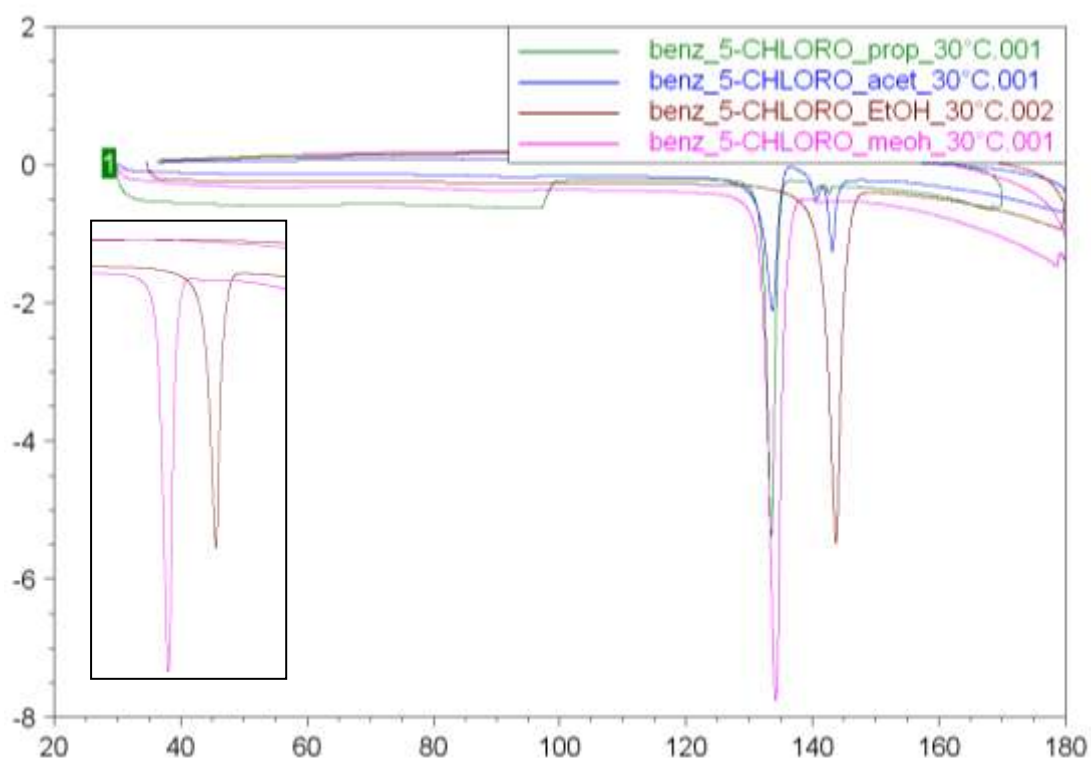


Fig. 4.65 – DSC thermogram of the product from co-crystallisation of benzimidazole and 5-chlorosalicylic acid at 30°C in propanol (-), acetone (-), ethanol (-) and methanol (-). Inset, selective polymorph growth has been achieved for two of the co-crystal polymorphs by recrystallisation from methanol (-) Form I and ethanol (-) Form III.

Further experiments were then set up to attempt to control the formation of the third possible polymorph and to promote the growth of diffraction quality crystals of all forms. Table 4.18 summarises the results of co-crystallisation experiments at various temperatures and solvents, Form I is the most obtainable form followed by Form III, however Form II is only produced in conjunction with Form I. The powder diffraction data, Figure 4.66a, highlights two clear Forms (I and III). Single crystal X-ray diffraction quality crystals were only obtained for Form I (Figure 4.66b)

	Methanol	Ethanol	Propanol	Acetone
10°C	Blue	Blue, Red	Blue	Blue, Red
20°C	Blue	Blue	Blue	Blue, Red
30°C	Blue	Yellow	Blue	Blue
35°C	Blue	Yellow	Blue	Blue

Table. 4.18 – Visual Summary of the products obtained from varying the crystallisation conditions, Form I (blue), Form II (red), Form III (yellow)

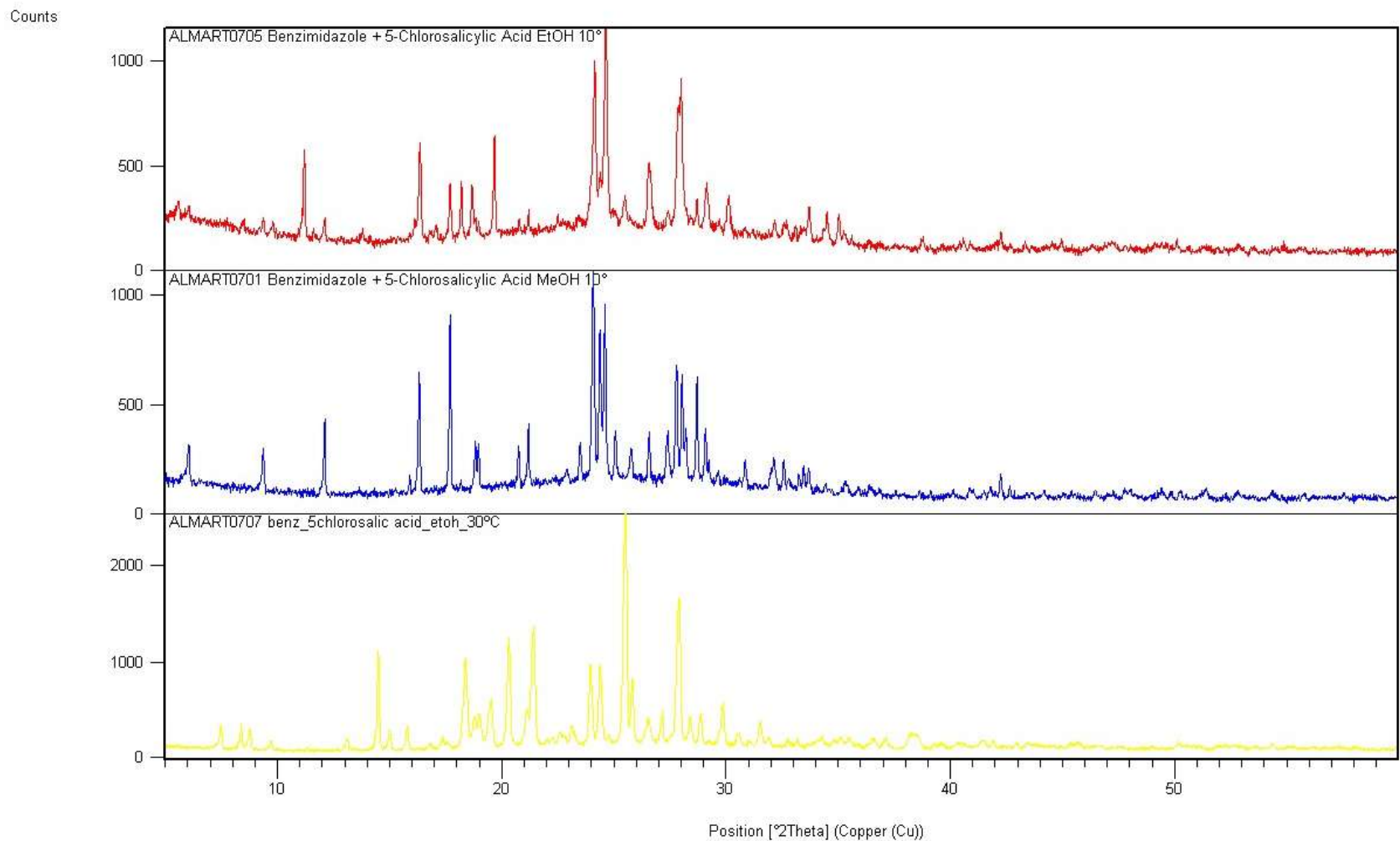
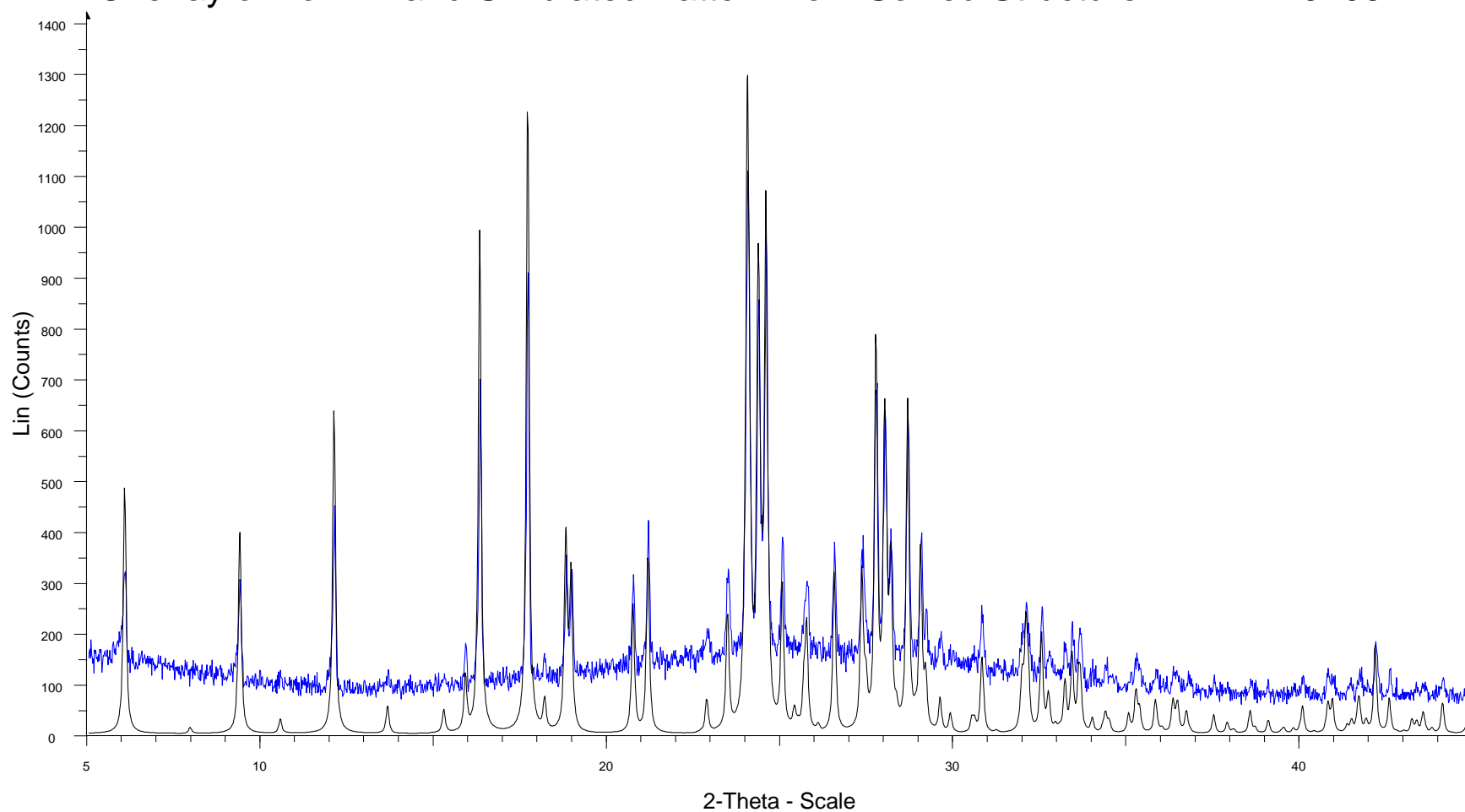


Fig. 4.66a – Powder patterns of the products of crystallisation from three different environmental conditions to promote growth of single component of; form I (blue) using methanol at 10°C, form I and II mix phase (red) using ethanol at 10°C and form III (yellow) using ethanol at 30°C. Two different products can clearly be identified from these powder patterns, while form II is mixed with form I.

Overlay of Form 1 and Simulated Pattern from Solved Structure ALMART0706



ALMART0701 Benzimidazole + 5-Chlorosalicylic Acid MeOH 10° - File: ALMART0701 Benzimidazole + 5-Chlorosalicylic Acid MeOH 10°.raw - Type: 2Th/Th locked - Start: 5.000 ° - End: 60.002 ° - Step: 0.017 ° - Step time: 240.5 s
Operations: Import
Simulated Powder Pattern From Solved Structure ALMART0706 - File: ALMART0706 Simulated Powder Pattern From Solved Structureb.raw - Type: 2Th/Th locked - Start: 5.000 ° - End: 50.000 ° - Step: 0.020 ° - Step time: 1. s - Te
Operations: Y Scale Mul 0.625 | Y Scale Mul 0.208 | Import

Fig. 4.66b – Powder x-ray diffraction pattern of benzimidazole and 5-chloro-2-hydroxybenzoic acid cocrystallised from methanol at 10°C (blue) overlaid with the simulated powder pattern from solved structure solution of form I.

Structure Description

The molecular ions, BZNH^+ and 5-chloro-2-hydroxybenzoate (5-Cl-2HBA^-) form a 1:1 molecular complex. The molecular complex was obtained using the solvent evaporation method, with a 1:1 stoichiometric mixture of benzimidazole (13mg) and 5-chlorosalicylic acid (17.5mg) dissolved in the minimum amount of methanol followed by evaporation at a constant temperature of 10°C using an Asynt hotplate. The crystals generated were block shaped and colourless. Single crystal X-ray diffraction data were obtained using a Rigaku R-axis/RAPID diffractometer at 100K, equipped with graphite monochromated $\text{Mo K}\alpha$ radiation ($\lambda = 0.71073 \text{ \AA}$). The structure was solved using SIR92³⁰ within the CRYSTALS³¹ program. The crystallographic data are summarised in Table 4.4. Figure 4.67 shows the BZNH^+ molecule created as described in Section 4.2.1 As in other examples discussed above, the equalisation of the internal bond lengths, $\text{N1}^{\delta+}\text{-C1 } 1.328(1)\text{ \AA}$ and $\text{N2}^{\delta+}\text{-C1 } 1.321(2) \text{ \AA}$, and bond angles, $\text{C1-N1}^{\delta+}\text{-C2 } 107.99(9)^\circ$ and $\text{C1-N2}^{\delta+}\text{-C7 } 108.23(9)^\circ$ is due to the protonation. The intramolecular hydrogen bond in the 5-Cl-2HBA^- molecules is relatively short with an $\text{O}\cdots\text{O}$ distance of $2.559(1)\text{ \AA}$ which is significantly shorter than the $\text{O}\cdots\text{O}$ distance of 2.577 \AA that is found in 5-chlorosalicylic acid caffeine molecular complex³⁵ (CSD reference CAFSAL). This is due to the intramolecular hydrogen bond being charged assisted, a result of the deprotonation of the 5-chlorosalicylic acid in the present case.

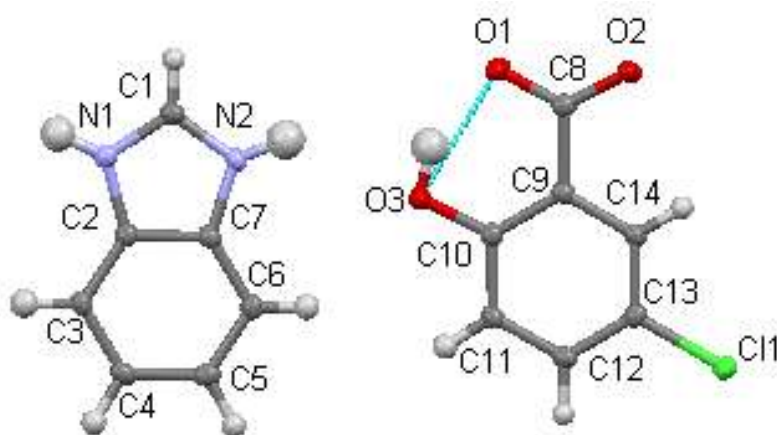


Fig. 4.67 – The benzimidazolium and 5-chloro-2-hydroxybenzoate molecules which are generated in the molecular complex with atom labelling.

Interaction	Length (Å) (D...A(Å))	For Hydrogen Bonds		
		D-H(Å)	H...A(Å)	D-H...A angle(°)
O3...O1	2.559(1)	0.89(1)	1.75(2)	150(1)
N1...O2	2.660(1)	0.89(2)	1.79(2)	165(1)
N2...O1	2.663(1)	0.92(1)	1.78(1)	162(1)
C1...O2	3.118(1)	0.92(1)	2.27(1)	153(1)
C6...O3	3.561(1)	0.92(1)	2.70(1)	156(1)
C6...C11	3.592(2)	0.92(1)	2.88(1)	135(1)
C11...C5	3.541(1)	-	-	-
$\pi \cdots \pi$ stacking	3.341	-	-	-

Table 4.19 – All the interactions that are present in the $\text{BZNH}^+ 5\text{-Cl-2-HBA}^-$ molecular complex

The main motif in the $\text{BZNH}^+ 5\text{-Cl-2-HBA}^-$ molecular complex is a four molecule hydrogen bonded ring consisting of alternating co-molecules with partially charge assisted $\text{N}^{\delta+}\text{-H}\cdots\text{O}^{\delta-}$ hydrogen bonds, which can be described by the graph set notation symbol R_4^4 (16) (Figure 4.68). These moderate strength hydrogen bonds are of length $\text{N1}^{\delta+}\text{-H}\cdots\text{O2}^{\delta-}$ 2.660(1)Å and $\text{N2}^{\delta+}\text{-H}\cdots\text{O1}^{\delta-}$ 2.663(1)Å (Table 4.19). This hydrogen bonded ring motif is identical to that seen in the $\text{BZNH}^+ 2\text{-HBA}^-$, it uses the same hydrogen bond pattern E, it has similar lengths (2.622(1) Å and 2.649(1) Å) and is described by the same graph set notation. The difference between the structures is the results of the effect of the weaker interactions on the packing.

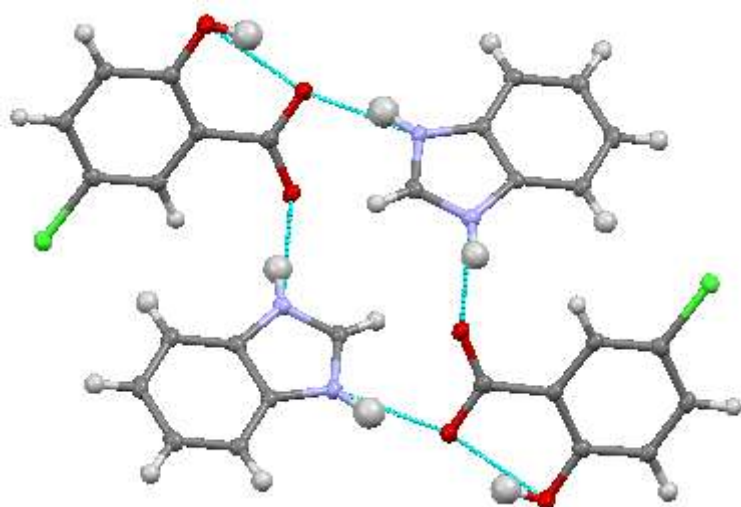


Fig. 4.68 – The main motif of the benzimidazolium 5-chloro-2-hydroxybenzoate molecular complex; a four molecule hydrogen bonded ring consisting of alternating co-molecules with partially charge assisted $N^{\delta+}-H\cdots O^{\delta-}$ hydrogen bonds.

There are two interactions that have the effect of stacking the rings upon one another creating a column of hydrogen bonded rings. This column runs along the *b*-axis and is held together by a weak hydrogen bond and $\pi\cdots\pi$ stacking interactions (Figure 4.69). The $\pi\cdots\pi$ stacking interactions are between the $BZNH^+$ molecules and of length 3.341(2)Å (between carbons C2 and C3) (Figure 4.66 black box). The weak hydrogen bond is one that is often seen in the molecular complexes involving $BZNH^+$ molecules, that is a hydrogen bond from the carbon sandwiched between the two nitrogens (C1) and a oxygen from the carboxylate group (O2) (Figure 66 red box). This hydrogen bond, $C1-H\cdots O2^{\delta-}$, has length of 3.118(1)Å and is the shortest of the weaker interactions that influence the packing in the molecular complex.

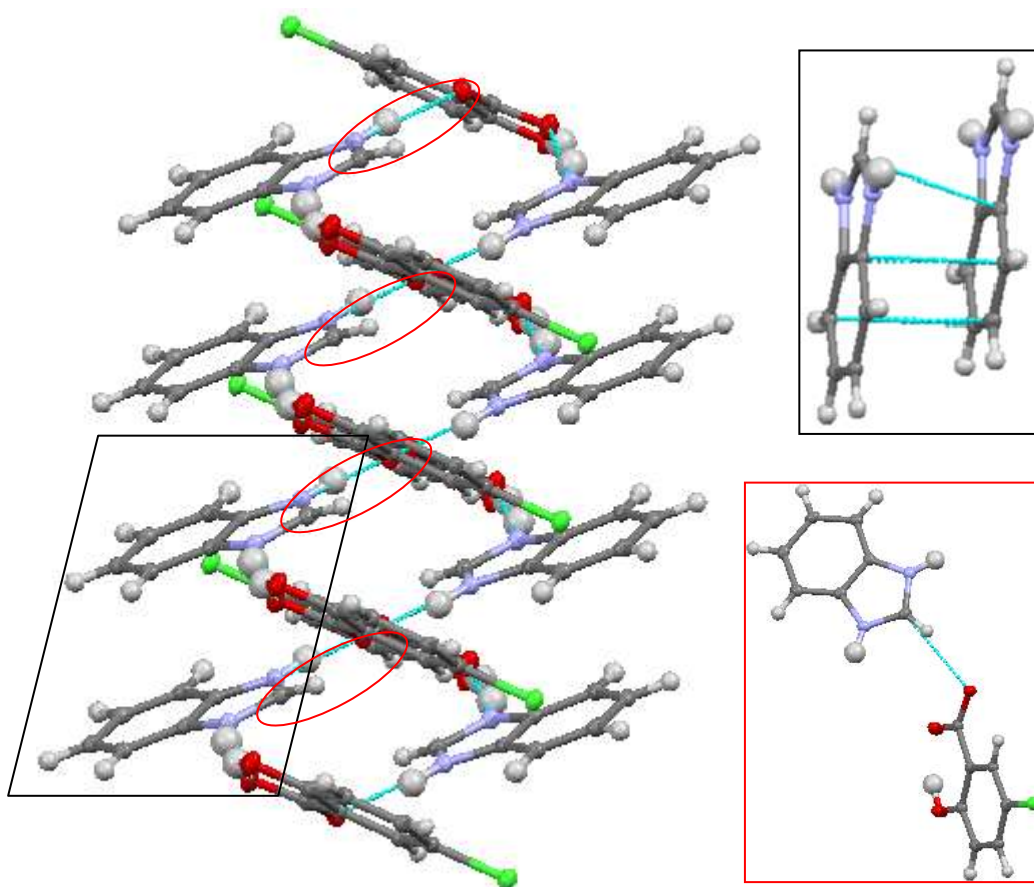


Fig. 4.69 – The main motif of the benzimidazolium 5-chloro-2-hydroxybenzoate molecular complex; the four molecule hydrogen bonded ring consisting of alternating co-molecules, are expanding along the *b*-axis by a weak hydrogen bond and $\pi\cdots\pi$ stacking interactions. Inset black box– An expanded image of the $\pi\cdots\pi$ stacking interactions that connect the hydrogen bonded rings together. Inset red box– An expanded image of the $\pi\cdots\pi$ stacking interactions that connect the hydrogen bonded rings together.

Expanding the structure along the *a*-axis, connecting the hydrogen bonded rings edge to edge, are two weak hydrogen bonds that form a bifurcated hydrogen bond (Figure 4.70). These weak hydrogen bonds are formed between a carbon of the BZNH⁺ and the hydroxyl oxygen, C6-H···O3, and carbon (C11) of the 5-Cl-2HBA⁻, C6-H···C11. The asymmetrical bifurcated hydrogen bond has the major component as the C6-H···O3 bond which has length 3.561(1)Å and minor component C6-H···C11 of length 3.595(2)Å. These weak hydrogen bonds expand the structure along the *a*-axis and are the only interactions that do so (Figure 4.71).

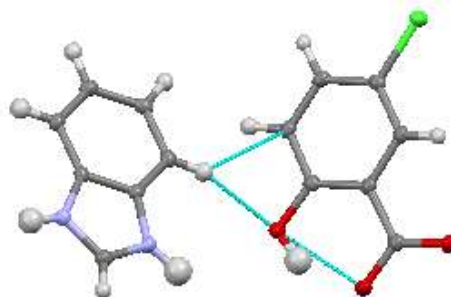


Fig. 4.70 – The two weak hydrogen bonds, C-H···C and C-H···O, which expand the structure along the *a*-axis.

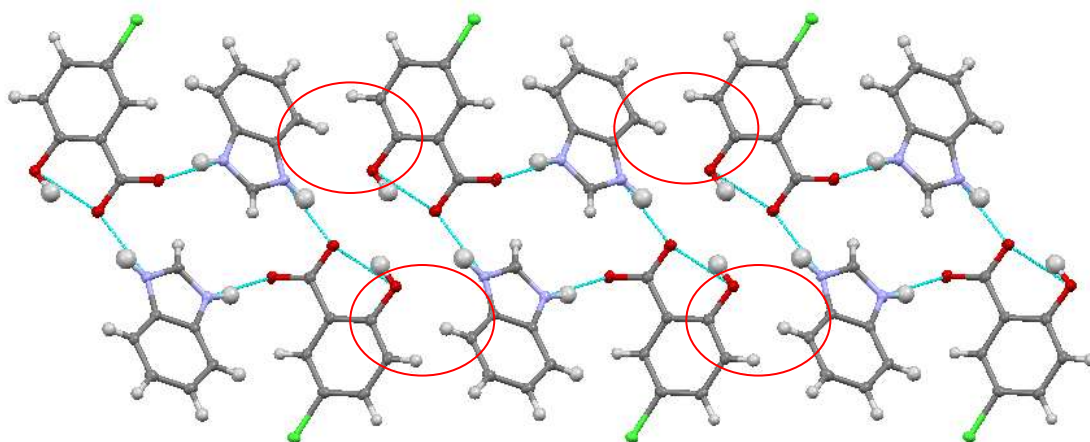


Fig. 4.71 – The main motif of the benzimidazolium 5-chloro-2-hydroxybenzoate molecular complex; four molecule hydrogen bonded ring consisting of alternating co-molecules, are expanding along the *a*-axis by two weak hydrogen bonds, C-H···C and C-H···O, that are circled in red.

The hydrogen bonded rings stack upon each other along the *b*-axis through $\pi\cdots\pi$ stacking interactions and a weak hydrogen bond (Figure 4.69). The *a*-axis is expanded by bifurcated weak hydrogen bonds (Figure 4.70) which leaves the *c*-axis that is expanded through halogen bonds (Figure 4.72). These halogen bonds, Cl1···H-C5, are of length 3.541(1)Å and are the only interactions that expand the structure along the *c*-axis.

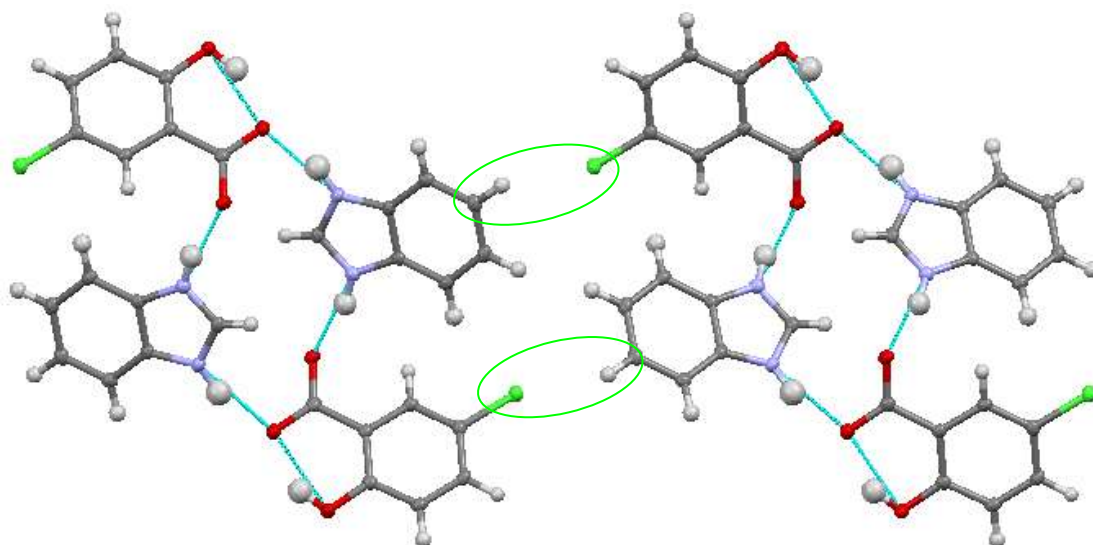


Fig. 4.72 – Halogen bonds, Cl \cdots H–C, connect the main motif of the benzimidazolium 5-chloro-2-hydroxybenzoate molecular complex along the *c*-axis (green circle).

4.5.3 Molecular Complex of Benzimidazole and L-Aspartic Acid 1:1

The molecular ions BZNH⁺ and aspartate form a 1:1 molecular complex with one another. The molecular complex was obtained using the solvent evaporation method, with a 1:1 stoichiometric mixture of BZN (12mg) and aspartic acid (14mg) dissolved in the minimum amount of methanol/water mixture followed by evaporation at room temperature. The crystals generated were needle shaped and colourless. Single crystal X-ray diffraction data were obtained using a Bruker-Nonius Kappa CCD diffractometer at 100K, equipped with graphite monochromated Mo K α radiation ($\lambda = 0.71073 \text{ \AA}$). The structure was solved using SIR92³⁰ within the CRYSTALS³¹ program. The crystallographic data are summarised in Table 4.3 and the inter- and intramolecular interactions are listed in Table 4.20.

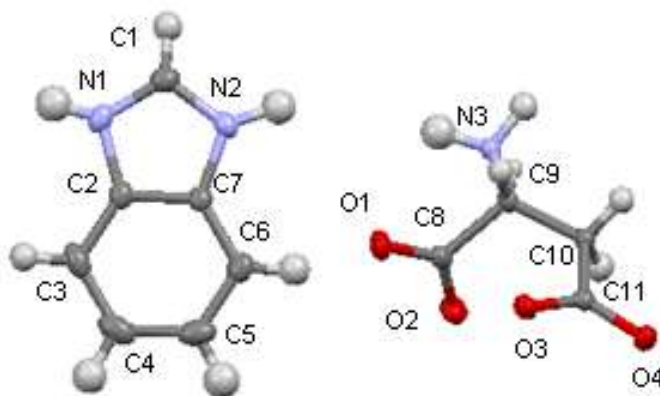


Fig. 4.73 – The benzimidazolium and aspartate molecules which are generated in the molecular complex with atom labelling.

Interaction	Length (Å) (D...A(Å))	For Hydrogen Bonds		
		D-H(Å)	H...A(Å)	D-H...A angle(°)
N1...O1	2.615(2)	0.97(3)	1.65(3)	170(2)
N2...O3	2.596(2)	0.87(3)	1.73(3)	177(3)
N3...O1	2.776(2)	0.87(2)	1.84(3)	166(2)
N3...O4	2.796(2)	0.95(3)	1.87(3)	172(2)
N3...O2	2.759(2)	0.95(3)	1.87(3)	137(2)
C1...O2	3.430(3)	0.94(2)	2.67(2)	138(2)
C1...O4	3.459(3)	0.94(2)	2.66(2)	144(2)
C5...O3	3.370(3)	0.94(3)	2.46(3)	161(2)
C5... π	3.672(3)	-	-	-

Table. 4.20 – The interactions that are found within the benzimidazolium aspartate molecular complex

In the molecular complex, the BZN molecule is protonated as discussed in section 4.3.1 forming a BZNH⁺ molecule (Figure 4.73). The BZNH⁺ bond lengths are delocalised reflected in the equalisation of the internal bond lengths, N1^{δ+}-C1 1.313(3)Å and N2^{δ+}-C1 1.318(3)Å, and bond angles, C1-N1^{δ+}-C2 107.2(2)° and C1-N2^{δ+}-C7 107.5(2)°.

The L-aspartic acid molecule has not only undergone deprotonation but also transferred the other carboxylic acid proton to the amine group. In its native crystal structure³⁶ (CSD reference LASPRT04) the L-aspartic acid already exists as the zwitterion (protonation of the amine from one of the carboxylic acid groups), however still contains one carboxylic acid group. The deprotonation of both carboxylic acid groups results in a negative charge that is found to be delocalised over both the carboxylate groups. This can be seen by the degree of normalisation of the bond lengths with comparison to the protonated form (Table 4.21).

	Aspartate (Å)	Aspartic Acid (Å)
C8-O1	1.259(2)	1.257(1)

C8-O2	1.238(2)	1.254(2)
C11-O3	1.250(2)	1.214(2)
C11-O4	1.2228(3)	1.315(1)

Table 4.21 – A comparison of the bond lengths found in the aspartate molecule in its molecular complex with benzimidazolium and those of the parent aspartic acid.

There are host of hydrogen bonds within the BZNH^+ aspartate molecular complex with lengths ranging from relatively strong distances of 2.596Å to relatively weak distances of 3.377Å. The BZNH^+ molecules are involved in the strongest hydrogen bonds which are two partially charge assisted $\text{N}^{\delta+}\text{-H}\cdots\text{O}^{\delta-}$ hydrogen bonds of lengths $\text{N1}^{\delta+}\text{-H}\cdots\text{O1}^{\delta-}$, 2.615(2) and $\text{N2}^{\delta+}\text{-H}\cdots\text{O3}^{\delta-}$ 2.596(2)Å. These hydrogen bonds combine to create a linear chain of alternating aspartate and BZNH^+ molecules that lie above and below the chain (Figure 4.74).

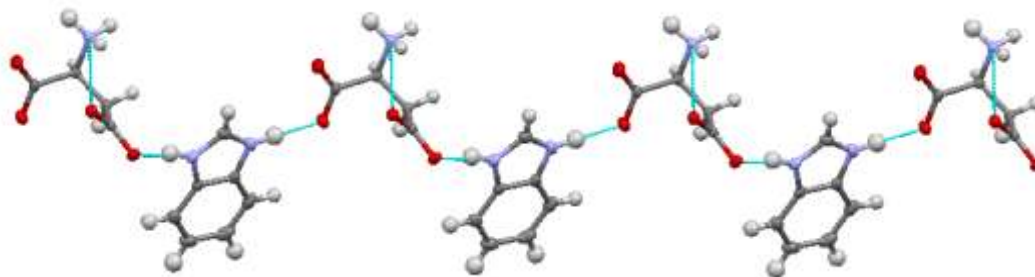


Fig. 4.74 – The main hydrogen bonds within the BZNH^+ aspartate molecular complex create a linear chain of alternating co-molecules.

The amine group on the aspartate molecule is involved in three hydrogen bonds that are all of similar strengths (Figure 4.75). These hydrogen bonds are the next most influential after those involving the BZNH^+ molecule. They are of lengths $\text{N3-H}\cdots\text{O1}^{\delta-}$, 2.776(2)Å (green), $\text{N3-H}\cdots\text{O4}^{\delta-}$, 2.796(2)Å (red) and $\text{N3-H}\cdots\text{O2}^{\delta-}$, 2.759(2)Å (blue).

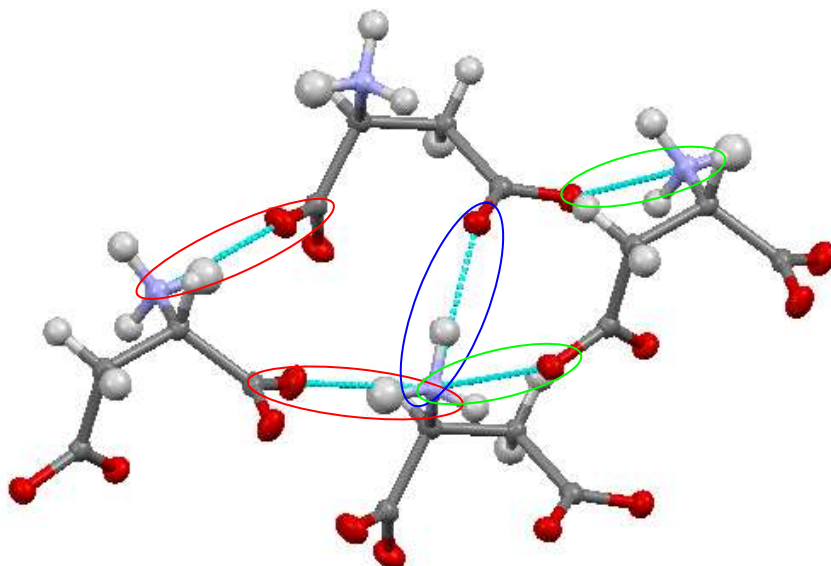


Fig. 4.75 – The amine group of the aspartate molecule is involved in three hydrogen bonds, N3-H \cdots O1 δ^- (green), N3-H \cdots O4 δ^- (red) and N3-H \cdots O1 δ^- (blue).

There are two weak hydrogen bonds that are influential within the structure. One is a three centred hydrogen bond (bifurcated) involving the carbon sandwiched between the nitrogens and an oxygen from each carboxylate group (Figure 4.76; a). These are of length C1-H \cdots O2 δ^- 3.430(3)Å and C1-H \cdots O4 δ^- 3.459(3)Å. The other weak hydrogen bond is also intermolecular and also involves a carboxylate oxygen (Figure 4.76; b). This hydrogen bond, C5-H \cdots O3 δ^- , is of length 3.370(3)Å and makes up the contingent of hydrogen bonds within this molecular complex



Fig. 4.76 – The weak hydrogen bonds within the BZNH $^+$ aspartate molecular complex: bifurcated hydrogen bonds (a) and C5-H \cdots O3 δ^- hydrogen bonds (b).

There are sets of lesser interactions that are influential within this structure, whose significance can be seen by looking at the extending structure. Figure 4.77 highlights how the linear chains of alternating co-molecules are connected through the hydrogen bonds involving the amine group. This has the effect of creating layers along the *b*-axis, with the first layer

being the linear chain (A), next the amine hydrogen bonds (B), back to linear chains (A), then the lesser interactions (C) before returning to A, then repeating this sequence B,A,C,A,B....

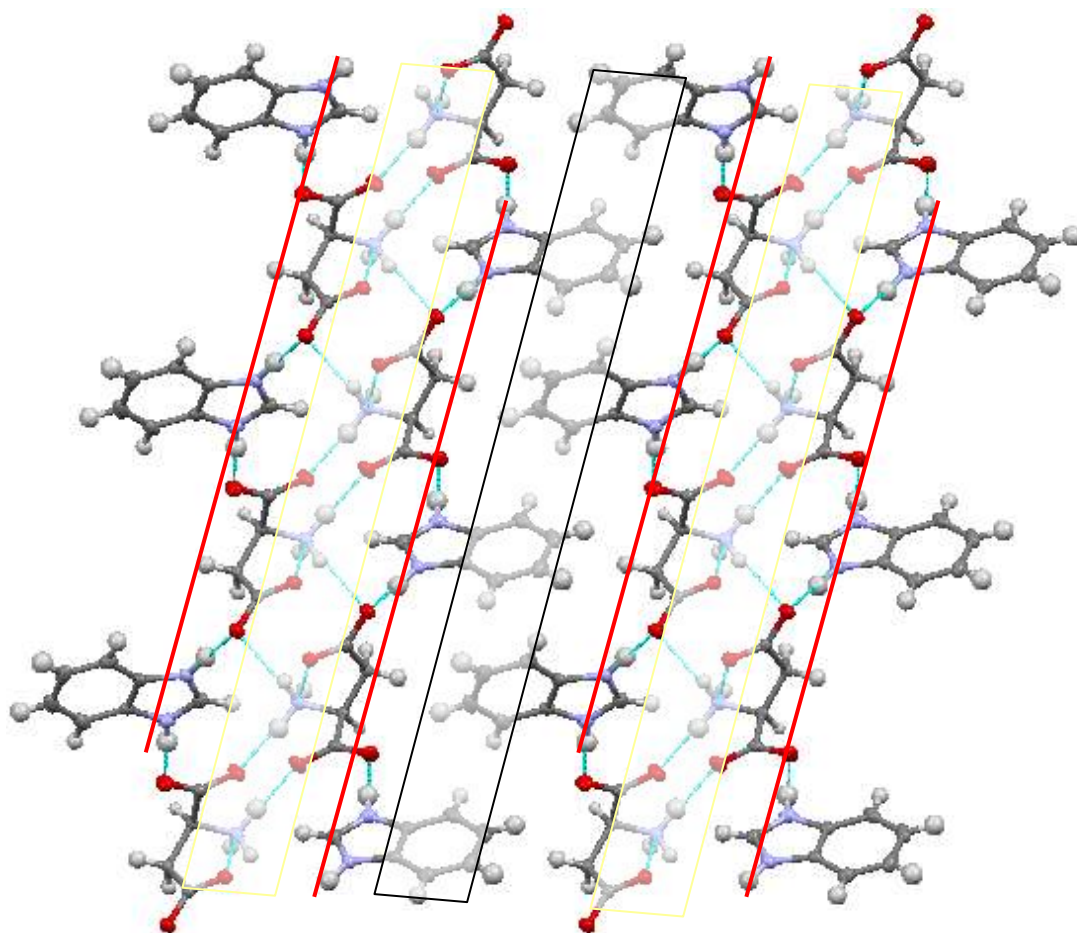


Fig. 4.77 – View along the *b*-axis of the expanded benzimidazolium aspartate molecular complex. The red line (-) indicates the chain of alternating co-molecule (Figure 4.74), the yellow box (-) indicates hydrogen bonds involving the amine group of the aspartate (Figure 4.75) and the black box is where the lesser interactions between the BZNH⁺ molecules operate(Figure 4.76).

The lesser interactions are C–H... π edge to face interactions involving the BZNH⁺ molecules. They are of length 3.622(3)Å (c) and 3.716(3)Å (d) (Figure 4.78) .

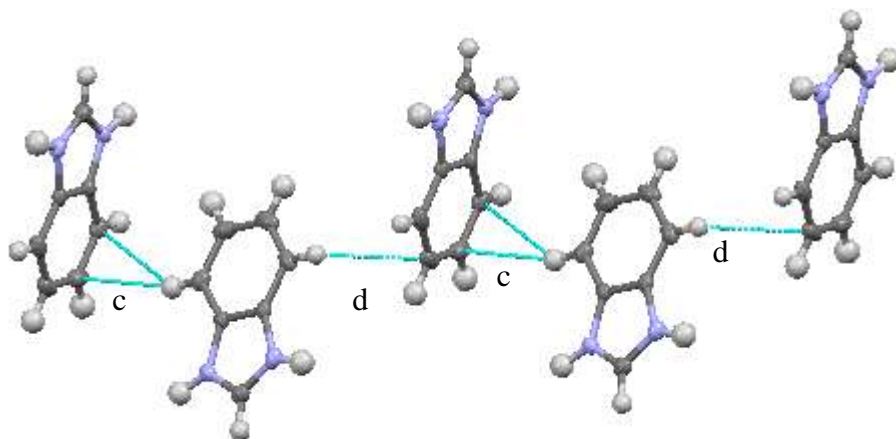


Fig. 4.78 – The C–H \cdots π edge to face interactions between the BZNH⁺ molecules.

4.6 Conclusions

Of all the possible hydrogen bonding patterns of the uncharged species (Figure 4.12) and charged species (Figure 4.13) and the many possibilities of potential hydrogen bond motifs and supramolecular synthons, there were only four unique hydrogen bonding patterns (Figure 4.79) and three hydrogen bond motifs (Figure 4.80) (excluding the hydrate for the hydrogen bonds) are observed.

From Figure 4.79, hydrogen bond 1 incorporates all N–H \cdots O hydrogen bonds which corresponds to hydrogen bond pattern E and F in Figures 4.12 and 4.13 and E and F in Table 4.3. This, as would be predicted, is the most influential intermolecular hydrogen bond between the co-molecules and can vary, quite considerably, in strength. This hydrogen bond, as will be displayed throughout the rest of the results sections, is robust, dependable and flexible. The O–H \cdots O hydrogen bond (Figure 4.79-2, Figure 4.12 and 4.13–G and Table 4.3-G) between a hydroxyl and carboxylate oxygen, is a very common hydrogen bond for crystal engineers for its dependability and flexibility. In this body of work it promotes the ladder motif and is the most influential hydrogen bond listed in Figure 4.79, as when there is potential for this type of hydrogen bond (not available in the 2-HBA molecular complexes) it forms and determines the rest of the structure. There is no better example than in the benzimidazole and 3,5-dihydroxybenzoic acid molecular complex, where the benzimidazole molecules seem to fit in where they are allowed. The other O–H \cdots O hydrogen bond, Figure 4.79-4, a carboxylic acid dimer (carboxylic acid and a carboxylate group) is only seen in the

BENZ⁺ 2-HBA⁻ 1:2 molecular complex, even though the carboxylic acid dimer is renowned in forming and is seen in many of the starting materials of the hydroxybenzoic acids and in other molecular complexes of which they are involved. The BZN dimer (Figure 4.79-3, Figure 4.12-C) only formed when there was an excess of BZN to the other co-molecule however examples in Chapters 5 and 7 will show that this is not always the case. For this hydrogen bond to form there needs to be a non protonated nitrogen atom.

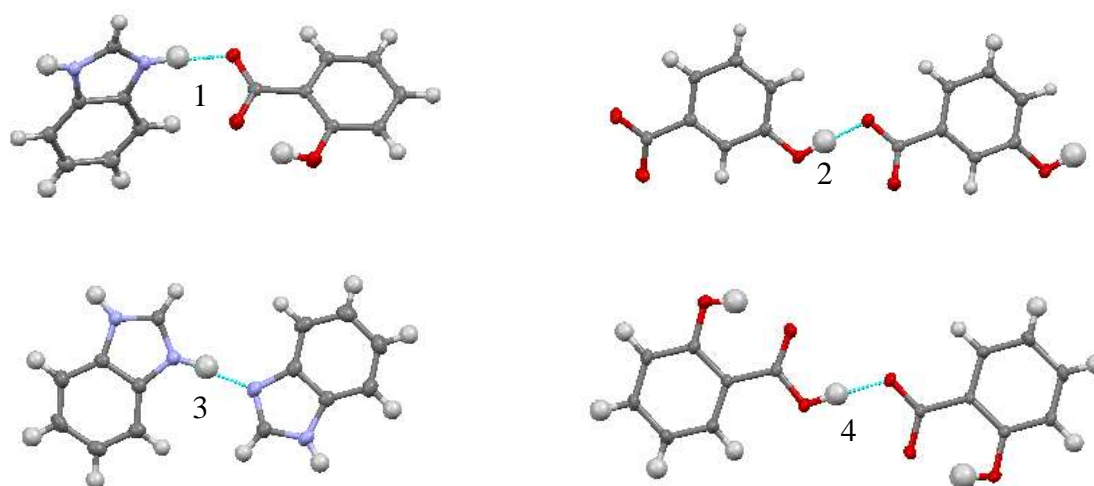


Fig. 4.79 – The four unique hydrogen bonds that were the only hydrogen bonds in all the crystal structures in Chapter 4, in order of occurrence 1, N^{δ+}–H···O^{δ-}, 2, O–H···O^{δ-}, 3, N^{δ+}–H··· N^{δ+}, 4, O–H···O.

Figure 4.80 shows the three motifs, hydrogen bond ring, chains of hydroxyl-benzoic acid dimers with connected BZN, and the ladder, with slight variations between the supramolecular synthons within the ladder structures. Firstly, the hydrogen bonded rings formed in the BENZH⁺ 2HBA⁻ 1:1 molecular complex, using solely hydrogen bond pattern 1, is regularly seen in other molecular complexes in chapters 5, 6 and 7. with some derivatives. On the other hand, the ladder motif is only seen in the hydroxybenzoic acid molecular complexes, which is due to the availability of the hydroxyl group to form hydrogen bond pattern G (2 in Figure 4.79). Within the ladder motifs, there are two slight derivatives, ladders with rungs of BZN molecules and ladders with alternative rungs of BZN molecules. These derivatives are neatly shown in the BZNH⁺ 3HBA⁻ polymorphs where they both adopt the different styles. It would not be surprising if more polymorphs of the BZN and 3- / 4-HBA molecular complexes adopting the ladder motifs not discovered during this work were found, for example BZNH⁺ 3-HBA⁻ 1:1 forming the alternative step ladder motif and the BZNH⁺ 4-HBA⁻ 2:1 forming the ladder with every step motif.

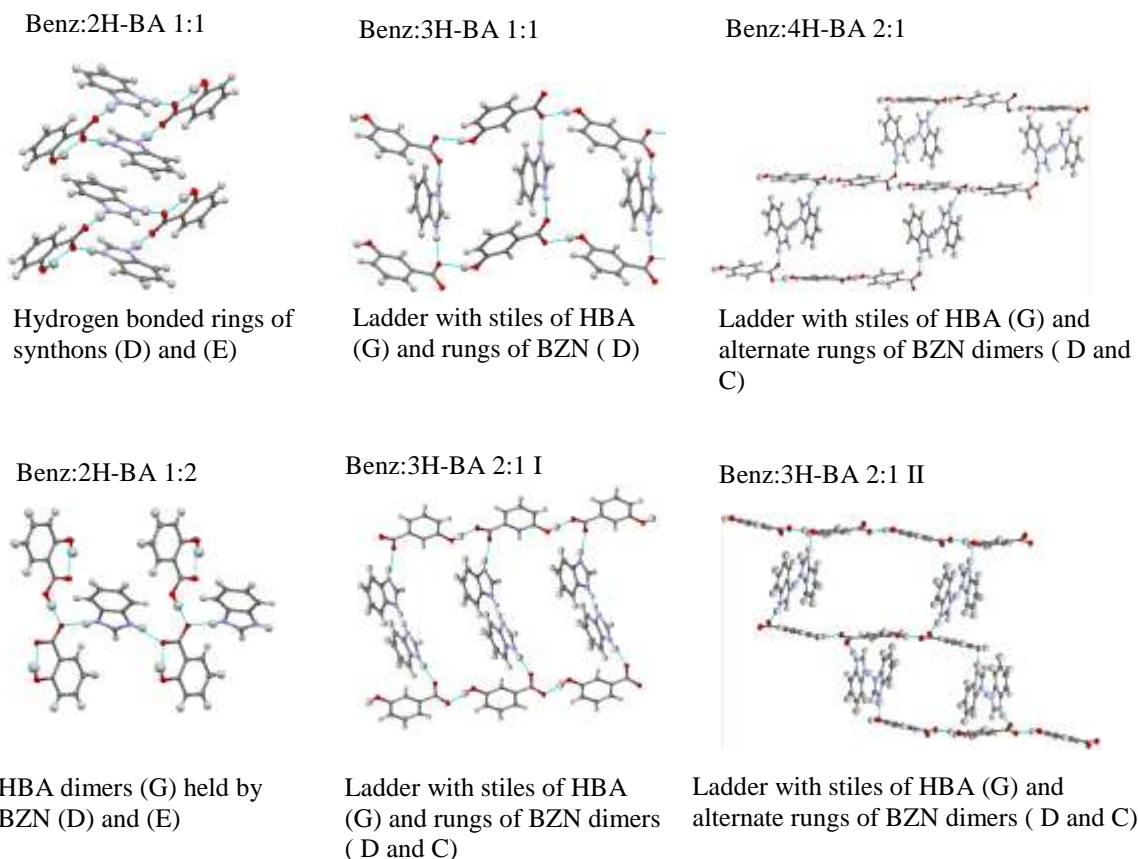


Fig. 4.80 – The motifs of the molecular complexes from Section 4.5 excluding benzimidazolium 4-hydroxybenzoate hydrate and benzimidazolium 3,5-dihydroxybenzoate. The three unique hydrogen bond motifs are shown, the hydrogen bonded rings ($\text{BENZH}^+ 2\text{HBA}^-$ 1:1), chains hydroxybenzoic acid dimers and the ladder motif.

Even with six new structures being determined with these set of molecules, I believe there are still a real possibility to obtain more, for example BZN and 3-HBA/4-HBA in a 1:2 ratio could adopt a dimer structure similar to the Benz:2H-BA 1:2 complex or the ladder motif. However due to the likely motifs that the structures would adopt, it would be highly unlikely for some structures to be obtained, for example BZN and 2-HBA in a 2:1 ratio is unlikely to occur as the 2-HBA would need to adopt the ladder motif. Also I do not think the BZN 4-HBA 1:1 molecular complex would occur as the geometry of the potential 4-HBA chains would be straight which would not allow the BZN to fit into the structure.

A weak hydrogen bond has been found in nearly all the structures, indicating a high degree of reliability. The carbon – oxygen hydrogen bond involving the carbon sandwiched between the protonated nitrogens can be shorter than normal carbon oxygen hydrogen bonds due to the

electronegative nature of the carbon with lengths as short as 3.091Å (normally around 3.2~3.5Å^{##}) However there are structures when this hydrogen bond lies within the normal range. These carbon-oxygen hydrogen bond always uses the carbon labelled C1 (or C8 when more than one BZN in the asymmetric unit) in structures and is found to be reliable in structures found throughout this project.

When scrutinising the ΔpK_a difference values (Table 4.4) for the molecular complexes obtained, it can be seen that the rule governing if a salt or co-crystal will form has been accurate. There was no ΔpK_a value under 0, therefore no co-crystals would be expected, which has occurred. The majority of the ΔpK_a values do lie within the 0~3 range that normally means prediction is impossible, however in these cases the salt form always prevails.

The solvent free grinding method, validated to an extent in the experiments described, is a very old method giving a new lease of life. There is debate over whether the term solvent free is correct (refer to Section 1.5) but there can be no debate that this technique works and is able to generate new materials and even materials unobtainable from normal solvent methods.

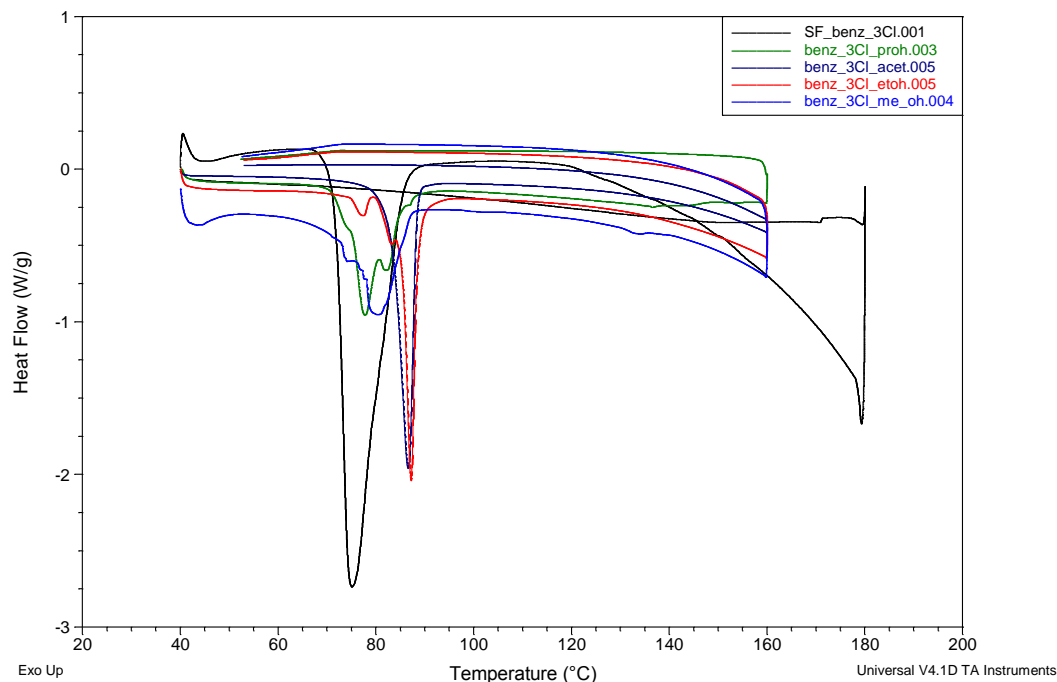
4.7 References for Chapter 4

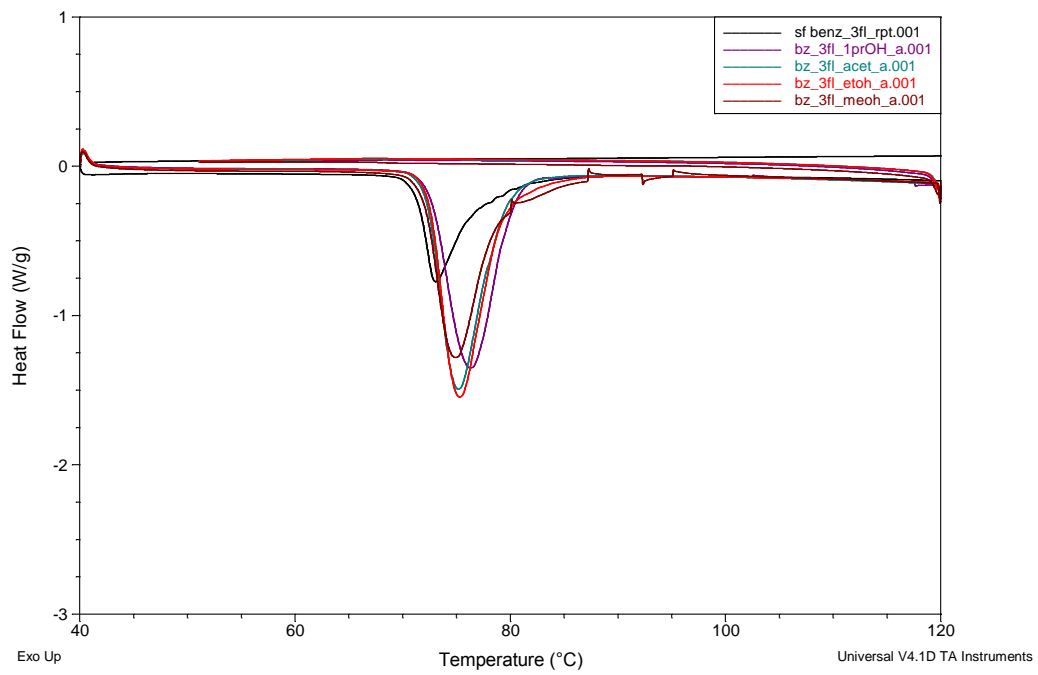
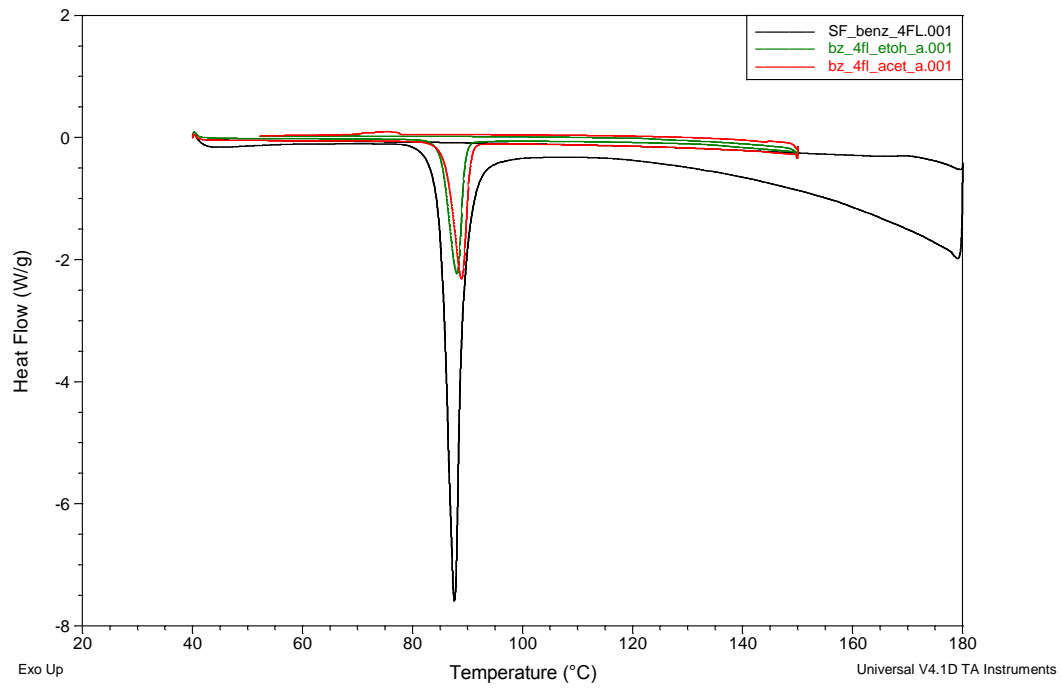
- (1) D. Braga, *Chemical Communications*, 2003, 2751-2754.
- (2) G. R. Desiraju, *Angewandte Chemie International Edition*, 1995, **107**, 2541-2557.
- (3) L. Brammer, G. Mi'nguez Espallargas and S. Libri, *CrystEngComm*, 2008, **10**, 1712.
- (4) M. Nishio, *CrystEngComm*, 2004, **6**, 130-158.
- (5) K. Steele, P. Shirodaria, M. O'Hare, J.D. Merrestt, W.G. Irwin, D.I.H. Simpson and H. Fister, *British Journal of Dermatology*, 2006, **118**, 537-544.
- (6) P. Munshi and T. N. Guru Row, *Acta Crystallographica section B*, 2006, **62**, 612-626.
- (7) C. López, R. M. Claramunt, M. Á. García, E. Pinilla, M. R. Torres, I. Alkorta and J. Elguero, *Crystal Growth & Design*, 2007, **7**, 1176-1184.
- (8) L. Du, W. Zeng, X. Liu and F.-F. Jian, *Acta Crystallographica section E*, 2009, **65**, 1791.
- (9) R.W.Gellert and I.-N.Hsu, *Acta Crystallographica section A*, 1981, **37**, 93.
- (10) M. Byres, P. J. Cox, G. Kay and E. Nixon, *CrystEngComm*, 2008, **11**, 135-142.
- (11) <http://extoxnet.orst.edu/pips/lactofen.htm>
- (12) <http://www.chemblink.com/products/99-06-9.htm>
- (13) J. A. McMahon, J. A. Bis, P. Vishweshwar, T. R. Shattock, O. L. McLaughlin and M. J. Zaworotko, *Zeitschrift für Kristallographie*, 2005, **220**, 340-350.
- (14) R. M. Gregson, C. Glidewell, G. Ferguson and A. J. Lough, *Acta Crystallographica section B*, 2000, **56**, 39-57.
- (15) C. M. Zakaria, A. J. Lough, G. Ferguson and C. Glidewell, *Acta Crystallographica section B*, 2004, **60**, 65-75.
- (16) B. Sarma, N. K. Nath, B. R. Bhogala and A. Nangia, *Crystal Growth & Design*, 2009, **9**, 1546-1557.
- (17) E. A. Heath, P. Singh and Y. Ebisuzaki, *Acta Crystallographica section C*, 1992, **48**, 1960-1965.
- (18) <http://www.indspec-chem.com/PRODUCTS/BRA/BRA.asp>
- (19) A. Parkin, M. Adam, R. I. Cooper, D. S. Middlemiss and C. C. Wilson, *Acta Crystallographica section B*, 2007, **63**, 303-308.
- (20) D.-D. Lin, J.-G. Liu and D.-J. Xu, *Acta Crystallographica section E*, 2006, **62**, 451-452.
- (21) L. R. MacGillivray and M. J. Zaworotko, *Journal of Chemical Crystallography*, 1994, **24**, 703-705.
- (22) M. Gdaniec, M. Gilski and G. S. Denisov, *Acta Crystallographica section C*, 1994, **50**, 1622-1626.
- (23) H. Lin, J. Chen, C. Huang and C. Wang, *International Journal of Cancer*, 2007, **120**, 2306-2316.
- (24) H. Babich, A. Sedletcaia and B. Kenigsberg, *Pharmacology & Toxicology*, 2003, **91**, 245-253.
- (25) Y. Nakamura, K. Torikai, Y. Ohto, A. Murakami, T. Tanaka and H. Ohigashi, *Carcinogenesis*, 2000, **21**, 1899-1907.
- (26) S. Guana, D. Gea, T. Liua, X. Maa and Z. Cuib, *Toxicology in Vitro*, 2009, **23**, 201-208.
- (27) J. Anderson, R. Gilardi, I. L. Karle, M. H. Frey, S. J. Opella, L. M. Gierasch, M. Goodman, V. Madison and N. G. Delaney, *Journal of the American Chemical Society*, 1983, **105**, 6609-6614.

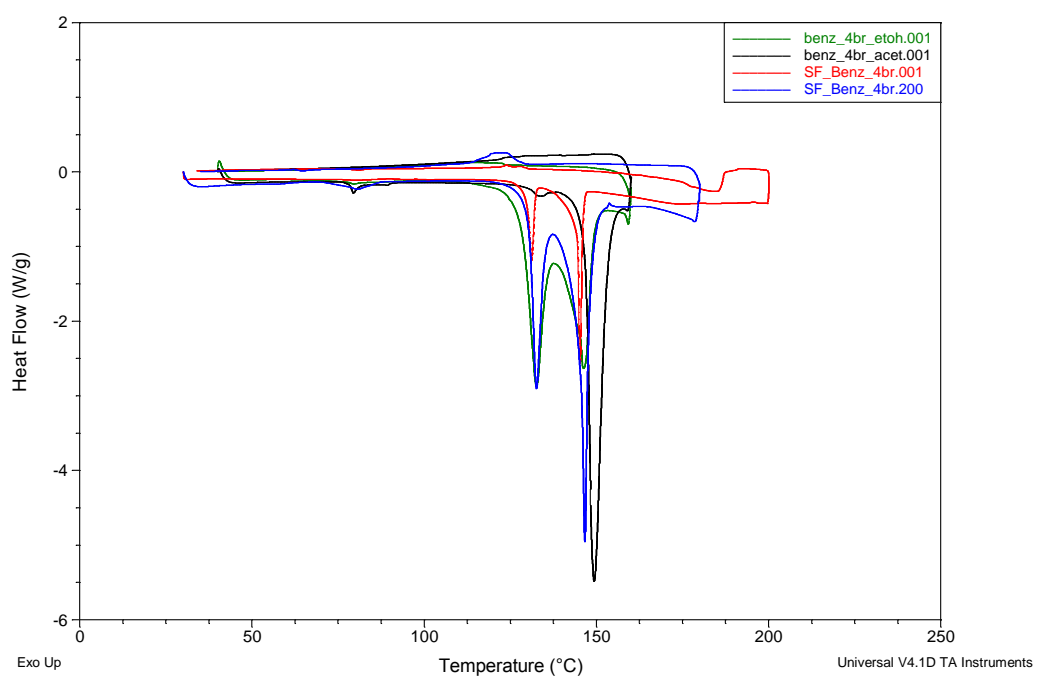
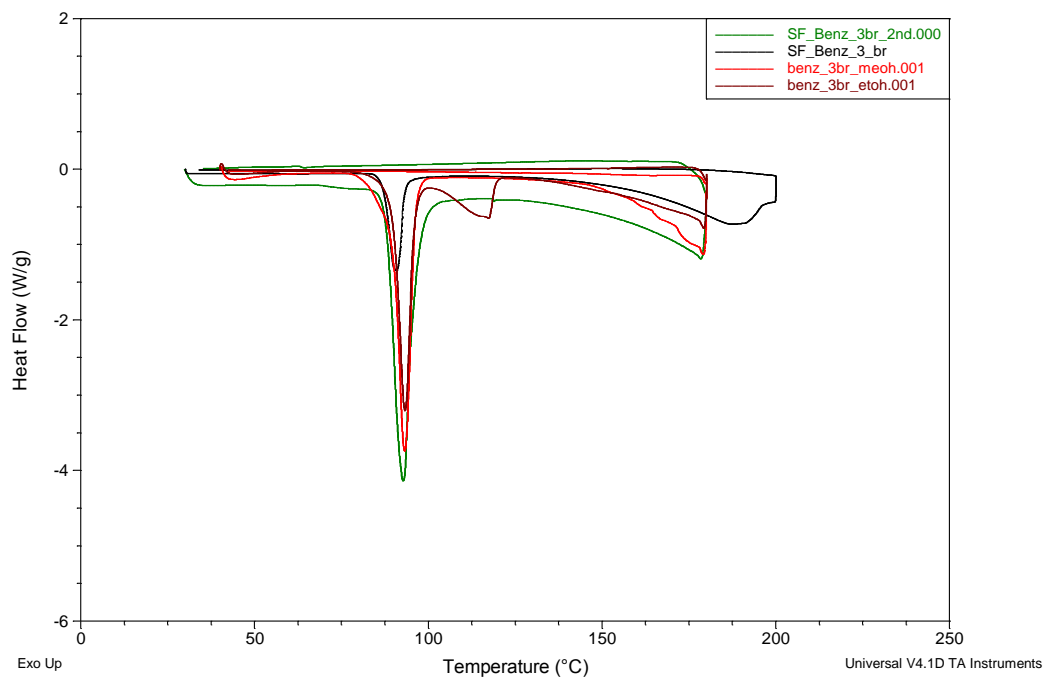
- (28) V. Aletrasa, N. Hadjiliadis, D. Stabakib, A. Karaliotab, M. Kamariotakib, I. Butlerc, J. C. Plakatourasd and S. Perlepesd, *Polyhedron*, 1997, **16**, 1399-1402.
- (29) X. Huang, J.-G. Liu and D.-J. Xu, *Acta Crystallographica section E*, 2006, **62**, 276-278.
- (30) A Altomare, G Cascarano, C Giacobozzo, A Guagliardi, M.C Burla and M. C. G Polidori, *Journal of Applied Crystallography*, 1994, **27**, 435-436.
- (31) D.J. Watkin, C.K. Prout, J.R Carruthers, P.W. Betteridge and R. I. Cooper, *Journal of Applied Crystallography*, 2003, **36**, 1487.
- (32) L Palatinus and G. Chapuis, *Journal of Applied Crystallography*, 2007, **40**, 786-790.
- (33) J Rohlicek and M Musak, *Journal of Applied Crystallography*, 2007, **40**, 600.
- (34) P. Totsatitpaisan, K. Tashiro and S. Chirachanchai, *The Journal of Physical Chemistry*, 2008, **112**, 10348-10358.
- (35) E. Shefter, *Journal of Pharmaceutical Sciences*, 1968, **57**, 1163-1168.
- (36) E. Bendeif and C. Jelsch, *Acta Crystallographica section C*, 2007, **63**, 361-364.

4.8 Appendix

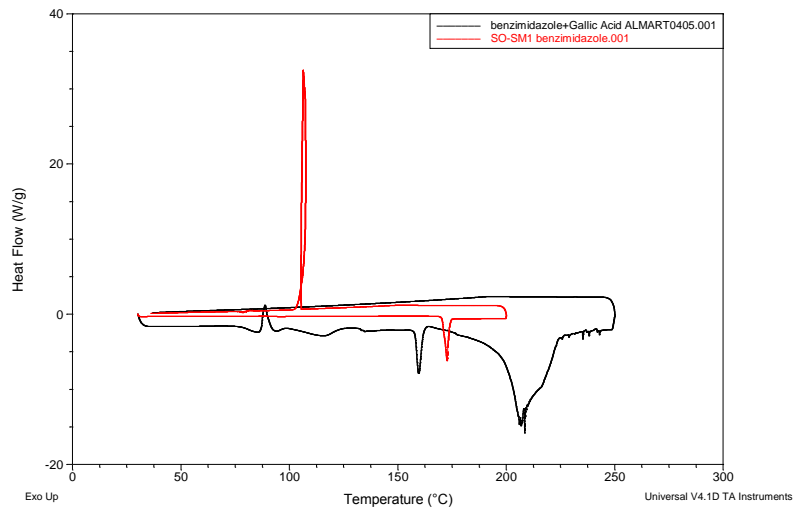
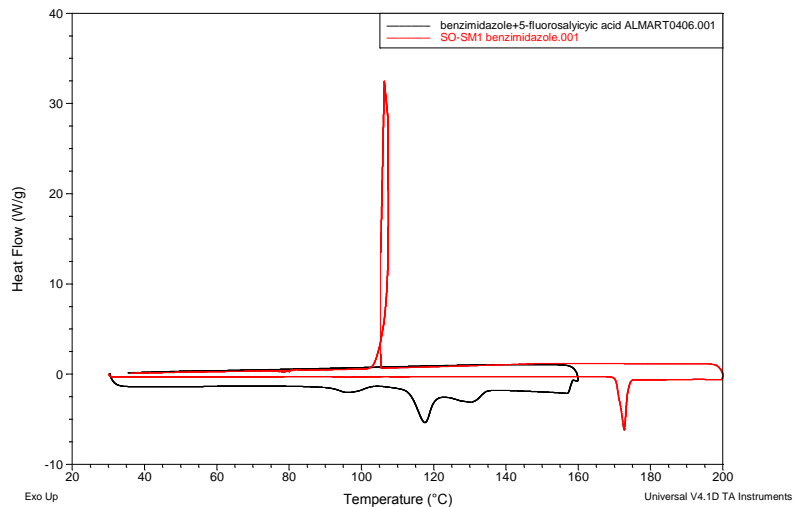
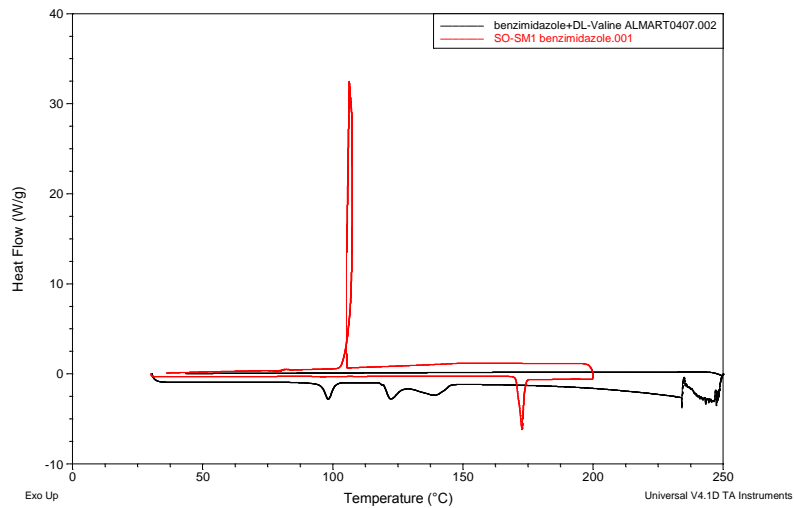
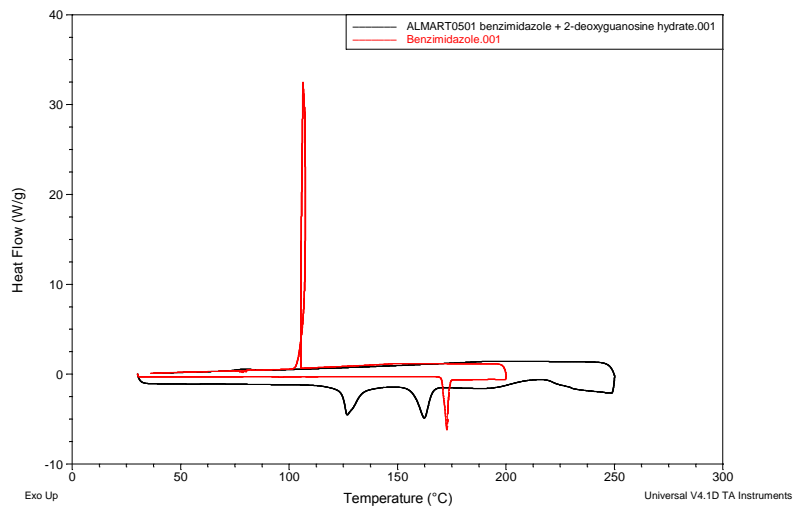
4.8.1 Appendix 4.A - DSC Thermograms of Solvent Free Co-crystallisations of BZN with Halo-BA

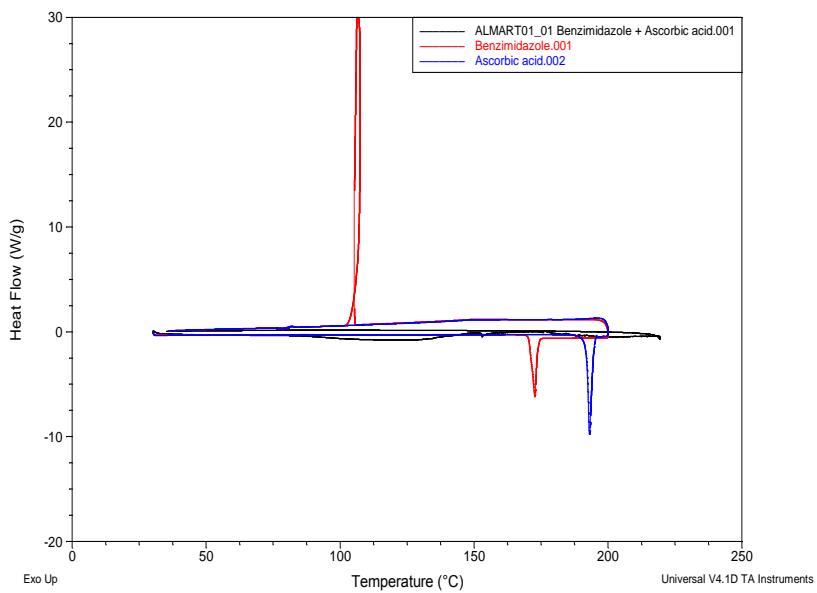
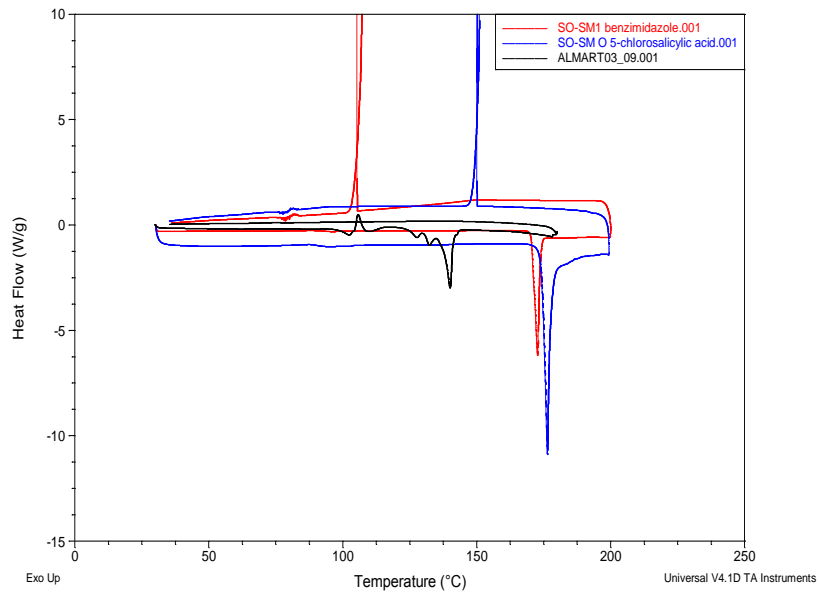
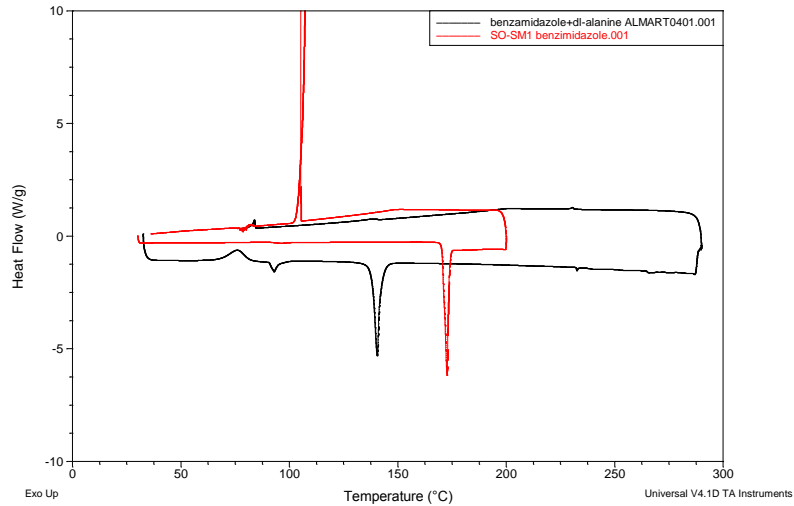
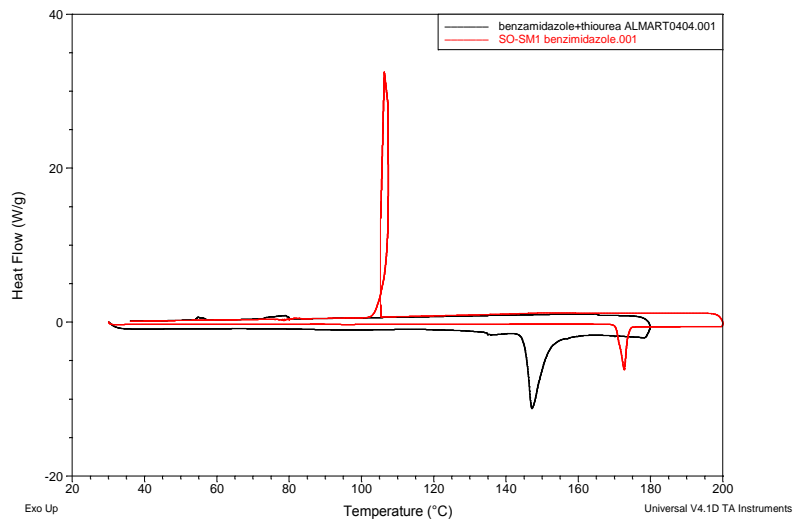






4.8.2 Appendix 4.B - DSC Thermograms of Solvent Free Co-crystallisations of BZN with a Range of Co-molecules





5 Solvent Mediated Molecular Complex Polymorphism and Isomorphic Formation

This chapter will focus on the co-crystallisation of benzimidazole with various halo-substituted benzoic acids. The primary aim of this work was to promote and control the formation of molecular complex polymorphs through varying crystallisation conditions including choice of solvent and crystallisation temperature. Powder X-ray diffraction (PXRD) and differential scanning calorimetry (DSC) were primarily used for characterisation of the resulting products due to difficulties in the growth and isolation of single crystals of all forms.

The theme of controlling the formation of polymorphs, as previously discussed at section 1.4.1, is of utmost importance to many different areas of industry. The quote by McCrone¹, “*the number of forms known for a compound is proportional to the time and money spent in research on the compound*” highlights the poor understanding of polymorph formation and the often serendipitous nature of discovery.

In addition to the molecular complex polymorphs obtained, isostructural series of compounds have been produced (refer to Section 1.4.3) where the sole chemical difference is the identity of the halogen atom; isostructures were however not obtained in a predictable manner.

This chapter will also look at the influence of halogen atoms involved in intermolecular interactions, including halogen bonding and halogen – π interactions. These weaker interactions are becoming increasingly important in molecular complex design, however they have historically been hard to use in crystal structure design due to their less directional and predictable nature (refer to Section 1.2.7).

5.1 Introduction

The complete series of mono-substituted iodo-, bromo-, chloro- and fluoro-benzoic acids have been used as co-molecules in the attempted synthesis of molecular complexes of benzimidazole. Halobenzoic acids themselves have many uses in the chemical industry, for

example 4-chlorobenzoic acid is used as an intermediate in the manufacturing of dyes, fungicides and pharmaceuticals². However it was not for these reasons alone that they were selected as co-molecules.

The carboxylic acid functional group found on halobenzoic acids is universally popular for crystal engineers as in many cases it forms predictable hydrogen bonds³. Benzoic acids are often found to produce hydrogen bonded dimers between the carboxylic acid groups, and this is always observed in the pure halobenzoic acid crystal structures. This dimer motif has also been found to persist in some molecular complexes.

The presence of halogens in molecules is also known to influence the crystal packing and so this aspect has also been investigated. As discussed (Section 1.2.7) halogen interactions have increasingly become an area of interest with much research concentrating on the manipulation of these interactions and their use in design of extended architectures.

5.1.1 2-Fluorobenzoic Acid

2-Fluorobenzoic acid (Figure 5.1) is of interest in metabolism studies⁴, however only one molecular complex of this material has been deposited in the Cambridge Structural Database (CSD). 4-(1H-pyrazol-1-ylmethyl)benzamide 4-fluorobenzoic acid (CSD reference OC1QEX) (Figure 5.2) was discovered by Aakeroy⁵ in 2006. The main supramolecular synthon is a double hydrogen bond between the carboxylic acid and carboxamide groups. It can also be noted that the fluorine atom on one of the fluorobenzoic acid groups is disordered over two sites; this also occurs in the 2-fluorobenzoic acid molecular complex generated during this project. There is no structure of 2-fluorobenzoic acid starting material in the CSD.

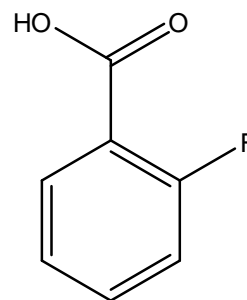


Fig. 5.1 – 2-fluorobenzoic acid.

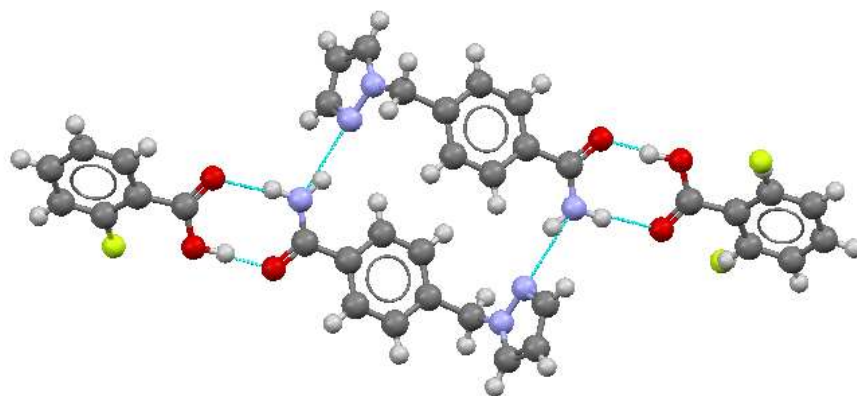


Fig. 5.2 – Basic building block of the 2-fluorobenzoic acid: 4-(1H-pyrazol-1-ylmethyl)benzamide molecular complex structure found in the CSD with a fluorine atom on one of the fluorobenzoic acid groups is disordered over two sites

5.1.2 3-Fluorobenzoic Acid

3-Fluorobenzoic acid (Figure 5.3), like 2-fluorobenzoic acid, has no known structural data and only one molecular complex structure in the CSD. 3-fluorobenzoic acid has been cocrystallised with 4-acetylpyridine (CSD reference HOLJAU) within the Wilson group in 2009⁶ (Figure 5.3). The only hydrogen bond within this structure is an O-H···N bond.

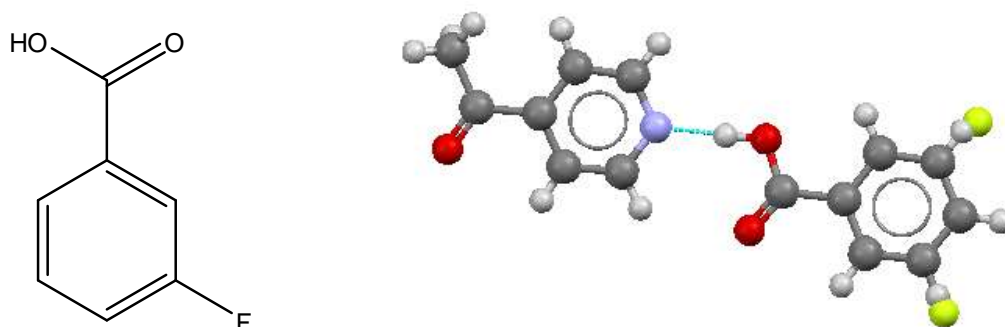


Fig. 5.3 – LHS, 3-fluorobenzoic acid; RHS, 3-fluorobenzoic acid : 4-acetylpyridine molecular complex with the fluorine atom disordered over two positions (common with fluorine atoms) explaining the overlap of the hydrogen and fluorine atoms.

5.1.3 4-Fluorobenzoic Acid

4-Fluorobenzoic acid is used as an intermediate for the production of pesticides and pharmaceuticals². The structure of the starting material was reported in 1992 (CSD reference

PFBZAD01)⁷ with a carboxylic acid dimer as the main supramolecular synthon (Figure 5.4). This structure also contains a halogen bond, F \cdots O-H, of 3.246Å which connects the linear carboxylic acid dimers.

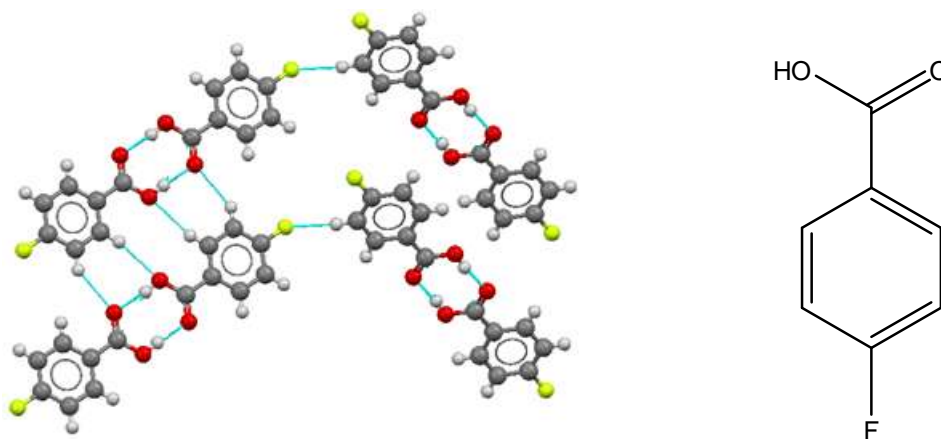


Fig. 5.4 – Basic building block of the 4-fluorobenzoic acid crystal structure, RHS, 4-fluorobenzoic acid.

4-fluorobenzoic acid has also been successfully cocrystallised with isonicotinamide in a one to one ratio (CSD reference ASAXUN)⁸ and as bis(N,N'-bis(2-fluorobenzylidene)ethylenediamine-N,N')-silver(i) 4-fluorobenzoate 4-fluorobenzoic acid solvate (CSD reference UCIWIN)⁹. The 4-fluorobenzoic acid: isonicotinamide molecular complex (Figure 5.5) contains heterodimers connected through an O-H \cdots N hydrogen bond. Of particular interest is that a 4-fluorobenzoic acid dimer is held together by a relatively strong halogen bond, F \cdots F, of distance 2.618 Å.



Fig. 5.5 – Basic building block of the 4-fluorobenzoic acid : isonicotinamide molecular complex.

5.1.4 2-Chlorobenzoic Acid

2-Chlorobenzoic acid is used as an intermediate in manufacture of drugs especially mefenamic acid and also in the manufacture of dyes and pigments. Its crystal structure was solved by Braga and co-workers in 2008¹⁰ (Figure 5.6).

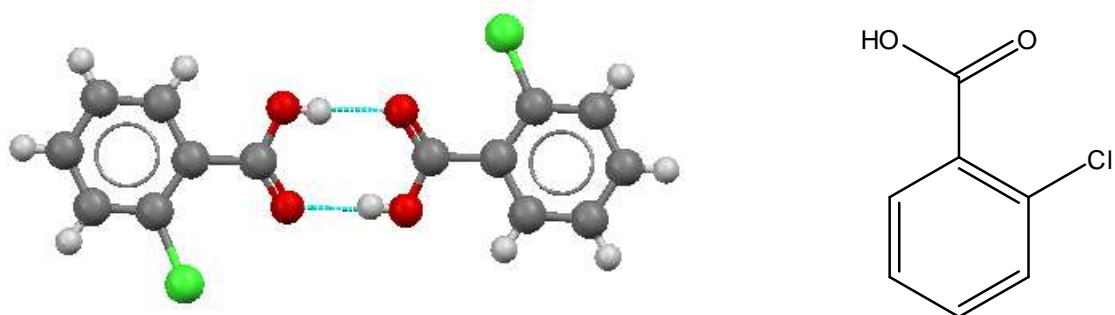


Fig. 5.6 – The carboxylic acid dimer that is the main supramolecular synthon in the 2-chlorobenzoic acid crystal structure; RHS, 2-chlorobenzoic acid.

During the same research, 2-chlorobenzoic acid was also successfully cocrystallised with 2-methylbenzoic acid (Figure 5.7). The carboxylic acid dimer is once again the main hydrogen bond motif with weaker hydrogen bonds building up the structure. Both independent molecules have the chloro and methyl substituents disordered over two sites of equal occupancy.

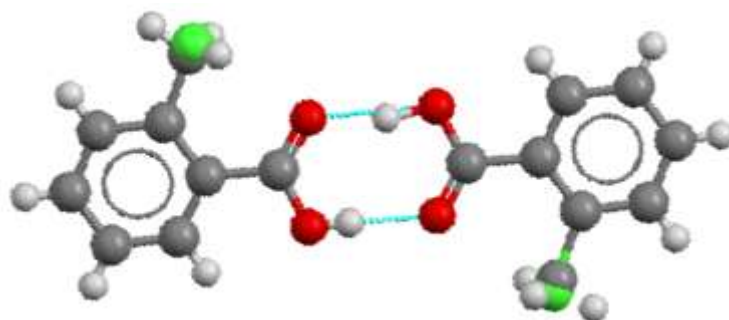


Fig. 5.7 – The main building block of the 2-chlorobenzoic acid : 2-methylbenzoic acid molecular complex. Both independent molecules have the chloro and methyl substituents disordered over two sites of equal occupancy

5.1.5 3-Chlorobenzoic Acid

3-Chlorobenzoic acid is used as a raw material in the production of the drugs loratadine¹¹ (antihistamine) and amfebutamone¹² (antidepressant). The structure of this molecule (Figure 5.8) was solved in 2003 (CSD reference MCBZAC01)¹³ at room temperature and to an R-factor of 6.29%. The carboxylic dimer has surprisingly been distorted from the normal planar geometry with the carboxylic groups lying at 87.3° to one another while still maintaining medium strength hydrogen bonds (2.558 Å). This must be a consequence of the Cl \cdots O-C halogen bond with the chlorine having a steric effect on the carboxylic dimer.

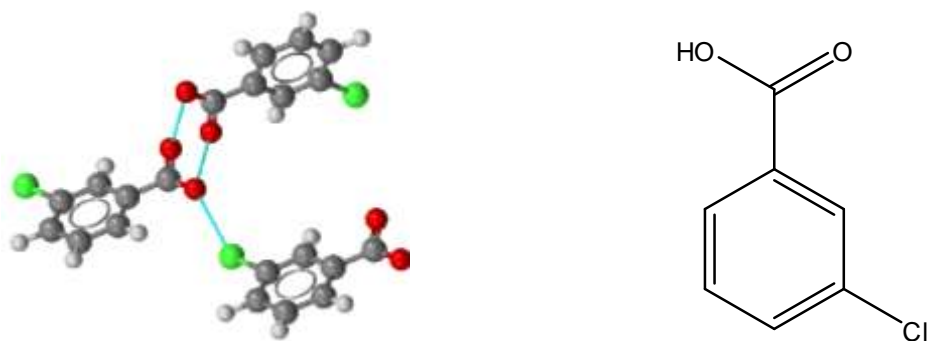


Fig. 5.8- Crystal structure of the 3-chlorobenzoic acid molecule; RHS, 3-chlorobenzoic acid.

3-Chlorobenzoic acid has successfully been cocrystallised with a range of co-molecules including 2,5-dibromo-1-(di-isopropylamido)-3,4-diphenyl-2,5-dihydrophosphole 1-oxide (CSD reference – EDUWOP)¹⁴, triphenylphosphine oxide (CSD reference – MACJEG)¹⁵, 2-picoline (CSD reference- ROKQEN)¹⁶ and hemikis((1RS,2RS,3RS)-3-N,N-dibenzylaminocyclohexane-1,2-diol N-oxide) (CSD reference – POYXOR)¹⁷ among others. Of particular interest is the 3-chlorobenzoic acid : 2-picoline N-oxide molecular complex (Figure 5.9), containing a simple O-H...O hydrogen bond as the main synthon and the halogen interaction assisting in expanding the structure.

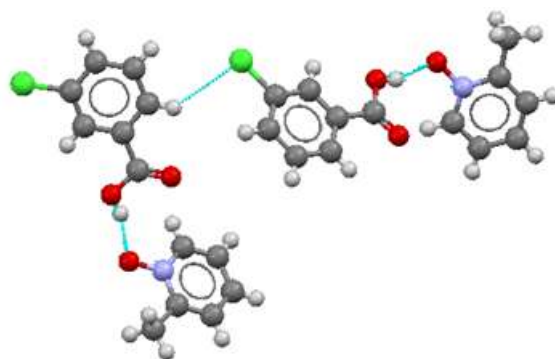


Fig. 5.9 – Building block of the 3-chlorobenzoic acid 2-picoline N-oxide molecular complex.

5.1.6 4-Chlorobenzoic Acid

4-Chlorobenzoic acid is probably the most industrially useful halobenzoic acid as it is used as an intermediate for manufacturing dyes, fungicides, pharmaceuticals and other organic chemicals and is also a preservative in adhesives and paints². The structure shows the carboxylic acid dimer, with dimers linked through halogen bonds of Cl...Cl 3.366(2)Å

distance in length (Figure 5.10). It has been studied with neutron diffraction by Wilson¹⁸ where it was found that the acidic proton is disordered over two sites with the occupancies changing with differing temperature.

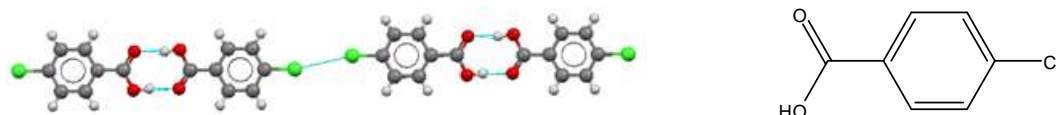


Fig. 5.10 – Structure of 4-chlorobenzoic acid highlighting the carboxylic acid dimer being held together by a chlorine-chlorine halogen bond, RHS, 4-chlorobenzoic acid.

This molecule has three molecular complexes reported in the CSD, N,N-dimethylformamide (CSD reference – ACERAC)¹⁹, (P)-tryptamine (CSD reference – FINZIM)²⁰ and 4-amino-N-(4,6-dimethyl-2-pyrimidinyl)benzenesulfonamide 4 (CSD reference – YIZQAA)²⁰ (Figure 5.11).

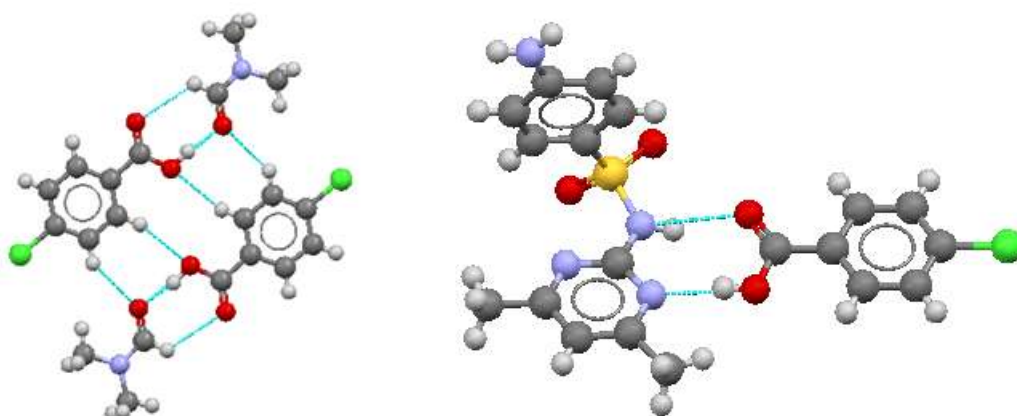


Fig. 5.11 – LHS, structure of the 4-chlorobenzoic acid : N,N-dimethylformamide molecular complex, RHS, 4-chlorobenzoic acid : sulfadimidine molecular complex.

5.1.7 2-Bromobenzoic Acid

There are no structures of any sort involving 2-bromobenzoic acid (Figure 5.12) in the CSD and information in the literature is limited to basic chemical properties.

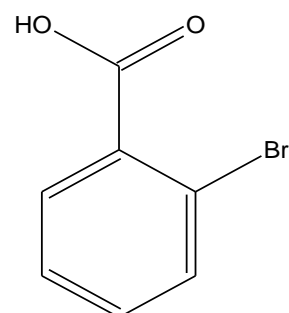


Fig. 5.12 – 2-bromobenzoic acid molecule.

5.1.8 3-Bromobenzoic Acid

There are limited uses and information on 3-bromobenzoic acid (Figure 5.13) acid in the literature, however it is involved in one structure reported in the CSD. Bis(bis(m2-3-bromobenzoato-O,O')-(2,2'-bipyridyl)-(3-bromobenzoato-O,O')-terbium(iii)) bis(3-bromobenzoic acid) dihydrate (CSD reference - TIDXAG)²¹ is a metal organic framework with six 3-bromobenzoic acid molecules coordinating to the terbium metal centre and one hydrogen bonding to a water molecule.

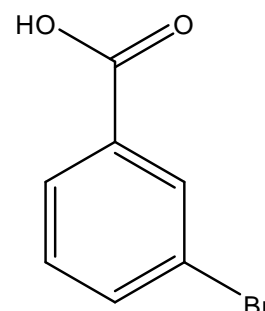


Fig. 5.13 – 3-bromobenzoic acid molecule.

5.1.9 4-Bromobenzoic Acid

4-Bromobenzoic acid is a known intermediate in the preparation of drugs, dyes and pigments²². Its structure was solved in 2004 with CSD reference - BRBZAP02²³ (Figure 5.14) showing that the carboxylic acid dimers are being held together by O··H-C hydrogen bonds (with C··O distances of 3.415(5)Å) to form layers. The layers are connected vertically by π - π stacking interactions with these columns of layers interacting with one-another through long-distance bromine – bromine interactions of 3.835 Å.

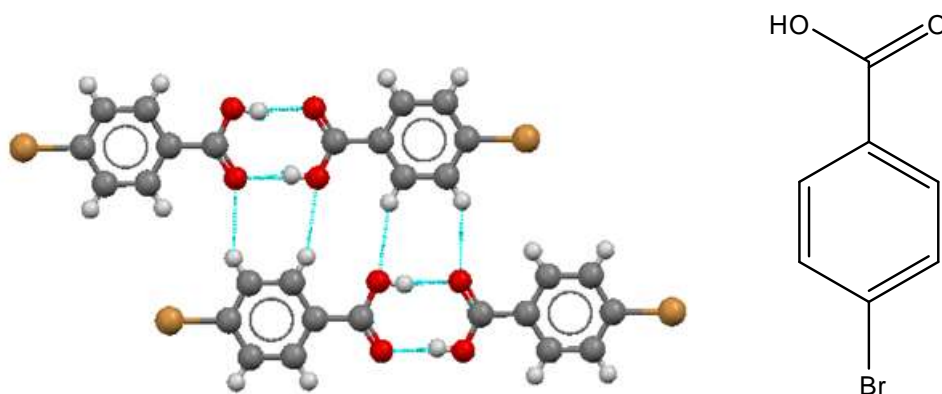


Fig. 5.14 – The 4-bromobenzoic acid structure highlighting the carboxylic acid dimers being held together by weak C-H··O hydrogen bonds; RHS, 4-bromobenzoic acid.

5.1.10 2-Iodobenzoic Acid

2-Iodobenzoic acid is a starting material for the preparation of iodosobenzoate (an oxidant which performs the synthesis of carbonyl compounds from primary/secondary alcohols) and flufenamic acid (with anti-inflammatory properties). Its structure was solved (Figure 5.15) in 2002²⁴, which showed how the carboxylic acid dimers are held together by I··I halogen bonds of 3.916Å in length. There are no other structures containing 2-iodobenzoic acid in the CSD.

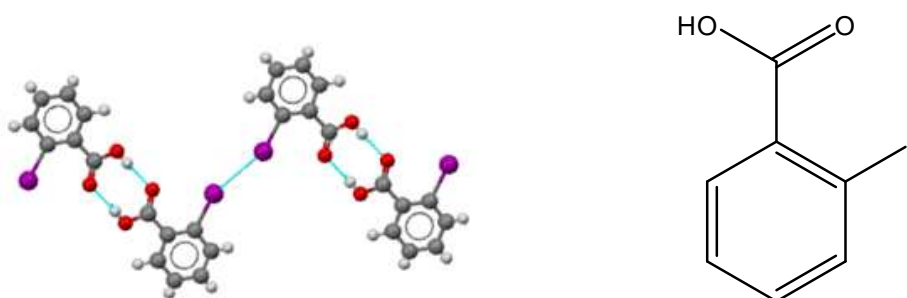


Fig. 5.15 – Structure of 2-iodobenzoic acid (CSD reference - OIBZAC01); the carboxylic acid dimer is held together by iodine-iodine halogen bonds. RHS, 2-iodobenzoic acid.

5.1.11 3-Iodobenzoic Acid

3-Iodobenzoic acid (Figure 5.16) is used in the organic synthesis of iodine-containing small molecules. There is no structural data for this molecule however it has been cocrystallised with N-carboxymethyl-N,N'-dimethylpiperazine (CSD reference SIXBAD)²⁵ (Figure 5.16), in which the 3-iodobenzoic acid does not form carboxylic acid dimers.

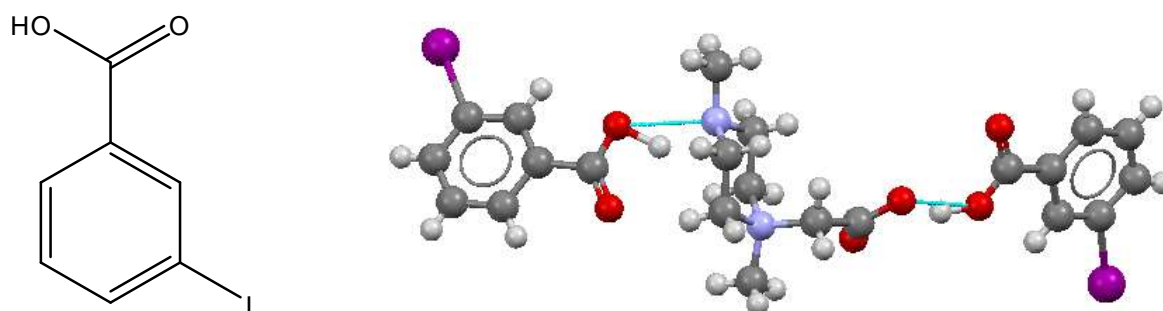


Fig. 5.16 – LHS- 3-iodobenzoic acid; RHS, structure of 3-iodobenzoic acid and N-carboxymethyl-N,N'-dimethylpiperazine molecular complex.

5.1.12 4-Iodobenzoic Acid

The structure of 4-iodobenzoic acid has been extensively studied by single crystal X-ray diffraction at various times (CSD references BENMOW, BENMOW01²⁶ and the BENMOW02²⁶ series) and over various temperatures (CSD references – BENMOW02 to BENMOW09)²⁷. There is a difference in the space group reported between the older structures (BENMOW and 01) and the newer structures (BENMOW02 series), however the difference is a $P2_1/n$ to $P2_1/a$ change between symmetrically equivalent structures.

The structure shown in Figure 5.17 shows that the carboxylic acid dimer is again the main hydrogen bond motif with I...I halogen bonds (distances ranging from 3.932(9)Å to 3.957(1)Å) connecting them together.

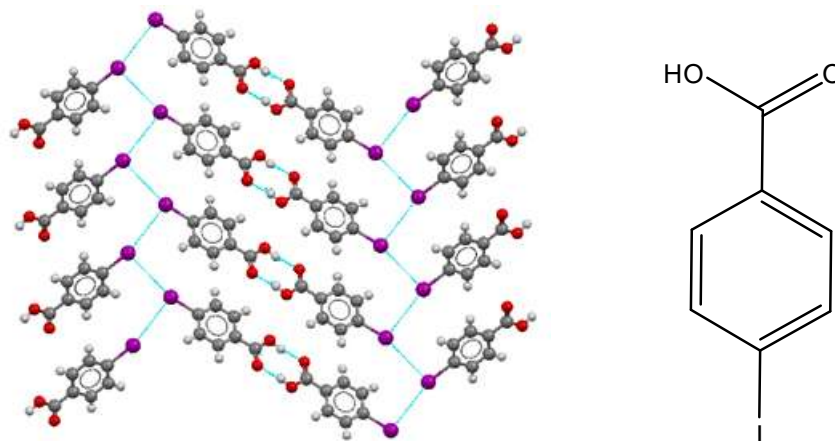


Fig. 5.17 – The structure of 4-iodobenzoic acid; carboxylic acid dimers are held together by iodine iodine interactions. RHS, 4-iodobenzoic acid.

4-Iodobenzoic acid is involved in four molecular complexes all from the same body of work by Aakeroy (2009)²⁸. These complexes are with 3-(2-amino-4-methylpyrimidin-6-yl)pyridine (AMP-P) toluene solvate (Figure 5.18, top left), 3-(AMP-P) 2,3,5,6-tetrafluoro (Figure 5.18, top right), 4-(AMP-P) (Figure 5.18, bottom left) and 1-(AMP-P) (Figure 18, bottom right). There are no carboxylic acid dimers formed in these structures, instead Figure 5.18 visually highlights the robustness of the carboxylate / amino-pyrimidine hydrogen bond motif throughout these systems.

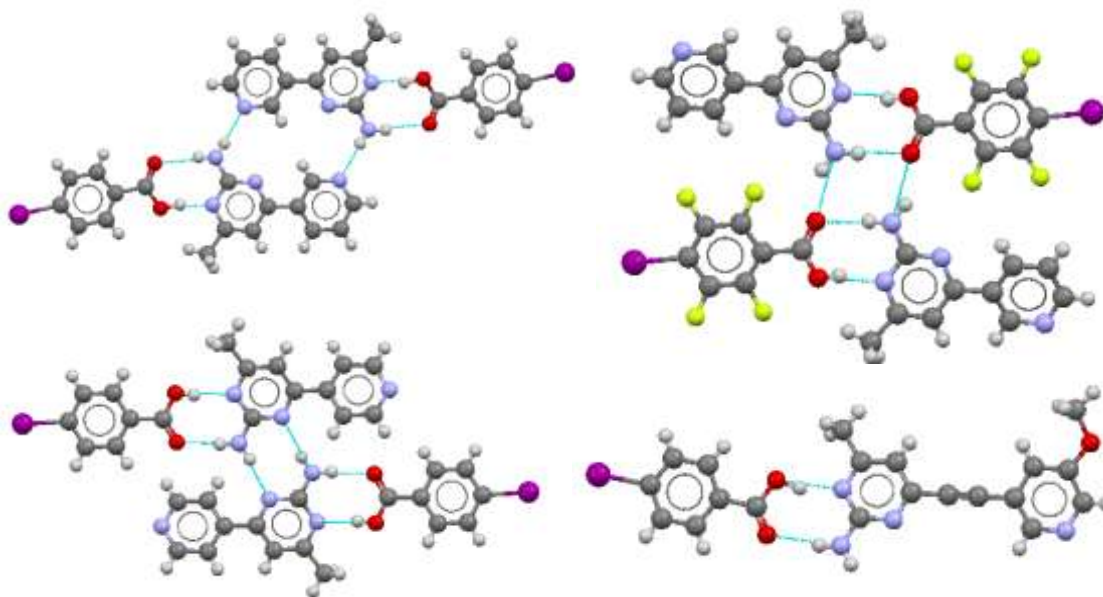


Fig. 5.18 – Top left, basic building block of the 3-(AMP-P) toluene 4-iodobenzoic acid solvate with CSD reference – COWHOM, top right, the 3-(AMP-P) 2,3,5,6-tetrafluoro 4-iodobenzoic acid molecular complex main hydrogen bond motif with CSD reference – COWHUS, bottom left, the molecular complex of 4-(AMP-P) 4-iodobenzoic acid which has CSD – reference COWJAA and lastly bottom right, 1-(AMP-P) 4-iodobenzoic acid with CSD reference – COWJOO.

5.2 Summary of Results

Benzimidazole has successfully been cocrystallised with a range of halo-benzoic acids (Table 5.1) generating a range of molecular complexes. These molecular complexes have been analysed, where possible, by single crystal X-ray diffraction and subsequently powder X-ray diffraction and DSC. Neutron diffraction data collected at the ILL Grenoble were also collected on several of these molecular complexes.

Benzimidazole	Ortho	Meta	Para
Fluorobenzoic Acid			
Chlorobenzoic Acid			
Bromobenzoic Acid			
Iodobenzoic Acid			

Table 5.1 – Summary of the successful (blue) and unsuccessful (grey) co-crystallisation experiments between benzimidazole and the various halobenzoic acids.

To date no solid material has been generated through the co-crystallisation of benzimidazole and 2-chloro/bromobenzoic acid, regardless of the solvent or temperature regime used. However, it is worthwhile to note that the co-crystallisation of these materials produces an oil-like substance suggesting that a low melting point complex may have been formed. All the benzimidazole and iodobenzoic acid co-crystallisation experiments produced only single components, regardless of the wide range of physical conditions used.

The main aim was to identify if these systems could generate molecular complex polymorphs and then selectively control the growth of each polymorph. Table 5.2 highlights the systems where molecular complex polymorphism occurred and could be selectively controlled through solvent and / or temperature changes. It can be seen that polymorphism has been confirmed in the systems that involve benzimidazole with 3-chlorobenzoic acid, 4-chlorobenzoic acid and 4-bromobenzoic acid.

Benzimidazole	Ortho	Meta	Para
Fluorobenzoic Acid	Yellow		
Chlorobenzoic Acid	Grey	Blue	Green
Bromobenzoic Acid	Grey	Yellow	Green
Iodobenzoic Acid	Grey		

Table 5.2 – Summary of the systems where molecular complex polymorphism was confirmed by single crystal data (blue), polymorphism identified using powder data (green), no polymorphism occurred (yellow) and no molecular complex generated (grey).

During analysis of the results, it was noted that there were many similarities between the different molecular complexes generated. The primary hydrogen bond in nearly all molecular complexes is a partially charge assisted $N^{\delta+}-H\cdots O^{\delta-}$ hydrogen bond with a proton transferring from the carboxylic acid group to the unprotonated nitrogen of the benzimidazole (Section 5.2.1). The consequence of the occurrence of the same supramolecular synthons generating the same motif, with the co-molecules only changing in the attached halogen atom, resulted in the identification of isostructures. Table 5.3 summarises where these isostructures have occurred.

Benzimidazole	Ortho	Meta	Para
---------------	-------	------	------

Fluorobenzoic Acid

Chlorobenzoic Acid

Bromobenzoic Acid

Iodobenzoic Acid



Table 5.3 –A summary of the molecular complexes that have generated isomorphous structures (blue and yellow), with grey indicating no isomorphism.

5.2.1 Benzimidazolium Ion

Where the crystallisation product is in a 1:1 stoichiometric ratio of benzimidazole and a carboxylic acid containing molecule, the benzimidazole is protonated through hydrogen transfer from the carboxylic acid group onto the normally unprotonated nitrogen atom in the five-membered ring, creating a benzimidazolium molecule (BZNH^+) (Figure 5.19). The effect of the proton transfer on the benzimidazolium molecule is a delocalisation of the charge across the five-membered ring, reflected in the equalisation of the internal bond lengths $\text{N}^{\delta+}-\text{C}-\text{N}^{\delta+}$ and bond angles $\text{C}-\text{N}^{\delta+}-\text{C}$ (Table 5.4). The delocalisation of the charge has the effect of creating a partial positive charge on both the nitrogens. This effect has been reported in many structures involving benzimidazole and imidazole.

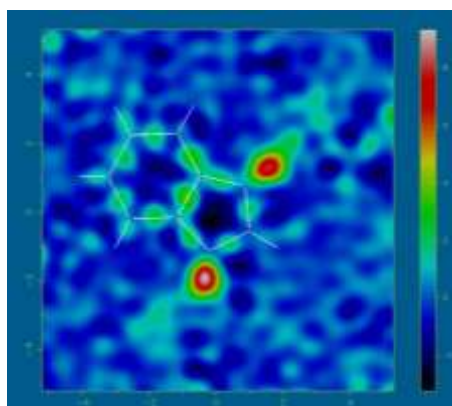
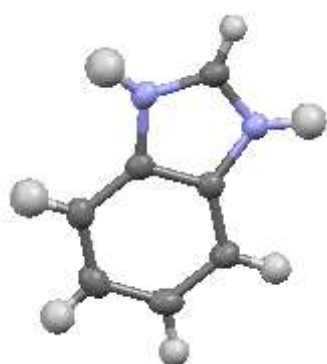


Fig. 5.19 – LHS, a typical benzimidazolium molecule where both nitrogens are protonated; RHS, the Fourier difference map generated where the H atoms located on a nitrogen atom have been omitted from the model, clearly shows that both nitrogen atoms are protonated.

The consequence for the co-molecule that has been deprotonated is the creation of a negative charge. The negative charge is found to be delocalised over the carboxylic acid group by consideration of the normalisation of the bond lengths in the carboxylate group.

Molecular Complexes	BZN 3-CIBA I	BZNH+ 3-CIBA-II	BZNH+ 4-CIBA-	BZNH+ 4-BrBA-	BZN 3-BrBA *	BZNH+ 2-FBA- 2-FBA	BZN BZNH+ 4-FBA- 4-FBA-
N-C(Å) <i>2nd molecule</i>	1.328(8)	1.329(2)	1.335(3) 1.334(2)	1.335(2) 1.327(3)	1.319(3)	1.3305(1)	1.359(3) 1.329(2)
N-C(Å) <i>2nd molecule</i>	1.358(9)	1.342(2)	1.340(2) 1.339(2)	1.328(3) 1.329(2)	1.335(3)	1.3252(1)	1.323(2) 1.331(3)
C-N-C(°) <i>2nd molecule</i>	107.5(4)	106.3(1)	107.8(1) 108.0(0)	107.2(2) 108.3(2)	106.6(2)	108.16	108.0(2) 107.9(2)
C-N-C(°) <i>2nd molecule</i>	105.2(5)	107.8(1)	108.6(1) 108.5(2)	108.3(2) 108.0(2)	108.0(2)	108.17	108.1(2) 104.4(2)

Table 5.4 – The N⁰⁺-C-N⁰⁺ bond lengths and C-N⁰⁺-C bond angles for the molecular complexes discussed in Chapter 5. *Note that BZN 3-BrBa has, on average, partial ionic species of the co-molecules

5.2.2 Primary Hydrogen Bonds

Consideration of the co-molecules involved in the successful generation of molecular complexes of benzimidazole would point to a series of possible hydrogen bonds that could be generated (Figure 5.20). All these hydrogen bonds have many examples in the Cambridge Structural Database and have been of interest in their own right.

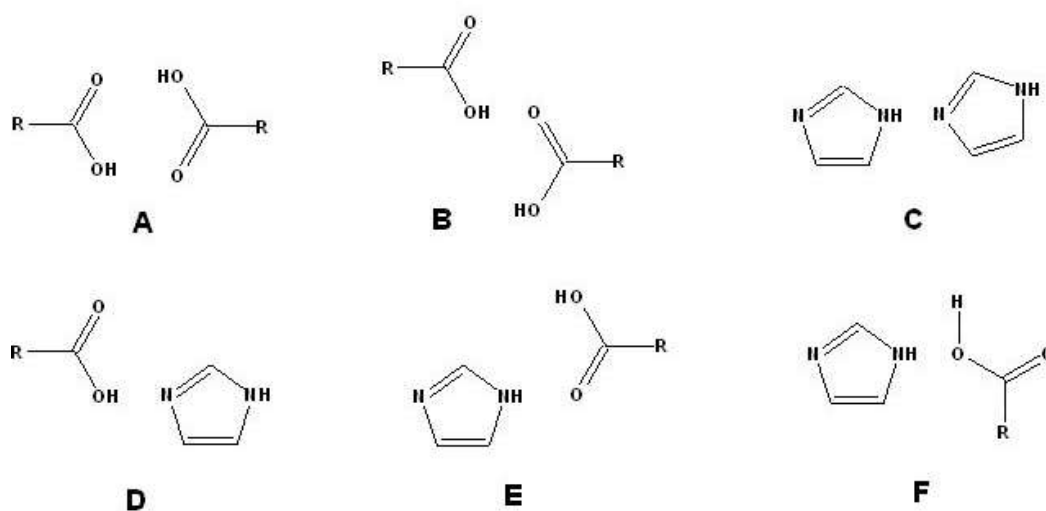


Fig. 5.20 – The potential homo-hydrogen bonds (A, B and C) and hetero-hydrogen bonds (D, E and F) that can be exhibited between a benzimidazole and carboxylic acid group.

As indicated, certain hydrogen bonding motifs appear in various different molecular complex structures. For ease of defining, the most prominent hydrogen bonds that appear in at least two of the structures will be outlined and labelled for future reference (Figure 5.21) and their scalar quantities given (Table 5.5). Note that this does not include secondary interactions that may play as influential a part in the structure as these primary hydrogen bonds.

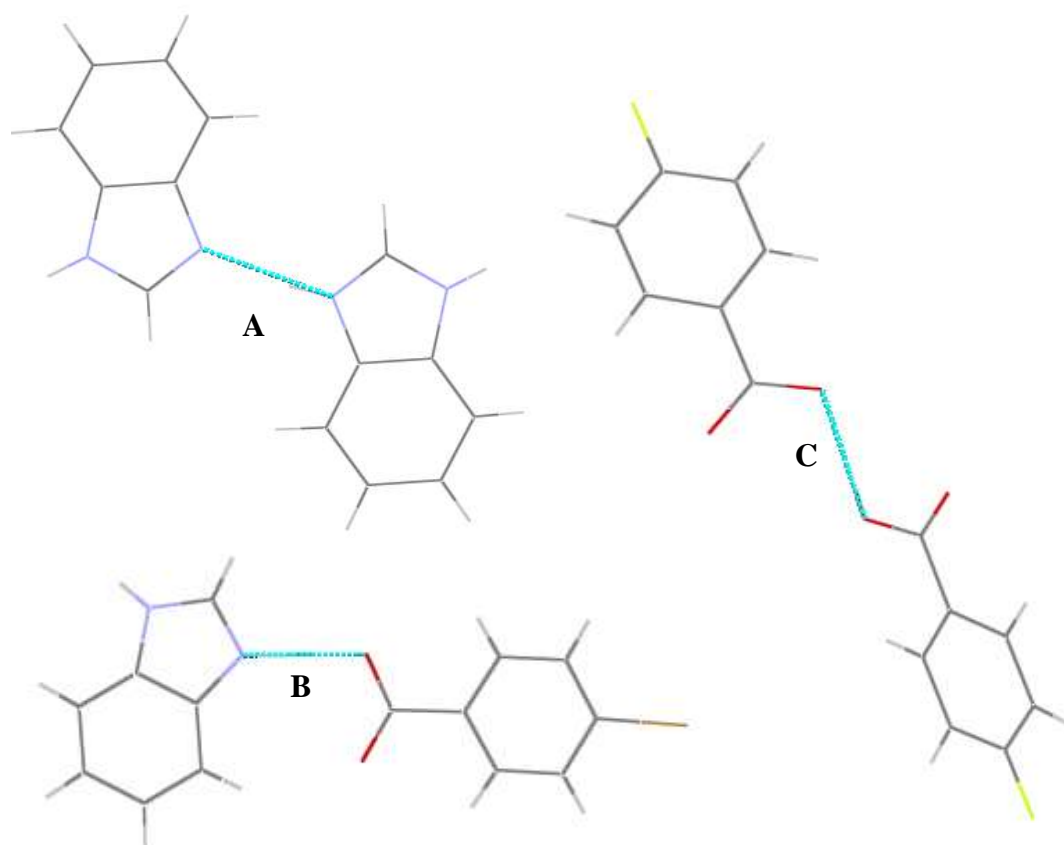


Fig. 5.21 - The most prominent hydrogen bonds within the benzimidazole : halobenzoic acid molecular complexes: N-H...N hydrogen bond (A), N-H...O hydrogen bond (B) and O-H...O hydrogen bond (C).

Molecular Complexes		BZN 3-CIBA I	BZNH+ 3-CIBA-II	BZNH+ 4-CIBA-	BZNH+ 4-BrBA-	BZN 3-BrBA*	BZNH+ 2-FBA- 2-FBA	BZN BZNH+ 4-FBA 4-FBA-
Hydrogen Bonds								
A, N ^{δ+} -H...N ^{δ-}	D...A(Å)	-	2.677(2)	-	-	2.693(3)	-	2.750(2)
	D-H(Å)	-	1.338(1)	-	-	0.76(5)	-	0.94(2)
	H...A(Å)	-	1.338(1)	-	-	1.94(5)	-	1.81(2)
	D-H...A angle(°)	-	180.00(9)	-	-	171(6)	-	179(2)
B, N ^{δ+} -H...O ^{δ-}	D...A(Å)	2.575(7) 2.760(5)	2.830(2)	2.606(2) 2.682(2) 2.642(2) 2.900(2) 2.832(2)	2.597(2) 2.667(2) 2.638(2) 2.850(2) 2.848(2)	2.843(3)	2.719(3) 2.691(3)	2.800(2) 2.687(2)
	D-H(Å)	0.95195) 0.950(5)	0.84(2)	0.93(2) 1.05(3) 0.97(2) 0.87(2) 0.87(2)	0.94(3) 0.78(2) 0.92(3) 0.77(2) 0.77(2)	0.80(4)	0.91(5) 0.90(4)	0.85(2) 0.93(2)
	H...A(Å)	1.640(5) 1.874(4)	2.00(2)	1.56(3) 1.80(2) 1.67(2) 2.15(2) 2.27(3)	1.65(3) 1.91(2) 1.72(3) 2.17(2) 2.36(3)	2.06(4)	1.85(4) 1.79(5)	2.13(3) 1.77(3)
	D-H...A angle(°)	166.5(3) 154.1(3)	172(3)	176(2) 169(3) 157(2) 144(2) 122(2)	178(3) 163(3) 147(2) 141.6(2) 123(2)	170(3)	162(4) 171(5)	135(2) 179(2)
C, OH...O ^{δ-}	D...A(Å)	-	2.492(2)	-	-	2.493(3)	2.5764(1)	2.528(2)
	D-H(Å)	-	1.246(1)	-	-	0.68(4)	0.856(5)	1.03(3)
	H...A(Å)	-	1.246(1)	-	-	1.82(4)	1.767(5)	1.50(3)
	D-H...A angle(°)	-	180.00(8)	-	-	169(5)	156.7(4)	177(3)

Table. 5.5 – The hydrogen bond scalar quantities, donor – acceptor (D...A), donor – hydrogen (D-H) and hydrogen – acceptor (H...A) distances, and hydrogen bond angle (D-H...A) for the molecular complexes discusses in Chapter 5. *Note that BZN 3-BrBa has, on average, partial ionic species of the co-molecules

5.3 Crystallographic Data

Compound	BZN 3-CIBA I	BZNH+ 3-CIBA- II	BZNH+ 4-CIBA-
Formula	C ₇ N ₂ H ₆ , C ₇ O ₂ ClH ₄	C ₇ N ₂ H _{6.5} , C ₇ O ₂ Cl, H _{4.5}	C ₇ N ₂ H ₆ , C ₇ O ₂ ClH ₄
ΔpKa (1:1)	1.69	1.69	1.53
Crystallisation Conditions	acetone, ~2-4°C	methanol, ~2-4°C	methanol, ~2-4°C
Molecular weight / gmol ⁻¹	274.70	274.45	274.71
Temperature (K)	100	100	100
Space Group	<i>P</i> -1	<i>P</i> 2 ₁ /c	<i>P</i> -1
<i>a</i> (Å)	3.802(6)	4.0009(6)	9.334(4)
<i>b</i> (Å)	12.358(13)	11.7056(17)	11.207(4)
<i>c</i> (Å)	14.706(14)	26.480(4)	12.230(5)
α (°)	109.37(2)	90	84.173(10)
β (°)	99.18(4)	94.074(8)	77.990(12)
γ (°)	101.46(3)	90	86.837(10)
Volume (Å ³)	619.5(13)	1237.0(3)	1243.8(9)
<i>Z</i>	2	4	4
θ range (°)	3.028-27.484	1.542-33.011	3.077-27.483
Completeness (%)	97.1	99.8	99.8
Refln Collected	2745	41466	28693
Independent	2745	4637	5698
Refln (obs.I>2sigma(I))	2745	3982	3982
R _{int}	0.096	0.071	0.046
Parameters	172	205	431
GooF on F ²	0.9044	1.0505	0.8945
R ₁ (Observed)	0.1372	0.0694	0.0344
R ₁ (all)	0.1372	0.0694	0.0520
wR ₂ (all)	0.1219	0.1553	0.0852

BZNH+ 4-BrBA-	BZN 3-BrBA*	BZNH+ 2-FBA- 2-FBA	BZN BZNH+ 4-FBA 4-FBA-
C ₇ N ₂ H ₆ , C ₇ O ₂ Br H ₄	C ₇ N ₂ H _{6.5} , C ₇ O ₂ Br H _{4.5}	C ₇ N ₂ H ₆ , C ₇ O ₂ F H ₄ , C ₇ O ₂ F H ₅	C ₇ N ₂ H ₆ , C ₇ O ₂ F H ₅
1.57	1.72	2.26	1.38
Ethanol, room temperature	Ethanol, ~2-4°C	Methanol, RT then ~2-4°C	Methanol, RT then ~2- 4°C
319.16	638.32	398.36	516.50
100	200	100	100
<i>P -1</i>	<i>P 2₁/c</i>	<i>P 2₁/c</i>	<i>P -1</i>
9.4515(5)	4.15350(10)	12.8630(8)	8.0327(4)
11.2228(5)	11.6939(2)	11.3722(8)	12.1791(7)
12.1857(5)	26.3600(5)	12.8196(8)	13.2117(8)
84.102(2)	90	90	89.525(4)
78.200(2)	93.8799(10)	103.134(3)	75.621(3)
86.568(2)	90	90	74.452(3)
1257.55(10)	1277.39(5)	1826.2(2)	1203.86(12)
4	2	4	2
3.051-27.481	1.549-27.442	1.626-28.088	1.594-30.665
99.5	99.7	99.5	97.7
29425	20237	46454	25201
5749	2925	4425	7294
5388	2378	3893	4496
0.031	0.086	0.53	0.052
431	220	1	431
0.9433	0.9669	1.0791	1.1595
0.0232	0.0336	0.0551	0.0491
0.0248	0.0446	0.0635	0.0889
0.0607	0.0990	0.1525	0.1575

Table. 5.6 – Crystallographic data for the molecular complexes discussed in Chapter 5. *Note that BZN 3-BrBa has, on average, partial ionic species of the co-molecules

5.4 Results and Discussion

5.4.1 Molecular Complex Polymorphism

The most interesting set of molecular complexes with regard to polymorphism are those containing benzimidazole and 3-chlorobenzoic acid. Three molecular complex polymorphs have been discovered using powder diffraction with two of those producing single crystal structures. There are possibly two benzimidazole : 4-chlorobenzoic acid molecular complexes, one producing single crystal data with the other having been identified through powder XRD and DSC. The same is true for the benzimidazole : 4-bromobenzoic acid molecular complexes, where two possible polymorphs have been identified.

5.4.1.1 Benzimidazole and 3-Chlorobenzoic Acid 1:1

Benzimidazole and 3-chlorobenzoic acid has been the most intensively studied system during this project. Co-crystallisation experiments have ranged from using a wide range of solvents, various different temperatures, evaporation occurring in different types of glassware, the use of solvent-free and solvent-drop grinding experiments. An array of analytical techniques were deployed in characterising the resulting products.

Initial experiments were set-up using just four different types of solvent, methanol, ethanol, propanol and acetone with evaporation occurring at room temperature. From these initial experiments three different products could already be observed to form, from the DSC (Figure 5.22) and X-ray powder diffraction data (Figure 5.23).

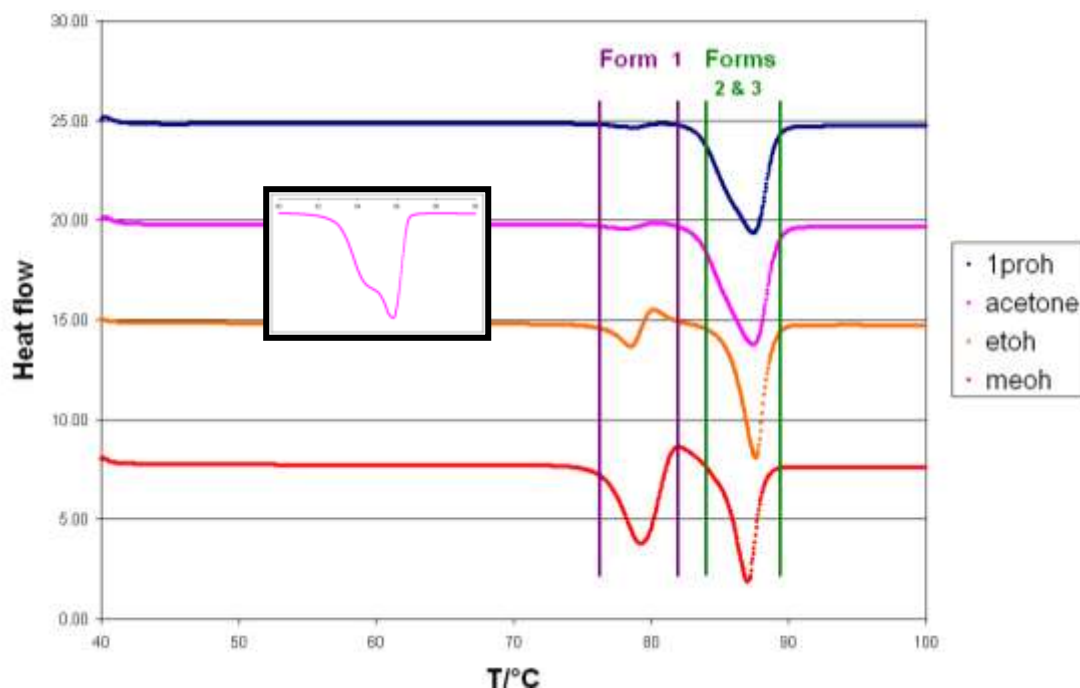


Fig. 5.22 – DSC data from the products of crystallisation of benzimidazole and 3-chlorobenzoic acid from four common solvents. Two different polymorphs can be clearly identified by two distinct melting points, but a third polymorph can also be identified in the samples crystallised from 1-propanol (1proh) and acetone. The shoulder on the principal peaks in these traces, representing the third polymorph, can be seen in the enlarged inset, taken from the acetone trace.

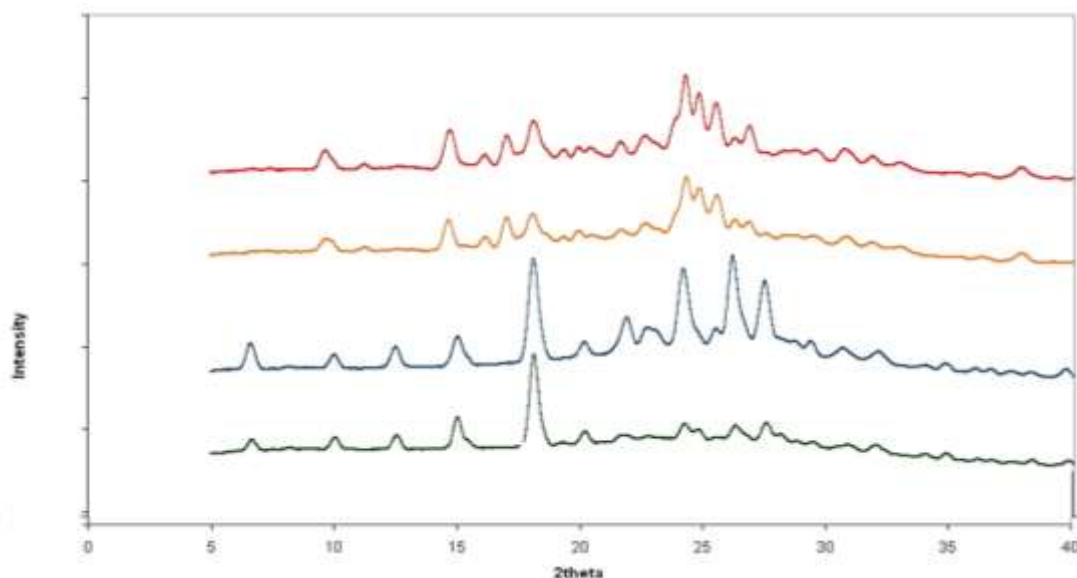


Fig. 5.23 – Powder patterns of the products of crystallisation from four common solvents propanol (-), acetone (-), methanol (-) and ethanol (-). Two different products can clearly be identified from these quick powder patterns (collected on the Rigaku R-axis/RAPID single crystal diffractometer) with crystallisation from propanol and acetone forming one product and methanol and ethanol the other.

Evidence of the third possible polymorph has been established using powder diffraction (Figure 5.24). These were identified after intensive studies into finding the optimal conditions to promote the growth of Form III. Acetone at 10°C using the Microvate and acetone at ~-2-4°C using the walk in fridge, gave for a period of time the Form III polymorph (which then transformed to Form I over a period of weeks).

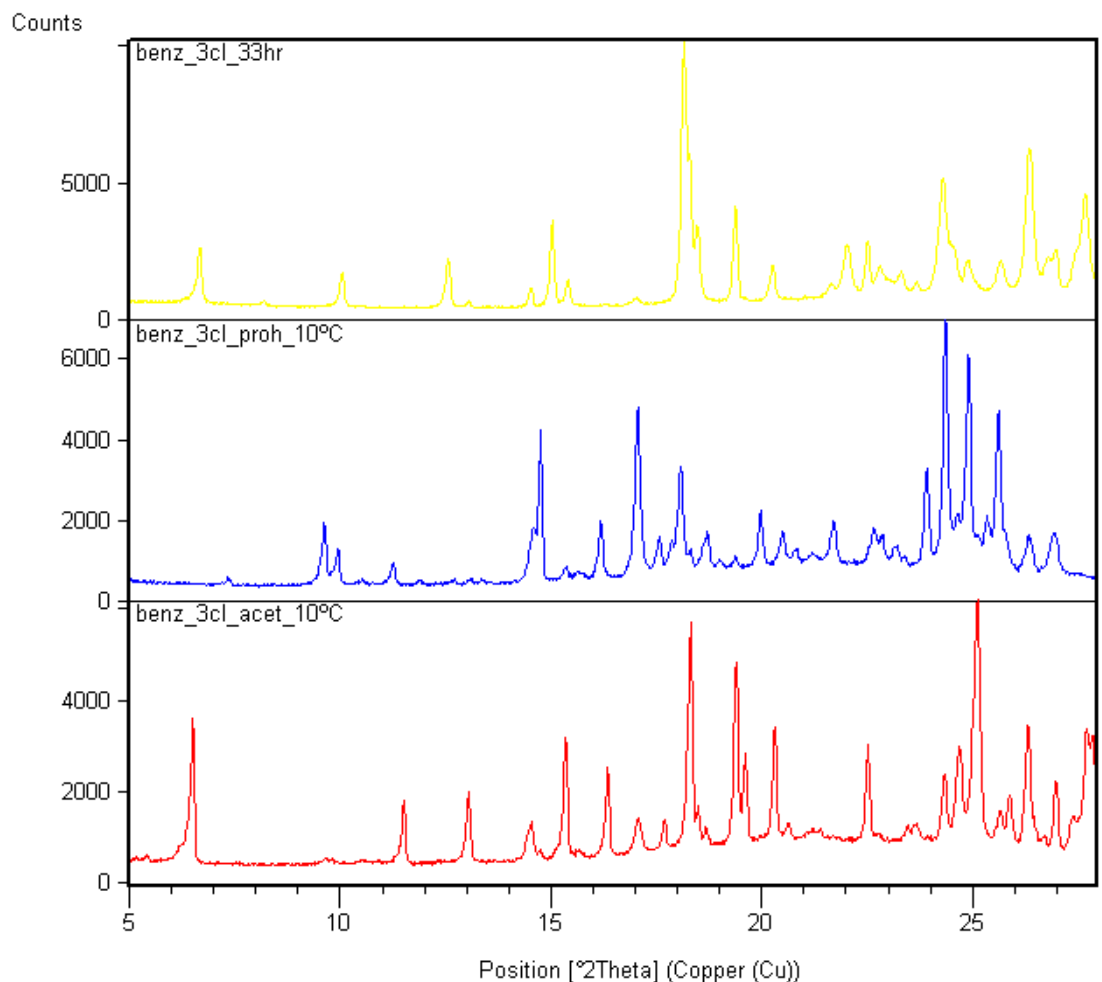


Fig. 5.24 – Powder patterns of the products of crystallisation from three different environmental conditions to promote growth of single component of; form I (blue) using propanol at 10°C, form II (yellow) using acetone at ~-2-4°C and form III (red) using acetone at 10°C. Three different products can clearly be identified from these powder patterns.

The aim was to promote selective growth of a particular molecular complex polymorph through controlling the conditions. This obviously required an extensive range of conditions to be explored initially to find the conditions that promoted selective growth. This then allowed the growth of crystals suitable for X-ray diffraction by exploiting these conditions. Table 5.7 gives a visual display showing the products observed by varying the experimental environmental conditions.

	Methanol	Ethanol	Propanol	Acetone
2~4°C	Yellow	Red	Blue	Yellow, Red
10°C	Yellow	Red	Blue	Yellow, Red
20°C	Yellow	Red	Blue, Red	Blue, Red
30°C	Blue	Red	Blue, Red	Red

Table 5.7 – The results of co-crystallisation experiments on the benzimidazole and 3-chlorobenzoic acid system in creating Form I (blue), Form II (yellow), Form III (red).

Unfortunately due to the limited conditions that promoted the growth of benzimidazole 3-chlorobenzoic acid molecular complex Form III, single crystals were never obtained. Thus, high quality powder X-ray diffraction data were acquired (Figure 5.25), collected over two days on the Bruker D8 diffractometer with varying exposure time with the aim of solving the structure from this data. Although the technique of solving crystal structures from powder data is still relatively new, it has proven very successful by using programs such as DASH (refer to Section 2.2.4). However, due to the many unknowns regarding the possible structure of Form III – including molecular stoichiometric ratio, proton transfer, solvent inclusion – a solution was never found.

benz_3cl_33hr [004]

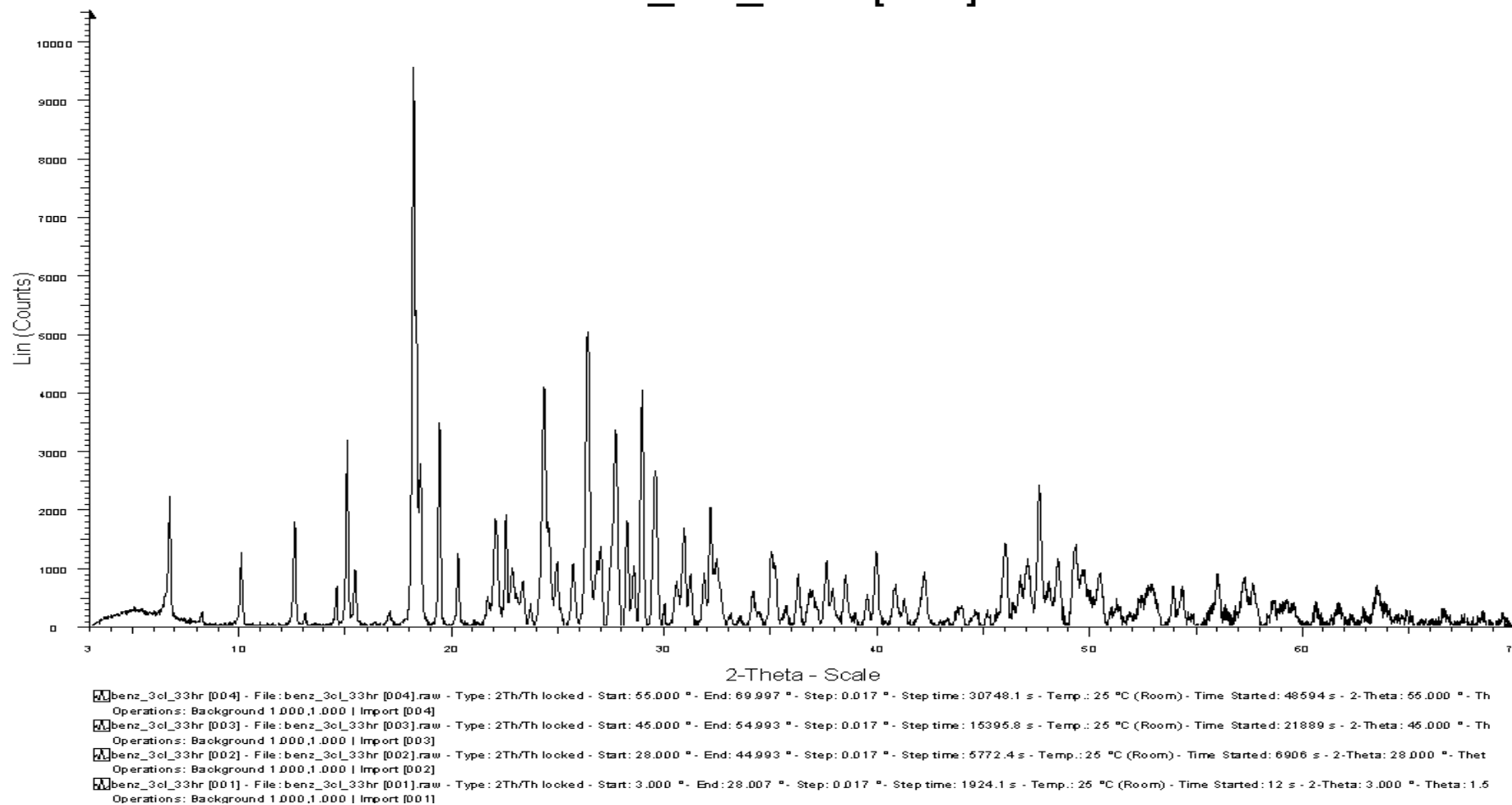


Fig. 5.25 – Powder pattern of benzimidazole and 3-chlorobenzoic acid Form III collected over a 33 hour period.

Two molecular complex polymorphs of benzimidazole and 3-chlorobenzoic acid have been analysed successfully by single crystal X-ray diffraction, Forms I and II. They display two very different hydrogen bonding motifs, although these motifs are not unexpected.

5.4.1.1.1 Benzimidazole : 3-Chlorobenzoic Acid Molecular Complex 1:1 Form I

The benzimidazole (BZN) : 3-chlorobenzoic acid (3-CIBA) Form 1 molecular complex is a equimolar material obtained using the solvent evaporation method. Using a 1:1 stoichiometric mixture of benzimidazole (12mg) and 3-chlorobenzoic acid (16mg) dissolved in the minimum amount of acetone followed by evaporation at a constant temperature of between 2 and 4°C using a walk in fridge gave crystals that were needle shaped and colourless. Single crystal X-ray diffraction data were obtained using a Rigaku R-axis/RAPID diffractometer at 100K, equipped with graphite monochromated Mo K α radiation ($\lambda = 0.71073 \text{ \AA}$). The structure was solved using SIR92 within the CRYSTALS program. The crystallographic data are summarised in Table 5.6. This is one of only two molecular complexes which contain BZN and a carboxylic acid containing molecule in a 1:1 ratio where proton transfer has not occurred (Table 5.4). The data quality is relatively poor and thus accurate hydrogen positions are not fully reliable. However there is no residual electron density observed around the unprotonated nitrogen atom of the BZN and is instead clearly associated with the carboxylic acid group (Figure 5.26).

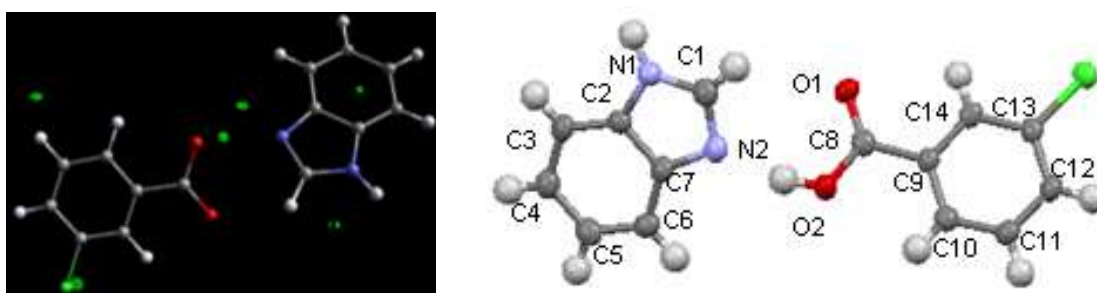


Fig. 5.26 – LHS, Fourier difference map of the residual electron density in BZN : 3-CIBA molecular complex with the proton associated with the carboxylic acid group removed, RHS, the BZN and 3-CIBA molecules involved in the molecular complex with associated atom labelling.

Interaction	Length (Å) (D...A(Å))	For Hydrogen Bonds		
		D-H(Å)	H...A(Å)	D-H...A angle(°)
N2...O2	2.575(7)	0.951(5)	1.640(5)	166(3)

N1...O1	2.760(6)	0.950(5)	1.874(4)	154(3)
C11...C11	3.325(3)	-	-	-
C1...O2	3.272(8)	0.950(6)	2.518(5)	136(4)
C10...O2	3.355(6)	0.951(4)	2.631(4)	132(3)

Table. 5.8 – The intermolecular interactions involved in the BZN : 3-CIBA Form I molecular complex

The result of the absence of proton transfer is that the BZN and 3-CIBA remain in their neutral state with no charge delocalised over the atoms and therefore no normalisation of bond lengths or angles.

There are two primary hydrogen bonds within this structure; both are slight derivatives of hydrogen bond B (Figure 5.21) with only the positioning of the hydrogen the difference. The shorter of the two has the hydrogen on the oxygen, O2-H...N2, which has length 2.575(7)Å while the other of length 2.760(6)Å has the hydrogen on the nitrogen, N1-H...O1 (see Table 5.5 for hydrogen bond data). The supramolecular synthons arrange themselves into an equimolar hydrogen bonded ring system that can be described by the graph set notation symbol R_4^4 (16). This hydrogen bonded ring system is the motif of the molecular complex and contains two occurrences of each co-molecule (Figure 5.27).

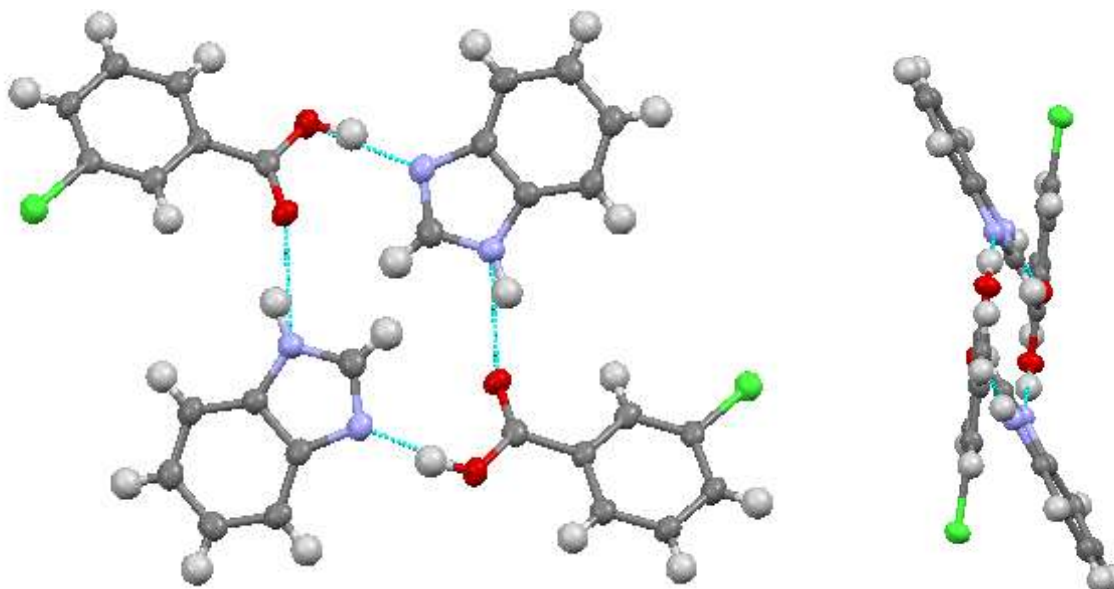


Fig. 5.27 – LHS, the main motif of the BZN : 3-CIBA Form I molecular complex; an equimolar hydrogen bonded ring system held together by N-H...O and O-H...N hydrogen bonds; RHS, view along the *b*- axis that highlights the spatial arrangement of the equimolar hydrogen bonded ring system.

The hydrogen bonded rings are expanded by weaker interactions in all directions. The most influential are chlorine–chlorine interactions that expand the structure along the *ab*-diagonal axis (Figure 5.28). These interactions are of length 3.325(3)Å and are highly directional.

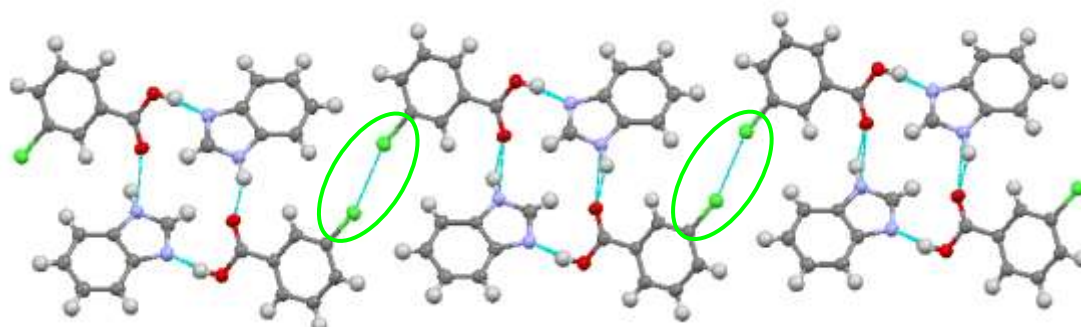


Fig. 5.28 – View along the *a*-axis of the BZN : 3-CIBA Form I molecular complex highlighting how the chlorine chlorine interaction connects the rings together (green circles).

The carbon located between the two nitrogens in the BZN molecule, a common hydrogen bond donor, is hydrogen bonded to an oxygen belonging to a different ring motif. Each of these carbons hydrogen bonds to an oxygen in opposite directions which results in stacks of hydrogen bonded rings which lie along the *a*-axis (Figure 5.29 LHS). This weak hydrogen bond, C1-H···O2, is of length 3.272(8)Å (Figure 5.29 RHS).

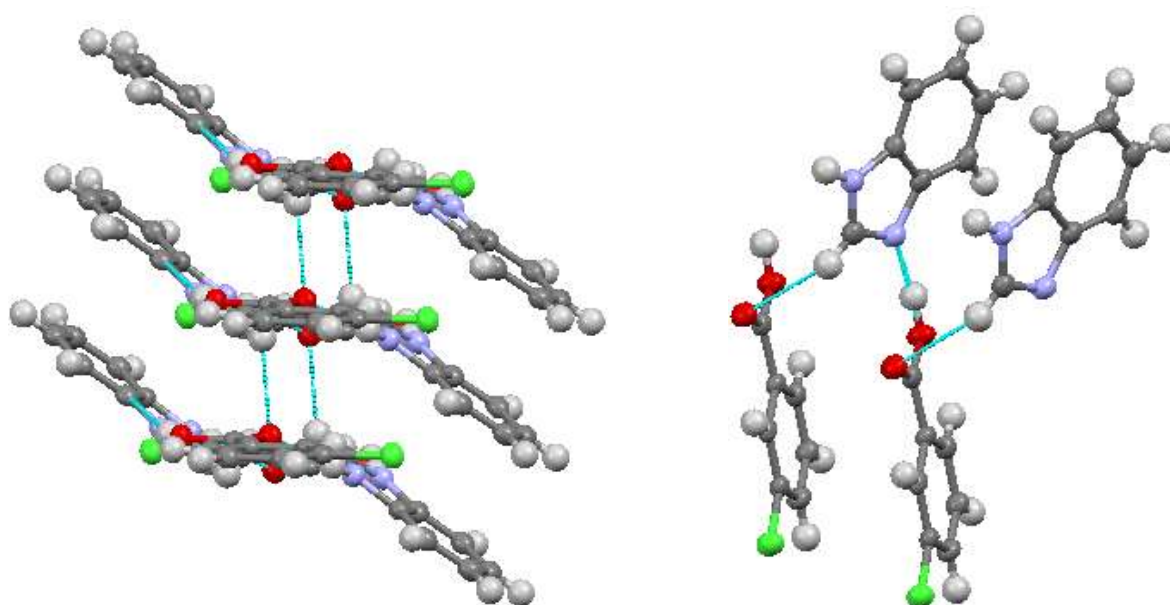


Fig. 5.29 – LHS, view along the *b*-axis of the BZN 3-CIBA Form I molecular complex highlighting how the hydrogen bonded rings stack upon one another. RHS, the weak hydrogen bond, C1-H···O2, which stacks the rings upon one another.

The weakest interaction present in the BZN : 3-CIBA Form I molecular complex expands the structure along the *b*-axis. This weak hydrogen bond exists between two 3-CIBA molecules of different rings and involves a carbon of the benzene ring and carbonyl oxygen, C10-H \cdots O2, that has length 3.355(6)Å (Figure 5.30).

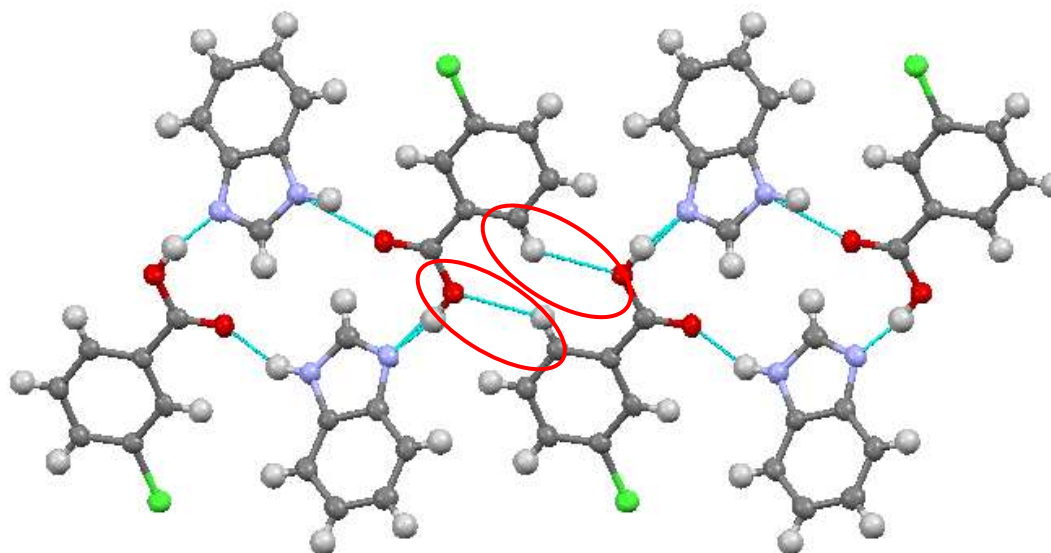


Fig. 5.30 – View along the *a*-axis of the BZN 3-CIBA Form I molecular complex. The hydrogen bonded rings, the main motif of the structure, are expanded along the *b*-axis by weak C-H \cdots O hydrogen bonds.

Figure 5.31 is a view of the extended structure of the BZN : 3-CIBA Form I molecular complex. The main motif, hydrogen bonded rings, (blue circle) are stacked upon one another through carbon oxygen hydrogen bonds as seen in Figure 5.27. These stacks of hydrogen bonded rings are expanded along the *b*-axis by another weak carbon oxygen hydrogen bond (Figure 5.30) (red circle) to create blocks. Lastly these blocks are connected through chlorine–chlorine interactions as describe in Figure 5.28 which completes the structure (green circle).

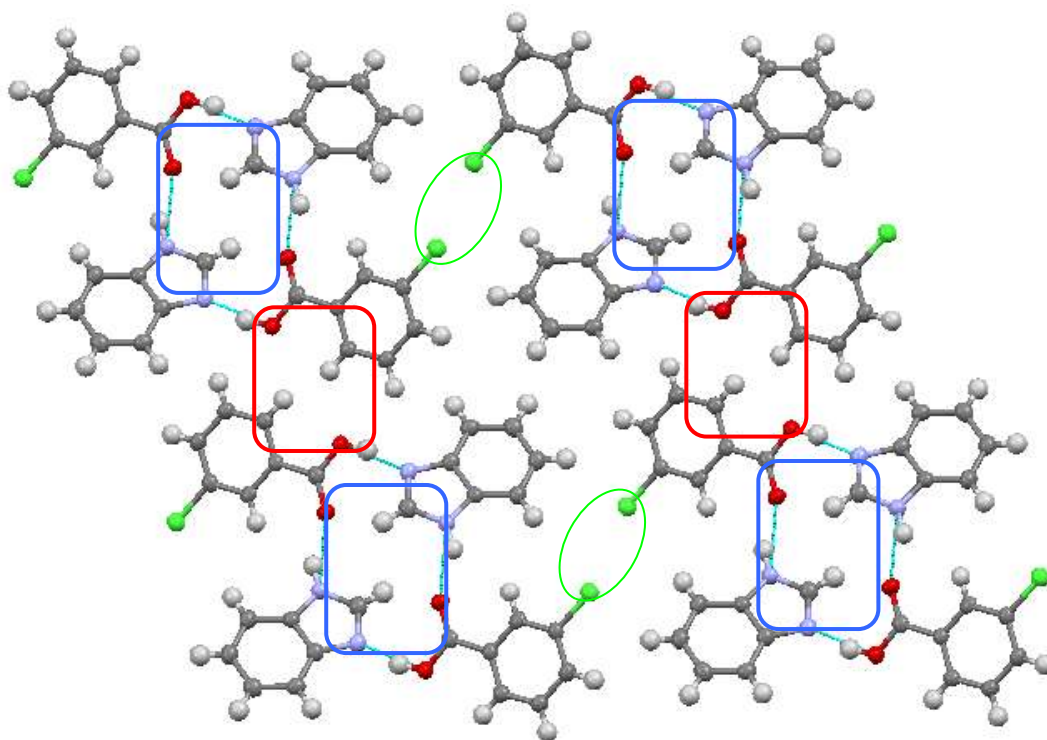


Fig. 5.31 – An extended view along the *a*-axis of the BZN 3-CIBA Form I molecular complex. The hydrogen bonded ring motif (blue circle), is expanded along the *b*-axis by weak C-H...O hydrogen bonds (red circle) and the *ab*-diagonal by chlorine-chlorine interactions.

5.4.1.1.2 Benzimidazole : 3-Chlorobenzoic Acid Molecular Complex 1:1 Form II

Form II of the benzimidazole (BZN) : 3-chlorobenzoic acid (3-CIBA) molecular complex contains the ionic species in a 1:1 ratio, where each benzimidazole has an average 0.5+ charge and each 3-chlorobenzoic acid an average 0.5– charge. The molecular complex was obtained using the solvent evaporation method, with a 1:1 stoichiometric mixture of benzimidazole (12mg) and 3-chlorobenzoic acid (16mg) dissolved in the minimum amount of methanol followed by evaporation at a constant temperature of between 2 and 4°C using a walk in fridge. This generated crystals that were blocky and colourless. Single crystal X-ray diffraction data were obtained using a Bruker ApexII diffractometer at 100K, equipped with graphite monochromated Mo K α radiation ($\lambda = 0.71073 \text{ \AA}$). The structure was solved using SUPERFLIP within the CRYSTALS program. The crystallographic data are summarised in Table 5.6.

Form II of the BZN : 3-CIBA molecular complex contains the ionic species of the co-molecules, rather than their neutral states found in Form I. The BZN molecule is partially

protonated through hydrogen transfer from the carboxylic acid group on the 3-CIBA molecule onto the normally unprotonated nitrogen atom in the five-membered ring forming a $\text{BZNH}^{0.5+}$ molecule (Figure 5.32). Therefore the 3-CIBA molecule retains a share of the proton forming a $3\text{-CIBA}^{0.5-}$ species. A centre of symmetry midway between two $\text{BZNH}^{0.5+}$ molecules means that the hydrogen atom in this group is disordered over two positions, and overall the two hydrogen-bonded benzimidazole molecules exhibit a total 1+ charge. Equally, the two $3\text{-CIBA}^{0.5-}$ molecules also have a proton positioned on a centre of symmetry and therefore the hydrogen atom in this hydrogen bond is disordered over two positions (Figure 5.33). The result of the proton transfer on the $\text{BZNH}^{0.5+}$ molecule is delocalisation of the partial charge across the five-membered ring which has the effect of creating a partial positive charge on both nitrogens (Table 5.4). The $3\text{-CIBA}^{0.5-}$ molecules also exhibit partial normalisation of the carbon oxygen bond lengths due to the partial deprotonation.

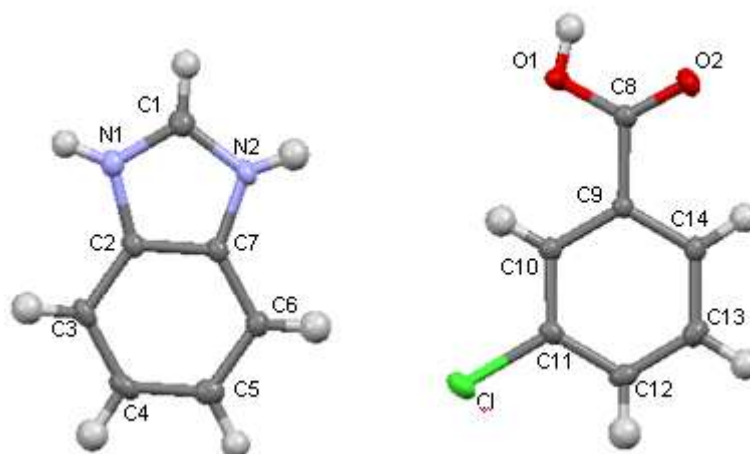


Fig. 5.32 – The co-molecules involved in the $\text{BZNH}^{0.5+} : 3\text{-CIBA}^{0.5-}$ molecular complex (BZN : 3-CIBA Form II) with atom labelling.

Interaction	Length (Å) (D...A(Å))	For Hydrogen Bonds		
		D-H(Å)	H...A(Å)	D-H...A angle(°)
O1...O1	2.494(1)	1.246(1)	1.246(1)	180(1)
N1...N1	2.676(1)	1.338(1)	1.338(1)	180(1)
N2...O1	2.830(1)	0.84(2)	2.00(2)	172(3)
C1...O2	3.074(1)	0.97(2)	2.17(2)	155(2)
C13...Cl1	3.354(1)	-	-	-
C12... π	3.724(1)	-	-	-

Table 5.9 – The interactions that are present within the BZN : 3-CIBA Form I molecular complex

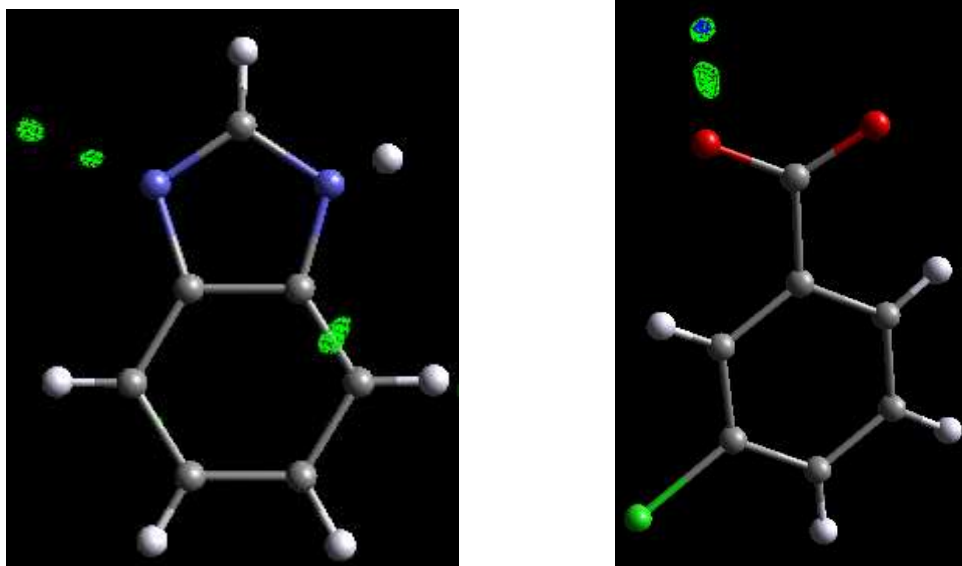


Fig. 5.33 – LHS, a MCE Fourier difference map generated where the H atoms located on the N atom have been omitted from the model, clearly showing that the proton is split over two sites; RHS, a MCE Fourier difference map generated where the H atoms located on the carboxylic acid group have been omitted from the model, again clearly showing that this proton is split over two sites.

The major difference between the polymorphs is the motifs they adopt. Form I adopts the 1:1 equimolar hydrogen bonded ring motif containing N-H \cdots O and O-H \cdots N hydrogen bonds, whereas the dominant Form II motif is a chain of alternate co-molecule dimers, linked together through N $^{\delta+}$ -H \cdots O $^{\delta-}$ hydrogen bonds (Figure 5.34).

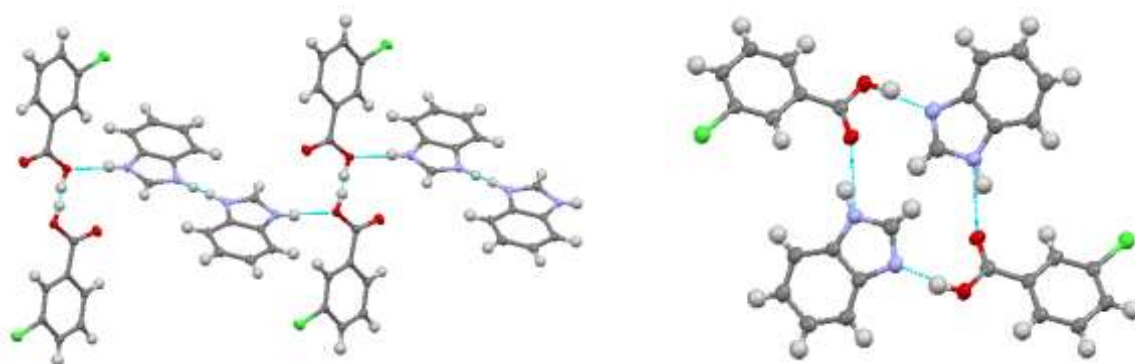


Fig. 5.34 – LHS, the supramolecular synthon of the BZN : 3-CIBA Form II molecular complex, co-molecule dimers, linked together through N $^{\delta+}$ -H \cdots O $^{\delta-}$ hydrogen bonds, RHS, the main motif of the BZN : 3-CIBA Form I molecular complex, an equimolar hydrogen bonded ring system held together by N-H \cdots O and O-H \cdots N hydrogen bonds.

The 3-CIBA $^{0.5-}$ dimer contains the strongest hydrogen bond within the structure, which has length O1 $^{\delta-}\cdots$ O1 $^{\delta-}$, 2.4944(3)Å. This is shorter than the distance found within the carboxylic

acid dimer of the 3-CIBA starting material (2.558(4)Å). The native BZN structure has N-H...N hydrogen bonds of length 2.8845(3)Å, in this case it is also shortened to 2.6757(3)Å. In both the BZNH^{0.5+} and 3-CIBA^{0.5-} the reason for the shortened hydrogen bond lengths is the presence of partially charged co-molecules, which creates a partially charge assisted hydrogen bond. The hydrogen bond that exists between the dimers, a N2^{δ+}-H...O1^{δ-} hydrogen bond, is on the long side at 2.8300(4)Å in comparison to other N^{δ+}-H...O^{δ-} interactions. Table 5.5 contains the full hydrogen bond details.

The molecular complex also contains a secondary supramolecular synthon that is an equimolar hydrogen bonded ring connecting two of the motifs together, that can be described by the graph set notation R_4^4 (14) (Figure 5.35). This supramolecular synthon uses two weak hetero-hydrogen bonds; one is the hydrogen bond that holds the dimers together, N2^{δ+}-H...O1^{δ-}(a), while the other uses the carbon most susceptible to hydrogen bonding and the other oxygen of the carboxylic acid group, C1-H...O2^{δ-} (b). This hydrogen bond has length 3.0740(3)Å and is the only interaction that oxygen O2 is involved in. The hydrogen bonded ring expands the structure along the *a*-axis, which can be seen in Figure 5.34 LHS, this has the effect of stacking the layers of the motif upon one another.

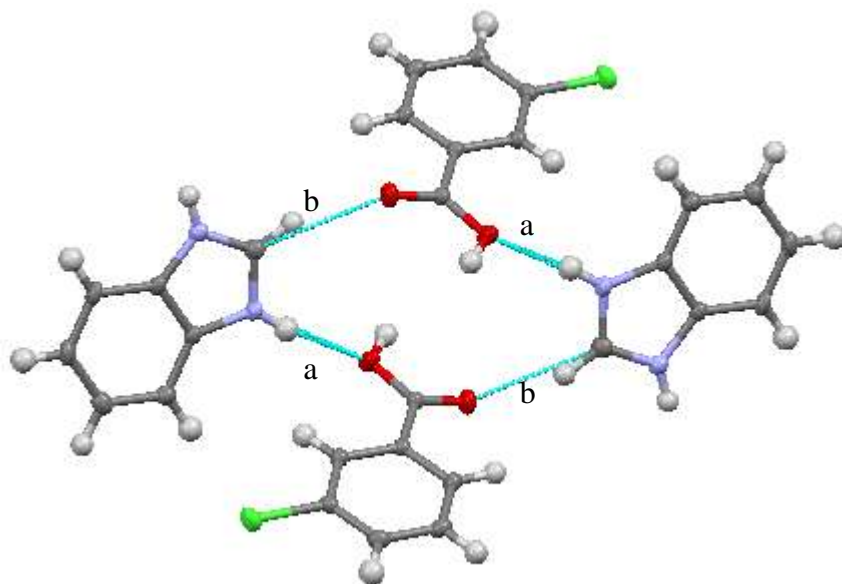


Fig. 5.35 – The secondary supramolecular synthon of the BZN : 3-CIBA Form II molecular complex that links the motifs together along the *a*-axis.

The *c*-axis is expanded through two weaker interactions that can be seen Figure 5.36. The most influential is a halogen bond between the chlorine and a carbon of another 3-CIBA^{0.5-} molecule (c). The C13-H...Cl halogen bond is of length 3.3536(3)Å which is of similar in

length to the chlorine–chlorine interaction found in Form I. The other lesser interaction is a C-H \cdots π bond between C12 of the 3-CIBA^{0.5-} molecule and the π -electrons of BZNH^{0.5+}. The length of this interaction is rather long at 3.7241(5)Å.

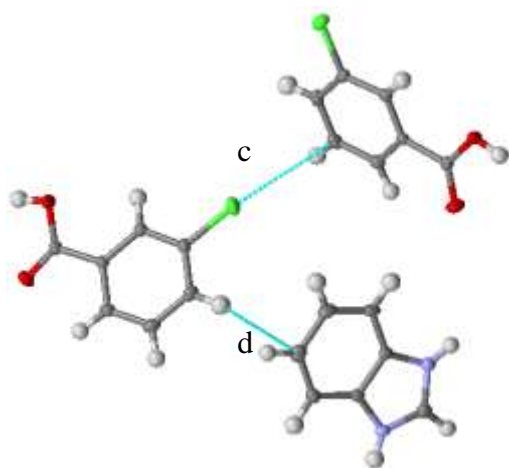


Fig. 5.36 – The lesser interactions c, halogen bond and d, C-H \cdots π interaction, that expand the structure along the *c*-axis.

The BZN : 3-CIBA Form II molecular complex has a motif that is a chain of alternate co-molecule dimers, linked together through N ^{$\delta+$} -H \cdots O ^{$\delta-$} hydrogen bond that expands the structure along the *b*-axis. The secondary supramolecular synthon, an equimolar hydrogen bonded ring of weak hydrogen bonds, expands the structure along the *a*-axis while the *c*-axis is expanded by a halogen bond and C-H \cdots π interaction (Figure 5.37). For comparison the main motif of the BZN 3-CIBA Form I molecular complex is hydrogen bonded rings which are stacked upon one another through weak carbon oxygen hydrogen bonds. These stacks of hydrogen bonded rings are expanded along the *b*-axis by another weak carbon oxygen hydrogen bond to create blocks which are expanding through chlorine–chlorine interactions (Figure 5.31).

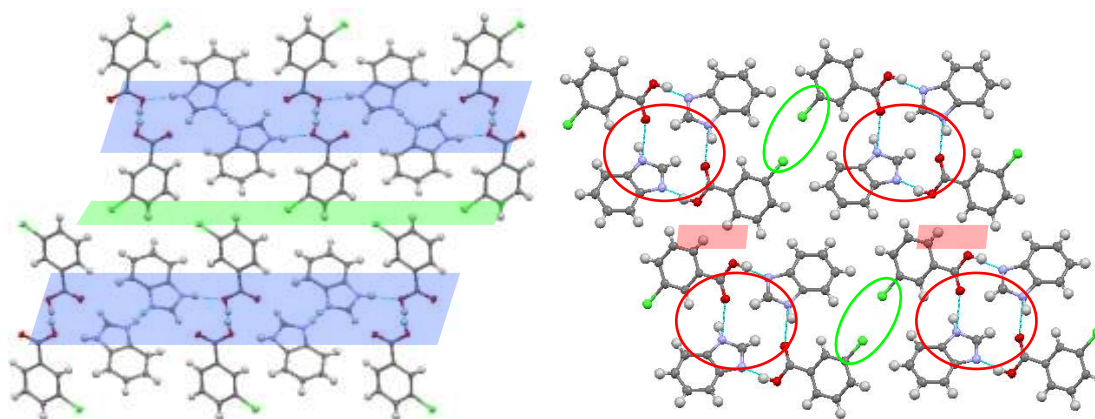


Fig. 5.37 – LHS, an extended view along the *a*-axis of the BZN : 3-CIBA Form II molecular complex. The motif, a chain of alternating co-molecule dimers (blue) is expanded along the *c*-axis via halogen bonds (green), RHS, an extended view along the *a*-axis of the BZN : 3-CIBA Form I molecular complex. The hydrogen bonded ring motif (red circle) is expanded along the *b*-axis by weak C-H...O hydrogen bonds (red box) and along the *ab*-diagonal by chlorine-chlorine interactions (green circle).

5.4.1.2 Molecular Complex of Benzimidazole and 4-Chlorobenzoic Acid 1:1.

The study into the benzimidazole and 4-chlorobenzoic acid system yielded two possible molecular complex polymorphs. The successful co-crystallisation experiments began by using the evaporation technique with just four different solvents at room temperature (Figure 5.38)

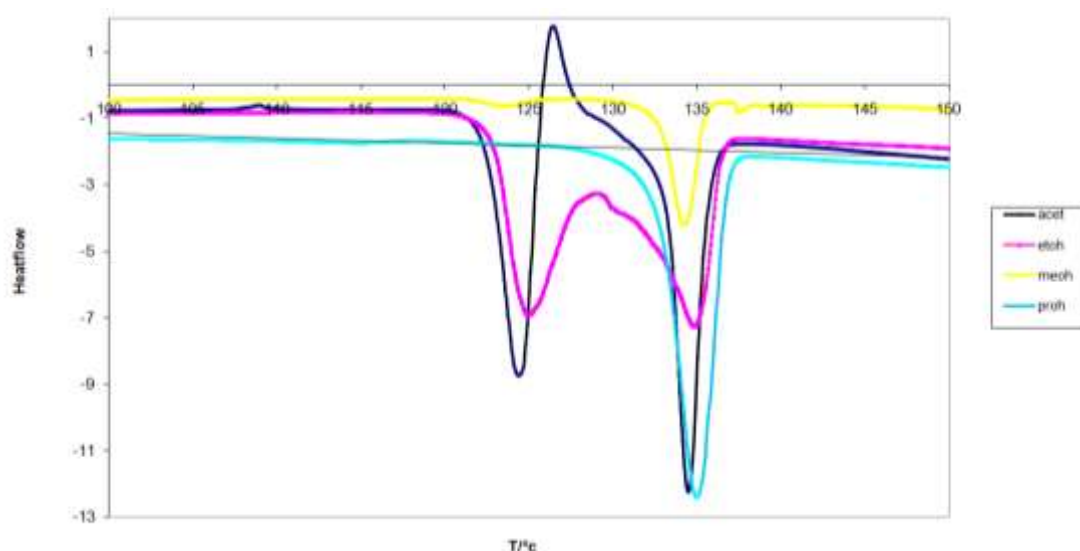


Fig. 5.38 – DSC thermogram of the products from benzimidazole and 4-chlorobenzoic acid co-crystallisations in acetone (-) ethanol (-), methanol (-) and propanol (-). It can clearly be seen that there are two distinct endothermic changes that relate to phase changes around 123°C and 132°C.

A more extensive study similar to that carried out for the benzimidazole and 3-chlorobenzoic acid system was undertaken with the aim to grow selectively each of the molecular complexes. A visual summary can be seen in Table 5.10.

	Methanol	Ethanol	Propanol	Acetone
Room T				
10°C				
20°C				
30°C				

Table 5.10 – The results from the co-crystallisation experiments between benzimidazole and 4-chlorobenzoic acid with Form I (high temperature phase) shaded in blue and Form II (low temperature phase) in red.

Powder X-ray diffraction studies of pure Form II resulted in an amorphous pattern, however experiments on what is thought to be a mixed phase, crystallised using acetone at room temperature, produced evidence for at least two forms (Figure 5.39).

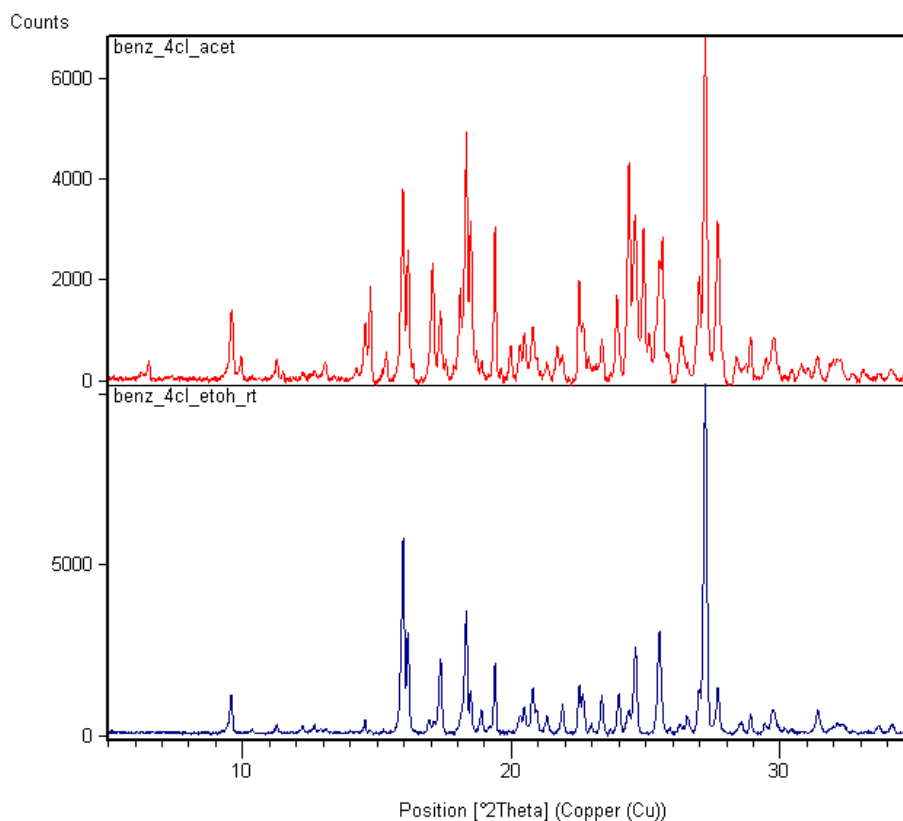


Fig. 5.39 - Powder patterns of the products of crystallisation from two different environmental conditions to promote growth of single component of Form I (blue) using ethanol at room temperature and a mixed phase of Forms I and II (red) using acetone also at room temperature.

From these findings, it should be possible to produce stable samples of Form II under the correct conditions. This is tentatively termed a polymorph here as there are many similarities with this molecular complex system and that of benzimidazole and 4-bromobenzoic acid where two polymorphic forms can be clearly identified.

The molecular ions, BZNH^+ and 4-ClBA^- form a 1:1 molecular complex with one another. The material was obtained using the solvent evaporation method, with a 1:1 stoichiometric mixture of benzimidazole (14mg) and 4-chlorobenzoic acid (16mg) in the minimum amount of acetone followed by evaporation at a constant temperature of $\sim 2\text{-}4^\circ\text{C}$ using a walk in fridge. The crystals generated were block shaped and colourless. Single crystal X-ray diffraction data were obtained using a Rigaku R-axis/RAPID diffractometer at 100K, equipped with graphite monochromated $\text{Mo K}\alpha$ radiation ($\lambda = 0.71073 \text{ \AA}$). The structure was solved using SIR92 within the CRYSTALS program. The crystallographic data are summarised in Table 5.6.

As described in Section in 5.2.1, a BZNH^+ molecule is generated through hydrogen transfer from the 4-ClBA (Figure 5.40). This has the effect of normalising the internal BZNH^+ carbon – nitrogen bond lengths (Table 5.4) and the carbon – oxygen bond lengths on the 4-ClBA^- (Table 5.11). There are two of each co-molecule within the asymmetric unit.

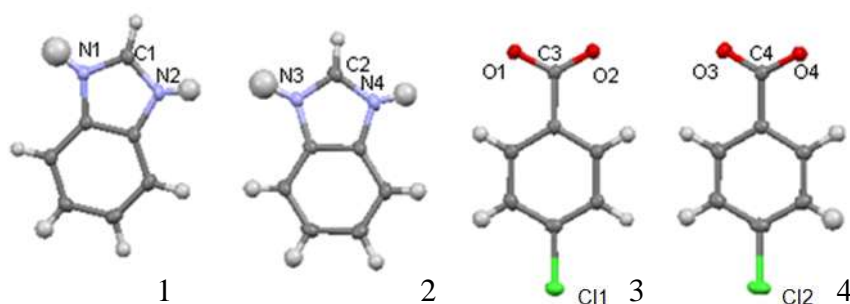


Fig. 5.40 - The molecular ions, two of each co-molecule BZNH^+ and 4-ClBA^- that make up this molecular complex, with atom labelling. The numbers, 1 to 4, designate their molecule number.

Molecule 3	
$\text{C3-O1}^{\delta-}$ (Å)	1.288(2)
$\text{C3-O1}^{\delta-}$ (Å)	1.250(2)
Molecule 4	
$\text{C3-O1}^{\delta-}$ (Å)	1.261(2)
$\text{C3-O1}^{\delta-}$ (Å)	1.271(2)

Table. 5.11 - The carbon – oxygen bond lengths within the two 4-ClBA^- molecules.

Interaction	Length (Å) (D...A(Å))	For Hydrogen Bonds		
		D-H(Å)	H...A(Å)	D-H...A angle(°)
N2...O1	2.900(2)	0.87(2)	2.15(2)	144(2)
N2...O2	2.832(2)	0.87(2)	2.27(3)	122(2)
N1...O3	2.642(2)	0.97(2)	1.67(2)	157(2)
N3...O4	2.682(2)	1.05(3)	1.80(2)	169(3)
N4...O2	2.606(2)	0.93(2)	1.56(3)	176(2)
Cl1... π	3.311	-	-	-
C...Cl2	3.412(1)	-	-	-

Table 5.12 – The inter- and intramolecular interactions found within the BZNH⁺ 4-ClBA⁻ molecular complex

The two 4-ClBA⁻ molecules have separate roles within the structure; one is involved in a hydrogen bonded ring, while the other acts to connect rings together. The same is seen with the BZNH⁺ molecules. The hydrogen bonded ring uses molecules 1 and 3, described by the graph set notation R_2^4 (8), that is made up of hydrogen bonds in the style of form B, through N2 ^{δ^+} -H...O1 ^{δ^-} and N2 ^{δ^+} -H...O2 ^{δ^-} hydrogen bonds. The nitrogen of the BZNH⁺ is involved in a double hydrogen bond of distance 2.900(2)Å and 2.832(2)Å (Table 5.12 for full interaction details) (Figure 5.41). This ring is one of the supramolecular synthons that make up the structure.

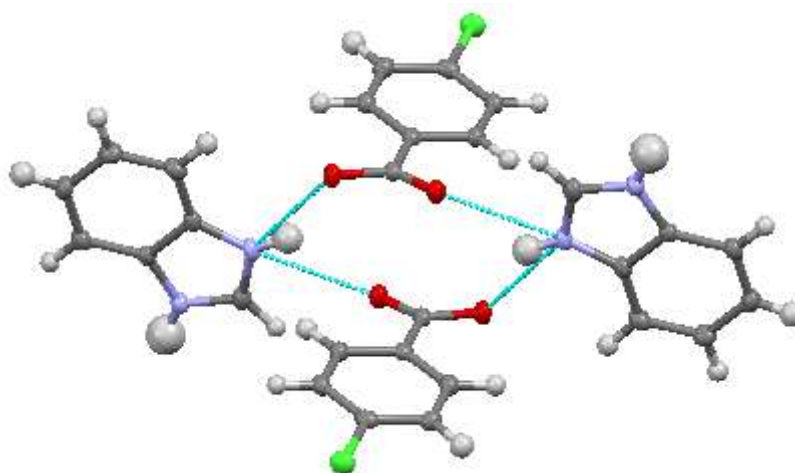


Fig. 5.41 – The supramolecular synthon, the hydrogen bonded rings, involves one of each co-molecule.

The hydrogen bonded rings are connected together by the other co-molecules, molecules 2 and 4. They achieve this by forming a greater ring network which is the main motif for this

molecular complex and described by the graph set notation symbol R_8^8 (32). Figure 5.42 shows the motif coloured in a way that the symmetry equivalent molecules are the same colour, thus the supramolecular synthon (small hydrogen bonded ring) is yellow and green while molecules 2 and 4 are red and blue respectively. Three moderate hydrogen bonds hold the two smaller rings together; a, $N^{\delta+}-H\cdots O^{\delta-}$ 2.642(2)Å, and b, $N^{\delta+}-H\cdots O^{\delta-}$ 2.682(2)Å and c $N^{\delta+}-H\cdots O^{\delta-}$, 2.606(2)Å (Table 5.5). It can be seen that the ring is not closed off to other hydrogen bonds, the $BZNH^+$ molecules involved in the supramolecular synthon (molecule 1) can further expand the structure to create the next motif (Figure 5.42 red circle).

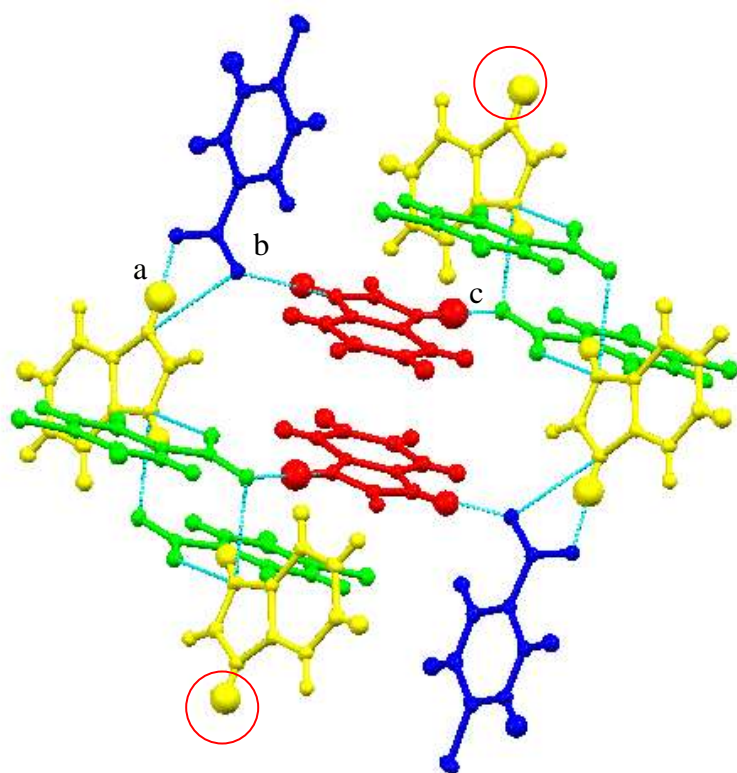


Fig. 5.42 – The motif of the $BZNH^+$ and $4-CIBA^-$ molecular complex with molecules coloured that are symmetry related, i.e. molecule 1 yellow, molecule 2 red, molecule 3 green and molecule 4 blue. Highlighted by a red circle is the $BZNH^+$ molecules that further expand the structure.

The only other significant interactions within the structure involve the chlorine atoms, the chlorine on molecule 4 is involved in a halogen– π interaction of length 3.311Å (measuring to a centroid position) with the other $4-CIBA^-$ molecule (Figure 5.43), while the chlorine on molecule 3 acts as the acceptor in a halogen bond with a C-H group on molecule 4 with length 3.415(2)Å.

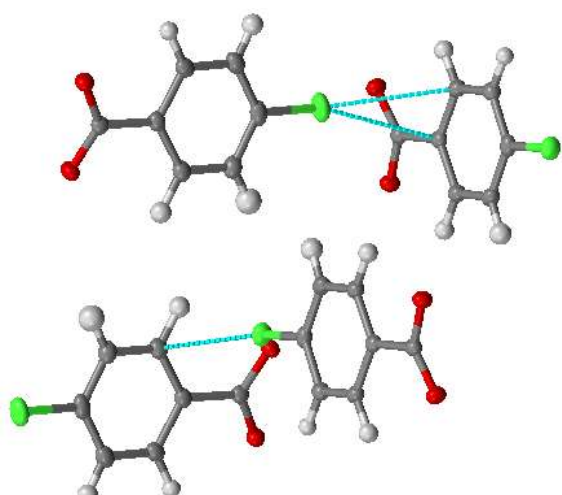


Fig. 5.43 – The halogen bond and halogen– π interactions that exist between the two 4-CIBA⁻ molecules.

The images in Figure 5.44 show the extended structure looking along the *b* and *c* axis. They both demonstrate that the motif, the extended ring network, expands the structure along the *b* and *c* directions while the halogen interactions connect the motifs together which therein expand the structure along the *c*-axis (green shaded area).

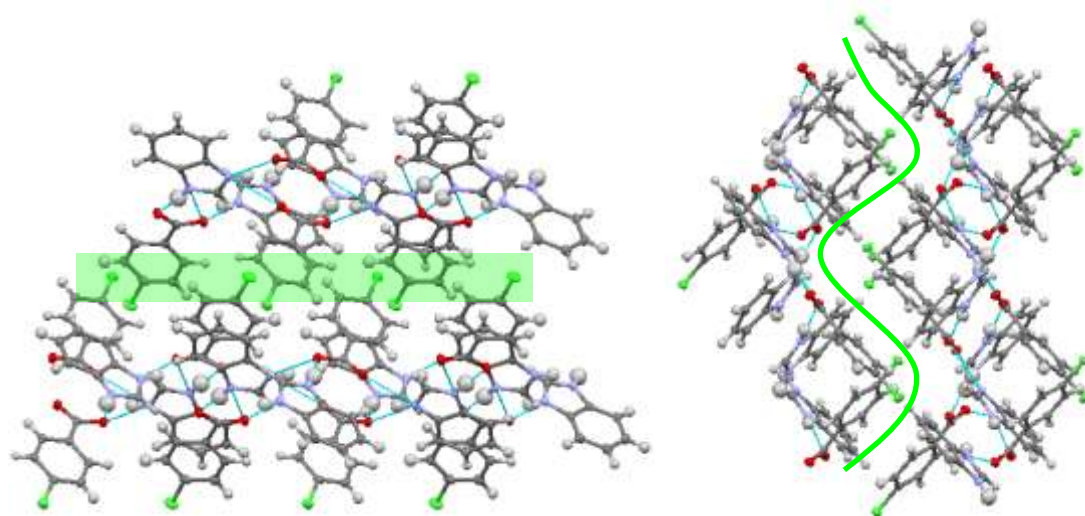


Fig. 5.44 – LHS, view along the *b*-axis of the BZNH⁺ : 4-CIBA⁻ molecular complex; RHS, view along the *c*-axis. Both images show the hydrogen bonded network that is held together by halogen interactions (green box and line).

5.4.1.3 Molecular Complex of Benzimidazole and 4-Bromobenzoic Acid 1:1

The benzimidazole : 4-bromobenzoic acid molecular complex does not just show similarities with the benzimidazole and 4-chlorobenzoic acid in terms of forming polymorphs, but their structures are also isomorphic.

Table 5.13 shows part of the range of crystallisation conditions used in trying to selectively grow each molecular complex polymorph. As can be seen from the DSC (Figure 5.45) and powder X-ray diffraction data (Figure 5.46), control of the different forms was relatively simple.

	Methanol	Ethanol	Propanol	Acetone
Room T				
20°C				
30°C				

Table 5.13 – The results from the co-crystallisation experiments between benzimidazole and 4-bromobenzoic acid with Form I (high temperature phase) shaded in blue and Form II (low temperature phase) in red.

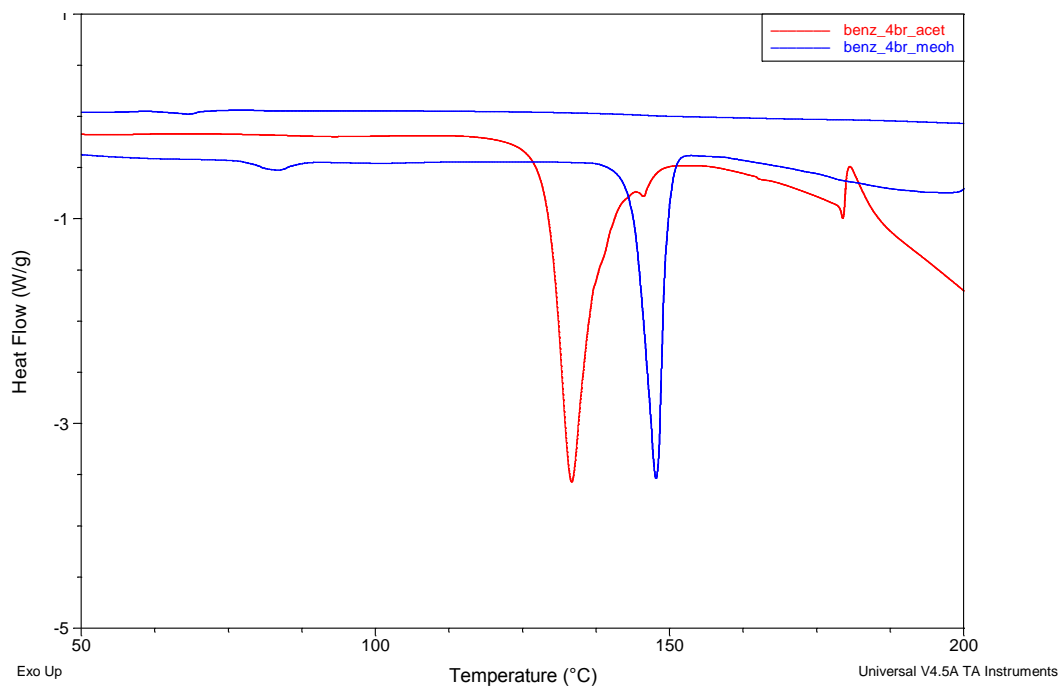


Fig. 5.45 – DSC thermogram of the products of benzimidazole and 4-bromobenzoic acid co-crystallisations in acetone (-) and methanol (-). It can clearly be seen that there are two distinct endothermic changes that relate to phase changes around 123°C and 142°C.

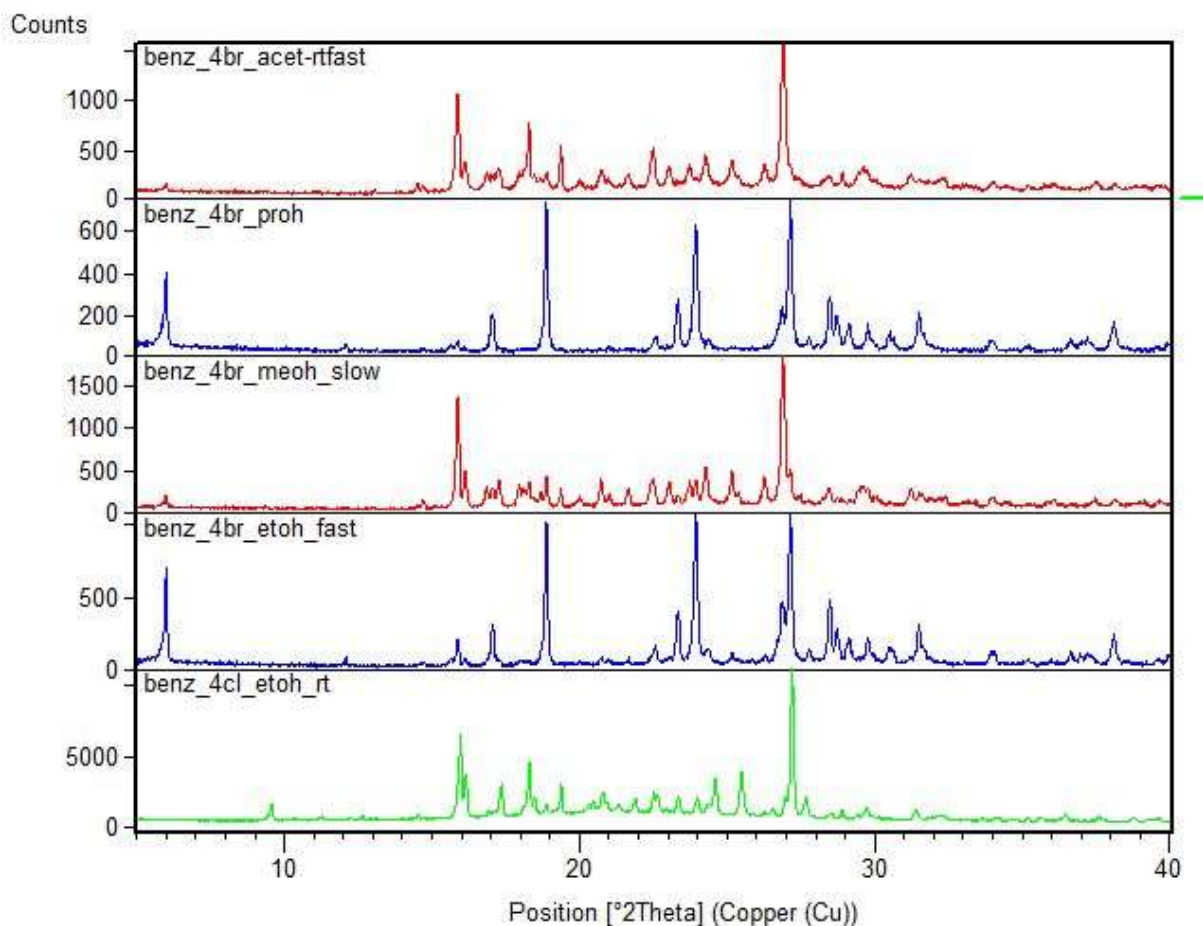


Fig. 5.46 - Powder patterns of the products of crystallisation from four different environmental conditions to promote growth of single component of Form I (blue) using propanol and ethanol and Form II (red) using acetone and methanol all at room temperature. The product pattern from the benzimidazole and 4-chlorobenzoic acid cocrystallisations

As stated, the molecular complex $\text{BZNH}^+ : 4\text{-ClBA}^-$ is an isostructure of the $\text{BZNH}^+ : 4\text{-BrBA}^-$ molecular complex. Therefore the report on this structure will give a brief description – refer to $\text{BZNH}^+ : 4\text{-ClBA}^-$ for full details. BZNH^+ and 4-BrBA^- form a 1:1 molecular complex with one another. The material was obtained using the solvent evaporation method, with a 1:1 stoichiometric mixture of benzimidazole (12mg) and 4-bromobenzoic acid (18mg) in the minimum amount of ethanol followed by evaporation at room temperature. The crystals generated were block shaped and colourless. Single crystal X-ray diffraction data were obtained using a Bruker Nonius Kappa diffractometer at 100K, equipped with graphite monochromated Mo $K\alpha$ radiation ($\lambda = 0.71073 \text{ \AA}$). The structure was solved using SIR92 within the CRYSTALS program. The crystallographic data are summarised in Table 5.6.

As described in Section 5.2.1 a BZNH^+ molecule is generated through hydrogen transfer from the 4-BrBA. This has the effect of normalising the internal BZNH^+ carbon – nitrogen bond lengths (Table 5.4) and the carbon – oxygen bond lengths.

As in the $\text{BZNH}^+ : 4\text{-ClBA}^-$ molecular complex the motif is an extended hydrogen bonded ring described by the graph set notation symbol R_8^8 (32). The motif is made up of two smaller equimolar hydrogen bonded rings (R_2^4 (8)) involving one pair of co-molecules. The other co-molecules join these rings together. All the interactions between the co-molecules are through moderate $\text{N}^{\delta+}\text{-H}\cdots\text{O}^{\delta-}$ hydrogen bonds. There are five unique $\text{N}^{\delta+}\text{-H}\cdots\text{O}^{\delta-}$ hydrogen bonds in the molecular complex and their scalar quantities are in Table 5.5. The motifs hydrogen bond run along the b - and c -axis while halogen bonds extend the structure along the a -axis (Figure 5.47).

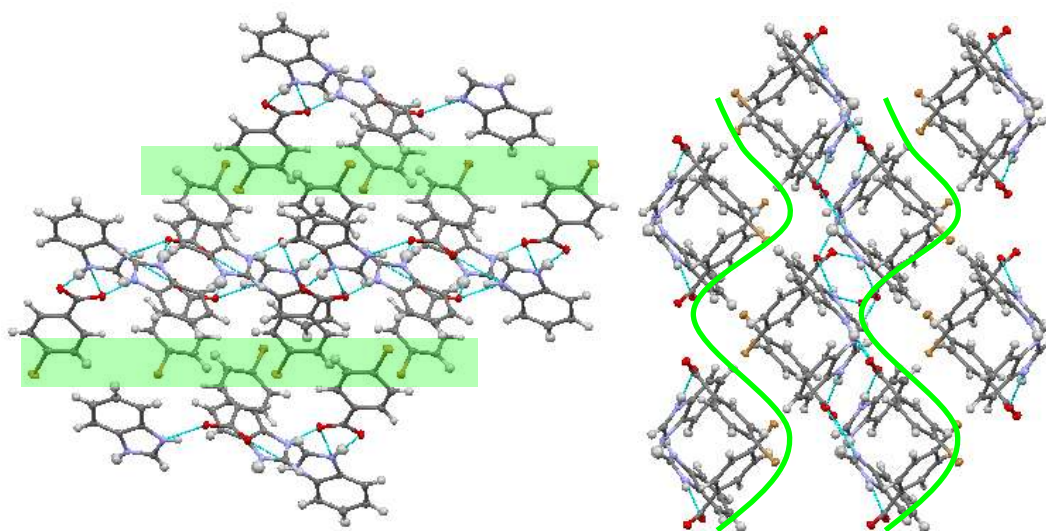


Fig. 5.47 – LHS, View along the b -axis of the $\text{BZNH}^+ : 4\text{-BrBA}^-$ molecular complex; RHS, view along the c -axis. Both images show the hydrogen bonded network that is held together by halogen interactions (green box and line).

5.4.2 Isomorphism

“Two crystals are said to be isomorphic if they have the same structure, but not necessarily the same cell dimensions nor the same chemical composition, and with a 'comparable' variability in the atomic coordinates to that of the cell dimensions and chemical

*composition*²⁹. Analysis of the molecular complexes generated between benzimidazole the halobenzoic acid series resulted in the serendipitous discovery of two series of isostructures as discussed in Section 5.2 (Table 5.3)

Benzimidazole	Ortho	Meta	Para
Fluorobenzoic Acid			
Chlorobenzoic Acid			
Bromobenzoic Acid			
Iodobenzoic Acid			

Table 5.3 –A summary of the molecular complexes – those that have generated isomorphous structures are coloured (blue and yellow) with grey indicating no isomorphism.

The benzimidazolium : 4-chlorobenzoate and benzimidazolium : 4 bromobenzoate molecular complexes also produced polymorphism and thus were discussed in Sections 5.4.2 and 5.4.3, respectively. The benzimidazole : 3-chlorobenzoic acid Form II (section 5.4.1.3) is the isomorphous partner of the benzimidazole : 3-bromobenzoic acid molecular complex.

5.4.2.1 Molecular Complex of Benzimidazole and 3-Bromobenzoic Acid 1:1

Co-crystallisation experiments between benzimidazole and 3-bromobenzoic acid produced a new molecular complex which has been identified by powder X-ray diffraction (Figure 5.48) and its structure determined by single crystal X-ray diffraction. DSC analysis was less conclusive in this case as it produced a thermogram similar to that from the product of the benzimidazole 3-chlorobenzoic acid co-crystallisation experiments (Appendix A) which produced three polymorphs. Although molecular complex polymorphism was found in the isostructural polymorphs of benzimidazolium : 4-chlorobenzoate and benzimidazolium : 4-bromobenzoate, the range of crystallisation conditions used have to date only produced a single form of benzimidazole : 3-bromobenzoic acid.

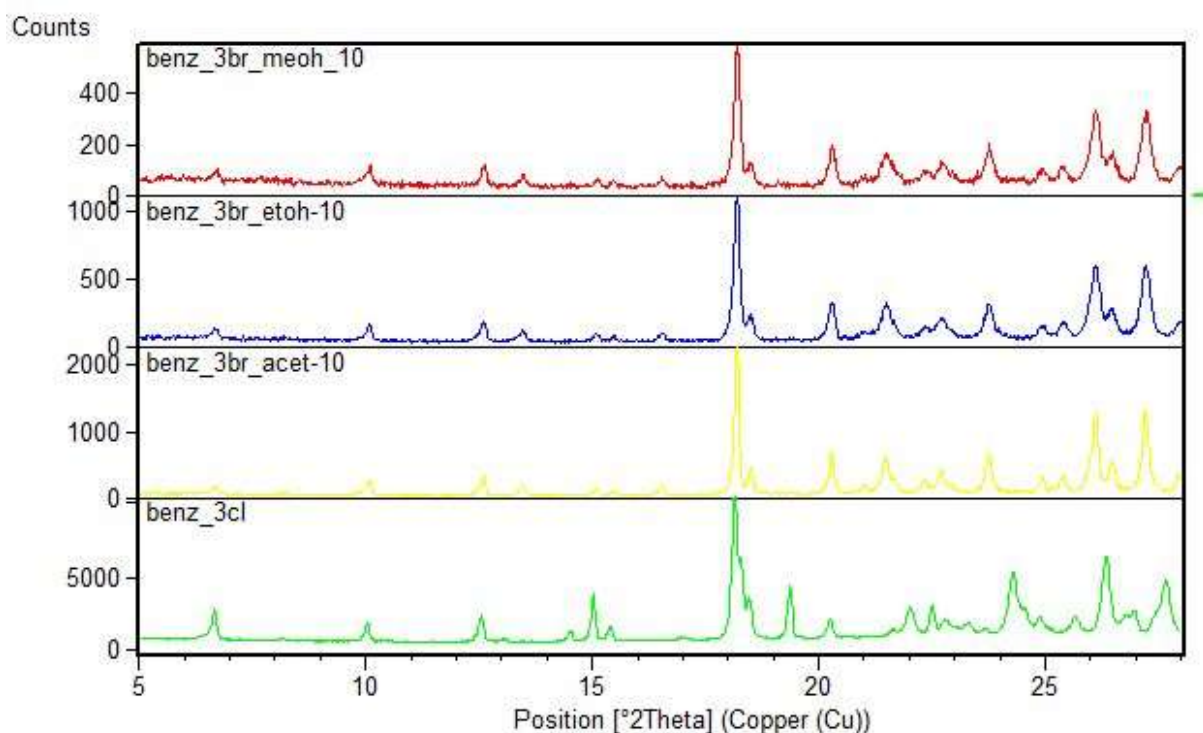


Fig. 5.48 – Powder patterns of the products of crystallisation from three different environmental conditions to promote the growth the benzimidazole : 3-bromobenzoic acid molecular complex using methanol at 10°C (red) ethanol at 10°C (blue) and acetone at 10°C (yellow). The powder pattern of Form II benzimidazole 3-chlorobenzoic acid, the corresponding isomorphous structure

The molecular complex contains, on average, the partial ionic species of benzimidazole (BZN) and 3-chlorobenzoic acid (3-CIBA) in a 1:1 ratio, where each benzimidazole has an average 0.5+ charge and each 3-chlorobenzoic acid an average 0.5– charge. This is a consequence of the presence of two of each type of molecule in the asymmetric unit where the H atom is disordered over two positions. The result of the proton transfer on the BZNH^+ molecule is delocalisation of the partial charge across the five-membered ring which has the effect of creating a partial positive charge on both the nitrogens (table 5.4). The 3-BrBA^- molecules also observe partial normalisation of the carbon oxygen bond lengths due to the partial deprotonation.

Block shaped colourless crystals were obtained using the solvent evaporation method, with a 1:1 stoichiometric mixture of benzimidazole (12mg) and 3-bromobenzoic acid (18mg) in the minimum amount of ethanol followed by evaporation at $\sim 2\text{--}4^\circ\text{C}$. Single crystal X-ray diffraction data were obtained using a Bruker Kappa diffractometer at 200K, equipped with graphite monochromated Mo $K\alpha$ radiation ($\lambda = 0.71073 \text{ \AA}$). The structure was solved using

SIR92 within the CRYSTALS program. The crystallographic data are summarised in Table 5.6.

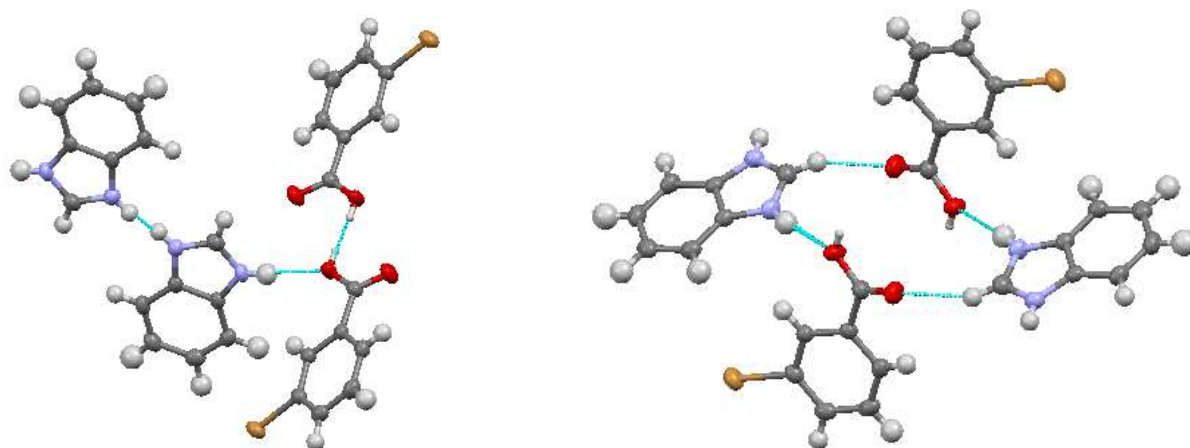


Fig. 5.49 – LHS, the supramolecular synthon of the $\text{BZNH}^+ : 3\text{-BrBA}^-$ molecular complex, dimers of each co-molecule are connected through a $\text{N}^{\delta+}\text{-H}\cdots\text{O}^{\delta-}$ moderate hydrogen bond, RHS, the secondary supramolecular synthon of that links the motifs together along the a -axis.

The primary supramolecular synthons, dimers of the co-molecules held together through a $\text{N}^{\delta+}\text{-H}\cdots\text{O}^{\delta-}$ moderate hydrogen bond (see Table 5.5 for hydrogen bond details) (Figure 49 LHS), connect along the b -axis to create a chain; this is the motif of the structure. These chains are held together through the secondary supramolecular synthon which is an equimolar hydrogen bonded ring made up of a weak $\text{C-H}\cdots\text{O}$ and moderate $\text{N}^{\delta+}\text{-H}\cdots\text{O}^{\delta-}$ hydrogen bond which expands the structure along the a -axis (Figure 5.49 RHS). The c -axis is expanded through lesser halogen and $\text{C-H}\cdots\pi$ bonds (Figure 5.50).

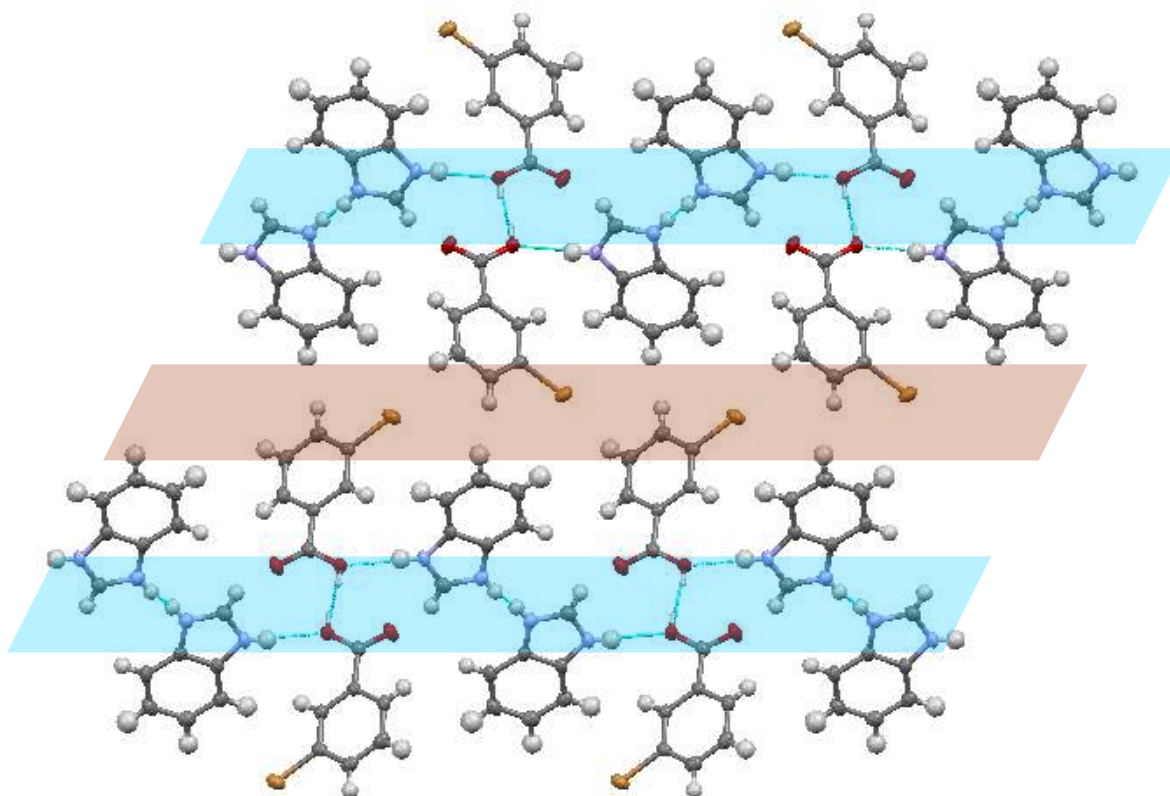


Fig. 5.50 – View along the a -axis of the extended structure of the $\text{BZNH}^+ : 3\text{-BrBA}^-$ molecular complex, the motifs (blue box) are held together through weak halogen and $\text{C-H}\cdots\pi$ interactions (brown box).

5.4.3 Benzimidazole and Fluorobenzoic Acid Structures

The co-crystallisations between benzimidazole and halobenzoic acids also produced two new molecular complexes involving fluorobenzoic acid.

5.4.3.1 Molecular Complex of Benzimidazole and 2-Fluorobenzoic Acid 1:2

A 1:1 stoichiometric mixture of BZN (12mg) and 2-fluorobenzoic acid (2-FBA) (14mg) dissolved in the minimum amount of methanol followed by evaporation at room temperature to generate an oil, which then was transferred to a walk in fridge, $\sim 2\text{-}4^\circ\text{C}$, to form a new molecular complex. The molecular complex consists of the molecular ions BZNH^+ and 2-fluorobenzoate (2-FBA^-) and the neutral molecule 2-fluorobenzoic acid that forms a 1:1:1 molecular complex with crystals that are block shaped and colourless (Figure 5.51). Single crystal X-ray diffraction data were obtained using a Bruker Apex II diffractometer at 100K, equipped with graphite monochromated $\text{Mo K}\alpha$ radiation ($\lambda = 0.71073 \text{ \AA}$). The structure was

solved using SIR92 within the WINGX program. The crystallographic data are summarised in Table 5.6. In this molecular complex as in others, hydrogen transfer from the carboxylic acid group on the 2-FBA molecule onto the normally unprotonated nitrogen atom in the five-membered ring forms BZNH^+ molecules (see Section 5.2.1). The result is a delocalisation of the charge across the five-membered ring as reflected in the internal bond lengths and angle (Table 5.4).

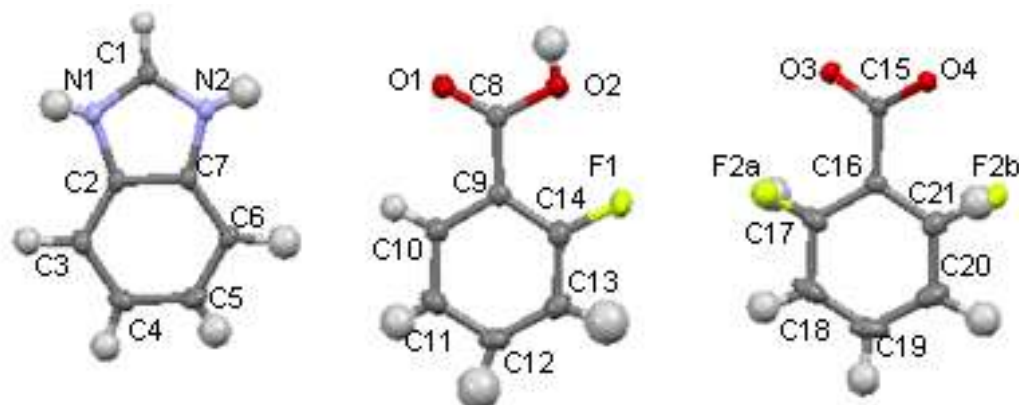


Fig. 5.51 – The BZNH^+ , 2-FBA and 2-FBA⁻ molecules, from left to right, that make up the $\text{BZNH}^+ : 2\text{-FBA}^- : 2\text{-FBA}$ molecular complex, with atom labelling.

Interaction	Length (Å) (D...A(Å))	For Hydrogen Bonds			C-O(Å)	2-FBA	2-FBA ⁻
		D-H(Å)	H...A(Å)	D-H...A angle(°)			
N1...O3	2.696(1)	0.90(4)	1.79(5)	171(5)	C-O(Å)	1.317(1)	1.255(1)
N2...O3	2.723(1)	0.91(4)	1.85(5)	162(5)		1.209(1)	1.264(1)
O2...O4	2.576(1)	0.85(5)	1.76(5)	156(4)			
C13...F1	3.347(1)	-	-	-	Twisting (°)	0.64	36.63
C1...O4	3.019(1)	0.93(3)	2.44(4)	120(3)			

Table 5.14 – LHS, The interactions that are involved in the molecular complex of BZN and 2-FBA, RHS, bond lengths and degree of twisting of the carboxylate group data for the 2-FBA and 2-FBA⁻ molecules.

The 2-FBA molecule retains the proton on the carboxylic acid group and thus there is no normalisation of bond lengths (Table 5.14). On the other hand the ionic species, 2-FBA⁻, has been deprotonated and the consequential bond normalisation has occurred. The 2-FBA⁻ ion is also disordered over two sites with the best model having occupancy levels of F2a:F2b, 0.75:0.25.

There are three primary hydrogen bonds within the $\text{BZNH}^+ : 2\text{-FBA} : 2\text{-FBA}^-$ molecular complex, two of form B and one of form A (Figure 5.52). The form B hydrogen bonds, $\text{N1}^{\delta+}\text{-H}\cdots\text{O3}^{\delta-}$ and $\text{N2}^{\delta+}\text{-H}\cdots\text{O3}^{\delta-}$, are moderate in strength with lengths $2.6955(2)\text{\AA}$ and $2.7226(1)\text{\AA}$ respectively (Table 5.5). The form A hydrogen bond between the 2-FBA and 2-FBA^- molecules is slightly shorter at $2.5764(1)\text{\AA}$.

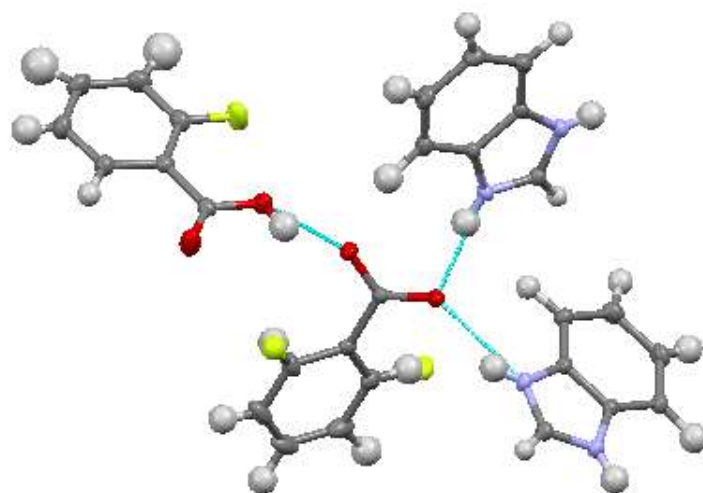


Fig. 5.52 – The primary hydrogen bonds within the $\text{BZNH}^+ : 2\text{-FBA} : 2\text{-FBA}^-$ molecular complex.

The form B hydrogen bonds between the molecular ions arrange their molecules into a zigzag chain along the b -axis, this is the motif of the structure (Figure 5.53).

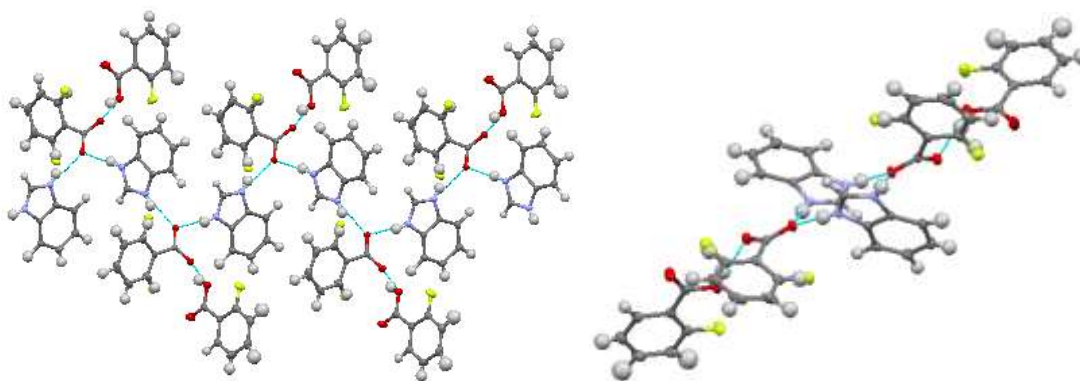


Fig. 5.53 – The motif of the $\text{BZNH}^+ : 2\text{-FBA} : 2\text{-FBA}^-$ molecular complex, zigzag chains between the BZNH^+ and 2-FBA^- co-molecules using the $\text{N-H}\cdots\text{O}$ form B hydrogen bond. LHS, view along the a -axis; RHS, view of the b -axis.

Connecting motifs together is achieved through weaker interactions, one of which is a $\text{C-H}\cdots\text{F}$ halogen bond that expands the structure along the ac -diagonal axis (Figure 5.54). This halogen bond is between two 2-FBA molecules, $\text{C13-H}\cdots\text{F1}$, and is $3.3466(2)\text{\AA}$ long.

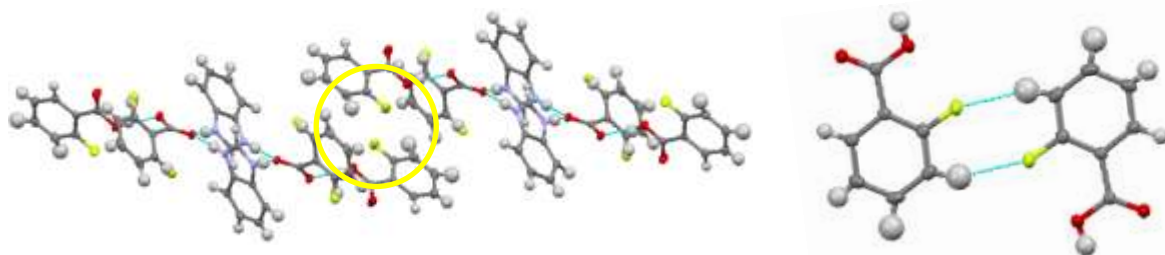


Fig. 5.54 – LHS, two motifs of the $\text{BZNH}^+ : 2\text{-FBA} : 2\text{-FBA}^-$ molecular complex held together along the *ac*-diagonal axis by halogen bonds (yellow circle); RHS, view of the halogen bonds, $\text{C-H}\cdots\text{F}$.

Expanding the structure along the *bc*-diagonal axis is a $\text{C-H}\cdots\text{O}$ weak hydrogen bond (Figure 5.55). The $\text{C1-H}\cdots\text{O4}$ interaction has length $3.0189(2)\text{\AA}$. There are other lesser interactions within the structure, however those are not significant and only assist in the interactions that have already been mentioned.

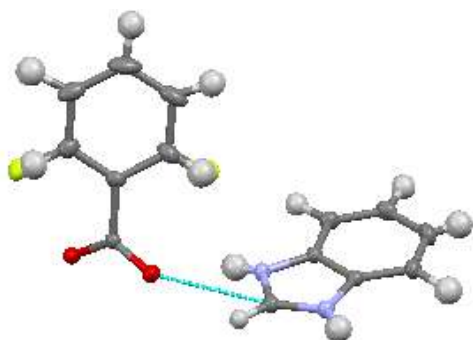


Fig. 5.55 – The $\text{C-H}\cdots\text{O}$ hydrogen bond that expands the structure along the *bc*-diagonal axis.

5.4.3.2 Benzimidazole and 3-Fluorobenzoic Acid

The co-crystallisation experiments between benzimidazole and 3-fluorobenzoic acid produced a powder which has been analysed using both DSC and powder X-ray diffraction (Figure 5.56). These patterns indicate that a new material has been formed with a melting point of 71°C , much lower than that for both 3-fluorobenzoic acid ($121\text{-}125^\circ\text{C}$) and benzimidazole ($170\text{-}172^\circ\text{C}$). A wide range of crystallisation environments were tried to promote crystal growth, unfortunately no crystals suitable for single crystal X-ray diffraction studies were generated. The X-ray powder pattern and main DSC thermogram of the molecular complex was generated using the solvent drop method with methanol as the solvent.

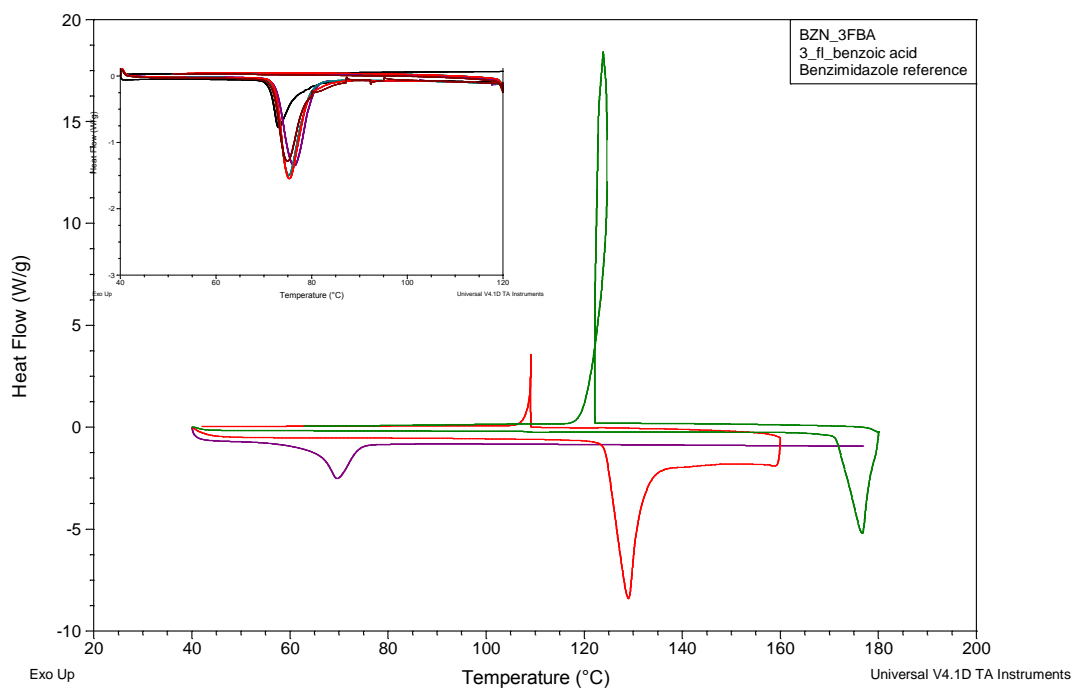
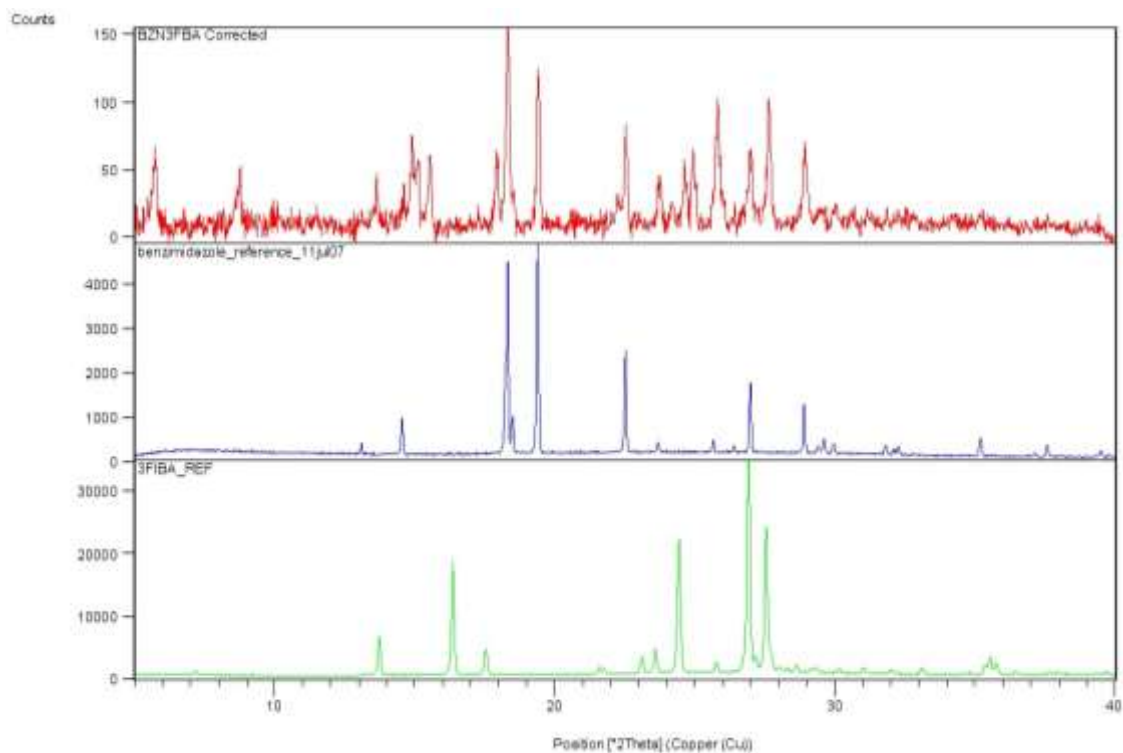


Fig 5.56 – top, X-ray powder diffraction patterns of benzimidazole : 3-fluorobenzoic acid (red), 3-fluorobenzoic acid (blue) and benzimidazole (green) clearly indicating a new product has been produced, bottom, DSC thermogram of the same materials; benzimidazole : 3-fluorobenzoic acid (purple), 3-fluorobenzoic acid (red) and benzimidazole (green) again indicating a new product is formed, insert, patterns of other co-crystallisations experiments.

5.4.3.3 Molecular Complex of Benzimidazole and 4-Fluorobenzoic Acid 1:1

The molecular complex between BZN and 4-fluorobenzoic acid (4-FBA) contains one of each co-molecule and one of each of their ionic forms in a 1:1:1:1 ratio. The molecular complex was obtained using the solvent evaporation method, with a 1:1 stoichiometric mixture of BZN (12mg) and 4-BA (12mg) dissolved in the minimum amount of acetone followed by evaporation at a constant temperature of between 2 and 4°C using a walk in fridge. The crystals generated were plate shaped and colourless. Single crystal X-ray diffraction data were obtained using a Bruker Apex II diffractometer at 100K, equipped with graphite monochromated Mo K α radiation ($\lambda = 0.71073 \text{ \AA}$). The structure was solved using SIR92 within the CRYSTALS program. The crystallographic data are summarised in Table 5.6 with the interactions involved in the molecular complex listed in Table 5.15.

This is the other example of a molecular complex which contains a BZN and a carboxylic acid containing molecule in a 1:1 ratio where proton transfer has not occurred. In this structure proton transfer occurs between one set of co-molecules but not the other (Figure 5.57). The result is that one BZN molecule has been protonated forming a BZNH⁺ molecule and one of the 4-FBA molecule-has been deprotonated forming a 4-FBA⁻ molecule. The consequence of the proton transfer on the molecular ions is discussed in Section 5.2.1, while one pair of BZN and 4-FBA molecules remain in their neutral state.

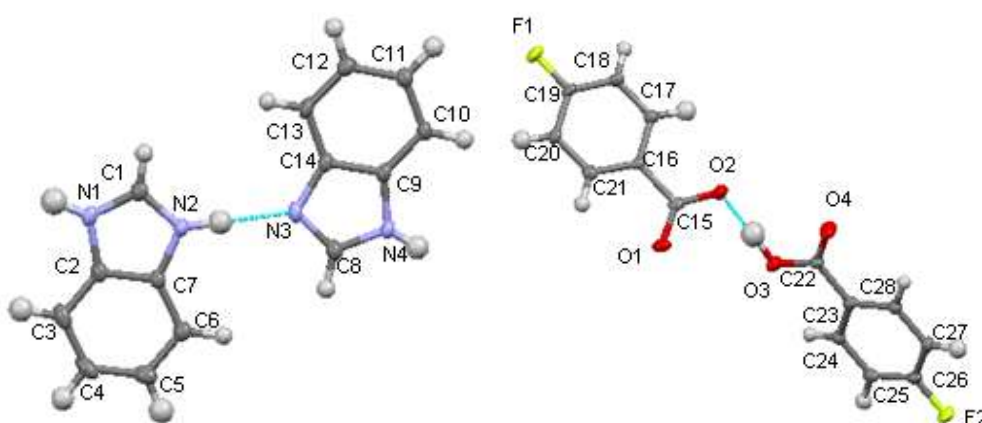


Fig. 5.57 – LHS, the BZNH⁺ and BZN dimers with atom labelling; RHS, the 4-FBA⁻ and 4-FBA dimers with associated labelling.

Interaction	Length (Å) (D...A(Å))	For Hydrogen Bonds		
		D-H(Å)	H...A(Å)	D-H...A angle(°)
N2...N3	2.750(3)	0.750(2)	1.81(2)	179(2)
O3...O2	2.528(3)	1.03(3)	1.50(3)	1.77(3)
F2...C4	3.191(3)	-	-	-
F1...C11	3.297(3)	-	-	-
C1...O1	3.287(2)	0.95(2)	2.55(2)	135(2)
C12... π	3.499	-	-	-

Table 5.15 – The interactions found in the BZN and 4-FBA molecular complex.

As can be seen in Figure 5.54, each neutral molecule and its ionic counterpart interact with one another using hydrogen bond forms A and B. These hydrogen bonds are two of the four primary hydrogen bonds in the molecular complex with length, N-H...N, 2.750(3)Å and ,O-H...O, 2.528(3)Å (see Table 5.15 for full hydrogen bond details). These hydrogen bonds have the effect of creating dimers of each co-molecule, which in turn are held together by the other primary hydrogen bond, form C, creating the supramolecular synthon. The two N-H...O hydrogen bonds differ slightly in their acceptor atom strengths, with one involving deprotonated carboxylate oxygen while the other involves the neutral carboxylic acid oxygen. This explains the differences in strengths, 2.687(2)Å and 2.800(2)Å. The supramolecular synthons combine to form a zigzag chain of co-molecules, the motif of this molecular complex (Figure 5.58).

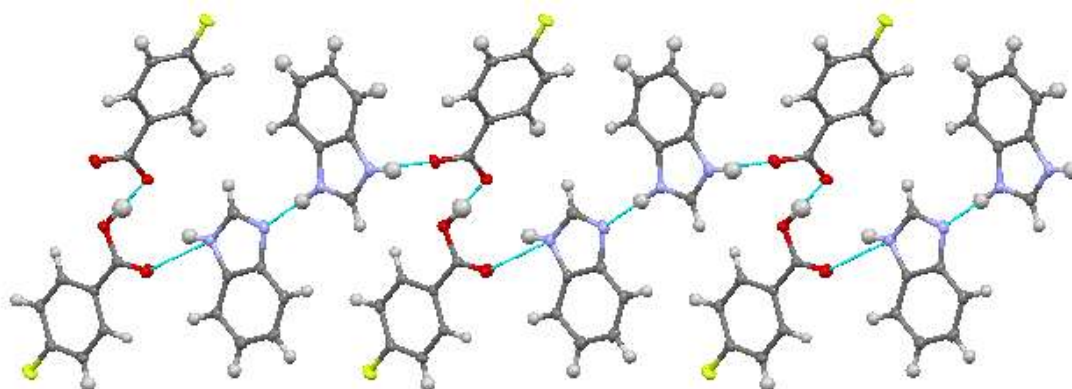


Fig. 5.58 – View along the *a*-axis of the BZN : 4-FBA molecular complex, showing the main motif, a zigzag chain of dimers held together by N^{δ+}-H...O^{δ-} hydrogen bonds that expand the structure along the *ab*-diagonal axis.

Connecting the chains along the *c*-axis are two halogen bonds of length *a*, 3.191(3)Å and *b*, 3.297(3)Å (Figure 5.59). These C-H...F halogen bonds are the only interactions that expand the structure along this direction.

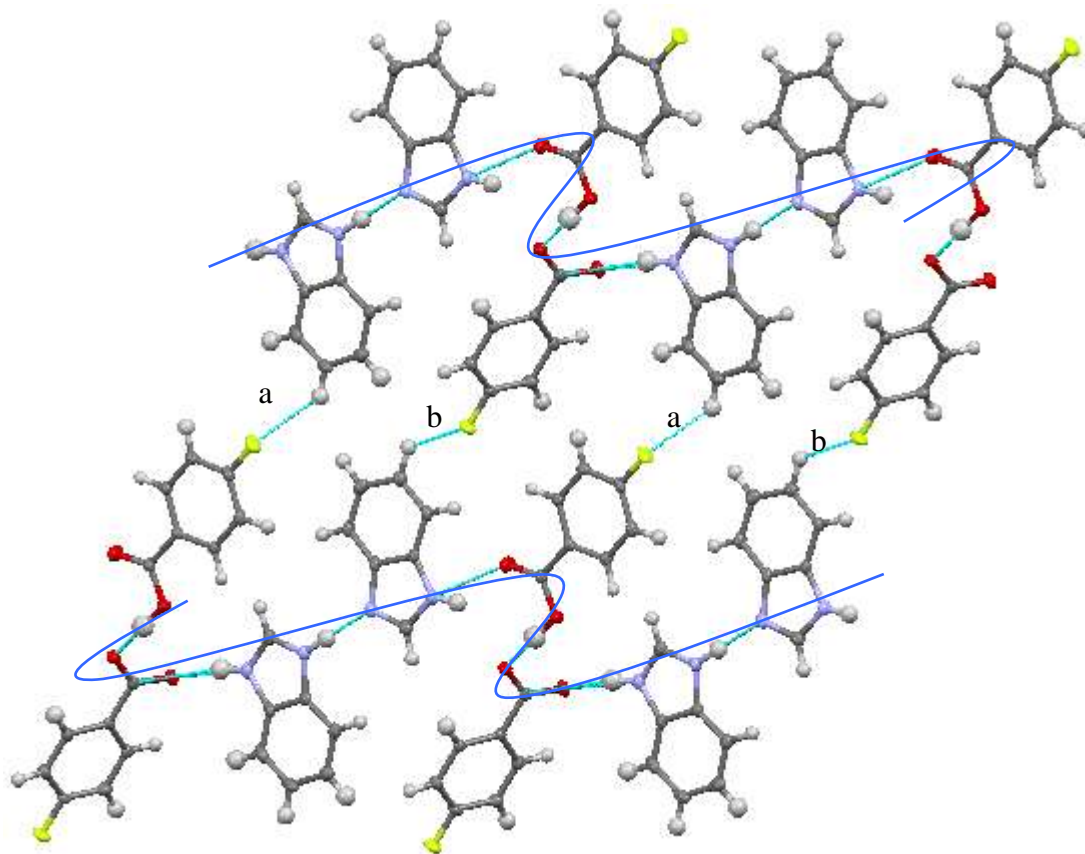


Fig. 5.59 – The *a*-axis of the BZN : 4-FBA molecular complex, showing the main motifs (blue line) held together along the *c*-axis by C-H...F halogen bonds (*a* and *b*).

The carbon located between the two protonated nitrogens of the BZNH⁺, C1, is involved in a weak hydrogen bond with the 4-FBA⁻ molecule (Figure 5.60). The C1-H...O1 hydrogen bond has length 3.287(2)Å and is helped to expand the structure along the *a*-axis by a C-H... π interaction of length 3.439Å (measured to a centroid between carbons, C19 and C20).

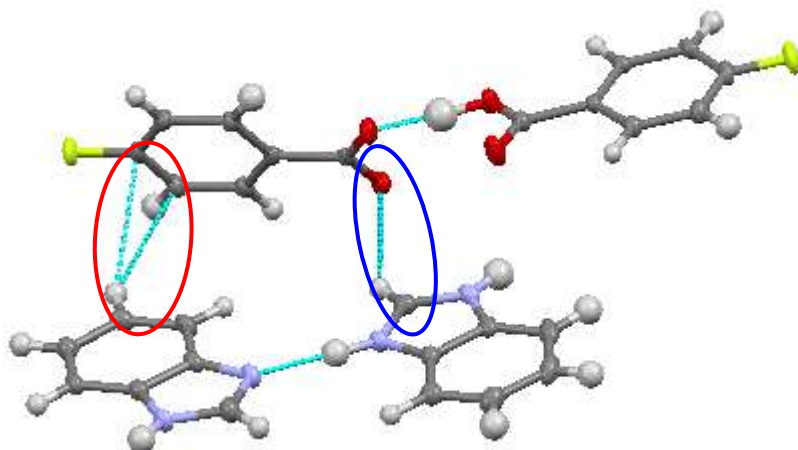
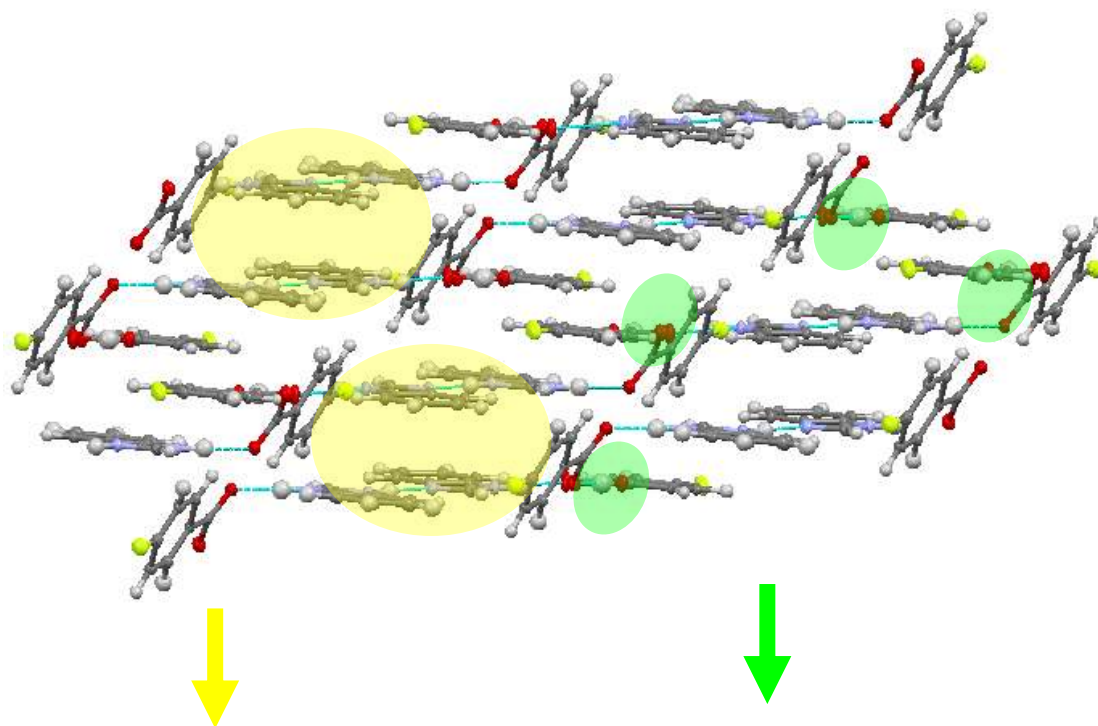


Fig. 5.60 – The *a*-axis is expanded by two interactions; a C-H...O weak hydrogen bond (blue circle) and a C-H... π interaction (red circle).

The structure is layered with the 4-FBA⁻ molecule the only molecule that does not lie along the *c*-axis and which promotes interactions between the layers. Figure 5.61 is an extended view along the *c*-axis which highlights two of the interactions between the layers, π ... π interactions (yellow circle) and C-H...O weak hydrogen bonds (green circle). The C-H...O weak hydrogen bonds, C-H...O2 and C-H...O3, have lengths 3.396(2)Å and 3.264(2)Å respectively, while the π ... π interactions are 3.360(4)Å in length.



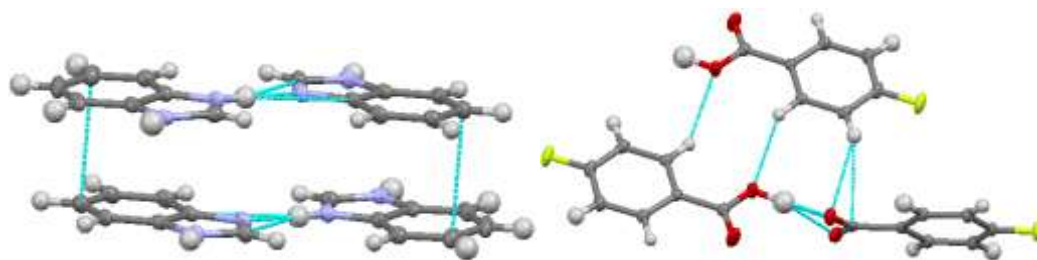


Fig. 5.61 –Top, view along the c-axis of the BZN: 4-FBA molecular complex which highlights the two types interactions that exist between the layers: a $\pi\cdots\pi$ stacking interaction between the BZN dimers (yellow circle) and the weak C-H \cdots O hydrogen bonds (green circle) between the 4-FBA molecules, bottom LHS, $\pi\cdots\pi$ stacking interactions, bottom RHS, C-H \cdots O weak hydrogen bonds.

5.5 Conclusions

The co-crystallisation experiments between benzimidazole and the halo-benzoic acid series resulted in the formation of seven previously undiscovered molecular complexes, benzimidazole with the following co-molecules: 2-fluorobenzoic acid, 4-fluorobenzoic acid, 3-chlorobenzoic acid, 4-chlorobenzoic acid, 3-bromobenzoic acid and 4-bromobenzoic acid. Co-crystallisation experiments between benzimidazole and 3-fluorobenzoic acid produced a new material identified through DSC and powder analysis, however structure determination was unfeasible. Two experiments produced oils, those between benzimidazole with 2-chlorobenzoic and 2-bromobenzoic acid while co-crystallisation experiments with the iodo range of halo-benzoic acids produced only starting materials.

The aim of the work was to investigate the occurrence of molecular complex polymorphism and to control selectively the form produced. The results show that polymorphism is common within molecular complexes, with three of the seven newly discovered systems showing evidence of this. Fortunately, controlled growth of a selective polymorph can be achieved through changes in crystallisation conditions, as shown for the three materials that showed polymorphism. Unfortunately, it only takes small changes in these conditions to promote other forms, for example co-crystallisations between benzimidazole and 3-bromobenzoic acid using acetone Form polymorph I at 30°C, but Form II at 20°C.

Whilst polymorphism can be unpredictable, the types of hydrogen bonds formed between the co-molecules are much less so. The three primary hydrogen bonds described in Section 5.3

are the only hydrogen bonds within these structures, which is also the case for those structures described in Chapter 4: “Towards selective molecular complex formation: challenging crystal engineering”. These dependable hydrogen bonds, N-H \cdots O, N-H \cdots N and O-H \cdots O, scalar quantities for which are given in Table 5.5, have slight ranges in length but always form the primary hydrogen bonds in the structures. In the case of benzimidazole with 3-chlorobenzoic acid, of the two forms that were structurally determined, Form I adopts the motif of chains of dimers while Form II adopts the motif of hydrogen bonded rings. All the other structures in the chapter falls into one of these two motifs, in an even split. No firm conclusions can be made to why a molecular complex forms a certain motif; further work would be needed.

When evaluating the ΔpK_a difference values (Table 5.6) for the molecular complexes obtained, it can be seen that the rule governing if a salt or co-crystal will form has been accurate. All of the cocrystallisations had ΔpK_a values within the 0~3 range that normally means prediction is impossible, which is the case as in the example of polymorphism within the BZN 3CL molecular complex, one form formed the co-crystal while the other formed the salt. The cases where the ratio of co-molecule was not 1:1, they tended to form a mixture of salt and co-crystal.

In all seven of the structurally determined molecular complexes the halogen atom is involved in either a halogen bond or other significant halogen interaction. These interactions tend to be individual in the role they adopt, they are often the only interaction that expands the structure in a particular direction. For example in the benzimidazole : 4-fluorobenzoic acid molecular complex the halogen bond is the only interaction that expands the structure along the *c*-axis. This body of work shows that the halogen bond is significant and is key in determining the overall packing in these structures.

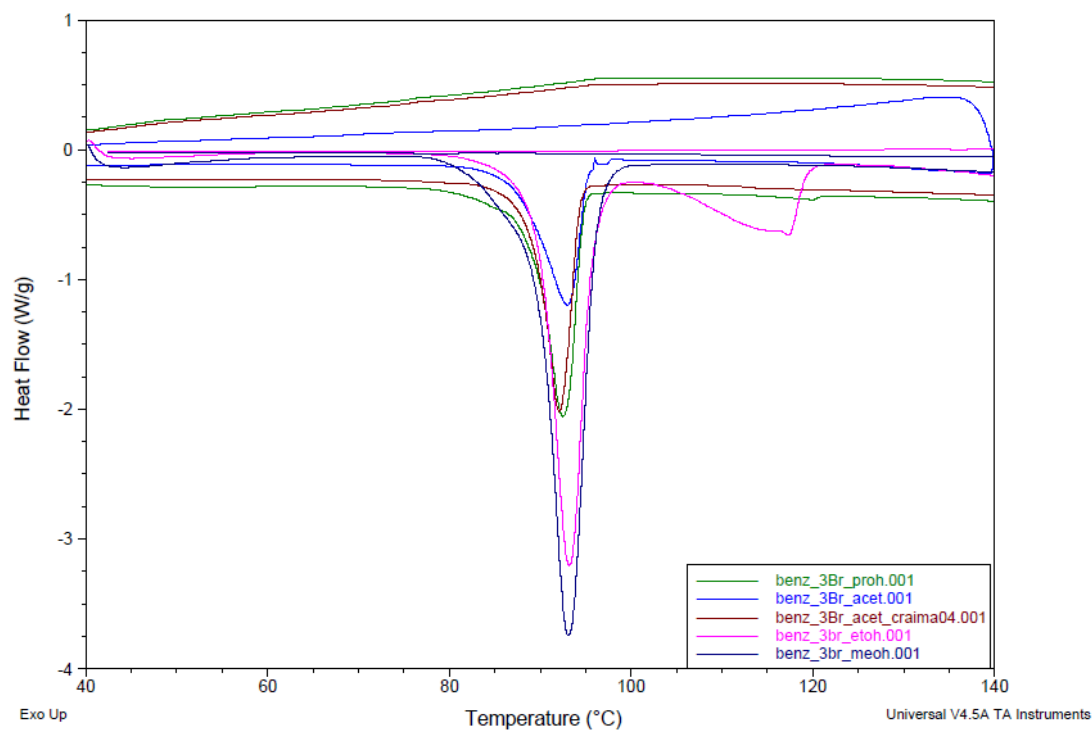
5.6 References for Chapter 5

- (1) W. C. McCrone, *Wiley Interscience, New York*, 1965, 725-726.
- (2) http://msds.chem.ox.ac.uk/CH/4-chlorobenzoic_acid.html
- (3) D. M. P. Mingos and M. Alajarin, *Springer*, 2004, **1**.
- (4) P. Goldman, G. W. A. Milne and M. T. Pignataro, *Archives of Biochemistry and Biophysics*, 1967, **118**, 178-184.

- (5) C. B. Aakeröy, J. Desper and B. M. T. Scott, *Chemical Communications*, 2006, 1445-1447.
- (6) G. A. Craig, L. H. Thomas, M. S. Adam, A. Ballantyne, A. Cairns, S. C. Cairns, G. Copeland, C. Harris, E. McCalmont, R. McTaggart, A. R. G. Martin, S. Palmer, J. Quail, H. Saxby, D. J. Sneddon, G. Stewart, N. Thomson, A. Whyte, C. C. Wilson and A. Parkin, *Acta Crystallograpica Section E*, 2009, **65**, 380.
- (7) M. Kubota and S. Ohba, *Acta Crystallograpica Section B*, 1992, **46**, 849-854.
- (8) C. B. Aakeröy, J. Desper and B. A. Helfrich, *CrystEngComm*, 2004, **6**, 19-24.
- (9) Y.-T. Li, G.-L. Zhang, C.-W. Yan, J.-M. Dou and D.-Q. Wang, *Polish Journal of Chemistry*, 2005, **79**, 1405-1413.
- (10) M. Polito, E. D'Oria, L. Maini, P. G. Karamertzanis, F. Grepioni, D. Braga and S. L. Price, *CrystEngComm*, 2008, **10**, 1848-1854.
- (11) G. G. Kay and A. G. Harris, *Clinical & Experimental Allergy*, 2009, **29**, 147-150.
- (12) D. M. Perrine, J. T. Ross, S. J. Nervi and R. H. Zimmerman, *Journal of Chemical Education*, 2000, **77**, 1479.
- (13) M.B.Hursthouse, D.E.Hibbs and V.N.Ramachandran, *Private Communication*, 2003.
- (14) J. Hydrio, M. Gouygou, F.c Dallemer, G. G. A. Balavoine and J. C. Daran, *European Journal of Organic Chemistry*, **2002**, 675-685.
- (15) K. A. Al-Farhan, *Acta Crystallograpica Section C*, 2003, **59**, 179-180.
- (16) R. Moreno-Fuquen, M. Grajales-Tamayo and M. T. d. Gambardella, *Acta Crystallograpica Section C*, 1997, **53**, 1635-1637.
- (17) C. Aciro, S. G. Davies, W. Kurosawa, P. M. Roberts, A. J. Russell and J. E. Thomson, *Organic Letters*, 2009, **11**, 1333-1336.
- (18) C. C. Wilson, X. Xu, A. J. Florence and N. Shankland, *New Journal of Chemistry*, 2006, **30**, 979-981.
- (19) X. Xu, A. R. Kennedy, A. J. Florence and N. Shankland, *Acta Crystallograpica Section E*, 2004, **60**, 1950-1951.
- (20) H. Koshima, M. Nagano and T. Asahi, *Journal of the American Chemical Society.*, 2005, **127**, 2455-2463.
- (21) Y.Q. Li, Y. L. Ju, Y. Zhang, C. Wang, T. Zhang and X. Li, *Chinese Journal of Inorganic Chemistry*, 2007, **23**, 969.
- (22) <http://www.sdichem.com/4-Bromo%20Benzoic%20Acid.htm>
- (23) M.Albrecht, S.Schmid and R.Frohlich, *Private Communication*, 2004.
- (24) T. Liwporncharoenvong and R. L. Luck, *Inorganica Chemica Acta*, 2002, **340**, 147-154.
- (25) M. Szafran, I. Kowalczyka and A. Katrusiaka, *Journal of Molecular Structure*, 2008, **875**, 244-253.
- (26) R. G. Baughman and J. E. Nelson, *Acta Crystallograpica Section C*, 1984, **40**, 204-206.
- (27) C. L. Nygren, C. C. Wilson and J. F. C. Turner, *The Journal of Physical Chemistry A*, 2005, **109**, 2586-2593.
- (28) C. B. Aakeroy, N. C. Schultheiss, A. Rajbanshi, J. Desper and C. Moore, *Crystal Growth & Design*, 2009, **9**, 432-441.
- (29) http://reference.iucr.org/dictionary/Isostructural_crystals

5.7 Appendix

5.7.1 Appendix A – DSC Thermograms of the Co-crystallisation Experiments of BZN and 3-BrBA.



Key – The thermograms relate to co-crystallisations of BZN : 3-BrBA in different solvent; propanol (green), acetone (blue), acetone (brown), ethanol (pink) and methanol (dark blue)

6 Increasing the Competition – The Introduction of Competing Hydrogen Bonding Sites

This chapter will investigate the effect of introducing nitrogen containing functional groups into the co-molecule on the supramolecular synthons obtained on co-crystallisation with benzimidazole and imidazole. The effect on proton transfer, hydrogen bonding motifs, crystallisation ratios, weaker interactions and the formation of solvates will be discussed.

The first focus will be on challenging the synthons and hydrogen bond motifs created by co-crystallisation of benzimidazole with co-molecules containing carboxylic- and hydroxyl-functional groups such as those found in Chapters 4 and 5, by introducing another basic nitrogen into the co-molecule. This additional basic nitrogen will take the form of carboxyl and hydroxyl substituted pyridines and should compete on two fronts: firstly with the other basic nitrogen on the benzimidazole for proton transfer; secondly for involvement in the potential hydrogen bonds. If left unprotonated, this will compete with the carboxylic acid group to be the primary hydrogen bond acceptor and if protonated, it will compete with the other protonated nitrogen on the benzimidazole for the primary hydrogen bond donor role.

The second section will look at electronic effects introduced in the previously reported molecular complexes of nitro-substituted benzoic acid molecular complexes with benzimidazole and imidazole. This particularly looks at effects such as the normalisation of the internal bond lengths, a consequence of the proton transfer, the strength of the hydrogen bonds with the variation in the position of the nitro group and the role of the weaker interactions that affect the packing of the structures.

6.1 Introduction

The co-molecules to be used in this chapter are picolinic acid, nicotinic acid, isonicotinic acid, hydroxypicolinic acids and nitrobenzoic acids. Of this range of compounds, the most widely recognizable is nicotinic acid, which is also known as vitamin B₃. Two of the nitro substituted benzoic acids are commercially important while of the hydroxy substituted picolinic acids 3-hydroxypicolinic acid is used as a matrix for nucleotides in mass spectrometry.

6.1.1 Picolinic Acid

Picolinic acid is used as an intermediate to produce pharmaceuticals (especially local anesthetics) and metal salts for the application of nutritional supplements. Picolinic acid is also a chelating agent in the body. The acid is believed to form a complex with zinc that facilitates the passage of zinc through the gastrointestinal wall and into the circulatory system¹. Picolinic acid has been studied by X-ray diffraction on three occasions, with the latest structure determination being in 1998 (CSD reference PICOLA02)². A hydrogen atom was found to be 50:50 disordered between the heteroatom in the ring and the carboxylic acid group (Figure 6.1). There are dimers of picolinic acid molecules linked through a single O–H···O hydrogen bond which are connected to one another by N–H···N hydrogen bonds (Figure 6.1) and weaker C–H···O hydrogen bonds. Picolinic acid has been complexed with a range of organometallic molecules including thalium³ and uranium⁴ among others, however of particular interest are the complexes it forms with other small organic molecules. One of the most recent complexes reported was with L-tartaric acid⁵ (CSD reference DULGIB) (Figure 6.2 LHS). The deprotonated form, picolinate, has been found in a range of structures coordinated to metals including; samarium, europium, holmium, erbium, yttrium⁶ and in hydrogen bonded complexes with other small

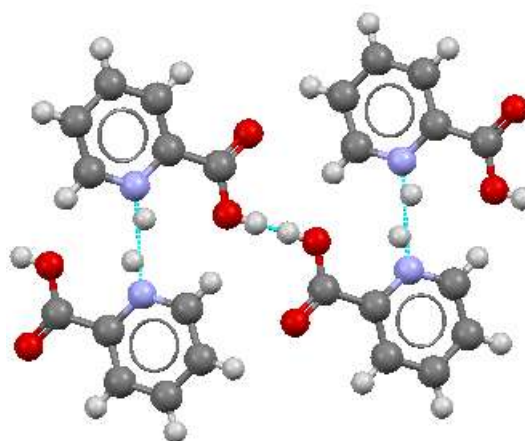


Fig. 6.1 – The structure of picolinic acid showing the main hydrogen bonds between the molecules. Proton disorder can be seen between the carboxylic acid hydrogen bond and the weaker N–H···H–N hydrogen bond.

organic molecules including 2-amino-5-methylpyridinium⁷ (CSD reference TUPVAC) (Figure 6.2 RHS).

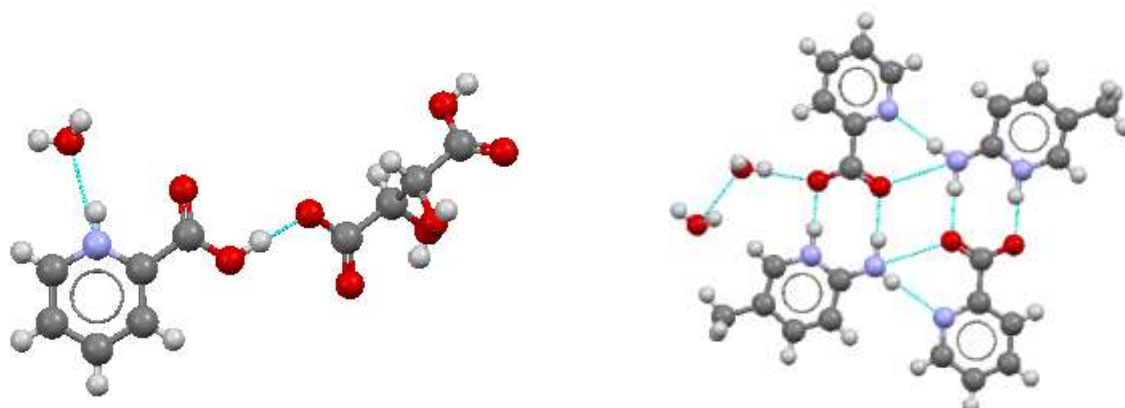


Fig. 6.2 – LHS, protonated picolinic acid : L-tartrate acid molecular complex; RHS, the molecular complex of picolinate and 2-amino-5-methylpyridinium, where the picolinic acid has been deprotonated.

6.1.2 3-Hydroxypicolinic Acid

3-Hydroxypicolinic acid is used as a matrix for nucleotides in MALDI mass spectrometry analyses. There is no reported crystal structure of 3-hydroxypicolinic acid or any molecular complexes with other organic molecules within the CSD. There are examples of the deprotonated form, 3-hydroxypicolinate, with metals and organic molecules including; thallium³, 2,4-diamino-(p-chlorophenyl)-6-ethylpyrimidinium⁸ and acetoguanaminium⁹ (CSD reference QUWXIQ) (Figure 6.3).

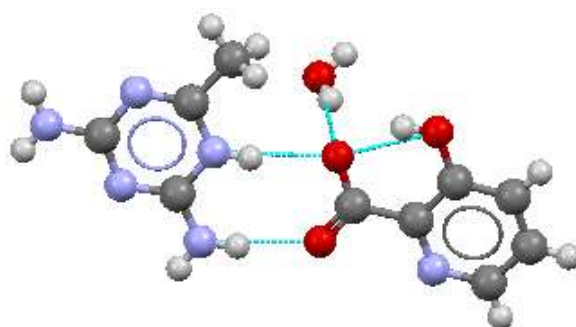


Fig. 6.3 – Basic building block of the acetoguanaminium 3-hydroxypicolinate monohydrate molecular complex.

6.1.3 6-Hydroxypicolinic Acid

6-Hydroxypicolinic acid has recently been used as a raw material in the pharmaceutical sector. Its structure was determined in 1998¹⁰ and is more properly referred to as 2-oxo-1,2-dihydropyridine-6-carboxylic acid (CSD reference POVFIIP) (Figure 6.4 LHS). A hydrated structure (CSD reference NIGZEJ01)¹¹ (Figure 6.4 RHS) contains the same double hydrogen bond unit, but with the hydrate molecules hydrogen bonding carbonyl and carboxylic groups.

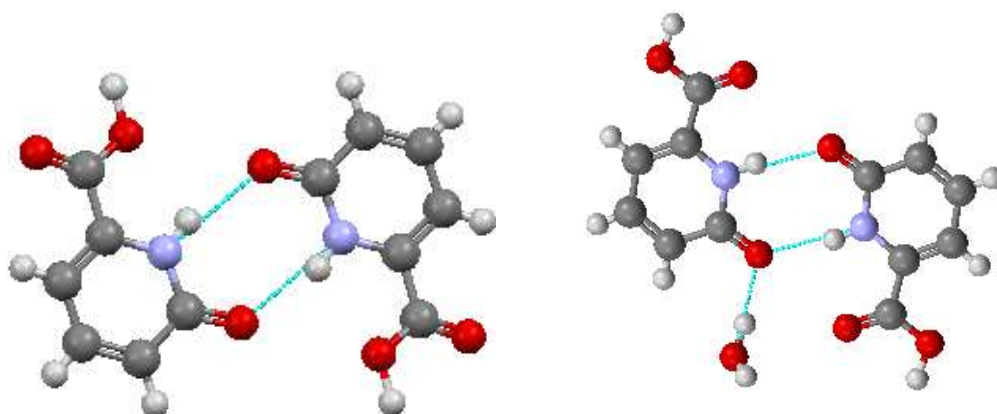


Fig. 6.4 – LHS, the structure of 6-hydroxypicolinic acid (2-oxo-1,2-dihydropyridine-6-carboxylic acid) and, RHS, a hydrate form.

There are examples of complexes involving the deprotonated form with small organic molecules including chloro- and bromo- substituted 2-amino-pyridinium⁷ (CSD references SUZNEH and SUYXIU) (Figure 6.5). There are also a large number of examples of 6-hydroxypicolinic acid complexes with metals for example; copper (CSD reference BOPXOU)¹², manganese (CSD reference EXOYIZ)¹³ and lanthanum (CSD reference PACSUI)¹⁴ to name but a few.

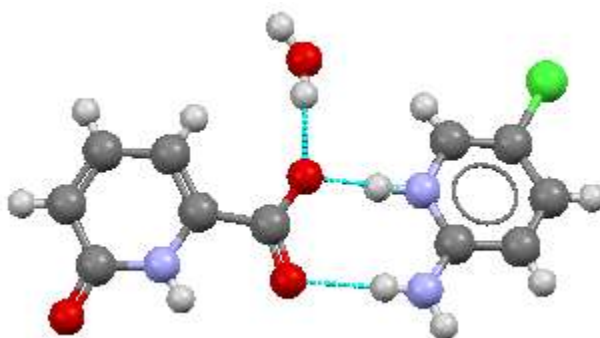


Fig. 6.5 – The molecules involved in the 6-hydroxypicolinic acid 2-amino-5-chloropyridinium molecular complex.

6.1.4 Nicotinic Acid

Nicotinic acid, also known as vitamin B₃, is one of the forty to eighty essential human nutrients. A lack of vitamin B₃ can lead to pellagra whose symptoms include high sensitivity to light, aggression, dermatitis and insomnia among a host of others but is classically referred to as the four D's: diarrhea, dermatitis, dementia and death. The first of the three published structures of nicotinic acid dates from 1953¹⁵. The most recent structure was published in 1983 by Schering et al¹⁶ (CSD reference NICOAC02) with the main hydrogen bond being between the nitrogen and the hydroxyl oxygen (Figure 6.6). There are only two structures of the neutral molecule contained in the CSD in complex with other small organic molecules. These are with 4-aminobenzoic acid (CSD reference SESLIM)¹⁷ and 3,5-dinitrobenzoic acid (CSD reference AWUDEB)¹⁸. Other molecular complexes in the CSD show examples of both cations, where the nitrogen is protonated⁵ (CSD reference DULGEX) (Figure 6.7 LHS), and anions, where the carboxylic acid group is deprotonated⁷ (CSD reference PUKDEF) (Figure 6.7 RHS). There are no examples of co-crystallisation products containing the zwitterionic form.

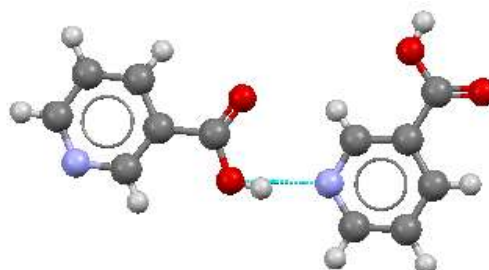


Fig. 6.6 – The nicotinic acid supramolecular synthon showing the dominating O-H...N hydrogen bond.

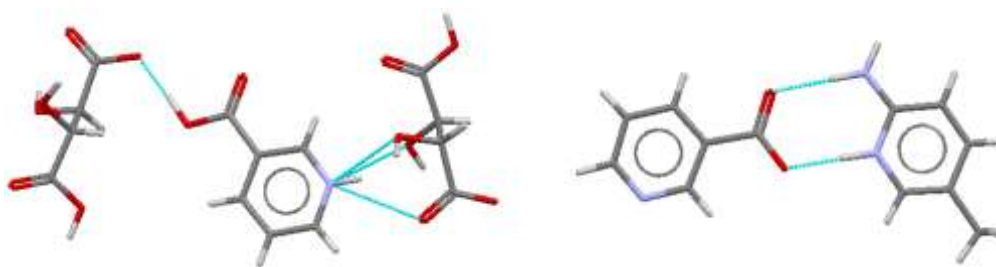


Fig. 6.7 – LHS, 3-carboxypyridinium hydrogen (2R,3R)-tartrate molecular complex where the nitrogen has been protonated; RHS, the molecular complex 2-amino-5-methylpyridinium nicotinate, where the carboxylic group on the nicotinic acid has been deprotonated.

6.1.5 Isonicotinic Acid

The structure of isonicotinic acid was determined in 1976 by Shimada et al¹⁹ (CSD reference ISNICA) and is found to have an O-H···N hydrogen bond (Figure 6.8 LHS). There are a host of structures where isonicotinic acid coordinates to metals, both through the basic nitrogen, for example with platinum²⁰ (CSD reference BOXJEE), and through the carboxylic group, for example with gadolinium²¹ (CSD reference RUBLIK). There are no structures of neutral isonicotinic acid with other small organic molecules reported in the CSD, however there are complexes of both the protonated cationic and deprotonated anionic forms. There are also examples where the zwitterion has been created by intramolecular proton transfer from the carboxylic acid group to the nitrogen. This has been found in a body of work by Zaworotko et al²² with co-molecules citric acid (CSD reference RUWGAS), gallic acid (CSD reference RUWGUM), quercetin (CSD reference RUWHUN) and 3,4-dihydroxybenzoic (Figure 6.8 RHS) acid (CSD reference RUWHOHO).

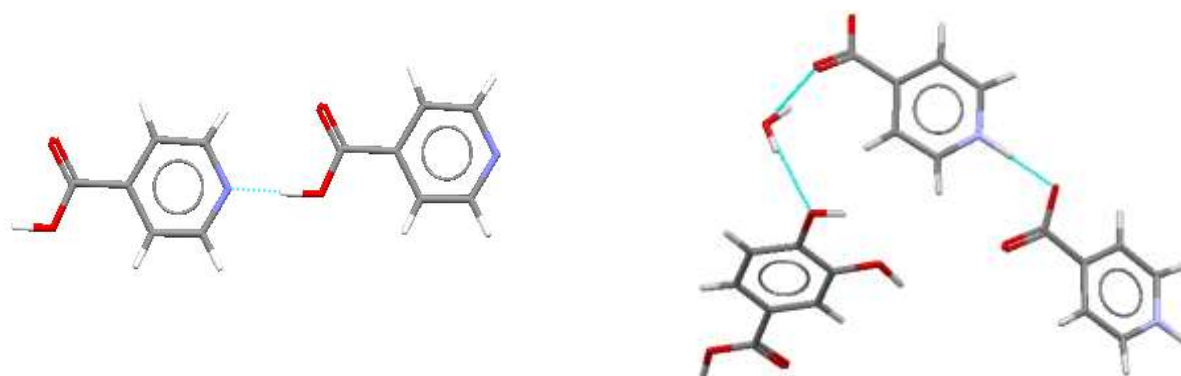


Fig. 6.8 – LHS, the O-H···N hydrogen bond in the crystal structure of isonicotinic acid; RHS, the molecular complex of isonicotinic acid protocatechuic acid monohydrate, with the zwitterionic form of isonicotinic acid.

6.1.6 2-Nitrobenzoic Acid

2-Nitrobenzoic acid is used as an intermediate in the manufacturing of pharmaceuticals, dyes and pigments. The most recent crystal structure of 2-nitrobenzoic acid was published by Portalone²³ in 2009 (Figure 6.9). The structure consists of a conventional hydrogen bonded carboxylic acid dimer ($R_2^2(8)$) with an inversion centre in the middle of the hydrogen bonded ring and the nitro groups twisted out of the plane. The crystal structure of 2-nitrobenzoic acid with benzimidazole in a 3:1 ratio has already been reported, creating the benzimidazolium 2-nitrobenzoate bis(2-nitrobenzoic acid)²⁴ molecular complex (Figure 6.9) (CSD reference

XIBWAH). In this structure one of the 2-nitrobenzoic molecules is disordered over two sites. In common with all structures involving benzimidazole and a carboxylic acid containing molecule, there has been proton transfer with the basic nitrogen of the benzimidazole absorbing a proton. The ratio of 3:1 among the constituent molecules is however unusual.

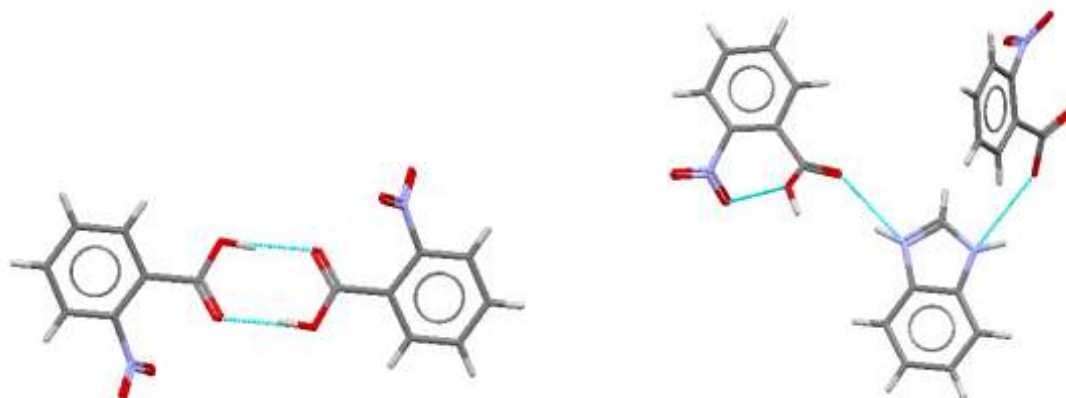


Fig. 6.9 – LHS, the hydrogen bonded dimer of 2-nitrobenzoic acid with the two molecules related by an inversion centre in the middle of the hydrogen bonded ring and the nitro- groups twisted out of the plane; RHS, the molecular complex of benzimidazolium 2-nitrobenzoate bis(2-nitrobenzoic acid) showing some of the hydrogen bonds between the molecules.

6.1.7 3-Nitrobenzoic Acid

3-Nitrobenzoic acid is a precursor to 3-aminobenzoic acid, which in turn is used to prepare some dyes. It is prepared by nitration of benzoic acid and is a factor of 10 times more acidic than benzoic acid itself. Its crystal structure was solved in 1990 by Domenicano²⁵ (CSD reference MNBZAC04) (Figure 6.10) and exhibits the common carboxylic acid dimer motif. The structure was solved at room temperature and this explains why the carboxylic acid hydrogen is found to be disordered over two positions. The molecular complex of 3-nitrobenzoic acid in a 1:1 ratio with both benzimidazole, creating the benzimidazolium 3-nitrobenzoate² molecular complex (CSD reference SUZZES) (Figure 6.11 LHS), and imidazole, producing the imidazolium 3-nitrobenzoate² molecular complex (CSD reference SUZZUI) have previously been reported (Figure 6.11 RHS).



Fig. 6.10 – The hydrogen bonded carboxylic acid dimer of benzimidazolium and 2-nitrobenzoic acid.



Fig. 6.11 – LHS, the supramolecular synthon of benzimidazolium and 3-nitrobenzoic acid; RHS, the supramolecular synthon of imidazolium and 3-nitrobenzoic acid.

Both of these molecular complexes show proton transfer from the carboxylic acid group to the unprotonated nitrogen of the co-molecule. They produce the common $N^{\delta+}-H\cdots O^{\delta-}$ hydrogen bond, but this creates two very different motifs. The benzimidazolium molecular complex forms zigzag chains, while the imidazolium molecular complex forms into a hydrogen bonded ring system.

6.1.8 4-Nitrobenzoic Acid

4-Nitrobenzoic acid is a precursor in the synthesis of the anaesthetic Procaine. Its crystal structure has been solved by single crystal X-ray and neutron diffraction (CSD references NBZOACO4 and NBZOAZ05²⁶, respectively). The crystal structure displays the common carboxylic acid dimer motif (Figure 6.12) with the protons in the hydrogen bond showing disorder at 302K.

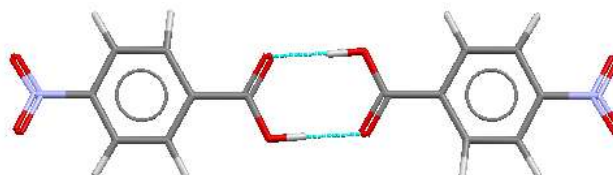


Fig. 6.12 - The hydrogen bonded dimer of 4-nitrobenzoic acid.

4-Nitrobenzoic acid has been co-crystallised with both benzimidazole and imidazole by Hashizume²⁷ in 2001. The benzimidazolium 4-nitrobenzoate molecular complex (CSD reference SUZZIW) exhibits the common $N^{\delta+}-H\cdots O^{\delta-}$ supramolecular synthon which creates a zigzag chains motif (Figure 6.13 LHS). The imidazolium 4-nitrobenzoate²⁸ molecular complex (CSD reference SABPEQ) also forms the $N^{\delta+}-H\cdots O^{\delta-}$ supramolecular synthon, however on this occasion the motif is the hydrogen bonded ring system that has been seen many times before (Figure 6.13 LHS). This is the same pattern as that observed for the 3-nitrobenzoic acid molecular complexes.



Fig. 6.13 –LHS, benzimidazolium 4-nitrobenzoate molecular complex that contains the synthon $N^{\delta+}-H\cdots O^{\delta-}$, which forms into zig-zag chains; RHS, the imidazolium 4-nitrobenzoate molecular complex also forms $N^{\delta+}-H\cdots O^{\delta-}$ hydrogen bonds, which in this case assemble to form hydrogen bonded rings.

6.2 Summary of Results

Molecular complexes of benzimidazole with a series of picolinic acids have been characterised in this work. This includes the first reported molecular complexes of 3-hydroxy- and 6-hydroxypicolinic acid with another small organic molecule. These new molecular complexes have formed in a variety of manners, with some forming as hemihydrates and solvates (Table 6.1). The increase in the competition has, as expected, increased the difficulty in predicting the main supramolecular synthons in the structure, to such an extent that it made structure solution difficult in the benzimidazolium picolinate hydrate molecular complex. This structure contains inherent disorder throughout the structure and the diffraction patterns showed strong diffuse scattering.

	Picolinic Acid	3-hydroxypicolinic acid	6-hydroxypicolinic acid
Benzimidazole	1:1 hydrate	1:1	1:1 & 1:1:2 acetic acid
Imidazole		1:1	

Table 6.1 – Summary of the molecular complexes successfully generated (blue) between benzimidazole and imidazole with picolinic acid and its mono-substituted hydroxyl derivatives. A diverse range of products was generated including a hemihydrate and solvate.

The attempted co-crystallisation of benzimidazole with nicotinic and isonicotinic acids only produced an unknown hydrated form of nicotinic acid in single crystal form (Table 6.2) and a series of powders. Powder diffraction measurements of the products were not completed; therefore it is still possible that molecular complexes with benzimidazole were produced but just did not produce single crystals.

	Picolinic Acid	Nicotinic Acid	Isonicotinic Acid
Benzimidazole	1:1 hydrate	Nicotinic acid hydrate	

Table 6.2 – Summary of the molecular complexes successfully generated (blue) between benzimidazole and picolinic, nicotinic and isonicotinic acids. Apart from the new molecular complex (benzimidazole : picolinic acid hydrate) only single crystals of a new hydrate of nicotinic acid was formed.

The aim of investigating the molecular complexes generated between benzimidazole and imidazole with mono-substituted nitrobenzoic acids was to understand the effect, if any, that the charged nitro-group has on the supramolecular synthons generated. The structures that have already been determined and deposited in the CSD are summarised in Table 6.3.

	2-Nitrobenzoic Acid	3-Nitrobenzoic Acid	4-Nitrobenzoic Acid
Benzimidazole			
Imidazole			

Table 6.3 – Summary of the molecular complexes found in the CSD. Blue shading corresponds to molecular complex found while grey represents no molecular complexes found.

6.2.1 Benzimidazolium

Where the crystallisation product is in a 1:1 stoichiometric ratio of benzimidazole and a carboxylic acid containing molecule, the benzimidazole is protonated through hydrogen transfer from the carboxylic acid group onto the normally unprotonated nitrogen atom in the five-membered ring creating a benzimidazolium molecule (BZNH^+) (Figure 6.14). The result of the proton transfer on the benzimidazolium molecule is a delocalisation of the charge across the five-membered ring, reflected in the equalisation of the internal bond lengths $\text{N}^{\delta+}$ - $\text{C}-\text{N}^{\delta+}$ and bond angles $\text{C}-\text{N}^{\delta+}-\text{C}$ (Table 6.4). The delocalisation of the charge has the effect of creating a partial positive charge on both the nitrogens. This effect is seen in all the molecular complexes that have been structurally determined and discussed in this chapter.

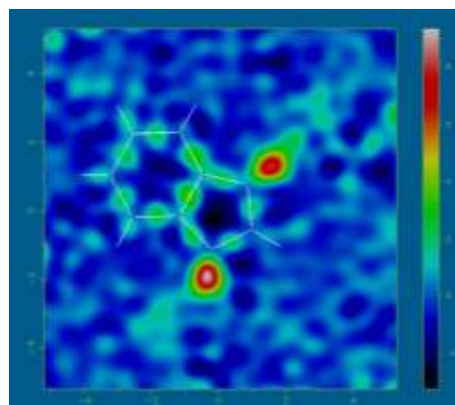
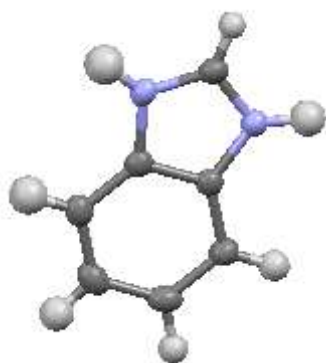


Fig. 6.14 – LHS, a typical benzimidazolium molecule where both nitrogens are protonated; RHS, the Fourier difference map generated where the H atoms located on a nitrogen atom have been omitted from the model, clearly showing that both nitrogen atoms are protonated.

The consequence for the co-molecule that has been deprotonated is the creation of a negative charge. The negative charge is found to be delocalised over the carboxylic acid group by consideration of the normalisation of the bond lengths in the carboxylate group.

Molecular Complexes	BZNH ⁺ PA ⁻ hemihydrate	BZNH ⁺ 3-HPA ⁻	IMIDH ⁺ 3-HPA ⁻	BZNH ⁺ 6-HPA ⁻	BZNH ⁺ 6-HPA ⁻ diacetic
N-C(Å) 1st 2 nd molecule	1.329(2)	1.331(3)	1.337(5) 1.333(5)	1.343(2)	1.341(3)
N-C(Å) 1st 2 nd molecule	1.334(2)	1.332(3)	1.337(5) 1.329(5)	1.330(2)	1.328(5)
C-N-C(°) 1st 2 nd molecule	107.0(3)	108.0(2)	108.0(3) 108.2(3)	107.7(1)	108.2(2)
C-N-C(°) 1st 2 nd molecule	106.1(3)	107.9(2)	108.2(3) 108.9(3)	108.2(1)	108.6(2)

Table 6.4 – The N^{δ+}-C-N^{δ+} bond lengths and C-N^{δ+}-C bond angles for the molecular complexes discussed in Section 6.5.

6.2.2 Hydrogen Bonding Motifs and Supramolecular Synthons

In contrast to the molecular complexes generated with the hydroxy- and halo-substituted benzoic acids (see Chapters 4 and 5) the introduction of another basic nitrogen into the system has led to the established hetero hydrogen bond, N^{δ+}-H^{δ+}...O^{δ-}, and homo hydrogen bonds,

$\text{O-H}\cdots\text{O}^{\delta-}$ and $\text{N-H}\cdots\text{N}^{\delta+}$, being challenged (Figure 5.21). This, along with the presence of the hydroxyl groups found in the hydroxypicolinic acid molecule leads to an increase in the number of hydrogen bonding patterns available for the molecules to adopt and thus an increased difficulty in predicting the supramolecular synthons which will form from this.

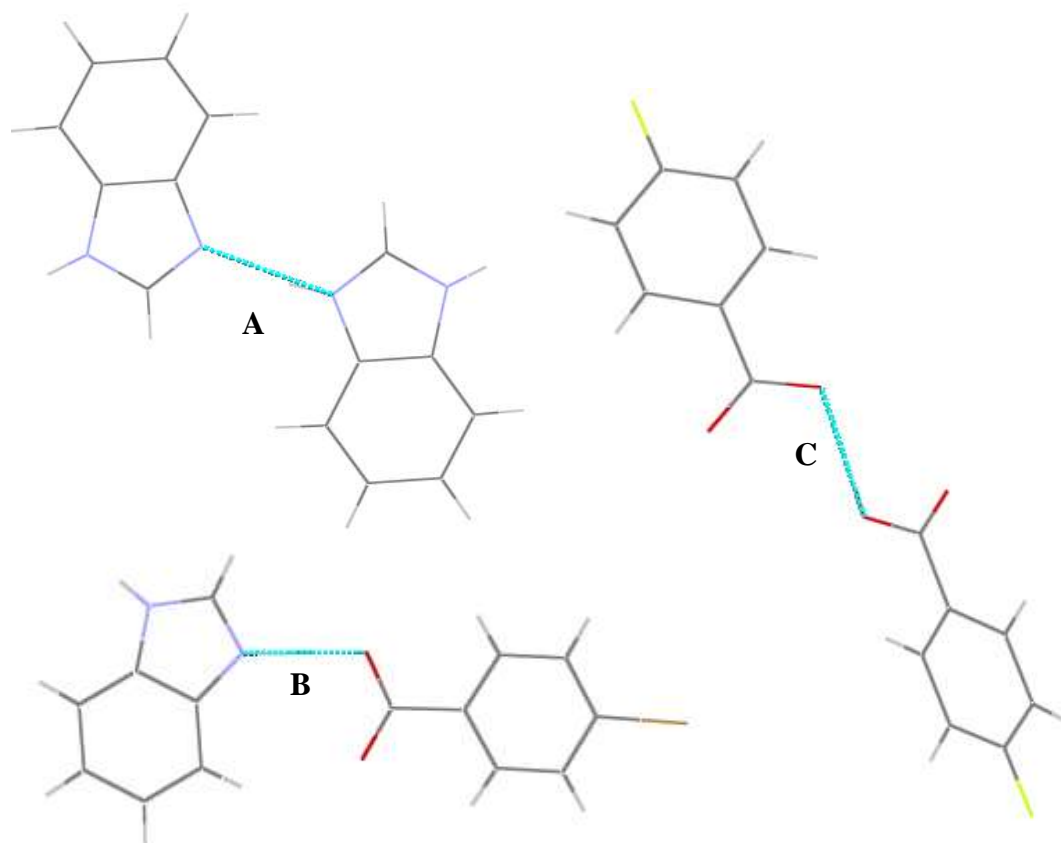


Fig. 5.21 – The most prominent hydrogen bonds within the benzimidazole : halobenzoic acid molecular complexes: an N-H...N hydrogen bond (A), an N-H...O hydrogen bond (B) and an O-H...O hydrogen bond (C).

6.3 Crystallographic Data

Compound	BZNH ⁺ PA ⁻ hydrate	BZNH ⁺ 3-HPA ⁻	IMIDH ⁺ 3-HPA ⁻
Formula	C ₇ N ₂ H ₇ , C ₆ O ₂ NH ₄ , OH ₂	C ₇ N ₂ H ₇ , C ₆ O ₃ NH ₄	C ₃ N ₂ H ₅ , C ₆ O ₃ NH ₄
ΔpKa (1:1)	4.54 / 0.15	4.39	5.85
Crystallisation Conditions	Methanol, ~2-4°C	Methanol, room temperature	ethanol, ~2-4°C
Mol. weight / gmol ⁻¹	259.26	257.25	207.19
Temperature (K)	100	100	100
Space Group	<i>F d d 2</i>	<i>P 2₁/n</i>	<i>C c</i>
<i>a</i> (Å)	34.511(7)	14.7485(11)	26.514(3)
<i>b</i> (Å)	9.2559(19)	5.0177(4)	3.7403(3)
<i>c</i> (Å)	15.824(3)	15.9323(11)	18.7022(15)
α (°)	90	90	90
β (°)	90	98.131(3)	94.043(3)
γ (°)	90	90	90
Volume (Å ³)	5054.81	1214.46(3)	1850.1(3)
Z	4	4	8
θ range (°)	3.104-27.502	3.525-27.482	3.081-27.478
Completeness (%)	99.6	99.7	99.4
Refln Collected	8135	16346	10876
Independent	1496	2677	2102
Refln (obs.I>2σ(I))	1333	1798	1702
R _{int}	0.046	0.052	0.0624
Parameters	244	216	327
GooF on F ²	1.3180	0.9693	0.9845
R ₁ (Observed)	0.0574	0.0503	0.065
R ₁ (all)	0.0657	0.0741	0.0597
wR ₂ (all)	0.2167	0.1418	0.0751

Compound	BZNH⁺ 6-HPA⁻	BZNH⁺ 6-HPA⁻ diacetic acid
Formula	C ₇ N ₂ H ₇ , C ₆ O ₃ NH ₄	C ₇ N ₂ H ₇ , C ₆ O ₃ NH ₄ , 2(CH ₄ O ₂)
Crystallisation Conditions	DMSO, room temperature	Acetic acid, ~-2-4°C
Molecular weight / gmol⁻¹	257.25	377.35
Temperature (K)	100	100
Space Group	<i>C</i> 2/ <i>c</i>	<i>P</i> -1
<i>a</i> (Å)	14.8393(13)	7.8162(6)
<i>b</i> (Å)	12.4978(10)	10.7954(8)
<i>c</i> (Å)	13.7739(12)	11.8566(8)
α (°)	90	61.624(2)
β (°)	113.328(4)	83.249(2)
γ (°)	90	78.779(2)
Volume (Å³)	2345.7(4)	863.05(11)
<i>Z</i>	8	2
θ range (°)	2.211- 30.569	3.086-27.484
Completeness (%)	97.2	99.6
Refn Collected	42210	17383
Independent	3502	3938
Refln (obs.I>2sigma(I))	2859	3244
R_{int}	0.0624	0.0359
Parameters	216	320
GooF on F²	1.2511	1.2582
R₁ (Observed)	0.0537	0.0622
R₁ (all)	0.0654	0.0776
wR₂ (all)	0.1905	0.1673

Table. 6.5 - Crystallographic data for the molecular complexes discussed in Chapter 6.

6.4 Structural Descriptions of the Molecular Complexes

6.4.1 Molecular Complex of Benzimidazole and Picolinic Acid

The molecular ions, BZNH^+ and picolinate (PA^-) form a 1:1 hydrate molecular complex. The molecular complex was obtained using the solvent evaporation method, with a 1:1 stoichiometric mixture of BZN (12mg) and picolinic acid (3-HPA) (12mg) dissolved in the minimum amount of methanol followed by evaporation at $\sim 2-4^\circ\text{C}$. The crystals generated were very large, block shaped and colourless. Single crystal X-ray diffraction data were obtained using a Rigaku R-axis/RAPID diffractometer at 100K, equipped with graphite monochromated Mo $K\alpha$ radiation ($\lambda = 0.71073 \text{ \AA}$). The structure was solved using SHELXS-97²⁸ within the WINGX²⁹ program. The crystallographic data are summarised in Table 6.5.

The crystals generated from the co-crystallisation experiments were large in all three dimensions, however, solving the structure proved difficult due to the large amount of disorder indicated by the strong diffuse scattering observed in the diffraction patterns (Figure 6.15).

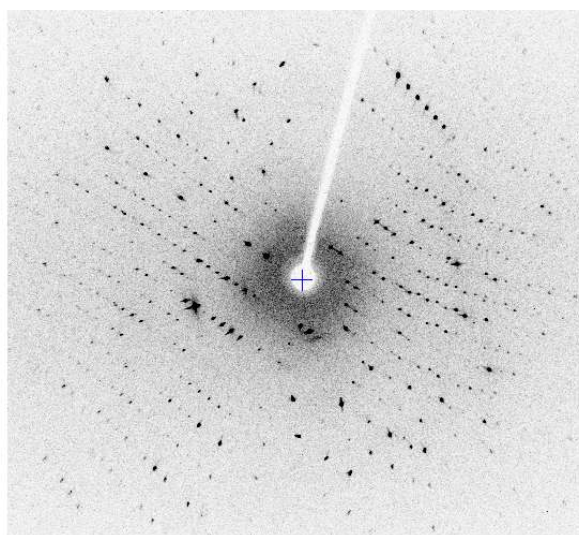


Fig. 6.15 – A diffraction pattern frame from the single crystal X-ray diffraction experiment on a crystal of the benzimidazole : picolinic acid molecular complex showing the strong diffuse scattering.

The model that best fits the experimental diffraction data is shown in Figure 6.16 LHS. The BZNH^+ and PA^- molecules adopt 50:50 disordered positions within layers. In practice, on a local level, this corresponds to having a plane with the BZNH^+ and PA^- molecules alternating with one another and forms chains of $\text{N-H}\cdots\text{O}$ hydrogen bonds. Within these planes, it is statistically possible for two of the benzimidazole molecules to lie adjacent to each other introducing a discontinuity in the hydrogen bonded chains. Alternatively, a vacancy could be present. It is not, however, possible for two picolinic acid molecules to lie adjacent to one another as two oxygen atoms would then come into very close contact ($\sim 1.7907(2)\text{\AA}$).

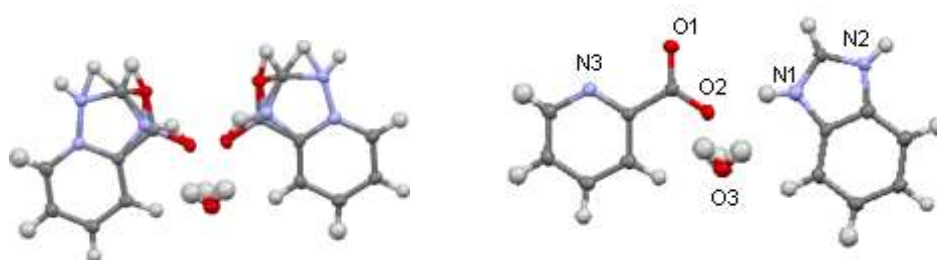


Fig. 6.16 – LHS, the disordered model for the benzimidazolium picolinate hydrate molecular complex; RHS, the likely hydrogen bonded unit when considering the local ordering, i.e. with the disorder removed.

The disordered water molecule also plays a role in the construction of these chains. There is one 50:50 disordered H atom on the water which lies approximately within the same plane. The location of this hydrogen bond is directly correlated to the location of the carboxylate group as it forms a hydrogen bond to whichever oxygen atom is not involved in the $\text{N-H}\cdots\text{O}$ hydrogen bond to the neighbouring benzimidazole molecule. The water molecule then acts as a hydrogen bond donor to a molecule in the plane below (Figure 6.17).

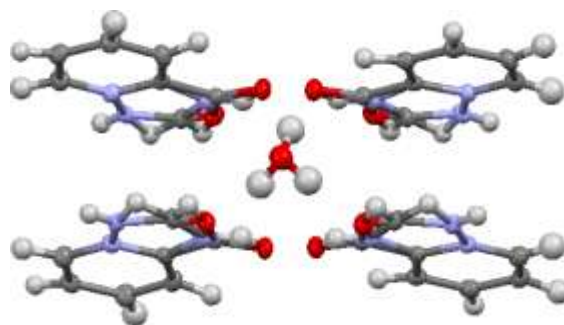


Fig. 6.17 – The water molecule connects the layers of alternately hydrogen bonded co-molecules together.

Another potential source of disorder could take the form of proton disorder in a similar manner to that found within the picolinic acid starting material and this could also be a driving force behind the observed diffuse scattering. In the pure picolinic acid crystal structure (Section 6.1.1), hydrogen disorder is found between the carboxylic acid group and the nitrogen heteroatom of the ring. Evidence of the occurrence of this effect in the present structure is inconclusive but it is most likely that there is no proton disorder. If the nitrogen was protonated, there would be a strong likelihood of hydrogen

bonding from this site, but there are no oxygen atoms within a hydrogen bonding distance. However, the disordered nature of this system would make it difficult to identify any electron density corresponding to a hydrogen on the heteroatom of the pyridine ring.

It is therefore most likely that the BZN molecule is protonated through hydrogen transfer from the carboxylic acid group on the PA molecule onto the normally unprotonated nitrogen atom in the five-membered ring forming a BZNH^+ molecule (Section 6.2.1). This form of proton transfer is common and would normally result in a delocalisation of the charge across the five-membered ring and the equalisation of the internal bond lengths. Although it is difficult to separate the positions of some of the atoms of the benzimidazole molecule from those of the picolinic acid molecule in this disordered situation, and some of the atoms have only been refined with isotropic thermal parameters, there is a clear equalisation of the bonds lengths with $\text{N}^{\delta+}-\text{C}$ 1.336(2) Å and $\text{N}^{\delta+}-\text{C}$ 1.320(2) Å, and bond angles, $\text{C}-\text{N}^{\delta+}-\text{C}$ 107.5° and $\text{C}-\text{N}^{\delta+}-\text{C}$ 107.1° (see Table 6.4 for comparisons). This delocalisation of charge can also be found in the carboxylate group of the picolinate molecules where the carbon oxygen bond lengths are comparable to those found in other deprotonated carboxylate groups within similar systems, with $\text{C}-\text{O}$ bond lengths of 1.256(2)Å and 1.268(2)Å.

The main hydrogen bonds in the $\text{BZNH}^+ \text{PA}^-$ molecular complex are charge assisted $\text{N}^{\delta+}-\text{H}\cdots\text{O}^{\delta-}$ hydrogen bonds that combine to create a flat chain of alternating co-molecules on a local length scale (Figure 6.18). The $\text{N}^{\delta+}-\text{H}\cdots\text{O}^{\delta-}$ hydrogen bonds are moderate in strength with $\text{N}^{\delta+}-\text{H}\cdots\text{O}^{\delta-}$ hydrogen bond lengths of 2.692(4)Å and 2.675(5)Å. The latter bond length can, however, only be taken as a guide value as the absolute position of one of the N atoms in the benzimidazole molecule is difficult to determine due to the close proximity of the disordered carboxylate carbon atom and thus it was only refined isotropically. It is likely that the N atom of the picolinic acid is involved in a asymmetric bifurcated hydrogen bond with the major $\text{N}^{\delta+}-\text{H}\cdots\text{O}^{\delta-}$ hydrogen bond length of 2.692(4)Å, and a corresponding minor hydrogen bond length of 3.061(4)Å. The atoms involved in this bifurcated hydrogen bond have both been refined with anisotropic displacement parameters.

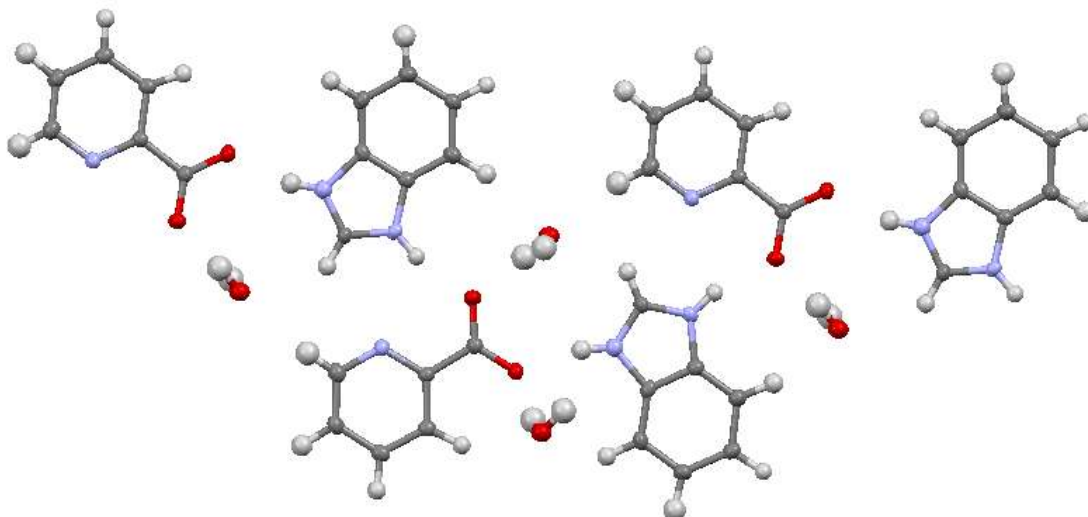


Fig. 6.18 – The main motif of the $\text{BZNH}^+ \text{PA}^-$ molecular complex is a flat chain of alternating hydrogen bonded co-molecules.

The water molecule has two 50:50 disordered positions for one of the H atoms and one ordered H position. Figure 6.19 shows that the disordered hydrogens on the water molecule point towards the oxygen atoms of the picolinate molecule approximately within the same plane. The fully occupied hydrogen points towards the picolinate on in a different plane. On a local length scale, the hydrogen will take the position closest to that of the picolinate molecule. One possible short-range order model is shown in Figure 6.20 where the water molecules form hydrogen bonded rings with the picolinate molecules in parallel chains. These moderate $\text{O}-\text{H}\cdots\text{O}^{\delta-}$ hydrogen bonds are of $\text{O}\cdots\text{O}$ length of $2.697(4)\text{\AA}$ and $2.891(6)\text{\AA}$ (both O atoms refined anisotropically).

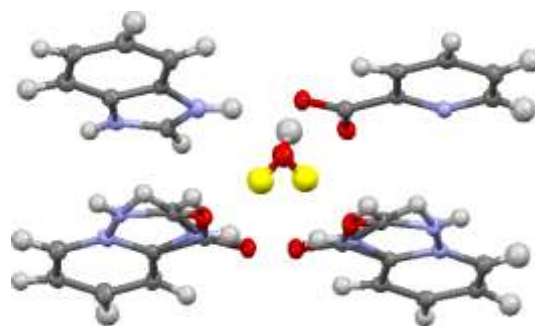


Fig. 6.19 – The water molecule, with two 0.5 occupied hydrogens (yellow) and one fully occupied hydrogen (white) connects the layers of alternately hydrogen bonded co-molecules together.

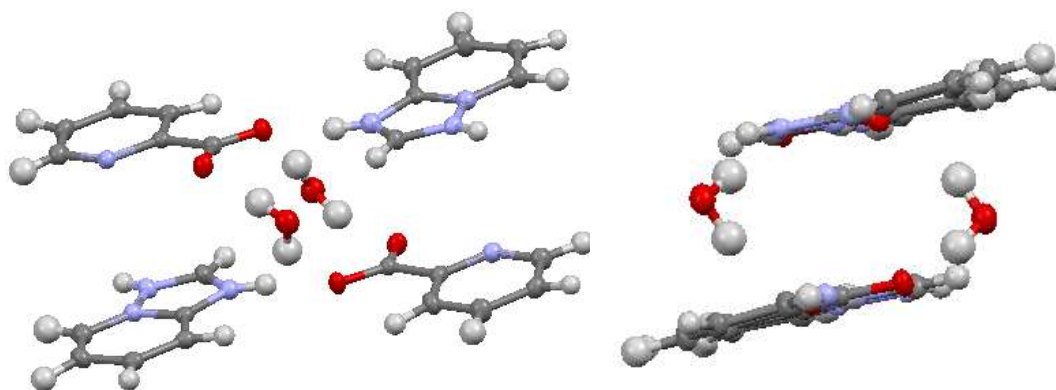


Fig. 6.20 – LHS, the hydrogen bonded ring (hydrogen bonds shown in blue) involving two water molecules and two picolinate molecules that connect two flat chains of hydrogen bonded $\text{BZNH}^+ \text{PA}^-$ molecules; RHS, view along the c -axis emphasising that the water molecule sits just out of the plane of the flat sheets of hydrogen bonded $\text{BZNH}^+ \text{PA}^-$ molecules.

The high level of disorder makes it harder to identify the weaker interactions within this system. However consideration of the extended structure (Figure 6.21) makes it possible to explain the main interactions in the structure and provide possibilities for the others. The main interactions between BZNH^+ and PA^- are the $\text{N}^{\delta+}-\text{H}\cdots\text{O}^{\delta-}$ hydrogen bonds that create flat chains along the c -axis, these sheets are then held together through water molecules effectively generating columns along the b -axis.

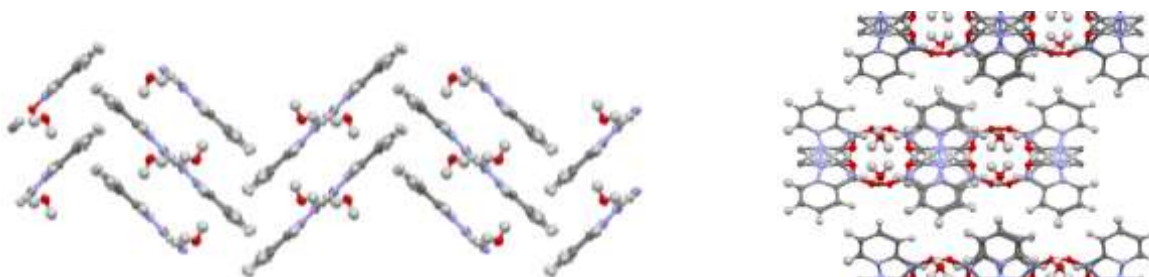


Fig. 6.21 – LHS, the view along the c -axis of the $\text{BZNH}^+ \text{PA}^-$ molecular complex showing the herringbone layers connected by water molecules; RHS, the view along the b -axis of the $\text{BZNH}^+ \text{PA}^-$ molecular complex showing the channels of water.

In the space between these columns there is only one clear interaction, a weak $\text{C}-\text{H}\cdots\text{O}^-$ hydrogen bond with $\text{C}\cdots\text{O}$ lengths of $3.381(2)\text{\AA}$ and $3.383(2)\text{\AA}$, depending on which position for the picolinic acid molecule is occupied, along the a -axis (Figure 6.22 LHS). There is also a strong possibility of some $\pi\cdots\pi$ stacking interactions as the distances between the rings are

$\sim 3.3083(5)\text{\AA}$ (between two N atoms) and the 5-membered ring section of the BZNH^+ molecules lie directly parallel to one another (Figure 6.22 RHS).

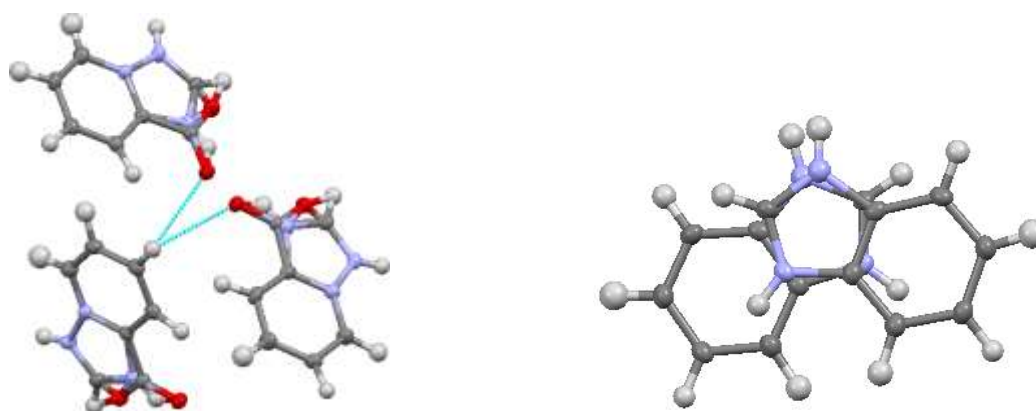


Fig. 6.22 – LHS, weak C–H \cdots O hydrogen bonds that lie along the *a*-axis; RHS, view showing that the BZNH^+ molecules lie directly parallel thus improving the chances of $\pi\cdots\pi$ stacking interactions.

6.4.2 Molecular Complex of Benzimidazole and 3-Hydroxypicolinic Acid 1:1

The molecular ions, BZNH^+ and 3-hydroxypicolinate (3-HPA^-), form a 1:1 molecular complex with one another (Figure 6.23). Single crystals were obtained using the solvent evaporation method, with a 1:1 stoichiometric mixture of BZN (12mg) and 3-hydroxypicolinic acid (3-HPA) (14mg) dissolved in the minimum amount of methanol followed by evaporation at room temperature. The crystals generated were cube shaped and colourless. Single crystal X-ray diffraction data were obtained using a Rigaku R-axis/RAPID diffractometer at 100K, equipped with graphite monochromated Mo $K\alpha$ radiation ($\lambda = 0.71073\text{\AA}$). The structure was solved using SIR92³⁰ within the CRYSTALS³¹ program. The crystallographic data are summarised in Table 6.5. In the molecular complex, the BZN molecule is protonated as discussed in Section 6.2.1. The resulting normalisation of the internal bond and angles is seen in Table 6.4. Within the molecular complex the 3-HPA^- molecules form an intramolecular hydrogen bond between the hydroxyl and carboxylate groups. This intramolecular hydrogen bond, $\text{O1-H}\cdots\text{O2}^{\delta-}$, is of moderate strength with an $\text{O}\cdots\text{O}$ distance of $2.537(3)\text{\AA}$ and is consistent with that found within the 2-hydroxybenzoic acid molecular complex ($2.551(3)\text{\AA}$, Section 4.5.1) and is shorter and stronger than found in its native crystal structure (2.622\AA), reflecting the charge assisted nature. In common with the other carboxylate groups that have been deprotonated, the resulting negative charge is found

to be delocalised over the group. This can be seen by consideration of the bond lengths in the carboxylate group, C8–O2^{δ-} 1.290(2)Å and C8–O3^{δ-} 1.240(2)Å. The consequence of the proton transfer is that there are now three possible hydrogen bond acceptor sites on the picolinate molecule: the two oxygens on the carboxylate group that have a partial negative charge and the pyridyl nitrogen which is naturally basic.

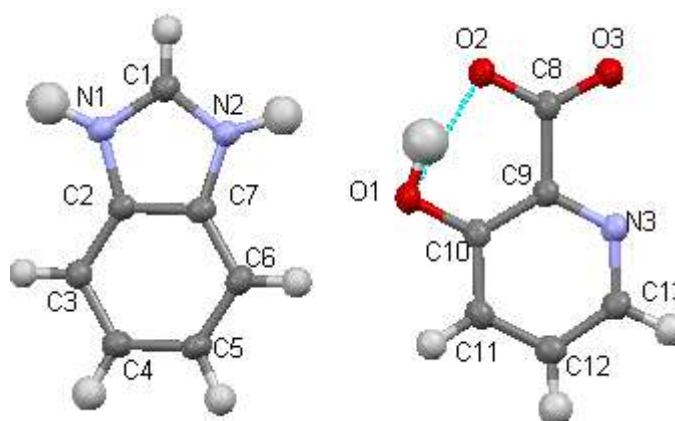


Fig. 6.23 – The atom labelling for the molecular complex of benzimidazolium (LHS) and 3-hydroxypicolinate. (RHS).

Interaction	Label	Length (Å) (D···A(Å))	For Hydrogen Bonds		
			D–H(Å)	H···A(Å)	D–H···A angle(°)
N1···O3	a	2.732(3)	1.06(3)	1.71(3)	163.0(3)
N2···N3	b	2.909(3)	1.04(3)	1.88(3)	168.1(3)
N2···O3	b	2.889(2)	1.04(3)	2.33(3)	112.4(2)
O3···C4		3.337(3)	1.00(2)	2.65(2)	125(2)
O3···C5		3.313(3)	0.99(2)	2.64(3)	125(2)
$\pi \cdots \pi$		3.260	-	-	-
C··· π		3.582(3)	-	-	-
C··· π		3.609(3)	-	-	-
C··· π		3.629(3)	-	-	-

Table. 6.6 – The interactions involved in the BZNH⁺ 3-HPA⁻ molecular complex with full data for the hydrogen bonds.

The primary hydrogen bonds in the BZNH⁺ 3-HPA⁻ molecular complex are; a partially charge assisted N^{δ+}–H···O^{δ-} hydrogen bond between the nitrogen of the BZNH⁺ and oxygen of the carboxylic acid group and a bifurcated N2^{δ+}–H···N3/O3^{δ-} hydrogen bond between the N2 of the BZNH⁺ and N3 and O3 of 3-HPA⁻ (Figure 6.24). The strongest hydrogen bond is the N–H···O hydrogen bond and this is of moderate strength, with an N···O distance of 2.732(3)Å, N–H 1.06(3)Å, O···H 1.71(3)Å and angle of 163.0(3)° (labelled a in Figure 6.24). The bifurcated bond has N···N and N···O distances of 2.909(3)Å and 2.889(2)Å, respectively

(labelled b in Figure 6.24) with hydrogen bond data shown in Table 6.6. This bifurcated hydrogen bond would be termed symmetrical with regard to the equal strengths of the interactions, however the position of the hydrogen promotes an asymmetrical nomenclature as the hydrogen bond angles are $168.1(3)^\circ$ and $112.4(2)^\circ$ respectively. Therefore this bifurcated hydrogen bond, and the others of a similar nature, will be termed asymmetrical.

The primary hydrogen bonds assemble the structure into an equimolar hydrogen bonded ring with alternating molecules which can be described by the graph set notation symbol R_4^4 (18) (Figure 6.23). This hydrogen bonded ring is the motif of the structure and is not dissimilar to the hydrogen bonded rings seen in Chapter 4. The difference is that the basic nitrogen on the 3-hydroxypicolinic acid is a more appealing acceptor than the oxygen.

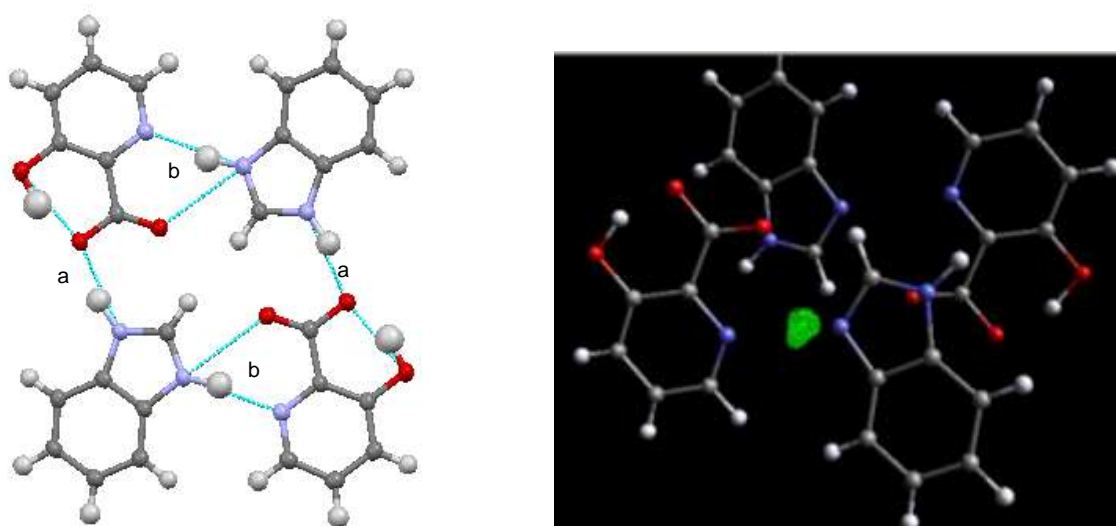


Fig. 6.24 – LHS, the supramolecular synthon for the $\text{BZNH}^+ \text{3-HPA}^-$ molecular complex; a hydrogen bonded ring system held together by partially charge assisted $\text{N}^{\delta+}-\text{H}\cdots\text{O}^{\delta-}$ and $\text{N}^{\delta+}-\text{H}\cdots\text{N}$ hydrogen bonds; RHS, the Fourier difference map (generated using MCE), where the hydrogen adjoining N2 has been removed from the model, showing the hydrogen atom to be clearly located on the N atom of the benzimidazolium molecule ion. The elongation of the electron density along the hydrogen bond illustrates the influence of the neighbouring oxygen molecule.

The motifs, equimolar hydrogen bonded rings, are connected by weaker interactions in all three dimensions. Along the *ac*-diagonal, the hydrogen bonded rings are stacked on top of one-another through staggered face-to-face π - π interactions of spacings between the closest molecules of 3.096\AA and 3.260\AA (Figure 6.25).

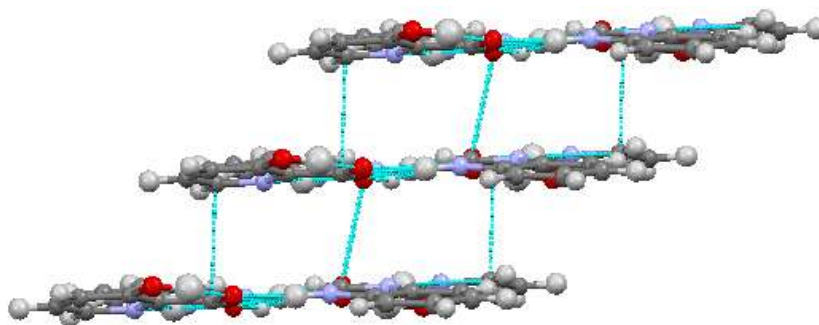


Fig. 6.25 – the stacking of the hydrogen bonded rings held together by π - π interactions.

The hydroxyl group of the 3-HPA⁻ molecule is involved in a DDHHA weak bifurcated hydrogen bond directed along the *c*-axis (Figure 6.25). The bifurcated hydrogen bond is symmetric with C \cdots O distances of 3.313(3)Å and 3.337(3)Å (Figure 6.26, inset).

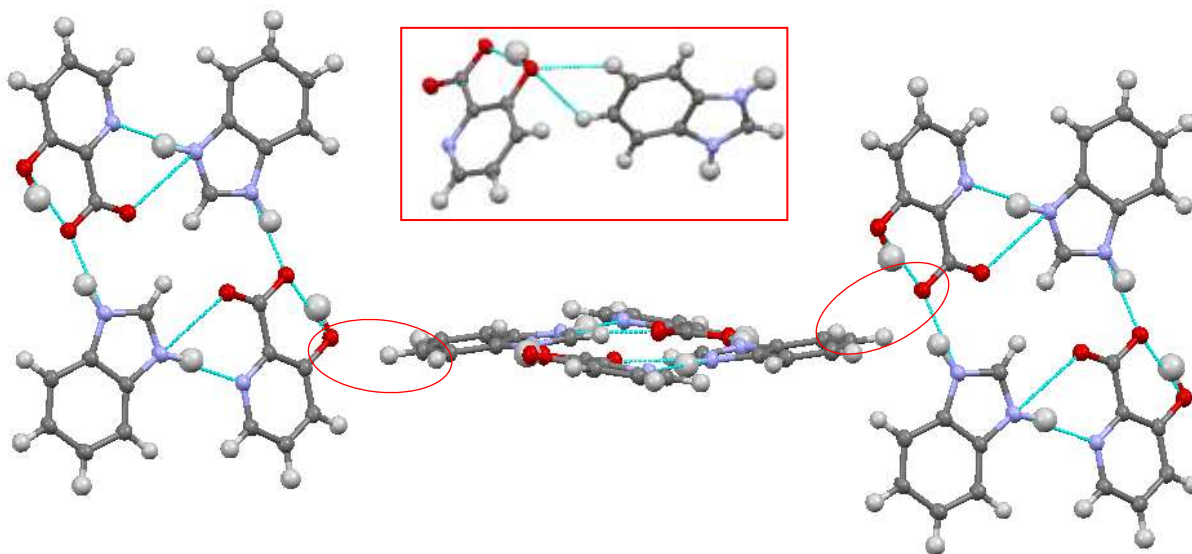


Fig. 6.26 – The supramolecular synthons of the BZNH⁺ 3-HPA⁻ molecular complex, are connected by weak bifurcated hydrogen bonds (circled in red) along the *c*-axis. Inset shows the bifurcated weak hydrogen bond circled in red in the main figure.

In addition, along the *ac*-diagonal there are weak C-H \cdots π bonds with C \cdots C distances of 3.582(3)Å, 3.609(3)Å and 3.629(3)Å (Figure 6.27). These are the only interactions that exist between the layers that expand the structure in this direction.



Fig. 6.27 – LHS, view of the *c*-axis of the BZNH⁺ 3-HPA⁻ molecular complex, which indicates the interactions between the layers (circled in yellow); RHS an expanded view of the interactions that hold the layers together, with C-H \cdots π interactions circled in yellow.

These three interactions, the π - π stacking interactions, the weak bifurcated hydrogen bonds, and the C-H \cdots π bonds, connect the motifs together to create the extended structure. Figure 6.28 illustrates the different roles that the intermolecular interactions play in the structure.

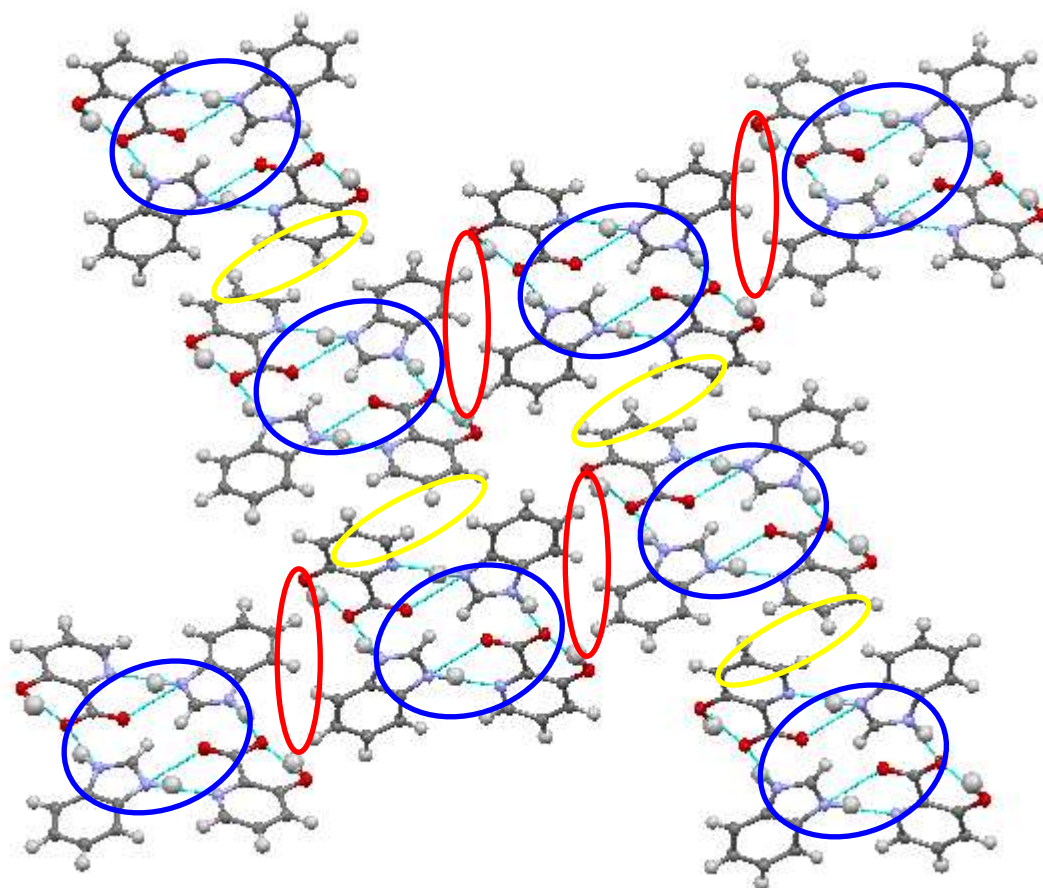


Fig. 6.28 – The intermolecular interactions in the BZNH⁺ 3-HPA⁻ molecular complex, with the supramolecular synthon circled in blue, the weak bifurcated hydrogen bonds in red and the C-H \cdots π contacts in yellow. The π - π stacking goes into the plane of the page.

6.4.3 Molecular Complex of Imidazole and 3-Hydroxypicolinic Acid 1:1

The molecular ions, IMDZH^+ and 3-hydroxypicolinate (3-HPA^-), form a 1:1 molecular complex with one another. Single crystals were obtained using the solvent evaporation method, with a 1:1 stoichiometric mixture of IMD (8mg) and 3-hydroxypicolinic acid (3-HPA) (14mg) dissolved in the minimum amount of methanol followed by evaporation at $\sim 2\text{-}4^\circ\text{C}$. The crystals generated were needle shaped and colourless. Single crystal X-ray diffraction data were obtained using a Rigaku R-axis/RAPID diffractometer at 100K, equipped with graphite monochromated Mo $K\alpha$ radiation ($\lambda = 0.71073 \text{ \AA}$). The structure was solved using SIR92³⁰ within the CRYSTALS³¹ program. The crystallographic data are summarised in Table 6.5. In the molecular complex, the IMD molecule is protonated through hydrogen transfer from the carboxylic acid group in the fashion seen in Section 6.2.1. The result of the proton transfer on the IMDH^+ molecule is a delocalisation of the charge across the five-membered ring, reflected in the equalisation of the internal bond lengths and bond angles (Table 6.4). There are two independent IMDH^+ and 3-HPA^- molecules in the asymmetric unit (Figure 6.29). Within the molecular complex the two independent 3-HPA^- molecules both form intramolecular hydrogen bonds between the hydroxyl and carboxylate groups with $\text{O}\cdots\text{O}$ distances of 2.517(4) and 2.525(4) \AA , respectively. These intramolecular hydrogen bonds are of moderate strength and are consistent with that found within the $\text{BZNH}^+ 3\text{HPA}^-$ molecular complex that had an $\text{O}\cdots\text{O}$ distance of 2.537(3) \AA (Table 6.7).

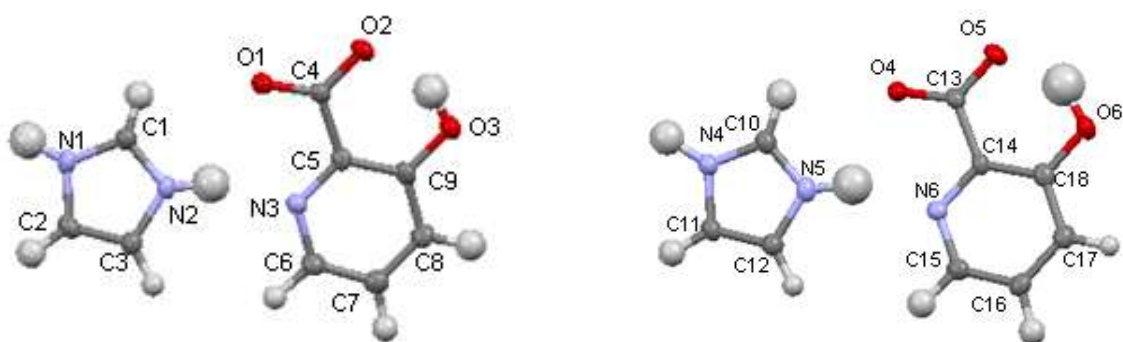


Fig. 6.29 – The atomic labelling for the two independent molecules of each type in the imidazolium 3-hydroxypicolinate molecular complex.

Interaction		Length (Å) (D...A(Å))	For Hydrogen Bonds		
			D-H(Å)	H...A(Å)	D-H...A angle(°)
N1...O4	a	2.651(4)	1.05(3)	1.60(3)	173(3)
N4...N1	a'	2.649(5)	0.95(3)	1.70(3)	179(2)
N2...N3	b	2.859(4)	1.00(3)	1.91(3)	157(2)
N3...O1	b	2.866(4)	1.00(3)	2.22(3)	121(2)
N5...N6	b'	2.786(5)	0.94(3)	1.88(3)	160(2)
N5...O4	b'	3.011(4)	0.94(3)	2.41(3)	121(2)
C2...O5		3.184(5)	0.98(4)	2.21(4)	171(3)
C11...O2		3.414(5)	0.98(4)	2.46(4)	165(3)
C17... π		3.707	-	-	-
C17... π		3.703	-	-	-
π ... π		3.274 / 3.403		-	-
π ... π		3.334 / 3.378		-	-

Table 6.7 – The three scalar quantities and bond angles of the hydrogen bonds and information of the interactions found in the IMDH⁺ 3-HPA⁻ molecular complex

The two primary hydrogen bonds in the IMDH⁺ 3-HPA⁻ molecular complex are a partially charge assisted N ^{δ^+} -H...O ^{δ^-} hydrogen bond between the nitrogen of the IMD⁺ and oxygen of the carboxylic acid group (a and a' in Figure 6.30)) and a bifurcated N ^{δ^+} -H...N/O ^{δ^-} hydrogen bond between the other nitrogen of the IMDH⁺ and the unprotonated nitrogen and oxygen of 3-HPA⁻ (b and b' in Figure 6.30). Whilst the hydrogen bonds are the same in this molecular complex as found in the BZNH⁺ 3HPA⁻ molecular complex, the motif is quite different. In the BZNH⁺ 3HPA⁻ structure the motif was a hydrogen bonded ring system (Figure 6.24). However, in the imidazole equivalent, the motif is a zigzag hydrogen bonded chain (Figure 6.30).

The N ^{δ^+} -H...O ^{δ^-} hydrogen bonds are of moderate strength with N...O distances of 2.651(4) and 2.649(5) Å (Table 6.8); these are slightly shorter than the N ^{δ^+} -H...O ^{δ^-} hydrogen bond found in the BZNH⁺ 3HPA⁻ structure which has an N...O distance of 2.732(3)Å. The bifurcated hydrogen bonds, b and b', are again similar to those seen in the BZNH⁺ 3HPA⁻

structure, with similar bond strengths (b' slightly less so) but vastly different hydrogen bond angles. Therefore these can be classified as asymmetrical bifurcated hydrogen bonds.

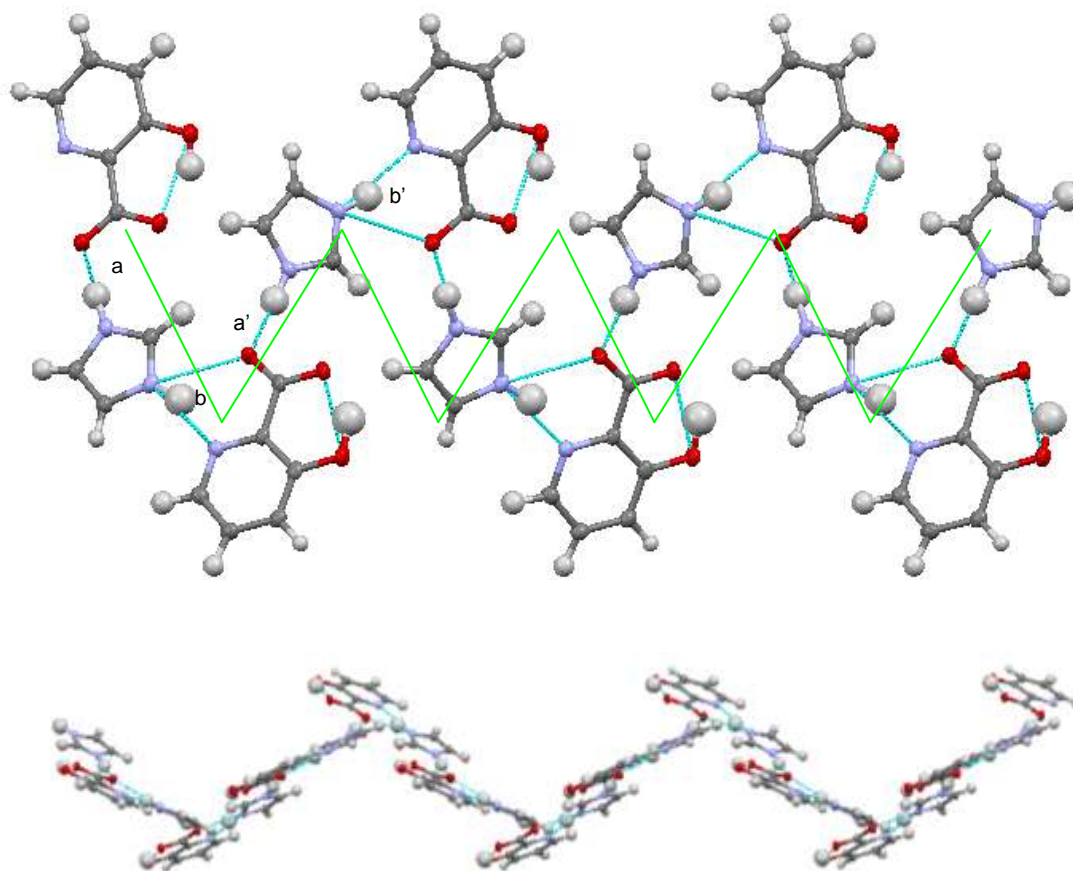


Fig. 6.30 – Top, view along the b -axis of the main motif of the IMDH^+ 3-HPA^- molecular complex, a zigzag chain of alternate co-molecules held together by partially charge assisted hydrogen bonds; bottom, view along the a -axis of the main motif of the IMDH^+ 3-HPA^- molecular complex.

The hydrogen bonded zigzag chains are connected along the ac -diagonal by weak $\text{C-H}\cdots\text{O}^{\delta-}$ hydrogen bonds to create layers (Figure 6.31 LHS) that have $\text{C}\cdots\text{O}$ distances of $3.184(5)\text{\AA}$ and $3.414(5)\text{\AA}$. The zigzag chains stack through staggered face-to-face $\pi\cdots\pi$ stacking interactions between like molecules (Figure 6.31 RHS). The distances between the layers have been calculated by creating a plane through the atoms in the ring and measuring the distance between these planes. The stacking distances are relatively short with IMDH^+ distances of 3.274\AA and 3.403\AA , and 3-HPA^- distances of 3.334\AA and 3.378\AA .

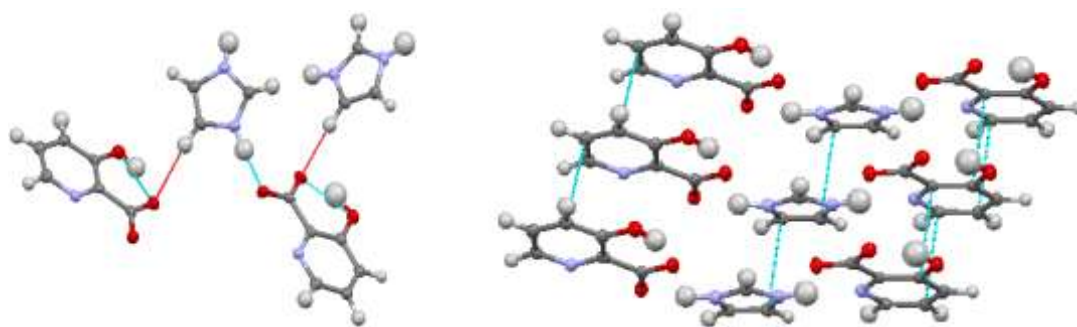


Fig. 6.31 – LHS, the C-H \cdots O $^{\delta-}$ hydrogen bonds (-) along the *ac*-diagonal, RHS, view along the *c*-axis of the staggered face-to-face $\pi\cdots\pi$ stacking interactions that extend the structure along the *b*-axis.

Figure 6.32 shows the extended structure of the IMDH $^+$ 3HPA $^-$ molecular complex. The green zigzag line indicates the main hydrogen bonded zigzag motif while the transparent blue box shows the weak hydrogen bonds that exist between the layers and with the assistance of the $\pi\cdots\pi$ stacking interactions into the plane of the paper along the *b*-axis. Parallel to the *b*-axis, there are also weak C-H $\cdots\pi$ interactions (Figure 6.30 yellow box) with distances of 3.707Å and 3.703Å, respectively (Figure 6.30 insert).

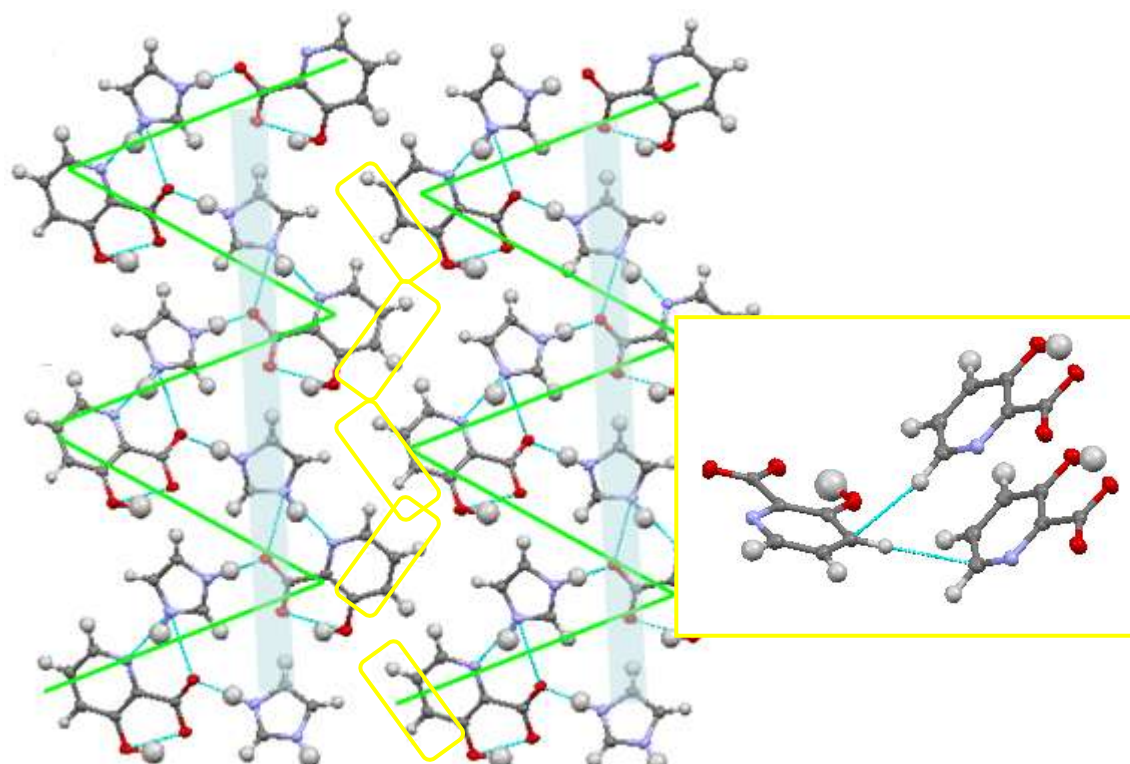


Fig. 6.32 – View along the *b*-axis of the extended IMDH $^+$ 3HPA $^-$ molecular complex. The main motif, the zigzag chains of alternate hydrogen bonded co-molecules, is shown by the green line (-) and the weak hydrogen bonds are located within the transparent blue box (-). Inset shows the C-H $\cdots\pi$ interactions that extend the structure along the *b*-axis.

6.4.4 Molecular Complex of Benzimidazole and 6-Hydroxypicolinic Acid 1:1

The molecular ions, BZNH^+ and 6-hydroxypicolinate, which is more accurately described as 2-oxo-1,2-dihydropyridine-6-carboxylic acid but will be referred to as the previous name (6-HPA $^-$) for consistency, form a 1:1 molecular complex with one another. Single crystals were obtained using the solvent evaporation method, with a 1:1 stoichiometric mixture of BZN (12mg) and 6-hydroxypicolinic acid (3-HPA) (14mg) dissolved in the minimum amount of DMSO followed by evaporation at room temperature. The crystals generated were block shaped and colourless. Single crystal X-ray diffraction data were obtained using a Bruker Apex II diffractometer at 100K, equipped with graphite monochromated Mo $K\alpha$ radiation ($\lambda = 0.71073 \text{ \AA}$). The structure was solved using SIR92³⁰ within the CRYSTALS³¹ program. The crystallographic data are summarised in Table 6.5.

The BZN molecule is protonated through hydrogen transfer from the carboxylic acid group on the 6-HPA molecule (Figure 6.33) resulting in a delocalisation of the charge across the five-membered ring (see Section 6.2.1). The effect of deprotonation on the 6-HPA $^-$ molecule is not in this case limited to changes in the carboxylate group; it also undergoes lactam - lactim tautomerism, where the hydrogen from the hydroxyl group (O3) transfers to the previously unprotonated nitrogen in the benzene ring (N3) (Figure 6.34). This form of tautomerism is also referred to as amide – imidic acid tautomerism and is found in heterocyclic rings, most commonly nucleobases such as guanine, thymine and cytosine³¹.

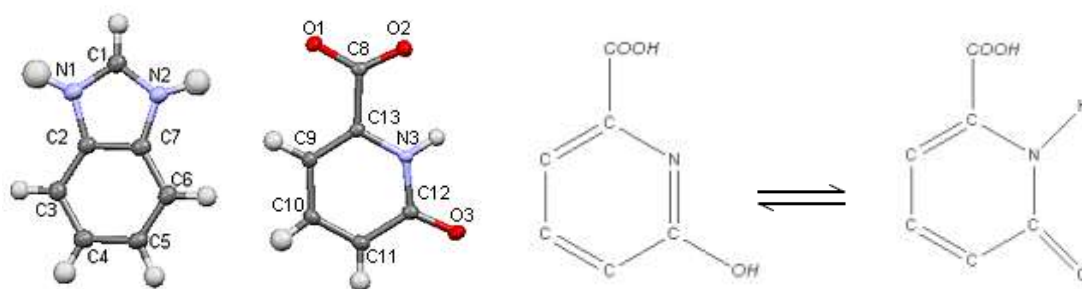


Fig. 6.33 – the benzimidazolium and 6-hydroxypicolinate molecule ions which are generated in the molecular complex, with atom labelling.

Fig. 6.34 – schematic diagram of the lactam - lactim tautomerism (imidic acid) that the 6-hydroxypicolinic acid molecule undergoes, forming 2-oxo-1,2-dihydropyridine-6-carboxylic acid.

Interaction	Label	Length (Å) (D...A(Å))	For Hydrogen Bonds		
			D-H(Å)	H...A(Å)	D-H...A angle(°)
N1...O4	f	2.644(2)	1.09(3)	1.56(3)	172.2(2)
N4...N1	g	2.640(2)	0.94(3)	1.74(3)	160.2(3)
N2...N3	e	2.915(2)	0.88(2)	2.05(2)	166.4(2)
C5...O2	h	3.302(2)	0.98(3)	2.34(3)	168(2)
C3...O1	i	3.183(2)	1.01(2)	2.42(2)	132(2)
C9... π		3.578	-	-	-
C10... π		3.588	-	-	-
π ... π		3.306	-	-	-

Table. 6.8 – The three scalar quantities and bond angles of the hydrogen bonds with labels and information of the interactions found in the BZNH⁺ 6-HPA⁻ molecular complex

There is one other example in the CSD where a 6-hydroxypicolinic acid has lost a proton (at the carboxylic acid) and undergone tautomerism (lactam-lactim), the metal organic framework with titanium as the metal centre (CSD reference RIYDEJ)³³. Within the 6-hydroxypicolinate molecule the carbon-oxygen distances differ quite substantially from other related molecules that are co-crystallised with benzimidazolium (Table 6.9). The most obvious difference is in regard to the hydroxyl carbon-oxygen length (C-O3); the oxygen here is deprotonated and forms a double bonded carbonyl bond to the ring. By comparing structures found within the CSD, in general, complexes involving hydroxypicolinic acids show that the carboxylic acid bond lengths tend not to be normalised as much as those that involve the hydroxybenzoic acid molecules. For the 6-hydroxypicolinate molecules this may be down to the loss of the conjugated benzene ring, however the 3-hydroxypicolinate still retains this conjugation.

Bond	BZNH ⁺ 6-HPA ⁻	BZNH ⁺ 6-HPA ⁻ di-acetic acid	BZNH ⁺ 3-HPA ⁻	IMIDH ⁺ 3-HPA ⁻	BZNH ⁺ 2-HBA ⁻	BZNH ⁺ 3-HBA ⁻
C-O1	1.2700(1)	1.273(2)	1.289(3)	1.284(2)	1.273(1)	1.270(1)
C-O2	1.2382(1)	1.251(4)	1.240(3)	1.244(2)	1.264(1)	1.260(1)
C-O3	1.2553(1)	1.280(3)	1.350(3)	1.367(2)	1.3552(2)	1.360(1)

Table 6.9 – The carbon-oxygen bond distances for six different molecular complexes. The numbering of the oxygen refers to Figure 6.31, with oxygens 2 and 3 always being on the same of the molecule.

Figure 6.33 shows that the basic nitrogens on the BZNH^+ and 6-HPA^- are all protonated. The consequence is that there are now three equal strength hydrogen bond donors shared between the two co-molecules. The BZNH^+ molecules contain two of these donor sites and no hydrogen bond acceptors, whereas there are three hydrogen bond acceptors and one hydrogen bond donor on the 6-HPA^- molecules. Therefore BZNH^+ can only form hydrogen bonds to molecules of a different type, and 6-HPA^- can only act as hydrogen bond donor to molecules of the same type.

A hydrogen bonded ring motif is formed which can be described by the graph set notation symbol R_6^6 (32) (Figure 6.35). The 6-membered hydrogen bonded ring is made up of two partially charge assisted 6-HPA^- dimers (e in Figure 6.35) with the BZNH^+ molecules linking these together through two partially charge assisted $\text{N}^{\delta+}\text{-H}\cdots\text{O}^{\delta-}$ (f in Figure 6.35) and $\text{N}^{\delta+}\text{-H}\cdots\text{O}$ (g in Figure 6.35) hydrogen bonds. These collectively form the main supramolecular synthon in the molecular complex with the partially charged assisted $\text{N}^{\delta+}\text{-H}\cdots\text{O}^{\delta-}$ and $\text{N}^{\delta+}\text{-H}\cdots\text{O}$ hydrogen bonds having relatively short $\text{N}\cdots\text{O}$ distances with respective bond angles of $2.644(2)\text{\AA}$ and $2.640(2)\text{\AA}$ (see Table 6.8 for full hydrogen bond data and list of interactions). This is relatively short in comparison to other $\text{N}^{\delta+}\text{-H}\cdots\text{O}^{\delta-}$ hydrogen bonds that tend to be of length 2.7\AA and above. The 6-HPA^- dimers, which equally could also be referred to as pseudo base pairs, are made up of partially charge assisted $\text{N-H}\cdots\text{O}^{\delta-}$ hydrogen bonds of length $2.915(2)\text{\AA}$ ($0.88(2)\text{\AA}$, $2.05(2)\text{\AA}$, $166.4(2)$) with an inversion centre located in the centre of the hydrogen bonded ring.

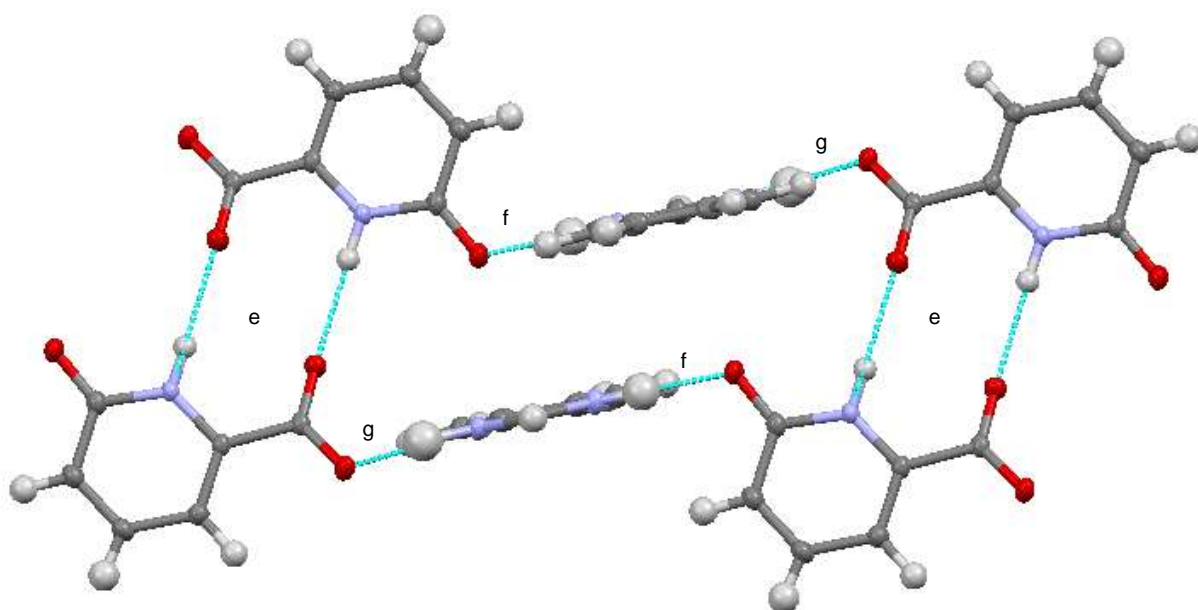


Fig. 6.35 – The main motif of the BZNH^+ 6-HPA^- molecular complex; a hydrogen bonded ring system held together by 6-HPA^- dimers (e) and partially charge assisted $\text{N}^{\delta+}\text{-H}\cdots\text{O}^{\delta-}$ (f) and $\text{N}^{\delta+}\text{-H}\cdots\text{O}$ (g) hydrogen bonds.

The 6-membered hydrogen bonded rings are connected by equivalent hydrogen bonds f and g, creating a chain along the *b*-axis (Figure 6.36). The 6-HPA^- molecules are coplanar and the BZNH^+ molecules lie at $\sim 77^\circ$ to this plane.

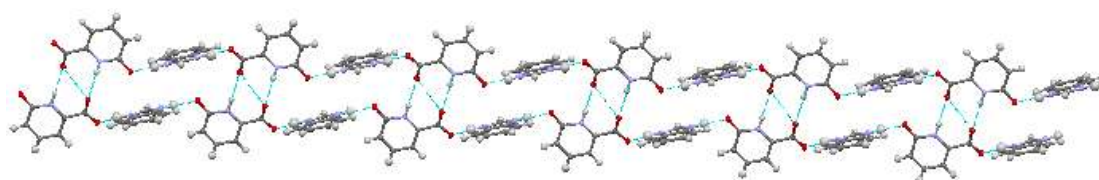


Fig. 6.36 – the chains of BZNH^+ 6-HPA^- rings along the *b*-axis, viewed along *a*.

These chains of hydrogen bonded rings are connected in all three-dimensions by an array of weaker interactions. Three of these interactions are shown in Figure 6.37, two of them promote a stacking of the motifs, while the other connects the stack motifs together. Firstly, the shortest of these interactions are weak hydrogen bonds involving the carbon located between the two nitrogens of the BZNH^+ molecule and one of the carboxylate oxygens, $\text{C1-H}\cdots\text{O1}^{\delta-}$ which is of $\text{C}\cdots\text{O}$ distance of $3.131(2)\text{\AA}$ (Figure 6.37 LHS). These connect a BZNH^+ of one chain and a 6-HPA^- of another. There are also $\pi\cdots\pi$ stacking interactions of approximate length 3.306\AA (measured between two planes created using the adjacent 6-HPA^-

molecules, LHS Figure 6.37) between 6-HPA⁻ molecules stacking the chains along the *c*-axis. These are the two interactions that are highlighted within the red circle in Figure 6.37, middle. Also between the chains, there are two C-H \cdots π interactions, C9-H \cdots π and C10-H \cdots π , with the aromatic hydrogens of 6-HPA⁻ acting as hydrogen bond donors and the aromatic ring of the BZNH⁺ acting as the π acceptor. The C \cdots C distances are 3.578(3) and 3.588(3) Å. (Figure 6.37 RHS).

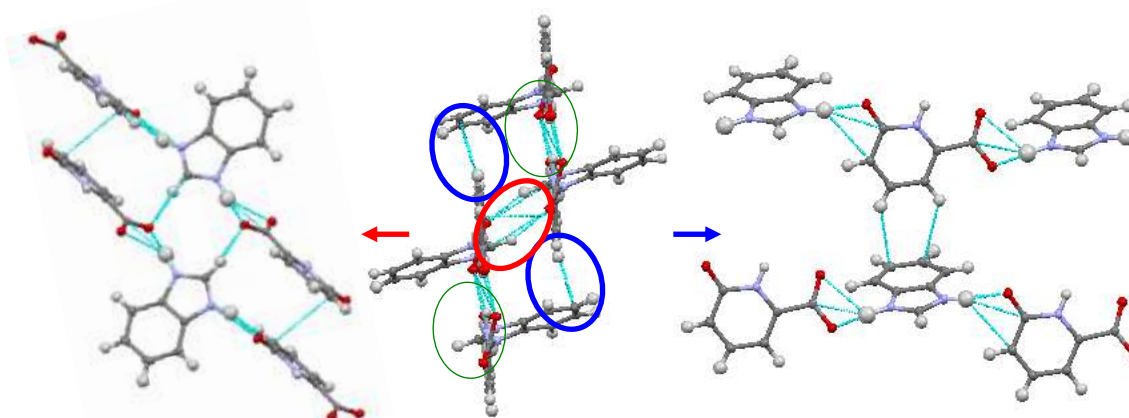


Fig. 6.37 – LHS, the weak hydrogen bonds C1-H \cdots O1 δ^- and $\pi\cdots\pi$ interactions between two chains. These are two interactions that stack the chains along the *a*-axis. Middle, view along the *b*-axis showing the stacking of the chains. Highlighted in red are the interactions viewed in Figure 6.33, LHS. Circled in blue are those interactions from Figure 6.33, RHS. The interactions within the green circle are the moderate hydrogen bonds involved in the hydrogen bond ring motif. RHS, the C-H \cdots π interactions are the blue dotted lines in the centre of the image.

The final significant interactions within the molecular complex are two weak hydrogen bonds. These are C-H \cdots O δ^- hydrogen bonds between the oxygens of the carboxylate group and carbons from the BZNH⁺ molecule and propagate along the *ac*-diagonal (Figure 6.38). These have C \cdots O distances of 3.302(2)Å (h in Figure 6.38) and 3.183(2)Å (i in Figure 6.38). The three molecules shown in Figure 6.38 are from three different chains.

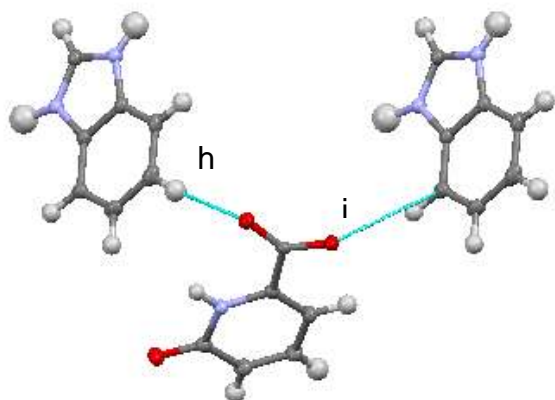


Fig. 6.38 – The C–H...O^{δ-} weak hydrogen bonds connect three different chains within the BZNH⁺ 6-HPA⁻ molecular complex.

6.4.5 Molecular Complex of Benzimidazole and 6-Hydroxypicolinic Acid Diacetic Acid Solvate 1:1:2

The molecular ions, BZNH⁺ and 6-hydroxypicolinate (IUPAC name, 2-oxo-1,2-dihydropyridine-6-carboxylic acid), (6-HPA⁻) form a 1:1:2 acetic acid molecular complex. Single crystals were obtained using the solvent evaporation method, with a 1:1 stoichiometric mixture of BZN (12mg) and 6-hydroxypicolinic acid (6-HPA) (14mg) dissolved in the minimum amount of acetic acid followed by evaporation at room temperature. The crystals generated were block shaped and brown. Single crystal X-ray diffraction data were obtained using a Rigaku R-axis/RAPID diffractometer at 100K, equipped with graphite monochromated Mo K α radiation ($\lambda = 0.71073 \text{ \AA}$). The structure was solved using SUPERFLIP³⁴ within the CRYSTALS³¹ program. The crystallographic data are summarised in Table 6.6. The BZN molecule is protonated through hydrogen transfer from the carboxylic acid group on the 6-HPA molecule as discussed in Section 6.2.1. Table 6.4 gives the resulting normalised bonds lengths and angles of the BZNH⁺ molecule (Figure 6.39). The 6-HPA⁻ molecule has also undergone lactam - lactim tautomerism, where the hydrogen from the hydroxyl group (O3) transfers to the previously unprotonated nitrogen in the pyridine ring (N3). The negative charge is delocalised over the carboxylate group; evidence for this is seen in the normalisation of the carbon oxygen bond lengths, C8–O1^{δ-} 1.273(2) Å and C8–O2^{δ-} 1.251(4)Å. The carbonyl group has a bond length of C12–O3 1.280(3)Å. There are also two distinct acetic acid molecules within the molecular complex; both retain their neutral properties.

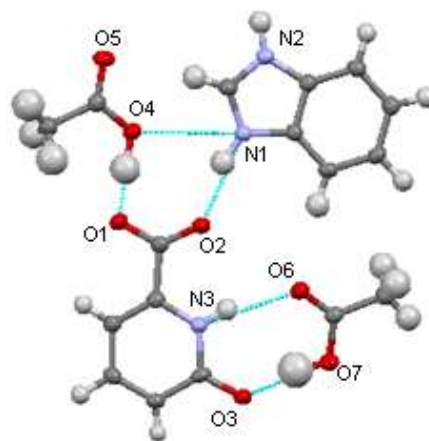


Fig. 6.39 – The benzimidazolium, 6-hydroxypicolinate and acetic acid molecules which are generated in the molecular complex, with atom labelling.

BZNH⁺ again only has hydrogen bond donor groups and the 6HPA⁻ has one donor and three acceptors. In addition, the acetic acid molecule has one traditional

donor and one acceptor sites; however protonated oxygens can act as both acceptors and donors. The presence of acetic acid disrupts the pseudo base-pairing of the 6-HPA⁻ which was present in the unsolvated complex, which instead forms heterodimers with the acetic acid molecules. The motif of the molecular complex is a linear chain of alternating co-molecules BZNH⁺ and 6-HPA⁻ with acetic acid molecules satisfying the remaining hydrogen bonding sites (Figure 6.40).

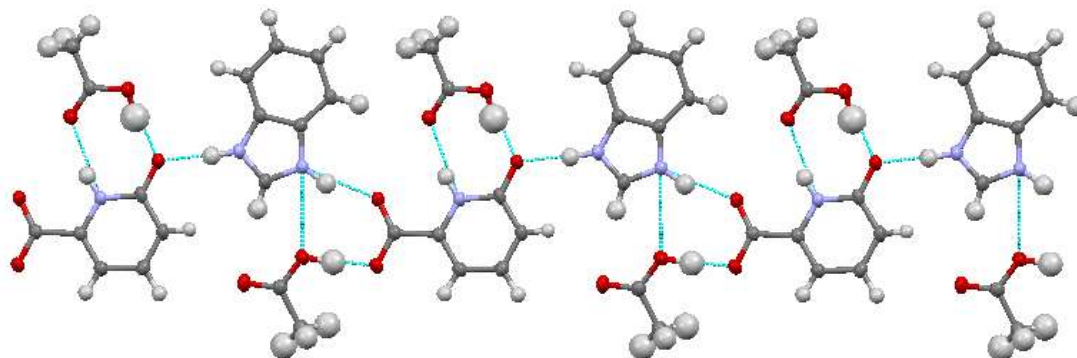


Fig. 6.40 – The hydrogen bonded chains of the BZNH⁺ : 6-HPA⁻ acetic acid solvate molecular complex is a flat linear chain of alternating hydrogen bonded co-molecules.

The linear chain of alternate BZNH⁺ and 6-HPA⁻ molecules are held together by two different partially charge assisted N–H⁺⋯O hydrogen bonds of approximately equal strength along the *ac*-diagonal. The first is between the BZNH⁺ and the carboxylate group, a, N1^{δ+}–H⁺⋯O4^{δ-}, of N⁺⋯O distance 2.762(4)Å, and the other between the BZNH⁺ and carbonyl group, b, N1^{δ+}–H⁺⋯O2 of N⁺⋯O distance 2.736(4)Å. The acetic acid molecules have two important roles in this structure. Firstly they are a key part of the main motif, the flat linear chain (Figure 6.41). One of the acetic acids creates a hydrogen bonded ring with graph set notation R_2^2 (8) by hydrogen bonding with the tautomeric nitrogen and carbonyl group of the 6-HPA⁻ (Figure 6.41, labelled c). These are of D⁺⋯A lengths of N3–H⁺⋯O6 2.915(4)Å and O7–H⁺⋯O3 2.606(4)Å. The other acetic acid hydrogen bonds to the carboxylate group, O4–H⁺⋯ O1^{δ-}, and is the strongest hydrogen bond in the structure with length of 2.498(4)Å (Figure 6.41 d)(Table 6.10).

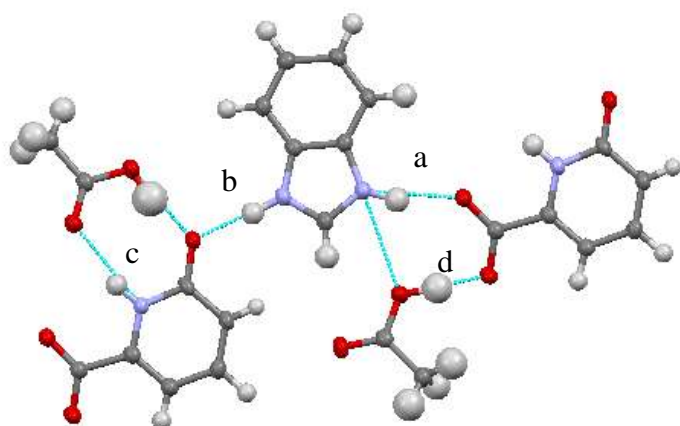


Fig. 6.41 – The hydrogen bonding scheme in the BZNH^+ 6-HPA^- acetic acid solvate molecular complex, highlighting the role of the acetic acid molecules in creating the linear chain.

Interaction	Label	Length (Å) (D...A(Å))	For Hydrogen Bonds		
			D-H(Å)	H...A(Å)	D-H...A angle(°)
N1...O4	a	2.762(4)	0.95(3)	1.79(3)	176.2(3)
N2...O3	b	2.736(4)	0.97(4)	1.82(4)	163.1(3)
N3...O6	c	2.915(4)	0.88(4)	2.06(4)	164.7(3)
O7...O2	c	2.606(4)	0.97(6)	1.66(7)	166.0(5)
N2...O3	d	2.498(4)	1.04(4)	1.46(4)	174.8(4)
O7...C		3.537(3)	0.98(5)	2.85(4)	131(3)
O5...C		3.601(3)	0.96(3)	2.73(3)	150(3)
$\pi \cdots \pi$		3.339	-	-	-
O4...C		3.366(4)	0.95(4)	2.46(4)	120(3)
O5...C		3.290(4)	0.96(3)	2.70(4)	161(4)

Table 6.10 – The three scalar quantities and bond angles of the hydrogen bonds a, b, c, d and list of the interactions between the molecules in the benzimidazole and 6-hydroxypicolinic acid diacetic acid solvate.

The other important role of the acetic acid molecules is connecting the structure along the *c*-axis. Figure 6.42 shows two of the motifs where the only interactions between them are C–H...O weak hydrogen bonds between acetic acid molecules (Figure 6.42 inset). These weak hydrogen bonds have lengths C...O7 3.575(3)Å and C...O5 3.601(3)Å respectively.

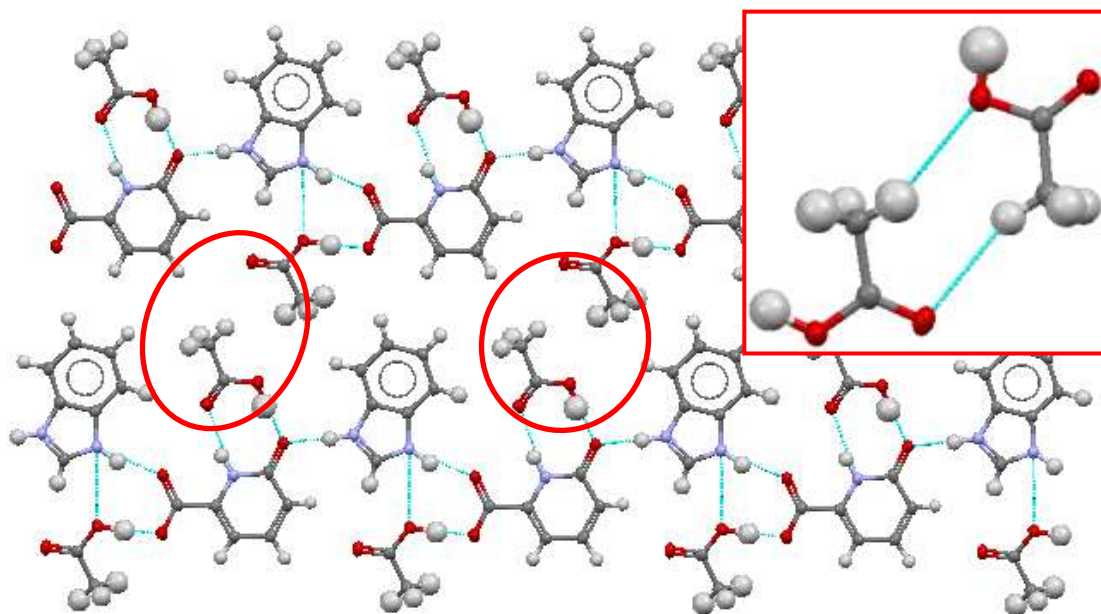


Fig. 6.42 – Two motifs of the BZNH^+ 6-HPA^- diacetic acid molecular complex showing how the two adjacent linear chains are connected along the c -axis through weak $\text{C-H}\cdots\text{O}$ hydrogen bonds (circled in red) between the acetic acid molecules; inset – expanded image of these hydrogen bonds.

With the linear chains extending the structure along the ab -diagonal and the weak hydrogen bonds connecting these chains along the c -axis, this creates a plane of molecules (Figure 6.43 LHS). These planes of molecules are connected along the ab -diagonal by $\pi\cdots\pi$ interactions and two hydrogen bonds. The hydrogen bonds are between the two independent acetic acid molecules (Figure 6.43 RHS). The $\text{C-H}\cdots\text{O}$ hydrogen bonds are weak with $\text{C}\cdots\text{O}$ lengths of $3.366(4)\text{\AA}$ and $3.290(4)\text{\AA}$. The $\pi\cdots\pi$ interactions is relatively short in length with the distance measured between two carbons at $3.339(4)\text{\AA}$ (red) and $3.886(3)$ (blue) in length (Figure 6.43 middle).

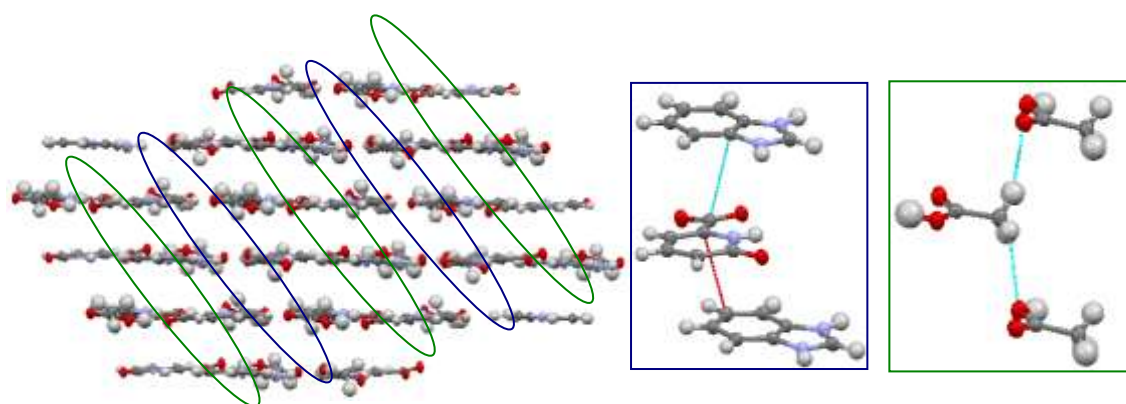


Fig. 6.43 – LHS, view along the c -axis showing the layered nature with the weaker interactions along the ab -diagonal, weak hydrogen bonds (light blue) and $\pi\cdots\pi$ interactions (dark blue); middle, the $\pi\cdots\pi$ interaction (blue); RHS, the weak $\text{C-H}\cdots\text{O}$ hydrogen bonds between the acetic acid molecules.

6.5 Systematic Structural Study of Nitrobenzoic acid : Benzimidazole / Imidazole Molecular Complexes

Molecular complexes of mono-substituted 2-, 3-, 4-nitrobenzoic acid have been generated with both benzimidazole and imidazole. Apart from the benzimidazolium 2-nitrobenzoate molecular complex, the rest of this family of structures was published in 2001 in a paper entitled *Two-component molecular crystals from N-heteroaromatics and nitrobenzoic acids* by Hashizume²⁷ (Table 6.11). The focus of this paper was on generating chiral crystals from achiral molecules. The method of co-crystallising two-component molecular crystals from organic acids and bases is one of the most promising methods in developing chiral crystals²⁸.

	2-Nitrobenzoic Acid	3-Nitrobenzoic Acid	4-Nitrobenzoic Acid
Benzimidazole	2:1		
Imidazole			

Table 6.11 – Summary of the molecular complexes found on the CSD. Blue shading corresponds to molecular complexes being present, while grey represents no molecular complexes found.

In this section, the electronic effects of the nitro group on the supramolecular synthons obtained will be investigated (Figure 6.44). As a result of the chemical bonding in the nitro group, the nitrogen atom is positively charged and each oxygen atom has a partial negative charge. For this reason the nitro group has a powerful attraction for electrons. This is in contrast to all the other molecular complexes reported in this work. Effects such as proton transfer, the normalisations on the internal bond lengths, the strength of the hydrogen bonds with the varying position of the nitro group and the influence of the nitro group in the packing arrangements of the structure will be discussed.

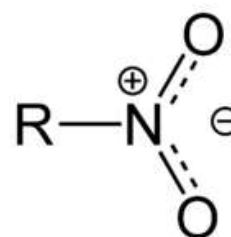


Fig. 6.44 – The structure of the nitro group.

6.5.1 Proton Transfer

The one common thread that runs through all the molecular complexes in this work is that where there is an equimolar ratio of carboxylic acid groups to BZN or IMD molecules in the molecular complex, then there will be proton transfer. The proton transfers from the carboxylic acid group to the unprotonated nitrogen on the BZN or IMD molecule and typically results in the normalisation of the internal bond lengths. In the four structures published by Hashizume²⁷ the molecular complexes all formed in a 1:1 ratio and so there was also 100% proton transfer (Figure 6.45).

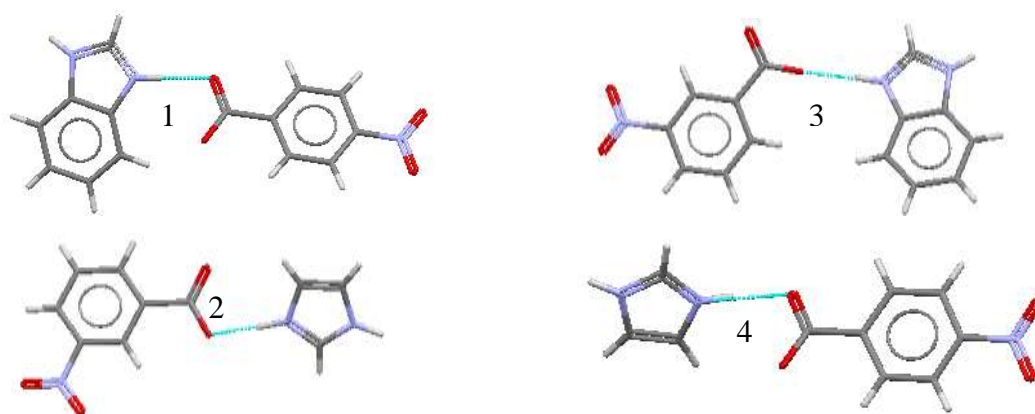


Fig. 6.45 – The structures of 1, benzimidazolium 4-nitrobenzoate 2, benzimidazolium 3-nitrobenzoate 3, imidazolium 3-nitrobenzoate 4, imidazolium 3-nitrobenzoate.

6.5.2 Normalisation of the Internal Bond Lengths and the Effect on Hydrogen Bond Length

The effect of proton transfer on the co-molecules involved are the normalisation of the bond lengths (carbon-oxygen and carbon-nitrogen for the carboxylate or imidazolium groups, respectively) and a delocalisation of the resulting charge across the functional group. Table 6.12 lists a range of similar molecular complexes, where the nitro group has been replaced with either a hydroxyl or halo group, with the resulting outcome on the internal and hydrogen bond lengths.

If the molecular complexes involving the nitrobenzoic acids are excluded, the C–O bond lengths are all similar with the minimum value being 1.230Å and the maximum 1.297Å. The mean value is 1.264Å. The carboxylic acid bond distances are normally ~1.36Å for a C–O single bond and ~1.23Å for a double bond, therefore the mean value found in the molecular

complexes corresponds to greater than double the single bond character and utilising the hydrogen bonds that were seen. This might be expected since the carboxylate oxygens are acting as the hydrogen bond acceptor within the structures. The nitrobenzoic acid molecular complexes (shaded yellow in Table 6.12) do not all follow this trend; the BZN-2NBA and BZN-3NBA fall within the range of the other molecular complexes by adopting more double bond characteristics, however, the other three structures exhibit much stronger single bond characteristics. Their carbon-oxygen bond lengths range from 1.314-1.329Å which is a little shorter than the normal 1.36Å length expected of a carbon oxygen single bond in a carboxylic acid. Similarly, the nitrogen-carbon bond lengths within the BZN and IMD molecules in most of the molecular complexes (i.e. not including the nitrobenzoic acid complexes) take a maximum value of 1.347Å, a minimum of 1.304Å and a mean of 1.330Å. This mean value has greater single bond characteristics when compared to the pure crystal structures of BZN and IMD which have C-N bond lengths of 1.315Å and 1.316Å for the double bond and 1.348Å and 1.336Å for single bonds, respectively. This again might be expected as both nitrogens have been protonated and act as the donors within the hydrogen bonds found in the crystal structures. However, once again, in the nitrobenzoic acid molecular complexes, the BZN and IMD molecules have carbon-nitrogen bond distances with different characteristics to those of the other molecular complexes. With carbon-nitrogen distances of between 1.250Å and 1.263Å, this is much more similar to that of a double bond and is even shorter than the double bond seen in the crystal structures of single component BZN and IMD. In these examples, as the bond lengths are short it might be expected that the nitrogens would be unprotonated; all complexes do, however, show proton transfer.

The N-H...O hydrogen bond distances of the nitrobenzoic acid molecular complexes are similar to those found in the other molecular complexes therefore there is no obvious effect on the hydrogen bond distances induced by the nitro group.

	C-O1(Å)	C-O2(Å)	N1-C(Å)	N2-C(Å)	HB1(Å)	HB2(Å)
BZN-2NBA ²⁴	1.214	1.273	1.319	1.308	2.728	2.887
BZN-3NBA ²	1.269	1.234	1.316	1.325	2.550	2.718
IMD-3NBA ²	1.328	1.314	1.252	1.258	2.644	2.745
BZN-4NBA ²	1.323	1.326	1.250	1.263	2.647	2.660
IMD-4NBA ²	1.320	1.329	1.256	1.256	2.644	2.742

BZN-6HPA	1.270	1.238	1.330	1.342	2.644	2.640
BZN-6HPA	1.273	1.251	1.341	1.328	2.763	n/a
BZN-3HPA	1.289	1.240	1.332	1.331	2.733	2.889
IMD-3HPS	1.284	1.244	1.337	1.337	2.649	3.011
BZN-2HBA	1.264	1.273	1.331	1.333	2.646	2.621
BZN-3HBA	1.260	1.270	1.330	1.325	2.697	2.700
BZN-4HBA	1.258	1.271	1.322	1.347	2.695	2.717
IMD-2HBA	1.247	1.279	1.304	1.317	2.699	2.729
IMD-3HBA	1.284	1.244	1.330	1.324	2.654	2.667
IMD-4HBA	1.25	1.28	1.33	1.33	2.66	2.74
BZN-3BrBA	1.230	1.292	1.332	1.335	2.843	n/a
BZN-4BrBA	1.239	1.283	1.329	1.328	2.597	2.848
BZN-3ClBA	1.297	1.237	1.341	1.326	2.282	n/a
BZN-4ClBA	1.251	1.288	1.334	1.339	2.642	2.688

Table 6.12. – List of molecular complexes where BZN = benzimidazole, IMD = imidazole, NBA = nitrobenzoic acid, HPA = hydroxypicolinic acid, HBA = hydroxybenzoic acid BrBA= bromobenzoic acid and ClBA = chlorobenzoic acid. The bond lengths C–O1, C–O2 represent the lengths in the carboxylate group and N1–C, N2–C the bond lengths between the nitrogen and central carbon in BZN and IMD. HB1 and HB2 represent the N–H···O hydrogen bond lengths between the nitrogens on the BZN or IMD and the carboxylate group.

6.5.3 Packing Effects

The nitro groups within the molecular complexes do not form the predominant interactions. They do however; form weaker hydrogen bonds with aromatic hydrogen atoms.

6.5.3.1 Benzimidazolium 3-Nitrobenzoate

These co-molecules generate a spiral structure of alternating benzimidazolium and 3-nitrobenzoate molecules connected through partially charged assisted $N^{\delta+}-H\cdots O^{\delta-}$ hydrogen bonds. Neighbouring spirals are connected via weak $C-H\cdots O^{\delta-}$ hydrogen bonds involving an oxygen of the nitro group and an aromatic hydrogen of the benzimidazolium of $C\cdots O$ distance of 3.553(6)Å (Figure 6.46).

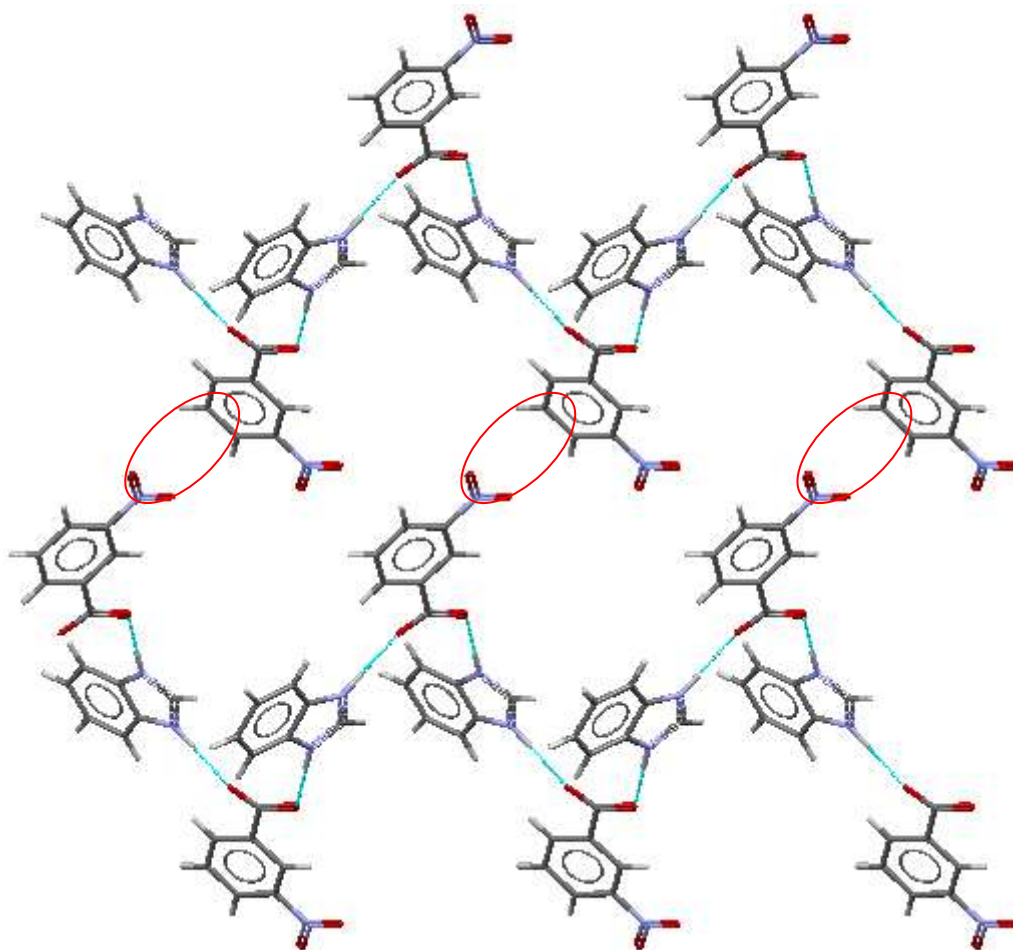


Fig. 6.46 – The benzimidazolium 3-nitrobenzoate molecular complex structure viewed along the *c*-axis. The spiral hydrogen bond motif runs along the *b*-axis with the weak C–H \cdots O $^{\delta-}$ hydrogen bonds (circled in red) connecting adjacent spirals.

6.5.3.2 Benzimidazolium 4-Nitrobenzoate

The benzimidazolium 4-nitrobenzoate structure adopts the same supramolecular synthons and motif as the benzimidazolium 3-nitrobenzoate molecular complex. Spirals of alternating co-molecules are held together by N $^{\delta+}$ –H \cdots O $^{\delta-}$ hydrogen bonds and are then connected to one another through weak C–H \cdots O $^{\delta-}$ hydrogen bonds. Again the acceptor atom is an oxygen of the nitro group, but in this case, the donor is an aromatic hydrogen atom from another 4-nitrobenzoate molecule (Figure 6.47).

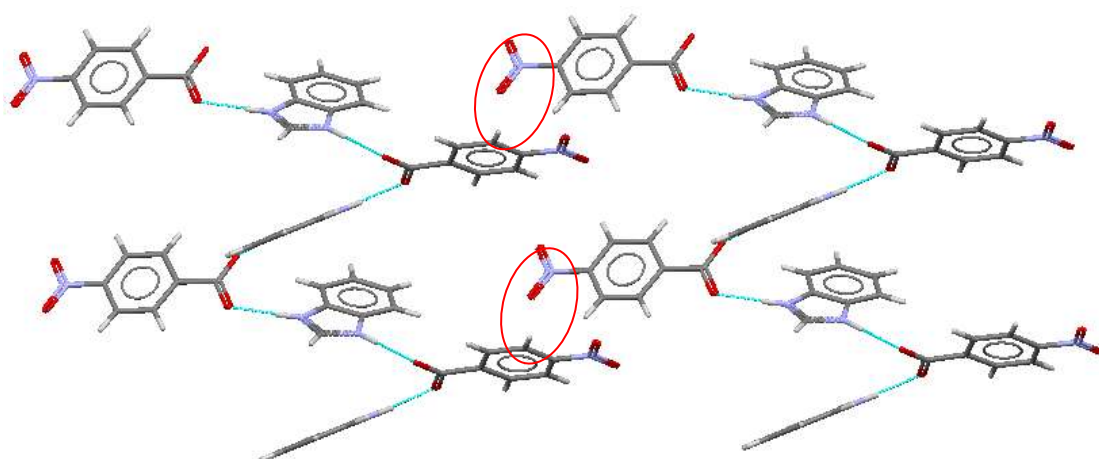


Fig. 6.47 – The benzimidazolium 4-nitrobenzoate molecular complex structure viewed along the *c*-axis. The spiral hydrogen bond motif runs along the *b*-axis with the weak C–H \cdots O $^{\delta-}$ hydrogen bonds (circled in red) connecting adjacent spirals.

6.5.3.3 Imidazolium 3-Nitrobenzoate

The main hydrogen bonds in the imidazolium 3-nitrobenzoate structure are two N $^{\delta+}$ –H \cdots O $^{\delta-}$ interactions between the carboxylate group and protonated nitrogens of the imidazolium. They arrange themselves into a four membered hydrogen bonded ring system containing two of each co-molecule. These hydrogen bonded rings are then connected through several C–H \cdots O $^{\delta-}$ weak hydrogen bonds involving the oxygens of the nitro group and $\pi\cdots\pi$ stacking interactions between the IMDH $^+$ molecules (blue circle) (Figure 6.48).

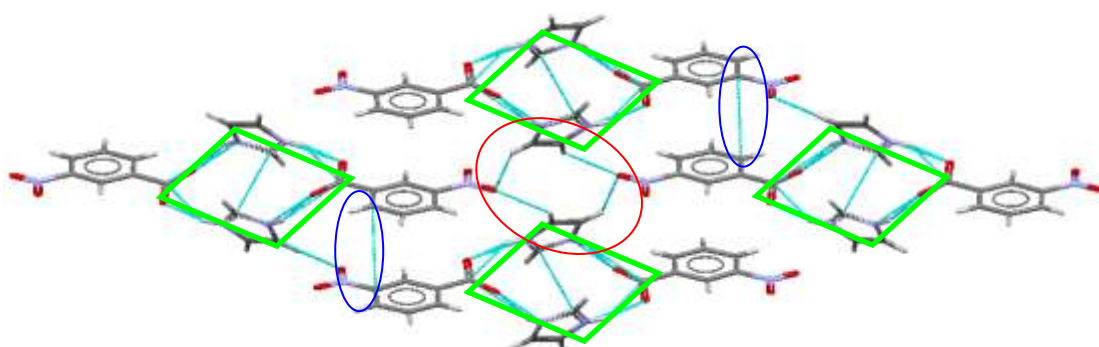


Fig. 6.48 – The imidazolium 3-nitrobenzoate molecular complex structure viewed along the *a*-axis. The hydrogen bonded rings (green boxes) are connected by weak carbon oxygen hydrogen bonds (circled in red) and $\pi\cdots\pi$ interactions (blue).

6.5.3.4 Imidazolium 4-Nitrobenzoate

The benzimidazole nitrobenzoic acid structures all share the same motif. The same can be said about the imidazolium structures. The imidazolium 4-nitrobenzoate molecular complex forms four membered hydrogen bonded rings held together by $N^{\delta+}-H\cdots O^{\delta-}$ hydrogen bonds. These rings are connected through $C-H\cdots O^{\delta-}$ weak hydrogen bonds involving the nitro group (Figure 6.49).

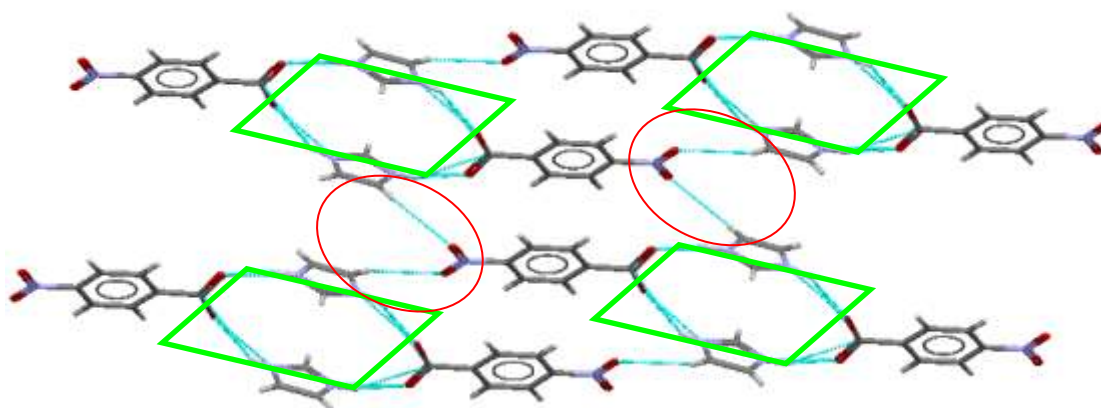


Fig. 6.49 – The imidazolium 3-nitrobenzoate molecular complex structure viewed along the *a*-axis. The hydrogen bonded rings (green boxes) are connected by weak carbon oxygen hydrogen bonds (circled in red).

6.6 Conclusions

The introduction of another basic atom into the system, in this case a nitrogen in the form of carboxyl and hydroxyl substituted pyridines, was intended to compete on two fronts; firstly with the other basic nitrogen on the benzimidazole for proton transfer, secondly for involvement in the potential hydrogen bonds. In regard to the proton transfer, in all the cases the proton from the carboxylic acid group has transferred to the benzimidazole molecule, as has been seen in all but two examples in this work (BZN : 3ClBA and BZN : 4FBA). However, this does not tell the whole story, as picolinic acid and 6-hydroxypicolinic acid have a history of undergoing tautomerisation with the proton transferring between the hydroxyl and the basic nitrogen. In both cases, within the molecular complex with benzimidazole, the co-molecule has undergone deprotonation with the proton transferring to the basic nitrogen of the benzimidazole. The result for the picolinic acid complex is that there is no proton available for tautomerisation to occur therefore it forms the zwitterion. The 6-

hydroxypicolinic acid molecule does have an available proton for tautomerisation and has occurred. Therefore proton transfer from the carboxylic acid group to the basic nitrogen of the same molecule would not be preferred over proton transfer from the hydroxyl group to the nitrogen within these two molecules.

When the basic nitrogen is unprotonated, the established N–H···O hydrogen bond is not favoured over a N–H···N hydrogen bond, with the N–H···O interaction forming the weaker part of a bifurcated hydrogen bond (Figure 6.50). Therefore it has competed with the carboxylic acid group to be the primary hydrogen bond acceptor and this designed intervention was successful.

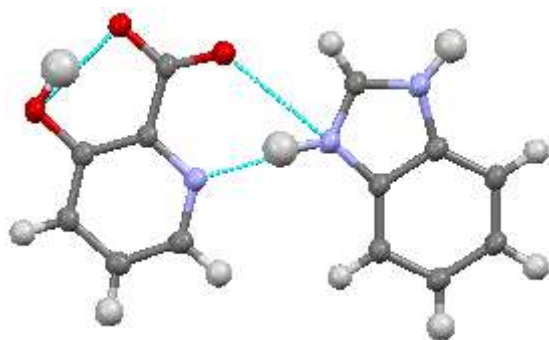


Fig. 6.50 – The bifurcated hydrogen bond of the $\text{BZNH}^+ : 3\text{-HPA}^-$ molecular complex, with the major component the N–H···N hydrogen bond and minor component being N–H···O.

The other possible outcome was that if the nitrogen was protonated, it would compete with the other protonated nitrogen on the benzimidazole for the primary hydrogen bond donor role. As the benzimidazole is found still to be protonated, the hydrogen bond donors from this molecule would be charged assisted and therefore still a more attractive prospect for hydrogen bond acceptors. With this being the case it was not surprising to see that in the benzimidazole and 6-hydroxypicolinic acid molecular complex the N atom of the pyridine was acting as a the donor in a hydrogen bond, however it was the weakest of the three primary hydrogen bonds within the structure at $2.915(2)\text{\AA}$. The solvate structure also had the named N atom within hydrogen bonds, it also produced one of the weaker hydrogen bonds in the structure and also had a length of $2.915(3)\text{\AA}$.

Scrutiny of the ΔpK_a difference values (Table 6.5) was not possible for molecular complexes containing the 6-hydroxypicolinic acid molecule as this value could not be obtained. For the molecular complexes where the values could be obtained the rule governing if a salt or co-

crystal will form has been accurate. All the ΔpK_a values lie above the 3 value that normally means a salt will be formed, which was the case.

The second part of the chapter focused on the benzimidazole and nitro-substituted benzoic acid series of molecular complexes. The object was to investigate if electronic properties affected structural features seen in other benzimidazole containing molecular complexes, for example proton transfer, the strength of the hydrogen bonds and the packing of the structures. As ever, proton transfer from the carboxylic acid group to the unprotonated N atom on the benzimidazole occurred, however the effect of this on the internal bond lengths of both the benzimidazole and carboxylate group was very different to previously seen. Whereas normally proton transfer promoted the normalisation of the N–C and C–O bond lengths, with distances around N \cdots C 1.33 Å and C \cdots O 1.25 Å representing N–C bond lengths a little shorter than characteristic single bonds and C–O lengths longer than characteristic double bond. In three out of the four molecular complexes containing 3- and 4-nitrobenzoic acid, the opposite effect was seen, with the N–C lengths adopting more double bond characteristics, N \cdots C 1.25 Å, and C–O greater single bond characteristics, 1.32 Å. These are the only molecular structures in all of the results generated in this work to behave in this way.

The nitro-groups always formed weaker interactions that connected the main supramolecular synthons or motifs together in a way similar to those seen in the halo substituted benzoic acid structures.

6.7 References for Chapter 6

- (1) G. W Evans and E. C. Johnson, *The Journal of Nutrition*, 1981, **111**, 68-75.
- (2) H Hosomi, S Takeda, H Kataoka and S. Ohba, *Acta Crystallographica section C*, 1998, **54**, 142-145.
- (3) M. Toma, A. Sánchez, J. S. Casas, J. Sordo, M. S. García-Tasende, E. E. Castellano, J. Ellena and I. Berdan, *Central European Journal of Chemistry*, 2003, **1**, 441-464.
- (4) A Cousson, J Proust and E. N. Rizkalla, *Acta Crystallographica section C*, 1991, **47**, 2065-2069
- (5) G Smith and U. D. Wermuth, *Acta Crystallographica section C*, 2010, **66**, 345-348.
- (6) D. Braga, S. L. Giaffreda, F. Grepioni, G. Palladion and M. Polito, *New Journal of Chemistry*, 2008, **32**, 820-828.
- (7) M Hemamalini and H. K. Fun, *Acta Crystallographica section E*, 2010, **66**, 49-50.
- (8) K Thanigaimani and P. T. Muthiah, *Acta Crystallographica section C*, 2010, **66**, 104-108.

- (9) K Thanigaimani, P Devi, P T Muthiah, D E Lynch and R. J. Butcher, *Acta Crystallographica section C*, 2010, **66**, 71-74.
- (10) K Sawada and Y. Ohashi, *Acta Crystallographica section C*, 1998, **54**, 1491-1493.
- (11) B. Kukoveca, Z. Popovića, G. Pavlovićb and M. R.Linarićc, *Journal of Molecular Structures*, 2008, **882**, 47-55.
- (12) B. Kukovec, Z. Popovi and G. Pavlovi, *Acta Chimica Slovenica*, 2008, **55**, 779-787.
- (13) G Q Bian, T Kuroda-Sowa, H Konaka, M Maekawa and M. Munakata, *Acta Crystallographica section C*, 2004, **60**, 338-340.
- (14) C. Sun, X. Zheng and L. Jin, *Journal of Inorganic and General Chemistry*, 2004, **630**, 1342-1347.
- (15) W B Wright and G. S. D. King, *Acta Crystallographica*, 1953, **6**, 305-317.
- (16) C. Scherlinger, *Acta Crystallographica section C*, 1983, **39**, 232-234.
- (17) S R Jebas and T. Balasubramanian, *Acta Crystallographica section E*, 2006, **62**, 5621-5622.
- (18) J Zhu and J. Zheng, *Jiegou Huaxue, Chinese Journal of Structural Chemistry.*, 2004, **23**, 417.
- (19) F Takusagawa and A. Shimada, *Acta Crystallographica section B*, 1976, **32**, 1925-1927.
- (20) R. H W Au, C.S A Fraser, D. J Eisler, M. C Jennings and R. J. Puddephatt, *Organometallics*, 2009, **28**, 1719-1729.
- (21) W. Chena, Z. Yaob, D. Liua, S. Yinga and J. Liua, *Journal of Coordination Chemistry*, 2009, **62**, 1553-1560.
- (22) P. Kavuru, D. Aboarayes, K. K Arora, H. D. Clarke, A. Kennedy, L. Marshall, T. T. Ong, J. Perman, T. Pujari, L. Wojtas and M. J. Zaworotko, *Crystal Growth & Design*, 2010, **10**, 3568-3584.
- (23) G. Portalone, *Acta Crystallographica section E*, 2009, **65**, 954.
- (24) Z L Wang and L. H. Wei, *Acta Crystallographica section E*, 2007, **63**, 2574-2575.
- (25) A. Domenicano, G. Schultz, I. Hargittai, M. Colapietro, G. Portalone, P. George and C. W. Bock, *Structural Chemistry*, 1988, **1**, 107-122.
- (26) M. Tonogaki, T. Kawata, S. Ohba, Y. Iwata and I. Shibuya, *Acta Crystallographica section B*, 1993, **49**, 1031-1039.
- (27) D. Hashizume, M. Iegaki, M. Yasui, F. Iwasaki, J. Meng, Z. Wen and T. Matsuura, *Acta Crystallographica section C*, 2001, **57**, 1067-1072.
- (28) G. M. Sheldrick, *Acta Crystallographica section A*, 2008, **64**, 112-122.
- (29) L. J. Farrugia, *Journal of Applied Crystallography*, 1999, **32**, 837-838.
- (30) A Altomare, G Cascarano, C Giacovazzo, A Guagliardi, M.C Burla and M. C. G Polidori, *Journal of Applied Crystallography*, 1994, **27**, 435-436.
- (31) D.J. Watkin, C.K. Prout, J.R Carruthers, P.W. Betteridge and R. I. Cooper, *Journal of Applied Crystallography*, 2003, **36**, 1487.
- (32) O. Bensaude, M. Chevrier and J. E. Dubois, *Journal of The American Chemical Society*, 1978, **100**, 7055-7060.
- (33) A. Touceda, *Polyhedron*, 2007, **4**, 1296-1302.
- (34) L Palatinus and G. Chapuis, *Journal of Applied Crystallography*, 2007, **40**, 786-790.

7 A Comparison Study of Benzimidazole and Imidazole Containing Molecular Complexes with a Range of Related Co-Molecules

This chapter aims to compare the molecular complexes generated between BZN and IMD and a range of co-molecules. The method adopted will consist of the direct comparison of a BZN molecular complex with the identical IMD molecular complex, and comparisons between BZN and IMD molecular complexes within a systematic series of co-molecules. There will be many different aspects to the comparisons, including hydrogen bond strength, physical properties and crystallographic information; however there will be one main theme throughout them all – crystal engineering. The comparisons will focus on the hydrogen bonding patterns and motifs taking into account the library of interactions that have been generated in the complexes discussed in previous chapters with the aim of explaining the structures generated.

The co-molecules can be split into four categories, with each category having different areas of interest and associated aims:

- the mono-hydroxy-benzoic acid series which have successfully been cocrystallised with BZN producing a library of hydrogen bonds with predictable motifs were used with IMD to further investigate the robustness and predictability of these motifs;
- a related set of compounds, aromatic dicarboxylic acids, were cocrystallised with BZN and IMD to test further the robustness of the hydrogen bonds and motifs generated with the hydroxy-benzoic acid materials;
- halo-substituted benzoic acids were cocrystallised with BZN to investigate the occurrence of polymorphism with an aim to control selectively the growth of individual forms. Cocrystallisations with IMD had a primary aim of investigating the influence of the halo- atom on the structure generated;
- experiments with a series of dicarboxylic acids with varying chain length and conjugation, for example fumaric and succinic acid, with both BZN and IMD were initially targeted at engineering network structures with differing pore sizes.

7.1 Introduction – Co-molecules

7.1.1 2-/ 3-/ 4-Hydroxybenzoic Acid

Refer to Sections 4.1.1 to 4.1.3, where these components are discussed.

7.1.2 4-Fluoro- / 4-Bromo- Benzoic Acid

Refer to Sections 5.1.3 and 5.1.9, where these components are discussed.

7.1.3 Phthalic Acid

Phthalic acid is an organic compound derived from benzene and used in the manufacture of dyes, perfumes, pharmaceuticals, and synthetic fibres. It was first discovered in 1836 by Auguste Laurent, who initially believed it was naphthalenic acid, before its nature was correctly determined years later. There are four entries of the same structure for phthalic acid in the CSD with differing R-factor and associated temperatures. Figure 7.1 displays the structure published by Ermer¹ (CSD ref PHTHAC02). The structure is made up of chains consisting of carboxylic acid dimers, which are held together through weaker interactions.

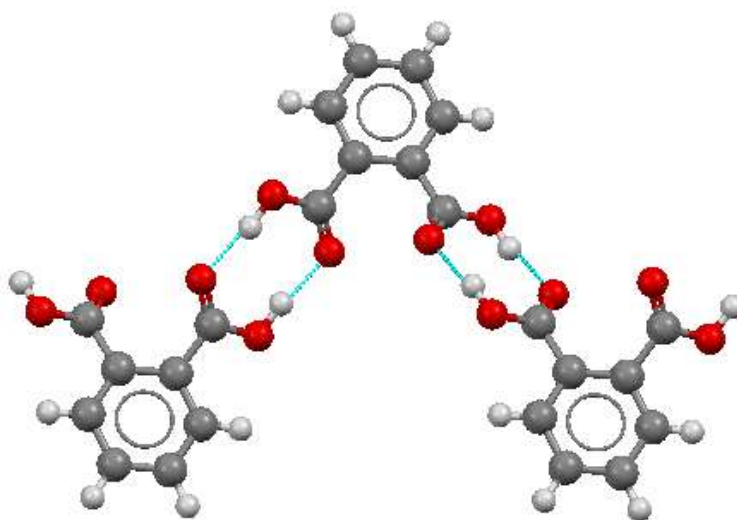


Fig. 7.1 – Structure of phthalic acid, which is seen to exploit the carboxylic acid dimer motif.

Phthalic acid is well studied and is found as a component in a large number of crystal structures, for example in organometallics with cobalt and chromium², and cocrystallised in its native structure with cinnamamide³ (CSD ref EBOSIX) and benzene-1,2-dicarboxylic acid⁴ (CSD ref EBOSIX02) (Figure 7.2). There are also molecular complexes with phthalic acid in its deprotonated state, phthalate, with other small organic molecules including 4,4'-iminodipyridinium⁵ (CSD ref BOGTAT) and 2,6-dimethylpyridinium⁶ (Figure 7.2) (CSD ref GUHREG). There are also many examples of complexes with the doubly deprotonated phthalate molecule.

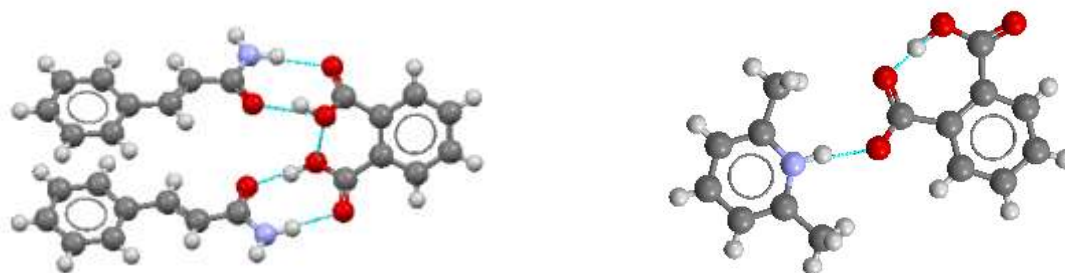


Fig. 7.2 – LHS, crystal structure of the molecular complex of phthalic acid and benzene-1,2-dicarboxylic acid; RHS, the phthalate ion in the ionic complex formed with 2,6-dimethylpyridinium.

7.1.4 Isophthalic Acid

The main use of isophthalic acid is in the production of the synthetic fibre, polybenzimidazole (PBI), which has an extremely high melting point and does not readily ignite, because of its thermal and chemical stability⁷. Therefore PBI is used to make protective clothing, for examples fire-fighter turnout coats and suits, astronaut space suits, high temperature protective gloves, welders' apparel, race driver suits, braided packing, and aircraft wall fabrics⁸. The crystal structure, solved by Derissen in 1974⁹ (CSD ref BENZDC01), is similar to that of phthalic acid, where the carboxylic acid groups form dimers that create chains, with the chains held together through lesser interactions (Figure 7.3).

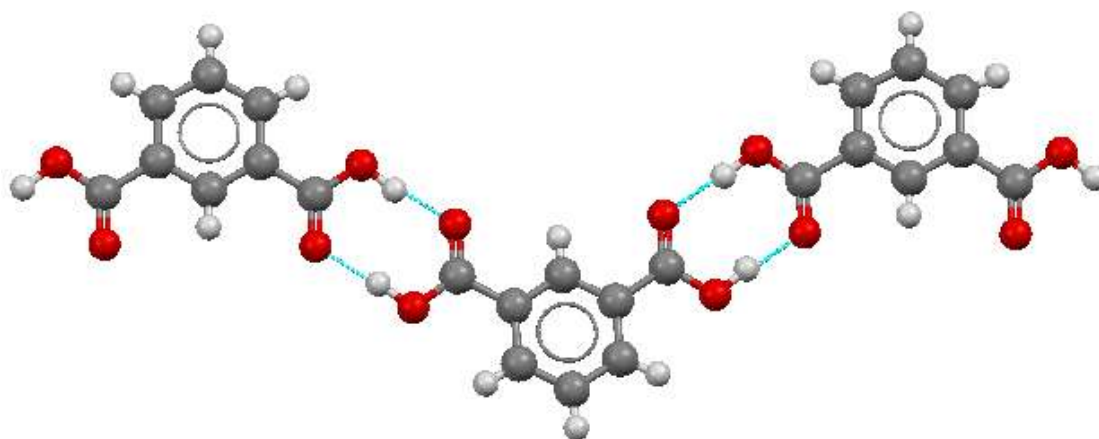


Fig. 7.3 – The crystal structure of isophthalic acid, which exhibits the common carboxylic acid dimer motif.

Many crystal structures of isophthalic acid in organometallic complexes have been deposited in the CSD, for example with lithium, sodium caesium and rubidium¹⁰. Importantly, molecular complex structures with both BZN¹¹ and IMD¹² have already been solved and deposited in the CSD. The BZN : isophthalic acid structure (CSD ref VARJAA) shown in Figure 7.4 exhibits hydrogen bonding ring motifs that combine to form a sheet. There are issues with the published structure: firstly it was undertaken at room temperature, the hydrogens have not all been accounted for and there is disorder on both co-molecules. The IMD : isophthalic acid complex (CSD ref MEQOOO), also shown in Figure 7.4, is a relatively well determined structure, however has it been solved at room temperature. The structure is made up of chains of alternate hydrogen bonded co-molecules. These chains also link through hydrogen bonds to chains above and below resulting in the stacking of these chains. These stacks are then linked through weaker interactions in the third direction.

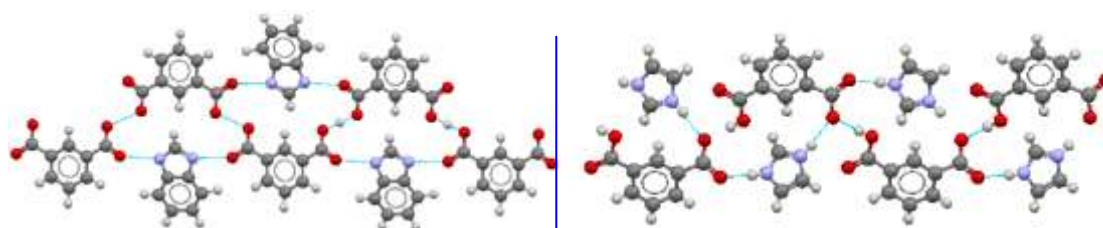


Fig. 7.4 – LHS, structure of the benzimidazole : isophthalic acid molecular complex; RHS, the structure of the imidazole : isophthalic acid molecular complex.

7.1.5 Terephthalic Acid

Nearly all the world's supply of terephthalic acid is used to make polyethylene terephthalate (PET), which has two main uses, in synthetic fibres (around 60% of market) and in liquid bottle holders (around 30%)¹³. This polymer is the sole material in the bottle industry with the major advantage of being recyclable back to its starting materials; it has resin identification code 1 (a set of symbols placed on plastics to identify the polymer type). Terephthalic acid has two other uses, of much lesser extent: in the production of polybutylene terephthalate (PBT) which is a thermoplastic engineering polymer used as an insulator in the electrical and electronics industries; and in research laboratories in engineering materials linked through hydrogen and coordination bonds. With terephthalic acid's major importance in industry, it is not surprising to see there are thirteen separate entries in the CSD. There are three known polymorphs, two different triclinic structures (CSD ref TEPHTH¹⁴ and TEPHTH12¹⁵) and a monoclinic structure (CSD ref TEPHTH13¹⁶) (Figure 7.5). All the structures have the same hydrogen bond pattern, a chain of terephthalic acid molecules connected through carboxylic acid dimers. The polymorphs differ in their packing arrangements.

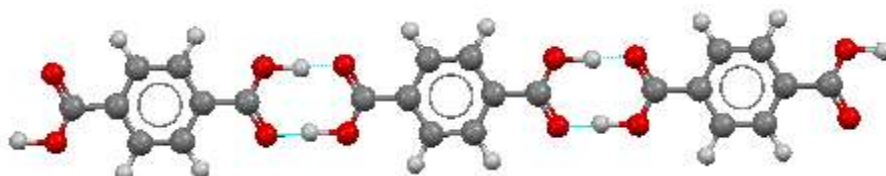


Fig. 7.5 – The carboxylic acid dimer that exists in all the terephthalic acid structures.

There are many compounds and complexes of terephthalic acid in the CSD: with metals including cadmium¹⁷ and with small organic molecules, most significantly imidazole¹⁸ (CSD ref HILSAX) (Figure 7.6). The structure of this imidazole : terephthalic acid complex consists of an interlinked hydrogen bonded network that expands in all three dimensions.

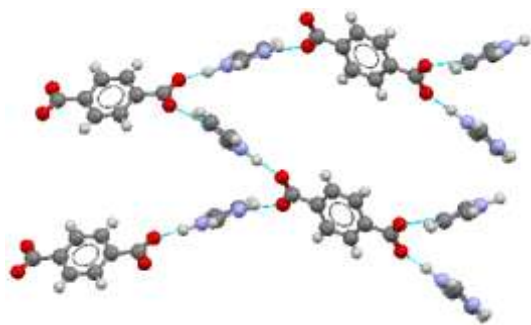


Fig. 7.6 – The imidazole : terephthalic acid molecular complex.

7.1.6 Fumaric acid

Fumaric acid is an unsaturated dicarboxylic acid with a four carbon chain, with the acid groups in *trans* position about the central C=C bond. They are in the *cis* conformation in the isomeric maleic acid. Fumaric acid has a fruit like taste and is a well known food additive. It is also used in the manufacturing of polyester resins and dyes. There are two polymorphs of the native structure, the latest was solved in 1966 by Brown¹⁸ (CSD ref FUMACC) (Figure 7.7), which adopts the carboxylic acid dimer motif that expands to form chains.

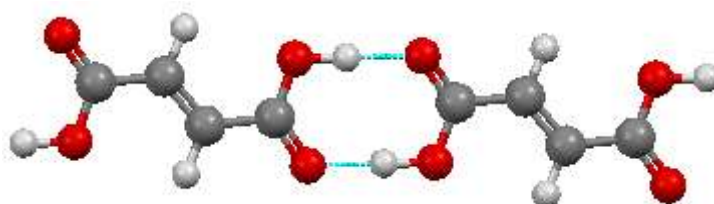


Fig. 7.7 – The carboxylic acid dimer motif adopted in the fumaric acid structure.

There are a few structures with fumaric acid as a component deposited in the CSD, of greatest importance is that with imidazole, imidazolium hydrogen fumarate. The structure was first solved in 2001 with CSD reference MEQPED¹² and adopts the ladder motif, with chains of fumaric acid and steps of imidazole (Figure 7.8).

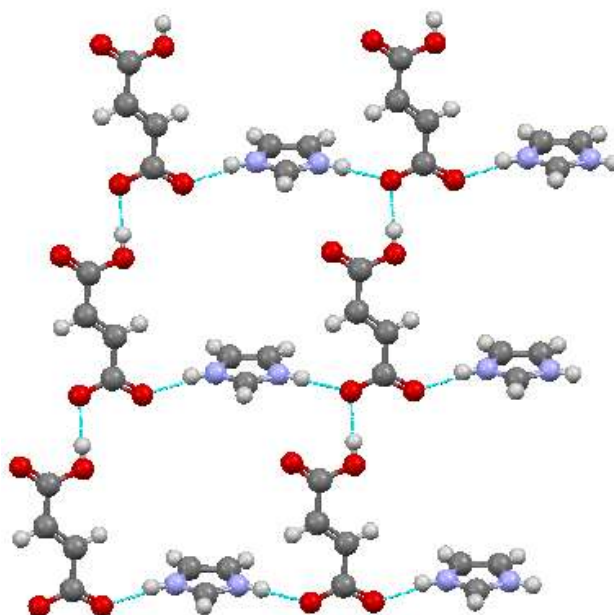


Fig. 7.8 – The ladder motif of the imidazolium hydrogen fumarate structure, with the uprights consisting of fumaric acid chains and the steps of imidazolium molecules.

7.1.7 Succinic acid

Historically succinic acid was known as spirit of amber and was used to ease rheumatic aches and pain. Nowadays it is used as a sweetener in the food industry¹⁹. It is the saturated form of fumaric acid. There are two polymorphs of succinic acid, a triclinic²⁰ (Figure 7.9 LHS) and a monoclinic form²¹ (Figure 7.9 RHS). They both are constructed by chains of succinic acid molecules using the carboxylic acid dimer (Figure 7.9 top), but differ in their packing arrangements.

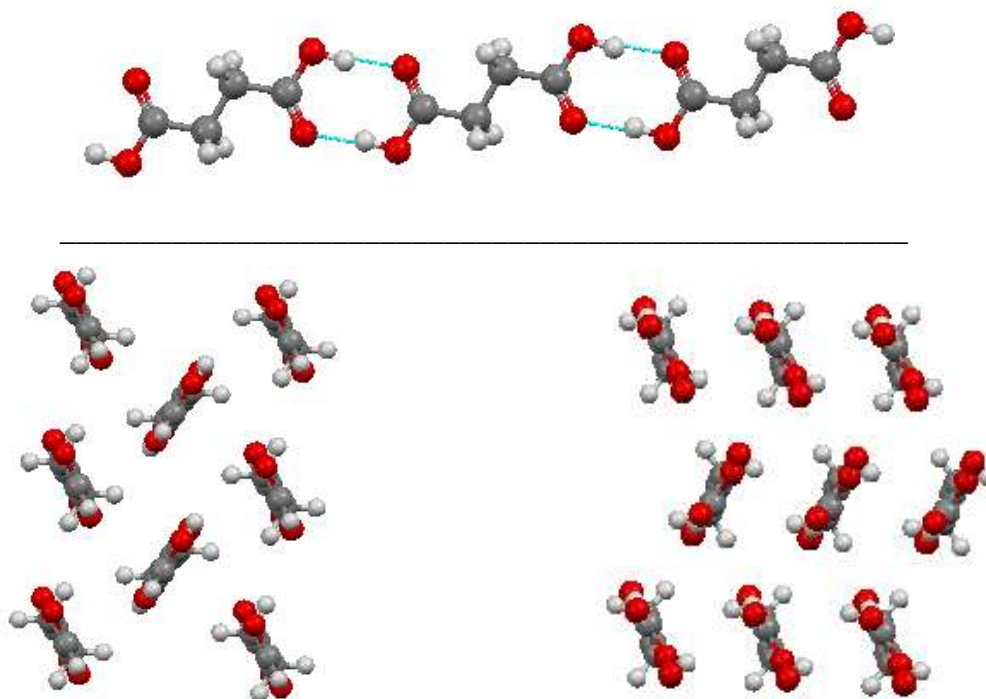


Fig. 7.9 – top, the carboxylic acid dimer that is the main hydrogen bonding pattern for both polymorphs of succinic acid, with the packing shown below, LHS, triclinic form, RHS, monoclinic form.

There are numerous examples of the occurrence of native succinic acid, and both its singly and doubly deprotonated forms in molecular complexes, of particular interest here is the imidazolium hydrogen succinate structure (Figure 7.10). This structure came from the body of work by MacDonald¹² that also reported the structures of imidazole with fumaric acid, isophthalic acid, malonic acid and a range of other carboxylic acids. This work found that proton transfer occurred and resulted in $N-H\cdots O$ hydrogen bonds being formed, and MacDonald summarised the structures as follows: *“These strong hydrogen bonds generate two types of chains that intersect at the anions and form polar hydrogen-bonded layers with four different motifs. These layers serve as scaffolds with which to control molecular packing in two dimensions for engineering the structures of crystals. All imidazolium cations function as multidentate proton donors by forming two or three $C-H\cdots O$ hydrogen bonds in addition to two $N-H\cdots O$ hydrogen bonds. Strong $O-H\cdots O$ and $N-H\cdots O$ hydrogen bonds define structure and connectivity within layers, while weaker $C-H\cdots O$ hydrogen bonds dominate interactions between layers in these salts”*¹².

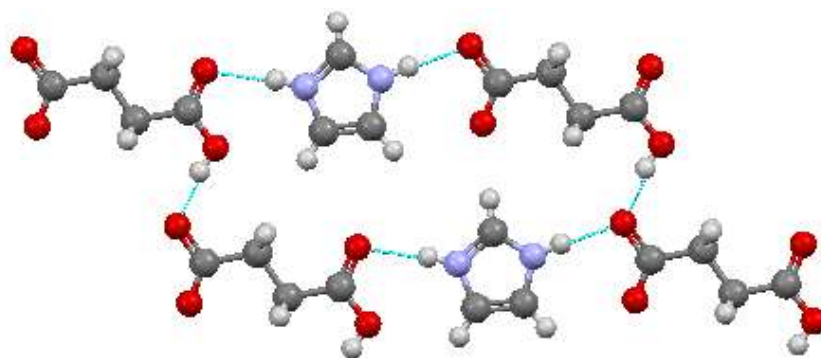


Fig. 7.10 – Basic building block of the imidazolium succinate ionic molecular complex.

7.1.8 Maleic acid

As stated, maleic acid is the *cis*- form of butenedioic acid and is primarily used in industry to form fumaric acid, the *trans*- form. There are two polymorphic forms of maleic acid which are both discussed by Jones²². Form I (CSD ref MALIAC12), shown in Figure 7.11, consists of sheets of hydrogen bonded maleic acid molecules with weaker interactions operating between the sheets. Form II has the same hydrogen bonding pattern, however the packing of the structure differs.

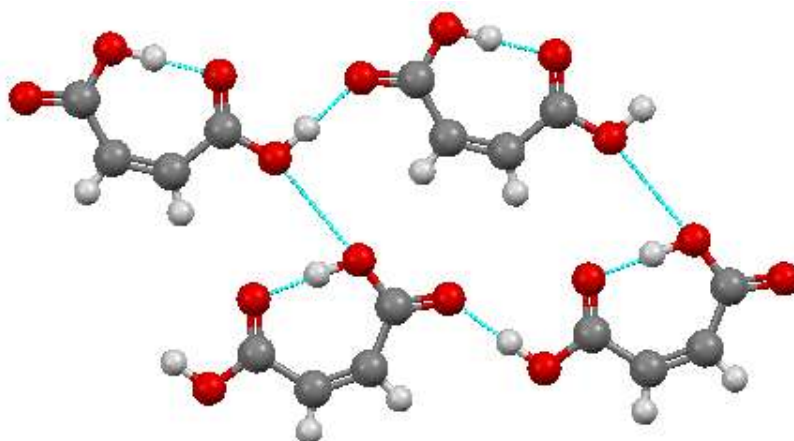


Fig. 7.11 – The structure of maleic acid Form I, showing the main hydrogen bonding pattern.

There are numerous molecular complexes containing maleic acid and its protonated form. Of most interest here is the molecular complex with imidazolium (Figure 7.12). This structure, first solved in 1972, was re-determined by both X-ray and neutron diffraction in 1980²³ (CSD ref IMZMAL12 & IMZMAL13). The structure adopts the 1:1 hydrogen bonded ring motif, using the charge assisted N-H \cdots O hydrogen bonds that result from the proton transfer.

Between the hydrogen-bonded rings are two interactions including C-H...O weak hydrogen bonds.

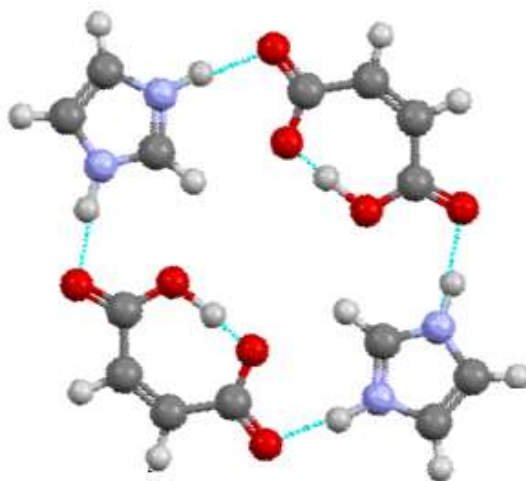


Fig. 7.12 – The hydrogen bonded ring motif of the imidazolium maleate molecular complex.

7.1.9 Malonic acid

Malonic acid is systematically known as propanedioic acid. Malonic acid is an important molecule within the body as it acts as a competitive inhibitor of succinate dehydrogenase in the respiratory electron transport chain. It has no real industrial applications in its native form. There are two polymorphic forms of malonic acid and two deuterium isotope induced polymorphs. The non-deuterated forms are triclinic²⁴ (CSD ref MALNAC02) and triclinic beta²⁵ (MALNIA04) and the deuterated forms are an orthorhombic alpha²⁶ (CSD ref MALNAC03) and triclinic gamma²⁷ (CSD ref MALNA08). All the different forms have the same basic building block, a carboxylic acid dimer (Figure 7.13), with the structures adopting different packing arrangements.

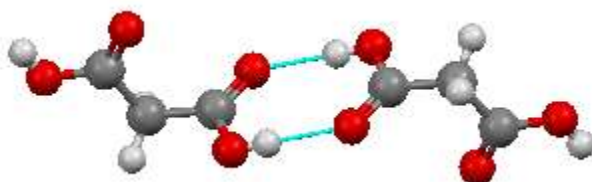


Fig. 7.13 – The basic dimeric hydrogen bonded building block of all the polymorphic forms of malonic acid.

The molecular complexes deposited within the CSD containing the deprotonated form of malonic acid, malonate, utilise a wide range of co-molecules, including metals and small organic molecules, such as neptunium²⁸, nickel²⁸ (CSD ref QARVAH), DL-histidine²⁹ (CSD ref CAMWOD) and most importantly for the work presented here, imidazole¹¹ (CSD ref. VARHOM). The malonate imidazolium hydrate complex (Figure 7.14) contains a disordered water molecule and disordered carboxylic acid groups. The structure adopts hydrogen bonded chains of alternate co-molecules which are held through hydrogen bonds to the water molecule in one direction to create a ladder style motif, while weaker hydrogen bonds form between the chains to create layers. A molecular complex containing malonic acid with benzimidazole has also been solved and published³⁰ (CSD ref MIZMUE). In this structure the main motif is a linear chain of hydrogen bonded alternate co-molecules (Figure 7.14). There are a few problems with the structure which are likely to stem from the fact that the diffraction experiment was undertaken at room temperature (20°C) and that the hydrogens were fixed geometrically and allowed to ride on the parent carbon atoms. There is thus no proton transfer presented in the published structure, which is unlikely as benzimidazole readily accepts protons from carboxylic acid groups when in a 1:1 molecular ratio, as is the case here. Also the carbon oxygen bond lengths are inconsistent, with double bonds apparently having longer distances than single bonds. The authors of this paper were focused on computational methods and used the diffraction experiment to support their measurements; unfortunately it was never considered that proton transfer might occur.

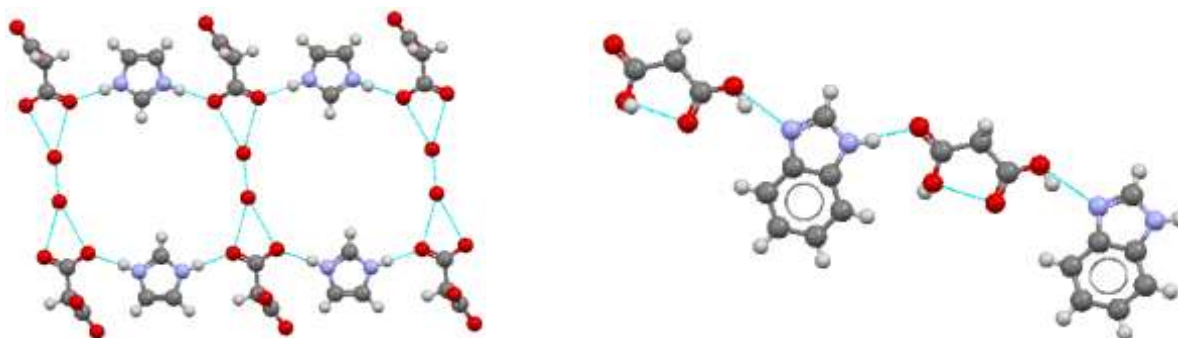


Fig. 7.14 – The imidazolium malonate hydrate structure consists of chains of alternate co-molecules connected through the disordered water molecules.

7.1.10 Benzoic Acid

Benzoic acid is a very important molecule, not necessarily in its native form but either in the salt form, where it is used as a food preservative as it inhibits the growth of mold/yeast³¹ or as a precursor to many important organic chemicals. Its structure was first solved in 1955, however the most accurate structure, determined by neutron diffraction, was published in 1996 by Wilson et al³² (Figure 7.15). The molecules adopt the carboxylic acid dimer motif, with the protons involved in the hydrogen bond disordered over two sites. The neutron experiment found that the occupancy levels on these two sites differed with varying temperature.

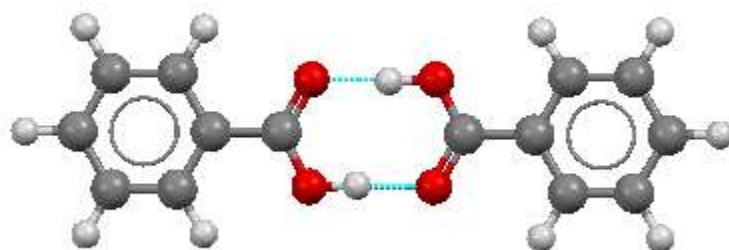


Fig. 7.15 – The carboxylic acid dimer that is the building block of the benzoic acid structure.

There are a host of materials that contain benzoic acid and / or its deprotonated form (benzoate), including salts, molecular complexes, organometallics and solvates. A molecular complex with imidazolium was published in 2006 (CSD ref HEPXUW) by Baruah et al³³. The structure adopts the linear chain motif with alternating hydrogen bonded co-molecules (Figure 7.16).

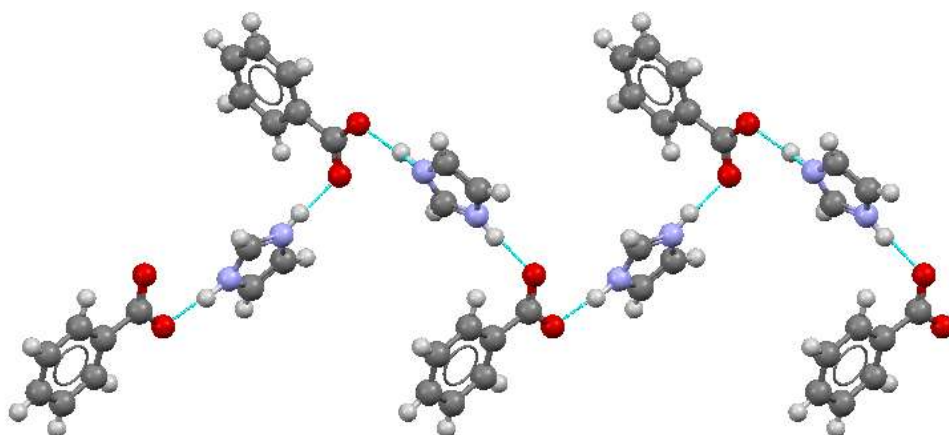


Fig 7.16 – The linear chain of alternating hydrogen bonded co-molecules that exists in the imidazolium benzoate molecular complex.

7.2 Summary of Results

Cocrystallisation reactions with IMD and BZN and a range of co-molecules have produced a series of molecular complexes. All of these have been analysed, primarily with single crystal X-ray diffraction.

As discussed in Chapter 4, BZN has successfully been cocrystallised with the mono-hydroxy substituted benzoic acids series producing a range of molecular complexes with predictable hydrogen bonding patterns. The successful cocrystallisation of IMD with the same mono-hydroxy substituted benzoic acids series is also reported here to produce new molecular complexes (Table 7.1). These new structures are all in a 1:1 molecular ratio, with proton transfer occurring (see Section 7.2.1) and utilising the hydrogen bond patterns that were seen within the other BZN structures studied.

	Imidazole	Source	Benzimidazole	Source
2-hydroxyBA	1:1	New	1:1 + 1:2	New
3-hydroxyBA	1:1	New	1:1 + 2:1	New
4-hydroxyBA	1:1	New	2:1	New

Table 7.1. – Summary of the molecular complexes generated between cocrystallisation experiments between BZN and IMD and the mono-substituted benzoic acid series. In the Source column of the table, “New” represents complexes previously undiscovered until this research and “CSD” means the complex already been structurally determined and deposited in the CSD.

Cocrystallisations with the aromatic dicarboxylic acids series produced previously undiscovered molecular complexes with BZN in a 1:1 molecular ratio (Table 7.2). The X-ray diffraction experiment of the BZN complex with terephthalic acid produced a suitable data set which resulted in a good quality structure, but problems with crystal quality, namely twinning, has resulted in poor data quality for the molecular complexes of BZN with isophthalic and phthalic acid. The structures of complexes of imidazole with terephthalic and isophthalic acid were previously known, but not with phthalic acid. Unfortunately at the time of writing no suitable crystals of IMD with phthalic acid have been produced.

	Imidazole	Source	Benzimidazole	Source
Terephthalic acid	1:1	CSD	1:1	New
Isophthalic acid	1:1	CSD	1:1	CSD (RD)
Phthalic acid	n/a	n/a	1:1	New

Table 7.2 – Summary of the molecular complexes that exist between IMD and BZN with aromatic dicarboxylic acids. In the Source column of the table, “New” represents molecular complexes generated for the first time during this research, “CSD” accounts for those that have already been solved while “RD” stands for re-determined, i.e. cases where a new X-ray diffraction experiment was attempted to get a improved data set than that available in the literature.

In Chapter 5, a wide range of new molecular complexes containing BZN and mono-substituted halo-benzoic acids were reported and the results discussed. Cocrystallisation experiments were also set-up using the mono-substituted halo-benzoic acid series with imidazole; the successful generation of molecular complexes with 4-fluoro- and 4-bromo-benzoic acids can be reported (Table 7.3). Unfortunately the other cocrystallisations did not produce suitable crystals for X-ray diffraction; however it is believed that with the correct crystallisation conditions that can be rectified. This section will also cover the cocrystallisation of IMD and BZN with benzoic acid and the resulting molecular complexes generated.

	Imidazole	Source	Benzimidazole	Source
4-fluoroBA	1:1	New	1:1	New
4-bromoBA	1:1	New	1:1	New
Benzoic acid	1:1	CSD	1:2	New

Table 7.3 – Summary of the successful cocrystallisations between IMD and mono-substituted halo-benzoic acid series with the corresponding BZN molecular complex.

Cocrystallisations with a range of dicarboxylic acids produced four new molecular complexes (Table 7.4); BZN with fumaric acid, succinic acid, maleic acid and IMD with malonic acid all in a 1:1 molecular ratio and all with associated proton transfer. A model that better represents the benzimidazole and malonic acid complex has also been produced. Structures containing IMD with fumaric, succinic, maleic acid and a malonic acid hydrate have already been solved and deposited in the CSD.

	Imidazole	Source	Benzimidazole	Source
Fumaric acid	1:1	CSD	1:1	New
Succinic acid	1:1	CSD	1:1	New
Maelic acid	1:1	CSD	1:1	New
Malonic acid	1:1 (1:1 hydrate)	New (CSD)	1:1	CSD (RD)

Table 7.4 – Summary of the successful cocrystallisation experiments between IMD and BZN with dicarboxylic acids. In the Source column of the table, “New” represents molecular complexes generated for the first time during this research, “CSD” accounts for those that have already been solved. “RD” represents the benzimidazole : malonic acid molecular complex structure which has been greatly improved in this work from that reported in the CSD.

7.2.1 Benzimidazolium, Imidazolium – Proton Transfer

As discussed in previous chapters, in cases where the crystallisation product is in a 1:1 stoichiometric ratio of BZN and a carboxylic acid containing molecule, the BZN is protonated through hydrogen transfer from the carboxylic acid group onto the normally unprotonated nitrogen atom in the five-membered ring, creating a benzimidazolium molecule (BZNH^+). The same process occurs with IMD in the presence of a carboxylic acid containing molecule in a 1:1 stoichiometric ratio; an imidazolium molecule is created (IMDH^+) (Figure 7.17). The result of the proton transfer on the IMDH^+ molecule is a delocalisation of the charge across the five-membered ring, reflected in the equalisation of the internal bond lengths $\text{N}^{\delta+}\text{-C}$ and bond angles $\text{C-N}^{\delta+}\text{-C}$. The delocalisation of the charge has the effect of creating a partial positive charge on both nitrogens. This effect has been reported in many structures involving BZN and IMD.

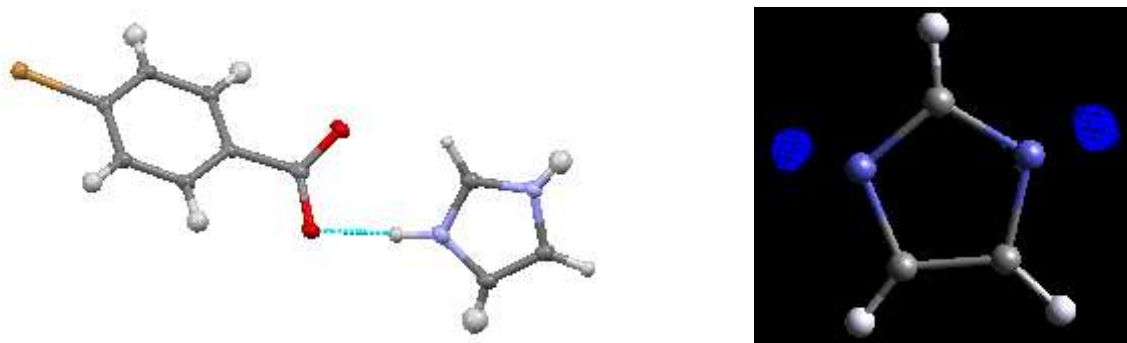


Fig. 7.17 – LHS, the imidazolium molecule with 4-bromobenzoate, in which both nitrogens are protonated. RHS, the MCE Fourier difference map generated where the H atoms located on a nitrogen atom have been omitted from the model, clearly showing that both nitrogen atoms are protonated.

The consequence for the co-molecule that has been deprotonated is the creation of a negative charge, which is delocalised over the carboxylic acid group resulting in equalisation of the C-O and C=O bond lengths in the carboxylate group.

7.2.2 Potential Hydrogen Patterns and Hydrogen Bond Motifs

The co-molecules involved in these studies have the same functional groups as those used in Chapters 4 and 5, pointing to a series of possible hydrogen bond patterns and supramolecular synthons identical to those seen in those chapters. Considering the formation of the molecular ion species and the hydrogen bonding patterns seen in structures discussed in previous chapters, a library of hydrogen bonding patterns and motifs can now be formed (Figure 7.18). It would be highly likely that the structures produced would adopt one of these hydrogen bonding patterns and likely to adopt one of the motifs. The motifs outlined are just the general trend, for example K represents the ladder motif which can also have a BZN dimer as the step and be a cross linked ladder, L represents the hydrogen bonded ring motif, which also has variances etc.

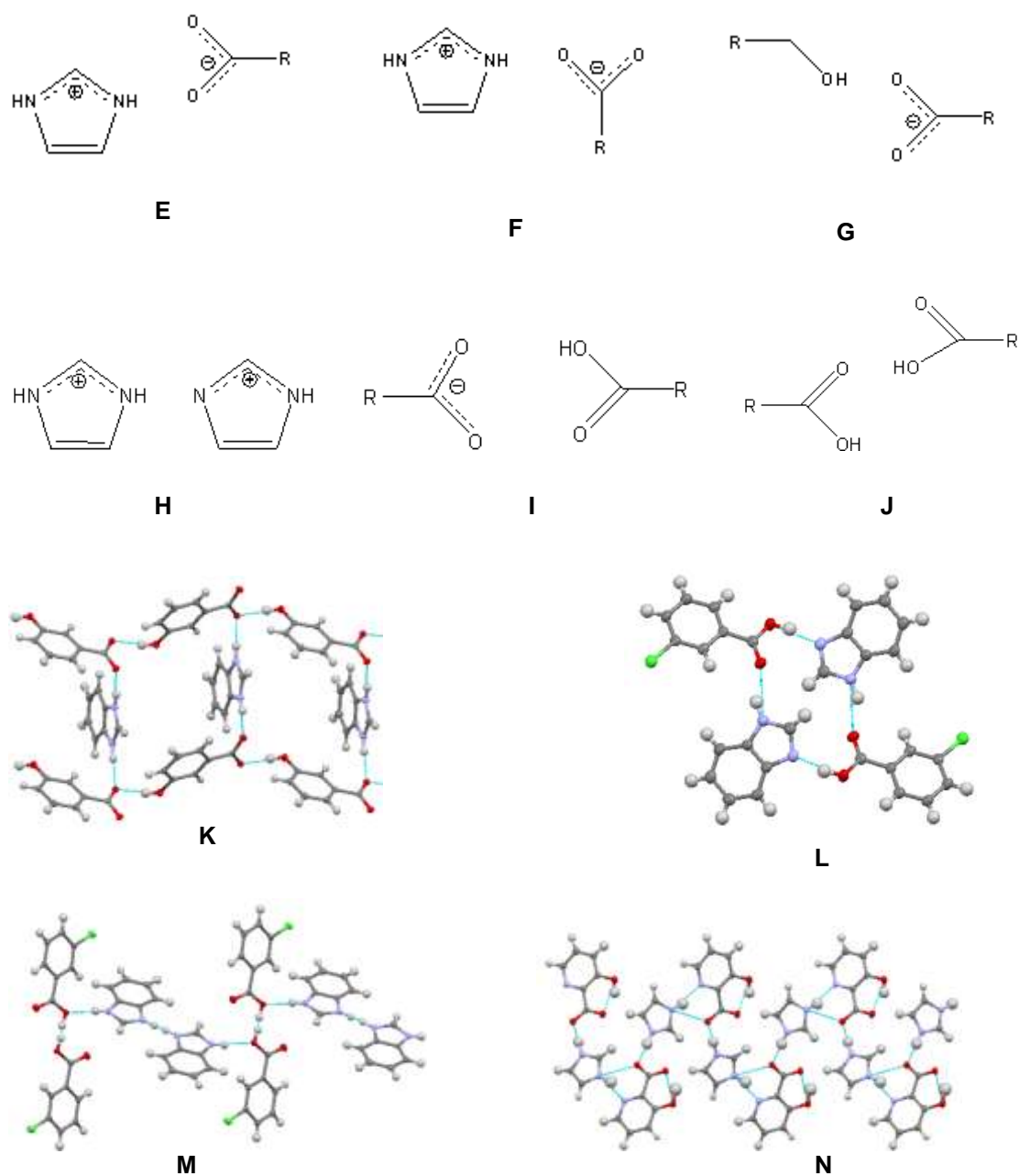


Fig. 7.18 – The library of hydrogen bond patterns that the molecular complexes are highly likely to adopt. E, F, G, H, I and J are all seen in other molecular complexes. The motifs are defined as the general descriptor of these interactions; K is the ladder motif, L is the hydrogen bonded ring motif, M is the co-molecule dimer motif while N is an example of a linear chain of alternate co-molecules.

7.3 Crystallographic Data

Compound	IMD 2-HBA	IMD 3-HBA	IMD 4-HBA	IMD 4-FBA	IMD 4-BrBA	IMD Malonate
Formula	C10 H10 N2 O3	C10 H10 N2 O3	C10 H10 N2 O3	C10 H9 F N2 O2	C10 H9 Br N2 O2	C6 H8 N2 O4
ApKa (1:1)	4.01	2.91	2.42	2.84	3.03	4.16
Cryst' Conditions	Methanol, ~2-4°C	Ethanol, RT	Methanol, ~2-4°C	Acetone, ~2-4°C	Methanol ~2-4°C	Acetone, ~2-4°C
M. weight / gmol ⁻¹	206.20	206.20	206.20	208.19	269.10	172.14
Temperature (K)	100	100	100	100	100	100
Space Group	<i>P bca</i>	<i>P 2₁/n</i>	<i>P 2₁/n</i>	<i>P 2₁/c</i>	<i>P n a 2₁</i>	<i>P 2₁/c</i>
<i>a</i> (Å)	11.0916(12)	8.1947(15)	9.1930(4)	12.7412(18)	9.18790(10)	9.3531(2)
<i>b</i> (Å)	10.9340(13)	12.604(2)	10.7841(4)	7.3249(11)	27.8801(3)	7.7079(2)
<i>c</i> (Å)	16.674(2)	9.889(2)	10.4544(4)	10.5181(16)	3.9500(5)	11.5136(7)
α (°)	90	90	90	90	90	90
β (°)	90	105.85(1)	112.790(2)	96.099(9)	90	113.9650(10)
γ (°)	90	90	90	90	90	90
Volume (Å ³)	2022.1(4)	982.6(3)	955.52(7)	976.193)	1011.83(13)	758.49(5)
Z	8	4	4	4	4	4
θ range (°)	2.443-24.815	2.683- 27.868	2.511-27.478	1.607-26.759	1.461-27.492	3.276-27.417
Completeness (%)	0.994	0.994	0.995	0.997	0.998	0.973
Reflections Collected	72325	10317	14100	15115	20365	7177
Independent	1733	2326	2183	2075	4335	1676
Refln (obs.I>2sigma(I))	1709	2319	1205	2067	4323	1673
R_{int}	0.057	0.61	0.093	0.115	0.052	0.028
Parameters	176	176	176	172	174	141
GooF on F ²	1.2876	1.0885	1.1913	0.9195	1.0232	1.0478
R_1 (Observed)	0.0427	0.0398	0.0573	0.0380	0.0320	0.309
R_1 (all)	0.0551	0.0732	0.0448	0.0693	0.0340	0.0324
wR_2 (all)	0.1012	0.1162	0.0471	0.0924	0.0874	0.0775

Table. 7.5 – Crystallographic data for the molecular complexes containing imidazolium.

Compound	BZN BA	BZN TerePHth	BZN PHth	BZN Fumarate	BZN succinate	BZN maelate	BZN malonate
Formula	C21 H18 N2 O4	C15 H12 N2 O4	C15 H12 N2 O4	C11 H12 N2 O4	C11 H12 N2 O4	C11 N2 H11 O4	C10 H10 N2 O4
ApKa (1:1)	1.34	2.02	2.64	2.50	1.37	3.70	2.7
Cryst' Conditions	Ethanol ~-2-4°C	Methanol~-2-4°C	Methanol, RT	Ethanol RT	Ethanol ~-2-4°C	Methanol, 40°C	Acetone ~-2-4°C
M. weight / gmol ⁻¹	362.38	284.27	284.27	234.01	235.87	234.21	222.20
Temperature (K)	100	100	100	100	100	100	100
Space Group	<i>P</i> 2 ₁ / <i>n</i>	<i>P</i> 2 ₁ / <i>c</i>	<i>P</i> 2 ₁ 2 ₁ 2 ₁	<i>P</i> -1	<i>P</i> 2 ₁ / <i>n</i>	<i>P</i> 2 ₁ / <i>n</i>	<i>P</i> -1
<i>a</i> (Å)	10.0661(3)	9.7610(2)	4.623(4)	3.7362(1)	9.6333(2)	12.8558(17)	3.7614(2)
<i>b</i> (Å)	16.8452(6)	7.96610(10)	11.254(10)	11.7687(3)	5.08570(10)	5.4500(6)	12.9268(5)
<i>c</i> (Å)	20.8572(5)	17.0597(3)	25.85(2)	11.7550(3)	21.8908(4)	15.4641(18)	21.1808(9)
α (°)	90	90	90	90.0212(11)	90	90	104.863(2)
β (°)	102.152(2)	98.2206(9)	90	90.5568(14)	97.2514(11)	91.516(4)	92.966(2)
γ (°)	90	90	90	91.9597(14)	90	90	94.865(3)
Volume (Å ³)	3457.41(8)	1312.88(4)	1344.9(20)	516.54(2)	1063.90(4)	1083.1(2)	988.94(8)
Z	8	4	4	2	4	4	4
θ range (°)	2.207-29.944	2.108-25.930	1.576-22.360	3.464-27.464	1.876-27.515	6-55	1.638-24.775
Completeness (%)	100	0.998	0.968	0.995	0.998	0.994	0.994
Reflections Collected	776600	25610	20069	10658	28914	12047	14831
Independent	7889	2545	1018	2343	2452	2459	3394
Refln (obs.I>2sigma(I))	4442	2545	1009	1711	2447	1796	3392
R _{int}	0.172	0.056	0.105	0.083	0.043	0.0624	0.0726
Parameters	487	238	190	192	200	194	349
Goof on F ²	0.9155	0.9457	1.0131	0.9532	0.9745	0.981	1.0090
R ₁ (Observed)	0.0484	0.0335	0.0356	0.0373	0.0347	0.0499	0.0433
R ₁ (all)	0.0959	0.0541	0.0547	0.0593	0.0471	0.0713	0.0726
wR ₂ (all)	0.0968	0.0853	0.0927	0.0957	0.0867	0.1211	0.0946

Table. 7.6 – Crystallographic data for the molecular complexes containing benzimidazolium. PHth represents phthalic acid i.e. TerePHth is terephthalic acid.

7.4 Imidazole with Mono Hydroxy Substituted Benzoic Acids

The three new molecular complexes generated, imidazolium 2-hydroxybenzoate ($\text{IMDH}^+ \text{2-HBA}^-$), imidazolium 3-hydroxybenzoate ($\text{IMDH}^+ \text{3-HBA}^-$) and imidazolium 4-hydroxybenzoate ($\text{IMDH}^+ \text{4-HBA}^-$), are all formed in a 1:1 molecular ratio, with the common proton transfer transformation occurring (Section 7.2.1). All these molecular complexes exhibit only three different hydrogen bonding patterns, G, E and F (Figure 7.18 extract). They also form a motif common between the structures, which is a hybrid of the ladder and linear chain motifs seen previously (M and N).

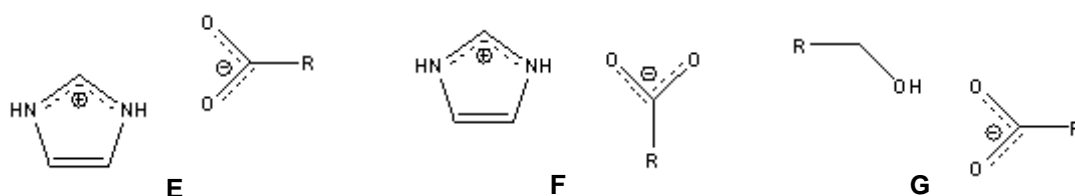


Fig. 7.18 extract – Extract from Figure 7.18 showing the hydrogen bonding patterns within the molecular complexes.

Since the structures of IMD and BZN with the mono-substituted HBA exhibit the same hydrogen bond patterns a comparison of their strengths can be undertaken (Table 7.7). This table highlights the similarity between the molecular complexes generated in terms of hydrogen bond strength, with no vast difference in lengths or angles.

Molecular Complexes		BZNH ⁺	BZNH ⁺	BZNH ⁺	IMDH ⁺	IMDH ⁺	IMDH ⁺
Hydrogen Bonds		2-HBA ⁻	3-HBA ⁻	4-HBA ⁻	2-HBA ⁻	3-HBA ⁻	4-HBA ⁻
N ^{δ+} - H····O ^{δ-} E and F	D···A(Å)	2.646(1)	2.700(1)	2.689(3)	2.729(2)	2.654(2)	2.739(3)
		2.621(1)	2.697(1)	2.717(2)	2.699(3)	2.667(2)	2.664(3)
	D-H(Å)	0.99(2)	0.88(1)	0.91(3)	0.96(3)	0.97(3)	0.94(3)
		0.99(2)	0.90(1)	0.93(3)	0.96(3)	0.91(2)	0.93(3)
	H···A(Å)	1.67(2)	1.82(1)	1.78(3)	1.78(3)	1.70(3)	1.85(3)
		1.64(2)	1.80(1)	1.79(3)	1.75(3)	1.78(3)	1.74(3)
	D-H···A angle(°)	169(2)	178(1)	173(3)	172(3)	169(2)	157(3)
		171(2)	173(1)	170(3)	171(3)	164(3)	174(3)
O-H····O ^{δ-} G	D···A(Å)	-	2.654(1)	2.602(2)	-	2.675(2)	2.614(3)
				2.605(2)			
	D-H(Å)	-	0.87(1)	1.02(3)	-	0.93(3)	0.98(4)
				0.94(3)			
H···A(Å)	-	1.79(1)	1.60(3)	-	1.76(3)	1.65(4)	
			1.69(3)				
D-H···A angle(°)	-	172(1)	166(3)	-	171(2)	170(4)	

Table 7.7 – The three scalar quantities and bond angles of the hydrogen bonds of N^{δ+}-H····O^{δ-} and O-H····O^{δ-} found in the molecular complexes presented in Chapter 7.

7.4.1 Molecular Complex of Imidazolium and 2-Hydroxybenzoic Acid 1:1

As the 2-hydroxybenzoic acid molecule contains an intramolecular hydrogen bond, which would be very difficult to break, of the three possible hydrogen bonding patterns, E, F and G, the latter would be very unlikely to occur for this complex. With only hydrogen bond patterns E and F remaining as possibilities, the question is how these will influence the overall structure.

Structure Description

The molecular ions, IMDH^+ and 2-hydroxybenzoate (2-HBA^-) form a 1:1 molecular complex. The molecular complex was obtained using the solvent evaporation method, with a 1:1 stoichiometric mixture of IMD (8mg) and 2-hydroxybenzoic acid (2-HBA) (14mg) dissolved in the minimum amount of methanol followed by evaporation at 2-4°C. The crystals generated were block shaped and colourless. Single crystal X-ray diffraction data were obtained using a Bruker-Apex II diffractometer at 100K, equipped with graphite monochromated Mo $K\alpha$ radiation ($\lambda = 0.71073 \text{ \AA}$). The structure was solved using SIR92 within the CRYSTALS program. The crystallographic data are summarised in Table 7.5. In the molecular complex, the IMD molecule is protonated through hydrogen transfer from the carboxylic acid group on the 2-HBA, as described in Section 7.2.1 (Figure 7.19). The result is that the internal bond lengths are normalised to $\text{N1}^{\delta+}\text{-C1}$ 1.304(3)Å and $\text{N2}^{\delta+}\text{-C1}$ 1.317(3) Å, and bond angles to $\text{C1-N1}^{\delta+}\text{-C2}$ 108.1(2)° and $\text{C1-N2}^{\delta+}\text{-C7}$ 107.7(2)°.

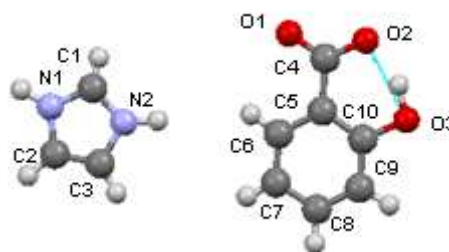


Fig. 7.19 – The imidazolium and 2-hydroxybenzoate ions which are generated in the molecular complex/salt, with atom labelling.

Interaction	Label	Length (Å) (D...A(Å))	For Hydrogen Bonds		
			D-H(Å)	H...A(Å)	D-H...A angle(°)
N2...O2	a	2.729(2)	0.96(3)	1.78(3)	172(3)
N1...O1	b	2.699(3)	0.96(3)	1.75(3)	171(3)
O3...O2		2.524	1.01(3)	1.56(3)	156(3)

O3...C3	c	3.301(4)	0.98(3)	2.48(3)	140(2)
C2... π	d	3.374	-	-	-
C1...O2	e	3.337(3)	0.89(2)	2.70(2)	130(2)
C8...O2	f	3.497(3)	0.97(2)	2.65(3)	145(2)

Table 7.8 – The three scalar quantities and bond angles of the hydrogen bonds and list of the interactions between the molecules in the $\text{IMDH}^+ \text{2-HBA}^-$ molecular complex..

The 2-HBA molecule retains the intramolecular hydrogen bond ($\text{O3-H}\cdots\text{O2}$) found within its native structure. The intramolecular hydrogen bond is relatively short, $\text{O}\cdots\text{O}$ distance of $2.524(2)\text{\AA}$, compared to that found in the native crystal structure, $\text{O}\cdots\text{O}$ distance of $2.6191(3)\text{\AA}$. This is due to the intramolecular hydrogen bond being charged assisted, a result of the deprotonation of the 2-HBA and is similar to that found in other 2-HBA^- molecular complexes reported in the CSD. The negative charge is found to be delocalised over the carboxylic acid group indicated by the normalisation of the bond lengths in the carboxyl group, $\text{C8-O1}^{\delta-}$ $1.248(3)\text{\AA}$ and $\text{C8-O2}^{\delta-}$ $1.278(2)\text{\AA}$.

The two hydrogen bonds within the structure (hydrogen bond patterns E and F) are both partially charged assisted $\text{N}^+\text{-H}\cdots\text{O}^-$ interactions of length (a) $2.729(2)\text{\AA}$ and (b) $2.699(3)\text{\AA}$ (Figure 7.20). These are the predominant interactions within the structure and combine to create an alternating chain of co-molecules forming arrow shapes (Figure 7.20 RHS).

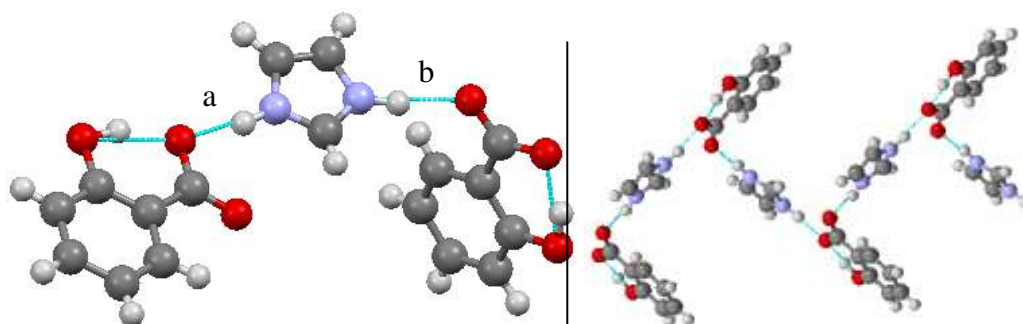


Fig. 7.20 – The two main hydrogen bonds within the molecular complex, a, $\text{N-H}\cdots\text{O}$ forming pattern E and b, $\text{N-H}\cdots\text{O}$ forming pattern F; RHS, the resulting arrow head chain of alternate co-molecules.

There are four weaker interactions that influence the expanded structure. The strongest is a $\text{C-H}\cdots\text{O}$ weak hydrogen bond, $\text{C3-H}\cdots\text{O3}$, of length $3.301(4)\text{\AA}$ that expands the structure along the *bc*-diagonal (Figure 7.21). Further supporting the packing along this diagonal is a $\text{C-H}\cdots\pi$

interaction of 3.574\AA (measured from C2 to a centroid between C7 and C8) (Figure 7.21 RHS).

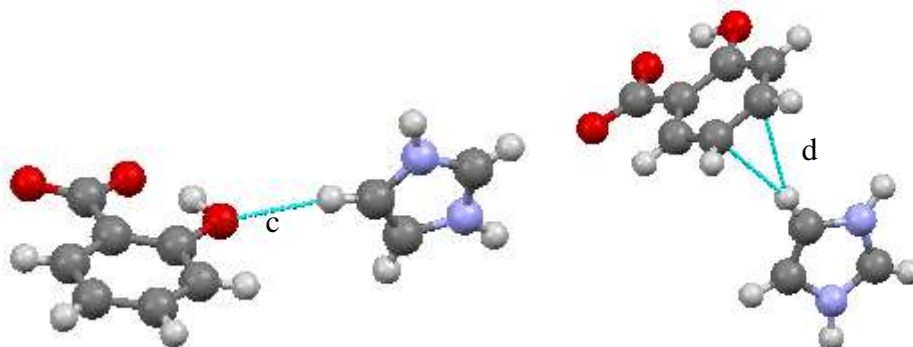


Fig. 7.21 – LHS, the weak C-H...O hydrogen bond, c, involving the hydroxyl oxygen, RHS, the C-H... π interaction, d, that expands the structure along the *bc* diagonal.

There is another weak hydrogen bond, from the carbon located between the nitrogens on the IMDH^+ and a carboxylate oxygen, C1-H...O2, which is of length $3.337(3)\text{\AA}$ (Figure 7.22). This interaction exists between the chains and interlinks them along the *a*-axis. The last of the weaker interactions that influence the structure is a C-H...O weak hydrogen bond involving the carboxylate oxygen (Figure 7.22 RHS). This hydrogen bond is weak at $3.497(3)\text{\AA}$ but is the only interaction that connects the chains along the *c*-axis.

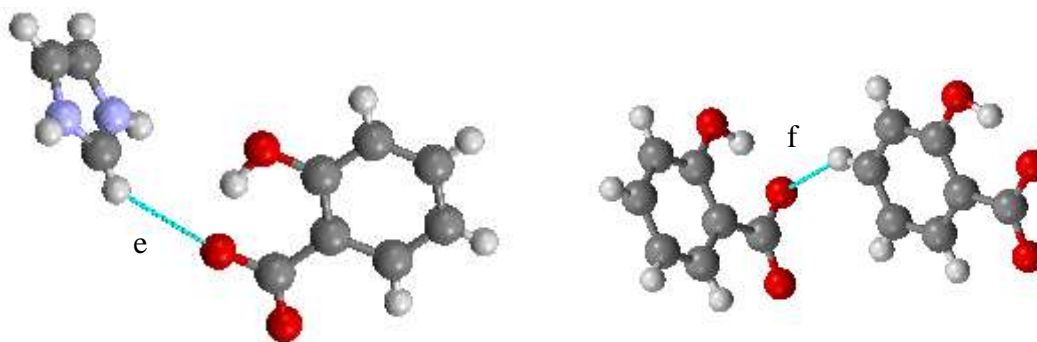


Fig. 7.22 – LHS, the C-H...O weak hydrogen bond, e, that connects two of the chains together, RHS, another C-H...O hydrogen bond, f, this time expanding the structure along the *c*-axis.

Figure 7.23 is a view of the expanded structure along the *b*-axis. In this figure the main hydrogen bonds, a and b, expand the chains in a zigzag fashion (blue line). Connecting the chains along the face of the figure are the weaker interactions e, C-H...O hydrogen bond, and f, C-H...O hydrogen bond (coloured in red). That leaves the weaker interactions c, C-H...O hydrogen bond and d, the C-H... π interaction that connect the chains perpendicular to Figure 7.23.

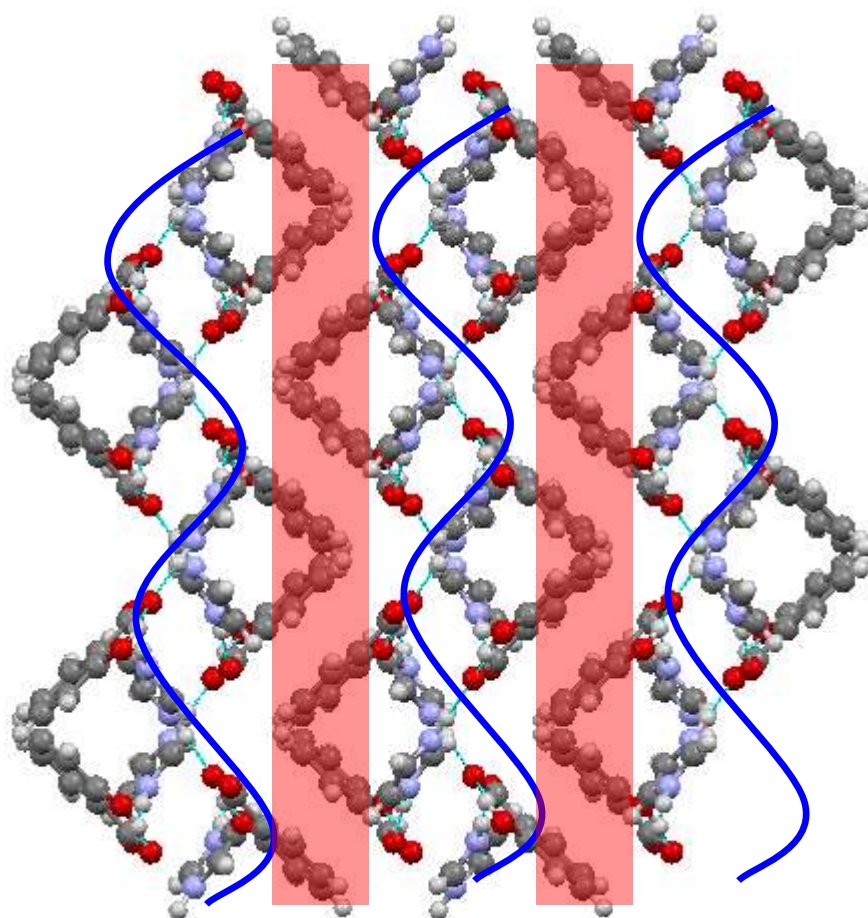


Fig. 7.23 – An expanded image of the $\text{IMDH}^+ 2\text{-HBA}^-$ molecular complex showing the hydrogen bonded chains (blue line) being connected by two $\text{C-H}\cdots\text{O}$ hydrogen bonds (red box).

7.4.2 Molecular Complex of Imidazolium and 3-Hydroxybenzoic Acid 1:1

Having the hydroxyl group in the 3-position on the benzoic acid molecule, removing the possibility of intramolecular hydrogen bond formation, will result in the hydroxyl group being available for medium strength intermolecular hydrogen bonds. In the BZN molecular complexes (see Chapter 4) the predominant hydrogen bond for this group was pattern G, a hydroxyl – carboxylate hydrogen bond. It is likely that this will be the case for the IMD structures and coupled with the hydrogen bond patterns seen in the $\text{IMDH}^+ 2\text{-HBA}^-$ molecular complex (and in every other structure containing BZN or IMD), E and F, there is a possibility for the ladder motif to form.

Structure Description

The molecular ions, IMDH^+ and 3-hydroxybenzoate (2-HBA^-) form a 1:1 molecular complex or salt. The molecular complex was obtained using the solvent evaporation method, with a 1:1 stoichiometric mixture of IMD (6mg) and 3-hydroxybenzoic acid (3-HBA) (14mg) dissolved in the minimum amount of ethanol and left to evaporate at room temperature. The crystals generated were block shaped and colourless. Single crystal X-ray diffraction data were obtained using a Bruker Apex II diffractometer at 100K, equipped with graphite monochromated Mo $K\alpha$ radiation ($\lambda = 0.71073 \text{ \AA}$). The structure was solved using SIR92 within the CRYSTALS program. The crystallographic data are summarised in Table 7.5.

Proton transfer has occurred (see Section 7.2.1 for details) resulting in the IMDH^+ anion having the N-C bonds and C-N-C angles normalised. This also creates an 3-HBA^- cation with the carboxylate group undergoing normalisation of the carbon-oxygen bond lengths (Figure 7.24). The intra-/intermolecular interactions with relevant data are listed in Table 7.9.

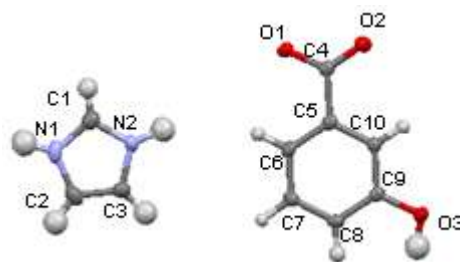


Fig. 7.24 – The imidazolium and 3-hydroxybenzoate ions which are generated in the molecular complex/salt, with atom labelling.

Interaction	Label	Length (Å) (D...A(Å))	For Hydrogen Bonds		
			D-H(Å)	H...A(Å)	D-H...A angle(°)
O3...O1		2.675(2)	0.93(3)	1.76(3)	171(2)
N2...O2		2.654(2)	0.97(3)	1.70(3)	169(2)
N2...O2		2.667(2)	0.91(2)	1.78(3)	164(3)
C1...O1	a'	3.345(2)	0.92(2)	2.69(2)	129(2)
C1...O2	b'	3.416(3)	0.92(2)	2.64(3)	142(2)
C7...O3		3.273(2)	1.02(2)	2.48(2)	133(1)

Table 7.9 – The three scalar quantities and bond angles of the hydrogen bonds and list of the interactions between the molecules in the $\text{IMDH}^+ 3\text{-HBA}^-$ molecular complex..

The main motif of the structure is a hydrogen bonded box consisting of two equivalents of each molecule acting as the sides with carboxylate groups as the corners (Figure 7.25). It can be seen that this shape is repeated along the *b*- and *c*-axis forming stacks of boxes. There are three unique hydrogen bonds within the structure that all occur at the corners of the boxes and

shape the structure (Figure 7.25 RHS). These three moderate hydrogen bonds are very similar in strength, O3-H \cdots O1 2.675(2)Å, O1-H \cdots N1 2.654(2)Å and O2-H \cdots N2 2.667(2)Å, and correspond to the common hydrogen bonding patterns G, E and F. There are no weaker interactions that help form these boxes. Interestingly, the hydrogen bond that is most directional is that between the carboxylate and the imidazole groups, which is the opposite situation to that found in the BZN structures where the hydroxyl - carboxylate hydrogen bond is the main hydrogen bond thus creating the chains seen in those structures.

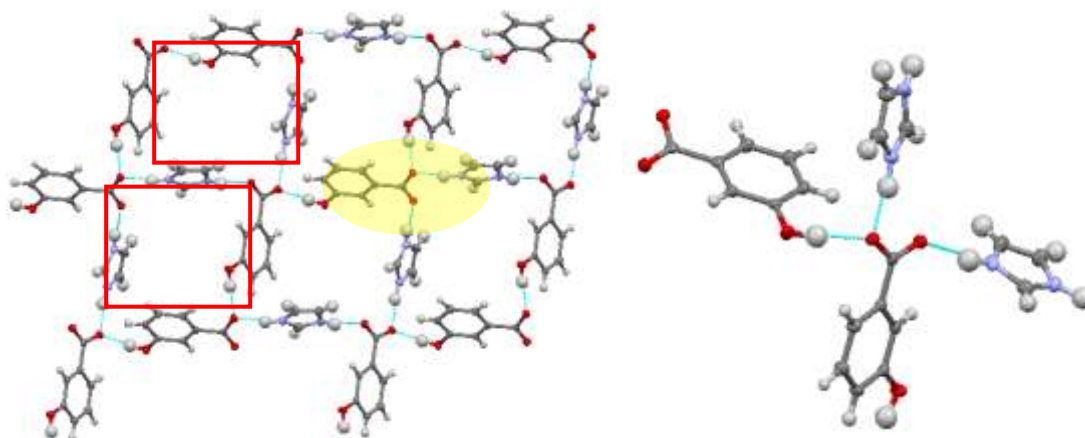


Fig. 7.25 – LHS, an expanded view of the $\text{IMDH}^+ 3\text{-HBA}^-$ molecular complex along the a -axis, it can be seen that the structure is made up of hydrogen bonded boxes (red box) stacked upon each other, RHS, a expanded view of the yellow circle highlighting the corners of each box with the three hydrogen bonds that originate from this point.

Connecting the motifs, 2D boxes stack upon one another, held together only by two weaker interactions. Firstly, a bifurcated hydrogen bond involving the carbon located between the two nitrogens of the IMDH^+ molecule and the oxygens involved in the hydroxyl – carboxylate hydrogen bond (Figure 7.26). The two interactions in this asymmetrical bifurcated hydrogen bond have similar lengths, with the hydrogen bond involving the partially negative oxygen slightly smaller: a' - 3.345(2)Å and b' - 3.416(3)Å. It is worth noting that the proton is directed towards the hydroxyl oxygen, which has the slightly longer hydrogen bond length. The bifurcated hydrogen bond expands the structure along the b -axis. Another weak hydrogen bond, C7-H \cdots O3, assists the bifurcated hydrogen bond in connecting the stacks along the b -axis (Figure 7.26 RHS). This weak hydrogen bond has a length of 3.273(2)Å.

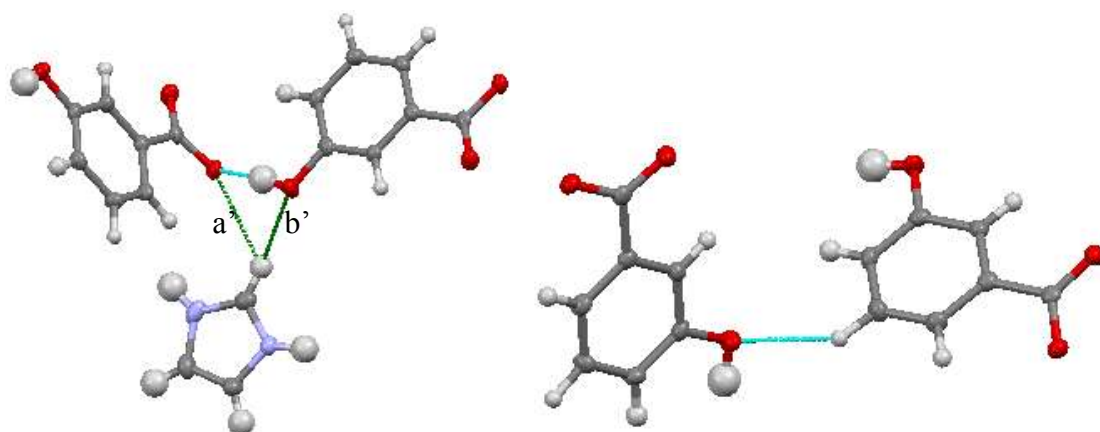


Fig. 7.26 – LHS, bifurcated hydrogen bond and RHS, C-H...O weak hydrogen bond that expands the stacks of boxes along the *b*-axis.

7.4.3 Molecular Complex of Imidazolium and 4-Hydroxybenzoic Acid 1:1

In this complex, the hydroxyl group is now in the 4-position on the benzoic acid molecule. This does not affect the motifs in the BZN structures so it is possible a similar motif to the $\text{IMDH}^+ 3\text{-HBA}^-$ structure will prevail. It will also be very likely that the same hydrogen bond patterns, E, F and G form with very little reason for this not to be the case.

Structure Description

The molecular ions, IMDH^+ and 4-hydroxybenzoate (4-HBA^-) form a 1:1 molecular complex or salt (Figure 7.27). The molecular complex was obtained using the solvent evaporation method, with a 1:1 stoichiometric mixture of IMD (6mg) and 4-hydroxybenzoic acid (4-HBA) (14mg) dissolved in the minimum amount of methanol followed by evaporation at 2-4°C in a cold room. The crystals generated were plate shaped and colourless. Single crystal X-ray diffraction data were obtained using a Bruker-Nonius Kappa diffractometer at 100K, equipped with graphite monochromated Mo $K\alpha$ radiation ($\lambda = 0.71073 \text{ \AA}$). The structure was solved using SUPERFLIP within the CRYSTALS program. The crystallographic data are summarised in Table 7.5. Proton transfer has

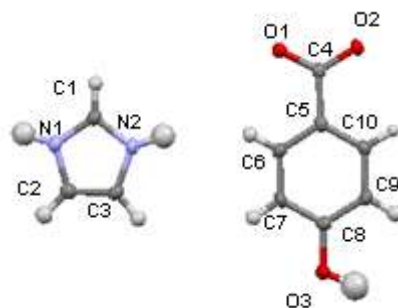


Fig. 7.27 – The imidazolium and 4-hydroxybenzoate ions which are generated in the molecular complex/salt, with atom labelling.

occurred (see Section 7.2.1 for details) resulting in the IMDH^+ anion having the N-C bonds and C-N-C angles normalised, N1-C1 1.332(4)Å, N2-C1 1.328(3)Å and C2-N1C1 108.7(2)°, C3-N2-C1 108.2(2)°. A similar effect is seen in the 4-HBA⁻ cation after the deprotonation leaving the negative charge delocalised across the carboxylate group resulting in the normalisation of the C-O bond lengths, C4-O1 1.259(4)Å and C4-O2 1.275(3)Å.

Interaction	Label	Length (Å) (D...A(Å))	For Hydrogen Bonds		
			D-H(Å)	H...A(Å)	D-H...A angle(°)
N1...O1	E	2.664(3)	0.93(3)	1.74(3)	174(3)
O2...O3	F	2.614(3)	0.98(4)	1.65(4)	170(4)
N2...O2	G	2.739(4)	0.94(3)	1.85(3)	157(3)
C1...π		3.838	-	-	-
C1...O1		3.073(3)	0.96(3)	2.45(2)	118(2)
N1...O1		3.537(3)	0.94(3)	2.62(3)	110(2)

Table 7.10 – The three scalar quantities and bond angles of the hydrogen bonds and list of the interactions between the molecules in the IMDH^+ 4-HBA⁻ molecular complex.

The IMDH^+ 4-HBA⁻ structure adopts the same motif as the IMDH^+ 3-HBA⁻, a hydrogen bonded box consisting of two equivalents of each molecule acting as the sides with carboxylate groups as the corners (Figure 7.28). The main difference is in the angles of the box. Within this structure they are close to 90° creating a very square box whereas in the 3-HBA⁻ structure the box is more of a parallelogram shape. The hydrogen bonds are the same as found in the 3-HBA⁻ structure following the patterns E, F and G (see Table 7.10 for details). They are of moderate strength and two of them are slightly shorter than the corresponding interactions in the 3-HBA⁻ structure at E, N-H...O 2.664(3)Å, F, N-H...O 2.739(3)Å and G, O-H...O 2.614(3)Å.

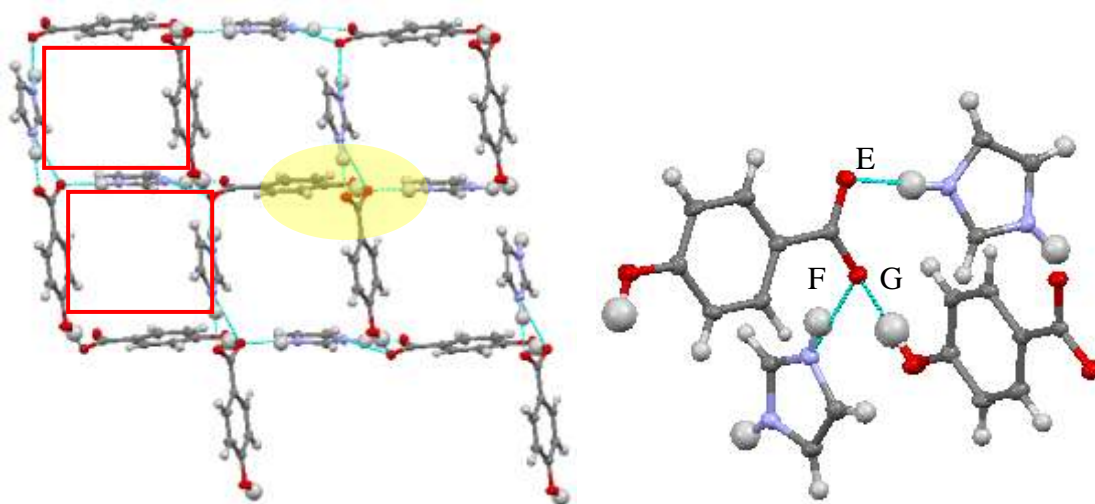


Fig. 7.28 – LHS, the view along the *c*-axis of the motif of the IMDH^+ 4-HBA^- molecular complex, hydrogen bonded squares (red box) stack upon one another, RHS, extract from the yellow circle which shows the corners of the boxes with hydrogen bonds E, F and G highlighted.

The stacks of boxes expand the structure along the *a*- and *b*-axes which leaves the expansion along the *c*-axis to be achieved by two weaker interactions. Figure 7.29 is the view along the *a*-axis when two stacks of boxes are expanded out. From this image the weaker interaction that expands the structure along the *c*-axis can be seen to be a $\text{C-H}\cdots\pi$ interaction of length 3.838\AA (measured from a centroid between carbons C6 and C7 to C1).

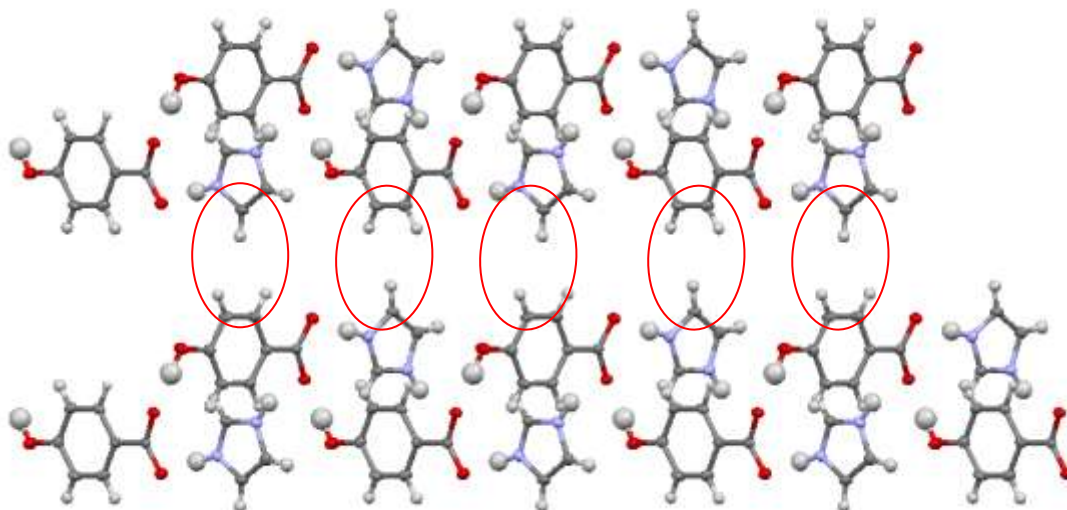


Fig. 7.29 – View along the *a*-axis showing two stacks of boxes held together along the *c*-axis by $\text{C-H}\cdots\pi$ interactions (circled in red).

Connecting the boxes along the *ac*-diagonal is a double hydrogen bond utilising the carbon located between the two nitrogens on the IMDH^+ and a nitrogen with the oxygen O1, C1-

H \cdots O1 and N1-H \cdots O1 (Figure 7.30). These hydrogen bonds are weak at 3.021(3)Å and 3.073(3)Å respectively and have the effect of packing the stacks of hydrogen bonded boxes along the *ac*-diagonal.

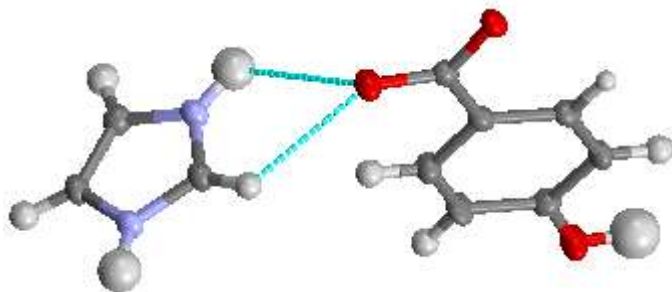


Fig. 7.30 – The double weak hydrogen bonds that expand the stacks of hydrogen bonded boxes along the *ac*-diagonal.

7.5 A Comparison of the Molecular Complexes of Imidazole and Benzimidazole with Halo Substituted Benzoic Acids

As discussed in Chapter 5, a whole range of new molecular complexes containing BZN and a mono-substituted halo-benzoic acid have been produced. Cocrystallisation experiments were also set-up using the mono-substituted halo-benzoic acid series with imidazole. This resulted in the successful generation of molecular complexes of imidazole with 4-fluoro- and 4-bromo- benzoic acids (Table 7.3). This section will look at the different hydrogen bond patterns produced but will focus on the roles of the halogen atom. The benzoic acid structures should help to highlight the roles that the halogen atoms play in the formation of a new molecular complex of different stoichiometry, a 1:2 benzimidazole : benzoic acid, which has been structurally determined.

	Imidazole	Source	Benzimidazole	Source
4-fluoroBA	1:1	New	1:1	New
4-bromoBA	1:1	New	1:1	New
Benzoic acid	1:1	CSD	1:2	New

Table 7.3 repeated - Summary of the successful cocrystallisations between IMD and mono-substituted halo-benzoic acid series with the corresponding BZN molecular complex.

The two newly characterised halo-substituted benzoic acid molecular complexes contain only the N-H...O hydrogen patterns E and F. Table 7.11 compares the distances of these hydrogen bonds with those in the benzimidazole counterparts. It can be seen that there is no real difference to the strength of the hydrogen bonds whether IMD or BZN is the co-molecule. This is also the case between the different IMD structures studied, where the hydrogen bond distances are a little shorter in the fluoro- complex compared to the bromo-substituted, but not by any significant margin.

Molecular Complexes		IMDH ⁺	BZNH ⁺	IMDH ⁺	BZNH ⁺	IMDH ⁺	BZNH ⁺
Hydrogen Bonds		4-FBA ⁻	4-FBA ⁻	4-BrBA ⁻	4-BrBA ⁻	BA ⁻	BA ⁻
N ^{δ+} - H····O ^{δ-} E and F	D···A(Å)	2.670(2) 2.626(2)	2.800(2) 2.687(2)	2.680(2) 2.710(2)	2.597(2) 2.667(2) 2.638(2) 2.850(2) 2.848(2)	2.613(3) 2.666(3)	2.776(4) 2.645(3) 2.766(4) 2.680(3)
	D-H(Å)	0.92(2) 0.99(2)	0.85(2) 0.93(2)	0.83(3) 0.93(3)	0.94(3) 0.78(2) 0.92(3) 0.77(2) 0.77(2)	1.02(6) 0.90(5)	0.88(3) 0.97(2) 1.06(3) 0.82(3)
	H···A(Å)	1.75(2) 1.64(2)	2.13(3) 1.77(3)	1.87(3) 1.78(3)	1.65(3) 1.91(2) 1.72(3) 2.17(2) 2.36(3)	1.63(5) 1.77(5)	1.99(2) 1.69(2) 1.85(2) 1.90(2)
	D-H···A angle(°)	173(2) 176(2)	135(2) 179(2)	165(3) 177(2)	178(3) 163(3) 147(2) 141.6(2) 123(2)	160(5) 173(5)	148(2) 168(2) 141(2) 157(2)

Table 7.11 – The three scalar quantities and bond angle of the hydrogen bonds of N^{δ+}-H····O^{δ-} found in the molecular complexes presented in section 7.5.

7.5.1 Molecular Complex of Imidazolium and 4-Fluorobenzoic Acid 1:1

The corresponding BZNH^+ structure with 4-FBA^- has dimers of each co-molecule connected to form zig-zag chains (as seen in Figure 5.58, repeated below). This sort of motif was seen in many of the BZNH^+ with halo-benzoic acid molecular complexes. It would be possible for this motif to prevail in the IMDH^+ structure, however this would require partial or no protonation to occur, which is unlikely.

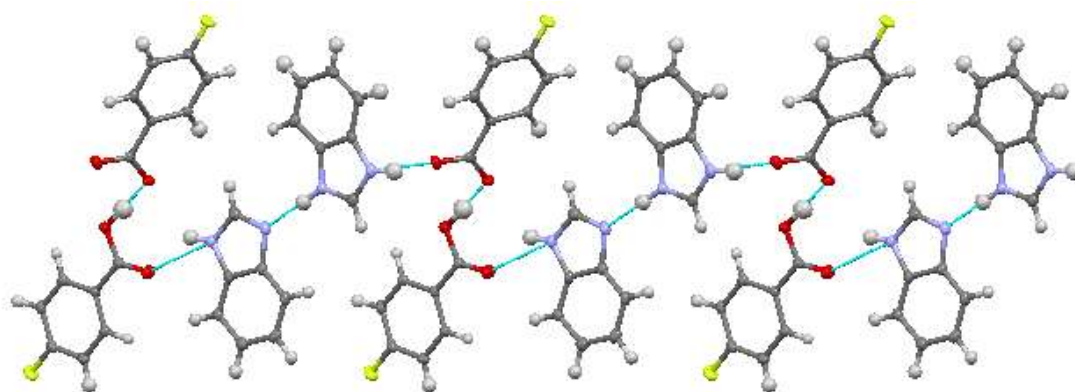


Fig. 5.58 repeated – View along the a -axis of the BZN 4-FBA molecular complex, showing the main motif, a zigzag chain of dimers held together by $\text{N}^{\delta+}\text{-H}\cdots\text{O}^{\delta-}$ hydrogen bonds that expand the structure along the ab -diagonal axis.

Structure Description

The molecular complex between IMD and 4-fluorobenzoic acid (4-FBA) contains one of each of their ionic forms in a 1:1 ratio, $\text{IMDH}^+ : 4\text{-FBA}^-$. The molecular complex was obtained using the solvent evaporation method, with a 1:1 stoichiometric mixture of IMD (6mg) and 4-fluorobenzoic acid (12mg) dissolved in the minimum amount of acetone followed by evaporation at a constant temperature of between 2 and 4°C using a walk in fridge. The crystals generated were block shaped and colourless. Single crystal X-ray diffraction data were obtained using a Bruker Apex II diffractometer at 100K, equipped with graphite monochromated Mo $K\alpha$ radiation ($\lambda = 0.71073 \text{ \AA}$). The structure was solved using SIR92 within the CRYSTALS program. The crystallographic data are summarised in Table 7.5. As described in Section in 7.2.1, a IMDH^+ molecule is generated through hydrogen transfer from the 4-FBA molecule (Figure 7.31 top). This has the effect of normalising the internal IMDH^+

carbon – nitrogen bond lengths, N1-C1 1.325(2)Å and N2-C1 1.320(2)Å, and the carbon – oxygen bond lengths on the 4-FBA⁻, C4-O1 1.256(2)Å and C4-O2 1.261(2)Å.

There are two main hydrogen bonds within the structure, both partially charged assisted N-H···O interactions that correspond to hydrogen bond patterns E and F (Figure 7.31). These two moderate hydrogen bonds (E, N1-H···O2, 2.687(2)Å F, N2-H···O1, 2.800(2)Å) combine to form spiral chains of alternating co-molecules along the *b*-axis that is the main motif of the structure (Figure 7.31 bottom LHS). Figure 7.31 RHS looks through one of the spiral chains highlighting the cyclical nature of the structure with Table 7.12 giving the hydrogen bond data.

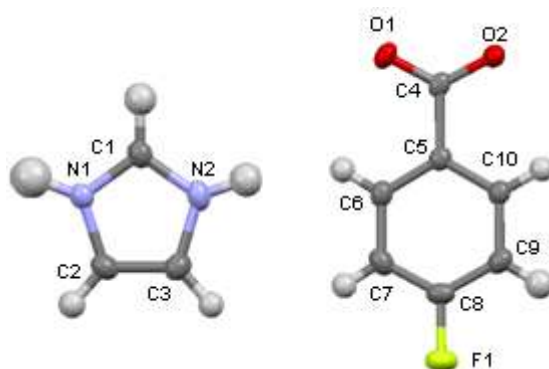


Fig. 7.31 – (top) The imidazolium and 4-fluorobenzoate ions which are generated in the molecular complex/salt, with atom labelling.

Interaction	Label	Length (Å) (D···A(Å))	For Hydrogen Bonds		
			D-H(Å)	H···A(Å)	D-H···A angle(°)
N1···O4	E	2.670(2)	0.92(2)	1.75(2)	173(2)
N2···O3	F	2.626(2)	0.99(2)	1.64(2)	176(2)
C1···O2		3.065(2)	1.02(2)	1.26(2)	147(1)
C9···F	M	3.490(2)	-	-	-
C2···F	N	3.547(2)	-	-	-

Table. 7.12 - The three scalar quantities and bond angles of the hydrogen bonds and list of the interactions between the molecules in the IMDH⁺ 4-FBA⁻ molecular complex.

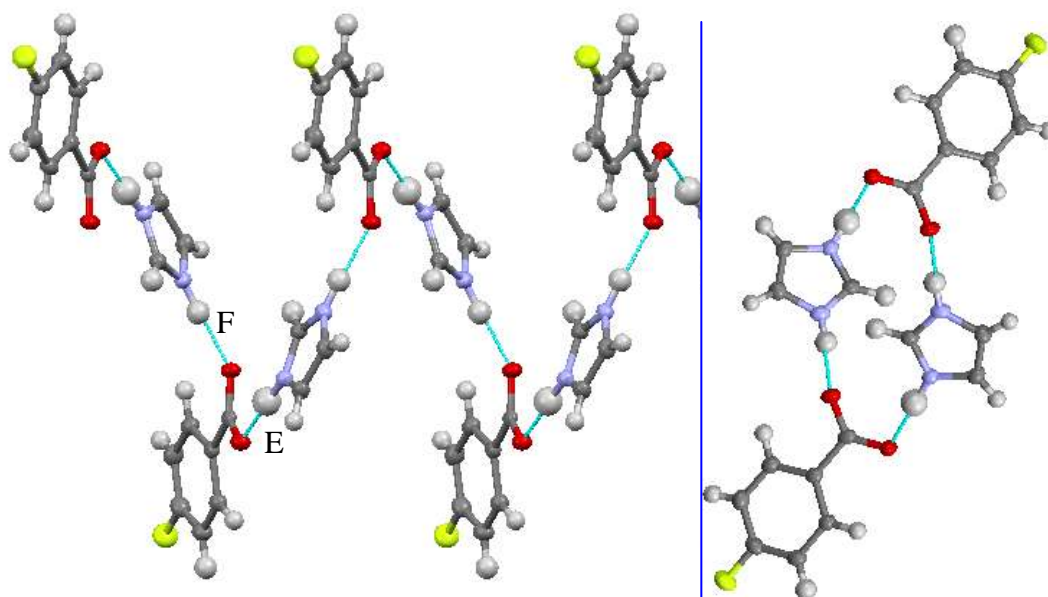


Fig. 7.31 – (bottom) LHS, the main motif of the $\text{IMDH}^+ 4\text{-FBA}^-$ molecular complex, a spiral chain of alternate co-molecules held together through $\text{N-H}\cdots\text{O}$ hydrogen bonds, E and F, RHS, view along the b -axis of an extended spiral chain showing its cyclical nature.

The third most common hydrogen bond donor of the IMD/BZN molecule, the carbon located between the nitrogens, is once again involved in a significant hydrogen bond in this structure. The $\text{C-H}\cdots\text{O}$ weak hydrogen bond is of a relatively short length for this type of hydrogen bond at $3.065(2)\text{\AA}$. It has the role of binding two spiral chains alongside one another (Figure 7.32).

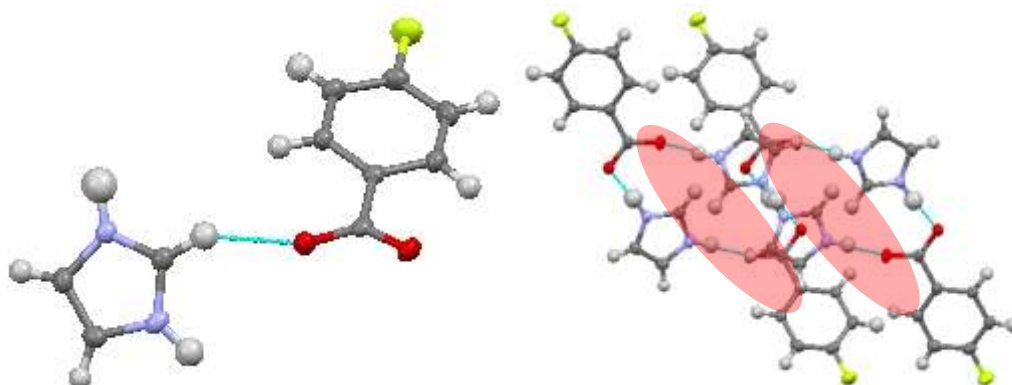


Fig. 7.32 – LHS, the $\text{C-H}\cdots\text{O}$ hydrogen bond that binds two spiral chains to one another, RHS, the effect the binding of the two spirals (red circle) has on the structure.

The main motif, the spiral chains, expands the structure along the b -axis, the $\text{C-H}\cdots\text{O}$ weak hydrogen bond then binds together two of the motifs. The structure is further expanded along the a - and c -axis through two weak hydrogen bonds of equal strength (Figure 7.33). Hydrogen

bond M, C9-H...F, has length of 3.490(2)Å while N, C2-H...F, has length 3.547(2)Å. These are the only interactions that expand the structure along the *a*- and *c*- axes.

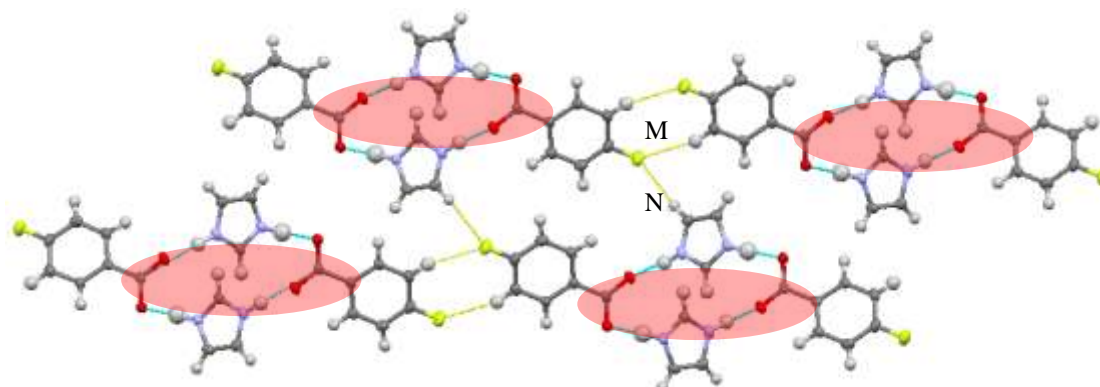


Fig. 7.33 – View along the *b*-axis of the extended structure of the IMDH⁺ 4-FBA⁻ molecular complex showing the spiral chains (highlighted in red) held together by weak hydrogen bonds (yellow lines) that connect the chains along the *a*- and *c*-axes.

7.5.2 Molecular Complex of Imidazolium and 4-Bromobenzoic Acid 1:1

The corresponding BZNH⁺ structure with 4-BrBA⁻ adopts a hydrogen bonded ring motif containing equal numbers of each co-molecule (as shown in Figure 5.56, repeated below). This sort of motif was seen in other BZNH⁺ with halo-benzoic acid molecular complexes and is considered likely to occur in the IMDH⁺ structures. The spiral chain motif, seen in the IMDH⁺ 4-FBA⁻ complex, utilises the most prominent hydrogen bonds available, E and F, N-H...O, to a better effect than in the BZNH⁺ 4-BrBA⁻ structure. In all the molecular complexes studied containing a halobenzoic acid, the halogen group is a significant factor in the extended structure and is highly likely to be so again.

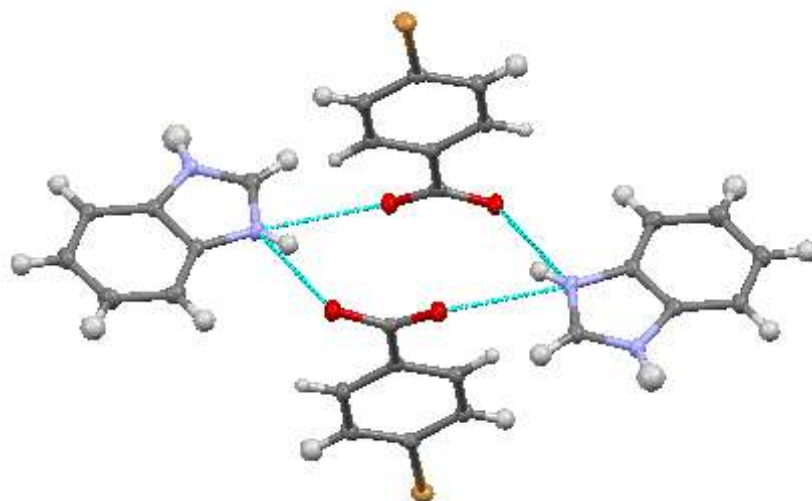


Fig. 5.56 repeated – The *b*-axis of the BZN 4-BrBA molecular complex, showing the main motif, a hydrogen bonded ring using $N^{\delta+}-H\cdots O^{\delta-}$ hydrogen bonds.

Structure Description

The molecular complex between IMD and 4-bromobenzoic acid (4-BrBA) contains one equivalent of each of their ionic forms in a 1:1 ratio, $IMDH^+ : 4-BrBA^-$. The molecular complex was obtained using the solvent evaporation method, with a 1:1 stoichiometric mixture of IMD (6mg) and 4-bromobenzoic acid (18mg) dissolved in the minimum amount of methanol followed by evaporation at a constant temperature of between 2 and 4°C using a walk in fridge. The crystals generated were plate shaped and colourless. Single crystal X-ray diffraction data were obtained using a Bruker Nonius Kappa diffractometer at 100K, equipped with graphite monochromated Mo $K\alpha$ radiation ($\lambda = 0.71073 \text{ \AA}$). The structure was solved using SUPERFLIP within the CRYSTALS program. The crystallographic data are summarised in Table 7.5. As described in Section in 7.2.1 a $IMDNH^+$ molecule is generated through hydrogen transfer from the 4-BrBA molecule (Figure 7.34). This has the effect of normalising the internal $IMDH^+$ carbon – nitrogen bond lengths, N1-C1 $1.331(3)\text{\AA}$ and N2-C1 $1.323(2)\text{\AA}$, and the carbon – oxygen bond lengths on the $4-FBA^-$, C4-O1 $1.287(2)\text{\AA}$ and C4-O2 $1.243(2)\text{\AA}$.

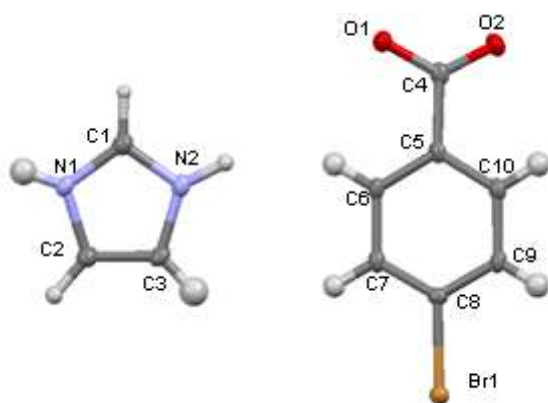


Fig. 7.34 – The imidazolium and 3-bromobenzoate ions which are generated in the molecular complex/salt, with atom labelling.

Interaction	Length (Å) (D...A(Å))	For Hydrogen Bonds		
		D-H(Å)	H...A(Å)	D-H...A angle(°)
N1...O2	2.680(2)	0.83(3)	1.87(3)	165(3)
N2...O2	2.710(2)	0.93(3)	1.78(3)	177(2)
C1...O1	3.129(2)	0.97(2)	2.63(2)	110(1)
C3...O1	3.183(2)	0.91(3)	2.34(3)	153(2)
C9...Br	3.831(2)	-	-	-
C7...Br	3.759(2)	-	-	-

Table. 7.13 - The three scalar quantities and bond angles of the hydrogen bonds and list of the interactions between the molecules in the $\text{IMDH}^+ 4\text{-BrBA}^-$ molecular complex.

The main motif in the $\text{IMDH}^+ 4\text{-BrBA}^-$ molecular complex is a zigzag chain of alternative co-molecules connected through moderate hydrogen bonds (Figure 7.35). These hydrogen bonds are partially charged assisted $\text{N}^{\delta+}\text{-H}\cdots\text{O}^{\delta-}$ interactions that correspond to hydrogen bond patterns E and F. They are of moderate strength with length $\text{N1-H}\cdots\text{O2}$ 2.680(2)Å and $\text{N2-H}\cdots\text{O2}$ 2.710(2)Å and runs along the *bc* diagonal (Table 7.13).

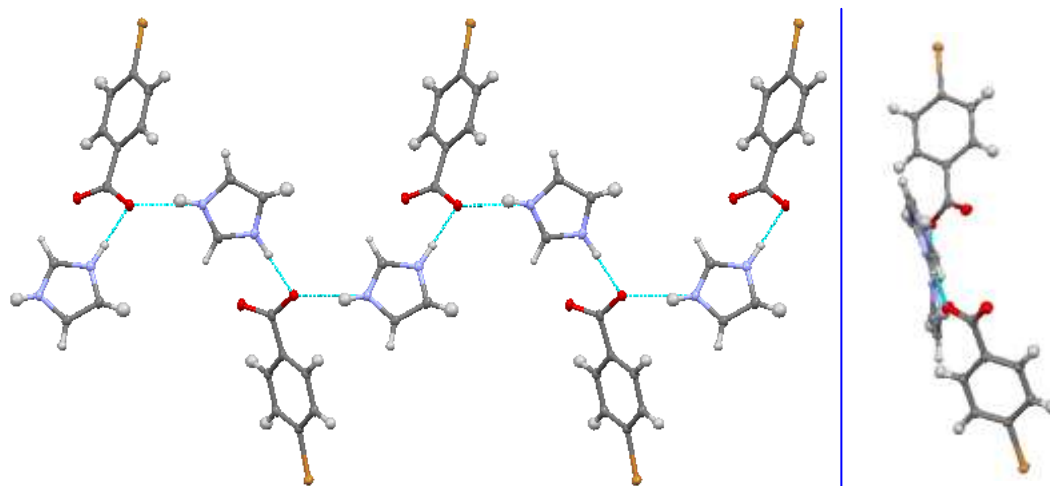


Fig. 7.35 – The main motif of the IMDH^+ 4-BrBA^- molecular complex, a zigzag chain of alternate co-molecules connected through moderate hydrogen bonds.

The motifs stack on top of one-another along the c -axis using weak $\text{C-H}\cdots\text{O}$ hydrogen bonds (Figure 7.36). These hydrogen bonds originate from the oxygen not involved in the moderate hydrogen bonds (O1) and connect to two separate carbons in the IMDH^+ molecule, C1 $3.129(2)\text{\AA}$ and C3 $3.183(2)\text{\AA}$ (Figure 7.36 RHS). The distances between both copies of the IMDH^+ and 4-BrBA^- molecules are too long for any π stacking interactions.

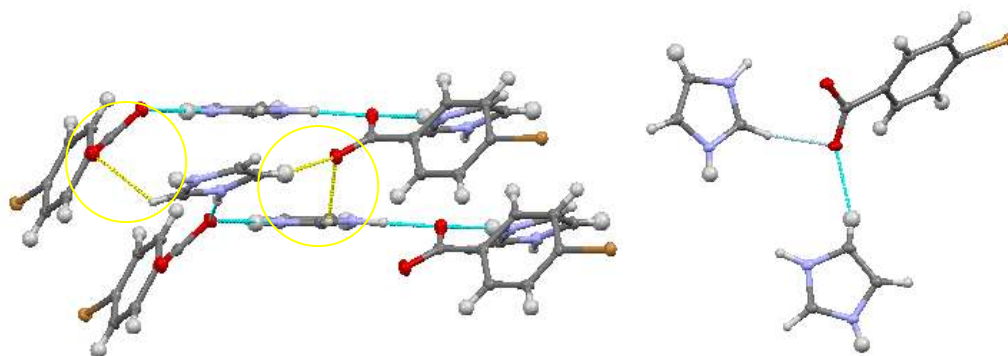


Fig. 7.36 – The motifs, zigzag chains of alternative co-molecules, are stacked upon one another along the c -axis held by weak $\text{C-H}\cdots\text{O}$ hydrogen bonds; RHS, the weak hydrogen bonds that exist between the layers.

The b -axis is expanded by interactions involving the bromine molecule which covers all the significant interactions within the structure (Figure 7.37). The bromine halogen bonds (brown circle) are of length $\text{C9-H}\cdots\text{Br}$ $3.831(2)\text{\AA}$ and $\text{C7-H}\cdots\text{Br}$ $3.759(2)\text{\AA}$ and are the only interactions that expand the structure along the b -axis.

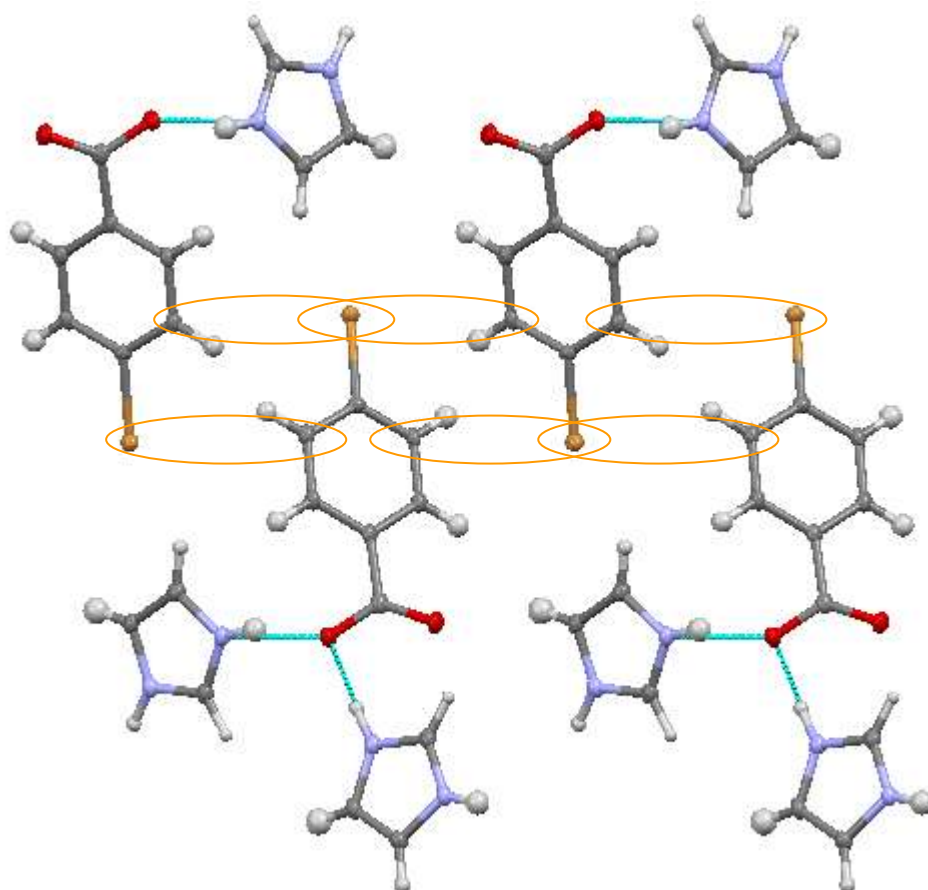


Fig. 7.37 – The halogen bonds, C-H...Br, that exist between the zigzag chains along the *b*-axis.

A view along the *a*-axis of the extended $\text{IMDH}^+ 4\text{-BrBA}^-$ molecular complex is shown in Figure 7.38. From this the main motif can be seen, zigzag chains held together through moderate N-H...O hydrogen bonds (blue line, Fig 7.35), and connected to another motif through C-H...O hydrogen bonds (red box, Fig 7.36) while they are further extended along the *b*-axis through halogen bonds (brown box, Fig. 7.37).

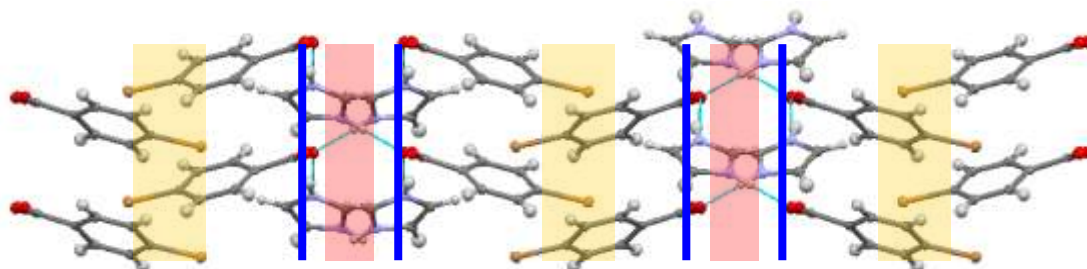


Fig. 7.38 – An extended image of the $\text{IMDH}^+ 4\text{-BrBA}^-$ molecular complex viewed along the *a*-axis, showing the main motif (blue line), the weaker C-H...O hydrogen bonds (red box) and the bromine halogen bonds (brown box).

7.5.3 Molecular Complex of Benzimidazole and Benzoic Acid 1:2

BZN has successfully been cocrystallised with benzoic acid (BA) forming a complex with a 1:1:1 molecular ratio of $\text{BZNH}^+ : \text{BA}^- : \text{BA}$. There are two unique molecules of each co-molecule, BZNH^+ , BA^- and BA within the unit cell. The molecular complex was obtained using the solvent evaporation method, with a 1:1 stoichiometric mixture of BZN (12mg) and benzoic acid (12mg) dissolved in the minimum amount of ethanol followed by evaporation at a constant temperature of between 2 and 4°C using a walk in fridge. The crystals generated were needle shaped and colourless. Single crystal X-ray diffraction data were obtained using a Bruker Nonius Kappa diffractometer at 100K, equipped with graphite monochromated Mo $K\alpha$ radiation ($\lambda = 0.71073 \text{ \AA}$). The structure was solved using SUPERFLIP within the CRYSTALS program. The crystallographic data are summarised in Table 7.6. As described in Section in 7.2.1 a BZNH^+ molecule is generated through hydrogen transfer from the BA molecule. This has the effect of normalising the internal carbon – nitrogen bond lengths and bond angles as seen in the nearly all the molecular complexes in this work. There is, however a 2:1 ratio in favour of BA over BZN molecules in this structure, with the effect that there are two BAs which are not deprotonated and two BAs which are deprotonated within the asymmetric unit. This results in six different molecules within the asymmetric unit. The effects on the carbon – oxygen bond distances are, as expected, quite profound (Table 7.14) with the deprotonated BA molecules having normalised bond lengths while the non-deprotonated retain the bond length variations characteristic of the native form.

	BA³²	Molecule 1	Molecule 2	Molecule 3	Molecule 4
C-O (Å)	1.288(3)	1.262(4)	1.316(4)	1.324(4)	1.262(4)
C=O (Å)	1.245(3)	1.263(3)	1.220(4)	1.225(4)	1.271(4)

Table 7.14 – The carbon –oxygen bond lengths of benzoic acid (BA)³² and the four benzoic acid molecules from the $\text{BZNH}^+ : \text{BA}^- : \text{BA}$ molecular complex.

The molecules involved in the proton transfer, BZNH^+ and BA^- , create partially charge assisted $\text{N}^{\delta+} - \text{H} \cdots \text{O}^{\delta-}$ hydrogen bonds between the nitrogen of the BZNH^+ and oxygen of the carboxylate group. These are of moderate strength, $a' - 2.978(3)\text{Å}$, $b' - 2.680(3)\text{Å}$, $c' - 2.924(3)\text{Å}$, $d' - 2.645(3)\text{Å}$ and arrange themselves into a 1:1 hydrogen bonded ring system that can be described by the graph set notation symbol R_4^4 (16). Attaching onto this inner ring

are the BA molecules that position themselves so that the hydroxyl oxygen hydrogen bonds to a deprotonated oxygen, $\text{O}-\text{H}\cdots\text{O}^{\delta-}$, and the carbonyl oxygen to a protonated nitrogen, $\text{N}^{\delta+}-\text{H}\cdots\text{O}$ (Figure 7.39). These hydrogen bonds are also moderate in strength with those involving the two oxygens slightly shorter, e' 2.570(3)Å, f' 2.776(4), g' 2.766(4)Å and h' 2.562(2)Å (Table 7.10). This creates a hydrogen bonded ring system, consisting of two occurrences of each molecule, BZNH^+ , BA^- and BA that can be described by graph set notation as $R_6^6(24)$. This hydrogen bonded ring, the motif of the molecular complex, is relatively flat apart from the benzene ring of molecules 1 and 3 that are $\sim 24.70^\circ$ tilted with respect to each other. There are two bifurcated hydrogen bonds ($g' : c'$ and $a' : f'$) within this structure that are borderline between being termed symmetrical or asymmetrical as the position of the hydrogen is relatively centred and the strengths of the interactions relatively equal (Table 7.15). Figure 7.39 has been produced by fixing the hydrogen atoms (found isotropically, placed on calculated positions and the thermal parameters fixed to 1.2 times to the atom to which they are bonded and no parameters refined during refinement) that are not involved in the main hydrogen bonds.

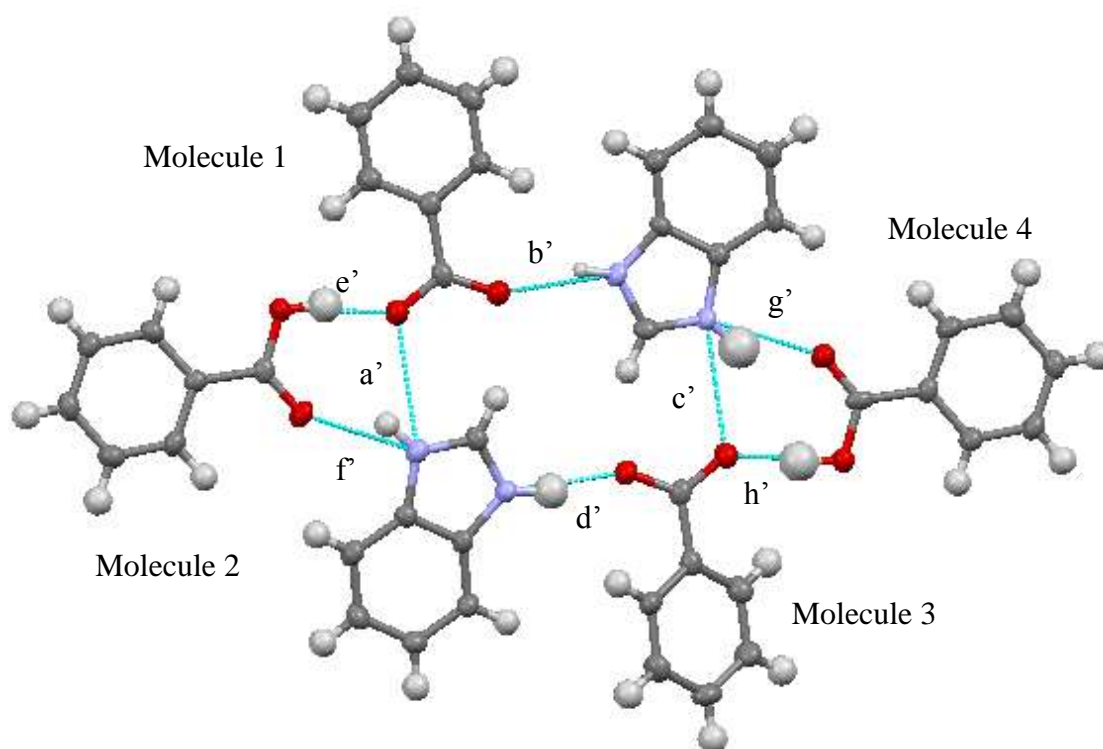


Fig. 7.39 – The motif of the $\text{BZNH}^+ : \text{BA}^- : \text{BA}$ molecular complex, an $R_4^4(24)$ hydrogen bond ring system containing two of each molecule held together by $\text{N}-\text{H}\cdots\text{O}$ (a' , b' , c' , d' , f' and g') and $\text{O}-\text{H}\cdots\text{O}$ (e' and h') hydrogen bonds. The BA and BA^- molecules are labelled 1 to 4.

Hydrogen Bonds	a'	b'	c'	d'	e'	f'	g'	h'
D...A (Å)	2.978(3)	2.680(3)	2.924(3)	2.645(3)	2.570(3)	2.776(4)	2.766(4)	2.562(2)
D-H (Å)	0.88(3)	0.82(3)	1.06(3)	0.97(2)	0.98(2)	0.88(3)	1.06(3)	0.97(2)
H...A (Å)	2.39(2)	1.90(2)	2.92(3)	1.68(2)	1.60(2)	1.99(2)	1.85(2)	1.59(2)
D-H...A angle (°)	124(2)	158(2)	123(2)	169(2)	173(1)	148(2)	142(2)	168(1)

Table 7.15 – The hydrogen bond data for all the moderate hydrogen bonds in the $\text{BZNH}^+:\text{BA}^-$: BA molecular complex.

The hydrogen bonded rings stack upon one another along the *a*-axis (Figure 7.40) held in place by two different interactions. The most significant are $\pi\cdots\pi$ interactions between the hydroxyl oxygens and the carbon located between the two nitrogens in the BZN (blue circle) and an oxygen from the deprotonated BAs with the same carbon (blue circle). These are relatively strong interactions at 3.009(4)Å (deprotonated oxygen) and 3.219(4)Å (protonated) respectively. There are also intermolecular $\pi\cdots\pi$ interactions, involving aromatic carbons from the co-molecules that have a length of 3.299(4)Å (red circle).

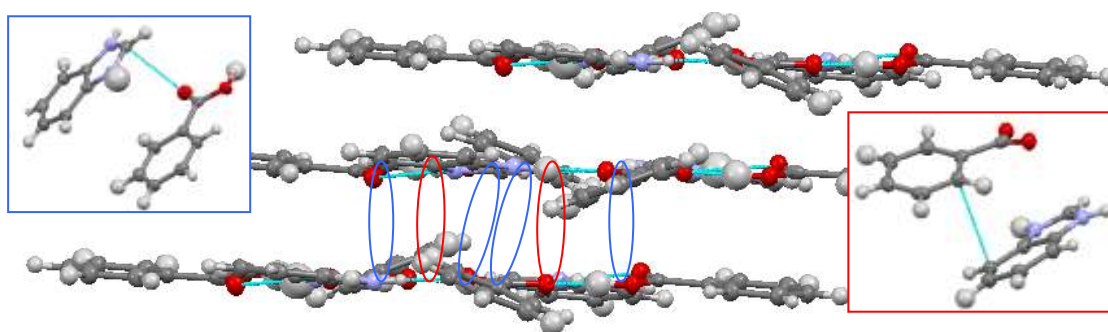


Fig. 7.40 – View along the *c*-axis highlighting the stacking behaviour of the motifs with the $\pi\cdots\pi$ interactions (red and blue ovals, and expanded in the blue and red boxes) that hold it them together.

The structure is expanded along the *b*-axis through C-H...O weak hydrogen bonds of 3.497(4)Å in length (Figure 7.41).

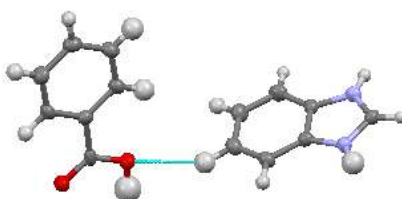


Fig. 7.41 – The C-H...O weak hydrogen bond that expands the structure along the *b*-axis.

Figure 7.42 highlights how the motifs, 6-membered hydrogen bonded rings, form a zigzag chain along the *b*-axis.

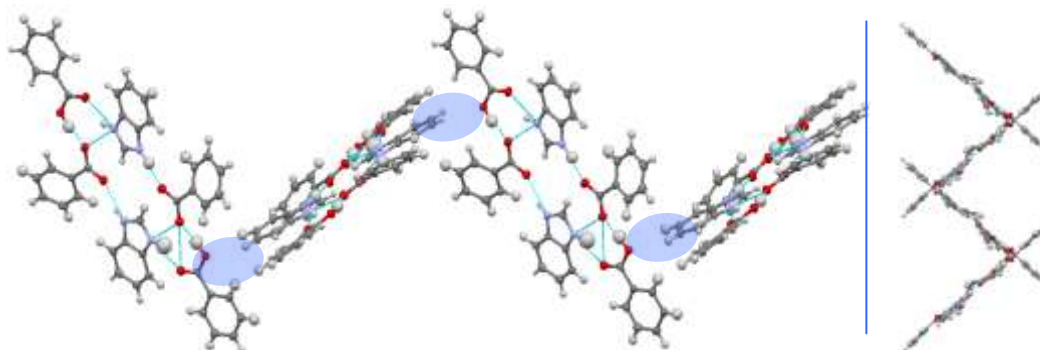


Fig. 7.42 – LHS, the blue shaded circles show where the C-H \cdots O weak hydrogen bonds (Figure 7.41) hold the motifs together; RHS, view along the *b*-axis highlighting the zigzag pattern formed by the motifs.

The two images shown in Figure 7.43 are viewed along the *a*-axis (LHS) and the *c*-axis (RHS) of the extended BZNH⁺ :BA⁻ : BA molecular complex. These highlight how the main motif, 6-membered hydrogen bonded rings, stack upon one another and that the weak C-H \cdots O hydrogen bonds extend the structure.

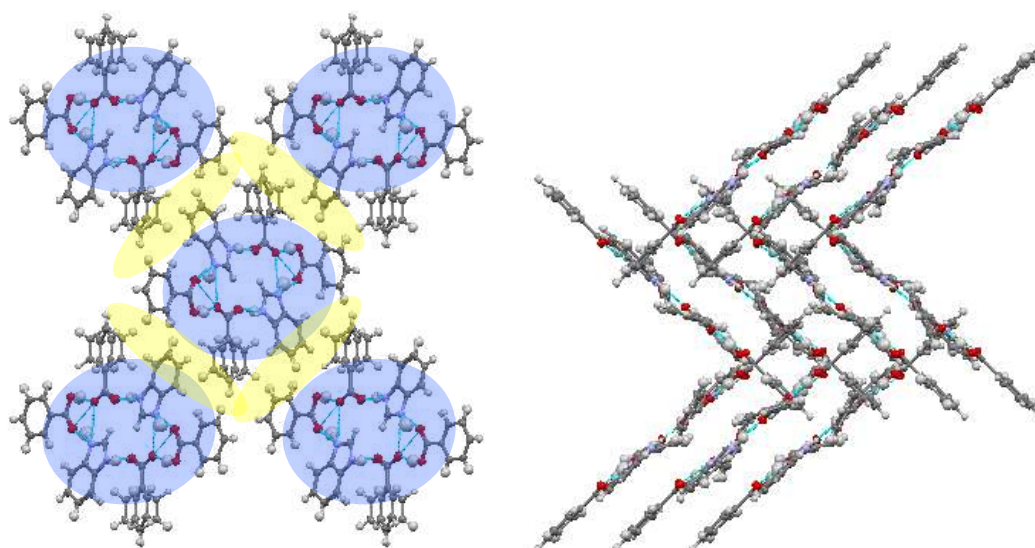


Fig. 7.43 – LHS, the *a*-axis, RHS, the *c*-axis of the extended structure showing how the main motif (blue areas) is expanded by weak C-H \cdots O hydrogen bonds (yellow areas).

7.5.3.1 Imidazolium Benzoate 1:1

The molecular ions, imidazolium and benzoate, form a 1:1 molecular complex that was published in 2006³³. The structure adopts the linear chain motif which, like other imidazolium molecular complexes, has a spiral nature (Figure 7.44). The chain is created through moderate N-H...O hydrogen bonds that utilise the hydrogen bond patterns E and F. The hydrogen bond distances are comparable to the benzimidazolium complex at E, N...O 2.613(3)Å and F, 2.666(3)Å compared to 2.645(3)Å and 2.776(4)Å in the imidazolium complex.



Fig. 7.44 – LHS, the linear chain of hydrogen bonded alternating co-molecules is the main motif in the imidazolium benzoate structure³³; RHS, shows the cyclical nature of the motif.

The motif is expanded throughout the structure by two interactions, the strongest is a weak hydrogen bond involving the carbon located between the nitrogens on the imidazolium molecule and an oxygen. The other is a weak carbon – carbon hydrogen bond of around 3.664(6)Å.

7.6 Molecular Complexes Containing Aromatic Dicarboxylic Acids and Benzimidazole

Cocrystallisations with the aromatic dicarboxylic acids series produced two previously undiscovered molecular complexes, benzimidazole : terephthalic acid and benzimidazole : phthalic acid (Table 7.2).

	Imidazole	Source	Benzimidazole	Source
Terephthalic acid	1:1	CSD	1:1	New
Isophthalic acid	1:1	CSD	1:1	CSD (RD)
Phthalic acid	n/a	n/a	1:1	New

Table 7.2 repeated – Summary of the molecular complexes that exist between IMD and BZN with aromatic dicarboxylic acids. “New” represents molecular complexes generated for the first time during this research, “CSD” accounts for those that have already been solved while “RD” stands for re-determined, i.e. cases where a new X-ray diffraction experiment was attempted to get a improved data set than that available in the literature.

The existence of two carboxylic acid groups on the benzoic acid brings potential similarities to the hydroxy-substituted benzoic acids molecular complexes with the real possibility of producing ladder style motifs. However there will also be a carboxylic acid group that is not deprotonated, increasing the number of potential hydrogen bond patterns. From Figure 7.18, it is essentially guaranteed that either hydrogen bond pattern E or F will be found in the structures. Within the iso- and terephthalic acid structures hydrogen bond patterns I, J and a full carboxylic acid dimer are the only options available for the carboxylic acid groups. When the second carboxylic acid is in the ortho position, as in phthalic acid, there is the likely option that the hydroxyl section will create an intramolecular hydrogen bond, as seen in the other molecular complexes involving phthalic acid that have been generated, therefore motif N, a linear chain of alternating co-molecules, is very possible. However the hydroxyl group may not form an intramolecular hydrogen bond, therefore will seek to adopt hydrogen bond patterns as found in the iso- and terephthalic acid complexes. For these structures the potential motifs are thus, in order of possibility, K, the ladder style (seen in the 3- and 4-hydroxybenzoic acid structures, L, the hydrogen bonded ring (as in benzimidazole and 2-hydroxybenzoic acid) then N the linear chain.

7.6.1 Molecular Complex of Benzimidazole and Phthalic Acid 1:1

The molecular ions, benzimidazolium and phthlate, form a 1:1 molecular complex with one another (Figure 7.45). Single crystals were obtained using the solvent evaporation method, with a 1:1 stoichiometric mixture of benzimidazole (12mg) and phthalic acid (16mg) dissolved in the minimum amount of methanol followed by evaporation at room temperature. The crystals generated were needle shaped and colourless. Single crystal X-ray diffraction

data were obtained using a Bruker Apex II diffractometer at 100K, equipped with graphite monochromated Mo K α radiation ($\lambda = 0.71073 \text{ \AA}$). The structure was solved using SUPERFLIP within the CRYSTALS program. The crystallographic data are summarised in Table 7.6. It can be seen that the data are only 96.8% complete with a theta range of 1.58-22.36 $^\circ$, therefore the hydrogens atoms have been fixed to reduce the number of parameters (found isotropically, placed on calculated positions and the thermal parameters fixed to 1.2 times to the atom to which they are bonded and no parameters refined during refinement).

In the molecular complex, the BZN molecule is protonated as discussed in section 7.2.1. The result is the normalisation of the internal bond lengths (N1-C1 1.321(6) \AA , N2-C1 1.326(5) \AA) and angles (C2-N1-C1 107.8(3) $^\circ$, C7-N2-C1 107.9(3) $^\circ$) and the creation of a positive charge that is delocalised over the 5-membered ring.

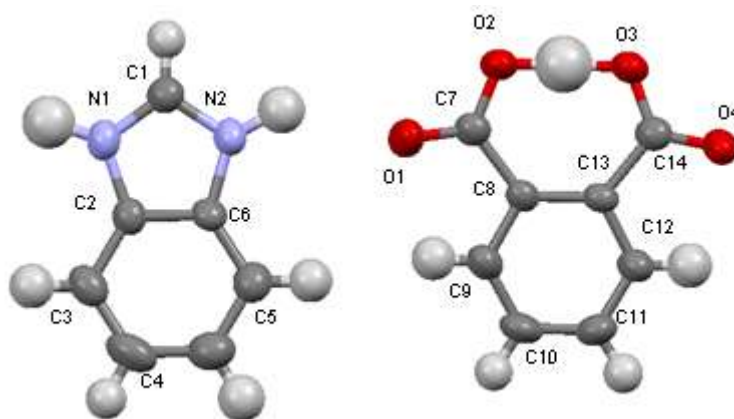


Fig. 7.45 – The molecules involved in the benzimidazolium phthalate molecular complex, with atom labelling.

Interaction	Length (D \cdots A(\AA))	For Hydrogen Bonds		
		D-H(\AA)	H \cdots A(\AA)	D-H \cdots A angle($^\circ$)
O2 \cdots O3	2.378(4)	1.179(3)	1.207(3)	170.6(2)
N1 \cdots O4	2.691(5)	1.001(3)	1.710(3)	165.7(2)
N2 \cdots O1	2.759(6)	1.000(3)	1.778(3)	165.0(2)
N2 \cdots O2	3.038(5)	1.000(3)	2.403(3)	120.7(2)
C4 \cdots O4	3.344(6)	0.909(5)	2.533(4)	148.9(3)
C10 \cdots O1	3.329(6)	0.943(4)	2.681(4)	126.5(3)
C5 \cdots π	3.847	-	-	-

Table. 7.16 - The three scalar quantities and bond angles of the hydrogen bonds and list of the interactions between the molecules in the benzimidazolium phthalate molecular complex.

Within the molecular complex the phthalic acid molecule is deprotonated, creating the phthalate species. Within this molecule an intramolecular hydrogen bond between the hydroxyl and carboxylate groups is formed, as in the other phthalate molecular complexes. This intramolecular hydrogen bond, O2 \cdots H \cdots O3, is strong with an O \cdots O distance of 2.378(4)Å which is consistent with the hydrogen bond found within the 2,6-dimethylpyridinium hydrogen phthalate molecular complex⁶, (2.398(2)Å). The intramolecular hydrogen bond results in the proton being shared over the two oxygens, this can be seen in the carbon – oxygen bond distances which have been slightly normalised, C1-O1 1.233(6)Å, C1-O2 1.275(5)Å, C8-O3 1.280(5)Å and C8-O4 1.243(6)Å. The structure adopts the linear chain of alternating co-molecules arranged in a spiral fashion (Figure 7.46). This motif, which is an example of the linear chain of alternate co-molecules of motif N, utilises the robust hydrogen bond pattern E, N-H \cdots O, only. The N-H \cdots O hydrogen bonds are moderate in strength, N1 \cdots O4, 2.691(5)Å, with an asymmetrical bifurcated hydrogen bond having distances of N2 \cdots O1, 2.756(5)Å and N2 \cdots O2, 3.038(5)Å (Table 7.16). The motif expands the structure along the *a*-axis.

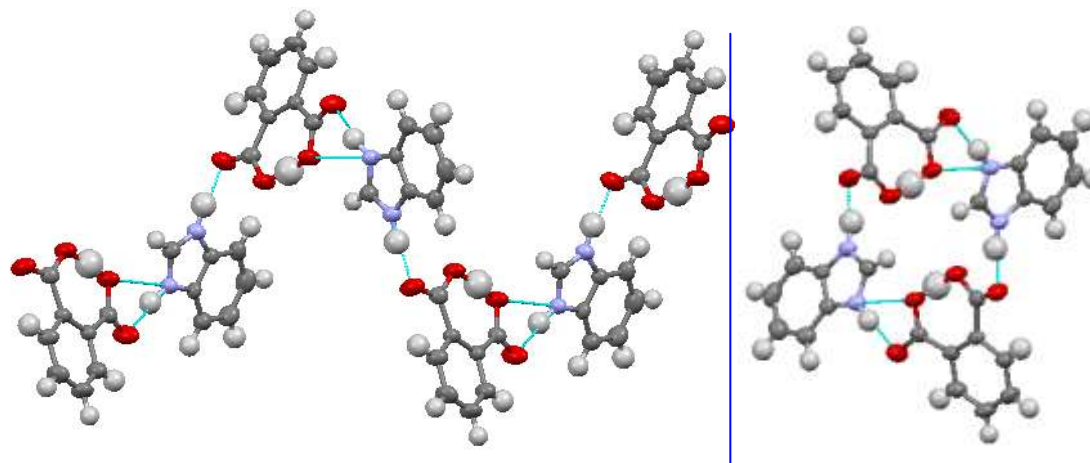


Fig. 7.46 – LHS, view of the main motif, linear chain of alternating hydrogen bonded co-molecules; RHS, view along the *a*-axis that highlights the spiral nature of the chain.

Expanding the structure along the *b*-axis is a C-H \cdots O hydrogen bond that connects the spiral chains together (Figure 7.47). This weak hydrogen bond, C4 \cdots O4, has length 3.344(6)Å and is the only interaction between the chains that expands the structure along the *b*-axis.

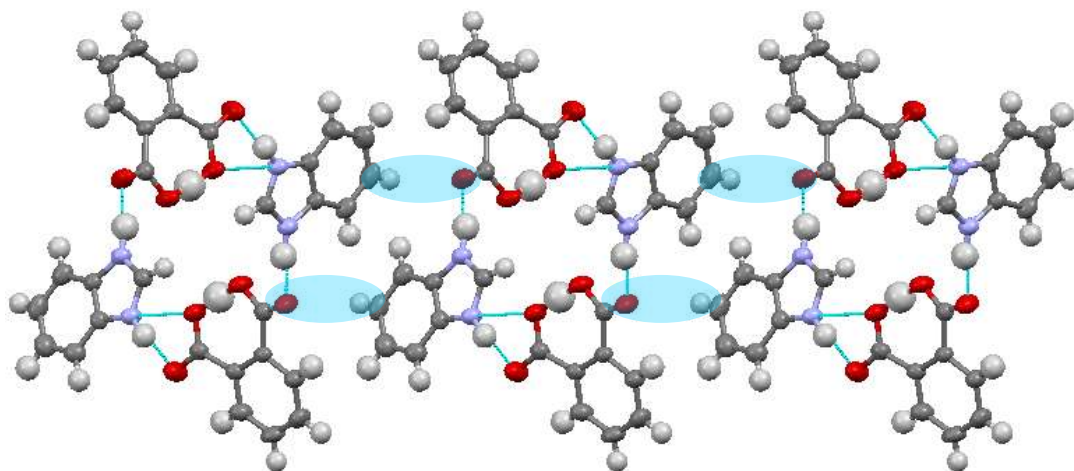


Fig. 7.47 – View along the *a*-axis of three motifs, spiral chains of alternating hydrogen bonded co-molecules, that are held together by C-H...O weak hydrogen bonds (blue circles).

Expanding the structure along the *c*-axis are two interactions involving three molecules. Again these interactions have the role of connecting two of the spiral chains together. The more significant of these is a C-H...O weak hydrogen bond, with C10...O1 distance of 3.329(6)Å (green line in Figure 7.48). The other interaction is a C-H... π interaction which is extremely weak at 3.847(7)Å in length (purple line in Figure 7.48).

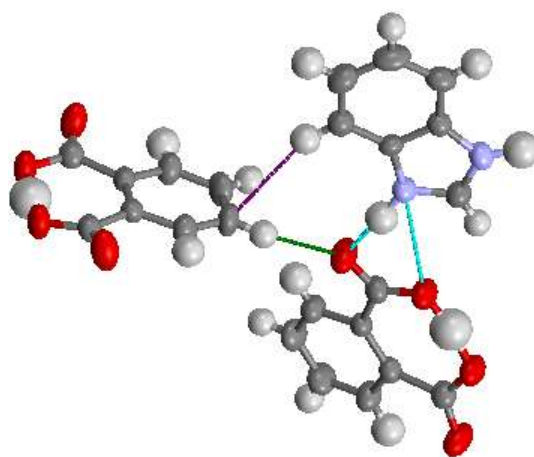


Fig. 7.48 – The weak hydrogen bond, C-H...O (green line) and C-H... π interaction (purple line), that expand the structure along the *c*-axis.

Figure 7.49 is the extended structure viewed along the *a*-axis. From this it can be seen that the motif (coloured in red) which extends along the *a*-axis, is expanded along the *b*-axis using the C-H...O weak hydrogen bonds (coloured in blue) and along the *c*-axis by the C-H...O (green) and C-H...C (purple) hydrogen bonds.

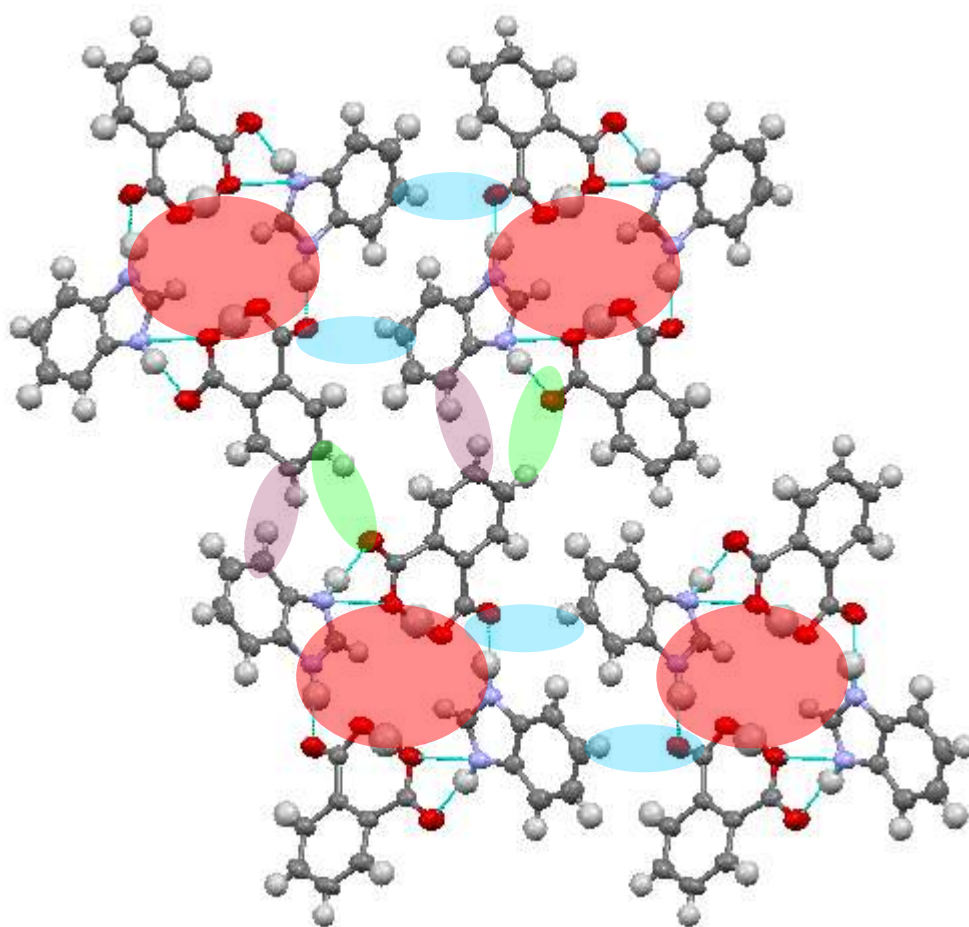


Fig. 7.49 – The extended structure viewed along the *a*-axis, showing how the motif (red) is expanded along the *b*-axis by weak C-H...O hydrogen bonds (blue) and finally along the *c*-axis by C-H...O (green) and C-H...C hydrogen bonds (purple).

7.6.2 Molecular Complex of Benzimidazole / Imidazole and Isophthalic Acid

Both the structures of the molecular complexes of benzimidazole¹¹ (CSD reference VARJAA) and imidazole¹² (CSD reference MEQQOO) with isophthalic acid are known (Table 7.17). Within the BZNH⁺ structure, both the co-molecules are disordered therefore accurate hydrogen positions are impossible to determine. Single crystal X-ray diffraction experiments performed during this project on crystals of the benzimidazole : isophthalic acid complex also proved difficult due to the poor quality crystals produced (twinning). Therefore, the data deposited in the CSD are used for the comparison work.

Complex	Space Gp	Cell Lengths (Å)	Cell Angles (°)	Volume / Z
BZN : isophthalic acid	$P 2_1/c$	10.157(4) 5.130(7) 26.067(6)	90 90.98(4) 90	1358.03 4
IMDH⁺ isophthalate	$P 2_1 2_1 2_1$	3.883(2) 14.015(2) 19.302(2)	90 90 90	1050.42 4

Table 7.17 – Basic crystal data for the benzimidazole : isophthalic acid molecular complex and the imidazolium isophthalate molecular complex.

The structures produced were in a 1:1 molecular ratio with proton transfer occurring in the imidazole complex but it is undetermined if it also occurred in the benzimidazole complex (Figure 7.50).

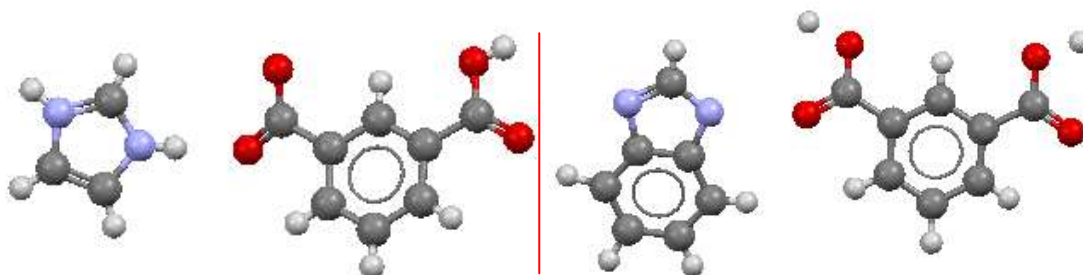


Fig. 7.50 – LHS, the molecules involved in the imidazolium isophthalate molecular complex; RHS, those involved in the benzimidazole isophthalic acid molecular complex, with the carboxylic acid protons in undetermined positions.

Structure Description

The benzimidazole : isophthalic acid molecular complex contains four unique hydrogen bonds utilising the hydrogen bond patterns E, N-H...O and J, O-H...O (Figure 7.51). These hydrogen bonds are moderate in strength, A', 2.637(5)Å, B', 2.482(4)Å, C', 2.492(4)Å and D', 2.601(5)Å, and arrange the structure into linear chains of alternate co-molecules using hydrogen bond E, that link together through hydrogen bond J. This chain, containing a double line of alternate co-molecules, expands the structure along the *a*-axis.

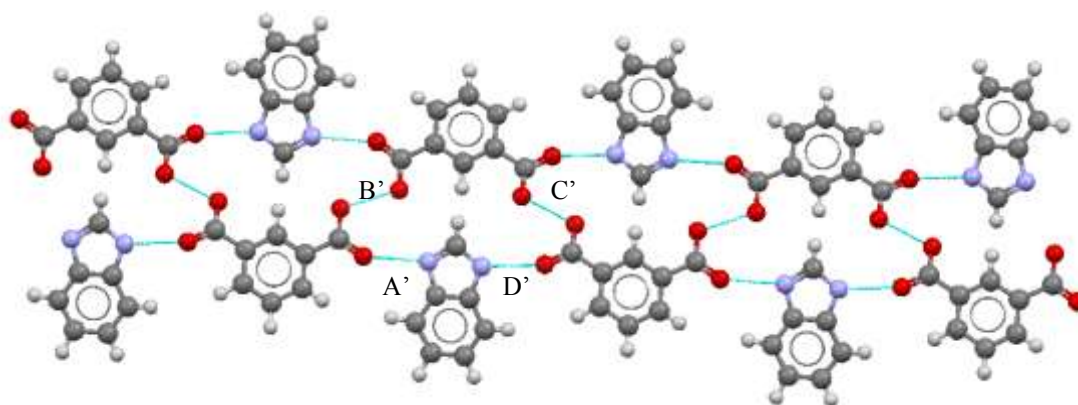


Fig. 7.51 – The main motif of the structure, a double linear chain of alternate co-molecules held together through N-H...O and O-H...O hydrogen bonds.

The structure is expanded by lesser interactions including C-H...C hydrogen bonds of 3.766(7)Å (Figure 7.52) that expand the structure along the *c*-axis and C-H...O interactions that stack the motifs upon one another.

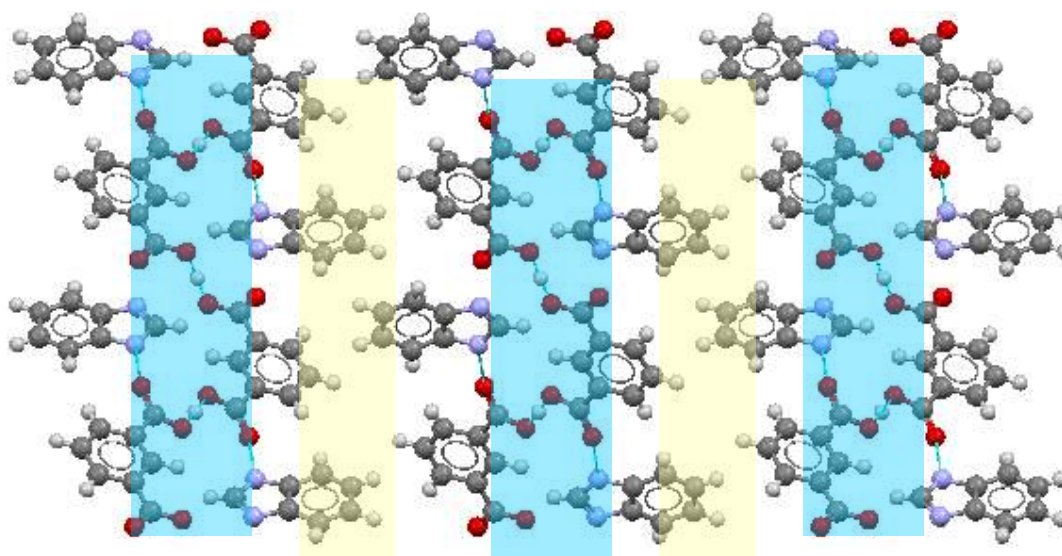


Fig. 7.52 – An extended structure showing the motifs (blue box) being expanded along the *c*-axis by carbon – carbon hydrogen bonds (yellow box).

The imidazolium isophthlate structure uses the same hydrogen bond patterns, E, N-H...O and J, O-H...O, however with one less moderate hydrogen bond. Whereas the benzimidazole structure has two of each of these hydrogen bonds, the imidazole structure has only one O-H...O hydrogen bond. The effect is that rather than having flat linear chains that can stack upon one another, the imidazole complex structure has linear chains of isophthlate molecules with imidazole molecules connecting these chains together (Figure 7.53).

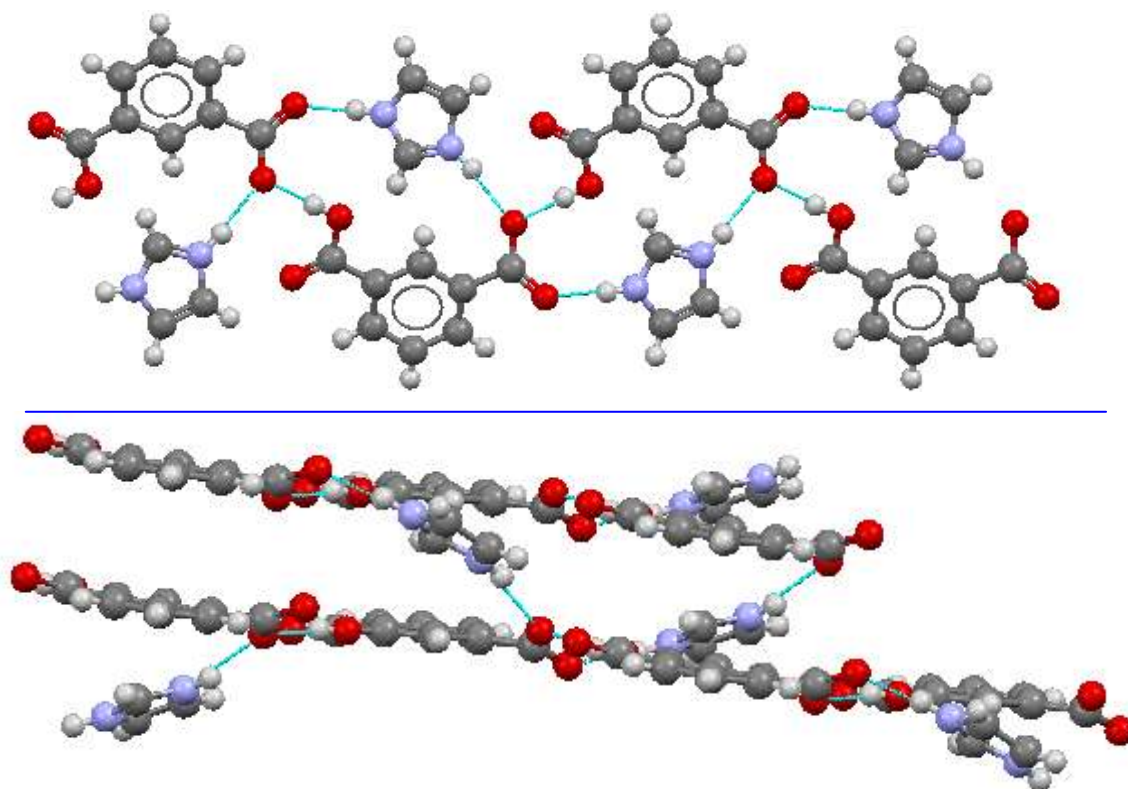


Fig. 7.53 – top, the view along the *a*-axis of the chains of isophthalic acid hydrogen bonding to the imidazolium molecule, bottom, view of the *b*-axis highlighting how the imidazolium molecule hydrogen bonds to two different chains on different layers.

The hydrogen bonds are moderate in strength, O \cdots O, 2.543(2)Å, N \cdots N, 2.858(3)Å and 2.651(2)Å and expand the structure along the *b*- and *c*-axes.

7.6.3 Molecular Complex of Benzimidazole / Imidazole and Terephthalic Acid

The molecular ions, benzimidazolium and terephthalate, form a 1:1 molecular complex with one another. Single crystals were obtained using the solvent evaporation method, with a 1:1 stoichiometric mixture of benzimidazole (12mg) and terephthalic acid (17mg) dissolved in the minimum amount of methanol followed by evaporation at ~-2-4°C in a cold room. The crystals generated were needle shaped and colourless. Single crystal X-ray diffraction data were obtained using a Bruker Nonius Kappa diffractometer at 100K, equipped with graphite monochromated Mo K α radiation ($\lambda = 0.71073$ Å). The structure was solved using SIR92 within the CRYSTALS program. The crystallographic data are summarised in Table 7.6.

The BZN molecule is protonated through hydrogen transfer from the carboxylic acid group on the terephthalic acid molecule (Figure 7.54) resulting in a delocalisation of the charge across the five-membered ring, N1-C1 1.332(2)Å, N2-C1 1.323(2)Å (section 7.2.1). The deprotonation of a carboxylic acid group, creating the terephthalate molecule, results in a negative charge on the carboxylate group that is normalised over the group, as seen in the carbon oxygen bond lengths, C8-O1 1.235(2)Å and C8-O2 1.277(1). The neutral carboxylic acid group retains its bond lengths, C14-O3 1.325(2)Å and C14-O4 1.217(2)Å.

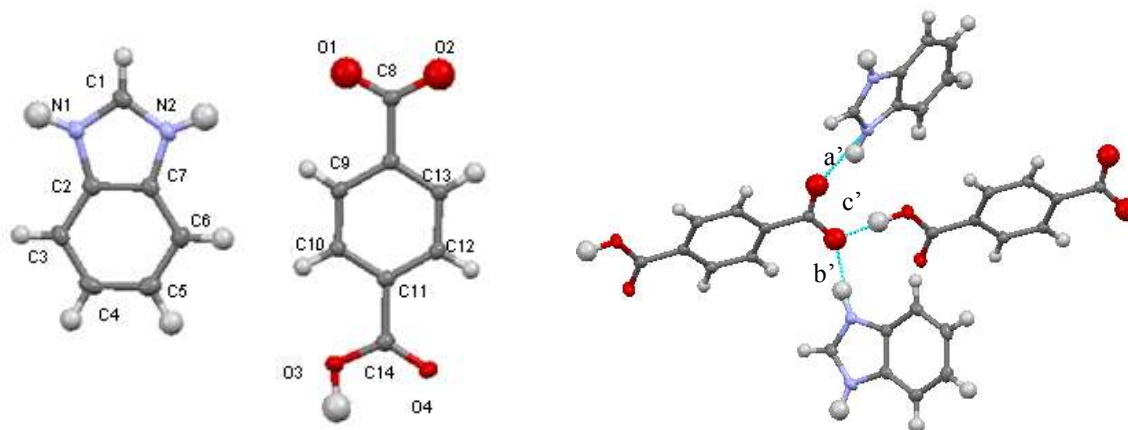


Fig. 7.54 – LHS, the benzimidazolium and terephthalate molecules involved in the molecular complex with atom labelling; RHS, the three main hydrogen bonds involved in the molecular complex, a' N-H \cdots O, b' N-H \cdots O and c' O-H \cdots O.

The benzimidazolium terephthalate molecular complex contains three distinct hydrogen bonds that adopt the hydrogen bonding patterns E, F and J (Figure 7.54 RHS). The strongest is the oxygen – oxygen hydrogen bond, c' O3-H \cdots O2, that has length of O \cdots O 2.580(1)Å. The two N-H \cdots O hydrogen bonds are similar in strength at a' N1-H \cdots O2, 2.635(2)Å and b' N2-H \cdots O1 2.699(1)Å (Table 7.18).

Interaction	Label	Length (Å) (D \cdots A(Å))	For Hydrogen Bonds		
			D-H(Å)	H \cdots A(Å)	D-H \cdots A angle(°)
O2 \cdots N2	a'	2.635(2)	0.96(2)	1.71(2)	158.9(2)
N2 \cdots O2	b'	2.699(1)	0.97(2)	1.74(2)	168.4(2)
C1 \cdots O1	c'	2.580(1)	1.04(2)	1.55(2)	172.8(2)
C1 \cdots O4		3.112(2)	1.00(1)	2.11(1)	174(1)

Table 7.18 – The hydrogen bond data for the hydrogen bonds in the benzimidazolium terephthalate molecular complex.

These three moderate hydrogen bonds arrange the structure into the ladder motif K, with uprights of terephthalic acid molecules that are bonded through the O-H...O hydrogen bonds and rungs of benzimidazolium molecules that utilise the N-H...O hydrogen bonds (Figure 7.55). This motif runs along the *a*- and *c*-axis and is common with the hydroxyl-benzoic acid molecular complexes.

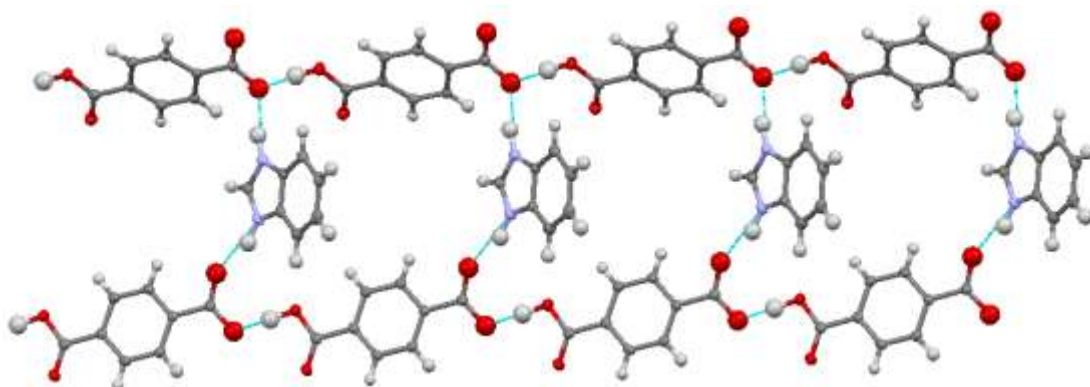


Fig. 7.55 – The main motif of the benzimidazolium terephthalate molecular complex, a ladder with uprights of terephthalate molecules and rungs of benzimidazolium molecules.

There is only one other significant interaction with this structure which expands the structure along the *b*-axis (Figure 7.56). A carbon – oxygen hydrogen bond, involving the carbon located between the two nitrogens and oxygen O4 (Figure 7.56 extract), is 3.112(2)Å in length.

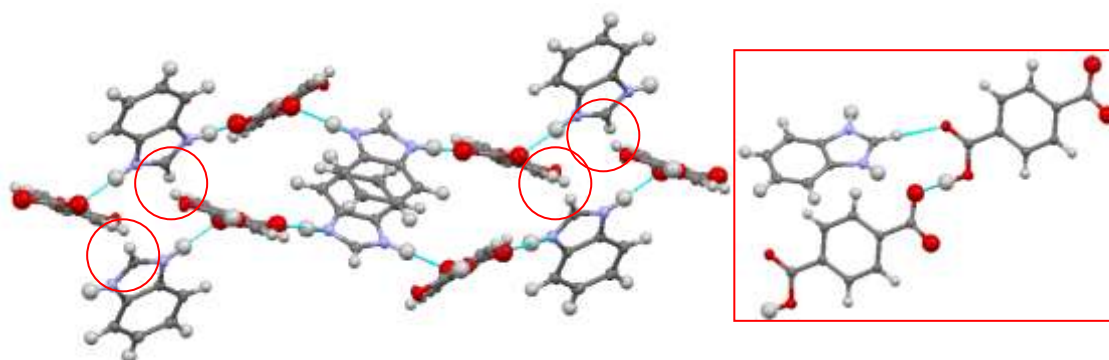


Fig. 7.56 – The main motif, a ladder of terephthalic acid uprights and benzimidazole rungs, stack upon one another through C-H...O hydrogen bonds (red circle); insert, blown-up image of the C-H...O hydrogen bond.

Figure 7.57 shows two images of the extended structure viewed along the *c*-axis (LHS) and *a*-axis (RHS). They both show how the motif expands the structure along the *a*- and *c*-axis while the weak C-H...O hydrogen bond stacks these chains on top of one another along the *b*-axis.

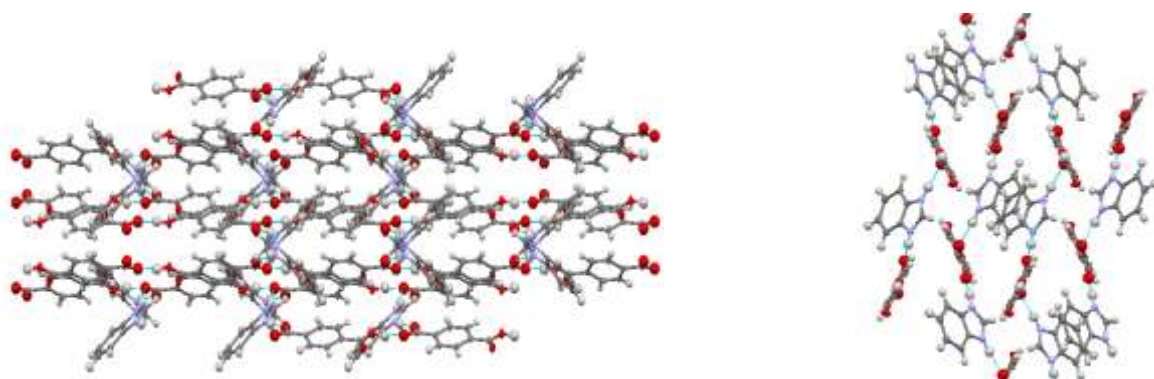


Fig. 7.57 – The extended structure of the benzimidazolium terephthalate molecular complex viewed along the *c*-axis (LHS) and *a*-axis (RHS).

Imidazole Structure

The structure of the imidazole : terephthalic acid molecular complex was published in 2007¹⁸ (Table 7.19). The structure adopts the spiral linear chain motif, with alternating co-molecules hydrogen bonded together, that expands the structure along the *b*-axis (Fig. 7.58). With the other carboxylic acid group still available for hydrogen bonding the chain also expands along the *ac* diagonal (Figure 7.59 LHS). A C-H...O weak hydrogen bond, the last significant interaction within the structure, connects the motif along the *a*-axis (Figure 7.59 RHS).

	Space Gp	Cell Lengths (Å)	Cell Angles (°)	Volume / Z
Imidazolium terephthalate	<i>P 2₁/n</i>	9.6288(6)	90	721.124
		8.3351(6)	113.8540(10)	
		9.8244(6)	90	2

Table 7.19 – Basic crystallographic data of the imidazolium terephthalate molecular complex.



Fig. 7.58 – LHS, the linear chain of alternating co-molecules that is the motif of the molecular complex; RHS, view along the *b*-axis highlighting the spiral nature of the chain.

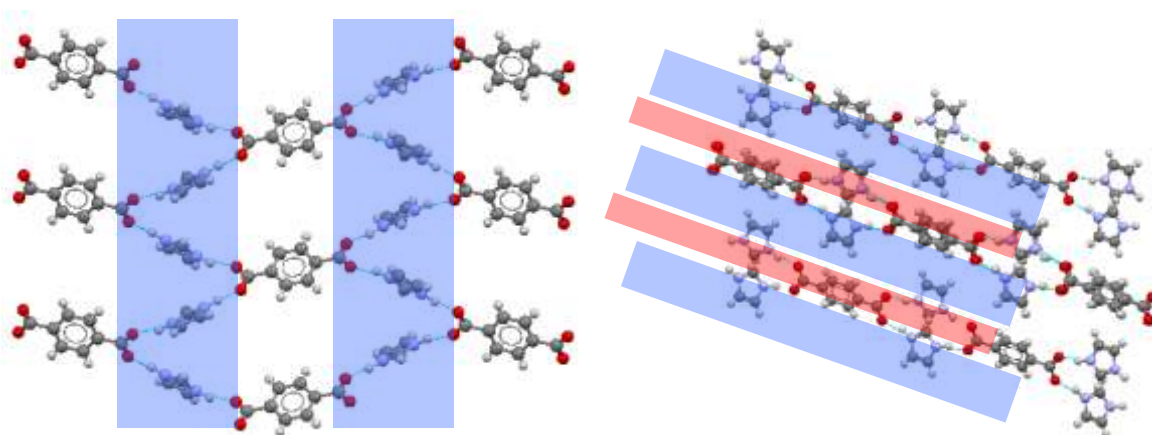


Fig. 7.59 – LHS, the motif, spiral chains (blue box), expands along the *b*-axis and *ac*-diagonal forming sheets; RHS, the C-H...O weak hydrogen bond (red box) connects these sheets together along the *a*-axis.

7.7 Benzimidazole and Imidazole Molecular Complexes with Non-Aromatic Dicarboxylic Acids

Cocrystallisations with a range of non-aromatic dicarboxylic acids produced four new molecular complexes (Table 7.4); BZN with fumaric, succinic, maleic acids and IMD with malonic acid, all in a 1:1 molecular ratio and all with associated proton transfer (Section 7.2.1). An improved model for the benzimidazole and malonic acid structure has been proposed over that which has been published. Structures containing IMD with fumaric, succinic and maleic acid and a malonic acid hydrate have already been solved and deposited in the CSD, and are discussed here for comparison purposes.

	Imidazole	Source	Benzimidazole	Source
Fumaric acid	1:1	CSD	1:1	New
Succinic acid	1:1	CSD	1:1	New
Maelic acid	1:1	CSD	1:1	New
Malonic acid	1:1 (1:1 hydrate)	New (CSD)	1:1	RD

Table 7.4 repeated – Summary of the successful cocrystallisation experiments between IMD and BZN with dicarboxylic acids. “New” represents molecular complexes generated for the first time during this research, “CSD” accounts for those that have already been solved, while “RD” stands for re-determined, i.e. cases where a new X-ray diffraction experiment was attempted to get a improved data set than that available in the literature.

The main hydrogen bonds in these molecular complexes will undoubtedly come from the nitrogens of the benzimidazole and imidazole molecules and the carboxylic acid group of the dicarboxylic acids series. Consideration of the many potential hydrogen bonds that could form between them can be reduced by using the library of hydrogen bond patterns that have constantly appeared in previous structures containing these characteristic hydrogen bond donor and acceptor groups. The hydrogen bond patterns that have been identified in previous chapters, E through to J (Figure 7.18 pattern extract, repeated below), have once again been utilised in the structures studied in this chapter, including the aromatic dicarboxylic acids which are very similar in terms of functional groups to the dicarboxylic acid series presented in this section. It is therefore highly likely that hydrogen bond patterns E, F and J will prevail in these structures. There will also be potential for carboxylic acid dimers, as seen in hydrogen bond pattern I, to be used in the hydrogen bonds.

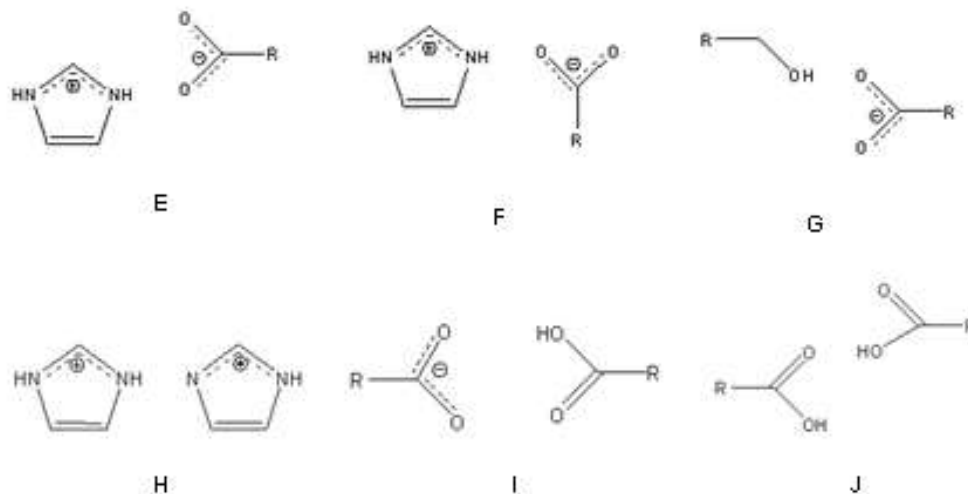


Fig. 7.18 pattern extract – the library of hydrogen bond patterns that the molecular complexes are highly likely to adopt – E, F, G, H, I and J – are all seen in other molecular complexes.

With regard to the potential motifs (Figure 7.18 motif extract, repeated below) that may be formed between the co-molecules, that will undoubtedly use hydrogen bond patterns E, F and I, there is a very high possibility that motif N, linear chain of alternate co-molecules, will be influential. There is also a possibility that the ladder motif may also appear, however this would only be an option where the chain is rigid and the carboxylic acid groups are in the

trans disposition, i.e. fumaric acid. A specific comment can be made with regard to the imidazole molecules, in which there has been a high tendency for these structure to adopt the linear chain motif, N, with a spiral nature. It would be no surprise if these structures once more adopted this nature of chain.

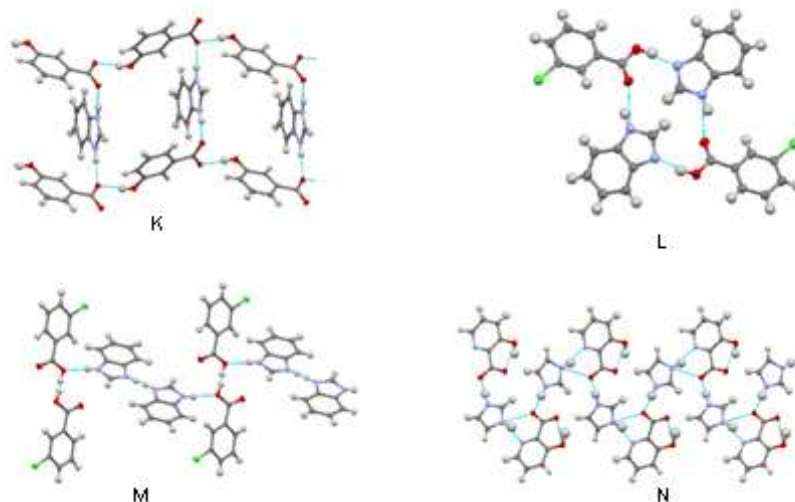


Fig. 7.18 motif extract – the motifs are the general modes of assembly of the molecules; K is the ladder motif, L is the hydrogen bonded ring motif, M is the co-molecule dimer motif while N is an example of a linear chain of alternate co-molecules.

7.7.1 Molecular Complexes of Benzimidazole and Imidazole with Fumaric Acid

Successful cocrystallisation experiments have produced the previously undetermined structure of benzimidazole with fumaric acid. The structure of the molecular complex salt imidazolium fumarate has previously been solved and published¹².

In this case, following the logic being applied throughout this work, there is a real possibility of formation of an influential N-H \cdots O hydrogen bond between the molecules, with it either adopting hydrogen bond pattern E or F. With one of the carboxylic acid groups undergoing deprotonation, there will be only one hydroxyl group in the structure. From the length of the carbon chain and the double bond on the chain, this hydroxyl group will be available for intermolecular hydrogen bonding. This would promote the possibility of hydrogen bond pattern I or J forming.

Benzimidazolium Fumarate

The molecular ions benzimidazolium and fumarate form a 1:1 molecular complex. The molecular complex was obtained using the solvent evaporation method, with a 1:1 stoichiometric mixture of benzimidazole (12mg) and fumaric acid (12mg) dissolved in the minimum amount of ethanol and left to evaporate at room temperature. The crystals generated were needle shaped and colourless. Single crystal X-ray diffraction data were obtained using a Bruker Nonius Kappa diffractometer at 100K, equipped with graphite monochromated Mo K α radiation ($\lambda = 0.71073 \text{ \AA}$). The structure was solved using SUPERFLIP within the CRYSTALS program. The crystallographic data are summarised in Table 7.5.

In the molecular complex, the benzimidazole molecule is protonated through hydrogen transfer from one of the carboxylic acid groups on the fumaric acid molecule, as described in Section 7.2.1 (Figure 7.60). The result is that the internal bond lengths are now normalised, with N1-C1 1.323(2) \AA and N2-C1 1.330(2) \AA , and bond angles to C1-N1 $^{\delta+}$ -C2 108.2(1) $^{\circ}$ and C1-N2 $^{\delta+}$ -C7 108.2(1) $^{\circ}$.

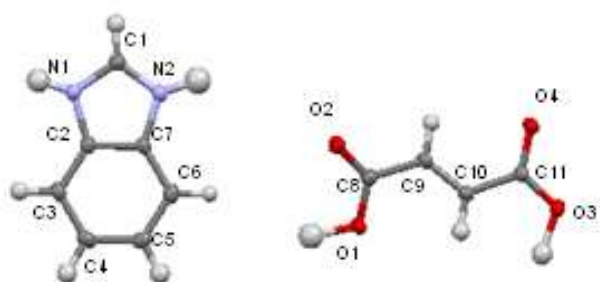


Fig. 7.60 – The benzimidazolium and fumarate ions (two protons are shown, but both have 0.5 occupancy levels) which are generated in the molecular complex/salt, with atom labelling.

Fumarate with	BZNH$^+$ (\AA)	IMDH$^+$ (\AA)
C8-C1	1.286(2)	1.309(1)
C8-O2	1.238(2)	1.212(1)
C11-O3	1.292(2)	1.238(1)
C11-O4	1.240(2)	1.269(1)

Table. 7.20 – The carbon oxygen bond lengths in the benzimidazolium fumarate and imidazolium fumarate molecular complex.

In its native form, the fumaric acid molecule adopts the carboxylic acid dimer with the hydroxyl groups in the molecule directed parallel to the molecule (Figure 7.61 LHS).

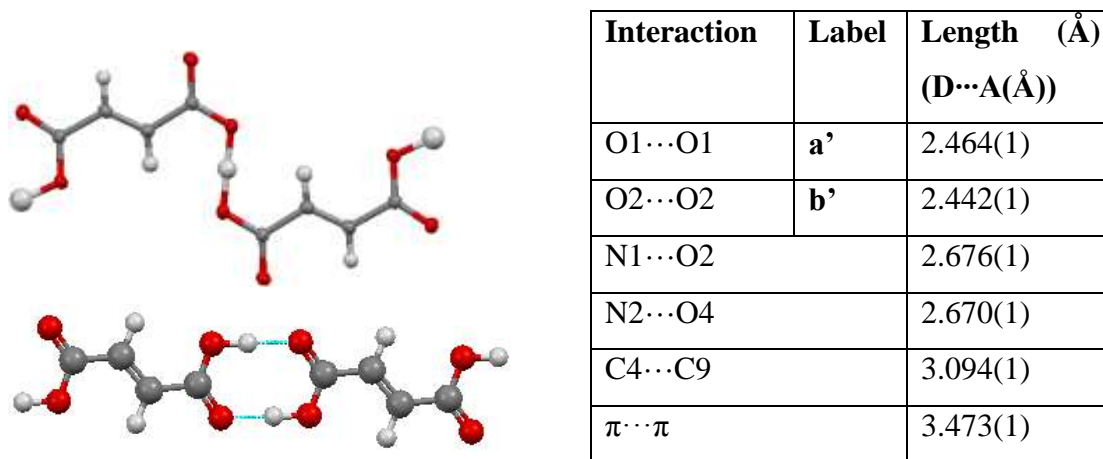


Fig. 7.61 – LHS, The carboxylic acid dimer of the fumaric acid structure; RHS, the hydrogen bond between the fumarate molecules of the benzimidazolium complex, with the shared proton split over the two sites.

Table 7.21 – A list of the hydrogen bonds and interactions in the benzimidazolium fumarate molecular complex.

Within the molecular complex with benzimidazolium, one of the carboxylic acid groups of the fumaric acid has been deprotonated. The result is that the remaining proton becomes shared over the two carboxylic acid groups (Figure 7.61 RHS). This can be seen in the partial normalisation of the carbon – oxygen bond lengths of the carboxylic acid groups (Table 7.20). In the imidazolium fumarate molecular complex proton transfer has also occurred however the remaining proton is only associated with one carboxylic acid which can be seen in the carbon – oxygen bond lengths. The shared protons, associated with the benzimidazolium complex, lie on an inversion centre between two of the same oxygen atoms, therefore each hydrogen within the asymmetric unit has a 0.5 occupancy levels, resulting in 1.0 occupancy levels over the hydrogen bond. The hydrogen bond involving the shared protons, a' O1·H·O1 and b' O3·H·O3, are of strong strength, a' 2.464(1) and b' 2.442(1), and creates a box comb chain of fumarate molecules along the *b*-axis (Figure 7.62)(Table 7.20). The box comb chain shape comes about because the one of the hydrogen bonds is “face to face”, a', while the other is “edge to edge”, b'.

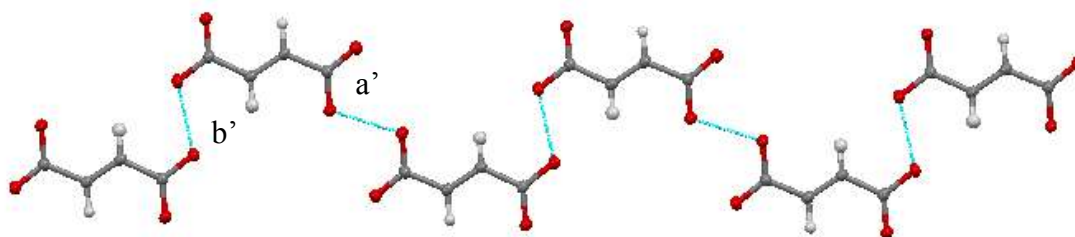


Fig. 7.62 – The box comb chain of fumarate molecules held together by oxygen – oxygen hydrogen bonds, a' and b' . The hydrogens on the carboxylic acid groups have been removed.

There are two other hydrogen bonds within the molecular complex, these follow the hydrogen bond pattern E, N-H \cdots O. These moderate hydrogen bonds of lengths N1 \cdots O2 2.6767(1) \AA and N2 \cdots O4 2.6702(1) create chains of alternating co-molecules along the b -axis (Figure 7.63).

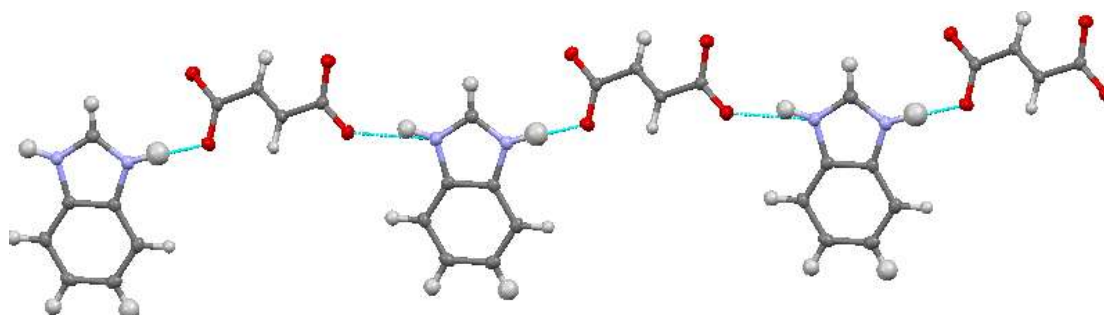


Fig. 7.63 – The co-molecules arrange themselves into hydrogen bonded alternating co-molecules which expand along the b -axis.

The two chains, fumarate chain (Figure 7.62) and the alternating co-molecule chain (Figure 7.63), combine to form interconnected layers, with the benzimidazole molecule connecting two of the fumarate chains together, this expands the structure along the a -axis (Figure 7.64 LHS). This has the effect of creating a column of layers interconnected by moderate hydrogen bonds that expands along the a - and b -axis (Figure 7.64 RHS).

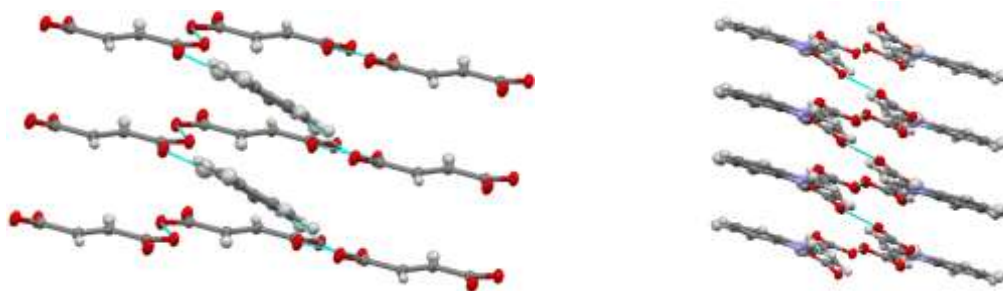


Fig. 7.64 – LHS, the benzimidazolium molecules connect the fumarate chains along the a -axis, resulting in the layers of fumarate and alternating co-molecules interconnecting to form columns of layers, RHS.

Between the columns are two very weak interactions which are shown in the inset to Figure 7.64. These interactions connect the columns together along the *c*-axis (Figure 7.65). The carbon – carbon hydrogen bond (red line) has length C4-H \cdots C9 3.594(1)Å while the $\pi\cdots\pi$ interaction between the benzimidazolium molecules is around 3.473(1)Å in length (green line).

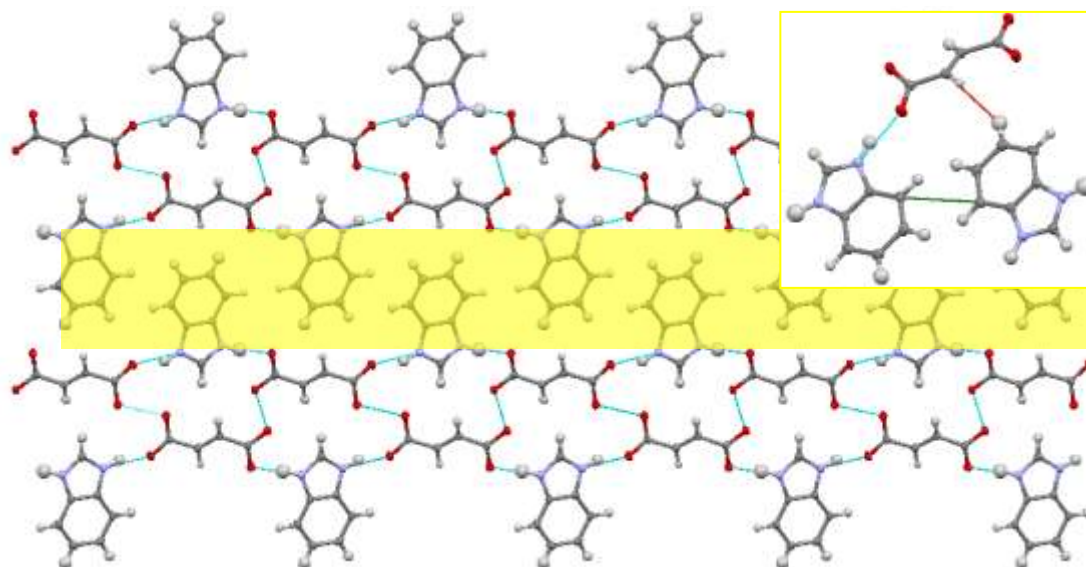


Fig. 7.65 – the columns consisting of interconnected chains of fumarate molecules and alternating co-molecules are expanded along the *c*-axis by lesser interactions (yellow box), inset, expanded view of the lesser interactions.

Imidazolium Fumarate

The imidazolium fumarate structure was first structurally determined in 2001¹². The structure contains a stoichiometric ratio of 1:1 of the ionic species of the co-molecules as proton transfer has occurred in the normal way (refer to Section 7.2.1). The result of the deprotonation on the fumarate molecule is different to that found in the molecule in the benzimidazole complex structure where the remaining proton was disordered over the carboxylic acid groups. In the imidazolium structure, the remaining proton is associated with only one oxygen therefore normalisation of the carbon – oxygen bond lengths has resulted in one of the carboxylic acids (Table 7.20). The imidazolium molecule undergoes the rearrangement mentioned in Section 7.2.1.

The motif of the imidazolium fumarate structure is an amalgamation of the ladder style and alternating linear chain style (Figure 7.66). With the fumarate molecules hydrogen bonding to one-another through the hydrogen bond pattern J, O-H...O, this creates chains of fumarate molecules with imidazolium molecules holding these chains together, i.e. the ladder motif. However, the fumarate molecules are not lined up to form long chains with one-another, but are “facing” the imidazolium molecules and are using the hydrogen bond pattern E to form alternating co-molecule linear chains. This amalgamated motif expands the structure along the *a*- and *c*-axis while the *b*-axis is expanded by $\pi\cdots\pi$ stacking interactions of distance 3.385(3)Å.

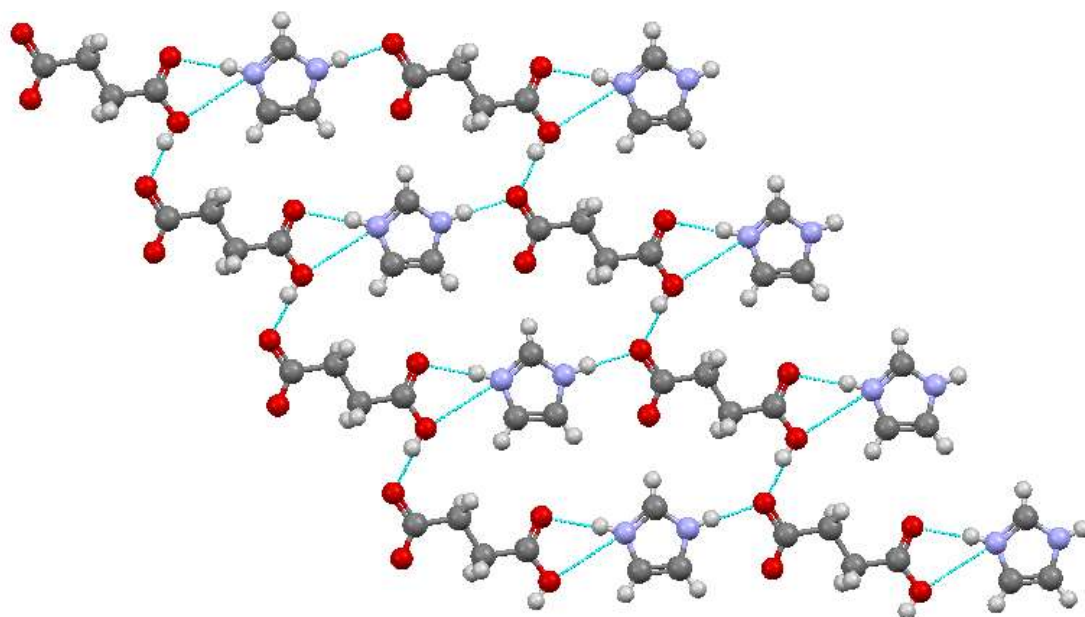


Fig. 7.66 – The main motif of the imidazolium fumarate molecular complex, an amalgamation of the ladder and linear chain motifs.

7.7.2 Molecular Complexes of Benzimidazolium and Imidazolium with Succinic Acid

The molecular ions benzimidazolium and succinate form a 1:1 molecular complex. The molecular complex was obtained using the solvent evaporation method, with a 1:1 stoichiometric mixture of benzimidazole (12mg) and succinic acid (12mg) dissolved in the minimum amount of ethanol and left to evaporate at a constant temperature of 2-4°C. The crystals generated were block shaped and colourless. Single crystal X-ray diffraction data were obtained using a Bruker Nonius Kappa diffractometer at 100K, equipped with graphite

monochromated Mo K α radiation ($\lambda = 0.71073 \text{ \AA}$). The structure was solved using SUPERFLIP within the CRYSTALS program. The crystallographic data are summarised in Table 7.6.

In the molecular complex, the benzimidazole molecule is protonated through hydrogen transfer from one of the carboxylic acid groups on the succinic acid molecule, as described in Section 7.2.1 (Figure 7.67). The result is that the internal bond lengths are now normalised, to N1 $^{\delta+}$ -C1 1.332(2) \AA and N2 $^{\delta+}$ -C1 1.328(2) \AA , and bond angles to C1-N1 $^{\delta+}$ -C2 108.3(1) $^{\circ}$ and C1-N2 $^{\delta+}$ -C7 108.3(1) $^{\circ}$.

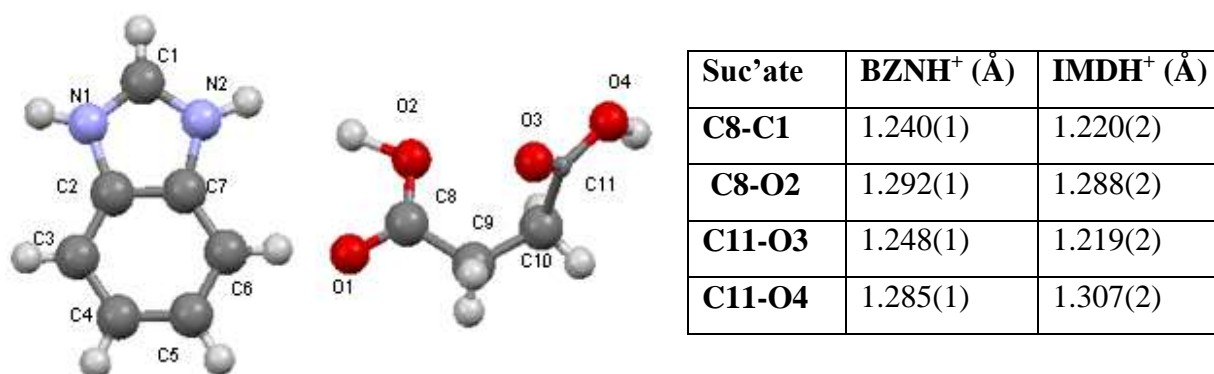


Fig. 7.67 –The benzimidazolium and succinate ions which are generated in the molecular complex/salt, with atom labelling.

Table. 7.22 – The carbon oxygen bond bonds in the benzimidazolium succinate and imidazolium succinate molecular complexes.

Interaction	Length (\AA) (D \cdots A(\AA))	For Hydrogen Bonds		
		D-H(\AA)	H \cdots A(\AA)	D-H \cdots A angle($^{\circ}$)
O2 \cdots O2	2.513(1)	1.256(1)	1.256(1)	180
O4 \cdots O4	2.443(1)	1.221(1)	1.221(1)	180
N1 \cdots O1	2.651(1)	0.97(2)	1.69(2)	172.7(2)
N2 \cdots O3	2.634(1)	0.95(2)	1.73(2)	158.1(2)
C5 $\cdots\pi$	3.550(2)	-	-	-

Table 7.23 – The hydrogen bond data for the hydrogen bonds in the benzimidazolium succinate molecular complex.

The succinate has two carboxylic acid groups, therefore only one has been deprotonated in order to fully protonate the benzimidazolium ion. The result is not full deprotonation of one

carboxylic acid group while the other retains its proton, but rather that the proton that is left is split over the two hydroxyl sites. The hydroxyl oxygen then hydrogen bonds to a symmetry-related oxygen through an inversion centre, therefore each hydrogen is 0.5 occupied within the asymmetric unit, but fully occupied over the hydrogen bond. The result on the carbon – oxygen bond lengths is still a degree of normalisation due to the deprotonation, which is similar to that found in the succinate ion in the imidazolium complex that has been fully deprotonated (Table 7.22).

The succinate molecule, as described, hydrogen bonds through an inversion centre using the hydrogen bond pattern J. There are two of these moderate hydrogen bonds, with length $O2\cdots O2$ 2.513(1)Å and $O4\cdots O4$ 2.443(1)Å. The proton is centred, with the hydrogen bond angle at 180°. These form chains of succinate molecules that run along the *a*-axis (Figure 7.68). The benzimidazolium ions have the role of connecting two of the chains together along the *b*-axis. This interaction uses N-H \cdots O moderate hydrogen bonds that can be described as types E and F, of length 2.651(1)Å and 2.634(1)Å (see Table 7.23 for full details). The motif is therefore the common ladder motif with uprights of succinate ions and rungs of benzimidazolium ions.

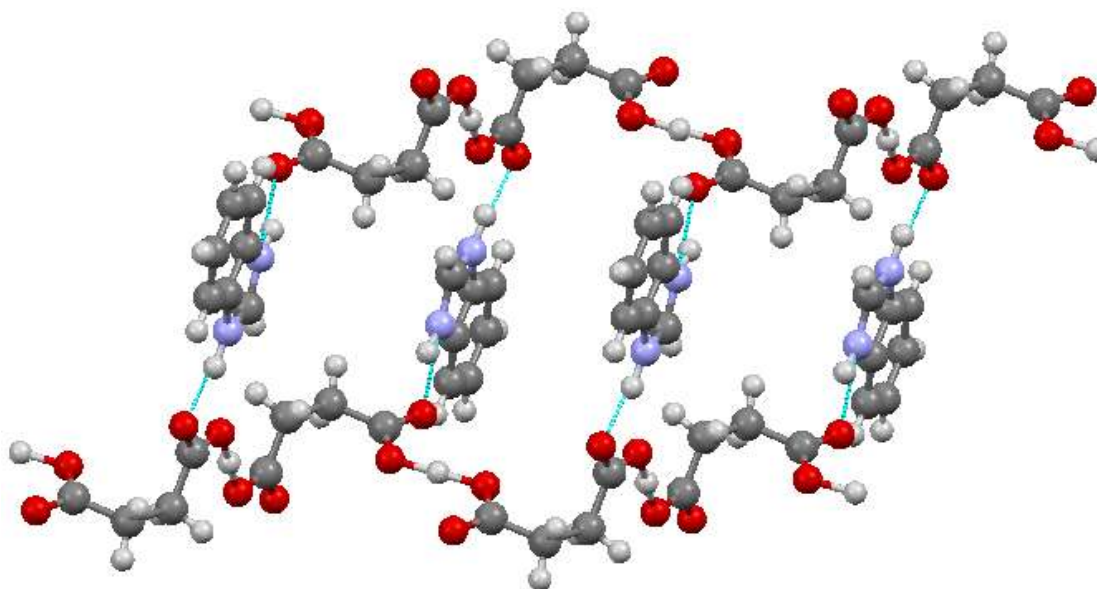


Fig. 7.68 – The main motif of the benzimidazolium succinate molecular complex, the ladder style with uprights of succinate ions and rungs of benzimidazolium ions.

Figure 7.69 is a view along the *b*-axis of the extended structure. From this it can be seen that the main motifs run perpendicular to the page, the ladder style motif (blue box) being expanded along the *c*-axis through C-H \cdots π interactions of 3.550(2)Å in length (red box). This

is the only other significant interaction with the structure – there are weak C-H \cdots O hydrogen bonds that exist between the adjoining chains, however these just support the moderate N-H \cdots O hydrogen bonds.

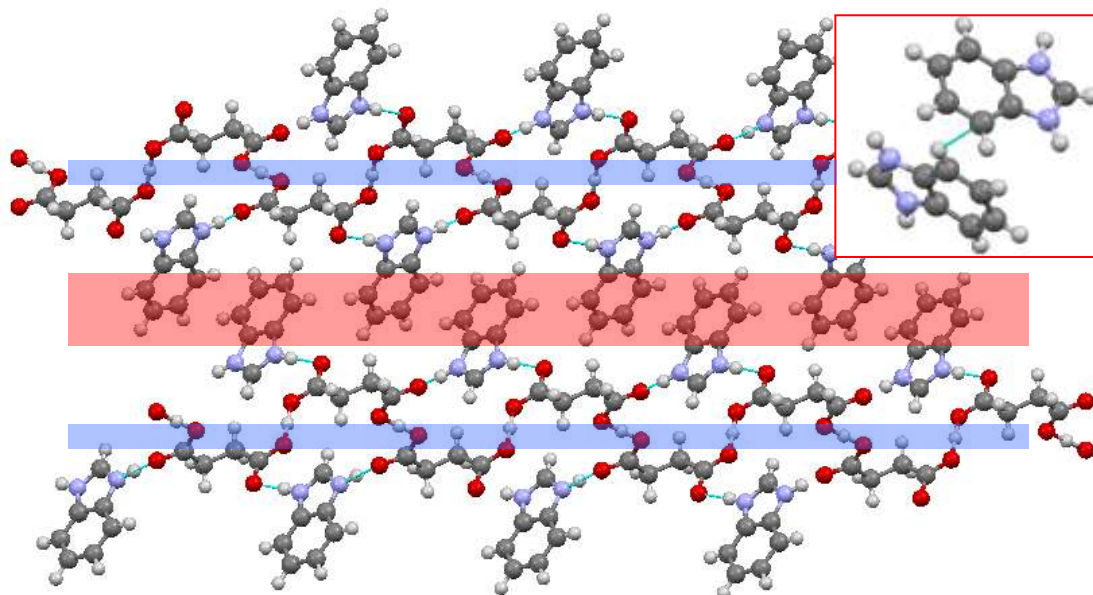


Fig. 7.69 – the extended structure of benzimidazolium succinate molecular complex viewed along the *b*-axis, highlighting how the main motif (blue line) extends along the *c*-axis through C-H \cdots π interactions (red box); inset, the C-H \cdots π interaction.

Imidazolium Succinate

The structure of the imidazolium succinate molecular complex¹² contains a 1:1 molecular ratio of co-molecules with proton transfer occurring (see Section 7.2.1). The hydrogen bonds between the co-molecules are partially charge assisted N-H \cdots O interactions (HB pattern E) of length 2.715(2)Å and 2.871(2)Å. They align the co-molecules into chains that run along the *ac*-diagonal (Figure 7.70).

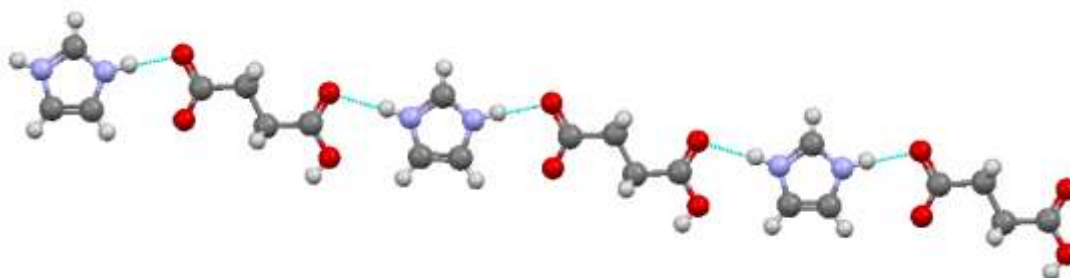


Fig. 7.70 – the chain that is created through the N-H···O hydrogen bonds between the co-molecules in the imidazolium succinate molecular complex.

The hydroxyl oxygen that remains on the non-protonated carboxylic acid group hydrogen bonds to an oxygen in an adjacent chain below (Figure 7.71). This hydrogen bond is the strongest in the molecular complex at O···O, 2.478(2)Å and expands the structure along the *a*-axis. Supporting this interaction are weaker carbon – oxygen hydrogen bonds involving the carbon located between the nitrogens and the currently non-hydrogen bonded oxygen (blue circle). This hydrogen bond has length C···O 3.082(2)Å and with the O-H···O interactions creates layers of co-molecules. These layers are then stacked upon another using very weak carbon – oxygen hydrogen bonds of length 3.358(3)Å.

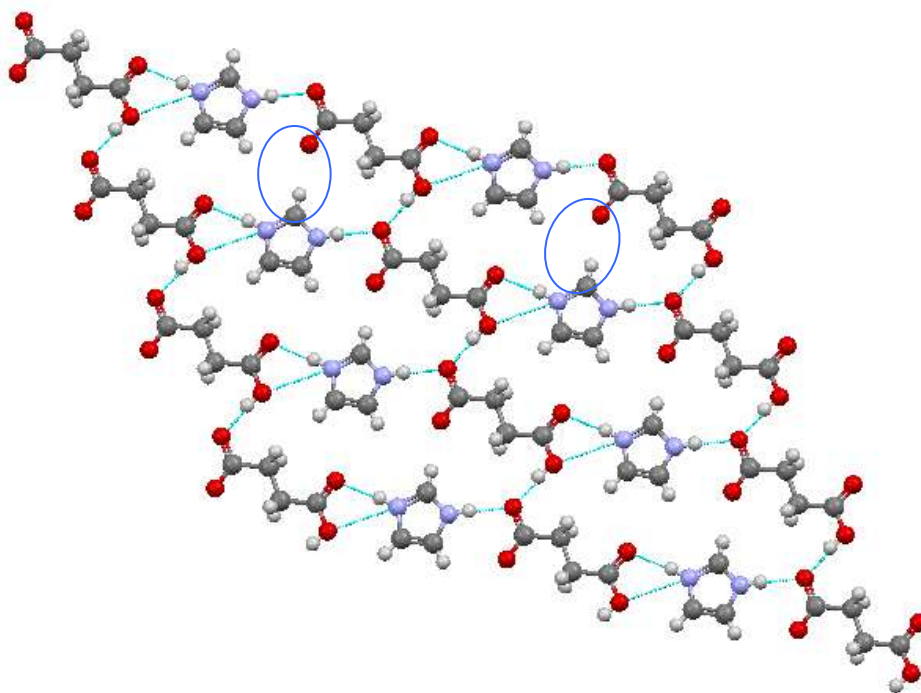


Fig. 7.71 – The main motif of the imidazolium succinate structure, layers consisting of linear chains of alternating co-molecules that expand along the *ac*-diagonal (chains) and *a*-axis.

7.7.3 Molecular Complexes of Benzimidazolium and Imidazolium with Maleic Acid

The molecular ions, benzimidazolium and maleate form a 1:1 molecular complex with one another. The molecular complex was obtained using the solvent evaporation method, with a 1:1 stoichiometric mixture of benzimidazole (14mg) and maleic acid (12.5mg) dissolved in

the minimum amount of methanol followed by evaporation at a constant temperature of 40°C using an Asynt hotplate. The crystals generated were block shaped and colourless.

Single crystal X-ray diffraction data were obtained using a Rigaku R-axis/RAPID diffractometer at 100K, equipped with graphite monochromated Mo K α radiation ($\lambda = 0.71073 \text{ \AA}$). The structure was solved using SIR92 within the CRYSTALS program. The crystallographic data are summarised in Table 7.6 with the hydrogen bond data and interaction listed in Table 7.24.

In the molecular complex, the benzimidazole molecule is protonated through hydrogen transfer from one of the carboxylic acid groups on the maleic acid molecule onto the normally unprotonated nitrogen atom in the five-membered ring forming a benzimidazolium molecule (Figure 7.72). This form of proton transfer is common in all molecular complexes involving benzimidazole and a carboxylic acid group containing molecule where the crystallisation product is in a 1:1 stoichiometric ratio. The result of the proton transfer on the benzimidazolium molecule is a delocalisation of the charge across the five-membered ring, reflected in the equalisation of the internal bond lengths, N1 $^{\delta+}$ -C1 1.325(3) \AA and N2 $^{\delta+}$ -C1 1.326(3) \AA , and bond angles, C2-N1 $^{\delta+}$ -C1 108.05(19) $^\circ$ and C7-N2 $^{\delta+}$ -C1 108.31(18) $^\circ$. The delocalisation of the charge has the effect of creating a partial positive charge on both the nitrogens. This effect has been reported in many structures involving benzimidazole and imidazole (see Section 7.2.1).

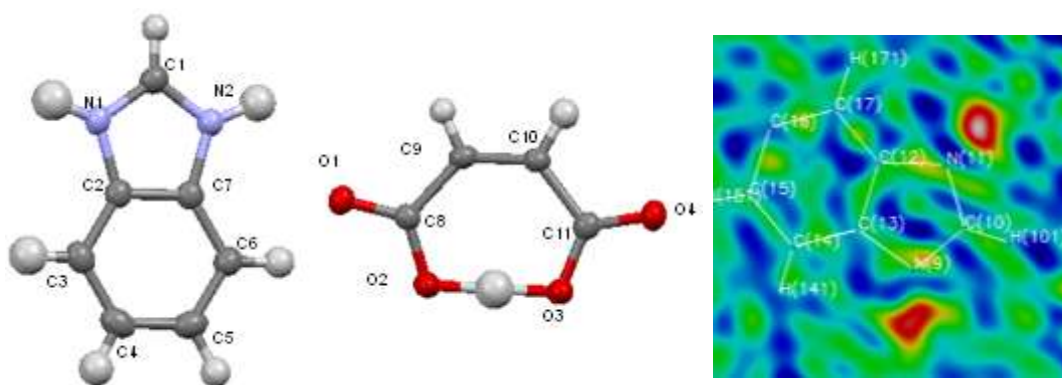


Fig. 7.72 – LHS, the benzimidazolium and maleate molecules which are generated in the molecular complex, with atom labelling. RHS, the Fourier difference map generated with the H atoms located on the N atoms omitted from the model; this clearly shows that both N atoms are protonated.

Interaction	Length (Å) (D...A(Å))	For Hydrogen Bonds		
		D-H(Å)	H...A(Å)	D-H...A angle(°)
O2...O3	2.405(3)	1.19(3)	1.229(3)	178(3)
N1...O1	2.751(3)	0.98(3)	1.77(3)	175(2)
N2...O4	2.691(3)	0.99(3)	1.71(3)	172(3)
C9...O2	3.275(3)	0.91(2)	2.65(2)	126(2)
C10...O3	3.501(3)	0.98(3)	2.64(3)	147(2)
C1...O4	3.175(3)	0.95(2)	2.23(2)	164(2)
C4...O1	3.517(3)	0.94(3)	2.60(3)	165(2)

Table 7.24 – The hydrogen bond data for the hydrogen bonds in the benzimidazolium succinate molecular complex.

The maleic acid molecule in its native crystal structure (refer to Figure 7.11) is configured such that there is an intramolecular hydrogen bond between the two carboxylic acid groups. Within the molecular complex with benzimidazolium this intramolecular hydrogen bond persists despite the proton transfer of a hydrogen atom to the benzimidazole. The intramolecular hydrogen bond is relatively short with an O...O distance of 2.405(3)Å which is significantly shorter than the O...O distance of 2.503Å that is found in maleic acid (polymorph MALIAC12)²² (used for comparisons hereafter). This is due to the intramolecular hydrogen bond being charge assisted, a result of the deprotonation of the maleic acid. The negative charge is found to be delocalised over the carboxylic acid groups, by consideration of the normalisation of the bond lengths in the carboxyl groups of the maleate molecule (Table 7.25). The delocalisation also results in the presence of partially charge assisted intermolecular hydrogen bonds involving O3 and O7.

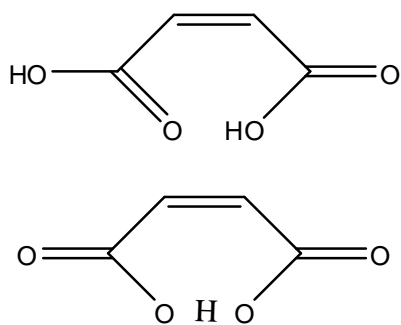


Fig. 7.73 – The maleic acid molecule (top) and the maleate ion (bottom) showing the differences in the bond characteristics.

	Maleate (Å)	Maleic Acid (Å)
C8-C9	1.437(3)	1.482(2)
C8-O1	1.244(2)	1.308(2)
C8-O2	1.289(2)	1.225(2)
C11-O3	1.291(3)	1.308(2)
C11-O4	1.237(3)	1.224(2)
C11-C10	1.492(3)	1.487(2)
C9-C10	1.334(3)	1.335(3)

Table 7.25 – A comparison of the bond lengths found in the maleate ion in its molecular complex with benzimidazolium and those of the neutral maleic acid molecule.

From Table 7.16, it can be seen the C6-O7 and C6-O8 bonds have undergone a complete character reversal. The single bond involved in the intramolecular hydrogen bond in the maleic acid (C8-O2) has now more double bond characteristics while the double bond in maleic acid (C8-O1) has more single bond characteristics (Figure 7.73). The proton that sits in the intramolecular hydrogen bond has an $O^{\delta-}$ -H distance of 1.18(3)Å and a $H \cdots O^{\delta-}$ distance of 1.22(3)Å. This indicates the hydrogen atom has an affinity for both oxygens and thus adopts an approximately central position within the hydrogen bond. However Fourier difference maps (Figure 7.74), directly imaging the electron density of the hydrogen atom in this intramolecular hydrogen bond, suggests that the hydrogen atom is positioned slightly closer to O2 in an asymmetric position; this is similar to the behaviour observed in the native structure of maleic acid.

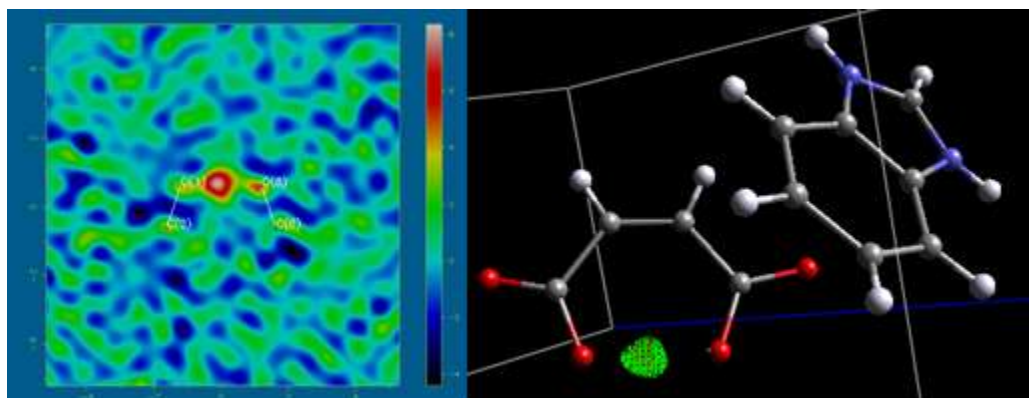


Fig. 7.74 – LHS, 2D Fourier difference map, RHS, 3D Fourier difference map (MCE); both images show a slightly asymmetric location of the hydrogen atom in the intramolecular hydrogen bond of the maleate molecule.

The main motif in the benzimidazolium maleate molecular complex is a zigzag chain of alternate co-molecules in the *ac* direction, motif N. This is constructed of alternating charge assisted $\text{N}^{\delta+}\text{-H}\cdots\text{O}^{\delta-}$ hydrogen bonds of lengths 2.751(3)Å and 2.691(3)Å. These hydrogen bonds are moderate in strength and utilise the hydrogen bond pattern E (Figure 7.75).

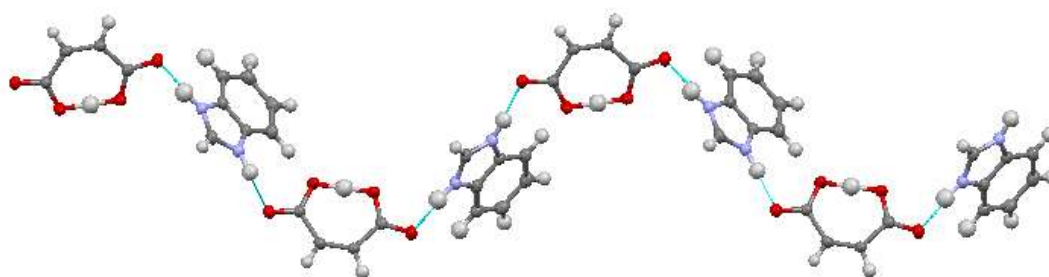


Fig. 7.75 – The main motif of the benzimidazolium maleate molecular complex; a chain of alternating co-molecules held together by alternating charge assisted $\text{N}^{\delta+}\text{-H}\cdots\text{O}^{\delta-}$ hydrogen bonds.

The zigzag chains are held together along the *b*-direction by weaker $\text{C-H}\cdots\text{O}^{\delta-}$ hydrogen bonds creating layers of these chains (Figure 7.76). These two weak hydrogen bonds have $\text{C}\cdots\text{O}^{\delta-}$ distances of 3.275(3)Å and 3.501(3)Å and $\text{C-H}\cdots\text{O}^{\delta-}$ angles of 126.3(2)° and 146.6(2)°, resulting in a staircase arrangement of the zigzag chains (Figure 7.76 insert).

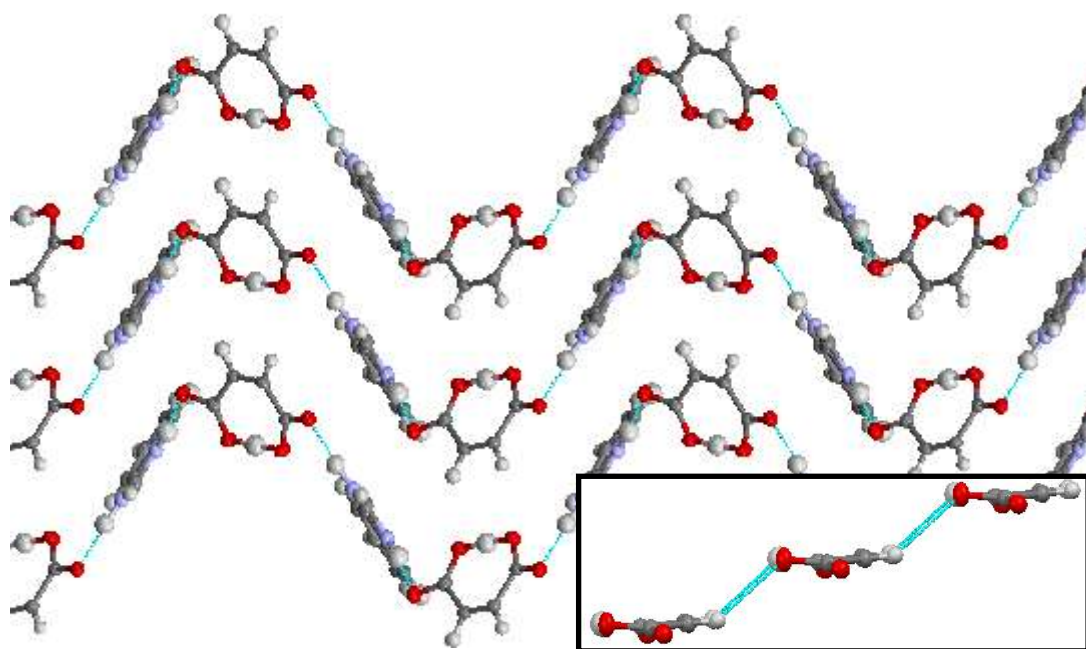


Fig. 7.76 – The zigzag chains that are the main synthon in the benzimidazolium maleate molecular complex are held together by weak hydrogen bonds connecting the maleate ions (insert).

Another C-H \cdots O $^{\delta-}$ hydrogen bond, is formed between the carbon located between the two nitrogens (C1) of the benzimidazole molecule and an oxygen (O4) on a maleate ion. With a C-H \cdots O $^{\delta-}$ length of 3.157(3) Å it can be classified as a weak hydrogen bond. These hydrogen bonds hold two layers together creating blocks of two layers of the main motif (Figure 7.77).

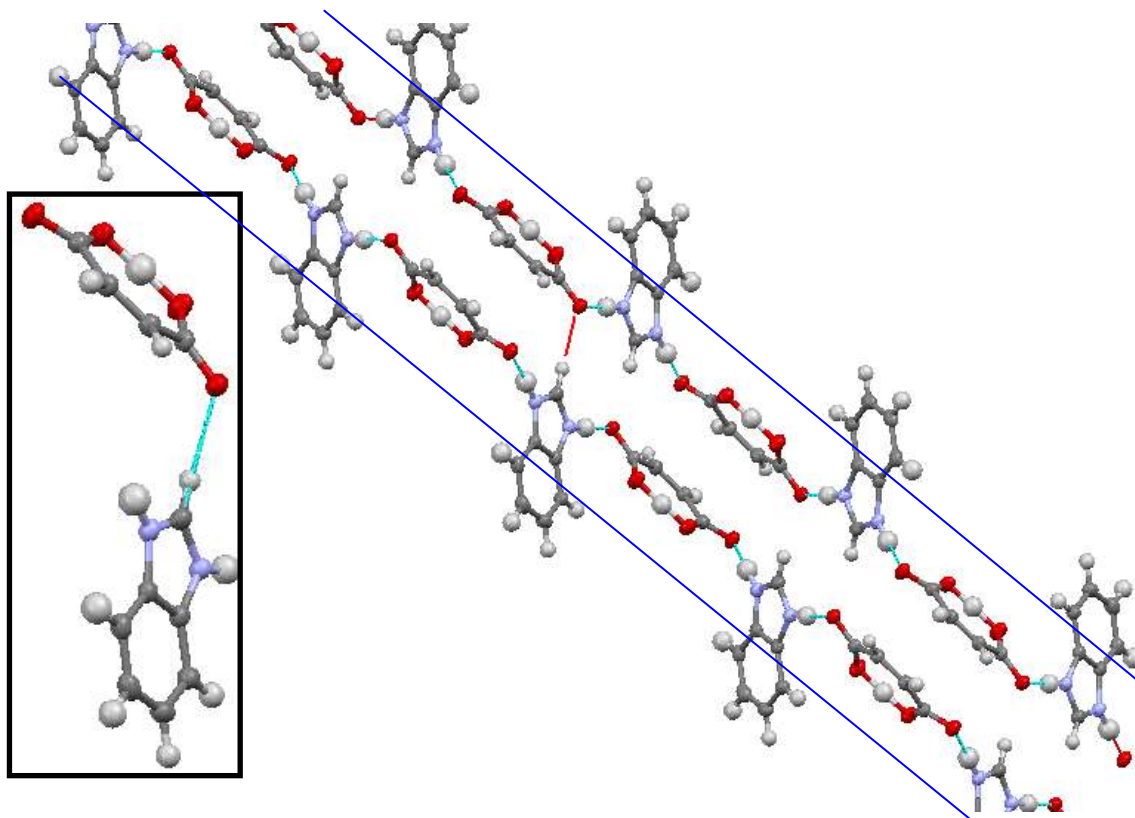


Fig. 7.77 – View along the *b*-axis showing the main motif (-) of the benzimidazolium maleate molecular complex connected by the C-H \cdots O $^{\delta-}$ hydrogen bond from the benzimidazolium molecule (-) (insert) to make a two layer block.

The blocks, consisting of the two layers of the main motif (Figure 7.77), are connected to one another through another weak hydrogen bond. This interaction is between an aromatic hydrogen on the benzene ring of the benzimidazolium (C4) and an oxygen involved in the intramolecular hydrogen bond (O1) of the maleate ion with a C \cdots O $^{\delta-}$ distance of 3.517(3)Å and a C-H \cdots O angle of 164.6(2) $^{\circ}$ (Figure 7.78). Figure 7.79 shows how the layers are held by these two weak hydrogen bonds in alternate fashion. The blue lines represent the chains of alternate co-molecules, red lines indicating the weak hydrogen

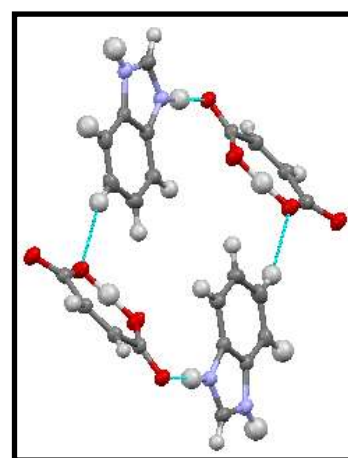


Fig. 7.78 - The weak hydrogen bond between the maleate and benzimidazolium ions.

bond seen in Figure 7.75 and the green lines indicate where the weak hydrogen bond in Figure 7.76 lies.

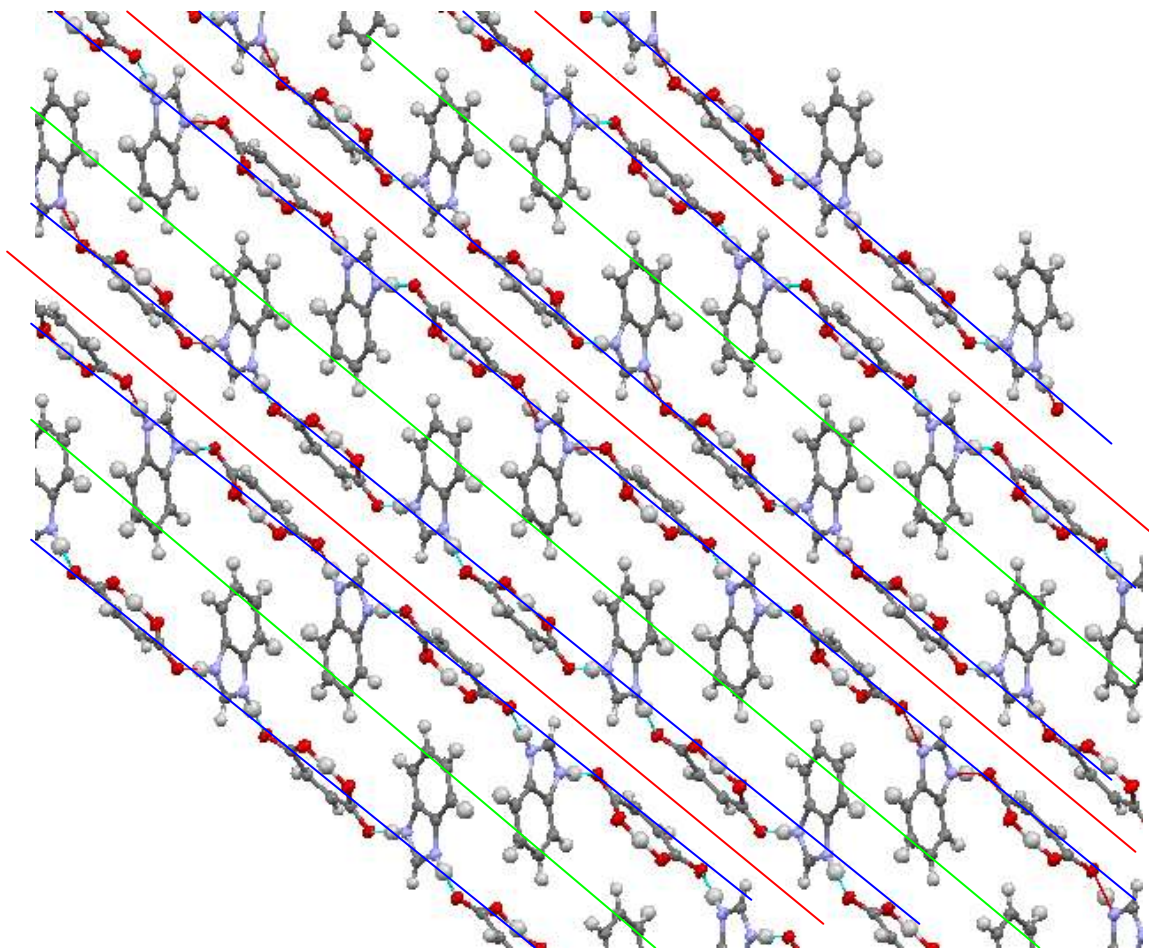


Fig. 7.79 – View along the *b*-axis of the expanded benzimidazolium maleate molecular complex. The blue line (-) indicates the planes of the main motif (Figure 7.75), the red line (-) indicates the weak hydrogen bond that holds the planes together in alternate layers (Figure 7.75) with the green line (-) indicating the other weak hydrogen bond (Figure 7.76).

Imidazolium Maleate

There are a few structures of the imidazolium maleate molecular complex within the CSD, the one that will be discussed was published in 1980 by Schlemper et al²³ (Table 7.26).

Maleate	Space Gp	Cell Lengths (Å)	Cell Angles (Å)	Volume (Å ³) / Z
BZNH⁺	<i>P 2₁/n</i>	12.858(2)	90	1083.1(2)
		5.450(2)	91.516(4)	
		15.454(2)	90	4
IMDH⁺	<i>P 2₁/c</i>	10.855(2)	90	853.47(2)
		5.518(1)	102.87(2)	
		14.616(4)	90	4

Table 7.26 – Some basic crystal data for the benzimidazolium maleate molecular complex and the imidazolium maleate molecular complex.

As in the benzimidazolium structure, there is proton transfer from the maleate to the imidazolium, which results in the maleate ion forming with the associated bond rearrangement taking place (Figure 7.72, Table 7.27). This results in two very strong hydrogen bond acceptor groups at each end of the maleate molecule, which when coupled with the two strong hydrogen bond donors within the imidazolium ion (N-H) it is almost certain that a hydrogen bond pattern of type E or F will prevail. The benzimidazolium maleate structure adopted the linear chain motif as did the imidazolium succinate structure, therefore there is a very strong chance that a linear hydrogen bonded chain with alternating co-molecules would be likely. The presence of two hydrogen bond acceptors on the end of the molecule rules out the ladder motif, but not the hydrogen bonded ring motif.

Figure 7.78 shows that the main motif of the imidazolium maleate is the hydrogen bonded ring motif (L) that is held together by partially charged assisted N-H...O interactions. These hydrogen bonds as moderate in strength with lengths of 2.783(3)Å (0.96(1)Å, 1.83(3)Å, 170.7(1)°) and 2.786(4)Å (0.98(1)Å, 1.81(2)Å 173.4(2)°), respectively.

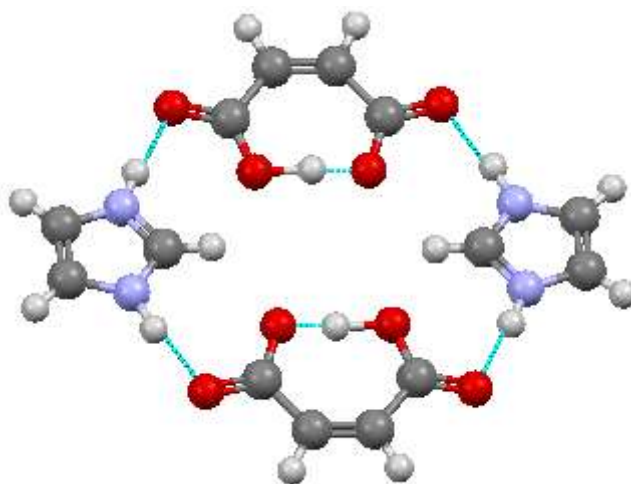


Fig. 7.80 – View along the *c*-axis of the motif of the imidazolium maleate structure, showing the hydrogen bonded ring.

There are only two lesser interactions that complete the significant interactions within the structure, both C-H \cdots O hydrogen bonds. The slightly weaker hydrogen bond expands the structure along the *ab*-diagonal which has length C \cdots O 3.2340(4)Å (Figure 7.81 blue circle). The other with length C \cdots O 3.1468(6)Å (red circle) expands the structure along the *ac*-diagonal, but more importantly, with an angle between the two adjoining hydrogen bonded rings of $\sim 68.7^\circ$. This allows for the hydrogen bonded rings to stack upon one-another (Figure 7.81 – RHS).

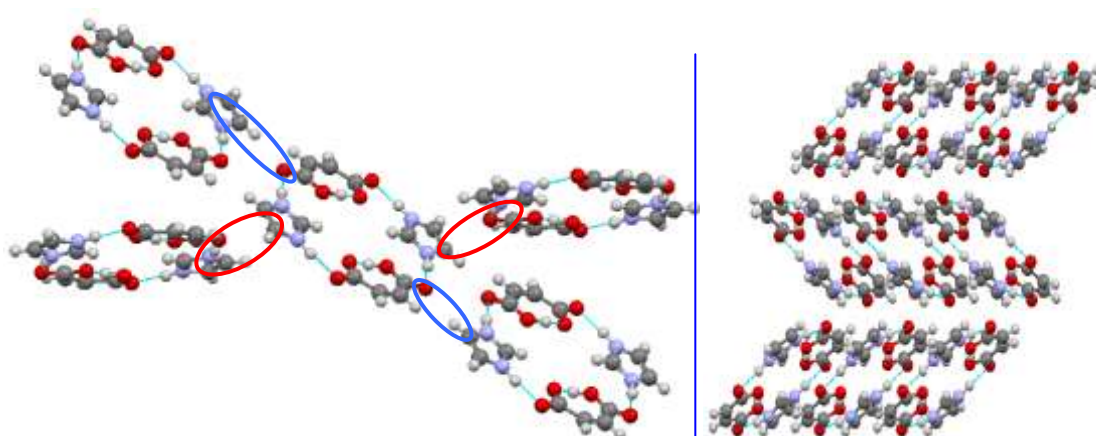


Fig 7.81 – LHS, the main motif, hydrogen bonded ring, are expanded by C-H \cdots O hydrogen bonds along the *ab*-diagonal (blue circle) and *ac*-diagonal (red circle); RHS, the view along the *a*-axis of an extended imidazolium maleate structure.

7.7.4 Molecular Complexes of Benzimidazole and Imidazole with Malonic Acid

Successful cocrystallisation experiments have produced the previously undetermined structure of imidazole with malonic acid and provided an enhanced model for the benzimidazole and malonic acid structure. In both structures there was proton transfer as described in Section 7.2.1 and each complex is in a 1:1 molecular ratio.

On the basis of previous findings, there will definitely be a N–H···O hydrogen bond between the molecules, with it adopting hydrogen bond pattern E or F. With one of the carboxylic acid groups undergoing deprotonation, there will be only one hydroxyl group in the structure, within the native structure of malonic acid there is no intramolecular hydrogen bond, and if this configuration is maintained, this hydroxyl group will be available for intermolecular hydrogen bonding. This would promote the possibility of hydrogen bond pattern I or J forming. The probable motifs would be K, the ladder style, or N the linear chain.

Malonate

The malonic acid molecule in its native crystal structure (refer to Section 7.1.9) is configured such that there is no intramolecular hydrogen bond between the two carboxylic acid groups. However within the molecular complex with benzimidazolium an intramolecular hydrogen bond is formed. The resulting intramolecular hydrogen bonds are relatively short with O···O distances of O2···O3 2.440(2)Å and O4···O5 2.449(2)Å which will be due to the delocalised negative charge. The intramolecular hydrogen bond was initially not proposed in the published structure³⁰; this new model explains the discrepancies in the carbon – oxygen bond lengths and positions the hydrogens more accurately. In contrast, the imidazolium malonate structure does not contain the intramolecular hydrogen bond but retains the native form with the hydrogen open for intermolecular hydrogen bonds (Figure 7.82). This is in line with the situation in imidazolium malonate hydrate, in which even though the hydrogen positions are unknown, the carbon – oxygen bond distances and overall bond geometry are similar (Table 7.27). There is no obvious reason for the differences in the malonate ion geometry between the different structures.

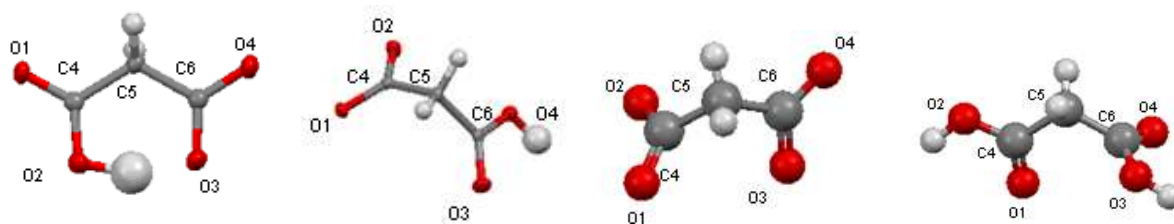


Fig. 7.82 – The malonate ion found in molecular complexes with (from left to right) benzimidazolium, imidazolium, imidazolium hydrate, and in its native form, with atom labelling.

	Malonate BZNH ⁺ (Å)	Malonate IMDH ⁺ (Å)	Malonate IMDH ⁺ Hydrate (Å)	Native Malonic Acid (Å)
C4-O1	1.234(2)	1.249(1)	1.240(6)	1.285(3)
C4-O2	1.292(3)	1.268(1)	1.250(5)	1.221(3)
C6-O3	1.270(3)	1.214(1)	1.208(7)	1.231(2)
C6-O4	1.251(3)	1.319(1)	1.285(6)	1.290(3)

Table 7.27 – A comparison of the bond lengths found in the malonate ions in their molecular complexes with benzimidazolium, imidazolium, imidazolium hydrate and in its native form.

Hydrogen Bond Data

Benzimidazolium Malonate					
Interaction	Label	Length (Å) (D...A(Å))	For Hydrogen Bonds		
			D-H(Å)	H...A(Å)	D-H...A angle(°)
N2...O1	a'	2.701(3)	0.95(3)	1.75(3)	173(2)
N3...O4	b'	2.676(3)	0.93(3)	1.75(3)	172(3)
C1...O4		3.242(3)	0.95(2)	2.31(2)	165(2)
C7...O6		3.229(3)	0.97(2)	2.26(2)	170(2)
C...O1		3.443(3)	0.96(2)	2.52(2)	162(2)
C...O3		3.369(3)	0.97(2)	2.42(2)	166(2)
$\pi \cdots \pi$		3.400(2)	-	-	-
Imidazolium Malonate					
Interaction		Length (Å) (D...A(Å))	For Hydrogen Bonds		
			D-H(Å)	H...A(Å)	D-H...A angle(°)
O4...O2		2.563(1)	0.94(2)	1.63(2)	174(2)
N1...O2		2.742(1)	0.90(2)	1.84(2)	165(2)

N2...O1	2.765(1)	0.92(2)	1.85(2)	173(2)
C1...O2	3.001(1)	0.95(2)	2.39(1)	150(1)

Table 7.28 – The hydrogen bond geometry data and interaction details for the benzimidazolium malonate and imidazolium malonate molecular complexes.

Benzimidazolium Malonate

The molecular ions, benzimidazolium and malonate form a 1:1 molecular complex with one another. The molecular complex was obtained using the solvent evaporation method, with a 1:1 stoichiometric mixture of benzimidazole (12mg) and malonic acid (10mg) dissolved in the minimum amount of acetone followed by evaporation at a constant temperature of 2-4°C in a walk-in fridge. The crystals generated were plate shaped and colourless.

Single crystal X-ray diffraction data were obtained using a Bruker Nonius Kappa diffractometer at 100K, equipped with graphite monochromated Mo K α radiation ($\lambda = 0.71073 \text{ \AA}$). The structure was solved using SIR92 within the CRYSTALS program. The crystallographic data are summarised in Table 7.6.

In the molecular complex, the benzimidazole molecule is protonated through hydrogen transfer from one of the carboxylic acid groups on the malonic acid forming a benzimidazolium molecule (Figure 7.83). The result of the proton transfer on the benzimidazolium molecule is a delocalisation of the charge across the five-membered ring, reflected in the equalisation of the internal bond lengths; N1-C1 1.333(3) \AA , N2 -C1 1.326(3) \AA , N3-C7 1.328(3) \AA , N4 -C7 1.329(3) \AA and bond angles; C2-N1-C1 108.3(2) $^\circ$ and C3-N2-C1 108.6(2) $^\circ$, C8-N3-C7 108.3(2) $^\circ$ and C9-N4-C7 108.4(2) $^\circ$. There are two of each co-molecule in the asymmetric unit. The deprotonation of the malonic acid molecule has resulted in an intramolecular hydrogen bond being formed (refer to *Malonate*, section 7.1.9) and the normalisation of the carbon – oxygen bond lengths.

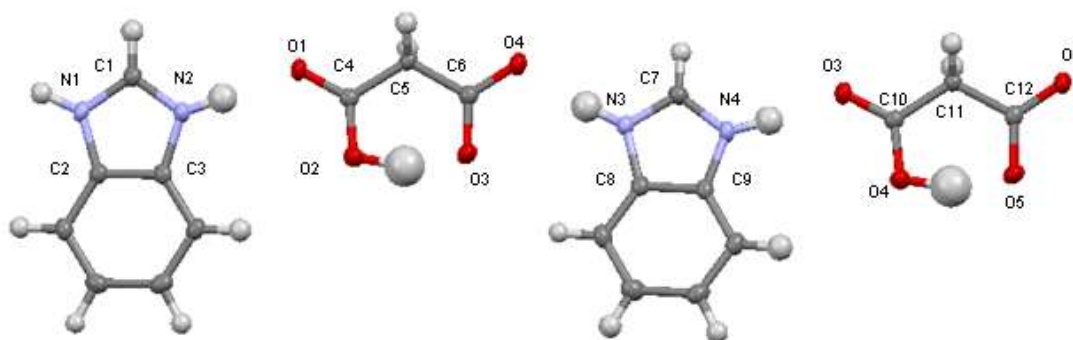


Fig. 7.83 – The benzimidazolium and malonate molecules which are generated in the molecular complex, with atom labelling.

There are two moderate hydrogen bonds within the structure, both are nitrogen – oxygen interactions and follow hydrogen bond pattern E. The hydrogen bonds have length $N2 \cdots O1$, a' , 2.701(3)Å and $N3 \cdots O4$, b' , 2.676(3)Å and align the co-molecules into a linear chain (Figure 7.84). This linear chain of alternating hydrogen bonded co-molecules is the motif of the structure, which follows motif N. Two of these motifs are connected along the b -axis by lesser $C-H \cdots O$ hydrogen bonds. This hydrogen bond involves the carbons located between the nitrogens on the two $BZNH^+$ molecules (C1 and C7) and oxygens O4 and O6, with lengths $C \cdots O$ 3.242(3) and 3.229(3)Å.

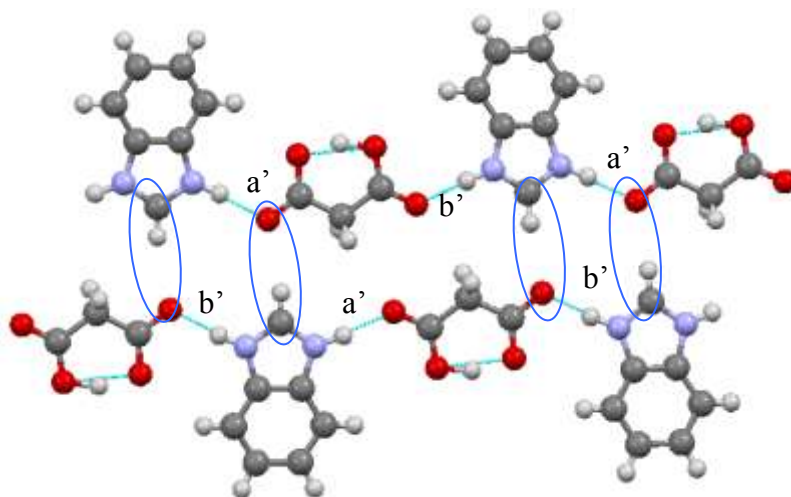


Fig. 7.84 – the main motif of the benzimidazolium malonate structure, linear chain of alternate hydrogen bonded co-molecules. Two of the motifs are connected together through carbon – oxygen hydrogen bonds (blue circle).

While the $C-H \cdots O$ hydrogen bonds shown in Figure 7.84 connect two chains together, this is just one part of the two different types of interactions that expand the structure along the b -axis, that work in an alternative fashion. The other interactions are also $C-H \cdots O$ hydrogen

bonds with lengths of 3.498(3) and 3.502(2)Å (Figure 7.85 red circle). This alternate interaction between the motifs runs along the *b*-axis creating a layer.

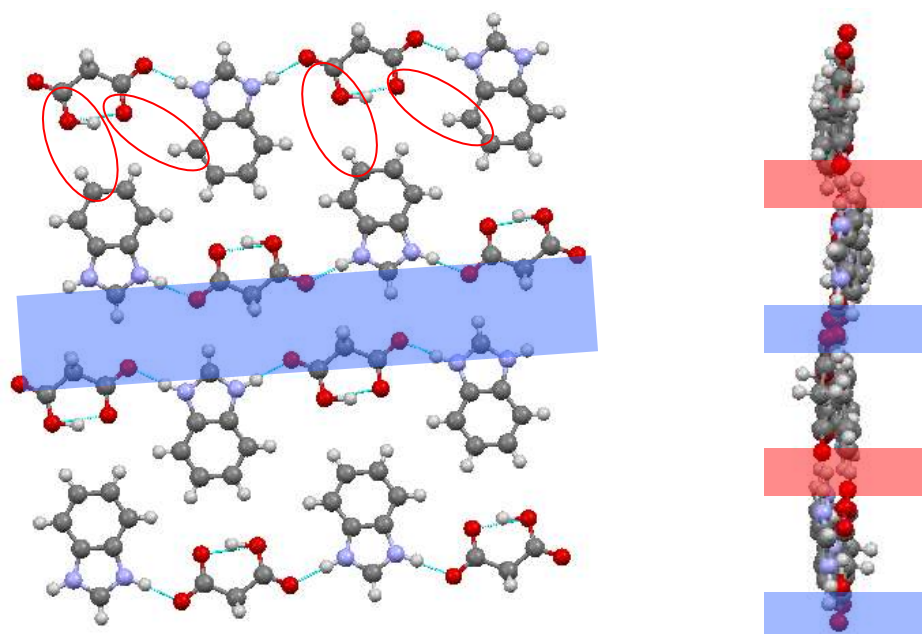


Fig 7.85 – RHS, the chains of motifs are held together along the *b*-axis by two alternating layers of interactions, a relatively stronger carbon – oxygen hydrogen bond (blue box), and a relatively weaker carbon – oxygen hydrogen bond (red circles); LHS, view of the *b*-axis with the interactions coloured in blocks to show the alternating layered nature.

Between these layers of motifs are two interactions that expand the structure along the *a*-axis. There is a C-H \cdots O hydrogen bond between two malonate molecules which have lengths C \cdots O 3.443(3)Å and 3.369(3)Å (Figure 7.86 yellow circle). The other interaction is $\pi\cdots\pi$ stacking interactions between the benzimidazolium molecules which have a length of around 3.400(2)Å (measured between the two closest benzimidazolium molecules). These are all the significant interactions within the benzimidazole malonate molecular complex.

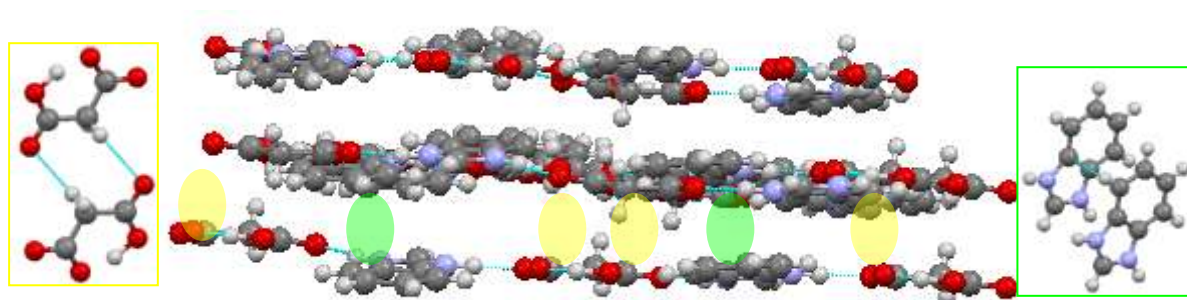


Fig. 7.86 – the *a*-axis is expanded by two lesser interactions that stack the layers of motifs upon one-another. The shortest is a C-H \cdots O hydrogen bond (yellow circle) while the other is a $\pi\cdots\pi$ stacking interaction between the

benzimidazolium molecules (green circle). Insert LHS, the C-H...O hydrogen bond; insert RHS, the $\pi\cdots\pi$ stacking interactions.

Imidazolium Malonate

The molecular ions, imidazolium and malonate form a 1:1 molecular complex with one another. The molecular complex was obtained using the solvent evaporation method, with a 1:1 stoichiometric mixture of imidazole (8mg) and malonic acid (10mg) dissolved in the minimum amount of acetone followed by evaporation at 2-4°C. The crystals generated were block shaped and colourless.

Single crystal X-ray diffraction data were obtained using a Bruker Nonius Kappa diffractometer at 100K, equipped with graphite monochromated Mo K α radiation ($\lambda = 0.71073\text{\AA}$). The structure was solved using SUPERFLIP within the CRYSTALS program. The crystallographic data are summarised in Table 7.6.

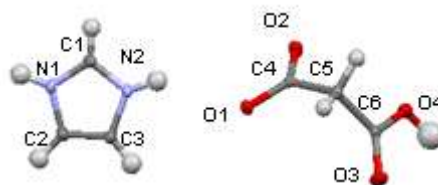


Fig. 7.87 – The imidazolium and malonate ions which are generated in the molecular complex/salt, with atom labelling.

As reported, the imidazole molecule is protonated through hydrogen transfer as shown in Section 7.2.1. The result is the creation of an imidazolium ion, with the positive charge being delocalised over the ion (Figure 7.87). This is reflected in the equalisation of the internal bond lengths, N1-C1 1.324(2) \AA and N2-C1 1.326(1) \AA , and bond angles, C2-N1-C1 108.4(1) $^\circ$ and C3-N2-C1 108.8(1) $^\circ$. The effect on the malonic acid molecule is that the carboxylic acid group that has been deprotonated, has a negative charge that is shared across the group. This can be seen in the normalisation of the carbon – oxygen bond lengths (refer to *Malonate*, section 7.1.9).

There are three moderate hydrogen bonds within the structure, two of which follow hydrogen bond pattern F, N-H...O, while the other adopts pattern I, O-H...O. The hydroxyl – carboxylate hydrogen bond, O4-H...O2 2.563(1) \AA , connects the malonate molecules together into chains. Connecting these chains together are the partially charge assisted N-H...O hydrogen bonds of length, N1...O2 2.742(1) \AA and N2-O1 2.765(1) \AA (see *Hydrogen Bond Data*, Table 7.28), As Figure 7.88 demonstrates, the motif of the structure is the ladder style with uprights of malonate molecules and rungs of imidazole. This ladder is not flat, but more

of a staircase shape due to the geometry of the malonate ion. The result is that the imidazole molecules lie on two levels.

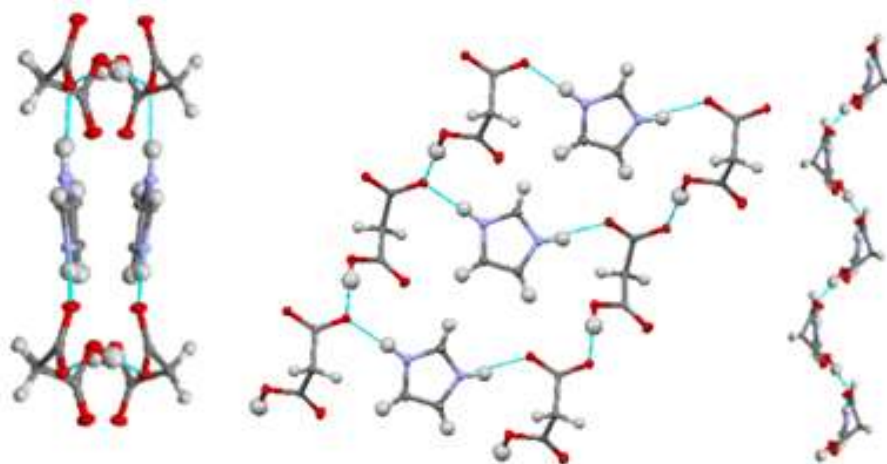


Fig. 7.88 – The main motif of the imidazolium malonate molecular complex, the ladder style with uprights of malonate ions and rungs of imidazolium, viewed along, LHS, the *c*-axis, middle, the *b*-axis, and RHS, the *a*-axis.

The motif expands along the *a*- and *c*-axis while the *b*-axis is expanded through C-H...O hydrogen bonds involving the carbon located between the nitrogens, and an oxygen – oxygen interaction. The hydrogen bond has a distance of C1...O2 3.001(1)Å (Figure 7.72 - green line) while the oxygen – oxygen interaction is on the limit of its sum of van der Waals radii (3.04Å) at 3.001(1)Å (Figure 7.89 - red line).

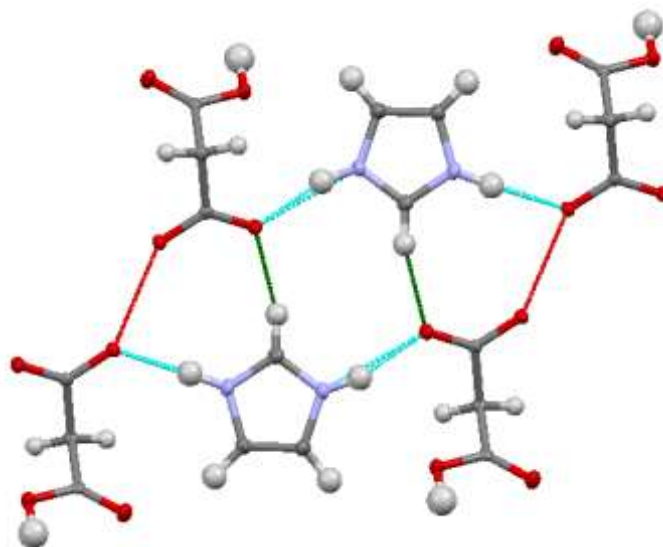


Fig. 7.89 – The motif of the structure (blue interactions) is expanded along the *b*-axis by C-H...O hydrogen bonds (green interaction) and an oxygen – oxygen interaction (red line).

Figure 7.90 shows the extended structure viewed along the c -axis (LHS) and b -axis (RHS). From these images the main motif, ladder style with uprights of malonate and rungs of imidazolium molecules (blue shading) can be seen to be expanded along the b -axis by the carbon – oxygen weak hydrogen bond (red shading).

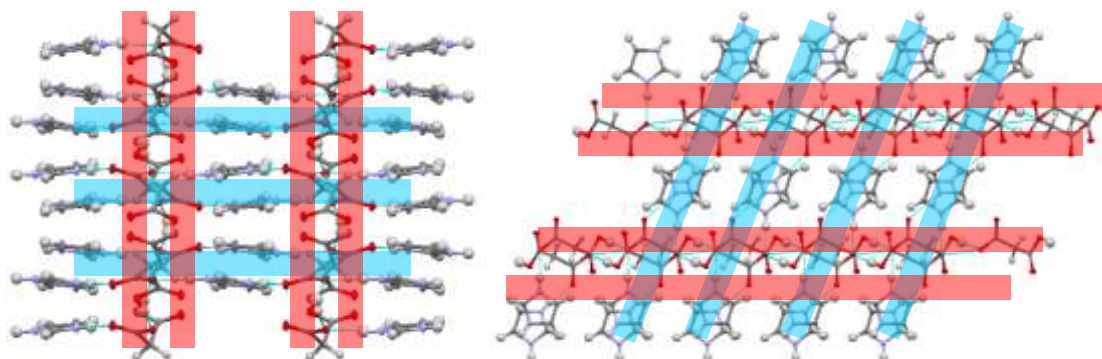


Fig. 7.90 – LHS, view along the c -axis of the extended structure; RHS, view along the b -axis of the extended structure, with the main motif (blue shading) being expanded along the b -axis by carbon – oxygen weak hydrogen bonds (red shading).

7.8 Conclusions

The library of hydrogen bond patterns shown in Figure 7.18 has featured in all the molecular complexes discussed in Chapter 7 with three of the four occurring more than once. This shows that the library of hydrogen bonding patterns is robust, dependable and in some cases very much predictable. There were also some slight derivatives of the motifs, for example the benzimidazolium : fumarate structure amalgamated the ladder and linear chain style. A majority of the imidazolium molecular complexes adopted the linear chain of hydrogen bonded alternating co-molecule motif with the addition of the chain having a spiral nature, for example in the imidazolium : 4-fluorobenzoic acid molecular complex (shown in Figure 7.31, repeated below).

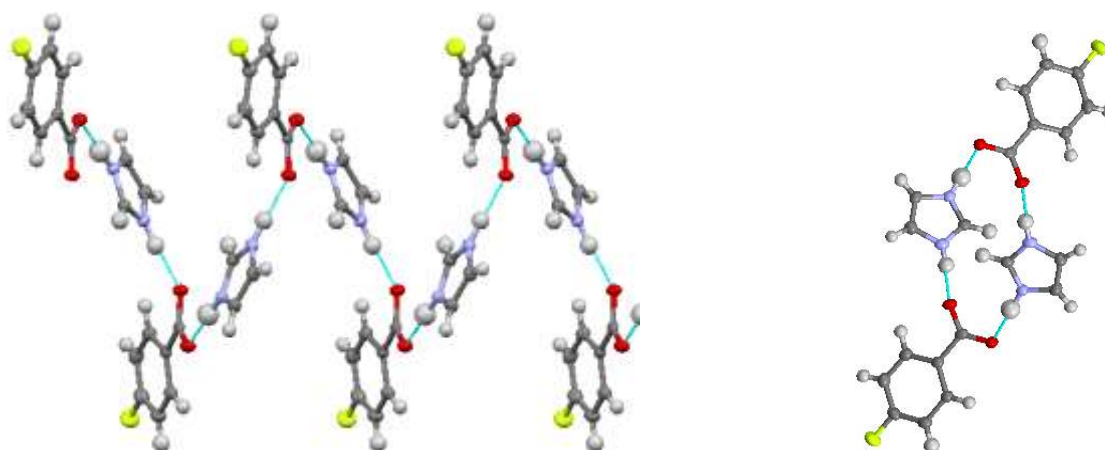


Fig. 7.31 repeated – LHS, the main motif of the $\text{IMDH}^+ 4\text{-FBA}^-$ molecular complex, a spiral chain of alternate co-molecules held together through $\text{N-H}\cdots\text{O}$ hydrogen bonds, E and F; RHS, view along the b -axis of an extended spiral chain showing its circular nature.

The halo-benzoic acid structures shown in this chapter, but also in Chapter 5, have shown the important nature of the halogen atoms in forming interactions. From these findings, the halogen interactions, including halogen bonds, have had little influence on formation of the main motif of the structure. However, they have contributed to the construction of a more stable structure by creating more robust interactions than corresponding non halogen-containing molecules. For example in the imidazolium 4-fluorobenzoate structure, the main motifs are expanded by halogen bonds of $\text{F}\cdots\text{C}$ distance of $3.490(2)\text{\AA}$ (Figure 7.91) while in the benzimidazolium succinate molecular complex, the interaction that has a similar role is a carbon – carbon hydrogen bond of $\text{C}\cdots\text{C}$ $3.552(1)\text{\AA}$ in length.



Fig. 7.91 – LHS, extract from **Fig. 7.33**, view along the b -axis of the extended structure of imidazole 4-fluorobenzoate showing the spiral chains held together by halogen bonds (yellow lines) that connect the chains along the a - and c -axis; RHS, extract from **Fig. 7.68** – the carbon - carbon weak hydrogen bond that expands the benzimidazolium succinate structure along the b -axis.

The aromatic dicarboxylic acids produced structures with benzimidazole and imidazole that utilised the library of hydrogen bonds and in one case, benzimidazolium : terephthalic acid,

produced the same motif as the corresponding mono-substituted hydroxy-benzoic acid structure.

The differences between the structures from BZN and IMD are evident, in no case did the main motif of equivalent complex structures stay the same. In every case between a BZN and IMD structure, there was both a different motif and a different packing arrangement. In one example, the malonate complexes, the co-molecule was rearranged (Figure 7.80, repeated below) between the different molecular complexes.

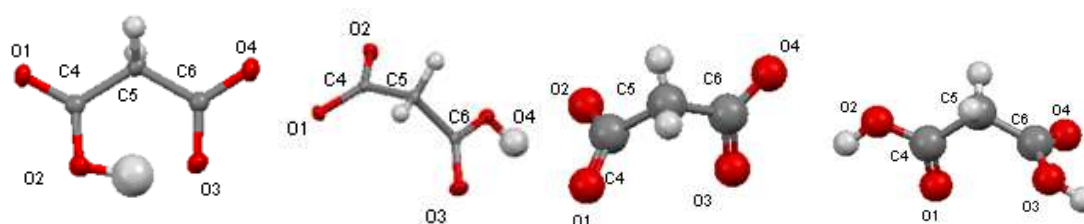


Fig. 7.82 repeated – the malonate ion found in molecular complexes with (from left to right) benzimidazolium, imidazolium, imidazolium hydrate, and in its native form, with atom labelling.

7.9 References for Chapter 7

- (1) O. Ermer, *Helvetica Chimica Acta*, 1981, **64**, 6.
- (2) D. Braga, A. Angeloni, L. Maini, A. W. Götz and F. Grepioni, *New Journal of Chemistry*, 1999, **23**, 17-24.
- (3) S. Ohba and Y. I. H. Hosomi, *Journal of the American Chemical Society*, 2001, **123**, 6349.
- (4) Y. Ito, H. Hosomib and S. Ohbab, *Tetrahedron* 2000, **56**, 6833-6844.
- (5) D. P. Martin and R. L. LaDuca, *Acta Crystallographica section E*, 2008, **64**, 2153.
- (6) Z. Jin, Y. Pan, D. Xu and Y. Xu, *Journal of Chemical Crystallography*, 1999, **30**, 119-122.
- (7) R. J. Sheehan, *Ullmann's Encyclopedia of Industrial Chemistry*, 2000.
- (8) H. Mera and T. Takata, *Ullmann's Encyclopedia of Industrial Chemistry*, 2005.
- (9) J. L. Derissen, *Acta Crystallographica section B*, 1974, **30**, 2764-2765.
- (10) W. Clegg and L. Russo, *Crystal Growth & Design*, 2009, **9**, 1158-1163.
- (11) D. R. Trivedi, A. Ballabh and P. Dastidar, *CrystEngComm*, 2003, **5**, 358-367.
- (12) J. C. MacDonald, P. C. Dorrestein and M. M. Pilley, *Crystal Growth & Design*, 2001, **1**, 29-38.
- (13) Ulrich K. Thiele; Polyester Bottle Resins, Production, Processing, Properties and Recycling, pp. 85 ff, Heidelberg, Germany, 2007
- (14) M. Bailey and C. J. Brown, *Acta Crystallographica*, 1967, **22**, 387-391.
- (15) A. Domenicano, G. Schultz, I. Hargittai, M. Colapietro, G. Portalone, P. George and C. W. Bock, *Structural Chemistry*, 1990, **1**, 107-122.

- (16) M. Led, J. Janczak and R. Kubiak, *Journal of Molecular Structures*, 2001, **595**, 77-82.
- (17) Wei LI, Ming-Xing LI, Xiang HE, Min SHAO and B.-L. AN, *Chinese Journal of Chemistry*, 2008, **26**, 2039-2044.
- (18) C. J. Brown, *Acta Crystallographica*, 1966, **21**, 1-5.
- (19) NNFCC Renewable Chemicals Factsheet: Succinic Acid
- (20) I.M.Dodd, S.J.Maginn, M.M.Harding, R.J.Davey (1998) *Private Communication*
- (21) V. R. Thalladi, M. Nüsse and R. Boese, *Journal of the American Chemical Society*, 2000, **122**, 9227-9236.
- (22) G. M. Day, A. V. Trask, W. D. S. Motherwell and W. Jones, *Chemical Communications*, 2006, 54-56.
- (23) B. Hsu and E. O. Schlemper, *Acta Crystallographica section B*, 1980, **36**, 3017-3023.
- (24) N. R. Jagannathan, S. S. Rajan and E. Subramanian, *Journal of Chemical Crystallography*, 1994, **24**, 75-78.
- (25) R. S. Gopalan, P. Kumaradhas, G. U. Kulkarni and C. N. R. Rao, *Journal of Molecular Structures*, 2000, **521**, 97-106.
- (26) R. G. Delaplane, W. I. F. David, R. M. Ibberson and C. C. Wilson, *Chemical Physics Letters*, 1993, **201**, 75-78.
- (27) R. K. McMullan, W. T. Klooster and H.-P. Weber, *Acta Crystallographica section B*, 2008, **64**, 230-239.
- (28) A. D. Burrows, R. W. Harrington, M. F. Mahon and S. J. Teat, *CrystEngComm*, 2005, **7**, 388-397.
- (29) N. T. Saraswathi and M. Vijayan, *Acta Crystallographica section B*, 2002, **58**, 734-739.
- (30) F. Jian, P. Zhao, Y. Li, X. Wang and Q. Yu, *International Journal of Quantum Chemistry*, 2008, **108**, 521-532.
- (31) A. D. Warth, *Applied and Environmental Microbiology*, 1991, **57**, 3410-3414.
- (32) C. C. Wilson, N. Shankland and A. J. Florence, *Journal of the Chemical Society, Faraday Transactions*, 1996, **92**, 5051-5057.
- (33) K. Dekaa, M. Laskara and J. B. Baruah, *Polyhedron*, 2006, **25**, 2525-2529.

8 Conclusions and Future Work

8.1 Hydrogen Bond Patterns/ Motifs

Of all the possible hydrogen bonding patterns, the many possibilities of potential hydrogen bond motifs that could be generated between the BZN and IMD and all the co-molecules used, surprisingly only four unique hydrogen bonding patterns and four hydrogen bond motifs can be used to describe every structure generated (Figure 8.1). This shows that the library of hydrogen bonding patterns is robust, dependable and in some cases very much predictable.

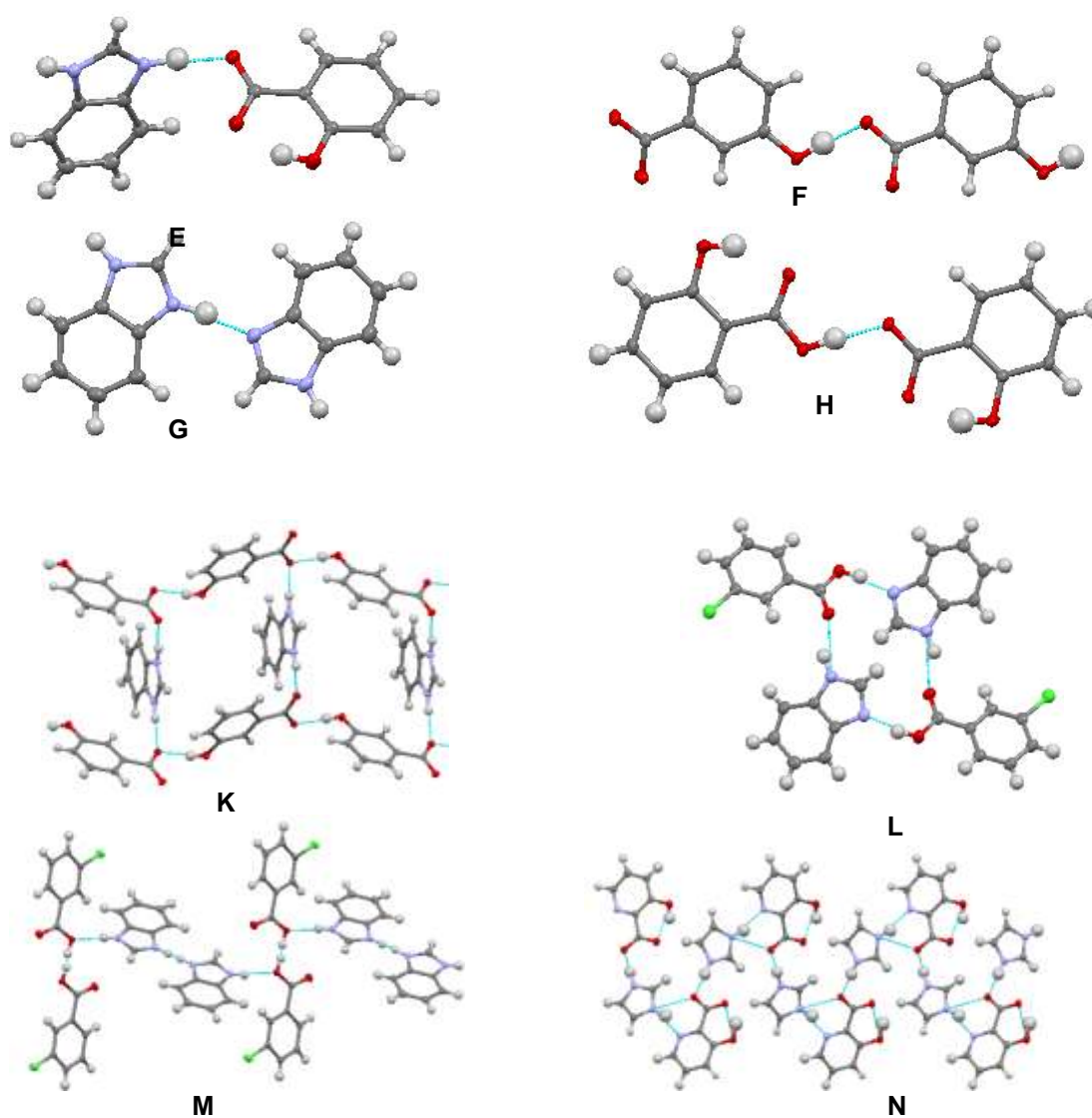


Fig. 8.1 – The library of hydrogen bond patterns that the molecular complexes discussed in this work are highly likely to adopt: **E** ($N^{\delta+}-H\cdots O^{\delta-}$), **F** ($O-H\cdots O^{\delta-}$), **G** ($N^{\delta+}-H\cdots N^{\delta+}$) and **H** ($O-H\cdots O$). The recurrent motifs found are defined as the general descriptor of these interactions: **K** is the ladder motif, **L** is the hydrogen bonded ring motif, **M** is the co-molecule dimer motif, while **N** is an example of a linear chain of alternate co-molecules.

Within this overall consistent picture of the outcomes of the attempts at “crystal engineering” in these families of structures, there are some variations that need to be accounted for. For example, the BZN : 3-/6-hydroxypicolinic acid molecular complex structures (Section 6.4) are found to adopt a nitrogen – nitrogen hydrogen bond involving the pyridine nitrogen that is partially, but not fully, described by hydrogen bond pattern H. There are also some slight deviations found within the motifs, for example the benzimidazolium fumarate structure amalgamates the ladder and linear chain style (Section 7.7.1). However even accounting for these, the re-occurrence of the hydrogen bond patterns / motifs shown in Figure 8.1 is remarkable. By using this library, the major hydrogen bonds and likely motifs in the molecular complexes of benzimidazole with any carboxylic acid containing co-molecule of similar size to those studies could be predicted, with some confidence. Given further time and more extensive investigation, more molecular complexes of BZN/IMD with carboxylic acid containing molecules could be produced and characterised. Further research could be carried out with a range of co-molecules that the findings in this work would predict to produce a molecular complex with benzimidazole; these could include *alpha*-hydroxy acids (glycolic acid, lactic acid and mandelic acid), tricarboxylic acids (citric acid, isocitric acid and aconitic acid), and keto acids (pyruvic acid, oxaloacetic acid and levulnic acids). There is also potential for BZN/IMD to be used with pharmaceuticals in producing molecular complexes/co-crystals. For example in this work BZN/IMD : salicylic acid (2-hydroxybenzoic acid) molecular complexes were produced. There are a vast amount of pharmaceutically active ingredients that contain carboxylic acid groups that could be utilised in such further investigations.

One rule that was followed during this research, and which was found to be useful, is that co-crystallisation experiments tended to be more successful between molecules of similar sizes/weights. While examples of complexes have been produced where this is not the case (imidazole : 3-hydroxypicolinic acid), there are many more examples where it was.

From Figure 8.1 it can be seen that hydrogen bond E incorporates all N–H···O hydrogen bonds. This, as would be predicted, is the most influential intermolecular hydrogen bond between the co-molecules and can vary, quite considerably, in strength. However this hydrogen bond, as has been seen throughout this work, is robust, dependable and flexible. The

O–H⋯O hydrogen bond between a hydroxyl and a carboxylate oxygen (F), is a very common hydrogen bond used by crystal engineers for its dependability and flexibility. In this body of work it promotes the ladder motif as it tends to be the shortest hydrogen bond of those listed in Figure 8.1 and therefore the most influential. This can be demonstrated, as when there is potential for this type of hydrogen bond (not available in the 2-HBA molecular complexes) to form, it does so, and thus determines the rest of the structure. There is no better example than in the benzimidazole and 3,5-dihydroxybenzoic acid molecular complex (Section 4.5.8), where the 3,5-dihydroxybenzoic acid molecules create a network of chains with the BZN molecules fitting in where possible. The other O–H⋯O hydrogen bond shown in Figure 8.1 – H, a carboxylic acid dimer (carboxylic acid and a carboxylate group) is seen in a few molecular complexes including $\text{BZNH}^+ : 2\text{-HBA}^-$ 1:2 and $\text{BZN} : \text{terephthalic acid}$ and represents the hydrogen bonds found between carboxylic acid groups in the series' investigated. The BZN dimer / nitrogen – nitrogen hydrogen bond (G), is the least predictable of all the hydrogen bonds, however it does always occur when there is a stoichiometric excess of BZN to the other co-molecules, in which case a non-protonated nitrogen is present. These recurrent and predictable hydrogen bonds have ranges in length, however one of these always forms the primary hydrogen bond in the structure.

A majority of the imidazolium molecular complexes produced during this work adopt the linear chain of hydrogen bonded alternating co-molecule motif (Figure 8.1 – N) with the chain adopting a spiral nature. This can be seen, for example, in the imidazolium : 4-fluorobenzoic acid molecular complex (Figure 7.31; repeated below). The spiral structure, most famously known from DNA, can be exploited at the molecular level to generate new materials, and in more recent investigations as a potential means of generating chirality in solid-state systems. The spirals tended to be held together by weak interactions, in this case halogen bonds, which can be altered (using different halogen atom) or replaced (by using methyl groups) to modify the structure selectively. This is one area where further research is required.

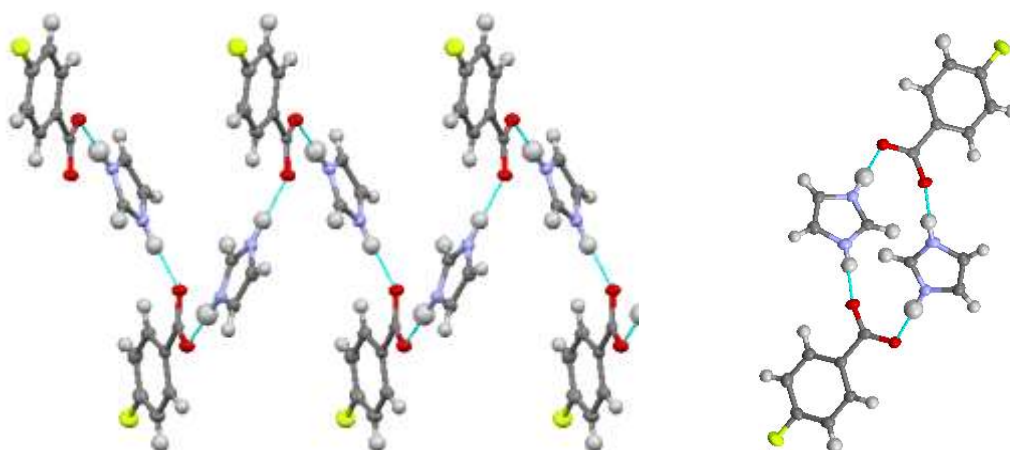


Fig. 7.31 repeated – LHS, the main motif of the $\text{IMDH}^+ 4\text{-FBA}^-$ molecular complex, a spiral chain of alternate co-molecules held together through $\text{N-H}\cdots\text{O}$ hydrogen bonds, types E and F, RHS, view along the b -axis of an extended spiral chain showing its circular nature.

8.2 Ladder Motif

The ladder motif, consisting of uprights of the carboxylic acid containing molecule and rungs of BZN, has a strong tendency to occur when there is potential for the carboxylic acid molecules to create a chain. For example, 4-hydroxybenzoic acid molecules can hydrogen bond to one-another through the hydroxyl-carboxylate hydrogen bond (Figure 8.1 – F), unlike the 2-hydroxybenzoic acid molecules where this is impossible. When generation of these chains was possible, the ladder motif prevailed. There is only one set of structures where the ladder motif was possible but did not occur, those comprising BZN/IMD with isophthalic acid. The resulting structures of these molecular complexes are found to maximise the hydrogen bond acceptor - donor pairing. If the chains had prevailed in these structures then there would have been a hydrogen bond acceptor site (oxygen) not involved in a hydrogen bond.

Figure 8.2 highlights all the molecular complexes that produced the ladder motif (apart from the benzimidazolium 3,5-dihydroxybenzoate molecular complex and associated hydrates), which as can be seen, is very flexible. There are variations of the motif, ranging from a “traditional” straight ladder, as in the $\text{IMD} : \text{malonate}$ structure, a wavy ladder as in $\text{BZN} : 3\text{-HBA}$ 1:1 and even a flat ladder, $\text{IMD} : \text{succinate}$. Also the differing ratios of co-molecules have resulted in different rung sizes, for example when there is an excess of BZN molecules

present, they pair together which results in the poles being further apart, therefore offering the potential to generate a more porous materials. The study using the series of BZN/IMD with dicarboxylic acid chains attempted to create materials with differing pore sizes with differing co-molecules. Unfortunately insufficient ladder structures were created to allow any conclusions to be formed. However it can be seen when comparing the structures shown in Figure 8.2 that there is potential to form materials with differing pore sizes. It is this flexibility in the motif that increases its potential uses; the ability to create networks with differing pore sizes is a strong area of interest for a range of industries. Therefore further work is required to develop further the ladder motif.

Within hydroxybenzoic acid complexes there are two slightly different variants: ladder with rungs of BZN molecules and ladder with alternate rungs of BZN molecules. These derivatives are neatly shown in the $\text{BZNH}^+ 3\text{HBA}^-$ polymorphs where the two forms adopt the different styles. It would not be surprising if more polymorphs of the $\text{BZN} : 3- / 4\text{-HBA}$ molecular complexes not discovered during this work were produced and found to adopt the ladder motifs, for example a $\text{BZNH}^+ 3\text{-HBA}^- 1:1$ polymorph forming the alternate step ladder motif and the $\text{BZNH}^+ 4\text{-HBA}^- 2:1$ polymorph forming the ladder with every step motif.

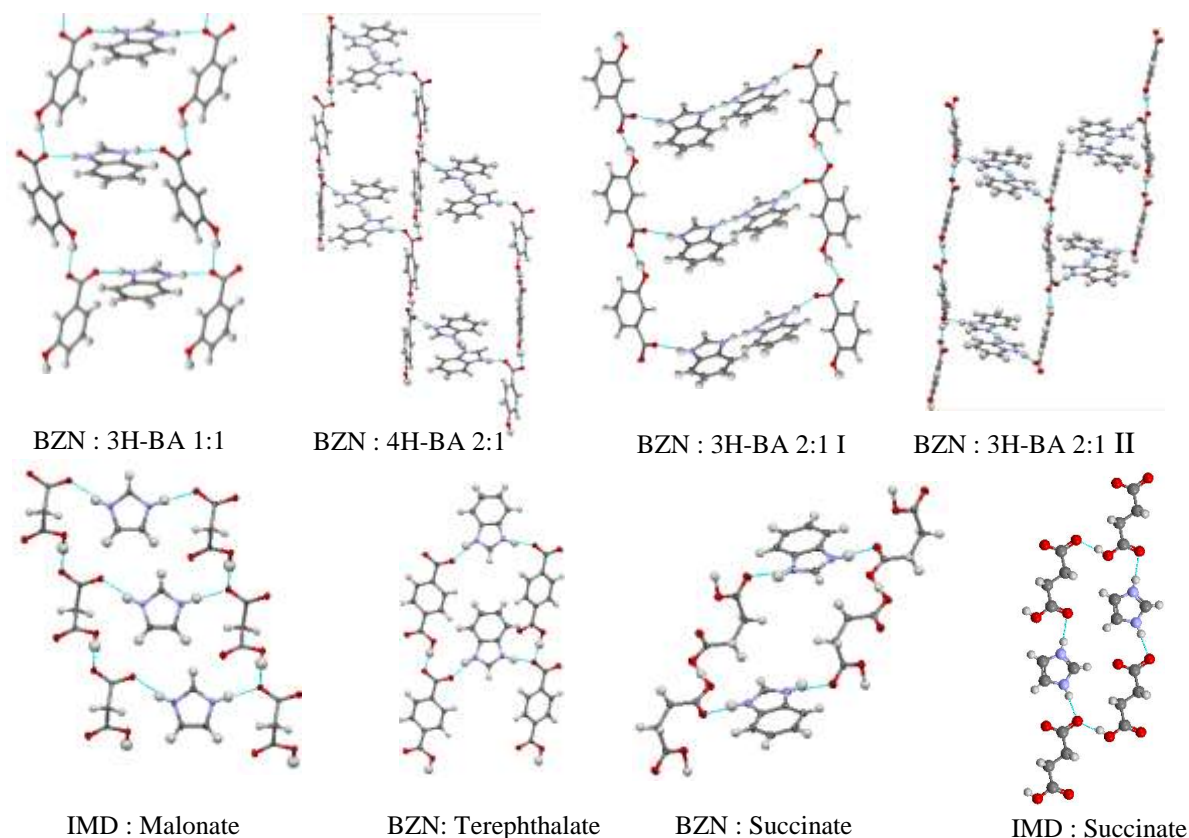


Fig. 8.2 – The molecular complexes that formed the ladder motif, with uprights of the carboxylic acid containing molecule and rungs of benzimidazole. From top to bottom, left to right, benzimidazolium : 3-hydroxybenzoate, benzimidazolium : 4-hydroxybenzoate 2:1, benzimidazolium: 3-hydroxybenzoate 2:1 Form I, benzimidazolium : 3-hydroxybenzoate 2:1 Form II, imidazolium : malonate, benzimidazole : terephthalate, benzimidazole : succinate and imidazolium : succinate.

8.3 Proton Transfer

Of the properties present in the molecular complexes produced, one aspect was found to be essentially certain to occur – proton transfer. Of all the molecular complexes produced and discussed, there were only two molecular complexes that showed no proton transfer, benzimidazole : 3-chlorobenzoic acid Form I and benzimidazole : 4-fluorobenzoic acid (in each of these structures there were two equivalents of each molecule, one pair formed the charged species while the other remained in their neutral states). In addition in these systems both diffraction experiments have questionable data quality (completeness value of around 97%) and no neutron diffraction experiments were undertaken, therefore there are still uncertainties over proton position.

However accepting the indicated proton transfer patterns, rationalising these is difficult. The empirical pKa rule, based on the ΔpK_a value, ($\Delta pK_a = pK_a(\text{base}) - pK_a(\text{acid})$), does not fully explain the outcome, since with pKa values for 3-chloroBA being 3.84 and that for 4-fluoroBA at 4.15, it would be predicted that other molecules within this range would also form the covalent molecular complex co-crystal rather than the salt when using the same solvent and temperature. For example, the pKa values for 4-bromobenzoic acid (3.96), 4-chlorobenzoic acid (4.00) and 3-hydroxybenzoic acid (4.08) are similar, but it is not the case that covalent complex co-crystals are formed. Attempts were made to use varying pH levels of the crystallisation solution to promote/discourage proton transfer, with the conclusion being that in basic conditions co-crystallisation experiments tended to be unsuccessful; however this is not universal. There is no question that further work is required on this aspect, with a wider range of pH levels, better controlled experimental conditions and a wider range of co-molecules utilised. However these limited results add another set of examples that call into question the robustness of the pKa rule.

In the systems studied, proton transfer has in general promoted hydrogen bonding between the BZN/IMD and carboxylic acid group due, primarily, to the proton transferring from the acid to the basic nitrogen. While a proton transferring from one group to another does not require a hydrogen bond or infer that a hydrogen bond will be created, in this work they went hand-in-hand. The proton transferring to the BZN/IMD resulted, in many cases, in there being only one hydrogen bond acceptor site for the donor sites to bond to, therefore only one possible hydrogen bond could occur. This charge assisted nitrogen-oxygen hydrogen bond (hydrogen bond pattern E in Figure 8.1) was very flexible but robust.

8.4 Solvent-Free Crystallisation/Co-crystallisation

The solvent free grinding method, validated to an extent in the experiments described during this work, is a very old method giving a new lease of life. There is debate over whether the term solvent-free is correct but there can be no debate that this technique works and is able to generate new materials and even materials unobtainable from normal solvent crystallisation methods. The acceptance of this technique has grown extraordinarily over a very short period of time recently, with it becoming common place in crystallisation groups (and a wide range of others) to perform solvent-free experiments when dealing with new molecules or trying to form previously unreachable forms. The drivers of this technique are the increase in speed and decrease in cost of reactions, however problems arise in forming uniform and stable products. With further work and a greater understanding of the mechanisms involved, these problems will be resolved and the utility of the technique increased still further.

8.5 Solvent Mediated Molecular Complex Polymorphism Formation

The co-crystallisation experiments between BZN and the halo-benzoic acid series resulting in the formation of seven previously undiscovered molecular complexes, however the primary aim of the work was to investigate the occurrence of molecular complex polymorphism and to selectively control the form produce. The results show that polymorphism is common within molecular complexes, with three of the seven newly discovered systems showing evidence of this. Controlled growth of a selective polymorph has also been achieved through changes in

crystallisation conditions, as shown for the three materials that showed polymorphism. However, it only takes small changes in these conditions to promote other forms, for example co-crystallisations between benzimidazole and 3-chlorobenzoic acid using acetone produced polymorph Form III at 30°C, but Form I and III were produced at 20°C (Table 5.7; repeated below).

	Methanol	Ethanol	Propanol	Acetone
2~4°C	Yellow	Red	Blue	Yellow, Red
10°C	Yellow	Red	Blue	Yellow, Red
20°C	Yellow	Red	Blue	Blue, Red
30°C	Blue	Red	Red	Red

Table. 5.7 repeated – The results of cocrystallisation experiments on the benzimidazole and 3-chlorobenzoic acid system in creating Form I (blue), Form II (yellow), Form III (red).

There are two examples where the structures have been fully determined for at least two of the possibly molecular complex polymorphs: BZN : 3ClBA (Figure 5.34, repeated below) and BZN : 3HBA 2:1 (Figure 4.39, repeated below). It can be seen that the structural differences are substantial, with two forms of the 3-chlorobenzoic acid complex in particular adopting a whole different motif.

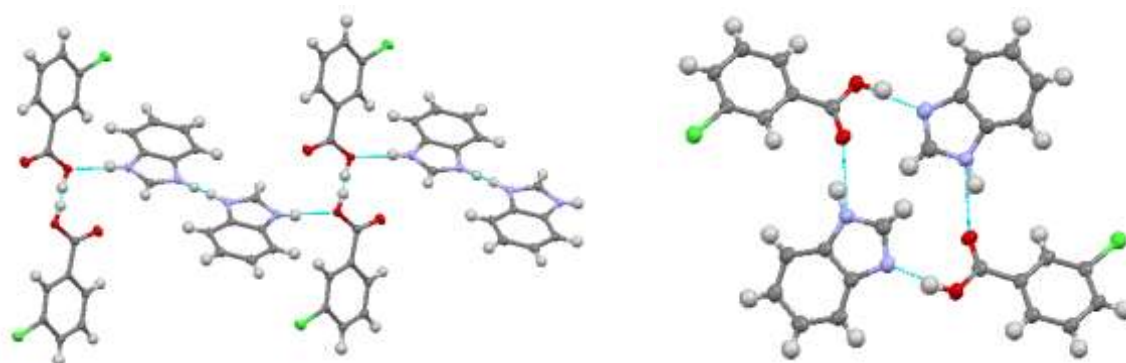


Fig. 5.34 repeated – LHS, the supramolecular synthon of the BZN : 3-CIBA Form II molecular complex, co-molecule dimers, linked together through $N^{\delta+}-H\cdots O^{\delta-}$ hydrogen bonds, RHS, the main motif of the BZN : 3-CIBA Form I molecular complex, an equimolar hydrogen bonded ring system held together by $N-H\cdots O$ and $O-H\cdots N$ hydrogen bonds.

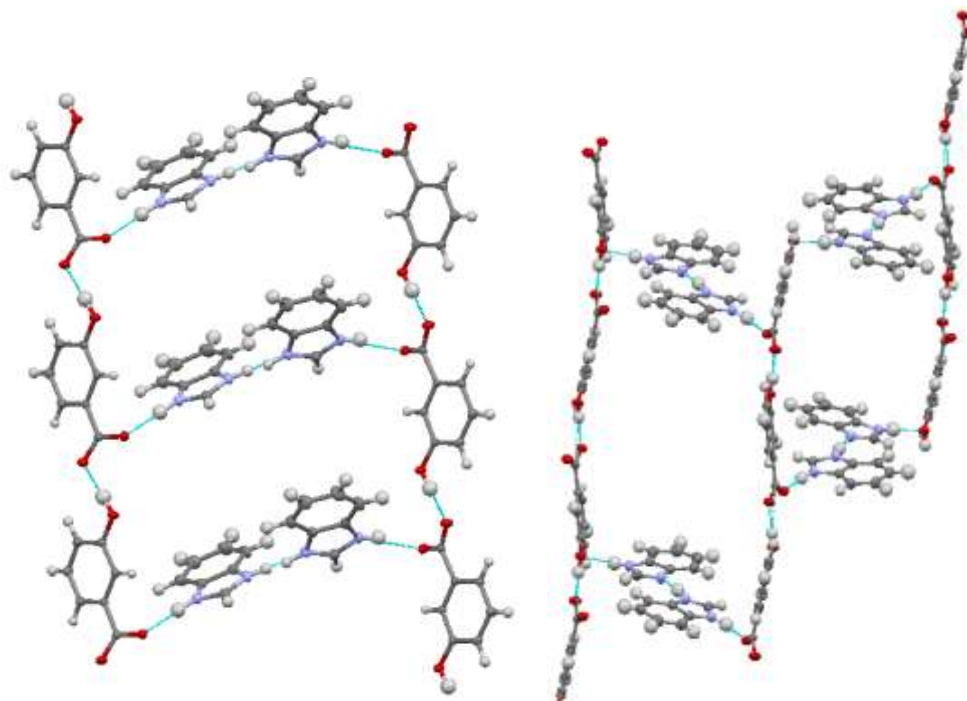


Fig. 4.39 repeated – LHS, Form II, the ladder structure consists of uprights of 3-hydroxybenzoate molecules and rungs of hydrogen bonded dimers of $BZNH^+$, RHS, Form I, the ladder structure consists of stiles of 3-hydroxybenzoate molecules and alternate rungs of hydrogen bonded dimers of $BZNH^+$.

8.6 Increasing the Competition – The Introduction of Competing Hydrogen Bonding Sites

The work presented in Chapter 6, which saw an introduction of another basic atom into the system, was to add competition within the system on two fronts; firstly with the other basic nitrogen on the BZN for proton transfer and for involvement in the potential hydrogen bonds. With regard to the proton transfer, in all cases studied the proton from the carboxylic acid group has transferred to the benzimidazole molecule, as has been seen in all but two examples in this whole work. There are some variations which are discussed in Chapter 6. When the basic nitrogen is unprotonated, the established $N-H\cdots O$ hydrogen bond is not favoured over a $N-H\cdots N$ hydrogen bond, with the $N-H\cdots O$ interaction forming the weaker part of a bifurcated hydrogen bond (Figure 6.50, repeated below). Therefore it has competed with the carboxylic

acid group to be the primary hydrogen bond acceptor and this designed intervention was successful.

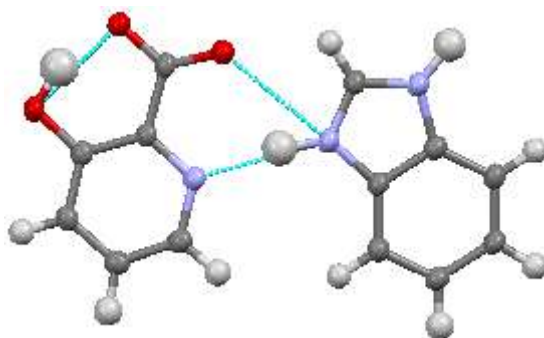


Fig. 6.50 repeated – The bifurcated hydrogen bond of the $\text{BZNH}^+ : 3\text{-HPA}^-$ molecular complex, with the major component the $\text{N-H}\cdots\text{N}$ hydrogen bond and minor component being $\text{N-H}\cdots\text{O}$.

The other possible outcome was that if the nitrogen was protonated, it would compete with the other protonated nitrogen on the benzimidazole for the primary hydrogen bond donor role. As the benzimidazole is found still to be protonated, the hydrogen bond donors from this molecule would be charged assisted and therefore still a more attractive prospect for hydrogen bond acceptors. With this being the case it was not surprising to see that in the benzimidazole and 6-hydroxypicolinic acid molecular complex the N atom of the pyridine was acting as a the donor in a hydrogen bond, however it was the weakest of the three primary hydrogen bonds within the structure at $2.915(2)\text{\AA}$. The solvate structure also had the named N atom within hydrogen bonds, which also produced one of the weaker hydrogen bonds in the structure and again had a length of $2.915(3)\text{\AA}$.

8.7 A Comparison Study of Benzimidazole and Imidazole Containing Molecular Complexes with a Range of Related Co-Molecules

The differences between the structures from BZN and IMD are evident; in no case did the main motif of equivalent structures stay the same. In every case between a BZN and IMD structure, there was different motif and different packing arrangement. In one example, the malonate complexes, the co-molecule was rearranged (Figure 7.80, repeated below) between the different molecular complexes. The only common features were in the hydrogen bond patterns that the structures adopted.

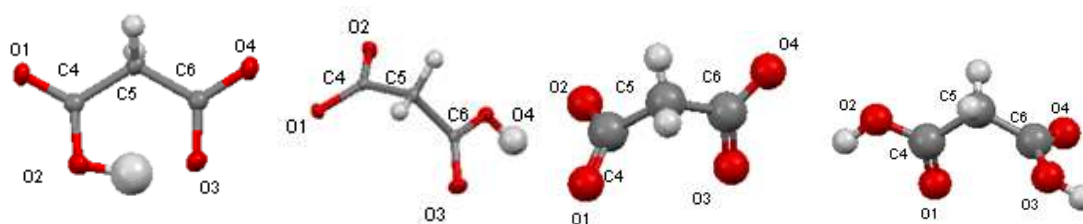


Fig. 7.80 repeated – the malonate ion found in the molecular complexes with (from left to right) benzimidazolium, imidazolium, imidazolium hydrate and its native form with atom labelling.

8.8 Halogen Bonding

The halogen containing structures shown in this work have shown the important nature of the halogen atoms in forming interactions. It does not appear that the halogen interactions, be they halogen bonds or other halogen-containing interactions, had much influence on the main motif of the structure. However they have contributed to the construction of a more stable structure by creating more robust interactions than those found in corresponding non-halogen containing molecules. For example in the imidazolium 4-fluorobenzoate structure, the main motifs are expanded by halogen bonds of $F\cdots C$ distance of $3.490(2)\text{\AA}$ (Figure 7.89, repeated below) while in the benzimidazolium succinate molecular complex, the interaction that has a similar role is a carbon- π interaction of $C\cdots C$ $3.552(1)\text{\AA}$ in length. From all the structures in Chapter 5 the halogen atom is involved in either a halogen bond or halogen interaction. These interactions tend to be individual in the role they adopt, they are the only interaction that expands the structure in a particular direction, for example in the benzimidazole 4-fluorobenzoic acid molecular complex the halogen bond is the only interaction that expands the structure in the *c*-direction. This body of work shows that the halogen bond is significant and is key in determining the overall packing.



Fig. 7.89 repeated – LHS, extract from **Fig. 7.33** View along the b-axis of the extended structure showing the spiral chains are held together by halogen bonds (yellow lines) that connect the chains along the *a*- and *c*-axis, RHS, extract from **Fig. 7.69** – insert, the C-H... π interaction

8.9 Concluding Remarks

The robustness of both hydrogen bond patterns and the more extended motifs adopted by the molecular complexes that contain these patterns gives real promise that a rational, more predictive, approach to crystal engineering can be generated in families of compounds such as those presented here. Subtle variations in choice of co-molecules and in crystallisation conditions has been shown to affect the crystal form adopted, both in terms of motifs and in some cases in polymorphic form adopted, including examples where polymorph control has been obtained. In particular, it has been found possible during this work actually to make predictions about likely molecular association and packing of molecular complex structures that have been borne out by subsequent experiments.